

Las Gallinas Creek

Hydrologic, Hydraulic and Coastal (HH&C)



U.S. Army Corps of Engineers

San Francisco District

Water Resources Section

December 2013

Table of Contents

Section	Page
Introduction	2
Evaluation of Flood Risk (1990)	3
Re-Evaluation of Flood Risk (2009 to Present)	4
Hydrologic Analysis (2009-2011)	4
Hydrology and Hydraulics and Coastal Analysis (2012)	5
Las Gallinas Creek Downstream Boundary Condition Analysis (2013)	7
Hydraulic Loading Analysis (2013)	8
References	9
Figure	
1. Study Area	3
Tables	
1. Difference in Peak Discharges Downstream of the Confluence of the North and South Forks for the 1990 and 2011 Hydrologic Analysis	5
2. Probabilities of Water Surface Elevations Being Exceeded Now and Fifty Years in the Future Based on Various Sea Level Rise Scenarios.	8
Appendices	
A. Fluvial and Tidal Flooding Analysis Section 205 Reconnaissance Study, Gallinas Creek, Marin County, California, USACE 1990.	
B. Las Gallinas Hydrologic Analysis, South Fork Drainage Basin Final Report, Noble Consultants and Multech Engineering Consultants, Inc, May 2009	
C. Las Gallinas Creek Hydrologic Analysis, Final Report, USACE, August 2011	
D. Final Report, Las Gallinas Creek H&H & Coastal Analysis, Noble Consultants, 2012	
E. Las Gallinas Creek – Downstream Boundary Conditions Analysis, USACE, 2013	
F. Las Gallinas Creek – Hydraulic Loading, USACE, 2013	

Introduction

Santa Venetia (Marin County, CA) was a tidal marsh area prior to being developed for residential use in the early 20th century. Due to the low initial elevation of the fill and the compressible nature of the underlying bay mud, this land has subsided and continues to subside. Extensive and reoccurring flooding in the 1940s-1950s led to the creation of Zone 7 of the Marin County Flood Control and Water Conservation District (District) in 1962. Since then, a system of levees and pump stations has been constructed to reduce the area's flood risk. Many of the constructed improvements were recommendations contained in the 1971 report Marin County Flood Control and Water Conservation District Zone 7 Long Range Plan for Drainage and Flood Control. Record high tides in San Francisco Bay led to extensive breaching of the levees in 1983 which inundated streets and homes with several feet of water. As a direct emergency response, wooden floodwalls were installed on top of many of the existing earthen levees along Gallinas Creek. These floodwalls increased the level of protection afforded by the levees by adding approximately two feet to their height; however, they were not representative of standard material or design typically used in floodwall construction. The Las Gallinas Creek levee helps protect Santa Venetia from flooding, inundation by high tides and rainfall-runoff storm events, both of which may be a persistent threat to the community as ground subsidence continues and sea levels rise. A map of the study area is shown in Figure 1.

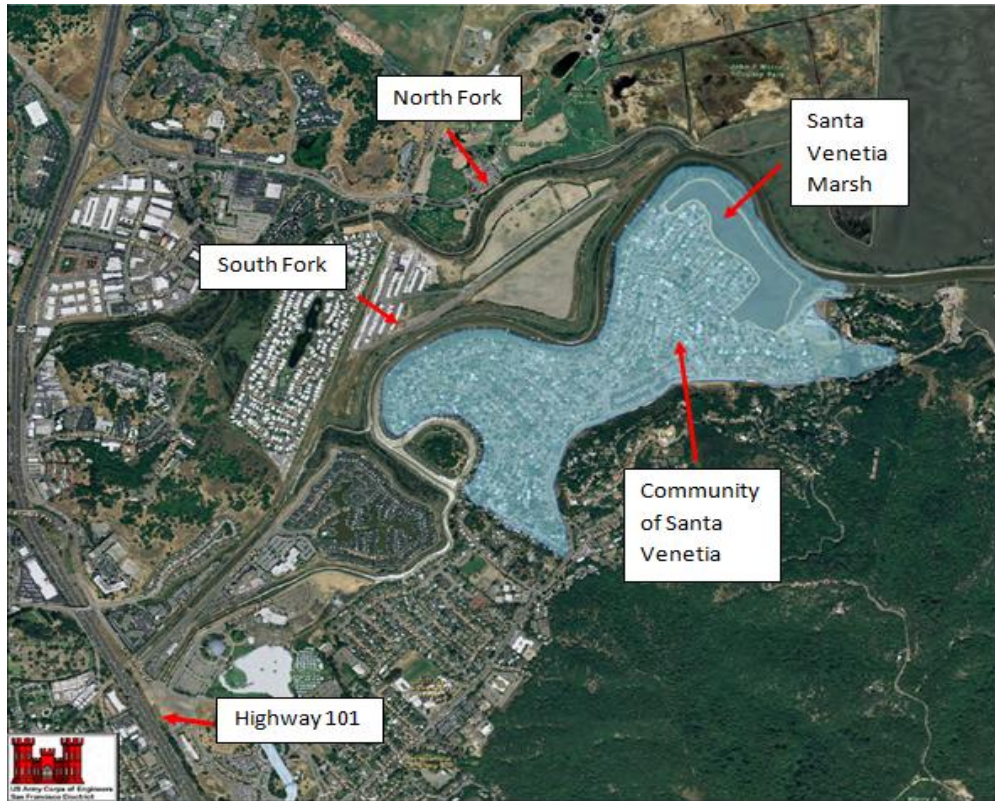


Figure 1. Study Area

Record high tides in San Francisco Bay led to extensive breaching of the levees in 1983 which inundated streets and homes with several feet of water. As a direct emergency response, wooden floodwalls were installed on top of many of the existing earthen levees along Gallinas Creek. These floodwalls increased the level of protection afforded by the levees by adding approximately two feet to their height; however, they were not representative of standard material or design typically used in floodwall construction.

Evaluation of Flood Risk (1990)

The likelihood of flooding due to overtopping of the levee and floodwall was studied by the U.S. Army Corps of Engineers, San Francisco District (USACE) and published as *Fluvial and Tidal Flooding Analysis Section 205 Reconnaissance Study, Gallinas Creek, Marin County, California* in 1990 (Appendix A). The results of the study concluded that the flood risk reduction benefits of a federal project would probably not be economically justifiable. The study implicitly assumed that the wooden floodwalls and levees would not breach due to

any level of hydraulic loading, even if they were overtopped. The levee and floodwall system could possibly breach under hydraulic loads up to and including overtopping of the system. Since a levee breach event would allow more water to inundate Gallinas Village than was estimated by the 1990 study, the flood risk and resulting damages may have been previously underestimated. Since 1990, the USACE has adopted probabilistic methods of defining risk and uncertainty in flood damage reduction studies and new methods of estimating future sea level rise.

Re-Evaluation of Flood Risk (2009 to Present)

USACE has since re-evaluated the level of flood risk in Gallinas Village due to failure of the existing levee and floodwall. The analysis has taken into consideration several factors, including: (1) hydrology of the Las Gallinas Creek watershed, (2) hydraulics of the South Fork of Las Gallinas Creek and Las Gallinas Creek downstream of the confluence with the North Fork, (3) coastal hydraulic processes acting on the Santa Venetia Marsh levee and the Las Gallinas Creek levee (which generally parallels Vendola Drive), (4) the probability of coincidence of rainfall-runoff events with high tide events, and (5) the potential for sea level rise. This summary provides an overview of the purpose and findings of each of the studies, which have been included herein as appendices.

Hydrologic Analysis (2009-2011)

The District provided geographic data related to topography, land use, imperviousness and soil type for use in the updated hydrology study *Las Gallinas Hydrologic Analysis, South Fork Drainage Basin, Final Report* (Appendix B) which was completed by Noble Consultants, Inc. (Noble) and Multech Engineering Consultants, Inc. in May 2009 for SPN. Eight frequency precipitation events were modeled based on rainfall data collected in San Rafael.

Stormwater runoff was routed through the watershed to determine peak flow rates at multiple points of interest throughout the study area. However, the Nobel Report only evaluated the South Fork Drainage basin. The Corps updated the 2009 hydrologic analysis to include the North Fork. The analysis was completed in August 2011, and the results of the revised analysis were published as the *Las Gallinas Creek Hydrologic Analysis, Final Report*. The complete report, which describes all of the methods, assumptions, and results

in detail, is included as Appendix C. The 1% annual chance exceedance (ACE) event, sometimes referred to as a 100-year flood, was previously estimated in the 1990 study to be 2,280 cfs downstream of the confluence of the north and south forks. The 2011 study estimated the mean 1% ACE event to be 3,159 cfs at the same location, with 90% confidence that the true 1% ACE value at the confluence is between 1,586 and 6,292 cfs. Table 1 shows the difference in peak discharges downstream of the confluence of the North and South Forks for the 1990 and 2011 hydrologic analysis.

Table 1. Difference in peak discharges downstream of the confluence of the North and South Forks for the 1990 and 2011 hydrologic analyses

Annual Chance Exceedance (ACE) Event	1990 Hydrologic Analysis (cfs)	2011 Hydrologic Analysis (cfs)
10%	1230	1843
2%	1960	2778
1%	2280	3159

Hydrology and Hydraulics (H&H) and Coastal Analysis (2012)

An analysis of riverine hydraulics of the South Fork of Las Gallinas Creek and the marsh levee (Appendix D) was performed by Noble Consultants, Inc. (Noble), for USACE. Peak flow values used in the simulation were derived from the 2011 USACE hydrology study. Model geometry was developed from topographic data provided by the District, with levee crest elevations measured at the top of the wooden floodwall. The downstream boundary condition, i.e. the tide level, was modeled to be between mean high water (MHW) and the 1-year maximum still water level, (i.e., between 3 and 4.4 feet NGVD 29).

Las Gallinas Creek levee performance, in terms of levee crest height (which includes the height of the wooden floodwall) relative to peak stage, was evaluated using current USACE Process for the National Flood Insurance Program (NFIP) Levee System Evaluation, dated 31 August 2010 (EC 1110-2-6067). The system in question must satisfy both criteria, the Risk Analysis (the Corps method), and the deterministic approach, (the FEMA method). Corps' guidance states that the target stage (top of levee/floodwall) needs to have at least 90% Conditional Non Exceedance Probability (CNP) for the 1% event and needs to meet

the deterministic check (FEMA check) for a 50% water surface profile plus 3 feet or more freeboard for the 90% CNP for the 1% event or it needs to have at least 95% CNP for the 1% event and feet or more freeboard. Although the probability of the levee containing the 1% ACE event is greater than 95%, and the levee is not expected to be overtopped even by the 0.2% ACE (500-year) event, the USACE levee performance criteria is not met under existing conditions. The levee and wooden floodwall do not meet the deterministic check.

A detailed coastal hydraulic analysis of the levee that borders the Santa Venetia Marsh, located on the eastern side of Santa Venetia, was also performed by Noble for USACE (Appendix D) as part of this document. The study took into account the normal tide cycle, storm surge, wind effects and sea level rise. Overtopping discharge rates were calculated for a variety of sea level rise and land subsidence scenarios. The study concluded that under existing sea level conditions, the marsh levee, which is higher than the creek levee (levee/floodwall structure adjacent to Las Gallinas Creek), will only be overtopped by coastal events that have less than 0.2% chance of occurring in any given year (i.e., a 500 year event), and the total overtopping flow rate would not exceed the interior drainage pump capacity. Three scenarios of conditions 50 years in the future were also simulated, with future sea levels rising according to: (1) historic rates, (2) a model developed by the International Panel on Climate Change (NRC Curve 1), and a USACE worst-expected case scenario (NRC Curve 3). A USACE geotechnical evaluation projected that the levee system will subside by a 0.2 feet over the course of the next 50 years (USACE SPN 2010). Pump capacity is expected to be exceeded by events with a 1% chance of occurring in any given year (i.e., a 100 year event) under all the future scenarios, with widely varying levels of severity. It was assumed that none of the levees would breach before or after overtopping by tidewaters, and that the interior drainage pumps would function normally. As a result, the projected flooding depths due to coastal events were generally minimal for all sea level rise scenarios.

Las Gallinas Creek Downstream Boundary Condition (DSBC) Analysis (2013)

Previous hydraulic modeling efforts described in the *Las Gallinas Creek H&H & Coastal Analysis* (Appendix E) used the mean higher high water (MHHW) as the downstream boundary condition (DSBC) at Las Gallinas Creek. The purpose of the Las Gallinas Creek Downstream Boundary is to establish a DSBC at the inlet to Las Gallinas Creek for hydraulic modeling that considers the full range of coastal water surface elevations (WSEs) and their statistical probabilities. In tidally influenced river reaches, such as the downstream portion of the Las Gallinas Creek, flood stage may be affected by coastal WSE. Therefore, it is necessary to incorporate both fluvial and coastal effects into a combined fluvial and coastal flood stage frequency analysis. Limited data is available at the Las Gallinas Creek inlet to establish a database of peak fluvial flow events to be used to evaluate the interaction of fluvial and coastal processes that could contribute to a combined coastal and fluvial flood event. Accordingly, available and proximal fluvial flow data from an adjacent watershed was used to estimate the statistical relationship between fluvial flow and the coastal parameters that contribute to the DSBC at the Las Gallinas Creek inlet. Fluvial flow information, which had an 8 year record, from Corte Madera Creek, located in the Ross Valley Watershed was used. This watershed was selected for use in this analysis based on a recommendation by the project sponsor, Marin County. The controlling parameters of coastal WSE to be used in the DSBC analysis have been identified as measured tide and wave setup. To establish the DSBC two approaches have been implemented. The methodology developed for these approaches is based on a collaborative effort with USACE teams, namely the Hydrologic Engineering Center and the San Francisco District, to develop a risk and uncertainty based analysis to statistically combine both fluvial and coastal contributions to the flood stage frequency curve. The first approach is a time series based methodology which assumes all of the controlling coastal parameters are statically independent of fluvial flow. The secondary approach used an event-based method which decouples measure tide into two parts: predicated tide and residual tide. The analysis concluded that both coastal DSVC approaches can be used to evaluate combined WSE of coastal and fluvial WSE in tidally influenced reaches of Las Gallinas Creek. Using the event based approach provides a slightly more conservative estimate of the coastal DSBC.

Hydraulic Loading Analysis (2013)

In order to quantify the effects of a significant rainfall-runoff event happening at the same time as a high tidewater event, a coincident frequency analysis (CFA) was performed. This analysis required the refinement of the coastal water surface elevations into a probability distribution function. The methods and results of the CFA are described in detail in Appendix F. The hydraulic model of the South Fork was run for a large number of combinations of flow rate and tidewater elevation of known probability of occurrence. The result was a water stage probability distribution curve at a location of the riverine levee and floodwall where geotechnical stability analyses have been performed. It was found that water surface elevations along the creek levee are tidally driven. The probability of the riverine levee being hydraulically loaded (i.e., the water surface elevation in the South Fork is greater than the ground elevation on the landward side of the levee) in any given year with existing conditions is about 10%. Worst-case scenario sea level rise projections indicate that the annual probability of hydraulic loading will rise to 50% by 2065. The existing and future water surface elevations in Las Gallinas Creek that account for both storm flow in the creek and coastal flood risk is presented in Table 2.

Table 2. Probabilities of water surface elevations being exceeded, now and fifty years in the future based on various sea level rise scenarios.

Annual Probability (%)	Year 0 Condition (ft, NGVD 29)	Year 50 Condition (ft NGVD 29)		
		Historic SLR	NRC 1	NRC 3
50	5.2	5.7	6.0	7.3
20	5.6	6.1	6.4	7.7
10	5.8	6.3	6.6	7.9
4	6.1	6.6	6.9	8.2
2	6.3	6.8	7.1	8.4
1	6.4	6.9	7.2	8.5
0.4	6.6	7.1	7.4	8.7
0.2	6.8	7.3	7.6	8.9

Note: Values highlighted in red exceed the existing wooden floodwall.

References

J. Warren Bute, Inc., 1971. *Marin County Flood Control and Water Conservation District Zone 7 Long Range Plan for Drainage and Flood Control*. Prepared for the Marin County Flood Control and Water Conservation District.

Kleinfelder, 2013. *Geotechnical Data Report, Las Gallinas Creek Levee*. Prepared for the Marin County Flood Control and Water Conservation District.

U.S. Army Corps of Engineers, San Francisco District, 1990. *Fluvial and Tidal Flooding Analysis Section 205 Reconnaissance Study, Gallinas Creek, Marin County, California*.

U.S. Army Corps of Engineers, San Francisco District, 2011. *Las Gallinas Creek Hydrologic Analysis, Final Report*.

Noble Consultants, Inc., 2012. *Final Report, Las Gallinas Creek H&H & Coastal Analysis*. Prepared for the U.S. Army Corps of Engineers, San Francisco District.

U.S. Army Corps of Engineers, San Francisco District, 2013. *Las Gallinas Creek – Downstream Boundary Condition (DSBC) Analysis*.

U.S. Army Corps of Engineers, San Francisco District, 2013. *Las Gallinas Creek – Hydraulic Loading Analysis*.

Appendix A



DEPARTMENT OF THE ARMY
SAN FRANCISCO DISTRICT, CORPS OF ENGINEERS
211 MAIN STREET
SAN FRANCISCO, CALIFORNIA 94105 - 1905

August 10, 1990

Design Branch

Mr. Romaine Repair
Marin County Flood Control
and Water Conservation District
P.O. Box 4186
San Rafael, California 94913-4186

RECEIVED
AUG 20 1990
Marin County Public Works

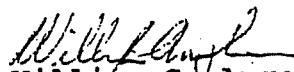
Dear Mr. Repair:

The San Francisco District of the U.S. Army Corps of Engineers has completed the hydraulic and hydrology analysis in support of the of Las Gallinas Creek Section 205 Reconnaissance Study.

The fluvial and tidal flooding analysis was based on the existing level of tidal protection and interior drainage system with the assumption that the degree of protection would be maintained at a comparable level in the future. Analysis of existing conditions considered in combination with assumed sea level rise (based on historic trends) and land subsidence indicate that impacts of tidal flooding to the Santa Venetia Community would be minimal.

Associated annual average flood damages would also be minimal. Consequently, it appears that it would be difficult to economically justify any project in the area. It is, therefore, the recommendation of the San Francisco District that the Section 205 Reconnaissance Study of Las Gallinas Creek be terminated at this time.

Please review the enclosed analysis and respond prior to September 15, 1990. If you concur that terminating the study is warranted, we would like to do so in a timely manner. Any questions or comments should be addressed to Ms. Lyn Hawkins.


William C. Angeloni
Chief, Planning/Engineering
Division

FLUVIAL AND TIDAL FLOODING ANALYSIS
SECTION 205
RECONNAISSANCE STUDY
GALLINAS CREEK
MARIN COUNTY, CALIFORNIA

INTRODUCTION

The purpose of this report is to determine the volume of runoff and wave overtopping that can cause ponding, and to determine the depth and location of the resultant ponding. This information will aid in the decision of which of two alternatives would prevent tidal related flooding and would benefit the Santa Venetia area. The first alternative would be to improve the existing floodwall/levee system which protects the Gallinas Village area, and the second alternative would be to construct a tide barrier 2,600 feet downstream from the confluence of the north and south forks.

FLUVIAL FLOODING ANALYSIS

I. Basin Description. The Las Gallinas Creek Basin (which is shown as Gallinas Creek on U.S.G.S maps) is located in the eastern portion of Marin County, approximately 14 miles north of San Francisco. The basin has a drainage area of 7.12 square miles, and is bounded by the San Rafael Creek Basin to the south, the Corte Madera Creek Basin to the west, Miller Creek to the north, and the China Camp State Park to the east. Basin elevations range from 666 feet NGVD to -1.5 feet NGVD at the Smith Ranch Airport. A basin and vicinity map are presented on Plate 1.

Gallinas Creek extends from San Pablo Bay to the confluence of its north and south forks. From this point the north fork is 1.2 miles long, and the south fork is about 4.6 miles long; however, the south fork of the creek is poorly defined beyond 1.8 miles above the confluence.

A levee system has been constructed along the north and south banks of the south and the north forks of Gallinas Creek. The area of concern, in the unincorporated area of Santa Venetia, is located adjacent to the south bank of the south fork. Due to the low elevation of the land, with respect to tidal stages in Gallinas Creek, the area has been subject to significant tidal flooding. The south fork of Gallinas Creek has overflowed its banks three times in recent years, once in 1982 and twice in 1983. The drainage system consists of five pump stations with a combined capacity of 162.5 c.f.s., a culvert with a capacity of 300 c.f.s., and an intercept with a capacity of 50 c.f.s. The drainage system has been improved by the recent addition of backup power; it is assumed that the pumps will operate when they are needed. The locations of the pump stations are shown on Plate 2.

Gallinas Creek

II. Precipitation. Normal annual precipitation (NAP) over the basin ranges from about 24.5 inches at the mouth of Gallinas Creek to about 34 inches at the higher elevations, with the basin averaging 29 inches.

III. Unit Hydrograph. Unit hydrographs for the Gallinas Creek Basin were developed using the District-wide S-curve hydrograph. Discharges were required at the downstream end of the 7.12 square mile basin, and for the sub-basin to the south of the south fork of the creek, which drains into the area which is subject to tidal flooding. The sub-basin has a drainage area of 1.04 square miles with a normal annual precipitation of 25.5 inches.

A 5-minute unit hydrograph and rainfall distribution was developed for the sub-basin, and a 15-minute unit hydrograph and rainfall distribution was developed for the basin.

Basin and sub-basin characteristics, which were used in deriving the unit hydrographs, are presented in the following tabulation:

Description	D.A. (sq mi)	L (mi)	L _{ca} (mi)	S (ft/mi)	n	Lag (hrs)	NAP (in)
Sub-basin	1.04	1.45	0.78	104	0.08	0.83	25.5
Basin	7.12	4.62	2.48	8.4	0.08	3.24	29.0

- Where:
- D.A. - Drainage area, in square miles;
 - L - Length of primary watercourse, in miles;
 - L_{ca} - Distance from the centroid of the basin to the downstream end of the basin measured along the primary watercourse, in miles;
 - S - Slope of primary watercourse, in feet per mile;
 - n - Basin roughness coefficient, dimensionless;
 - Lag - Time from the start of runoff to the point where 50 percent of the ultimate discharge reaches the index point, in hours;
 - NAP - Normal annual precipitation.

IV. Peak Discharge vs. Frequency Curves. There are no streamgaging records in the Gallinas Creek Basin from which peak discharge versus frequency curves could be developed. Therefore, peak discharge versus frequency relationships were developed by synthetic means, by applying the unit hydrographs which were developed to statistically determined rainfall amounts. Precipitation amounts, which were

used to calculate peak discharges for the basin and sub-basin, were based on statistical rainfall data developed by the California Department of Water Resources (DWR) for the nearby NWS raingage "San Anselmo." The statistical rainfall data were adjusted for use in each sub-basin by the ratio between the normal annual rainfall at the raingage and that of each sub-basin. The DWR statistical rainfall data for the San Anselmo raingage are presented in the following tabulation:

San Anselmo Rainfall Data ^{1/}

Statistical Rainfall (Inches)

Rainfall Duration (hours)	for the sub-basin, and a 15-minute unit hydrograph and Duration of 10-Year, 50-Year, 100-Year, and 500-Year			
	Event	Event	Event	Event
0.083	0.29	0.39	0.43	0.54
0.167	0.40	0.54	0.60	0.73
0.250	0.57	0.77	0.85	1.05
0.500	0.83	1.11	1.23	1.52
1.0	1.27	1.71	1.89	2.30
3.0	2.68	3.61	3.99	4.95
6.0	4.02	5.41	5.99	7.35

^{1/} Complied from rainfall records 1958 through 1986.
 * NAP for San Anselmo Station is 41.9 inches.

Based on the results of previous studies, which included the reproduction of flood hydrographs recorded by streamgaging stations in other hydrologically similar basins, the following initial and minimum loss rates, in units of inch per hour, were adopted for use in developing discharges hydrographs for a recent San Rafael Creek hydrologic study; the adopted values were also used for this study:

Event	Loss Rates (inch per hour)	
	Initial Loss	Minimum Loss
10-year	0.22	0.12
50-year	0.19	0.09
100-year	0.18	0.08
500-year	0.16	0.06

Base flow rates, in cubic feet per second per square mile (CSM), which were based on the results of previous studies, are tabulated below:

<u>Event</u>	<u>Base Flow Rates (CSM)</u>
10-year	6
50-year	5
100-year	6
500-year	9

Adopted peak discharges for the sub-basin and the basin are plotted graphically on Plate 3 and are tabulated below:

<u>Index Point</u>	<u>PEAK DISCHARGES (Cubic-Foot per Second)</u>				
	<u>D.A.</u> (sq mi)	<u>10-yr</u>	<u>50-yr</u>	<u>100-yr</u>	<u>500-yr</u>
Sub-basin: South Fork of Gallinas Creek, Vendola Drive	1.04	320	490	550	730
Basin: Gallinas Creek, 2,600 feet downstream from the confluence	7.12	1,230	1,960	2,280	3,060

V. Fluvial Flooding. Topographic maps, obtained from the Marin County Flood Control and Water Conservation District (MCFCWCD) and the City of San Rafael Department of Public Works, were used to develop area-elevation-capacity curves of the Gallinas Village area. Then, subtracting the capacity of the existing drainage system (the pumps, culvert, and intercept) from the peak discharges for the sub-basin, it was determined that the inflow would exceed the capacity of the drainage system by 41.5 c.f.s. and 216.5 c.f.s. during the 100-year and 500-year events, respectively. The discharges were then converted to volumes. Using the volumes and the area-elevation-capacity curves, the water surface elevations and ponding depths were determined. Under existing conditions, the water surface would reach an elevation of 3.15, and 4.10 feet during the 100- and 500-year events, respectively. The corresponding depths of ponding would be 0.15 foot and 1.1 feet (see Plate 4).

If a 41.5 c.f.s. pump was installed to protect against the 100-year inflow, and the 500-year event occurred, the water surface elevation would reach 4.0 feet, and the residual flooding would reach a depth of 1.0 feet.

This analysis and the following tidal flooding analysis were limited to the sub-basin.

TIDAL FLOODING ANALYSIS

VI. Procedure

A. Introduction. This analysis is similar to the analysis developed and used for the San Francisco Bay Shoreline Study, which was reviewed and approved by the U.S. Army Corps of Engineers, South Pacific Division.

B. Tide Elevation Determination. Tide elevations used for this study were taken from the Flood Insurance Study (FIS) for the City of San Rafael, California, dated November 1, 1983. The 100- and 500-year tide elevations are the same as the 100- and 500-year tide elevations found in the San Francisco District's report, San Francisco Bay Tidal Stage vs. Frequency Study, October 1984.

Listed below are the stillwater heights which were adopted for the study reach.

	<u>10-Year Tide</u>	<u>50-Year Tide</u>	<u>100-Year Tide</u>	<u>500-Year Tide</u>
Existing Conditions	5.6	6.2	6.4	6.7
Future Conditions ^{1/}	5.9	6.5	6.7	7.0

^{1/} Sea-level rise based on historic trends. For a 50-year analysis period, 0.3 foot was added to the existing tide conditions.

C. Runup Determination

1. Wind Fetch Length Determination. In order to determine wind-induced wave runup, the distance over which the wave develops must be determined. This distance is called the fetch length, which for this study is 10.6 miles.

The fetch length was determined using the National Oceanic and Atmospheric Administration's (N.O.A.A.) 1:40,000 scale nautical chart of the San Pablo Bay, printed 1979.

2. Wind Caused Wave Runup Determination. The computer program WRUP (Wave Runup by Noble Software, Inc.) was used to determine the wave runup (R), wave runup elevation (NGVD) (R_e), wave period (T), and deepwater wave height (H'_0). The program requires the following inputs:

- Stillwater tide elevation (NGVD)
- Elevation at toe of levee (NGVD)
- Approach slope and roughness
- Fetch length (miles)
- Wind speed (mph)

The stillwater tide elevations are shown in Section VI. A. The approach and levee slopes and roughness coefficient were determined by field surveys and observations. Based on this information, the adopted approach slope for all reaches was 1 vertical (V) on 1000 horizontal (H), with an adopted corresponding roughness coefficient of 1.0. The adopted levee slope for all reaches was 1V on 2H, with an adopted corresponding roughness coefficient of 0.90. The wave runup values computed by the WRUP computer program are tabulated in Section VII, Description of Results. Wave runup values are represented by the parameter R.

C. Overtopping Elevations. With the known stillwater tide and the computed wave runup elevation, the study area was analyzed for its overtopping potential. The study area was divided into two major reaches, Reach 1 and Reach 2, as shown on Plate 5. The analysis was based upon levee crest elevations which were surveyed on March 29, 1989; the crest elevations reflect improvements which have been made to the levee system since the January 1982 flood event. Reach 1 extends from Station 4+85 to Station 25+15. Potential levee overtopping due to stillwater tides and to wind-generated runup will occur from Station 4+85 to Station 12+75 (Sub-Reach 1-A to Sub-Reach 1-G). It was determined that the effects of wind-generated waves will be dissipated by Station 12+75, and that the remaining portion of Reach 1 will only be subject to overtopping by high stillwater tide levels. Reach 2 extends from Station 25+50 to Station 98+00 and is only subject to overtopping by high stillwater tide levels. Only two areas were found to be susceptible to overtopping by high tides. Any levee section in a reach that could potentially be overtopped was identified, measured, and given a sub-reach identification number. The data for Reach 1 and Reach 2 are tabulated below:

Reach 1

<u>Sub-Reach Number</u>	<u>Average Levee Elevation (feet)</u>	<u>Length of Sub-Reach (feet)</u>	<u>Overtopping Potential</u>
1-A	5.6	70	Wind and Tide
1-B	7.3	80	Wind and Tide
1-C	6.1	85	Wind and Tide
1-D	5.7	215	Wind and Tide
1-E	6.0	60	Wind and Tide
1-F	6.3	220	Wind and Tide
1-G	6.7	55	Wind and Tide
1-H	6.4	70	Tide Only
1-I	5.3	70	Tide Only
1-J	5.5	100	Tide Only
1-K	6.1	85	Tide Only
1-L	5.9	100	Tide Only
1-M	6.3	140	Tide Only

Reach 2

<u>Station</u>	<u>Average Levee Elevation (feet)</u>	<u>Length of Depression ^{1/} (feet)</u>	<u>Overtopping Potential</u>
66+40	6.35	30	Tide Only
97+40	5.95	70	Tide Only

^{1/} Shown for the 100-year event.

2. Levee Overtopping Volumes Computer Program. A computer program had been written for an earlier study so the calculations could be performed on the IBM-PC. The program prompts the user for reach and sub-reach input variables that are needed for the calculations. These inputs are shown below:

For the entire reach-

- Reach titles
- Event tide height (wind and tide)
- Year tide height (tide only)
- Event wind speed and duration
- Event wind runup (calculated by program WRUP)
- Empirical constant Q_0 (USACE Shore Protection, Manual, 7-34, page 7-55)

For each sub-reach-

- Sub-reach identifier
- Levee height and length
- Tide durations for the weir flow component of both the wind induced wave overtopping condition and the tidal weir flow overtopping condition.

The program outputs all the parameter information that was input and the overtopping volumes in acre-feet. The volumes that are output are delineated by the overtopping condition for which they were calculated.

D. Floodplains. Topographic maps were used to develop area-elevation-capacity curves, as described in Section V. The computed overtopping volumes would be used to determine tidal-flooding ponding elevations.

VII. Description of Results

This section of the report contains a physical description of the reach and a short discussion of the tidal hydraulics of the reach. Also contained in this section are the input parameters, and the results of the wave runup computation performed by the program WRUP.

REACH 1

Reach 1 extends from Station 4+85 to Station 25+15, as shown on Plate 5. The WRUP data are tabulated below.

	<u>Wind Speed</u> (mph)	<u>Deepwater Wave Height</u> H' (feet)	<u>Wave Period</u> T (sec)	<u>Wave Runup</u> R (feet)
Elevation at Toe: -2.7				
Fetch Length: 10.6 miles	15	1.5	3	3.0

Homes along Reach 1 are protected by two levee systems. The outer levee is 2,550 feet long and has a minimum elevation of 5.2 feet. The inner levee is 2,650 feet long and has a minimum elevation of 7.6 feet. A seasonal wetland, which has an area of 17.56 acres, lies between the two levees. Tidal waters will overtop the outer levee until the water surface reaches the tidal elevation. Tidal waters will not overtop the inner levee in this reach.

REACH 2

The remaining levee (Reach 2) along Vendola Drive is higher than the 100-year tide elevation with the exception of two low spots where tidal waters can overtop the system (see Plate 5). The first low spot is located at Station 66+40, which is 320 feet west of the Vendola Drive and Marby Way intersection. The second low spot is located at Station 97+40, which is 40 feet upstream of Santa Margarita Island on Adrian Way. Using the levee overtopping volumes computer program and the area-capacity curve, the overtopping volume, discharge, elevation, and depth of ponding were determined for existing and future conditions and are tabulated below.

Existing Conditions

<u>Event</u>	<u>Overtopping Volume</u> (acre-feet)	<u>Average Discharge</u> (c.f.s.)	<u>Elevation</u> (feet)	<u>Depth of Ponding</u> (feet)
10-year	0.03	0.36	3.00	---
50-year	2.40	15.20	3.30	0.30
100-year	4.64	26.14	3.50	0.50
500-year	13.56	71.17	4.20	1.20

Future Conditions^{2/}

<u>Event</u>	<u>Overtopping Volume (acre-feet)</u>	<u>Average Discharge (c.f.s.)</u>	<u>Elevation (feet)</u>	<u>Depth ^{1/} of Ponding (feet)</u>
10-year	0.39	3.25	3.00	---
50-year	6.72	36.80	3.80	0.80
100-year	13.56	71.17	4.15	1.15
500-year	23.47	98.60	4.50	1.50

1/ Depth of ponding if the pumps were not operating.

2/ Sea-level rise based on historic trends. For a 50-year analysis period, 0.3 foot was added to the existing tide conditions.

Pump stations 1 and 2, which have a total capacity of 80 c.f.s., should be able to handle the volume of water overtopping the system for most events (both stations have back-up power systems and should be operable). The only exception to this is the future 500-year condition in which case 4.43 acre-feet would not be pumped out. This will cause some ponding in the lower elevations (see Plate 5).

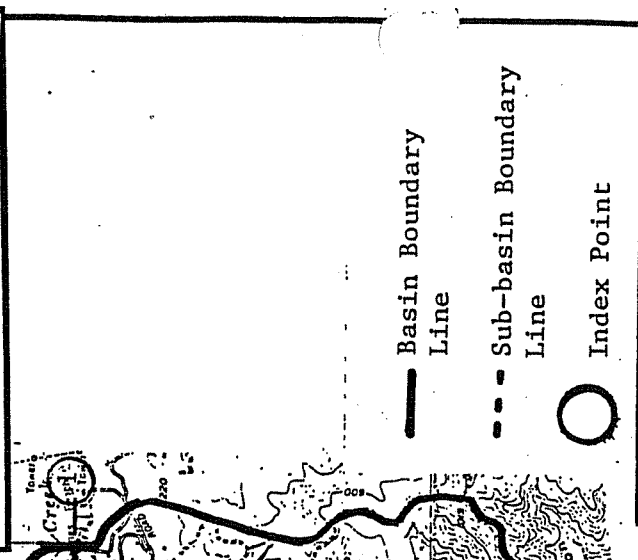
The above analysis did not incorporate freeboard. In our analysis, the floodwall/levees were studied in their existed state. This is similar to methodology used for the San Francisco Bay Shoreline Study tidal-flooding analysis.

Land subsidence and future sea-level rise were considered in combination as a potential future condition. However, we felt that some action would be taken locally to protect against future flooding caused by continued future subsidence. Therefore, we felt that this scenario was not a reasonable without-project future-condition.

VIII. Tide Barrier Alternatives. Personnel from the Marin County Flood Control and Water Conservation District have stated that the elevation of the levees on the north side of Gallinas Creek vary from 7 to 8 feet and have not been overtopped by tidal waters since they were improved. A representative from the Smith Ranch Airport has stated that the levees surrounding the airport have not been overtopped by tidal waters in recent years. Therefore, a tide barrier, which would be located 2,600 feet downstream from the confluence of the north and south forks, would appear not to produce any flood-damage reduction benefits from adjoining areas. Therefore, since the tidal barrier would be expected to be much more costly than the levee/floodwall alternative, we would recommend that the tide barrier be dropped from further consideration.

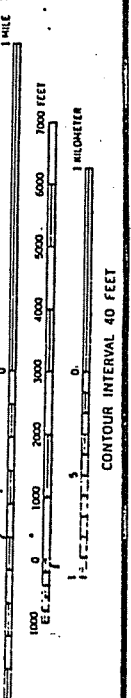
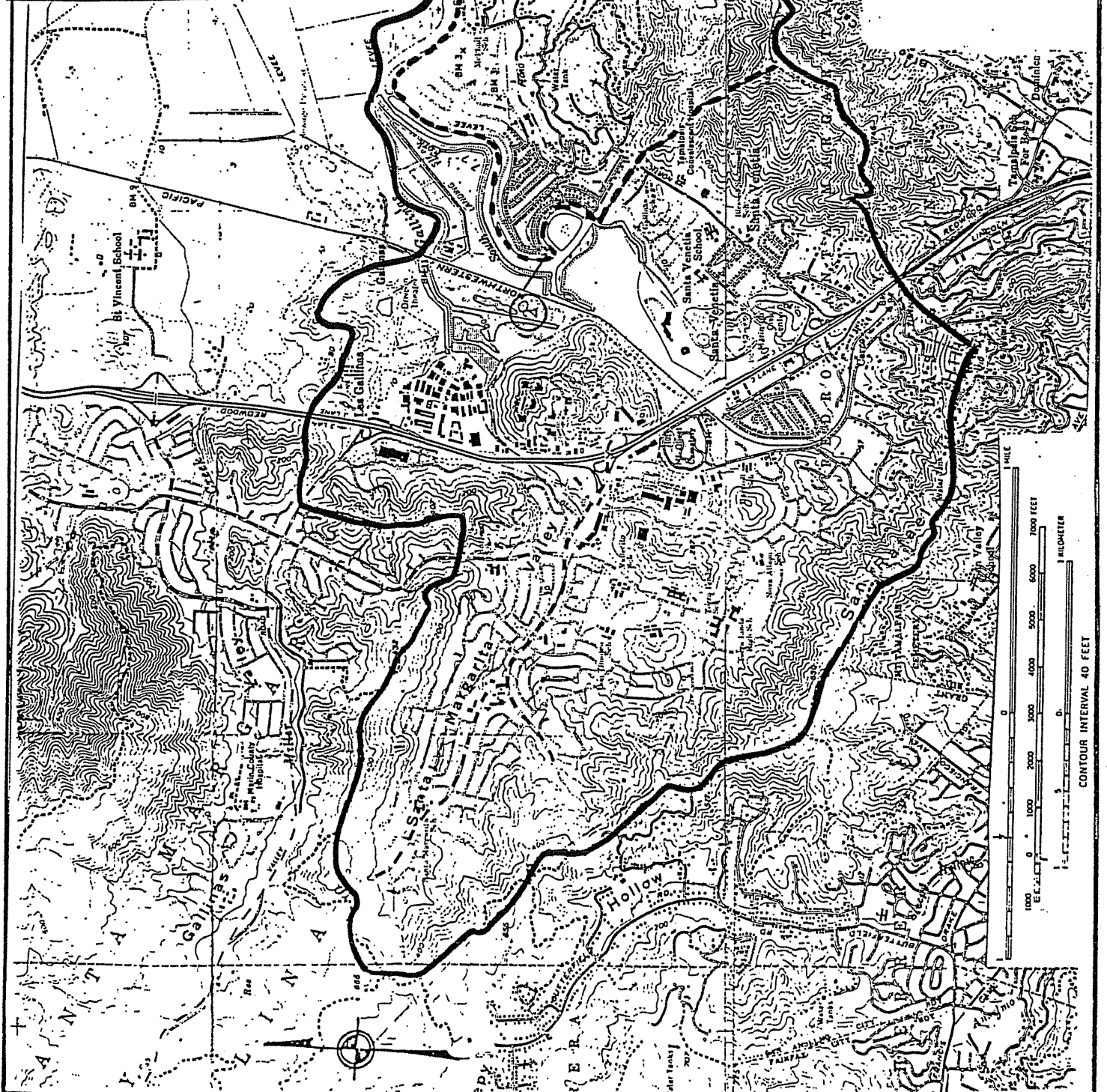
SUMMARY

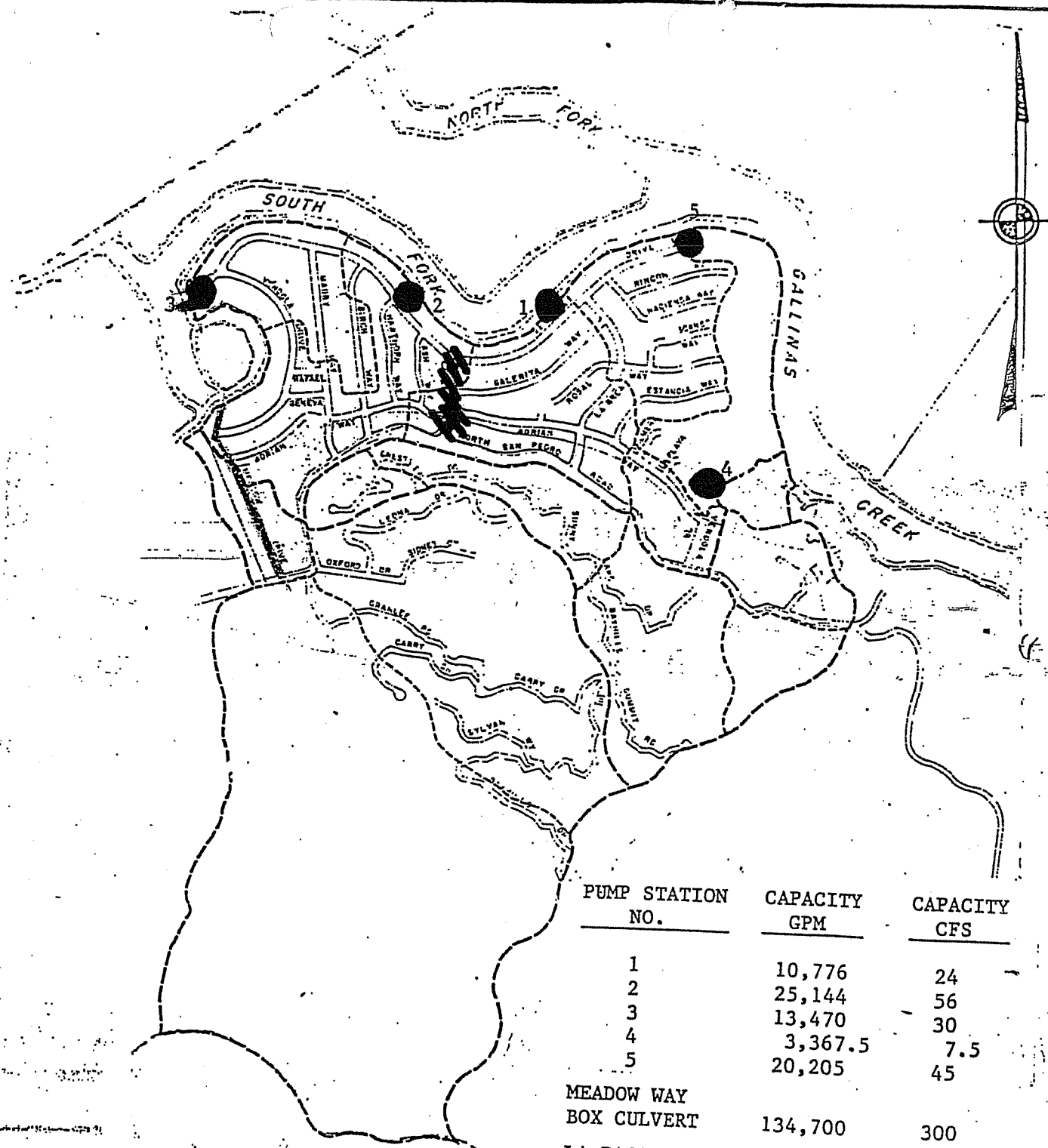
IX. The fluvial and tidal flooding analysis indicates that the impacts of tidal flooding would be relatively minor, assuming that the existing pumping system works; tidal flooding would only exceed existing pumping capacities during the 500-year event for future conditions. A more significant problem is the interior runoff, which would produce ponding depths of 0.15 foot for the 100-year event and 1.1 feet for the 500-year event without improvements being made to the existing local drainage system. This problem would not be solved by the proposed levee/floodwall alternative. Additionally, it should be recognized that the Corps has no authority to be involved in reducing the interior flooding problem in the absence of the storm-damage reduction (i.e. tidal flooding) project.



Gallinas Creek
 Marin County, California
 BASIN MAP

IN SHEET
 U.S. ARMY ENGINEER DIST. SAN FRANCISCO C OF E
 DRAWN BY JL
 TO ACCOMPANY REPORT
 CHECKED DATE MAY 1990

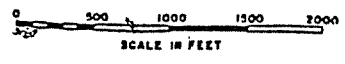




PUMP STATION NO.	CAPACITY GPM	CAPACITY CFS
1	10,776	24
2	25,144	56
3	13,470	30
4	3,367.5	7.5
5	20,205	45
MEADOW WAY BOX CULVERT	134,700	300
LA PASADA INTERCEPT	22,450	50

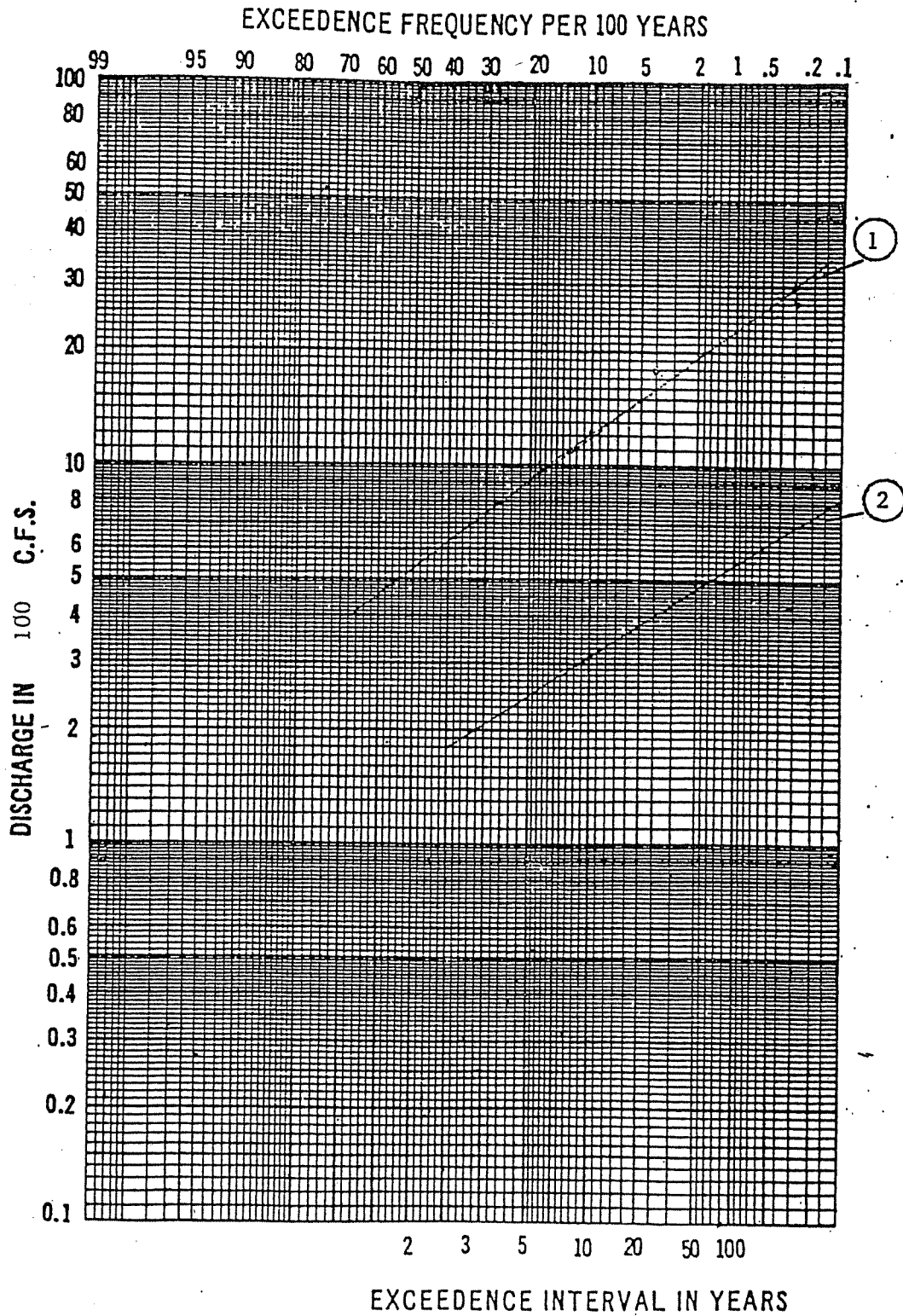
LEGEND

- BOUNDARY OF MAJOR DRAINAGE AREA
- BOUNDARY OF DRAINAGE AREAS
- PUMP STATION
- MEADOW WAY BOX CULVERT
- LAS PASADA INTERCEPT



Gallinas Creek
 Marin County, California
 PUMP STATION LOCATION MAP

1/4 SHEET SHEET NO.
 U.S. ARMY ENGINEER DIST., SAN FRANCISCO, C OF E
 DRAWN: JL FILE NO.
 TRACED:
 CHECKED: TO ACCOMPANY REPORT
 DATED May 1990



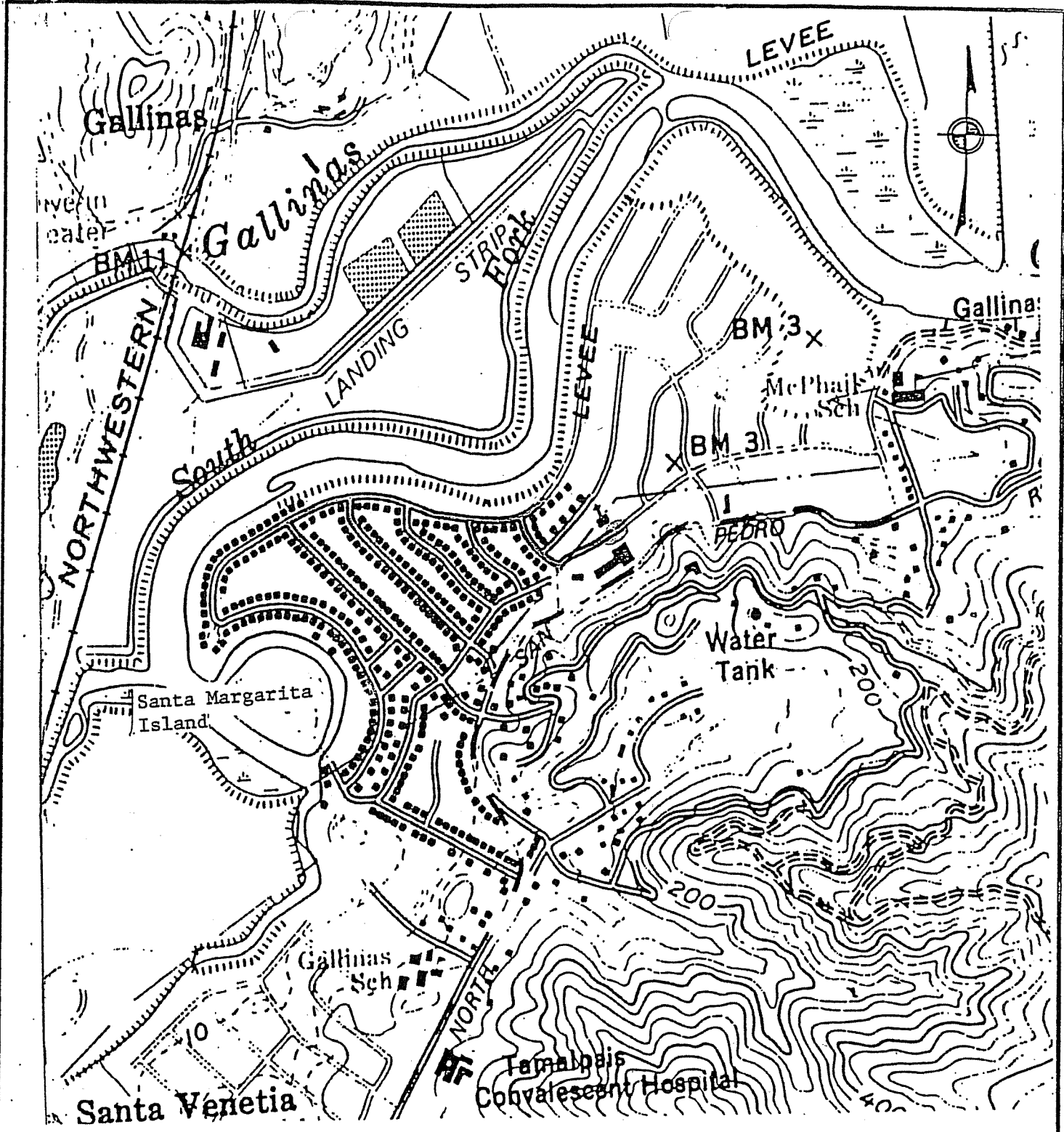
Index Point	Description	Drainage Area
1	Basin	7.12 sq. mi.
2	Sub-basin	1.04 sq. mi.

Gallinas Creek
Marin County, California

PEAK DISCHARGE VS.
FREQUENCY CURVES

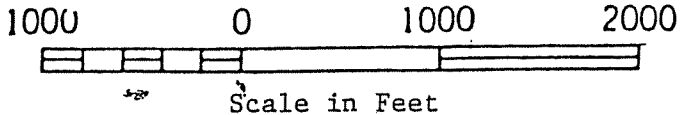
U.S. ARMY ENGINEER DIST., SAN FRANCISCO, CALIF. FILE NO. 6 OF 8
DRAWN: JL
TRACED:
CHECKED:
TO ACCOMPANY REPORT
DATED May 1990

SPW FORM 34
1 APR 72



Legend

■ 100-Year Floodplain -
Ponding due to fluvial runoff



Gallinas Creek
Marin County, California
100-Year Fluvial Floodplain

IN SHEET _____ SHEET NO. _____
U.S. ARMY ENGINEER DIST., SAN FRANCISCO, C OF E
DRAWN: JL
TRACED: _____ FILE NO. _____
CHECKED: _____ TO ACCOMPANY REPORT
DATED May 1990

Appendix B

**Las Gallinas Creek Hydrologic Analysis
South Fork Drainage Basin
Final Report**



**Prepared For:
U.S. Army Corps of Engineers
San Francisco District**



**Prepared By:
Noble Consultants, Inc.
&
Multech Engineering Consultants, Inc.**

May 2009

Table of Contents

1.0	INTRODUCTION	1
2.0	PHYSICAL SETTING	2
2.1	Las Gallinas Creek Watershed.....	2
2.2	Drainage System within Santa Venetia Valley.....	3
3.0	HEC-GEOHMS ANALYSIS	7
3.1	GIS Data.....	7
3.2	Preliminary Delineation of Drainage Subbasins.....	8
3.3	Modification of Delineated Subbasins.....	10
3.3.1	Alteration of Man-Made Structures.....	10
3.3.2	Final Delineation of Drainage Subbasins	11
4.0	HEC-HMS ANALYSIS.....	14
4.1	Model Basin Map.....	14
4.1.1	Drainage Subbasins.....	14
4.1.2	Drainage Channels.....	14
4.1.3	Drainage Junctions.....	16
4.1.4	Pump Stations	16
4.2	Rainfall Intensity-Duration-Frequency Curves.....	17
4.3	Losses.....	23
4.3.1	Hydrologic Soil Group Classification.....	23
4.3.2	Land Use/treatment Classification.....	25
4.3.3	Hydrologic Conditions.....	26
4.3.4	Antecedent Soil Moisture Condition	27
4.3.5	Estimates of SCS Curve Number.....	27
4.3.6	Impervious Ratio.....	30
4.3.7	Initial Abstraction	32
4.4	Clark Unit Hydrograph	32
4.4.1	Time of Concentration	33
4.4.2	Storage Coefficients.....	33
4.5	Muskingum Channel Routing.....	35
4.6	Hydrologic Simulations	38
4.7	Sensitivity Analysis	44
4.8	Present and Future Hydrologic Conditions.....	48
4.9	Simulated Results.....	48
5.0	RISK ANALYSIS.....	51
5.1	Log-Pearson III Distribution.....	51
5.2	HEC-FDA Simulations	54
5.3	Analyzed Results	54
6.0	SUMMARY	58
7.0	REFERENCES	60

List of Tables

Table 1. Capacities of Pump Stations	4
Table 2. Rainfall Depths for Specified Durations for Selected Frequencies	18
Table 3. Composite <i>CN</i> Values for Individual Subbasins for Different AMC Values.....	30
Table 4. Impervious Ratios for Individual Subbasins.....	32
Table 5. Initial Abstractions for Individual Subbasins with Different AMC	33
Table 6. Times of Concentration and Storage Coefficients for Subbasins	34
Table 7. Channel Routing Coefficients for AMC Value of 2.5	37
Table 8. HEC-HMS Simulation Results for AMC Value of 2.5	39
Table 9. HEC-HMS Simulation Results for AMC Value of 2	45
Table 10. HEC-HMS Simulation Results for AMC Value of 3	46
Table 11. Changes in the 100-year Discharges for Different AMC Values	47
Table 12. Peak Discharges of Different Frequencies at Three Locations along the South Fork.....	51
Table 13. Synthetic Distribution Parameters for Three Locations on the South Fork.....	52
Table 14. Confidence Limits for Junction 8 on the South Fork.....	55
Table 15. Confidence Limits for Junction 7 on the South Fork.....	56
Table 16. Confidence Limits for Junction 2 on the South Fork.....	57

List of Figures

Figure 1. Project Area – Santa Venetia Valley	1
Figure 2. Las Gallinas Creek Watershed	2
Figure 3. Drainage System in Santa Venetia Valley.....	3
Figure 4. Portable Pump Located at Meadow Drive.....	4
Figure 5. Housing Facility of Pump Station No. 3	5
Figure 6. Drainage Route of Pump Station No. 5	5
Figure 7. Outlets at Pump Station No. 5	6
Figure 8. DEM Comparison between County and USGS.....	7
Figure 9. Drainage Basin of South Fork	8
Figure 10. DEM Domain and Drainage Routes.....	9
Figure 11. Preliminary Subbasin Delineation Derived from GeoHMS	9
Figure 12. South Fork Subbasin Delineation.....	12
Figure 13. South Fork Watershed with Google Image Overlay	12
Figure 14. Drainage Network of HEC-HMS Model.....	15
Figure 15. Original Rainfall Intensity–Duration-Frequency Curves for the San Rafael Civic Center Station.....	17
Figure 16. Refined Rainfall Intensity–Duration-Frequency Curves for the San Rafael Civic Center Station.....	18
Figure 17. Temporal Distribution for the 2-year 24-hour Design Storm.....	19
Figure 18. Temporal Distribution for the 5-year 24-hour Design Storm.....	19
Figure 19. Temporal Distribution for the 10-year 24-hour Design Storm.....	20

Figure 20. Temporal Distribution for the 25-year 24-hour Design Storm.....	20
Figure 21. Temporal Distribution for the 50-year 24-hour Design Storm.....	21
Figure 22. Temporal Distribution for the 100-year 24-hour Design Storm.....	21
Figure 23. Temporal Distribution for the 200-year 24-hour Design Storm.....	22
Figure 24. Temporal Distribution for the 500-year 24-hour Design Storm.....	22
Figure 25. Soil Group Classification by the County of Marin.....	24
Figure 26. Soil Group Classification Adopted in the Present Study.....	25
Figure 27. Land Use Patterns of the Watershed	26
Figure 28. Spatial Distribution of Curve Number in Individual Subbasins for AMC 2...	28
Figure 29. Composite Curve Numbers for Individual Subbasins for AMC 2	29
Figure 30. Distribution of Impervious Area in the Watershed	31
Figure 31. Assigned K_C values with Respect to Impervious Ratios of Subbasins	35
Figure 32. Computed Hydrograph for the 2-year Flood for AMC Value of 2.5	40
Figure 33. Computed Hydrograph for the 5-year Flood for AMC Value of 2.5	40
Figure 34. Computed Hydrograph for the 10-year Flood for AMC Value of 2.5	41
Figure 35. Computed Hydrograph for the 25-year Flood for AMC Value of 2.5	42
Figure 36. Computed Hydrograph for the 50-year Flood for AMC Value of 2.5	42
Figure 37. Computed Hydrograph for the 100-year Flood for AMC Value of 2.5	43
Figure 38. Computed Hydrograph for the 200-year Flood for AMC Value of 2.5	43
Figure 39. Computed Hydrograph for the 500-year Flood for AMC Value of 2.5	44
Figure 40. Fitted Log-Pearson Type III Distribution for Junction 8 in the South Fork....	52
Figure 41. Fitted Log-Pearson Type III Distribution for Junction 7 in the South Fork....	53
Figure 42. Fitted Log-Pearson Type III Distribution for Junction 2 in the South Fork....	53
Figure 43. Confidence Limits for Junction 8 at the South Fork of Las Gallinas Creek ..	55
Figure 44. Confidence Limits for Junction 7 at the South Fork of Las Gallinas Creek ...	56
Figure 45. Confidence Limits for Junction 2 at the South Fork of Las Gallinas Creek ...	57

1.0 INTRODUCTION

A small flood damage reduction project in the unincorporated area of Santa Venetia under Section 205 of the 1984 Flood Control Act is being undertaken by the Corps of Engineers, San Francisco District. The study area, as illustrated in Figure 1, is located in southeastern Marin County approximately 14 miles north of San Francisco. The study area extends along the South Fork of Las Gallinas Creek from the confluence with North Fork of the Creek to approximately 500 feet upstream of Margarita Island. The site is bound to the east by San Pablo Bay and on the south by steep-sloped foothills of the San Pedro Ridge. This report summarizes the results of a hydrologic analysis in developing the flow frequency curves and flood hydrographs at key designated locations for the 2-yr, 5-yr, 10-yr, 25-yr, 50-yr, 100-yr, 200-yr and 500-yr events using hydrologic models of HEC-GeoHMS, HEC-HMS and HEC-FDA that were developed by the Hydrologic Engineering Center (HEC). The information is needed for the flood control planning of the study area, particularly the Santa Venetia Village that is situated in the low-lying area on the south side of the South Fork.

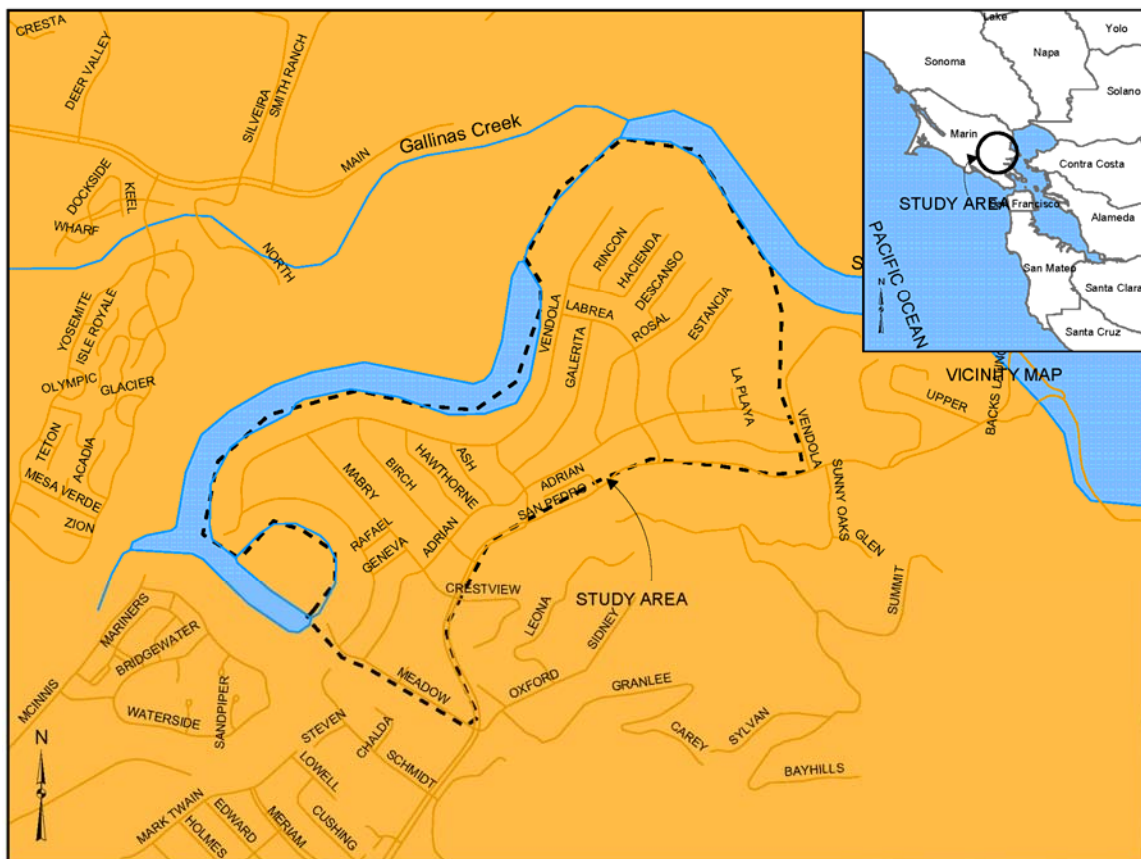
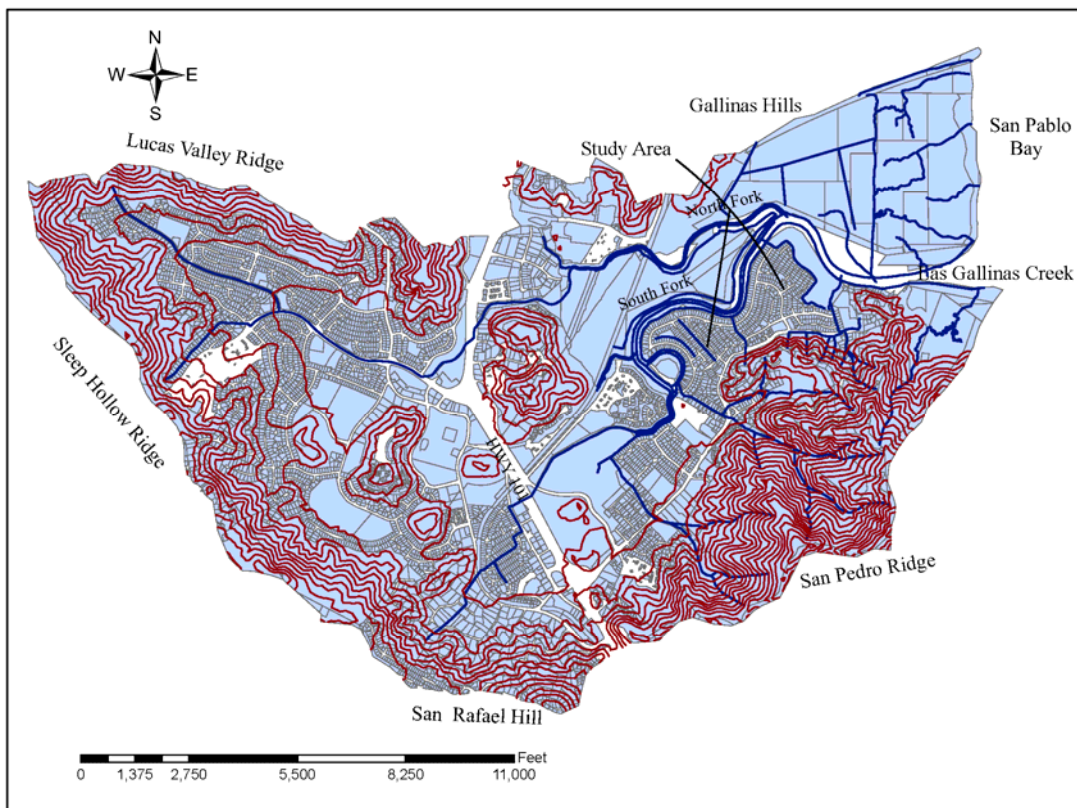


Figure 1. Project Area – Santa Venetia Valley

2.0 PHYSICAL SETTING

2.1 Las Gallinas Creek Watershed

The Las Gallinas Creek is comprised of the North Fork and the South Fork joining near the east end of the Smith Ranch Airport. The adjoining creek continues eastward for about 7,000 feet and empties into San Pablo Bay. The creek basin has a drainage area of approximately 7.5 square miles, and is bounded by the San Rafael Creek Basin to the south, the Corte Madera Creek Basin to the west, Miller Creek to the north and China Camp State Park to the east. Basin elevations range from approximately 1,000 feet, National Geodetic Vertical Datum (NGVD) to 1.5 feet, NGVD at the Smith Ranch Airport. Figure 2 shows the approximate boundary of the Las Gallinas Creek watershed.



Source: County of Marin

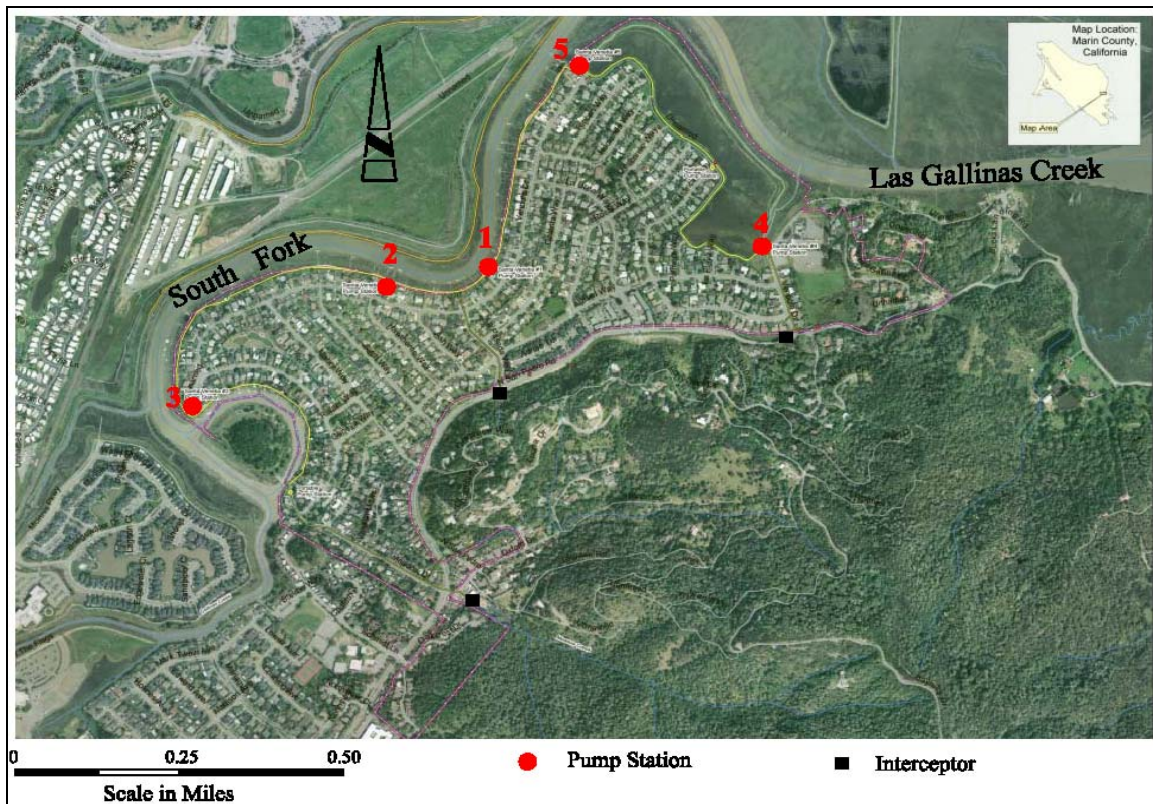
Figure 2. Las Gallinas Creek Watershed

The Las Gallinas Creek watershed is broken into an upper- and lower-watershed. The upper watershed is located west of Highway 101 while the lower watershed is located east of the highway (see Figure 2). Most of the upper watershed drains into the North Fork of Las Gallinas Creek. Ridge flanks are steep-sloped with gentler slopes extending across and down the valley bottom of the upper watershed. The boundary between the upper and lower watersheds marks the approximate extent of tidal influence in the lower creek-slough channel system. The lower watershed is bounded on the south

by the San Pedro Ridge and to the north by the Gallinas Hills (See Figure 2). Between Highway 101 and San Pablo Bay, the main-stem Gallinas Creek occupies a tidally influenced earthen and leveed channel named the South Fork. Most of the Santa Venetia Valley including the hillside along the San Pedro Ridge drains into the South Fork. The present hydrologic study focuses on the South Fork watershed upstream of the confluence with the North Fork.

2.2 Drainage System within Santa Venetia Valley

The drainage system within the Santa Venetia Valley has been altered by construction of culverts and underground drainage pipes to ensure that all flows drain toward either the South Fork or the main channel of Las Gallinas Creek. Three drainage interceptors were also installed to directly bypass surface runoffs from hillsides located on the south of the valley along the San Pedro Ridge into the South Fork or the creek's main channel without draining into the valley. The locations of the interceptors are shown in Figure 3. Five permanent pump stations situate along the South Fork to increase the drainage capacity. In addition, 2 to 3 small portable pump stations (see Figure 4) are also provided to supplement the drainage capacity during the winter rainy season. The discharge capacity of each permanent pump station is presented in Table 1, while individual locations are illustrated in Figure 3.



Source: Marin County

Figure 3. Drainage System in Santa Venetia Valley



Figure 4. Portable Pump Located at Meadow Drive

Table 1. Capacities of Pump Stations

Pump Station ID	Capacity (cfs)
1	63.4
2	40.5
3	38.0
4	5.00
5	45.0

A site investigation was conducted on February 5, 2009 to validate the GIS information provided by the County including pump stations, drainage routes and general geographic setting within the study area. Figure 5 shows, for example, the housing facility for Pump Station No. 3, while Figures 6 and 7 respectively depict a drainage route with its catchment and the discharge outlet for Pump Station No. 5.



Figure 5. Housing Facility of Pump Station No. 3



Figure 6. Drainage Route of Pump Station No. 5



Figure 7. Outlets at Pump Station No. 5

3.0 HEC-GEOHMS ANALYSIS

The Geospatial Hydrologic Modeling Extension (HEC-GeoHMS) is a software package for use with the ArcGIS system to analyze digital terrain information (e.g., Digital Elevation Model) for delineating drainage subbasins and other pertinent data inputs that are to be used in the application of Hydrologic Modeling System (HEC-HMS). Specifically, HEC-GeoHMS transforms the drainage paths and watershed boundaries into a hydrologic data structure including the HEC-HMS basin model, physical watershed and stream characteristics, and background map file that represents the watershed response to precipitation.

3.1 GIS Data

GIS data within the Las Gallinas Creek watershed including Digital Elevation Model (DEM), soil information, storm drain system, creek delineation and land use were obtained from the County of Marin. The DEM with a grid size of 10 feet by 10 feet was derived from black and white aerial photographs that were taken in 1997 by the County. Since the project area has been well urbanized by 1997, it is not expected that a significant change of terrain geometry has been changed. Nevertheless, a comparison was made between the County's DEM and the DEM directly downloaded from the USGS Seamless Data Distribution System (USGS, 2009) that has a grid size of 98.4 feet by 98.4 feet (30m by 30m). Figure 8 shows a comparison of the two DEMs that were projected onto the California State Plane system, Zone III. The figure validates the accuracy of the County's DEM with a much finer grid resolution. The County DEM data set was then used for the GeoHMS analysis.

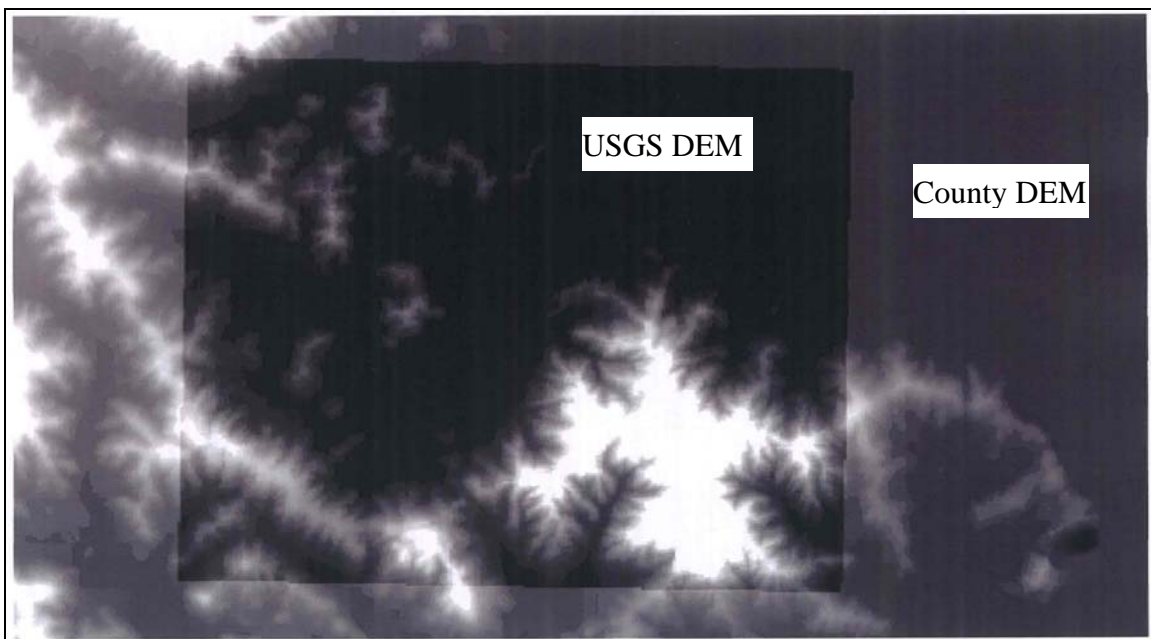


Figure 8. DEM Comparison between County and USGS

3.2 Preliminary Delineation of Drainage Subbasins

The entire drainage basin for the South Fork including the Railroad, Auditorium and Northbridge Channels were initially defined, based on the topographic contours that were derived from the DEM. Several discussions with County personnel regarding the drainage routes on the west side of Highway 101 and hillsides to the south were also conducted. Figure 9 illustrates the defined boundary of the drainage basin. The clipped DEM and the associated drainage routes for the South Fork were then used for the GeoHMS application to delineate the drainage subbasins for the study area.

Figure 10 shows the DEM domain and the drainage routes used in the GeoHMS application. The terrain process executed in the GeoHMS model consists of delineation of flow direction and flow accumulation, stream definition, and catchment representation. Basin Characteristics such as drainage length, slope, flow path and basin centroid information including elevation and its flow path were also derived. The preliminary drainage subbasins that were directly delineated from the GeoHMS process are shown in Figure 11.

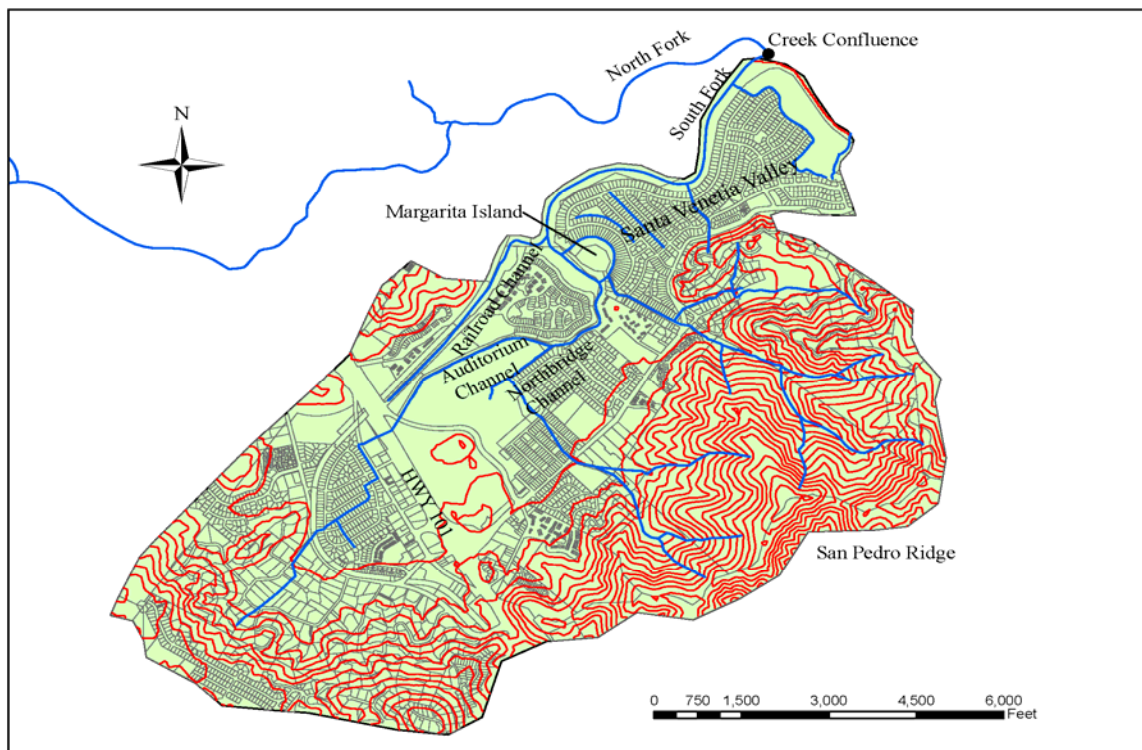


Figure 9. Drainage Basin of South Fork

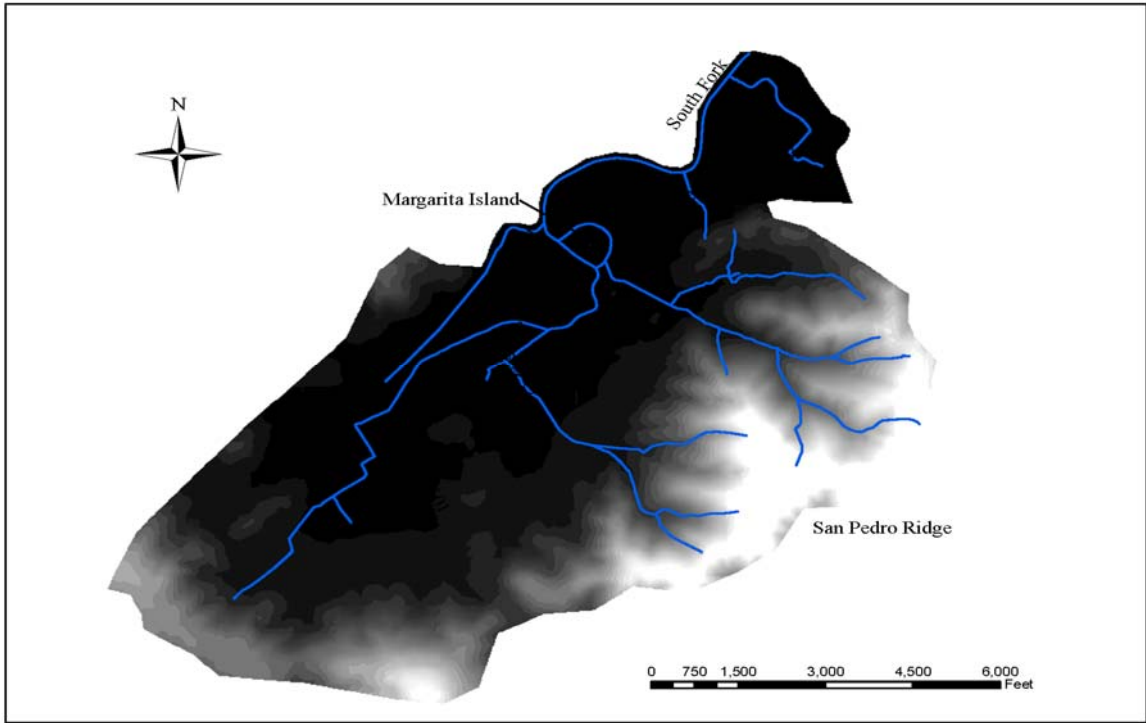


Figure 10. DEM Domain and Drainage Routes

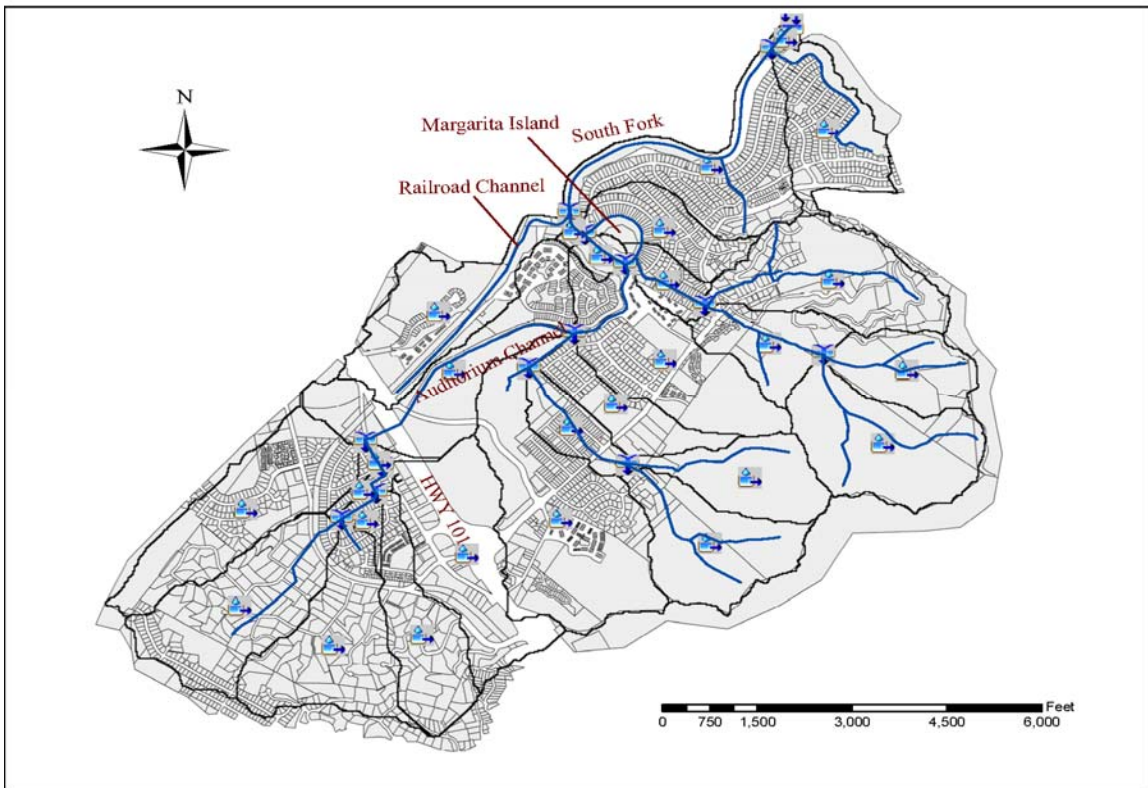


Figure 11. Preliminary Subbasin Delineation Derived from GeoHMS

3.3 Modification of Delineated Subbasins

3.3.1 Alteration of Man-Made Structures

The natural drainage pattern for the Las Gallinas Creek watershed has been altered by man-made structures such as Highway 101, roads, streets, storm drain systems, levees, etc. Therefore, the drainage network of the watershed was modified from the GeoHMS preliminary depiction to accurately delineate the drain basins by taking into account those man-made effects, as briefly described in the following sections.

Highway 101

Highway 101 runs in a northwest-southeast direction to separate the South Fork watershed into the upper west portion and the lower east portion. The west portion is drained by a small channel originating in the San Rafael Hill and passes the Highway 101 embankment through a 12 feet by 7.5 feet box culvert that is located at Auditorium Channel (See Figure 9). Due to obstruction by the Highway 101 embankment, the entire western portion of the watershed now drains through this box culvert to enter the lower portion of the watershed. In other words, this box culvert is the only outlet for the subbasin west of Highway 101. It is noted that the culvert has a capacity of 628 cfs (Marin County, 1998).

Northwestern Railroad

Northwestern Pacific Railroad runs southward across the northern portion of the South Fork watershed, underpasses Highway 101 and makes an arc turning southeastward toward the south end of the upper watershed west of Highway 101 (See Figure 11). East of Highway 101, a small channel called Railroad Channel runs parallel south of the railroad, which enters the South Fork at the downstream end. The channel also collects the runoff from the hill just north of the railroad.

Road Embankment

A road embankment often forms a dividing border between subbasins. For example, McInnis Parkway parallel to Northwestern Pacific Railroad and located on the south side of the Railroad Channel is the dividing border between the subbasin north and south of the parkway.

Levees

Levees are built along the south bank of the South Fork to provide flood protection for Gallinas Village and along the north bank to protect the San Rafael Airport. Levees typically obstruct surface runoff and alter drainage patterns.

Street Drainage System

The urban street drainage system within the Santa Venetia Valley consists of street gutters, drainage inlets, catch basins, and storm drains including hillside interceptors to collect and convey storm runoff. These drainage systems alter the natural drainage pattern and were taken into account in delineating subbasins. For example, subbasin delineation of Gallinas Village is made based on the street drainage systems, which lead to individual pump stations.

3.3.2 Final Delineation of Drainage Subbasins

Incorporating the effects of the above-mentioned man-made structures, the South Fork watershed can be delineated into 14 subbasins as respectively shown in Figures 12 and 13. These subbasins include G-1, G-2, G-3, and G-5 for Gallinas Village; W310, W380, and W390 for the hill side south of North San Pedro Road; W340 along Meadow Drive; W370 and W410 for the Northbridge channel; W400 for the Auditorium Channel; W350 for Margarita Island; W330 for the Railroad Channel; and W470 for the portion west of Highway 101. It is noted that Subbasin G-4, shown in Figure 12, drains to Pump Station No. 4, which discharges runoff to Gallinas Creek downstream of the confluence between the South Fork and the North Fork. Therefore, Subbasin G-4 is outside the watershed of the present study. A brief description of each subbasin is provided as follows.

Subbasin G-1: It is situated in the west end of Gallinas Village and has a drainage area of 0.0372 mi². Storm runoff from this subbasin drains to Pump Station No.3 where it is discharged into the South Fork.

Subbasin G-2: This subbasin is situated southeast of G-1 in Gallinas Village with a drainage area of 0.0867 mi². Storm runoff from this subbasin drains to Pump Station No.2 where it is discharged into the South Fork.

Subbasin G-3: It is situated east of G-2 in Gallinas Village and has a drainage area of 0.0702 mi². Storm runoff from this subbasin drains to Pump Station No.1 where it is discharged into the South Fork.

Subbasin G-5: This subbasin that is situated in the northeast end of Gallinas Village has a drainage area of 0.0587 mi². Storm runoff from this subbasin drains to Pump Station No.5 where it is discharged into the South Fork.

Subbasin W310: It is situated in the hillside south of North San Pedro Road with a drainage area of 0.0297 mi². Storm runoff from this subbasin is intercepted by La Pasada Hillside Drain. The storm drain initially consists of twin 30-in diameter drains running the length of La Pasada and transitions to a 42-in diameter pipe at Vendola Drive passing between 507 and 601 Vendola Drive to discharge directly into the South Fork without interacting with the runoff in Gallinas Village.

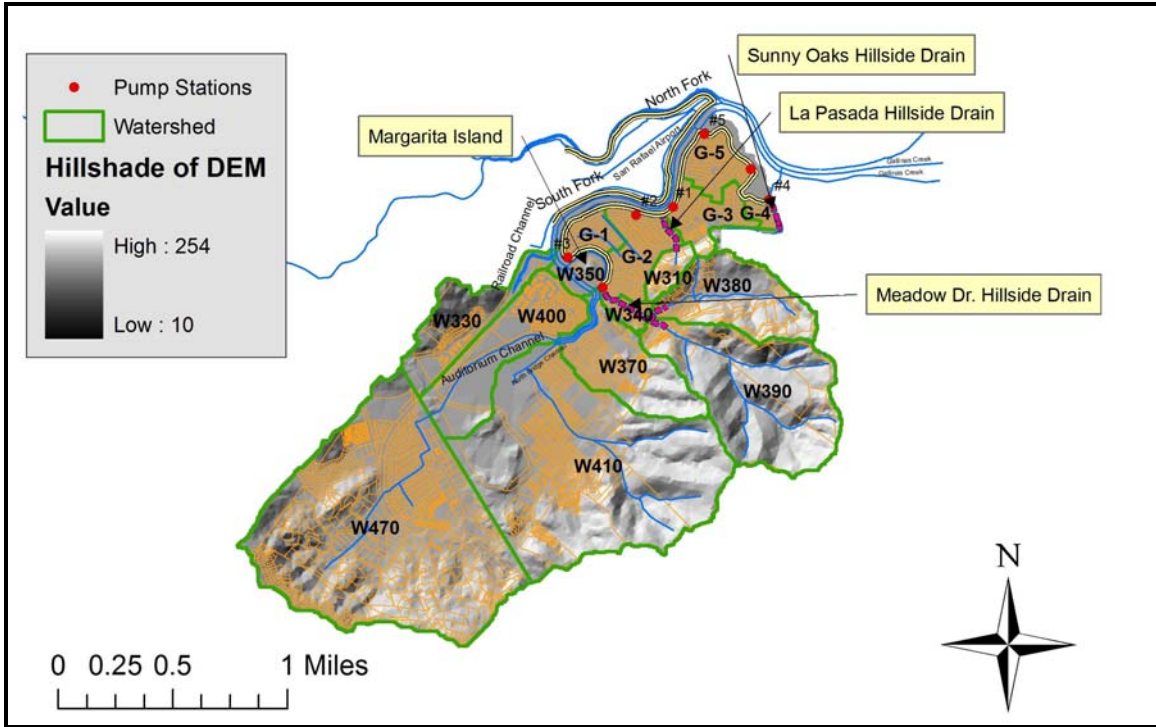


Figure 12. South Fork Subbasin Delineation



Figure 13. South Fork Watershed with Google Image Overlay

Subbasin W330: It is situated mostly north of the Railroad Channel and has a drainage area of 0.1308 mi². Storm runoff from this subbasin drains to the Railroad Channel, which in turn flows into the South Fork.

Subbasin W340: It is situated along Meadow Drive south of North San Pedro Road with a drainage area of 0.0221 mi². Storm runoff from this subbasin discharges directly into the South Fork at the east end of Margarita Island.

Subbasin W350: This subbasin consists of Margarita Island and the surrounding water. It has a drainage area of 0.0385 mi². Storm runoff from this subbasin discharges directly into the South Fork.

Subbasin W370: It is situated south of W340 with a drainage area of 0.1675 mi². Storm runoff from this subbasin discharges directly into the South Fork just upstream of Margarita Island.

Subbasin W380: The subbasin is situated southeast of W310 in the hillside south of North San Pedro Road. It has a drainage area of 0.1754 mi². Storm runoff from this subbasin is intercepted by the Meadow Drive Hillside Drain, which a 7 feet by 4 feet culvert is running the length of Meadow Drive starting south of North San Pedro and discharging directly into the South Fork at the end of Meadow Drive.

Subbasin W390: This subbasin is situated south of W380 in the hillside south of North San Pedro Road. It has a drainage area of 0.3631 mi². Storm runoff from this subbasin is also intercepted by the Meadow Drive Hillside Drain and discharged directly into the South Fork.

Subbasin W400: The subbasin that has a drainage area of 0.1970 mi² is situated northeast of Highway 101, northwest of W370 and 410, and east of W330. Storm runoff from this subbasin discharges into the Auditorium Channel upstream from its confluence with the Northbridge Channel.

Subbasin W410: This subbasin is situated south of W370. It includes the Marin County Civic Center, the San Rafael Civic Center Lagoon, Children's Island, and a large portion of hillside. The drainage area is 0.7478 mi². Storm runoff from this subbasin discharges into the Northbridge Channel upstream of the confluence with the Auditorium Channel.

Subbasin W470: The subbasin is situated west of Highway 101 with a drainage area of 0.8521 mi². Storm runoff from this subbasin drains through the box culvert at Highway 101 and enters the Auditorium Channel.

4.0 HEC-HMS ANALYSIS

The modified subbasins of the South Fork watershed were incorporated in the HEC-HMS to form an integrated hydrological system for storm runoff simulations. Pertinent elements of the modeling system are described in the following sections.

4.1 Model Basin Map

The model basin map is a network of hydrological elements for the runoff simulations including subbasins, channels, and flow junctions. Figure 14 shows the model basin map for the South Fork watershed, which includes 14 subbasins, 13 junctions, and 11 channels.

4.1.1 Drainage Subbasins

The runoff simulations were first performed for individual subbasins to generate runoff hydrographs at their outlets including G-1, G-2, G-3, G-5, W310, W330, W340, W350, W370, W380, W390, W400, W410, and W470 that are shown in Figure 12. The subbasins are previously described in Section 3.3.2.

4.1.2 Drainage Channels

Runoff hydrographs generated at the subbasin outlets are routed through connecting channels to the downstream locations, called junctions, where they are combined with runoff hydrographs from other subbasins. The connecting channels between subbasin outlets and downstream junctions are identified with “Reach” numbers, which include Reach 1, 2, 3, 4, 5, 6, 7, 8, 9, 10, and 11 as shown in Figure 14. They are described below:

Reach 1: The Auditorium Channel from the Highway 101 culvert to the confluence with the Northbridge Channel.

Reach 2: A segment of the South Fork from the Auditorium Channel-Northbridge Channel confluence to the Meadow Drive Hillside Drain outfall.

Reach 3: The entire Meadow Drive Hillside Drain.

Reach 4: A segment of the South Fork from the Meadow Drive Hillside Drain outfall to the outfall at Pump Station No. 3.

Reach 5: A segment of the South Fork from the Pump Station No. 3 outfall to the confluence with the Railroad Channel.

Reach 6: The entire La Pasada Hillside Drain.

Reach 7: A segment of the South Fork from the Railroad Channel confluence to the outfall of Pump Station No. 2.

Reach 8: A segment of the South Fork from the Pump Station No. 2 outfall to the La Pasada Hillside Drain outfall.

Reach 9: A segment of the South Fork from the outfall of Pump Station No. 1 to the Pump Station No. 5 outfall.

Reach 10: A segment of the South Fork from the La Pasada Hillside Drain outfall to the Pump Station No. 1 outfall.

Reach 11: A segment of the South Fork from the outfall of Pump Station No. 5 to the confluence with the North Fork.

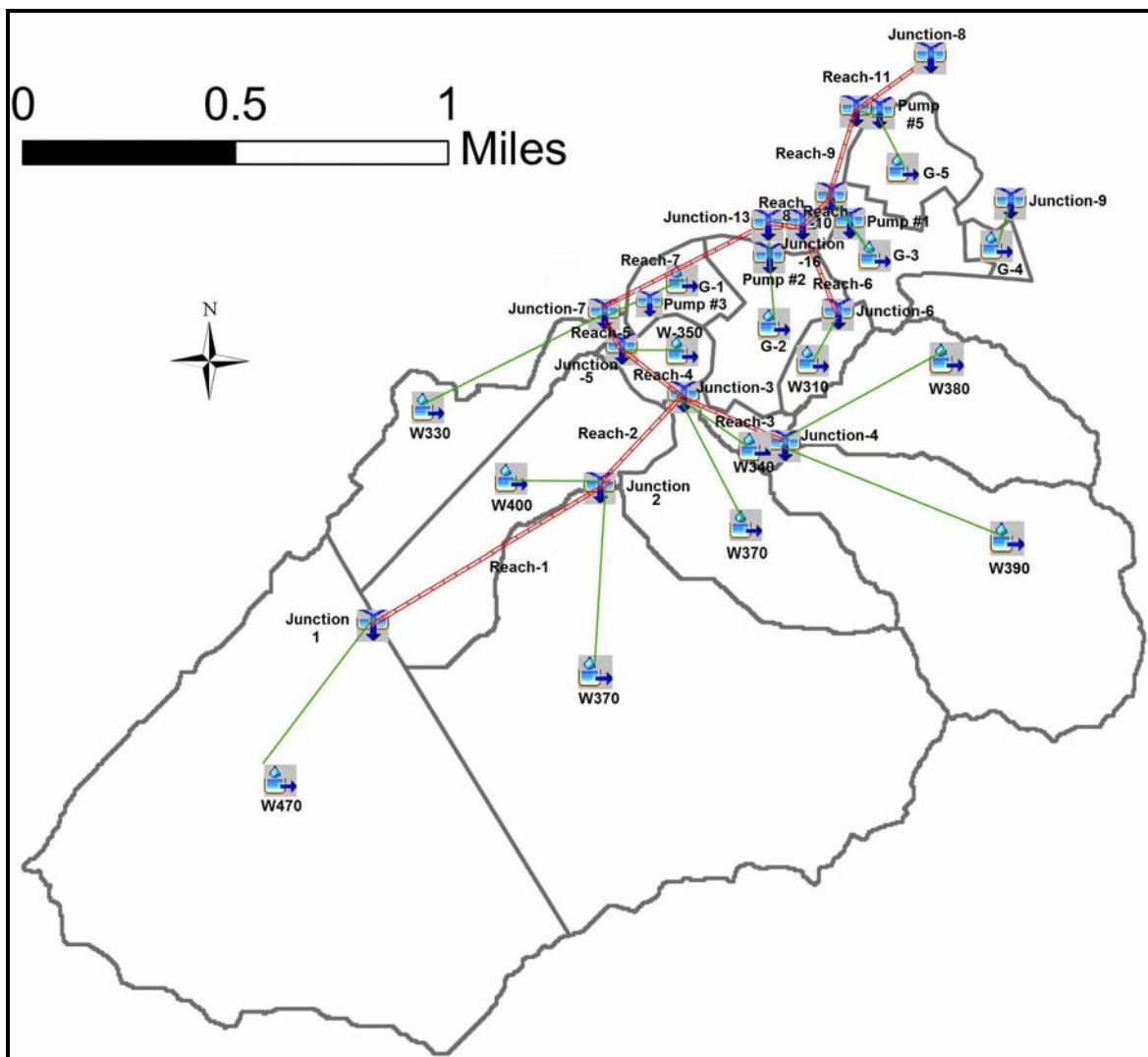


Figure 14. Drainage Network of HEC-HMS Model

4.1.3 Drainage Junctions

There are 13 junctions in the drainage networks as shown in Figure 14. They are described below:

Junction 1: The Highway 101 culvert, which receives runoff from Subbasin W470 west of Highway 101.

Junction 2: The confluence of the Auditorium Channel and Northbridge Channel where the South Fork begins.

Junction 3: The location where the Meadow Drive Hillside Drain outfall enters the South Fork.

Junction 4: The upstream inlet of the Meadow Drive Hillside Drain where runoffs from Subbasins W380 and W390 enter.

Junction 5: The location where the outfall of Pump Station No. 3 enters the South Fork.

Junction 6: Inlet to the La Pasada Hillside Drain where runoffs from Subbasin W310 enter.

Junction 7: The location where the Railroad Channel water discharges into the South Fork.

Junction 8: The confluence of the South Fork and the North Fork.

Junction 9: The outfall of Pump Station No. 4 (Note: This junction is outside the watershed of the South Fork).

Junction 13: The location in the South Fork where the outfall of Pump Station No. 2 enters.

Junction 14: The location in the South Fork where the outfall of Pump Station No. 1 enters.

Junction 15: The location in the South Fork where the outfall of Pump Station No. 5 enters.

Junction 16: The location in the South Fork where the outfall of the La Pasada Hillside Drain enters.

4.1.4 Pump Stations

There are 5 permanent pump stations in Gallinas Village along with 2 to 3 portable pump stations. In this hydrologic analysis, only permanent pump stations were considered, as the capacities of these portable ones are unknown, nevertheless, typically

small. Permanent pump stations are designated as junctions receiving runoffs from the associated subbasins. Pump Stations No. 1, 2, 3, and 5 discharge into the South Fork while Pump Station No. 4 discharges into the Las Gallinas Creek, which is the main channel downstream of the confluence of the South Fork and the North Fork (i.e., it is not included in the present study area).

4.2 Rainfall Intensity-Duration-Frequency Curves

Storm runoffs for the watershed were simulated in response to specified rainfall hyetographs. In the present hydrologic study, rainfall hyetographs were derived for a 24-hour storm duration with 2-year, 5-year, 10-year, 25-year, 50-year, 100-year, 200-year, and 500-year recurrence frequencies. The rainfall hyetographs were established based on the rainfall intensity-duration-frequency (IDF) curves that were deduced from the rainfall data at the San Rafael Civic Center station (Station No. E20-7880-20) for the recorded period between 1964 and 1994 with missing data in the 1968-74 period. The original IDF curves display irregularities for the durations of 10 minutes and 1,440 minutes as shown in Figure 15. The dips at the 10-minute duration imply that the corresponding changes of rainfall intensities are lower than those for the 15-minute duration, which are inconsistent with a critical storm pattern. Therefore, the rainfall intensities for 10-minute duration were interpolated based on the values for the 5-minute and 15-minute durations. Similarly, the rainfall intensities for the 1,440-minute duration were extrapolated from the values of the 360 minute and 720 minute durations. The refined IDF curves are shown in Figure 16.

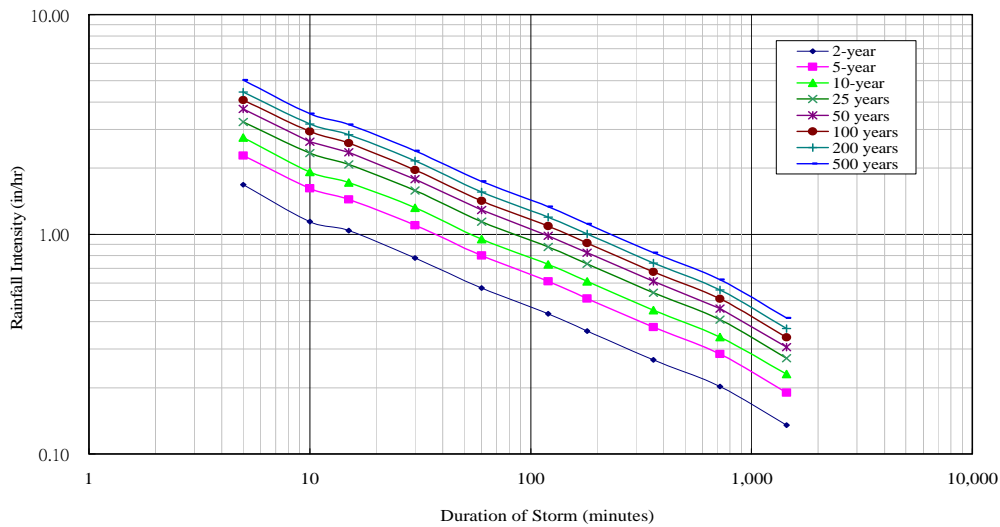


Figure 15. Original Rainfall Intensity–Duration–Frequency Curves for the San Rafael Civic Center Station

The derived rainfall intensity-duration-frequency curves were subsequently used to establish the 24-hour synthetic frequency storms for use in the HEC-HMS model. The frequencies include 2-, 5-, 10-, 25-, 50-, 100-, 200-, and 500-year recurrence intervals. The shortest time period of the storms is 5 minutes, which is also taken to be the time

step of the runoff simulation. The time that the peak intensity of the design storm will occur is assigned to be 50% of the storm duration, namely 12 hours from the start of the storm. Table 2 shows the depth values for the frequencies analyzed and Figures 17 to 24 show the temporal distribution of the 2-, 5-, 10-, 25-, 50-, 100, 200-, and 500-year design storms, respectively. For each frequency, the same design storm was applied to all subbasins in the HEC-HMS model.

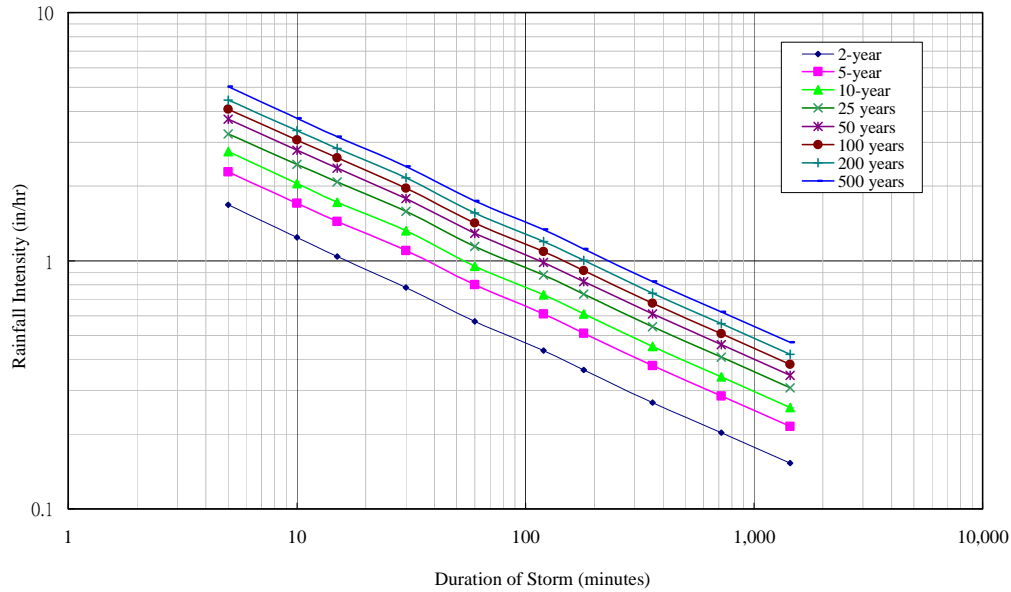


Figure 16. Refined Rainfall Intensity–Duration–Frequency Curves for the San Rafael Civic Center Station

Table 2. Rainfall Depths for Specified Durations for Selected Frequencies

Frequency	Rainfall Depth (in) for Selected Duration									
	5 min	10 min	15 min	30 min	60 min	120 min	180 min	360 min	720 min	1440 min
2 years	0.140	0.207	0.260	0.390	0.570	0.870	1.090	1.610	2.430	3.668
5 years	0.190	0.284	0.360	0.550	0.800	1.220	1.530	2.270	3.420	5.153
10 years	0.230	0.341	0.430	0.660	0.950	1.460	1.830	2.710	4.080	6.143
25 years	0.270	0.408	0.520	0.790	1.140	1.750	2.200	3.250	4.900	7.388
50 years	0.310	0.465	0.590	0.890	1.290	1.970	2.470	3.660	5.510	8.295
100 years	0.340	0.512	0.650	0.980	1.420	2.180	2.740	4.050	6.100	9.188
200 years	0.370	0.558	0.710	1.080	1.560	2.390	3.010	4.440	6.690	10.080
500 years	0.420	0.626	0.790	1.200	1.740	2.670	3.350	4.950	7.460	11.243

Source: Marin County

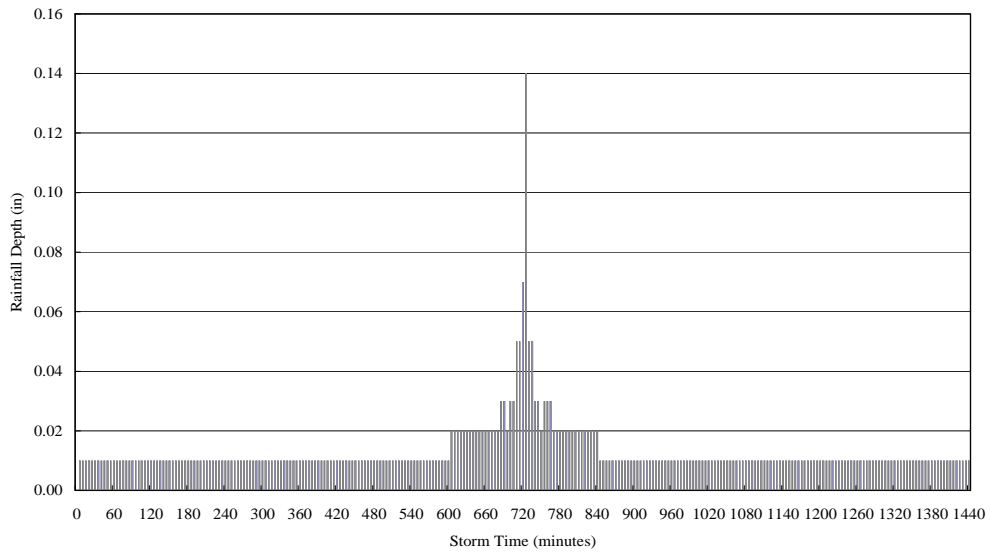


Figure 17. Temporal Distribution for the 2-year 24-hour Design Storm

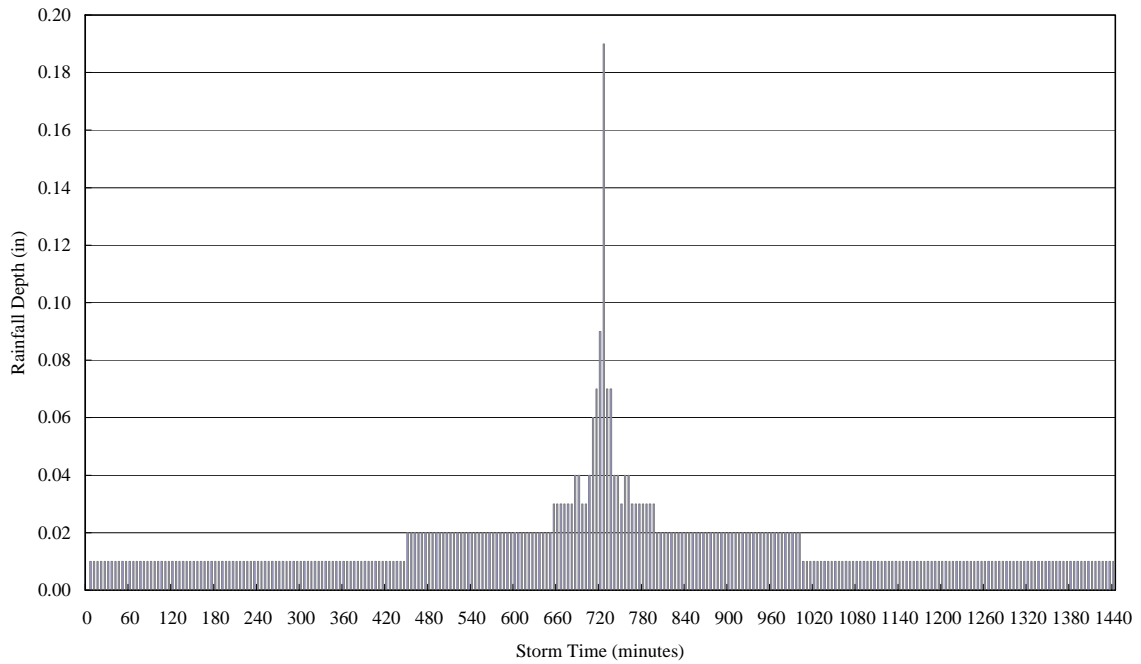


Figure 18. Temporal Distribution for the 5-year 24-hour Design Storm

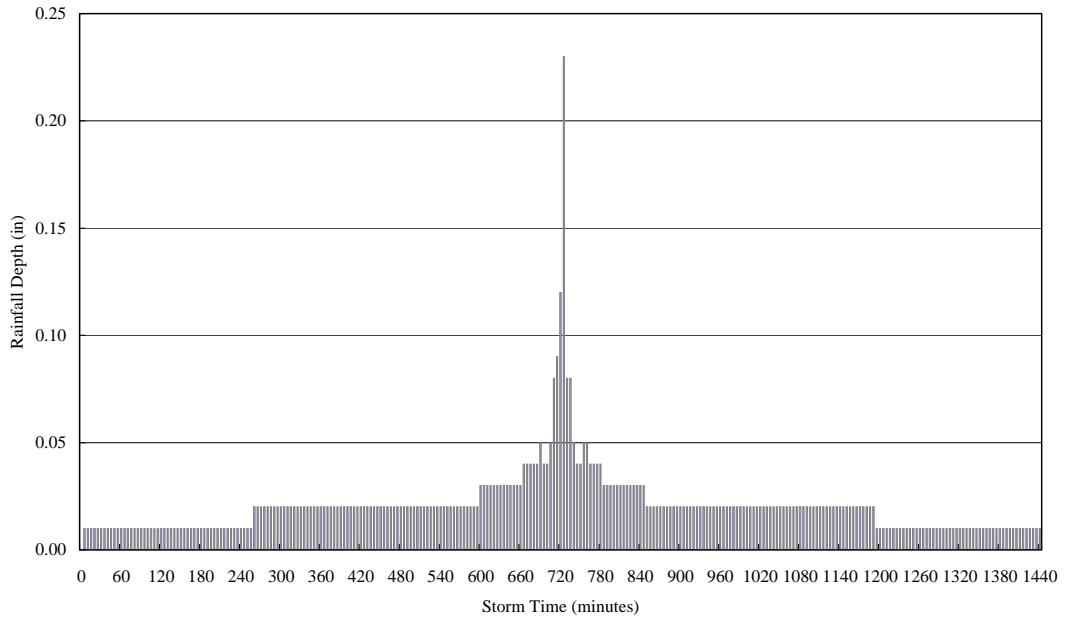


Figure 19. Temporal Distribution for the 10-year 24-hour Design Storm

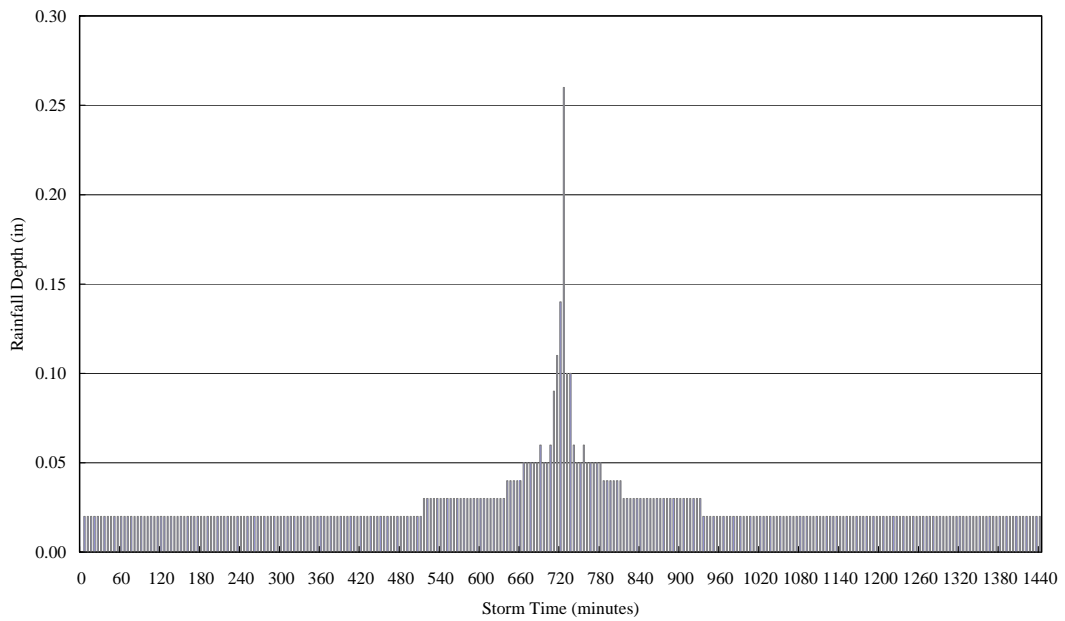


Figure 20. Temporal Distribution for the 25-year 24-hour Design Storm

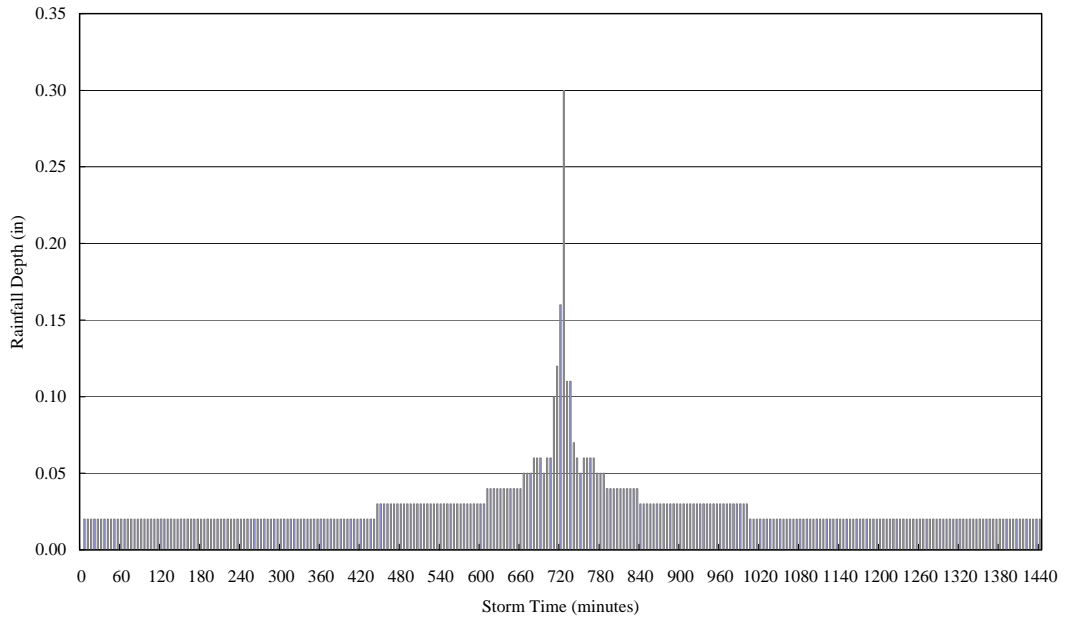


Figure 21. Temporal Distribution for the 50-year 24-hour Design Storm

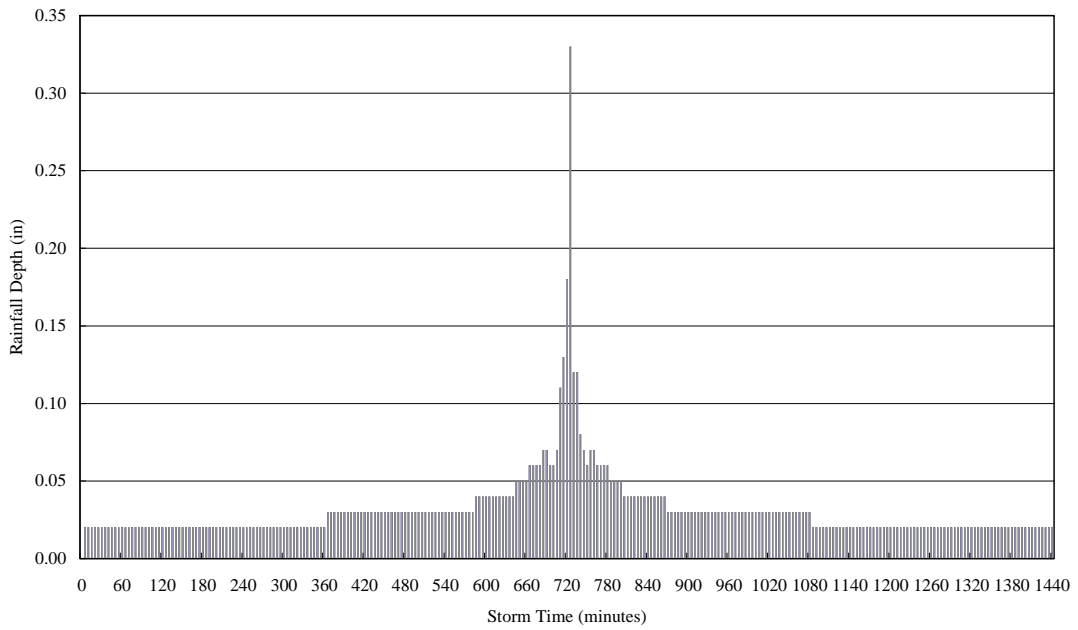


Figure 22. Temporal Distribution for the 100-year 24-hour Design Storm

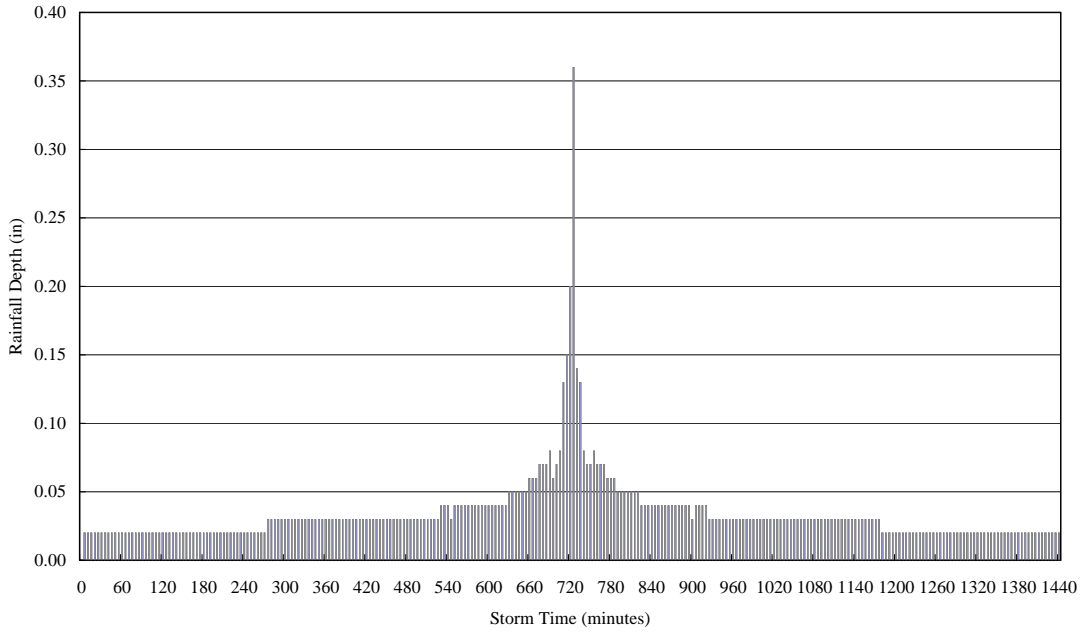


Figure 23. Temporal Distribution for the 200-year 24-hour Design Storm

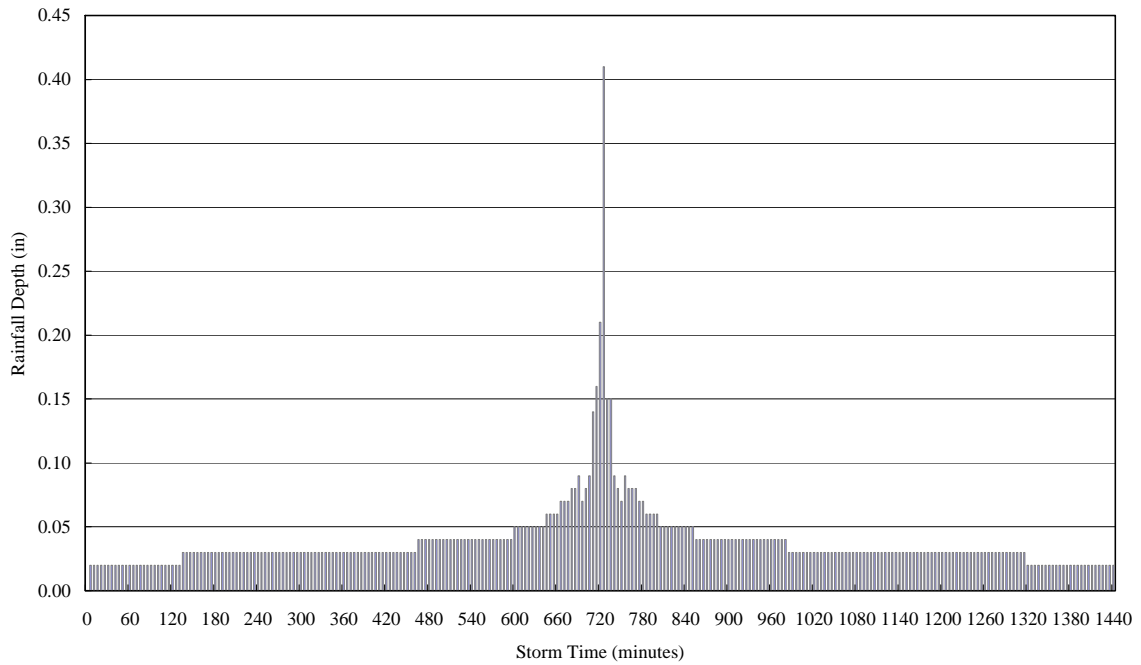


Figure 24. Temporal Distribution for the 500-year 24-hour Design Storm

4.3 Losses

Storm runoff occurs only after a rainfall depth exceeds losses. In other words, the runoff is formed by excess rainfall, which is equal to the rainfall depth minus the losses. In the present study, the Soil Conservation Service (now the Natural Resources Conservation Service) curve number method was used to track the losses during the storm. The method separates the losses into initial abstraction and incremental losses during the storm. The initial abstraction represents the amount of rainfall that must fall before excess rainfall occurs.

In the present analysis, the initial abstraction, denoted as I_a , was estimated as 0.2 times the potential retention (S), which was calculated from the SCS curve number as follows:

$$S = \frac{1000}{CN} - 10 \quad (1)$$

In the above equation, S is the potential retention in inches, and CN is the curve number. The incremental losses represent the infiltration depths during computation time intervals and are calculated as the difference in infiltration volume at the end of two adjacent time intervals. The infiltration loss at the end of each time interval is a function of rainfall depth, runoff volume, initial abstraction, and potential retention and is ultimately a function of rainfall depth and curve number. In other words, the curve number and the design storm together define both initial abstraction and incremental losses during the storm. The Soil Conservation Service developed a procedure to estimate the curve number based on soil group, the land use/land treatment class, the hydrologic condition, and the antecedent soil moisture condition. They are described in the following sections.

4.3.1 Hydrologic Soil Group Classification

The SCS developed a soil classification system that consists of four different groups identified as A, B, C, and D in the order of decreasing infiltration rate. Soil characteristics associated with each group are as follows:

Group A: Deep sand, deep loess, aggregates silts

Group B: Shallow loess, sandy loam

Group C: Clay loams, shallow sandy loam, soils low in organic content, and soils usually high in clay

Group D: Soils that swell significantly when wet, heavy plastic clays, and certain saline soils

The soil group classification of the South Fork watershed has been defined by the County of Marin as shown in Figure 25. It can be seen from Figure 25 that while portions

of the watershed are classified as Groups C and D, a significant portion remains unclassified due to lack of data. In the present study, the unclassified portion in the low-lying area, which is dominated by bay mud, is classified as Group D, while the portion in the upper area is classified as Group C as shown in Figure 26.

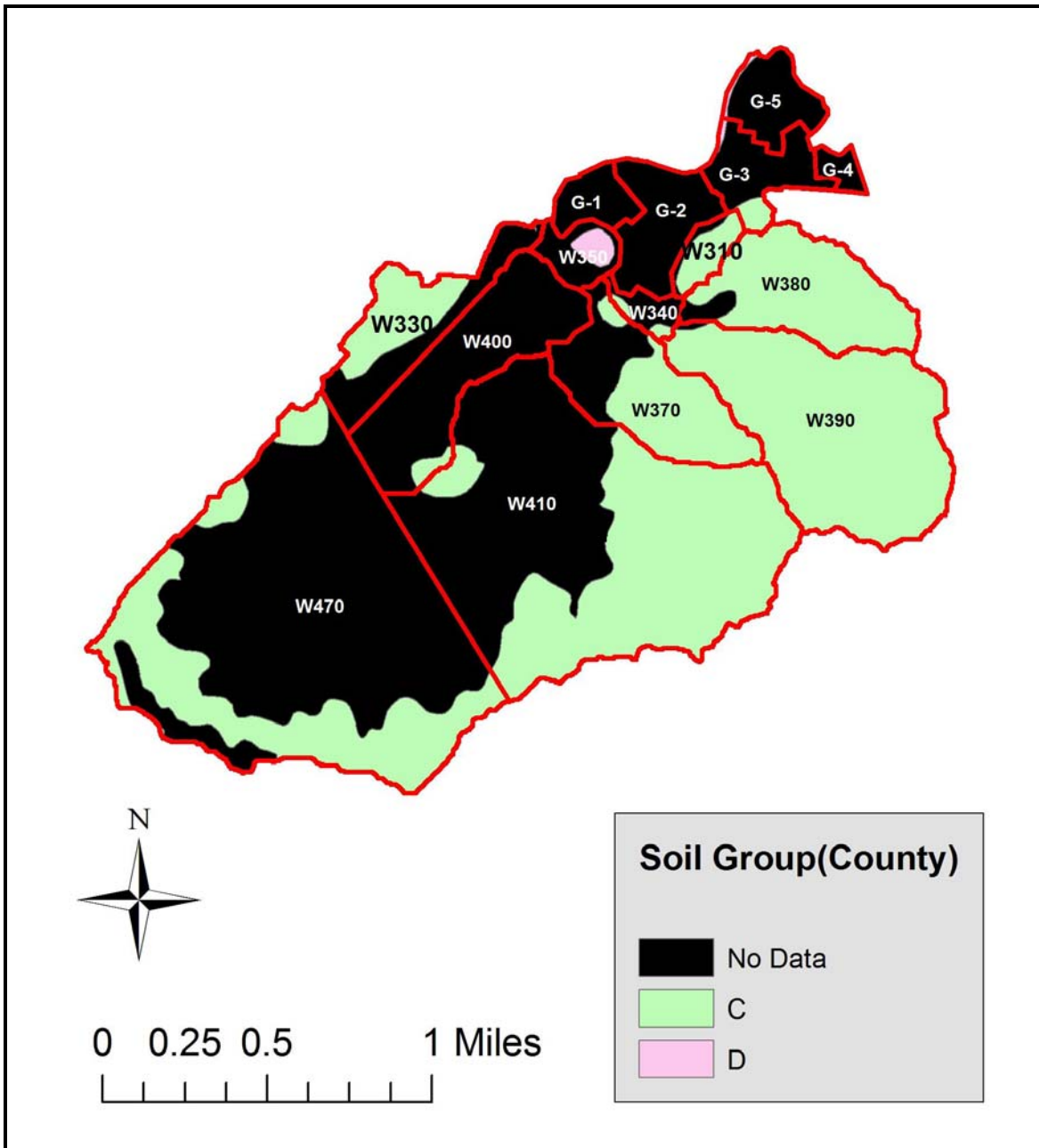


Figure 25. Soil Group Classification by the County of Marin

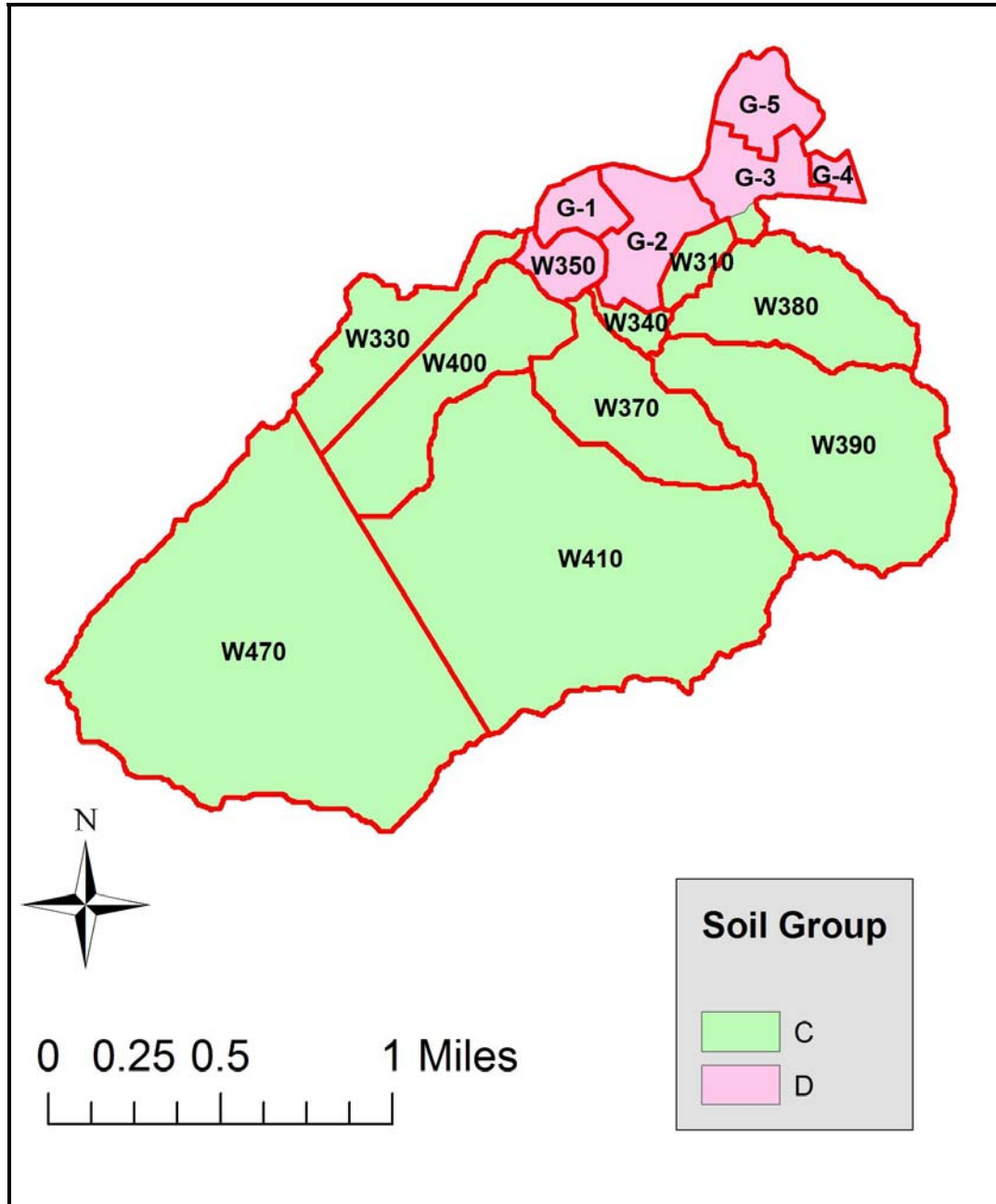


Figure 26. Soil Group Classification Adopted in the Present Study

4.3.2 Land Use/treatment Classification

The SCS has identified more than 20 general land use/treatment classes for estimating different curve numbers. In this hydrologic analysis, land use data provided by the County of Marin were used to develop the land-use pattern in the watershed and

categorized into 8 classes including employment areas, infrastructure, residential, urban open, forest land, rangeland, wetlands, and water. The distribution of those land uses is shown in Figure 27.

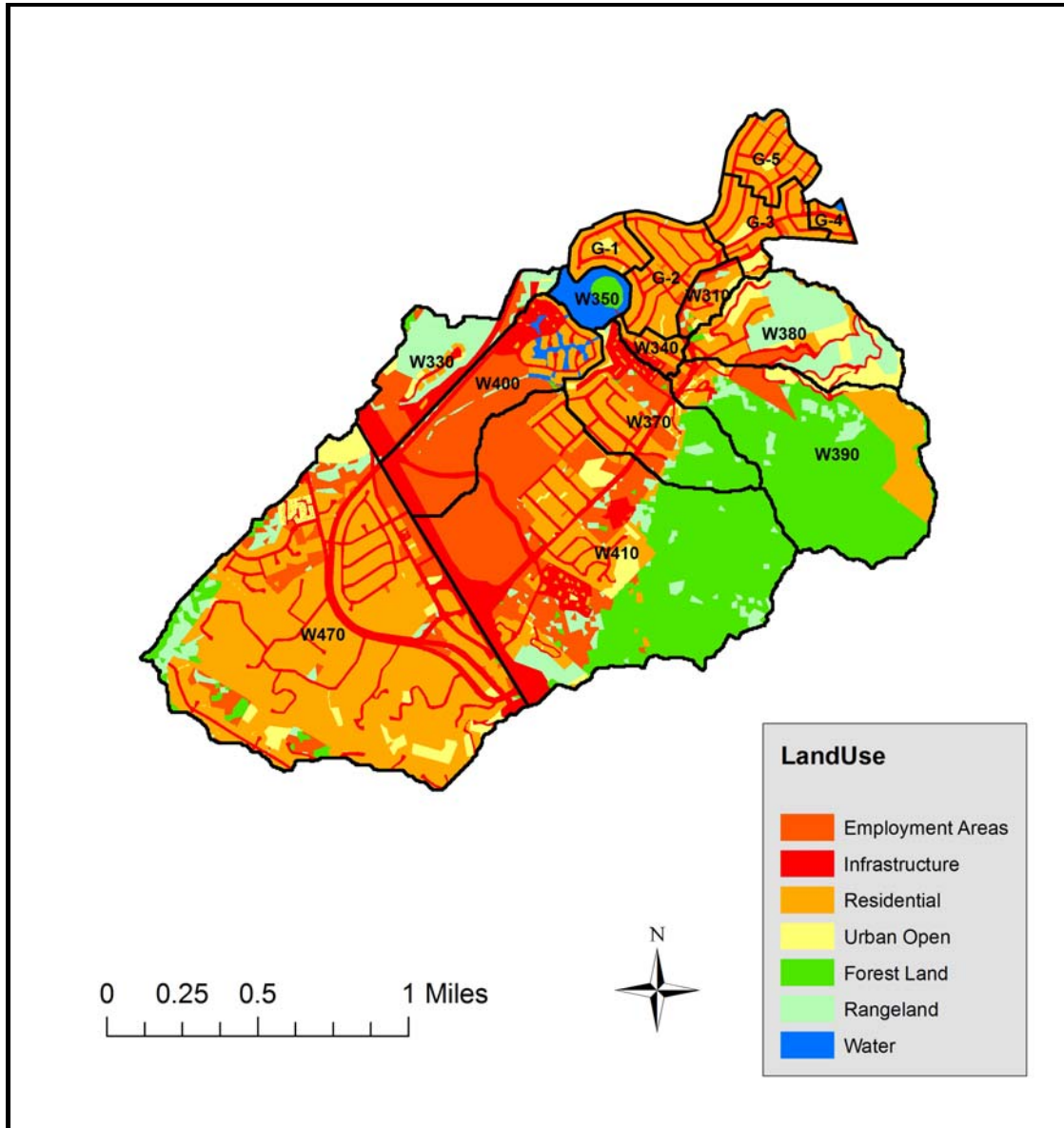


Figure 27. Land Use Patterns of the Watershed

4.3.3 Hydrologic Conditions

The infiltration capacity of a given soil is affected by vegetation/ground cover and quality and density of that cover. To refine the cover type, it is classified into the following hydrologic conditions:

Poor: Heavily grazed or regularly burned areas. Less than 50% of the ground surface is protected by plant or brush and tree canopy.

Fair: Moderate cover with 50 to 75% of the ground surface protected by vegetation.

Good: Heavy or dense cover with more than 75% of the ground surface protected by vegetation.

The hydrologic conditions of the South Fork watershed were determined from a field trip on February 5, 2009 and a review of the Google image of the study area. The entire South Fork watershed can be categorized to be in good hydrologic conditions.

4.3.4 Antecedent Soil Moisture Condition

Antecedent soil moisture has a significant effect on the volume and rate of storm runoff. The SCS developed three antecedent soil moisture conditions (AMC) with the designated values of 1, 2, and 3. They are described as follows:

Condition 1: Soils are dry but not to wilting point; satisfactory cultivation has taken place.

Condition 2: Average conditions.

Condition 3: Saturated soil; heavy rainfall or light rainfall/low temperatures have occurred within the last 5 days.

In the present hydrologic study, a sensitivity analysis that was performed for the HEC-HMS simulations, using different AMC values, is discussed in Section 4.7.

4.3.5 Estimates of SCS Curve Number

The curve numbers within each subbasin were estimated based on the combined effect of soil group, land use/treatment, hydrologic condition, and antecedent soil moisture condition, as individually discussed in the previous sections. Assuming the soil moisture condition is for the AMC value of 2, the spatial distribution of curve number within individual subbasins is shown in Figure 28. It can be seen from the figure that the Gallinas Village, including G-1, G-2, G-3, G-4, and G-5, is predominantly residential with a *CN* of 80, while the hillside south of North San Pedro Road is predominantly forest with a *CN* of 41 or 48. The information shown in Figure 28 was used to calculate the composite *CN* values for individual subbasins by weighting the areas of different *CN* values. The results are shown in Figure 29. The deduced composite *CN* values in individual subbasins for other AMC values ranging from 1.25 to 3 are shown in Table 3. It is noted from Table 3 that the higher the AMC value is, the greater the *CN* value is estimated.

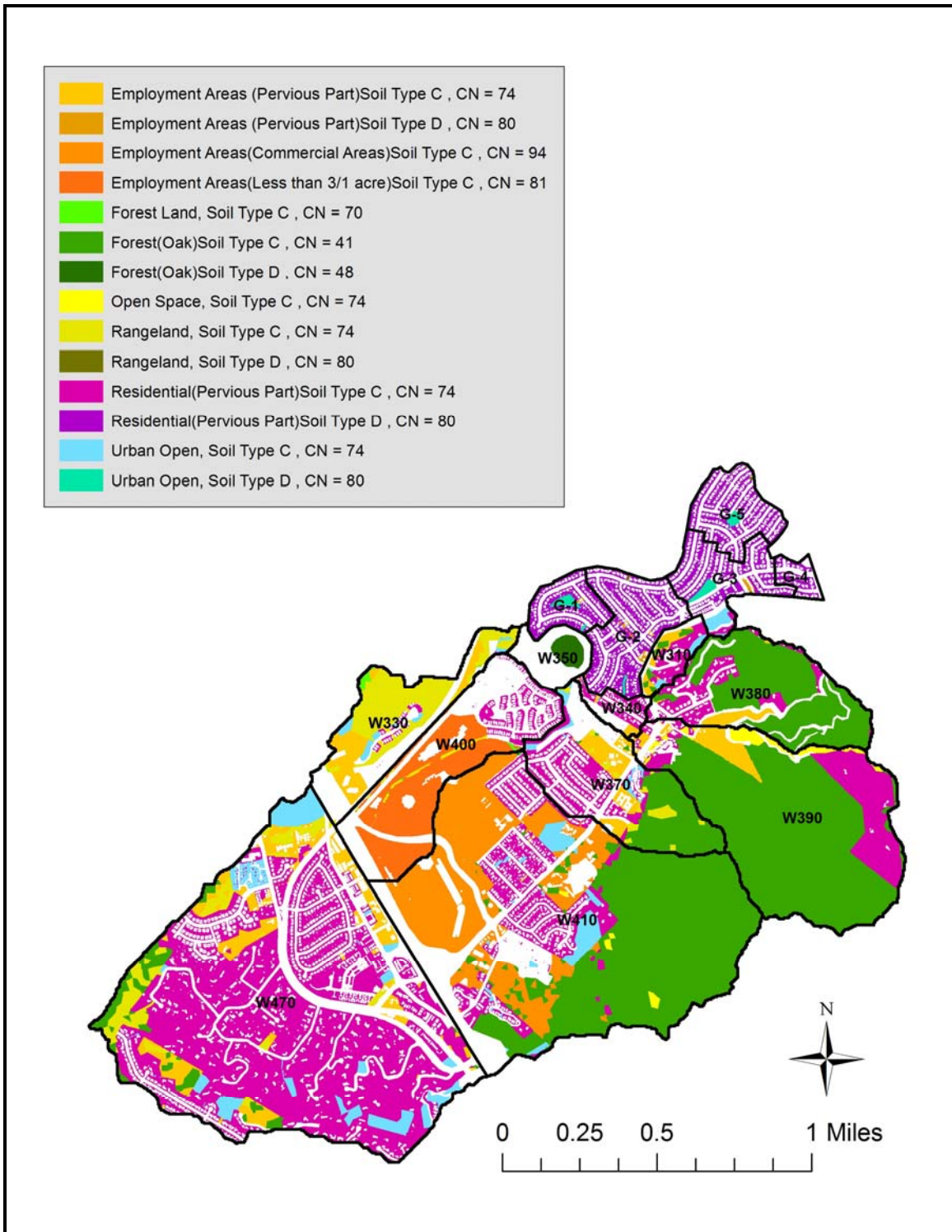


Figure 28. Spatial Distribution of Curve Number in Individual Subbasins for AMC 2

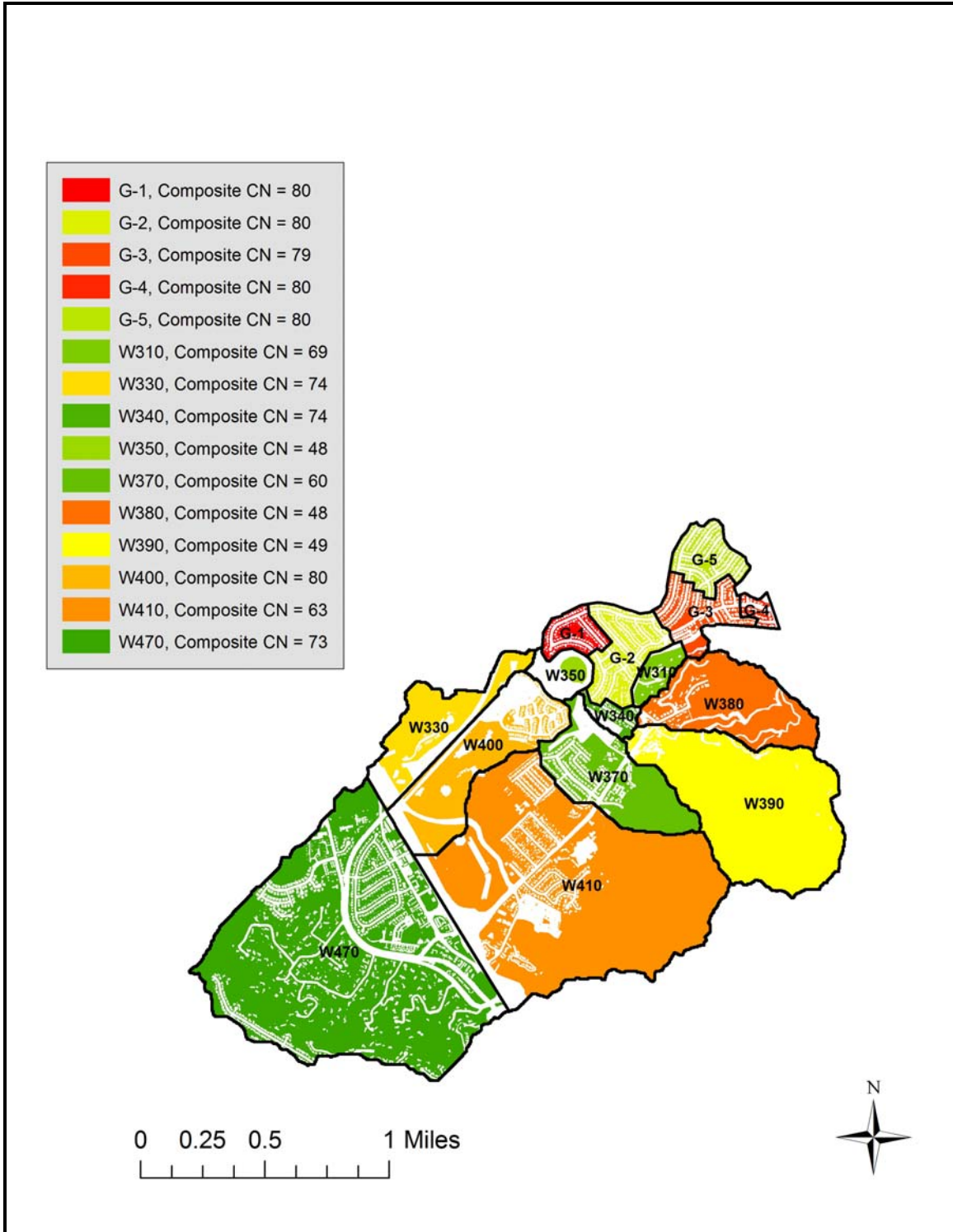


Figure 29. Composite Curve Numbers for Individual Subbasins for AMC 2

Table 3. Composite *CN* Values for Individual Subbasins for Different *AMC* Values

Subbasin	AMC Value							
	1.25	1.5	1.75	2	2.25	2.5	2.75	3
G-1	67	71	76	80	84	87	91	94
G-2	67	71	76	80	84	87	91	94
G-3	66	70	75	79	83	86	90	93
G-4	67	71	76	80	84	87	91	94
G-5	67	71	76	80	84	87	91	94
W310	55	59	64	69	73	77	81	84
W330	60	65	69	74	78	82	86	90
W340	60	65	69	74	78	82	86	90
W350	35	39	42	48	53	58	62	67
W370	45	50	55	60	65	69	74	78
W380	35	39	42	48	53	58	62	67
W390	36	40	44	49	54	59	64	68
W400	67	71	76	80	83	87	90	94
W410	52	56	59	63	67	70	74	78
W470	59	64	68	73	77	81	85	89

4.3.6 Impervious Ratio

Infiltration will only occur in pervious areas of the watershed. Therefore, no loss calculations were carried out on the impervious area, all rainfall on the impervious portion of each subbasin becomes excess rainfall and subject to direct runoff. The impervious ratio is expressed in terms of the percent of the area. The impervious area typically includes building, infrastructure (such as roads), and water body. Figure 30 shows the distribution of the impervious area in the watershed. The impervious ratios for individual subbasins are shown in Table 4. The high impervious ratio of 78% for subbasin W350 that includes Margarita Island and the surrounding waterway is due to a large portion of the area being classified as water body.

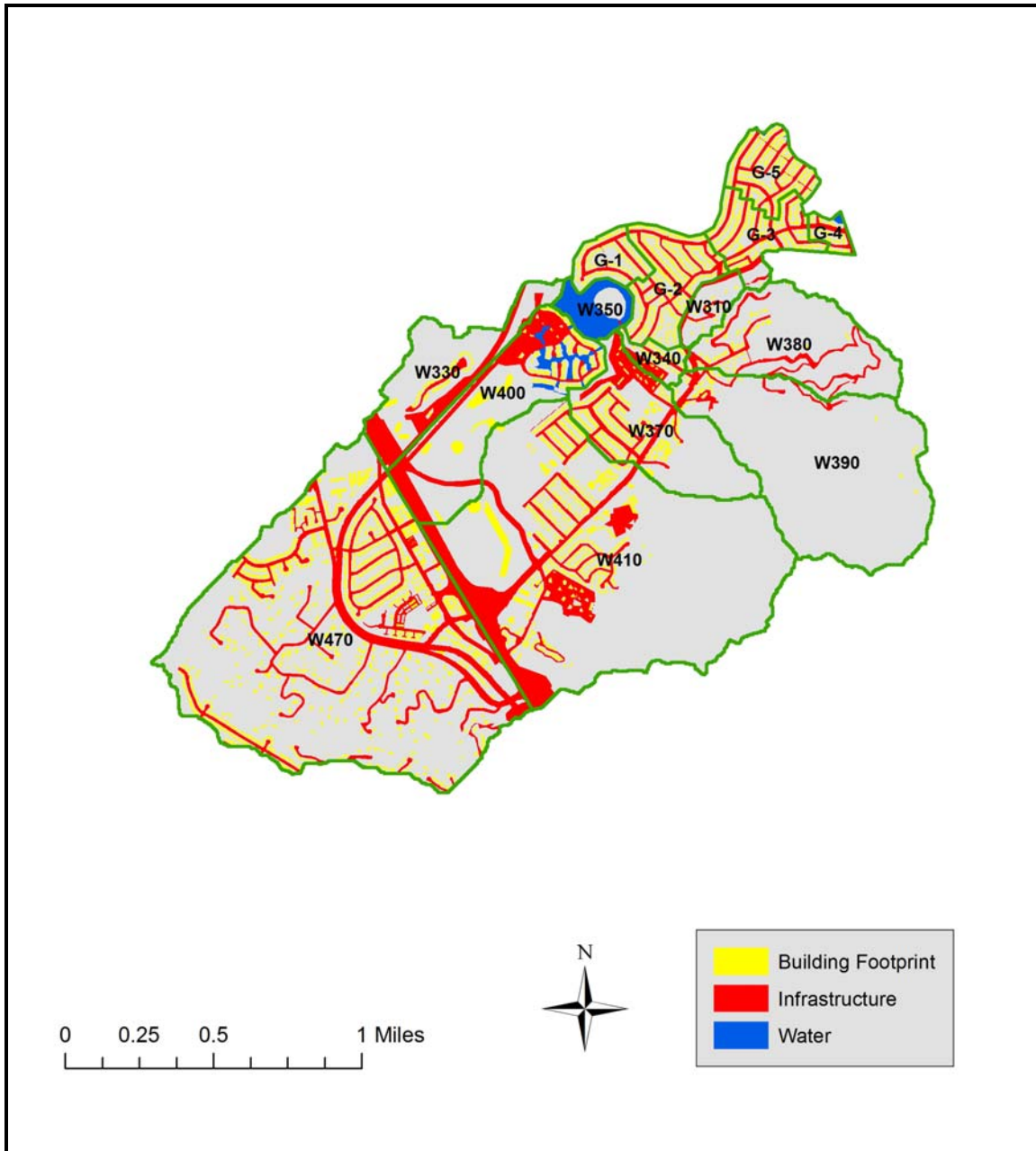


Figure 30. Distribution of Impervious Area in the Watershed

Table 4. Impervious Ratios for Individual Subbasins

Subbasin	Total Area		Impervious Area		Impervious Ratio
	mi ²	ft ²	mi ²	ft ²	
G-1	0.0372	1,036,345	0.0141	394,307	38
G-2	0.0867	2,416,929	0.0404	1,127,483	47
G-3	0.0702	1,958,242	0.0334	931,420	48
G-4	0.0145	403,348	0.0083	230,649	57
G-5	0.0587	1,637,224	0.0295	821,852	50
W310	0.0297	828,911	0.0074	206,041	25
W330	0.1308	3,645,242	0.0435	1,212,749	33
W340	0.0221	617,378	0.0115	319,620	52
W350	0.0385	1,073,232	0.0300	837,121	78
W370	0.1675	4,668,635	0.0531	1,480,028	32
W380	0.1754	4,889,600	0.0272	759,618	16
W390	0.3631	10,123,200	0.0142	394,626	4
W400	0.1970	5,490,841	0.0819	2,284,220	42
W410	0.7478	20,848,716	0.1616	4,506,452	22
W470	0.8521	23,754,790	0.2424	6,758,796	28

4.3.7 Initial Abstraction

The initial abstraction I_a that is defined as 0.2 of the calculated potential retention can be directly calculated from curve number, while the curve number is a function of the AMC value in addition to soil group, land use/treatment, and hydrologic condition. Table 5 shows the estimated initial abstractions for individual subbasins, based on the computed composite CNs with different AMC values. It can be seen from Table 5 that, as the AMC value increases, CN increases and I_a decreases.

4.4 Clark Unit Hydrograph

In the runoff simulation of a watershed, the excess rainfall hyetograph is transformed to a runoff hydrograph through a transfer function called the unit hydrograph. In the present hydrologic study, the Clark unit hydrograph was used as the transfer function. The Clark unit hydrograph method first develops a hydrograph based on the time-area curve. It is then routed through a linear reservoir to account for storage attenuation effect of each subbasin. The Clark unit hydrograph is defined by two parameters including time of concentration and storage coefficient. The time of concentration, denoted by t_c , is defined as the time between the end of excess rainfall and the point of inflection of the falling limb of the runoff hydrograph. Storage coefficient, denoted by R , represents the storage effect of a basin.

Table 5. Initial Abstractions for Individual Subbasins with Different AMC

Sub-basin	AMC=1.25		AMC=1.5		AMC=1.75		AMC=2		AMC=2.25		AMC=2.5		AMC=2.75		AMC=3	
	CN	I_a (in)	CN	I_a (in)	CN	I_a (in)	CN	I_a (in)	CN	I_a (in)	CN	I_a (in)	CN	I_a (in)	CN	I_a (in)
G-1	67	0.985	71	0.817	76	0.632	80	0.500	84	0.381	87	0.299	91	0.198	94	0.128
G-2	67	0.985	71	0.817	76	0.632	80	0.500	84	0.381	87	0.299	91	0.198	94	0.128
G-3	66	1.044	70	0.862	75	0.678	79	0.529	83	0.413	86	0.324	90	0.221	93	0.145
G-4	67	0.985	71	0.817	76	0.632	80	0.500	84	0.381	87	0.299	91	0.198	94	0.128
G-5	67	0.985	71	0.817	76	0.632	80	0.500	84	0.381	87	0.299	91	0.198	94	0.128
W310	55	1.616	59	1.390	64	1.125	69	0.899	73	0.728	77	0.582	81	0.469	84	0.381
W330	60	1.339	65	1.082	69	0.902	74	0.706	78	0.566	82	0.441	86	0.327	90	0.224
W340	60	1.333	65	1.077	69	0.899	74	0.703	78	0.564	82	0.439	86	0.326	90	0.222
W350	35	3.733	39	3.115	42	2.726	48	2.153	53	1.782	58	1.468	62	1.202	67	0.974
W370	45	2.419	50	2.016	55	1.636	60	1.333	65	1.077	69	0.899	74	0.703	78	0.564
W380	35	3.733	39	3.115	42	2.726	48	2.153	53	1.782	58	1.468	62	1.202	67	0.974
W390	36	3.552	40	2.966	44	2.595	49	2.048	54	1.702	59	1.403	64	1.149	68	0.930
W400	67	0.996	71	0.821	76	0.640	80	0.509	83	0.408	87	0.297	90	0.217	94	0.123
W410	52	1.848	56	1.583	59	1.410	63	1.155	67	0.996	70	0.844	74	0.695	78	0.572
W470	59	1.411	64	1.145	68	0.961	73	0.754	77	0.610	81	0.479	85	0.361	89	0.253

4.4.1 Time of Concentration

Times of concentration t_c for subbasins in the present study were calculated using Kirby Hathaway's formula:

$$t_c = 0.01377 \frac{(nL)^{0.47}}{s^{0.235}} \quad (2)$$

where: L is the length of the flow path in feet; n is Manning's watershed roughness coefficient; and s is the average slope in ft/ft, which is taken as the slope of the flow path between the 25% and 75% points of the path length. Manning's n is taken to be 0.07 for rural subbasins and 0.03 for urbanized subbasins. Table 6 shows the computed times of concentration for individual subbasins.

4.4.2 Storage Coefficients

The storage coefficient R is often estimated based on an acceptable routing indicator K_C defined as $K_C = R/(t_c + R)$. This indicator affects the peaking characteristics

of hydrographs. The larger the value of K_C is, the smaller the peaking of the runoff hydrograph will be. In general, smaller K_C values correspond to more urbanized basins, while larger K_C values correspond to undeveloped rural basins. Since the impervious ratio typically increases with the degree of urbanization within a basin, the K_C values in the present study are assigned smaller values for subbasins with large impervious ratios as respectively shown in Table 6 and Figure 31. It is noted, however, that K_C is assigned 0.8 for Subbasin W350 of Margarita Island, which has little urbanization. On the other hand, the high impervious ratio for this subbasin is due to a large portion of the water area. The resulting R values for subbasins are also shown in Table 6.

Table 6. Times of Concentration and Storage Coefficients for Subbasins

Subbasin	Length (L) ft	Slope (s)	n	t_c hr	Impervious Ratio %	K_C	R hr
G-1	2,135	0.0001	0.03	0.847	38	0.65	1.573
G-2	2,526	0.0022	0.03	0.443	47	0.65	0.822
G-3	2,536	0.0005	0.03	0.634	48	0.65	1.178
G-4	799	0.0050	0.03	0.213	57	0.65	0.395
G-5	2,128	0.0001	0.03	0.846	50	0.65	1.571
W310	560	0.3956	0.07	0.096	25	0.70	0.224
W330	4,783	0.0016	0.07	0.964	33	0.70	2.250
W340	1,755	0.0062	0.03	0.293	52	0.65	0.544
W350	4,783	0.0016	0.07	0.964	78	0.80	3.857
W370	6,111	0.0741	0.07	0.438	32	0.70	1.021
W380	4,899	0.0824	0.07	0.385	16	0.80	1.539
W390	6,145	0.1191	0.07	0.393	4	0.80	1.570
W400	4,771	0.0020	0.03	0.610	42	0.65	1.134
W410	7,663	0.0600	0.07	0.512	22	0.70	1.194
W470	7,152	0.0377	0.07	0.552	28	0.70	1.289

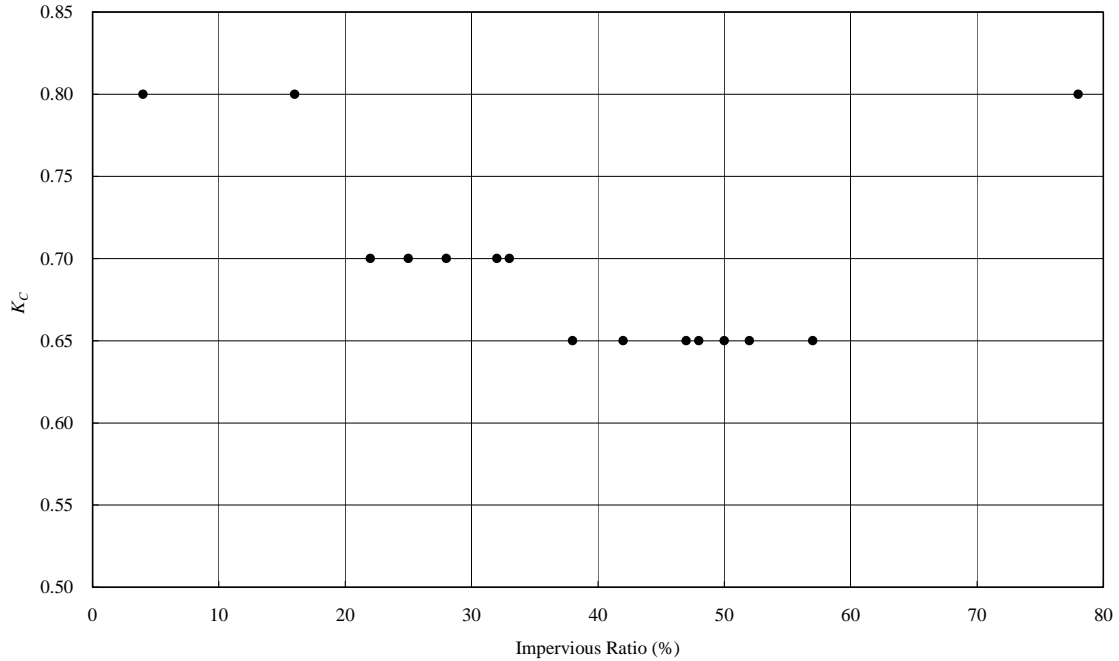


Figure 31. Assigned K_C values with Respect to Impervious Ratios of Subbasins

4.5 Muskingum Channel Routing

The runoff in channels is subjected to further storage attenuation. In the present study, the Muskingum method was used to account for this effect when appropriate. The method involves determining the outflow hydrograph at the downstream end of a channel, based on the inflow hydrograph, by solving the following equations:

$$O_2 = C_o I_2 + C_1 I_1 + C_2 O_1 \quad (3)$$

where:

- I_1 = Inflow discharge at t_1
- I_2 = Inflow discharge at $t_2 = t_1 + \Delta t$
- O_1 = Outflow discharge at t_1
- O_2 = Outflow discharge at $t_2 = t_1 + \Delta t$

The coefficients in Eq. 3 are expressed as follows:

$$C_o = -\frac{Kx - 0.5\Delta t}{K - Kx + 0.5\Delta t} \quad (4)$$

$$C_1 = \frac{Kx + 0.5\Delta t}{K - Kx + 0.5\Delta t} \quad (5)$$

$$C_2 = \frac{K - Kx - 0.5\Delta t}{K - Kx + 0.5\Delta t} \quad (6)$$

In the above equations, x and K are routing coefficients. Specifically, x is a weighting factor for the upstream inflow, while $(1-x)$ is the weighting factor for the downstream outflow; K is the storage coefficient of the channel. C_o , C_1 , and C_2 can be calculated with specified x , K and Δt . In general, x is taken as 0.2 for a natural channel, while K is estimated by the travel time through the channel reach. In the present hydrologic study, x is taken as 0.2, Δt is taken as 5 minutes (equal to 0.08 hour), and values of K were estimated separately for individual routing reaches as shown in Table 7. They are described below:

Reach 1 - The Auditorium Channel reach extending from the Highway 101 culvert (Junction 1) to the confluence with the Northbridge Channel (Junction 2) is approximately 3,500 feet. K was estimated at 0.71 hour as the travel time through the reach with the calculated velocity of 1.37 ft/sec, based on the 100-year peak inflow discharge of 502 cfs that was computed from the present HEC-HMS simulations for Subbasin W470 with an AMC value of 2.5 and the previously deduced cross section data (CSW, 1982).

Reach 2 - The South Fork from the Auditorium Channel-Northbridge Channel confluence (Junction 2) to the Meadow Drive Hillside Drain outfall (Junction 3) is 1,770 feet long. K was estimated at 0.40 hour as the travel time through the reach with the calculated velocity of 1.24 ft/sec, based on the 100-year peak inflow discharge of 930 cfs that was computed from the present HEC-HMS simulations with an AMC of 2.5 and the previously deduced cross section data (CSW, 1982).

Reach 3 - The Meadow Drive Hillside Drain (from Junction 4 to Junction 3) is a 7 feet by 4 feet box culvert of 1,620 feet long. K was estimated at 0.11 hour as the travel time through the reach with the calculated velocity of 4.25 ft/sec under full flow condition based on the 100-year peak inflow discharge of 170 cfs computed for Subbasins W380 and W390 from the present HEC-HMS simulations with an AMC value of 2.5.

Reach 4 - The South Fork from the Meadow Drive Hillside Drain outfall (Junction 3) to the outfall of Pump Station No. 3 (Junction 5) is 860 feet long. K was estimated at 0.19 hour as the travel time through the reach using the calculated velocity of 1.24 ft/sec for Reach 2.

Reach 5 - The South Fork from the Pump Station No. 3 outfall (Junction 3) to the confluence with the Railroad Channel (Junction 7) is 851 feet long. K was estimated at 0.19 hour as the travel time through the reach using the calculated velocity of 1.24 ft/sec for Reach 2.

Reach 6 - The La Pasada Hillside Drain (from Junction 6 to Junction 16) that is a twin 30-in diameter drain is 1,060 ft long. K was estimated at 0.09 hour as the travel

time through the reach with the calculated velocity of 3.46 ft/sec under a full flow condition based on the 100-year peak inflow discharge of 35 cfs for Subbasin W310 that was computed from the present HEC-HMS simulations with an AMC value of 2.5.

Table 7. Channel Routing Coefficients for AMC Value of 2.5

Reach No	V Ft/sec	L ft	K hr	x	Δt hr	C_o	C_1	C_2
1	1.37	3,500	0.71	0.2	0.08	-0.164	0.301	0.863
2	1.24	1,770	0.40	0.2	0.08	-0.105	0.337	0.768
3	4.25	1,620	0.11	0.2	0.08	0.162	0.497	0.341
4	1.24	860	0.19	0.2	0.08	0.016	0.410	0.574
5	1.24	851	0.19	0.2	0.08	0.018	0.411	0.571
6	3.46	1,060	0.09	0.2	0.08	0.242	0.545	0.213
7	1.24	2,670	0.60	0.2	0.08	-0.150	0.310	0.840
8	1.24	520	0.12	0.2	0.08	0.136	0.482	0.382
9	1.24	1,700	0.38	0.2	0.08	-0.100	0.340	0.759
10	1.24	254	0.06	0.2	0.08	0.347	0.608	0.044
11	1.24	865	0.19	0.2	0.08	0.015	0.409	0.576

Reach 7 - The South Fork from the Railroad Channel confluence (Junction 7) to the outfall of Pump Station No. 2 (Junction 13) is 2,670 feet long. K was estimated at 0.60 hours as the travel time through the reach using the calculated velocity of 1.24 ft/sec for Reach 2.

Reach 8 - The South Fork from the outfall of Pump Station No. 2 (Junction 13) to the La Pasada Hillside Drain outfall (Junction 16) is 520 feet long. K was estimated at 0.12 hour as the travel time through the reach using the calculated velocity of 1.24 ft/sec for Reach 2.

Reach 9 - The South Fork from the outfall of Pump Station No. 1 (Junction 14) to the outfall of Pump Station No. 5 (Junction 15) is 1,700 feet long. K was estimated at 0.38 hour as the travel time through the reach using the calculated velocity of 1.24 ft/sec for Reach 2.

Reach 10 - The South Fork from the La Pasada Hillside Drain outfall (Junction 16) to the outfall of Pump Station No. 1 (Junction 14) is 254 feet long. K was estimated at 0.06 hour as the travel time through the reach using the calculated velocity of 1.24 ft/sec for Reach 2. It is noted that no routing was performed for this reach due to the short reach length.

Reach 11 - The South Fork from the outfall of Pump Station No. 5 (Junction 15) to the confluence with the North Fork (Junction 8) is 865 feet long. *K* was estimated at 0.19 hour as the travel time through the reach using the calculated velocity of 1.24 ft/sec for Reach 2.

As noted above, the velocities for Reaches 4, 5, and 7 to 11 were assumed to be the same as that for Reach 2. The values for *K* were then calculated based on individual reach lengths.

4.6 Hydrologic Simulations

Hydrologic simulations using the HEC-HMS model with parameters developed in this analysis were respectively performed for the 2-, 5-, 10-, 25-, 50-, 100-, 200-, and 500-year floods. Base flow rates are considered negligible in the present model study (Note: The base flow rates for the 10-, 50-, 100-, and 500-year floods were estimated to be only in the range of 6 cfs to 9 cfs for Las Gallinas Creek downstream of the confluence of the North Fork and the South Fork (USACE-SFD, 1990)). The computed peak discharges at key locations are summarized in Table 8 for the AMC value of 2.5. The flood hydrographs at Junction 8, shown herein as an example case, are presented in Figures 32 through 39. The total drainage area for this junction located at the confluence of the North Fork and the South Fork Channels is 2.98 mi². It is noted that the 100-year peak discharge of 67 cfs from Subbasin G-2 exceeds the capacity of 40.5 cfs for Pump Station No. 2. However, since an existing intertie was designed to be capable of transferring 22 cfs between Pump Stations No. 2 and No. 3 (Nute Engineering, 1998), the ponding effect for Pump Station 2 would be minimal and, therefore, was not considered in the present HEC-HMS model.

The 2-year Flood Event

The peak discharge for the 2-year flood at the confluence of the North Fork and the South Fork was computed to be 297 cfs. The computed hydrograph is shown in Figure 32.

The 5-year Flood Event

The peak discharge for the 5-year flood at the confluence of the North Fork and the South Fork was computed to be 564 cfs. The computed hydrograph is shown in Figure 33.

The 10-year Flood Event

The peak discharge for the 10-year flood at the confluence of the North Fork and the South Fork was computed to be 757 cfs. The computed hydrograph is shown in Figure 34.

Table 8. HEC-HMS Simulation Results for AMC Value of 2.5

Element	Drainage Area mi ²	Q ₂ cfs	Q ₅ cfs	Q ₁₀ cfs	Q ₂₅ cfs	Q ₅₀ cfs	Q ₁₀₀ cfs	Q ₂₀₀ cfs	Q ₅₀₀ cfs
G-1	0.037	6	11	14	17	19	21	24	27
G-2	0.087	21	34	43	53	60	67	74	83
G-3	0.070	14	23	29	36	41	46	51	57
G-4	0.014	5	8	10	12	14	15	17	19
G-5	0.059	11	17	22	27	31	34	38	42
Junction-1	0.852	128	232	304	386	447	502	559	634
Junction-13	2.818	284	544	731	951	1,110	1,265	1,422	1,628
Junction-14	2.918	293	560	751	976	1,139	1,298	1,459	1,669
Junction-15	2.977	298	567	760	986	1,150	1,310	1,472	1,683
Junction-16	2.848	285	546	734	955	1,114	1,270	1,428	1,634
Junction-2	1.797	224	417	553	711	824	933	1,044	1,188
Junction-3	2.525	254	494	667	872	1,020	1,164	1,310	1,502
Junction-4	0.539	15	48	77	114	142	170	200	240
Junction-5	2.601	262	507	684	893	1,043	1,191	1,340	1,534
Junction-6	0.030	8	16	21	27	31	35	39	45
Junction-7	2.731	276	532	716	932	1,089	1,242	1,397	1,599
Junction-8	2.977	297	564	757	982	1,146	1,305	1,466	1,676
Junction-9	0.014	5	8	10	12	14	15	17	19
Pump #1	0.070	14	23	29	36	41	46	51	57
Pump #2	0.087	21	34	43	53	60	67	74	83
Pump #3	0.037	6	11	14	17	19	21	24	27
Pump #4	0.014	5	8	10	12	14	15	17	19
Pump #5	0.059	11	17	22	27	31	34	38	42
W310	0.030	8	16	21	27	31	35	39	45
W330	0.131	16	29	38	47	55	61	68	77
W340	0.022	6	10	13	16	18	20	22	25
W350	0.038	5	7	9	11	13	14	16	18
W370	0.167	20	40	54	71	83	95	107	123
W380	0.175	7	19	28	41	50	59	69	82
W390	0.363	8	30	49	74	92	111	131	158
W400	0.197	40	66	83	103	118	131	145	162
W410	0.748	74	154	213	283	336	385	437	503
W470	0.852	128	232	304	386	447	502	559	634

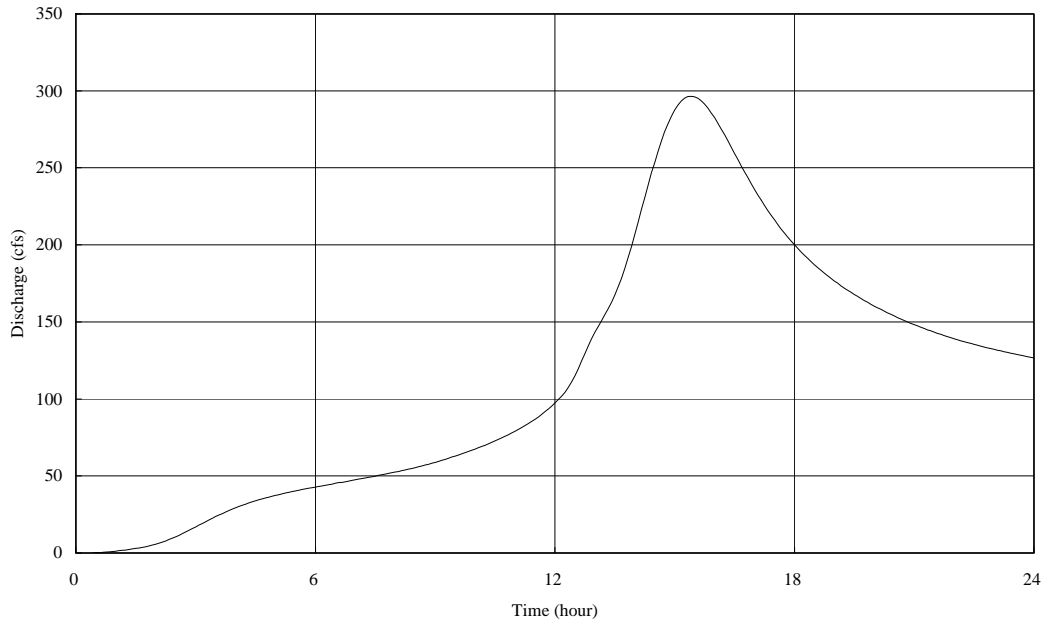


Figure 32. Computed Hydrograph for the 2-year Flood for AMC Value of 2.5

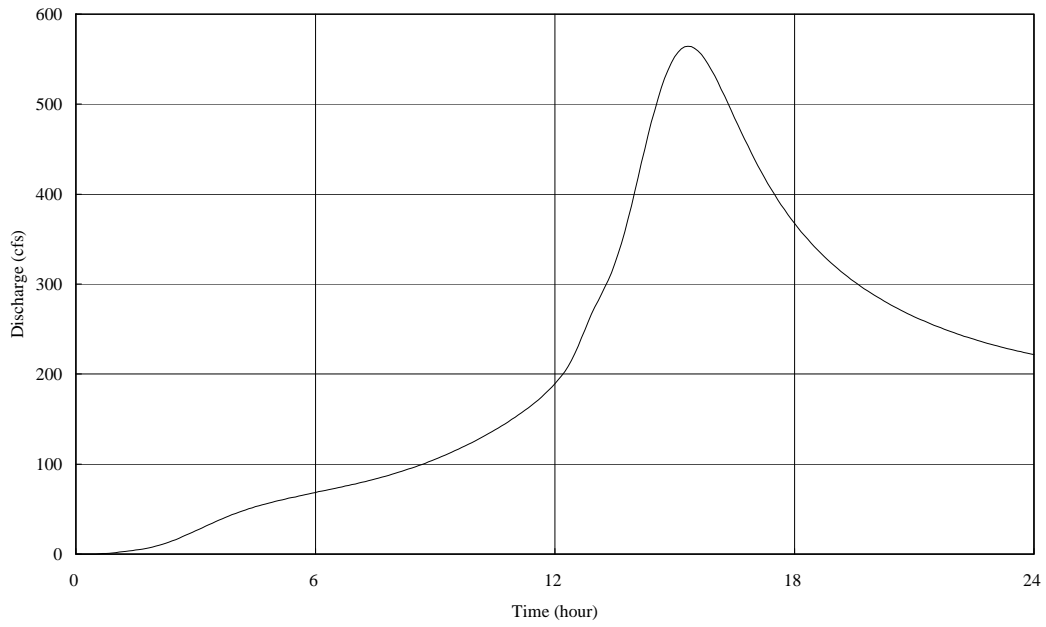


Figure 33. Computed Hydrograph for the 5-year Flood for AMC Value of 2.5

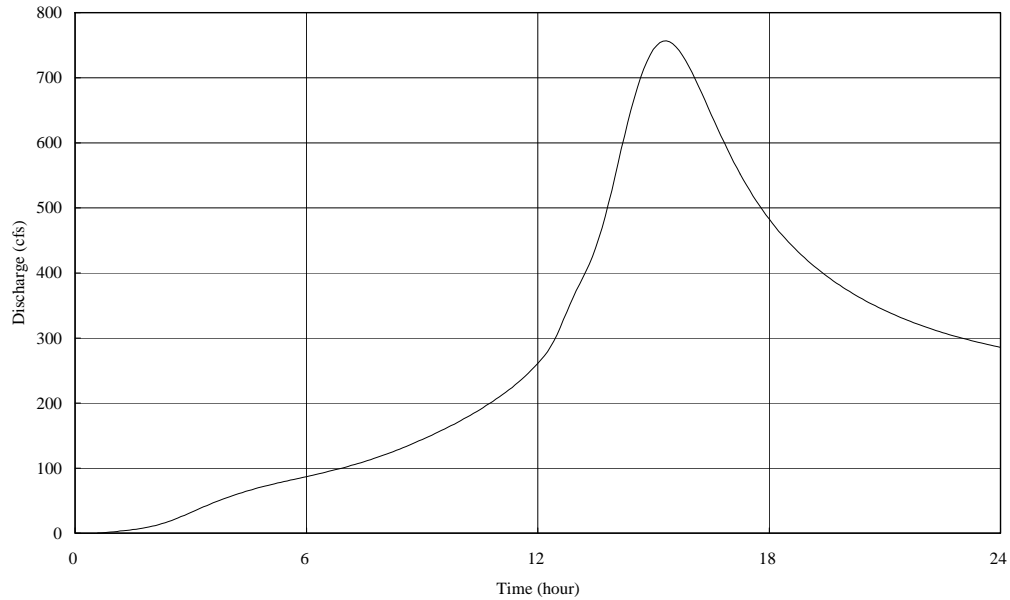


Figure 34. Computed Hydrograph for the 10-year Flood for AMC Value of 2.5

The 25-year Flood

The peak discharge for the 25-year flood at the confluence of the North Fork and the South Fork was computed to be 982 cfs. The computed hydrograph is shown in Figure 35.

The 50-year Flood

The peak discharge for the 50-year flood at the confluence of the North Fork and the South Fork was computed to be 1,146 cfs. The computed hydrograph is shown in Figure 36.

The 100-year Flood

The peak discharge for the 100-year flood at the confluence of the North Fork and the South Fork was computed to be 1,305 cfs. The computed hydrograph is shown in Figure 37.

The 200-year Flood

The peak discharge for the 200-year flood at the confluence of the North Fork and the South Fork was computed to be 1,466 cfs. The computed hydrograph is shown in Figure 38.

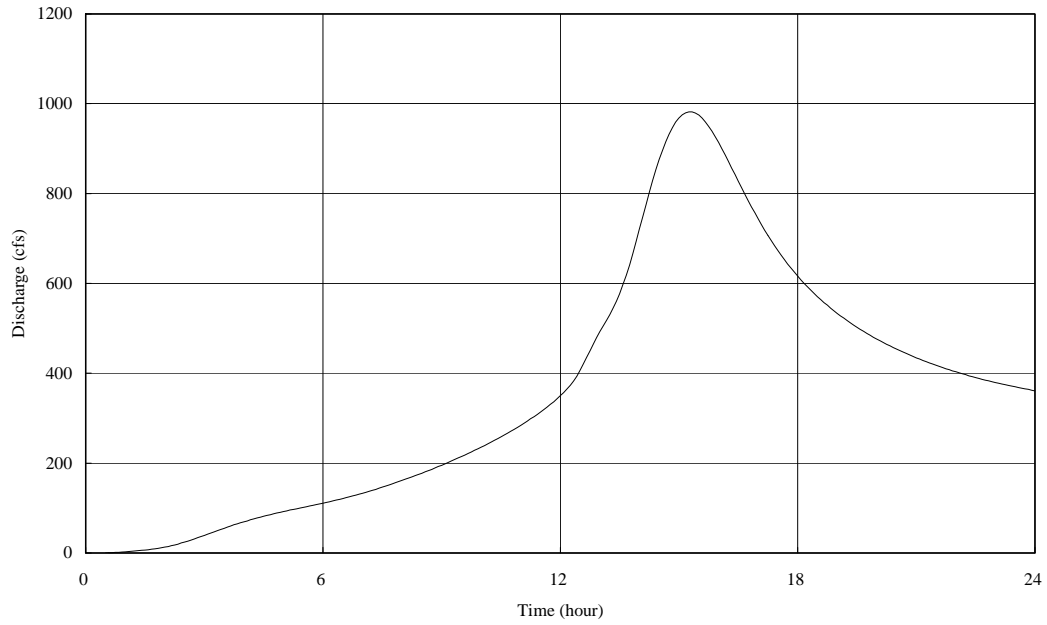


Figure 35. Computed Hydrograph for the 25-year Flood for AMC Value of 2.5

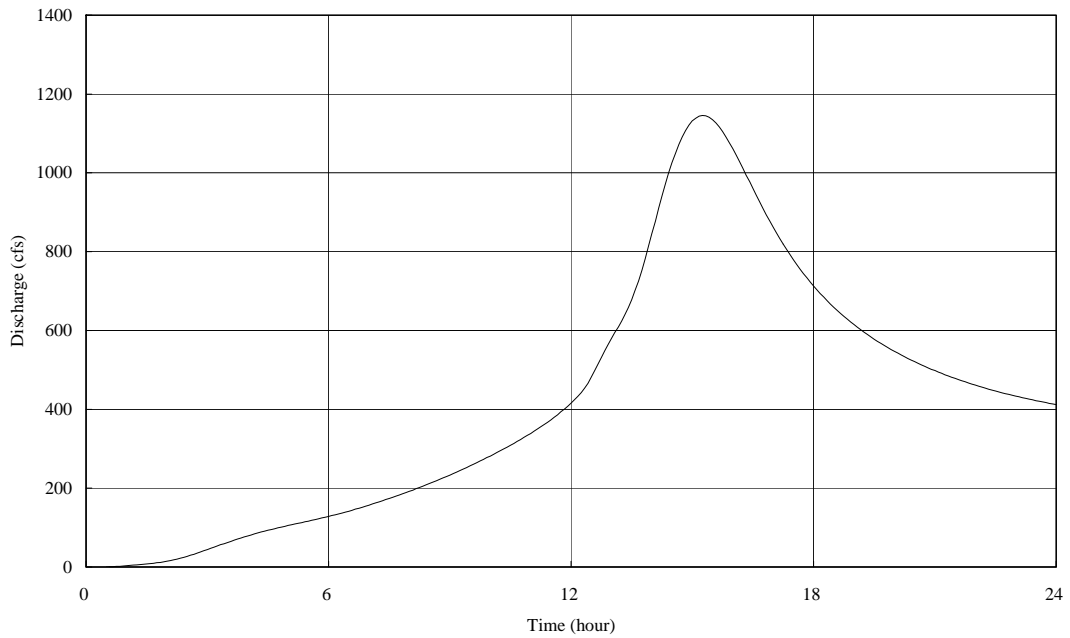


Figure 36. Computed Hydrograph for the 50-year Flood for AMC Value of 2.5

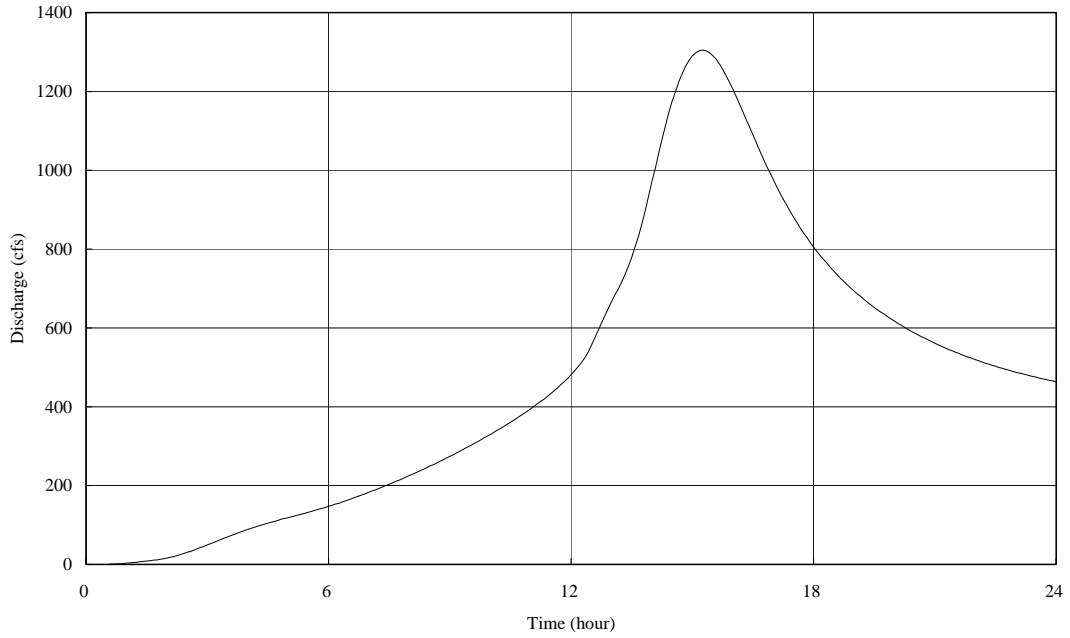


Figure 37. Computed Hydrograph for the 100-year Flood for AMC Value of 2.5

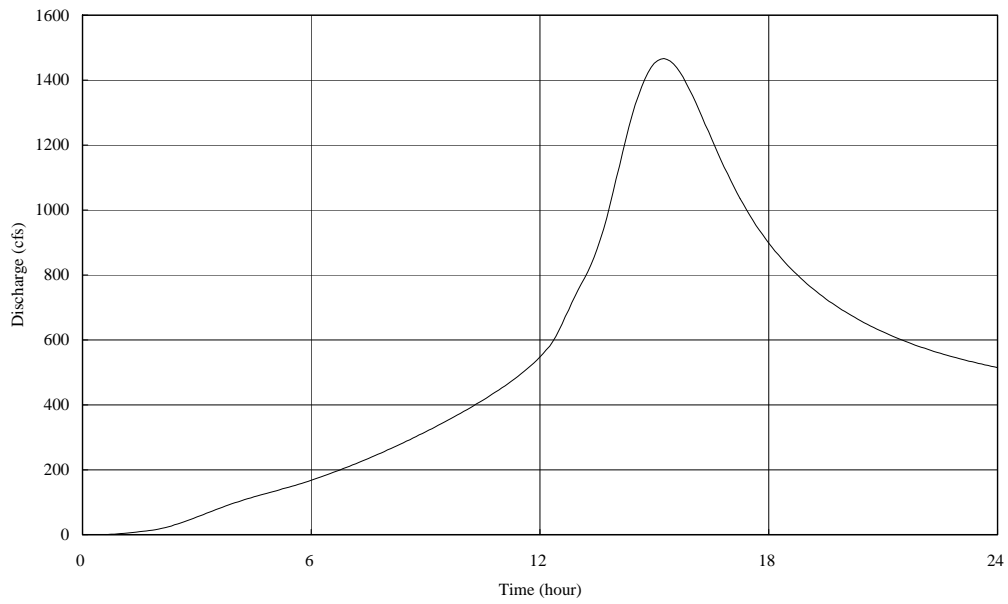


Figure 38. Computed Hydrograph for the 200-year Flood for AMC Value of 2.5

The 500-year Flood

The peak discharge for the 500-year flood at the confluence of the North Fork and the South Fork was computed to be 1,676 cfs. The computed hydrograph is shown in Figure 39.

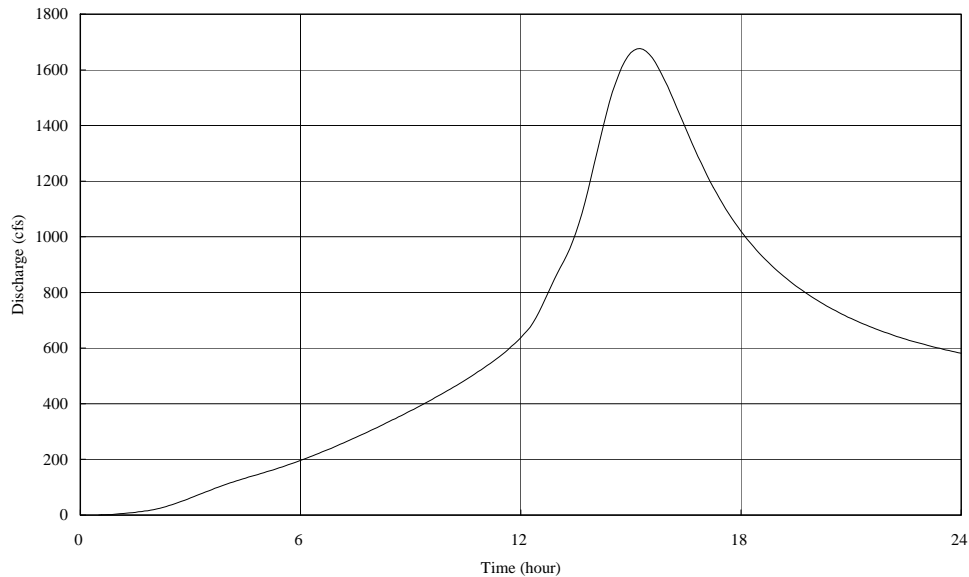


Figure 39. Computed Hydrograph for the 500-year Flood for AMC Value of 2.5

4.7 Sensitivity Analysis

A sensitivity analysis was conducted to investigate the effect of AMC on the simulation results. Simulation results for the AMC values of 2 and 3 are shown in Tables 9 and 10, respectively. A comparison of the discharges presented in Table 8 for AMC 2.5, Table 9 for AMC 2, and Table 10 for AMC 3 shows that runoff discharges increase with increasing AMC value for all recurrence frequencies. It is noted that AMC 2, for example, denotes the case for the AMC value of 2. The changes for the 100-year discharges between AMC 2, AMC 2.5 and AMC 3 are shown in Table 11. It can be seen from Table 11 that the changes from AMC 2 to AMC 2.5 and from AMC 2.5 to AMC 3 are less than 14% of the discharges for AMC 2.5, except for the hillside subbasins south of North San Pedro Road including W380 and W390. The relatively large changes for W350 (Margarita Island) create only negligible effect on the discharge at the outlet of the South Fork watershed (Junction 8). It is noted that at the watershed outlet (Junction 8) the changes in the 100-year discharges from AMC 2.5 are only 12% for AMC 2 and 10% for AMC 3. Based on the results of this sensitivity analysis and recognizing that major storms typically occur during the wet seasons in Northern California, it is therefore suggested that runoff discharges computed by HEC-HMS for different flood events, using the AMC 2.5 condition, be adopted.

Table 9. HEC-HMS Simulation Results for AMC Value of 2

Element	Drainage Area mi ²	Q ₂ cfs	Q ₅ cfs	Q ₁₀ cfs	Q ₂₅ cfs	Q ₅₀ cfs	Q ₁₀₀ cfs	Q ₂₀₀ cfs	Q ₅₀₀ cfs
G-1	0.037	5	9	12	16	18	20	22	25
G-2	0.087	18	31	39	50	57	64	71	80
G-3	0.070	12	21	27	34	39	44	48	55
G-4	0.014	4	7	9	11	13	15	16	18
G-5	0.059	9	16	20	25	29	33	36	41
Junction-1	0.852	98	193	260	340	399	454	510	584
Junction-13	2.818	221	442	611	815	965	1,113	1,264	1,463
Junction-14	2.918	229	457	630	839	992	1,144	1,298	1,502
Junction-15	2.977	234	464	638	849	1003	1,156	1,312	1,517
Junction-16	2.848	222	444	614	819	969	1,118	1,270	1,469
Junction-2	1.797	175	348	475	626	736	843	951	1,094
Junction-3	2.525	195	397	553	742	881	1,018	1,159	1,344
Junction-4	0.539	9	25	45	73	95	119	144	178
Junction-5	2.601	203	410	569	762	903	1,043	1,187	1,375
Junction-6	0.030	6	13	18	23	28	31	35	41
Junction-7	2.731	214	431	597	797	945	1,090	1,239	1,435
Junction-8	2.977	233	462	636	846	1,000	1,152	1,307	1,511
Junction-9	0.014	4	7	9	11	13	15	16	18
W310	0.030	6	13	18	23	28	31	35	41
W330	0.131	13	24	33	42	49	56	63	72
W340	0.022	5	9	11	14	17	19	21	24
W350	0.038	4	7	9	11	12	14	15	17
W370	0.167	16	32	44	60	71	82	94	109
W380	0.175	6	12	19	28	36	43	52	63
W390	0.363	4	14	26	45	60	76	92	115
W400	0.197	34	59	76	96	111	124	138	156
W410	0.748	55	124	177	242	291	338	387	452
W470	0.852	98	193	260	340	399	454	510	584

Table 10. HEC-HMS Simulation Results for AMC Value of 3

Element	Drainage Area mi ²	Q ₂ cfs	Q ₅ cfs	Q ₁₀ cfs	Q ₂₅ cfs	Q ₅₀ cfs	Q ₁₀₀ cfs	Q ₂₀₀ cfs	Q ₅₀₀ cfs
G-1	0.037	7	12	15	18	20	22	25	27
G-2	0.087	23	36	45	55	62	69	76	84
G-3	0.070	16	25	31	38	43	48	52	58
G-4	0.014	5	8	10	12	14	16	17	19
G-5	0.059	12	19	23	28	32	35	39	43
Junction-1	0.852	162	271	344	426	486	541	597	670
Junction-13	2.818	366	652	851	1,079	1,242	1,400	1,560	1,767
Junction-14	2.918	377	670	873	1,106	1,273	1,434	1,597	1,809
Junction-15	2.977	381	677	881	1,116	1,284	1,447	1,611	1,823
Junction-16	2.848	367	655	854	1,083	1,247	1,406	1,566	1,773
Junction-2	1.797	283	490	631	790	905	1,014	1,124	1,268
Junction-3	2.525	332	598	782	995	1,147	1,294	1,443	1,636
Junction-4	0.539	30	76	112	155	188	219	252	295
Junction-5	2.601	341	612	800	1,016	1,172	1,322	1,473	1,670
Junction-6	0.030	10	18	23	29	34	38	42	47
Junction-7	2.731	358	640	836	1,060	1,221	1,377	1,534	1,738
Junction-8	2.977	380	674	878	1,111	1,279	1,441	1,604	1,816
Junction-9	0.014	5	8	10	12	14	16	17	19
W310	0.030	10	18	23	29	34	38	42	47
W330	0.131	20	33	42	52	59	66	73	82
W340	0.022	7	11	13	16	19	21	23	25
W350	0.038	5	7	9	12	13	15	16	18
W370	0.167	27	49	64	82	95	107	120	136
W380	0.175	12	27	39	53	64	74	85	99
W390	0.363	19	49	73	102	124	145	167	196
W400	0.197	45	72	89	108	123	136	149	167
W410	0.748	99	191	255	330	384	435	487	555
W470	0.852	162	271	344	426	486	541	597	670

Table 11. Changes in the 100-year Discharges for Different AMC Values

Location	Q ₁₀₀ (cfs)			Difference in Q ₁₀₀ against AMC2.5 (%)	
	AMC2	AMC 2.5	AMC 3	Between AMC 2 and AMC 2.5	Between AMC 3 and AMC 2.5
G-1	20.1	21.4	22.3	-6	4
G-2	63.6	66.7	68.8	-5	3
G-3	43.6	45.8	47.5	-5	4
G-4	14.6	15.2	15.6	-4	3
G-5	32.5	34.1	35.3	-5	4
Junction-1	453.6	502.2	540.9	-10	8
Junction-13	1112.7	1265.1	1400.3	-12	11
Junction-14	1144.0	1297.8	1434.4	-12	11
Junction-15	1156.2	1309.9	1446.7	-12	10
Junction-16	1117.8	1270.1	1406.0	-12	11
Junction-2	842.5	933.3	1014.1	-10	9
Junction-3	1018.2	1163.9	1294.4	-13	11
Junction-4	118.9	170.4	219.0	-30	29
Junction-5	1043.3	1190.5	1321.8	-12	11
Junction-6	31.4	35.1	37.8	-11	8
Junction-7	1090.2	1242.2	1377.0	-12	11
Junction-8	1151.6	1305.0	1440.8	-12	10
Junction-9	14.6	15.2	15.6	-4	3
W310	31.4	35.1	37.8	-11	8
W330	55.8	61.4	65.9	-9	7
W340	18.7	19.8	20.7	-6	5
W350	13.5	14.1	14.6	-4	4
W370	82.2	95.2	107.0	-14	12
W380	43.4	59.2	74.0	-27	25
W390	75.6	111.4	145.0	-32	30
W400	124.0	131.0	135.7	-5	4
W410	337.8	385.4	435.0	-12	13
W470	453.6	502.2	540.9	-10	8

4.8 Present and Future Hydrologic Conditions

Various discussions with County personnel indicate that there will be no further urban development in the Santa Venetia Valley basin. Therefore, the impact of land development will remain unchanged for future conditions. However, there could be effects from global warming (IPCC, 2007). There is no scientific agreement whether the annual precipitation in Northern California will increase in the future, but there exists a general consent that the rainfall intensity for individual storm events will be greater. This would result in alteration of the design storm. Such a change would probably cause an increase in predicted peak flows. Also, the predicted sea level rise ranging from the low end of 0.5 feet to the upper limit of about 2 feet or more at the end of the next 50 years would potentially affect any runoff discharge rate through outfalls that are subject to tidal influence. However, since most of the runoffs in the Gallinas Valley basin are pumped into the creek, the impact due to tidal action will be minimal. On the other hand, the rising temperature resulting from global warming may cause more evapotranspiration. This could result in various degrees of reduction in the antecedent soil moisture (AMC) number. Such a reduction would lower predicted peaks.

4.9 Simulated Results

The HEC-HMS simulations for the South Fork watershed were performed in the present study. In the simulations, the watershed is subdivided into 14 subbasins. They are connected by 13 junctions and 11 channels to form the drainage network in the model. Design storms for 2-, 5-, 10-, 25-, 50-, 100-, 200-, and 500-year frequencies were established based on the rainfall intensity-duration-frequency curves deduced from rainfall data collected at the San Rafael Civic Center station (Station No. E20-7880-20). Runoff losses were estimated using the SCS method consisting of initial abstracts and subsequent incremental losses during the storms based on the composite SCS curve numbers for subbasins with considerations of soil group classification, land use/treatment classification, hydrologic conditions, and antecedent soil moisture conditions. Impervious ratios of subbasins were determined based on the GIS data provided by the County of Marin and were incorporated in the model. The Clark unit hydrograph was used to transform excess rainfall into the runoff hydrographs from individual subbasins. Times of concentration for the Clark unit hydrograph were calculated using Kirby Hathaway's formula and storage coefficients estimated based on the routing indicator which is related to the degree of urbanization represented by impervious ratios of individual subbasins. Modeled flows were routed through the connecting channels using the Muskingum method to account for the channel storage effects. The AMC 2.5 condition was adopted in the present simulations. A sensitivity analysis was performed by comparing the results for the AMC 2.5 condition with those for the AMC 2.0 and AMC 3.0 conditions. The simulation results are summarized as follows:

- Runoff hydrographs were simulated for the 2-, 5-, 10-, 25-, 50-, 100-, 200-, and 500-year frequencies based on the AMC 2.5 condition. The simulated peak

discharges are shown in Table 8 for runoffs from the subbasins and at various junctions. Specifically, peak discharges for the watershed outlet at the confluence of the South and North Forks (Junction 8) are 297 cfs, 564 cfs, 757 cfs, 982 cfs, 1,146 cfs, 1,305 cfs, 1,466 cfs, and 1,676 cfs for the 2-, 5-, 10-, 25-, 50-, 100-, 200-, and 500-year floods, respectively. Peak discharges at the location of the South Fork where the Railroad Channel enters (Junction 7) are 276, cfs, 532 cfs, 716 cfs, 932 cfs, 1,089 cfs, 1,242 cfs, 1,397 cfs, and 1,599 cfs, respectively. And, peak discharges at the confluence of the Auditorium Channel and the Northbridge Channel where the South Fork begins (Junction 2) are 224 cfs, 417cfs, 553 cfs, 711 cfs, 824 cfs, 933 cfs, 1,044 cfs, and 1,188 cfs, respectively.

- A sensitivity analysis was conducted to investigate the effect of the AMC condition on peak discharges by comparing the results from AMC 2.5 with those from AMC 2 and AMC 3. The results indicate that changes in peak discharge from AMC 2 to AMC 2.5 and from AMC 2.5 to AMC 3 are less than 14% of the peak discharges for AMC 2.5, except for the hillside subbasins south of North San Pedro Road including W380 and W390. Further, at the watershed outlet (Junction 8), changes in the 100-year peak discharge from AMC 2.5 are only 12% for AMC 2 and 10% for AMC 3. Based on the results of this sensitivity analysis and recognizing that major storms generally occur in the wet seasons in Northern California, it is suggested that the peak discharges based on the AMC 2.5 condition be adopted.
- There will be no further urban development in the Santa Venetia Valley basin and, therefore, the simulated results for the present conditions may be adopted for the future conditions.

Since there is no standard criterion in selecting the storm duration, a 24-hour design storm was used in the HEC-HMS simulations. To further evaluate the simulated discharges in relation to a selected design storm, the HEC-HMS simulations under 6-hour and 12-hour storm durations for the 100-year recurrence-interval scenario were also performed. A comparison of the modeled peak discharges at the confluence of the South and North Forks (Junction 8) is presented as follows.

- a) The 100-year 24-hour storm with AMC 2.5: $Q = 1,305$ cfs
- b) The 100-year 12-hour storm with AMC 2.5: $Q = 1,098$ cfs
- c) The 100-year 6-hour storm with AMC 3: $Q = 999$ cfs.

It is indicative that the modeled peak discharge for the 24-hour storm duration is the most conservative estimate among the three cases. The results show that the peak discharge at the confluence of the South and North Forks decreases with the shortened storm durations. With a critical storm pattern that was applied in the present study, the rainfall intensity reaches its peak at the mid point of the design storm while maintaining the same 5-minute depth of 0.34 inches (see Table 2). The 5-minute depth of 0.34 inches occurs at the 12th hour for the 24-hour storm, the 6th hour for the 12-hour storm, and the 3rd hour for the 6-hour storm. As the elapse time increases for longer storm duration, the soil becomes moister during the 5-min peak-intensity time interval. This in turn results in

a lower infiltration rate within the peak-intensity time interval and consequently a higher peak discharge. Also, based on past observations in the Bay area the AMC 3 condition is more appropriate than the AMC 2.5 condition for a 6-hour storm because the watershed generally tends to be wetter when a shorter intensive storm occurs during the wet season. Therefore, the antecedent soil moisture of 3 was used for the 6-hour storm duration.

5.0 RISK ANALYSIS

Risk analyses were performed for the flood hydrology established for the South Fork at the following three representative locations: (1) the watershed outlet, namely, the confluence of the South and North Forks denoted as Junction 8, (2) the junction where the Railroad Channel and the South Fork meets denoted as Junction 7, and (3) the confluence of the Auditorium Channel and Northbridge Channel where the South Fork begins denoted as Junction 2. The computed peak discharges for 8 different frequencies at these three identified locations from the HEC-HMS model simulations are shown in Table 12.

Table 12. Peak Discharges of Different Frequencies at Three Locations along the South Fork

Location	Q ₂ cfs	Q ₅ cfs	Q ₁₀ cfs	Q ₂₅ cfs	Q ₅₀ cfs	Q ₁₀₀ cfs	Q ₂₀₀ cfs	Q ₅₀₀ cfs
Junction-2	224	417	553	711	824	933	1,044	1,188
Junction-7	276	532	716	932	1,089	1,242	1,397	1,599
Junction-8	297	564	757	982	1,146	1,305	1,466	1,676

5.1 Log-Pearson III Distribution

The flood frequency distribution for the South Fork may be expressed by a Log-Pearson Type III distribution as follows:

$$X = \bar{X} + KS \quad (7)$$

where:

X = Logarithm of flood discharge

\bar{X} = Mean of the distribution in logarithm

S = Standard deviation of the distribution in logarithm

K = Frequency factor, which is a function of exceedance probability p and skew G .

This distribution may be represented by a synthetic distribution with the parameters, G_s , S_s , and \bar{X}_s that can be obtained from the 0.50-, 0.10-, and 0.01-exceedance probabilities using the following equations:

$$G_s = -2.5 + 3.12 \frac{\text{Log}(Q_{0.01}/Q_{0.10})}{\text{Log}(Q_{0.10}/Q_{0.5})} \quad (8)$$

$$S_s = \frac{\text{Log}(Q_{0.01}/Q_{0.50})}{K_{0.01} - K_{0.50}} \quad (9)$$

$$\bar{X}_s = \text{Log}(Q_{0.5}) - K_{0.5}(S_s) \quad (10)$$

where $Q_{0.5}$, $Q_{0.1}$ and $Q_{0.01}$ are the discharges for the 0.50-, 0.10-, and 0.01-exceedance probabilities. The parameters that were determined using the above equations for the three locations are listed in Table 13.

Table 13. Synthetic Distribution Parameters for Three Locations on the South Fork

Location	\bar{X}_s	S_s	G_s
Junction 8 - the South Fork watershed outlet	2.4301	0.3771	-0.6840
Junction 7 - the point where Railroad Channel flows into the South Fork	2.3964	0.3859	-0.6973
Junction 2 - the confluence of Auditorium Channel and Northbridge Channel where South Fork begins	2.3083	0.3654	-0.6942

Reasonable agreements of the fitted synthetic distributions with the computed discharges from the HEC-HMS simulations are respectively shown in Figures 33, 34, and 35 for Junctions 8, 7, and 2.

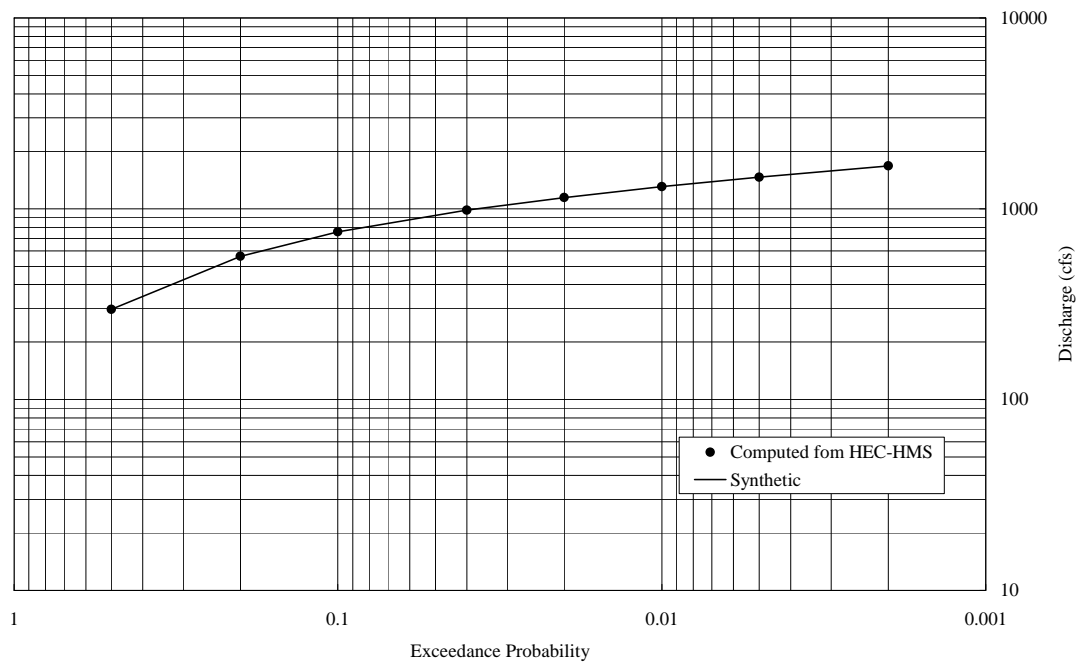


Figure 40. Fitted Log-Pearson Type III Distribution for Junction 8 in the South Fork

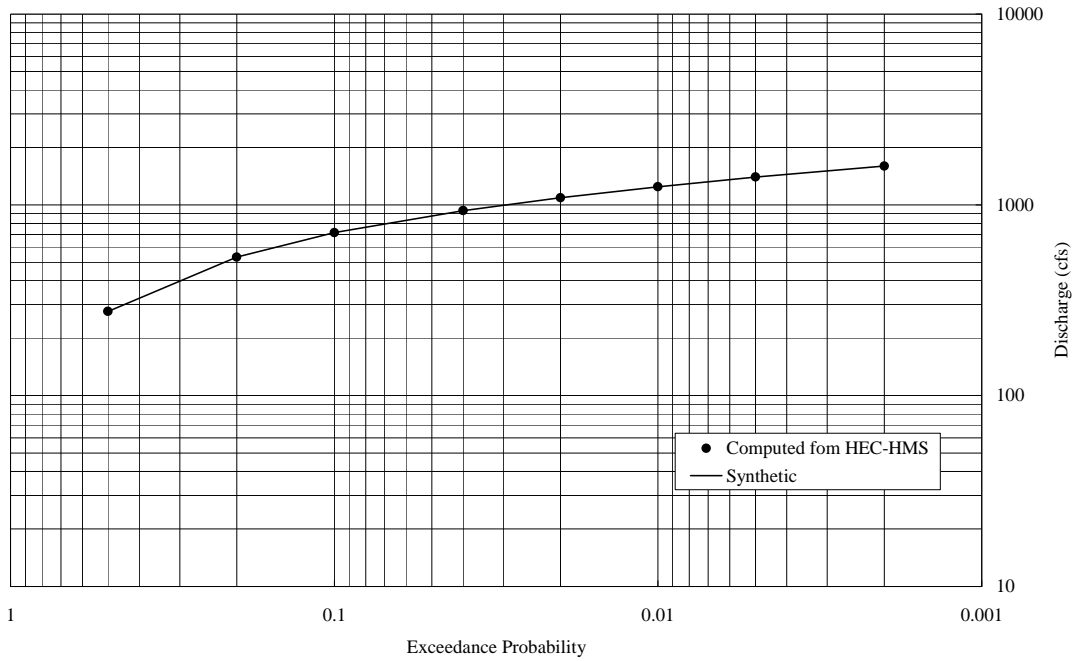


Figure 41. Fitted Log-Pearson Type III Distribution for Junction 7 in the South Fork

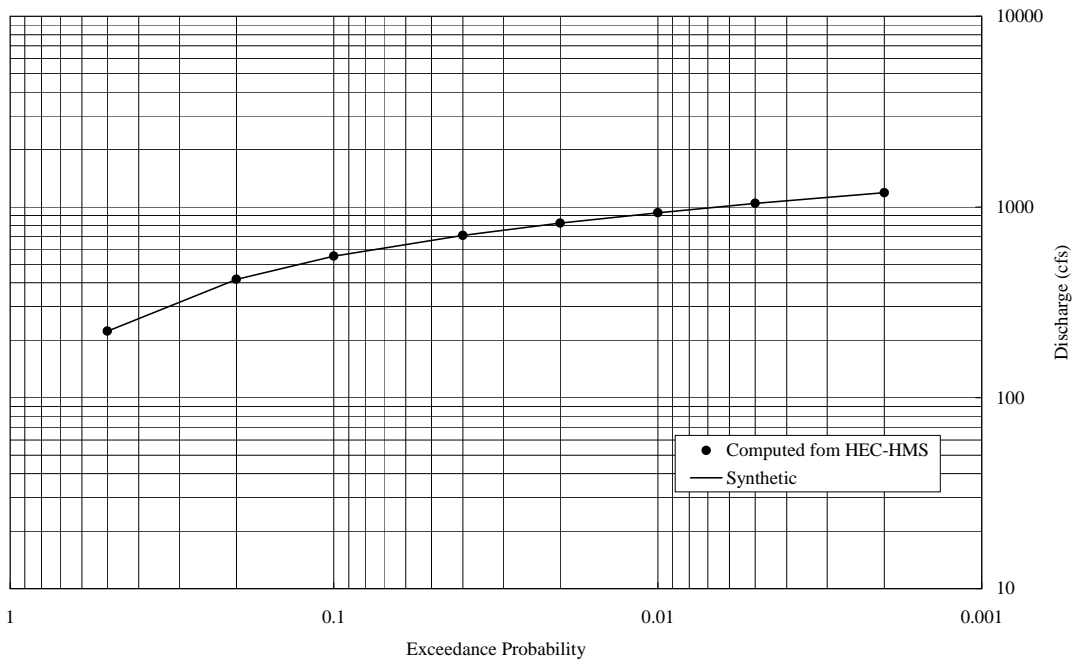


Figure 42. Fitted Log-Pearson Type III Distribution for Junction 2 in the South Fork

5.2 HEC-FDA Simulations

The uncertainty associated with the discharge-probability function can be displayed with confidence limits on the derived synthetic function. The general form of the confidence limits is specified as follows:

$$Up,c(X) = \bar{X} + S(K^U_{P,C}) \quad (11)$$

$$Lp,c(X) = \bar{X} + S(K^L_{P,C}) \quad (12)$$

where \bar{X} and S are the logarithmic mean and standard deviation of the estimated Log-Pearson Type III discharge-probability function, and $K^U_{P,C}$ and $K^L_{P,C}$ are the upper and lower confidence coefficients. It is noted that P is the exceedance probability of X , and c is the probability that $Up,c > X$ and that $Lp,c < X$. $K^U_{P,C}$ and $K^L_{P,C}$ can be estimated using the following equations:

$$K^U_{P,C} = \frac{K_{G,P} + \sqrt{K^2_{G,P} - ab}}{a} \quad (13)$$

$$K^L_{P,C} = \frac{K_{G,P} - \sqrt{K^2_{G,P} - ab}}{a} \quad (14)$$

where

$$a = 1 - \frac{z_c^2}{2(N-1)} \quad (15)$$

$$b = K^2_{G,P} - \frac{z_c^2}{N} \quad (16)$$

z_c is the standard normal deviate, N is the record length, and $K_{G,p}$ is Pearson Type III coordinate expressed in number of standard deviations from the mean for skew G and exceedance probability P . \bar{X} , S , and G are taken to be \bar{X}_s , S_s , and G_s , respectively. Since the discharges for different frequencies are estimated with a rainfall-runoff-routing model, N is taken to be 13 years as the equivalent record length to be consistent with the Corps' guideline (USACE, 1996), which specifies N to be in the range from 10 to 15 years.

5.3 Analyzed Results

Based on the above-described methodology, the error bounds in terms of confidence limits surrounding the 50-, 20-, 10-, 4-, 2-, 1-, 0.5, and 0.2-percent events are respectively shown in Table 14 and Figure 36 for Junction 8, in Table 15 and Figure 37 for Junction 7, and in Table 16 and Figure 38 for Junction 2.

Table 14. Confidence Limits for Junction 8 on the South Fork
(The South Fork Watershed Outlet)

Exceedance Probability	Discharge (cfs)	Discharge (cfs) of Confidence Limit Curves			
		95%	75%	25%	5%
0.999	8	1	3	15	20
0.990	23	6	12	37	47
0.950	56	22	34	79	95
0.900	85	40	57	114	134
0.800	135	76	99	175	203
0.700	185	113	141	236	275
0.500	297	197	233	381	459
0.300	451	303	353	603	766
0.200	567	375	437	782	1,033
0.100	754	484	568	1,094	1,525
0.040	986	609	721	1,506	2,219
0.020	1,150	692	826	1,813	2,762
0.010	1,305	768	923	2,113	3,311
0.004	1,495	858	1,039	2,492	4,025
0.002	1,631	920	1,120	2,772	4,568
0.0001	2,122	1,136	1,405	3,827	6,700

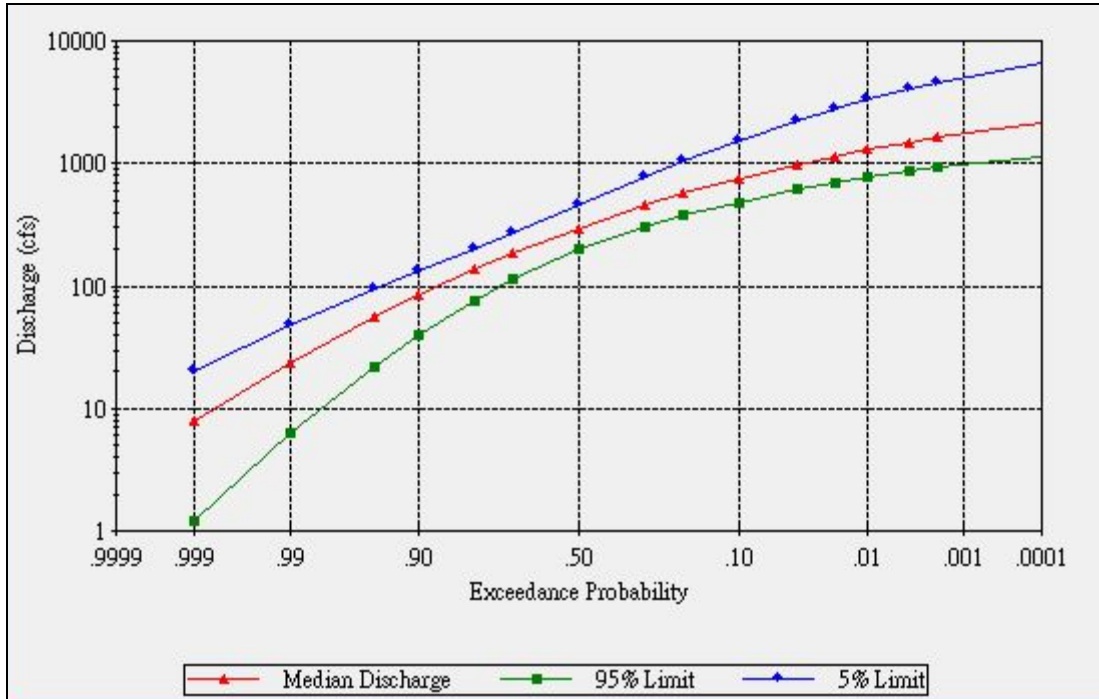


Figure 43. Confidence Limits for Junction 8 at the South Fork of Las Gallinas Creek
(The South Fork Watershed Outlet)

Table 15. Confidence Limits for Junction 7 on the South Fork
(Confluence of Railroad Channel)

Exceedance Probability	Discharge (cfs)	Discharge (cfs) of Confidence Limit Curves			
		95%	75%	25%	5%
0.999	7	1	2	13	17
0.990	20	5	10	33	42
0.950	50	19	30	71	85
0.900	76	35	51	103	122
0.800	123	68	90	160	187
0.700	170	103	129	218	255
0.500	276	182	216	356	431
0.300	423	281	329	569	727
0.200	533	350	409	742	986
0.100	713	454	534	1,043	1,465
0.040	936	572	680	1,442	2,143
0.020	1,093	651	780	1,740	2,673
0.010	1,242	723	872	2,030	3,208
0.004	1,423	808	982	2,396	3,903
0.002	1,553	867	1,060	2,666	4,430
0.0001	2,019	1,069	1,328	3,673	6,484

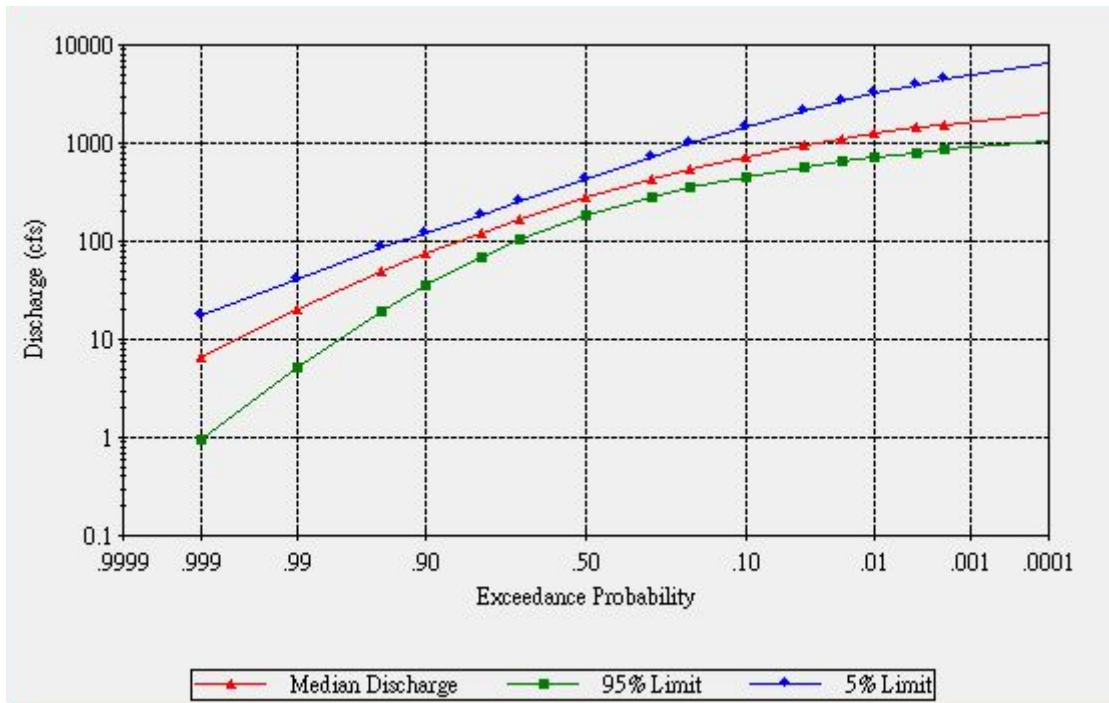


Figure 44. Confidence Limits for Junction 7 at the South Fork of Las Gallinas Creek
(Confluence of Railroad Channel)

Table 16. Confidence Limits for Junction 2 on the South Fork
(Confluence of Auditorium Channel and Northbridge Channel)

Exceedance Probability	Discharge (cfs)	Discharge (cfs) of Confidence Limit Curves			
		95%	75%	25%	5%
0.999	7	1	3	12	16
0.990	19	5	10	30	38
0.950	44	18	28	62	74
0.900	66	32	45	88	103
0.800	105	60	77	134	155
0.700	142	88	109	179	208
0.500	224	151	177	285	341
0.300	336	228	265	445	561
0.200	418	281	325	572	749
0.100	551	359	419	790	1,090
0.040	713	447	527	1,074	1,563
0.020	827	506	600	1,284	1,929
0.010	933	559	668	1,486	2,294
0.004	1,062	621	747	1,740	2,764
0.002	1,154	664	803	1,926	3,118
0.0001	1,482	811	996	2,615	4,484

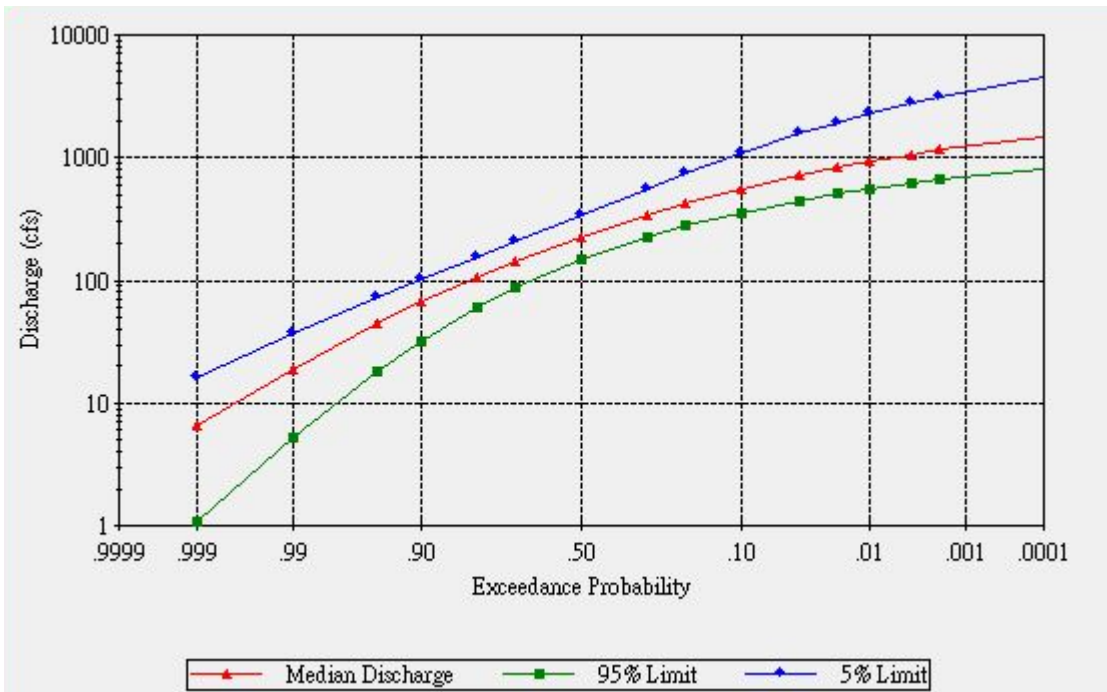


Figure 45. Confidence Limits for Junction 2 at the South Fork of Las Gallinas Creek
(Confluence of Auditorium Channel and Northbridge Channel)

6.0 SUMMARY

A hydrologic analysis using three HEC models (i.e., HEC-GeoHMS, HEC-HMS & HEC-FDA) was performed for the South Fork watershed to determine peak discharges at various locations along the South Fork of Las Gallinas Creek. A brief summary of this analysis is presented in the following.

- The HEC-GeoHMS was applied to delineate the preliminary drainage subbasins within the South Fork watershed as shown in Figure 11, based on the DEM with a grid size of 10 feet by 10 feet and various GIS-based information such as watershed boundary, creek delineation, drainage routes, etc. that were provided by the County of Marin.
- Modification of the deduced preliminary subbasins was made to reflect human alteration of the drainage pathways for flood control as well as a major corridor (i.e., Highway 101) that interferes in the natural drainage route for the South Fork watershed.
- A HEC-HMS model that was developed for the South Fork watershed consists of 14 subbasins, 13 junctions, and 11 channels to form the drainage network, as illustrated in Figure 14. Design storms were established based on the rainfall intensity-duration-frequency curves for the rainfall station at San Rafael Civic Center (Station No. E20-7880-20). Losses were estimated using the SCS method with considerations of soil group classification, land use/treatment classification, hydrologic conditions, and antecedent soil moisture conditions. Impervious ratios were determined based on the GIS data provided by the County of Marin and were incorporated in the model. The Clark unit hydrograph was used to transform excess rainfall into the runoff hydrographs from individual subbasins. Modeled flows were routed through the connecting channels using the Muskingum method to account for channel storage effects. The case of AMC 2.5 was adopted in the simulations.
- Runoff hydrographs were simulated for key locations along the South Fork for the 2-, 5-, 10-, 25-, 50-, 100-, 200-, and 500-year flood events based on the AMC 2.5 condition. Table 8 presents the simulated results for the subbasins as well as at various locations of interest. Specifically, peak discharges for the watershed outlet at the confluence of the South and North Forks (Junction 8) were computed to be 297 cfs, 564 cfs, 757 cfs, 982 cfs, 1,146 cfs, 1,305 cfs, 1,466 cfs, and 1,676 cfs for the 2-, 5-, 10-, 25-, 50-, 100-, 200-, and 500-year floods, respectively. Peak discharges at the location of the South Fork where the Railroad Channel enters (Junction 7) are 276, cfs, 532 cfs, 716 cfs, 932 cfs, 1,089 cfs, 1,242 cfs, 1,397 cfs, and 1,599 cfs, respectively. And, peak discharges at the confluence of the Auditorium Channel and the Northbridge Channel where the South Fork begins (Junction 2) are 224 cfs, 417cfs, 553 cfs, 711 cfs, 824 cfs, 933 cfs, 1,044 cfs, and 1,188 cfs, respectively.

- A sensitivity analysis was conducted to investigate the effect of the AMC condition on peak discharges. The results, as listed in Table 11, indicate that changes in peak discharge from AMC 2 to AMC 2.5 and from AMC 2.5 to AMC 3 are less than 14% of the peak discharges for AMC 2.5, except for the hillside subbasins south of North San Pedro Road including Subbasins W380 and W390. For the watershed outlet (Junction 8), changes in the 100-year peak discharge from AMC 2.5 are only 12% for AMC 2 and 10% for AMC 3. Based on the results of this sensitivity analysis and recognizing that major storms typically occur in the wet seasons in Northern California, it is suggested that the peak discharges based on the AMC 2.5 condition be adopted.
- There will be no further urban development in the Santa Venetia Valley basin and, therefore, the simulation results for the present conditions may be adopted for the future conditions.
- The HEC-FDA model was used to determine the error bounds for the 2-, 5-, 10-, 25-, 50-, 100-, 200-, and 500-year flood events at three key locations along the South Fork including the confluence of the South and North Forks (Junction 8), the junction of the Railroad Channel and the South Fork (Junction 7), and the confluence of the Auditorium Channel and the Northbridge Channel where the South Fork begins (Junction 2). The confident limits at these three locations are presented in Tables 14 to 16 and also shown in Figures 43 through 45.

7.0 REFERENCES

- Coleman, Selmi & Wright (CSW), 1982. “Civic Center North Hydrologic Report for the Upper Reach of the South Fork of Gallinas Creek”, prepared for the First National State Bank of New Jersey, May 26, 1982.
- Conatser, Neal. Marin County, 2009. Personal Communication.
- Hydrologic Engineering Center (HEC), 2009. <http://www.hec.usace.army.mil/>
- Hydrologic Engineering Center (HEC), 2008. “Hydrologic Modeling System HEC-HMS”, User’s Manual, Version 3.3, January 2008.
- Hydrologic Engineering Center (HEC), 2003. “Geospatial Hydrologic Modeling Extension HEC-GeoHMS”, User’s Manual, Version 1.1, December 2003.
- Hydrologic Engineering Center (HEC), 1998. “HEC-FDA Flood Damage Reduction Analysis”, User’s Manual, Version 1.0, January 1998.
- Intergovernmental Panel on Climate Change (IPCC), 2007. “The Physical Science Basis – Work Group I Report, Chapter 5 Observations: Oceanic Climate Change and Sea Level”, IPCC Fourth Assessment report.
- Kamman & Hydrology & Engineering, Inc., 2004 “ Gallinas Creek Restoration Feasibility Study and Conceptual Design Report, Marin County, California”, prepared for San Pablo Bay Watershed Restoration Program Partners, December 2004..
- Marin County, 1998. “Drainage Report for San Rafael Meadows Flood Control Zone 6”, prepared by Marin County Flood Control, September 1998
- Nute Engineering, 1999 “Pump Station No.1 and Intertie Pipeline Completion Predesign Study, Marin County Flood Control and Water Conservation District – Zone 7” prepared for Marin County.
- Nute Engineering, 1998. “ Vendola Driver Intertie Storm Drain and Pump Station Configuration Study, Marin County Flood Control and Water Conservation District – Zone 7” prepared for Marin County.
- Nute Engineering, 1971. “Long Range Plan for Drainage and Flood Control, Marin County Flood Control and Water Conservation District – Zone 7, Marin County, California”, prepared for Marin County.
- USGS, 2009. Seamless Data Distribution System, <http://seamless.usgs.gov/index.php>

USACE, 1996. "Risk-Based Analysis for Flood Damage Reduction studies", EM-1110-2-1619, August 1996.

USACE-SFD, 1990. "Fluvial and Tidal Flooding Analysis, Section 205, Reconnaissance Study, Gallinas Creek, Marin County, California", August 10, 1990.

Appendix C

**Las Gallinas Creek
Hydrologic Analysis
Final Report**



**U.S. Army Corps of Engineers
San Francisco District**



August 2011

Table of Contents

1.0	INTRODUCTION	2
2.0	PHYSICAL SETTING	2
2.1	Las Gallinas Creek Watershed	2
2.2	Drainage System within Santa Venetia Valley	3
3.0	HEC-GeoHMS ANALYSIS	6
3.1	GIS Data	6
3.2	Preliminary Delineation of Drainage Sub-basins	7
3.3	Alterations Due to Man-Made Structures	7
3.4	Final Delineation of Drainage Sub-basins	8
4.0	HEC-HMS ANALYSIS	8
4.1	Model Basin Map	8
4.1.1	Drainage Sub-basins, Junctions, & Reaches	11
4.1.2	Pump Stations	11
4.2	Rainfall Intensity-Duration-Frequency Curves	11
4.3	Losses	23
4.3.1	Hydrologic Soil Group Classification	23
4.3.2	Land Use/treatment Classification	24
4.3.3	Hydrologic Conditions	24
4.3.4	Antecedent Runoff Condition	25
4.3.5	Estimates of SCS Curve Number	25
4.4	Clark Unit Hydrograph	27
4.4.1	Time of Concentration	27
4.4.2	Storage Coefficients	27
4.5	Channel Routing	29
4.6	Hydrologic Simulations	32
4.7	Present and Future Hydrologic Conditions	32
4.8	Simulated Results	32
4.9	Sensitivity Analysis	36
5.0	RISK ANALYSIS	36
5.1	Equivalent Length of Record	37
6.0	Summary	44
7.0	REFERENCES	45

1.0 INTRODUCTION

A small flood damage reduction project in the unincorporated area of Santa Venetia is being undertaken by the Corps of Engineers, San Francisco District, under Section 205 of the 1984 Flood Control Act. The study area is located in southeastern Marin County approximately 14 miles north of San Francisco. It extends along the South Fork of Las Gallinas Creek from the confluence with North Fork of the Creek to approximately 500 feet upstream of Margarita Island (**Plate 1**, at the end of the report). The site is bound to the east by San Pablo Bay and on the south by steep-sloped foothills of the San Pedro Ridge. This report summarizes the results of a hydrologic analysis in developing the flow frequency curves and flood hydrographs at key designated locations for the 50%, 20%, 10%, 4%, 2%, 1%, 0.5% and 0.2% probability events using models of that were developed by the Hydrologic Engineering Center (HEC).

2.0 PHYSICAL SETTING

2.1 Las Gallinas Creek Watershed

Las Gallinas Creek is located in the City of San Rafael, CA, and originates in open space owned by Marin County, above the community of Terra Linda. It has two forks (North and South), which join near the east end of the Smith Ranch Airport. The adjoined creek continues eastward for about 7,000 feet and flows into San Pablo Bay. The creek basin has a drainage area of approximately 7.2 square miles, and is bounded by San Rafael Creek Basin to the south, Corte Madera Creek Basin to the west, Miller Creek to the north and China Camp State Park to the east. Basin elevations range from over about 1000 feet in the headwaters of Meadow Creek in the southeast corner of the watershed to about 4 feet (NAVD 88) at Smith Ranch Airfield. A watershed overview is shown in Plate 2.

The watershed is broken into upper and lower sections, with upper part located west of Highway 101, and the lower part located east of the highway (**Plates 2 & 3**). Most of the upper watershed drains into the North Fork. Ridge flanks are steep-sloped with gentler slopes extending across and down the valley bottom of the upper watershed. The boundary between the upper and lower watersheds marks the approximate extent of tidal influence in the lower creek-slough channel system. The lower watershed is bounded on the south by the San Pedro Ridge and to the north by the Gallinas Hills. Between Highway 101 and San Pablo Bay, both forks occupy tidally influenced earthen and leveed channels. Most of the Santa Venetia Valley, including the hillside along the San Pedro Ridge drains into the South Fork.

Mean annual precipitation at the San Rafael Civic Center weather station, in the lower watershed, is 34.29 inches. The length of record at the gage is 23 years (1964 to 1994, missing 1968 to 1974 & 1991). The elevation at this gage is 120 feet (NAVD 88).

2.2 Drainage System within Santa Venetia Valley

The drainage system within the Santa Venetia Valley has been altered by construction of culverts and underground drainage pipes to ensure that all flows drain toward either the South Fork or the main channel of Las Gallinas Creek. Three drainage interceptors were installed to directly bypass surface runoffs from hillsides located on the south of the valley along the San Pedro Ridge into the South Fork or the creek's main channel without draining into the valley. Five permanent pump stations are situated along the South Fork to increase the drainage capacity. The locations of the interceptors and permanent pump stations are shown in **Plate 4**. In addition, 2 to 3 small portable pump stations are used periodically to supplement the drainage capacity during the winter rainy season. An example of a portable pump deployed by the County is shown in **Figure 2.1**. Note that portable pumps are not considered in the hydrologic analysis. The discharge capacity of each permanent pump station (Pump Station No. 1 through No. 5) is presented in **Table 2.1**. Failure of the permanent pumps was not considered in this hydrologic analysis. Peak capacity of the pumps is small relative to peak flood flows, particularly for the less frequent events when pump failure would be more likely. Interior drainage pumps in the North Fork watershed were not investigated in this study, which is primarily concerned with the Santa Venetia Valley.

Table 2.1. Capacities of Pump Stations

Pump Station ID	Capacity (cfs)	Sub-Basin at Outlet
1	63.4	G3
2	40.5	G2
3	38.0	G1
4	5.00	G4
5	45.0	G5

A site investigation was conducted on February 5, 2009 to validate the GIS information provided by the County including pump stations, drainage routes and general geographic setting within the study area. Pump Station No. 3 is shown as an example of a typical housing facility in **Figure 2.2**. **Figures 2.3 and 2.4** depict a drainage route with its catchment and the discharge outlet for Pump Station No. 5.



Figure 2.1. Portable Pump Located at Meadow Drive



Figure 2.2. Housing Facility of Pump Station No. 3



Figure 2.3. Drainage Route of Pump Station No. 5



Figure 2.4. Outlets at Pump Station No. 5

3.0 HEC-GeoHMS ANALYSIS

The Geospatial Hydrologic Modeling Extension (HEC-GeoHMS) is a software package for use with the ArcGIS system to analyze digital terrain information (e.g., digital elevation model) for delineating drainage sub-basins and quantifying other pertinent data inputs that are to be used in the HEC-Hydrologic Modeling System (HEC-HMS). Specifically, HEC-GeoHMS transforms the drainage paths and watershed boundaries into a hydrologic data structure including the HEC-HMS basin model, physical watershed and stream characteristics, and background map file. The resulting numerical model predicts the watershed response to precipitation.

3.1 GIS Data

GIS data within the Las Gallinas Creek watershed, including: the digital elevation model (DEM), soil information, storm drain system, creek delineation and land use were obtained from the County of Marin. The DEM, with a grid size of 10 feet by 10 feet, was derived from black and white aerial photographs that were taken in 1997 by the County. Since the project area has been well urbanized by 1997, it is not expected that a significant change of terrain geometry has occurred. Nevertheless, a comparison was made between the County's DEM and the DEM directly downloaded from the USGS Seamless Data Distribution System (USGS, 2009) that has a grid size of 98.4 feet by 98.4 feet (30m by 30m). A comparison of the two DEMs that were projected onto the California State Plane system, Zone III, is shown in **Figure 3.1**. The figure validates the accuracy of the County's DEM with a much finer grid resolution. The County DEM data set was used for the GeoHMS analysis. The terrain of the watershed is shown in greater detail in **Plate 5**.



Figure 3.1. DEM Comparison between County and USGS

3.2 Preliminary Delineation of Drainage Sub-basins

The terrain process executed in the GeoHMS model consists of delineation of flow direction and flow accumulation, stream definition, and catchment representation. Basin Characteristics such as drainage length, slope, flow path and basin centroid information including elevation and its flow path were also derived. As is often the case in this type of analysis, the preliminary drainage sub-basins that were generated using GeoHMS were not completely realistic, as they do not capture all of the effects of man-made structures. Several discussions with County personnel regarding the drainage routes on the west side of Highway 101 and hillsides to the south were conducted to improve the accuracy of the sub-basin delineation.

3.3 Alterations Due to Man-Made Structures

The natural drainage pattern for the Las Gallinas Creek watershed has been altered by man-made structures such as Highway 101, roads, streets, storm drain systems, levees, etc. Therefore, the drainage network of the watershed was modified from the GeoHMS preliminary depiction to accurately delineate the drainage basins by taking into account those man-made effects, as briefly described in the following sections.

Highway 101

Highway 101 runs in a northwest-southeast direction to separate the South Fork watershed into the upper west portion and the lower east portion. The west portion is drained by a small channel originating in the San Rafael Hill and passes the Highway 101 embankment through a 12 feet by 7.5 feet box culvert that is located at Auditorium Channel (Plate 2). Due to obstruction by the Highway 101 embankment, the entire western portion of the watershed now drains through this box culvert to enter the lower portion of the watershed. In other words, this box culvert is the only outlet for the sub-basin west of Highway 101. It is noted that the culvert has a capacity of 628 cfs (Marin County, 1998). The Highway 101 bridge over the North Fork is approximately 7 feet high and 30 ft wide, with an estimated capacity of 2000 cfs.

Northwestern Railroad

Northwestern Pacific Railroad runs southward across the northern portion of watershed, underpasses Highway 101 and makes an arc turning southeastward toward the south end of the upper watershed west of Highway 101 (See **Plate 3**). East of Highway 101, a small channel called Railroad Channel runs parallel south of the railroad, which enters the South Fork at the downstream end. The channel also collects the runoff from the hill just north of the railroad.

Levees

Levees typically obstruct surface runoff and alter drainage patterns. Levees are built along the south bank of the South Fork to provide flood protection for Gallinas

Village and along the north bank of the South Fork to protect the San Rafael Airport (Plate 3).

Street Drainage System

The urban street drainage system within the Santa Venetia Valley consists of street gutters, drainage inlets, catch basins, and storm drains including hillside interceptors to collect and convey storm runoff. These drainage systems alter the natural drainage pattern and were taken into account in delineating sub-basins. Sub-basin delineation of Gallinas Village was made based on the street drainage systems, which lead to individual pump stations (**Plate 3**).

3.4 Final Delineation of Drainage Sub-basins

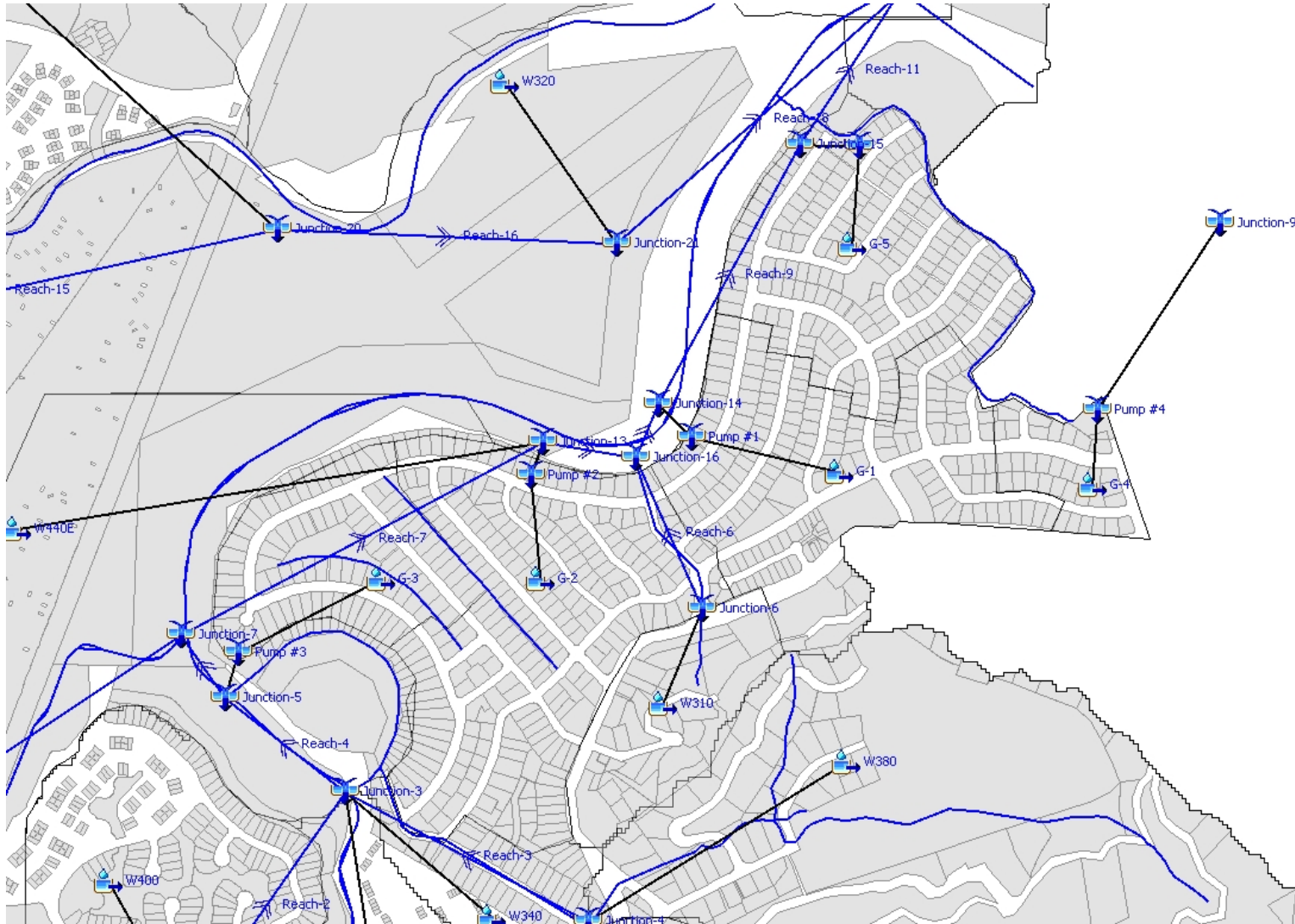
A brief description of each sub-basin is provided below. North Fork sub-basins have an “N” at the end of the name. Sub-basins in Las Gallinas Village begin with “G”. Aerial photography and street map views of the final sub-basin delineations are presented in **Plates 6 and 7**.

4.0 HEC-HMS ANALYSIS

The modified sub-basins of the Las Gallinas watershed were incorporated into HEC-HMS to form an integrated hydrological system for storm runoff simulations. Pertinent elements of the modeling system are described in the following sections.

4.1 Model Basin Map

The model basin map is a network of hydrological elements for the runoff simulations including sub-basins, channels, and flow junctions. **Figure 4.1** shows the model basin map for watershed. **Figure 4.2** provides a close-up view of the Gallinas Village model layout.



4.2. Close-up of Gallinas Village model layout in HEC-HMS

4.1.1 Drainage Sub-basins, Junctions, & Reaches

The HEC-HMS model developed for the watershed consists of 34 sub-basins, 21 junctions, and 18 channel reaches. The runoff simulations were first performed for individual sub-basins to generate runoff hydrographs at their outlets including all sub-basins that are shown in **Plates 6 & 7**. Runoff hydrographs generated at the sub-basin outlets are routed through connecting channels to the downstream locations, called junctions, where they are combined with runoff hydrographs from other sub-basins. The connecting channels between sub-basin outlets and downstream junctions are identified with reach numbers (1 – 19). Junctions & Reaches are displayed in **Figures 4.1 and 4.2**.

4.1.2 Pump Stations

There are 5 permanent pump stations in Gallinas Village along with 2 to 3 portable pump stations. In this hydrologic analysis, only permanent pump stations were considered, as the capacities of the portable ones are unknown. Permanent pump stations are designated as junctions receiving runoff from the associated sub-basins. Pump Stations No. 1, 2, 3, and 5 discharge into the South Fork while Pump Station No. 4 discharges into the Las Gallinas Creek, which is the main channel downstream of the confluence of the South Fork and the North Fork. The pump station locations are shown in **Plate 4**.

4.2 Rainfall Intensity-Duration-Frequency Curves

Storm runoff for the watershed were simulated in response to specified rainfall hyetographs. Rainfall hyetographs were derived for a 24-hour storm duration with 50%, 20%, 10%, 4%, 2%, 1%, 0.5% and 0.2% probabilities using the Frequency Storm method in HEC-HMS. This method is used to develop a precipitation event where precipitation depths for various durations within the storm have a consistent exceedance probability. Using this method, a partial duration hyetograph was created for each probability event. Input parameters include storm duration (24 hours), intensity position (50-percent), storm area, and statistical rainfall depths for 5 min, 15 min, 1 hour, 2 hour, 3 hour, 6 hour, 12 hour, and 24 hour durations.

The rainfall depths for specified durations for each probability were taken from rainfall intensity-duration-frequency (IDF) curves for the San Rafael Civic Center station (Station No. E20-7880-20). The San Rafael Civic Center station is located near the center of the watershed in sub-basin W400 (**Plates 6 & 7**). The statistical dataset used for this gage came from the Jim Goodridge Rainfall Depth-Duration Frequency Analysis for California Rain Gages and was compiled with support from the California Department of Water Resources (**Table 4.1**).

The original IDF curves from the data in **Table 4.1** are displayed in **Figure 4.3**. Revised values were interpolated to a linear configuration on the logarithmic scale (**Figure 4.4**). Revised and adopted precipitation depths are presented in **Table 4.2**. This procedure aided in smoothing out the generated hyetographs in HMS. It is recommended that this

type of analysis be expanded in future hydrology studies to create more smooth and uniformly curved hyetographs.

Figures 4.5 to 4.12 show the temporal distribution of the 50%, 20%, 10%, 4%, 2%, 1%, 0.5% and 0.2% probability design storms, respectively. For each frequency, the same design storm was applied to all sub-basins in the HEC-HMS model.

The rainfall depths provided by the County of Marin were compared to the rainfall depths provided in NOAA Atlas 14 for reasonableness. **Table 4.3** provides the NOAA Atlas 14 precipitation frequency (PF) estimates based on frequency analysis of partial duration series (PDS) to use as a comparison and a check for **Table 4.2**. The numbers in parenthesis in **Table 4.3** are PF estimates at lower and upper bounds of the 90% confidence interval. The probability that precipitation frequency estimates (for a given duration and average recurrence interval) will be greater than the upper bound (or less than the lower bound) is 5%. In general, the Jim Goodridge rainfall depths are within the 90% confidence bands of the NOAA estimates.

Table 4.1. Rainfall Depth by Return Year for Selected Durations (in)

Return Year	Rainfall Depth (in)									
	5 min	10 min	15 min	30 min	1 hr	2 hr	3 hr	6 hr	12 hr	1 day
2-YR	0.14	0.19	0.26	0.39	0.57	0.87	1.09	1.61	2.43	3.25
5-YR	0.19	0.27	0.36	0.55	0.8	1.22	1.53	2.27	3.42	4.56
10-YR	0.23	0.32	0.43	0.66	0.95	1.46	1.83	2.71	4.08	5.45
25-YR	0.27	0.39	0.52	0.79	1.14	1.75	2.2	3.25	4.9	6.55
50-YR	0.31	0.44	0.59	0.89	1.29	1.97	2.47	3.66	5.51	7.36
100-YR	0.34	0.49	0.65	0.98	1.42	2.18	2.74	4.05	6.1	8.15
200-YR	0.37	0.53	0.71	1.08	1.56	2.39	3.01	4.44	6.69	8.94
500-YR	0.42	0.59	0.79	1.2	1.74	2.67	3.35	4.95	7.46	9.97

Source: Rainfall Depth-Duration Frequency Analysis for California Rain Gages, Jim Goodridge.

Table 4.2. Revised/Adopted Statistical Rainfall Depths for Selected Durations (in)

Return Year	Rainfall Depth (in)									
	5 min	10 min	15 min	30 min	1 hr	2 hr	3 hr	6 hr	12 hr	1 day
2-YR	0.14	0.21	0.26	0.39	0.57	0.87	1.09	1.61	2.43	3.668
5-YR	0.19	0.28	0.36	0.55	0.8	1.22	1.53	2.27	3.42	5.153
10-YR	0.23	0.34	0.43	0.66	0.95	1.46	1.83	2.71	4.08	6.143
25-YR	0.27	0.41	0.52	0.79	1.14	1.75	2.2	3.25	4.9	7.388
50-YR	0.31	0.47	0.59	0.89	1.29	1.97	2.47	3.66	5.51	8.295
100-YR	0.34	0.51	0.65	0.98	1.42	2.18	2.74	4.05	6.1	9.188
200-YR	0.37	0.56	0.71	1.08	1.56	2.39	3.01	4.44	6.69	10.08
500-YR	0.42	0.63	0.79	1.2	1.74	2.67	3.35	4.95	7.46	11.24

Table 4.3. NOAA PDS-Based Precipitation Frequency Estimates, 90% Confidence Intervals (in)

Probability	50%	20%	10%	4%	2%	1%	0.50%	0.20%
5-min	0.176 (0.157-0.200)	0.223 (0.198-0.254)	0.264 (0.232-0.304)	0.323 (0.272-0.387)	0.371 (0.305-0.456)	0.423 (0.338-0.535)	0.479 (0.370-0.627)	0.56 (0.412-0.769)
10-min	0.253 (0.225-0.287)	0.32 (0.284-0.365)	0.378 (0.332-0.435)	0.463 (0.390-0.554)	0.532 (0.438-0.654)	0.607 (0.484-0.767)	0.687 (0.531-0.898)	0.803 (0.590-1.10)
15-min	0.306 (0.272-0.347)	0.387 (0.343-0.441)	0.457 (0.402-0.526)	0.56 (0.472-0.670)	0.644 (0.529-0.791)	0.734 (0.586-0.928)	0.831 (0.642-1.09)	0.971 (0.714-1.33)
30-min	0.456 (0.406-0.518)	0.578 (0.512-0.658)	0.683 (0.599-0.786)	0.836 (0.705-1.00)	0.961 (0.790-1.18)	1.1 (0.875-1.39)	1.24 (0.958-1.62)	1.45 (1.07-1.99)
60-min	0.657 (0.585-0.746)	0.832 (0.738-0.948)	0.983 (0.863-1.13)	1.2 (1.02-1.44)	1.38 (1.14-1.70)	1.58 (1.26-2.00)	1.79 (1.38-2.34)	2.09 (1.54-2.87)
2-hr	0.999 (0.889-1.13)	1.26 (1.12-1.44)	1.49 (1.31-1.72)	1.82 (1.54-2.19)	2.09 (1.72-2.57)	2.38 (1.90-3.01)	2.69 (2.08-3.52)	3.14 (2.31-4.31)
3-hr	1.26 (1.12-1.43)	1.6 (1.41-1.82)	1.88 (1.65-2.16)	2.29 (1.93-2.75)	2.63 (2.16-3.23)	2.99 (2.39-3.78)	3.37 (2.61-4.41)	3.92 (2.89-5.39)
6-hr	1.86 (1.66-2.12)	2.35 (2.09-2.68)	2.77 (2.43-3.19)	3.36 (2.84-4.03)	3.84 (3.16-4.72)	4.35 (3.47-5.50)	4.89 (3.78-6.39)	5.65 (4.16-7.76)
12-hr	2.73 (2.43-3.10)	3.48 (3.08-3.96)	4.1 (3.60-4.72)	4.98 (4.20-5.96)	5.67 (4.67-6.97)	6.4 (5.11-8.09)	7.17 (5.54-9.37)	8.24 (6.06-11.3)
24-hr	3.7 (3.33-4.20)	4.75 (4.26-5.40)	5.62 (5.00-6.44)	6.82 (5.89-8.05)	7.76 (6.58-9.33)	8.73 (7.24-10.7)	9.74 (7.88-12.3)	11.1 (8.68-14.6)

* Estimates at upper bounds are not checked against probable maximum precipitation (PMP) estimates and may be higher than currently valid PMP values

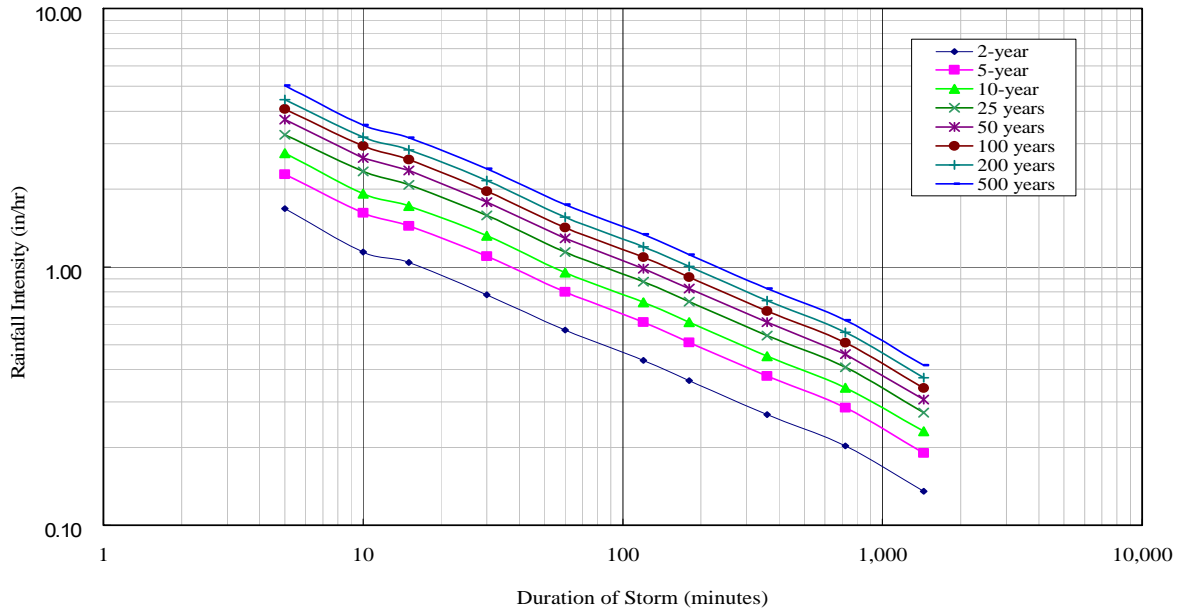


Figure 4.3. Rainfall Intensity–Duration-Frequency Curves for the San Rafael Civic Center Station

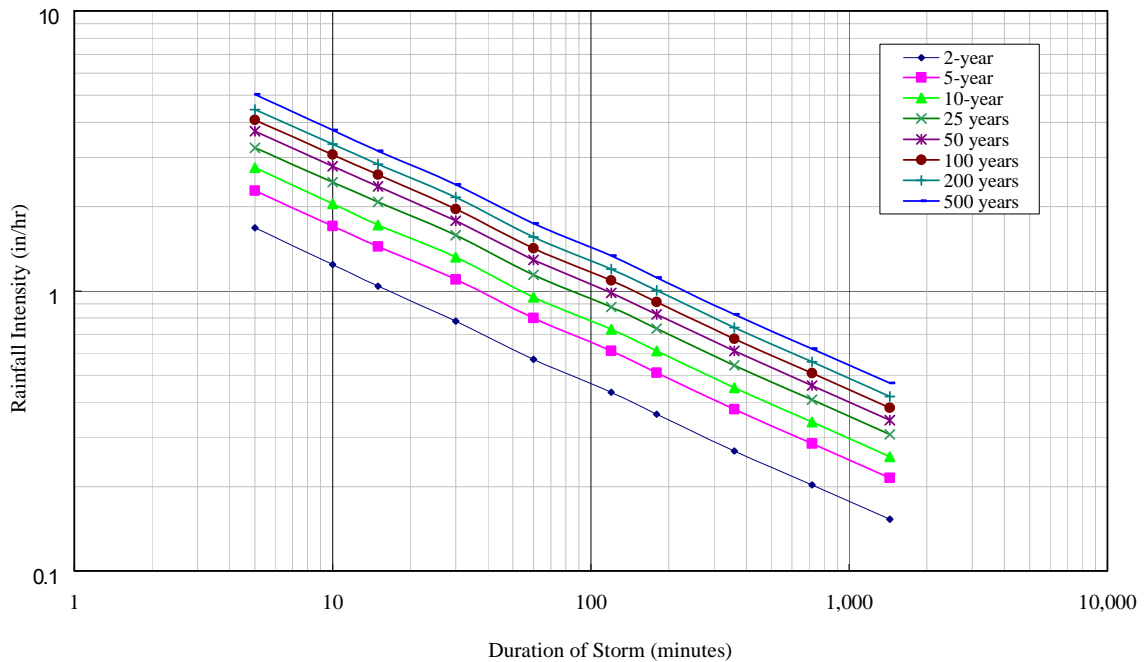


Figure 4.4. Refined Rainfall Intensity–Duration-Frequency Curves for the San Rafael Civic Center Station

Figure 4.5. Temporal Distribution for the 50% probability 24-hour Design Storm

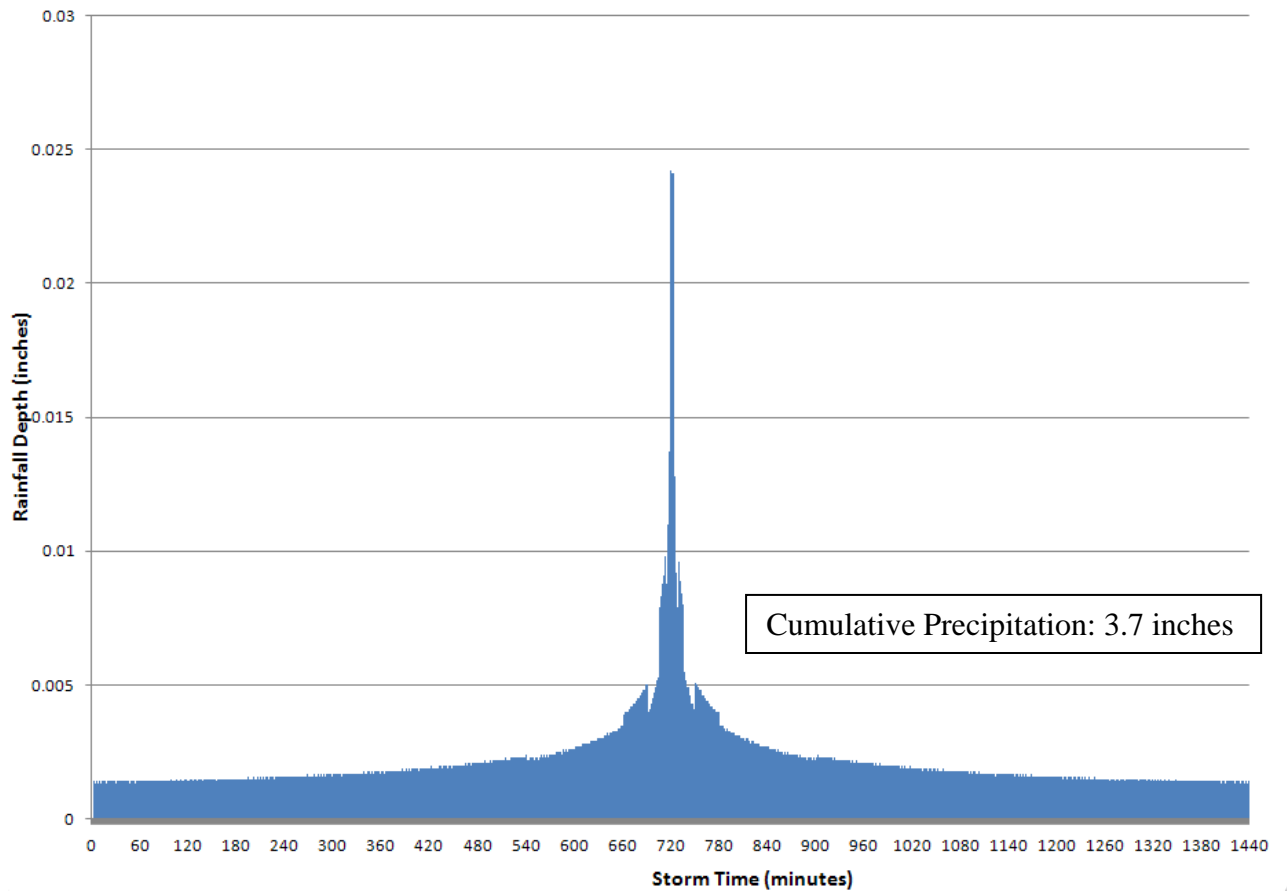


Figure 4.6. Temporal Distribution for the 20% probability 24-hour Design Storm

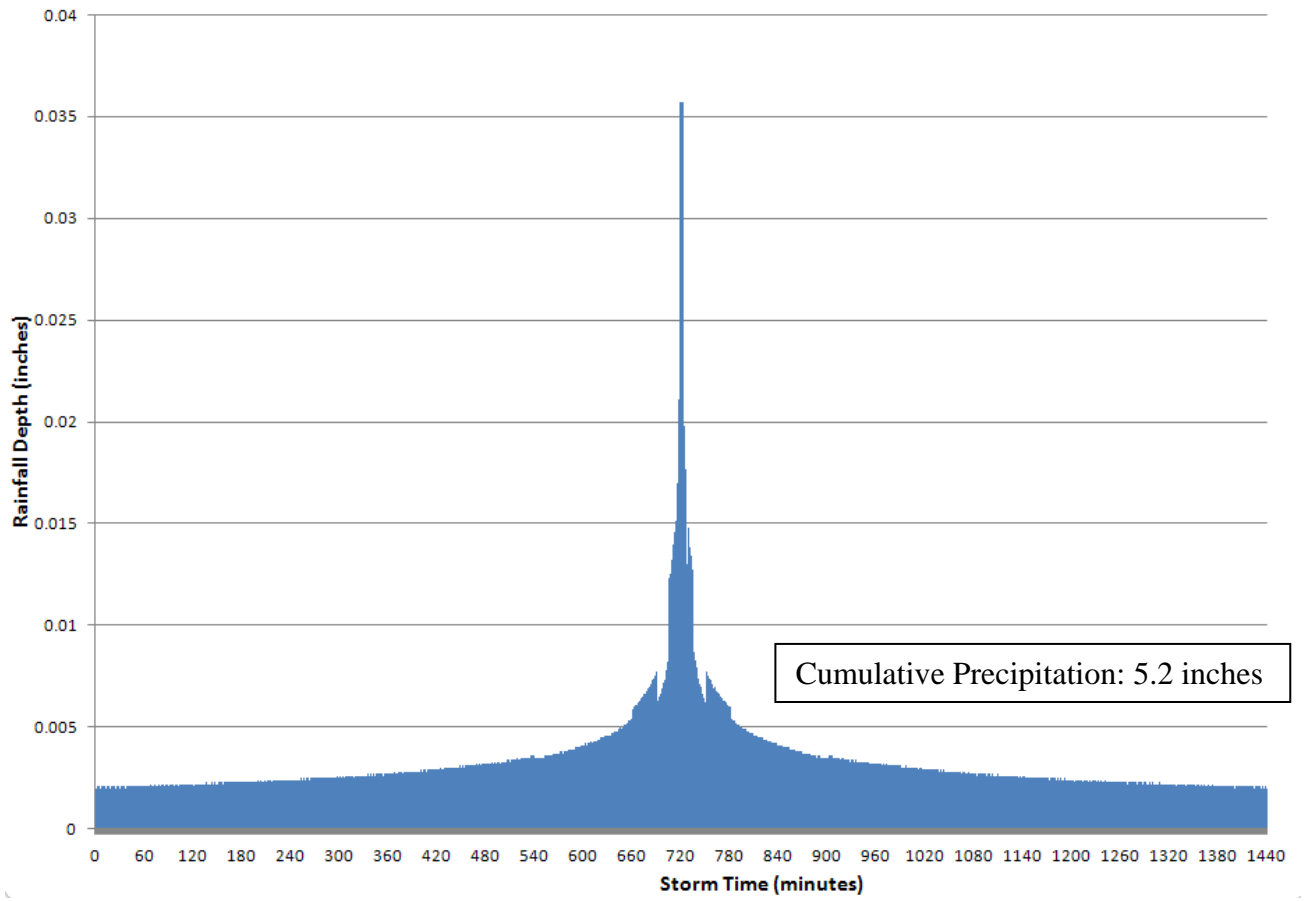


Figure 4.7. Temporal Distribution for the 10% probability 24-hour Design Storm

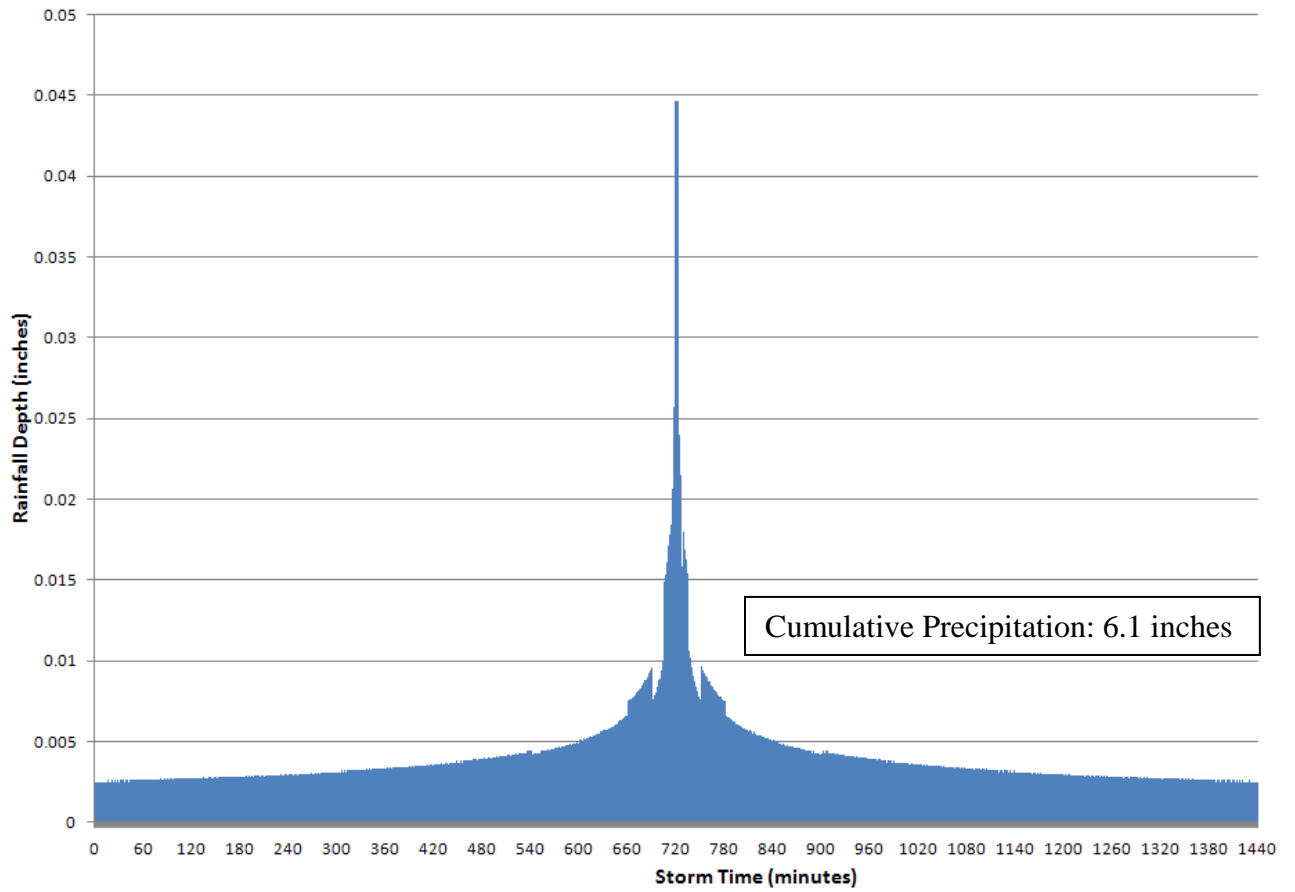


Figure 4.8. Temporal Distribution for the 4% probability 24-hour Design Storm

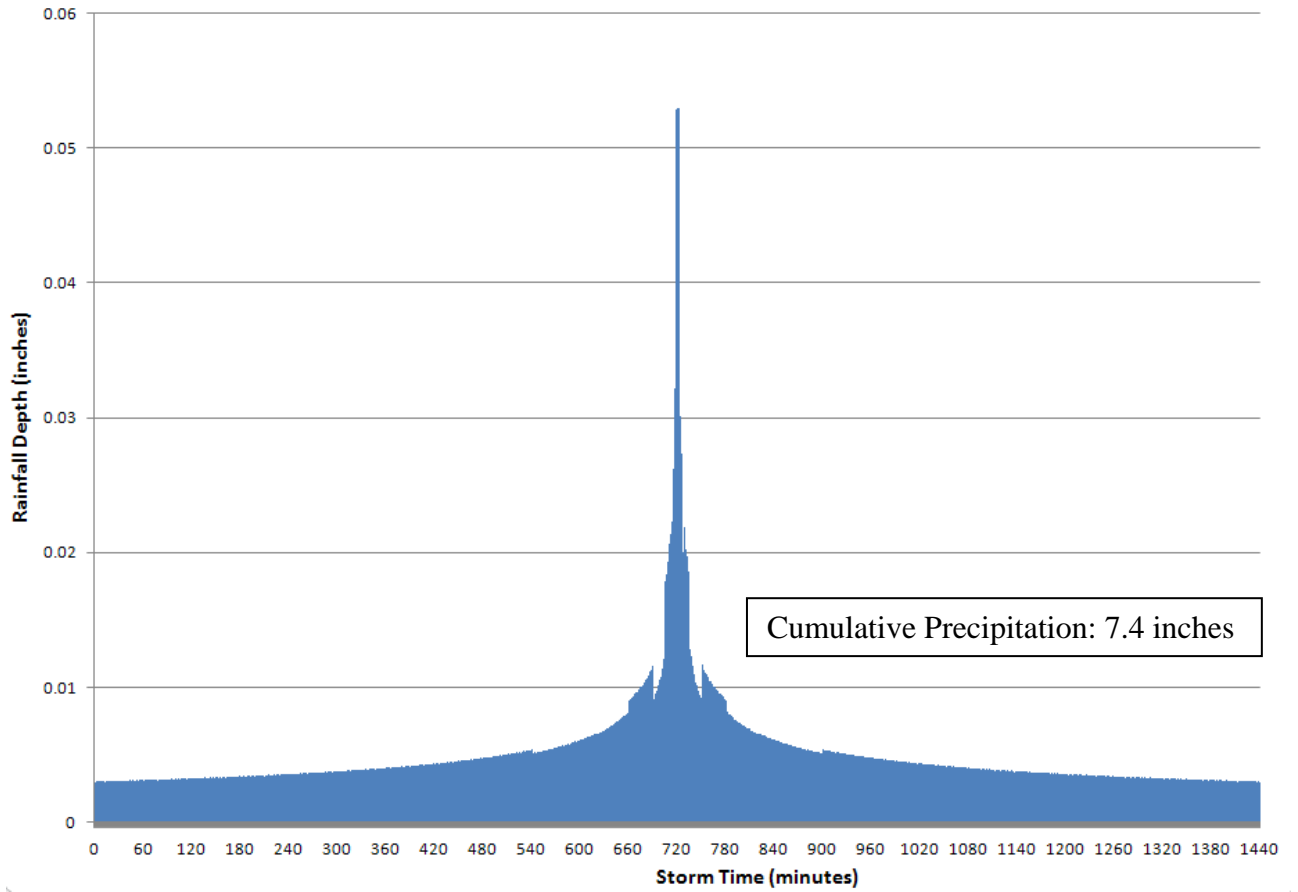


Figure 4.9. Temporal Distribution for the 2% 24-hour Design Storm

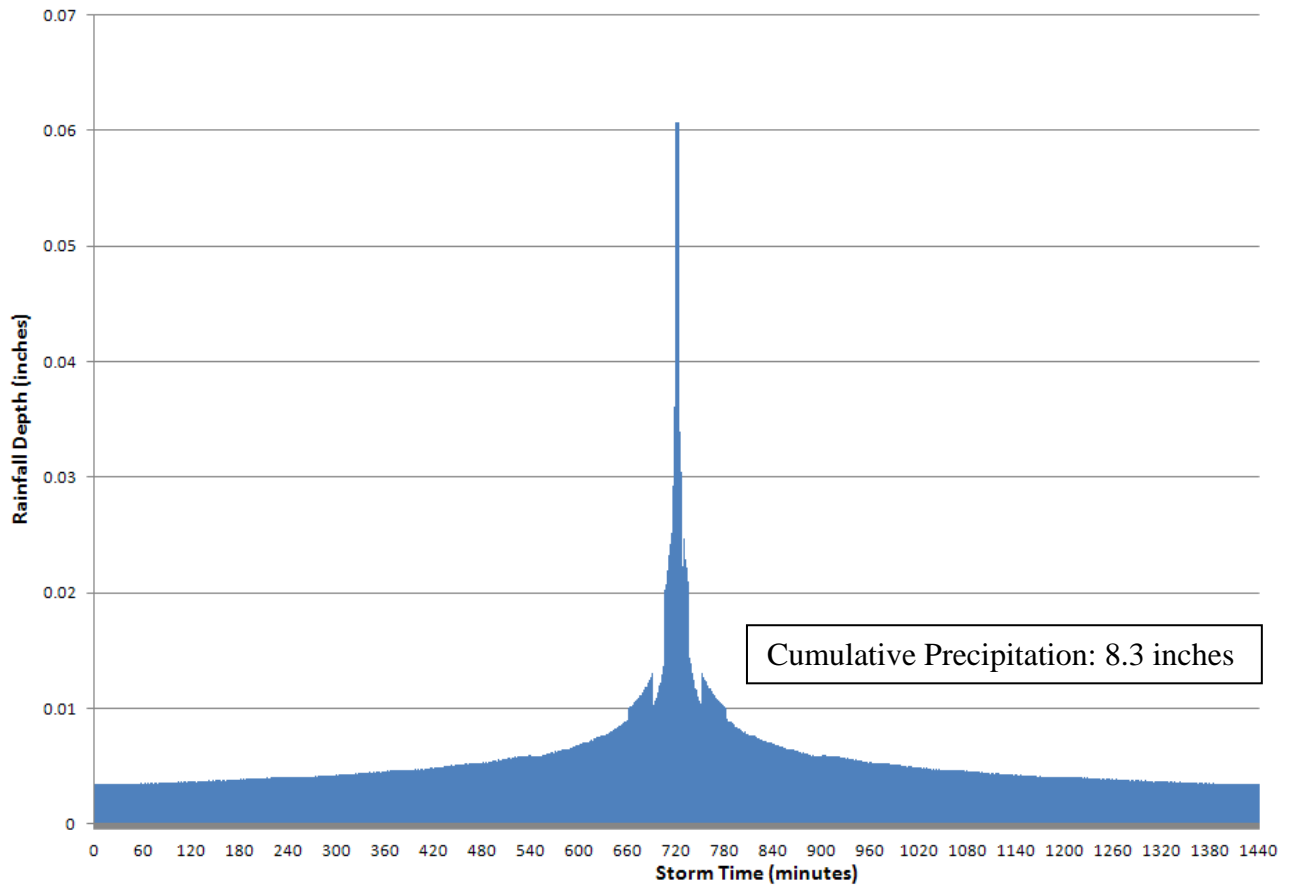


Figure 4.10. Temporal Distribution for the 1% probability 24-hour Design Storm

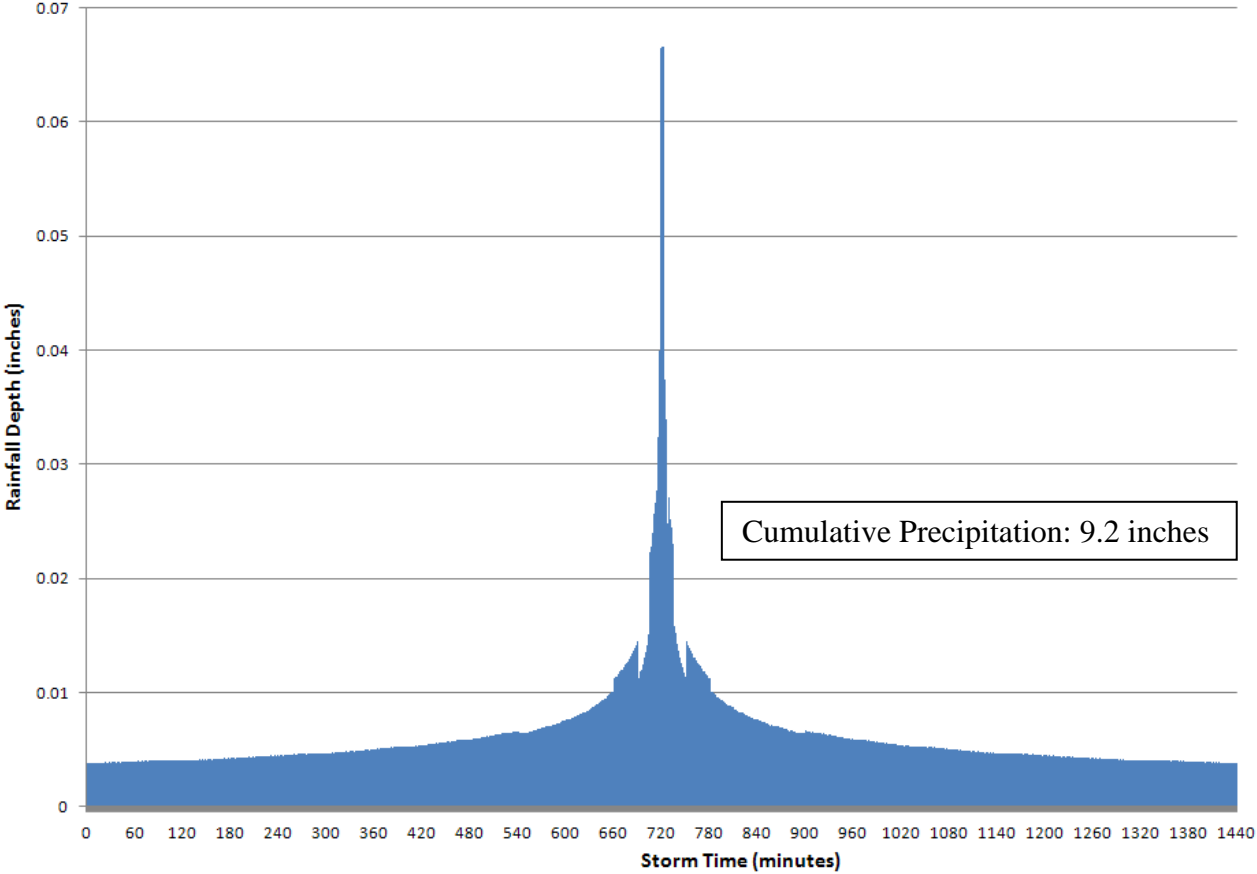


Figure 4.11. Temporal Distribution for the 0.5% 24-hour Design Storm

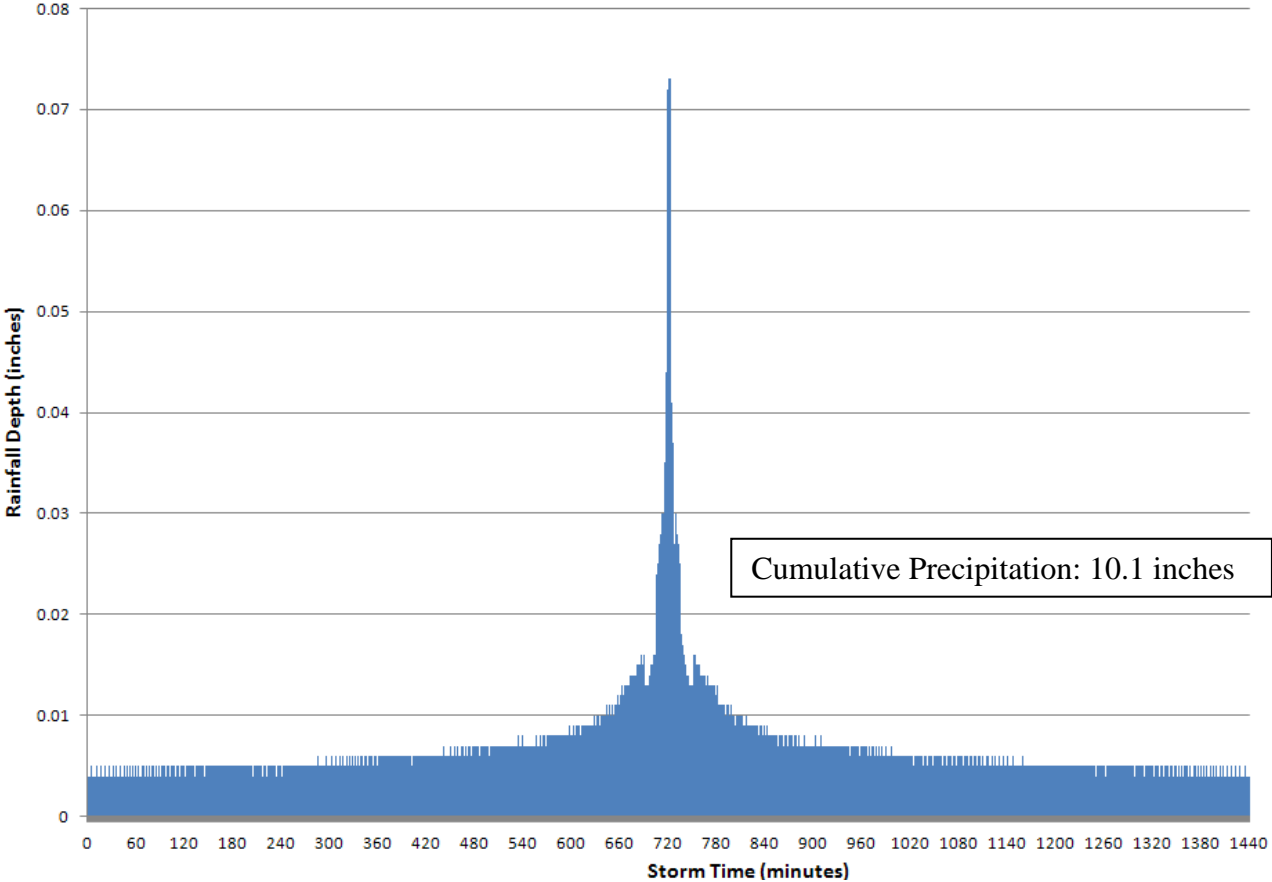
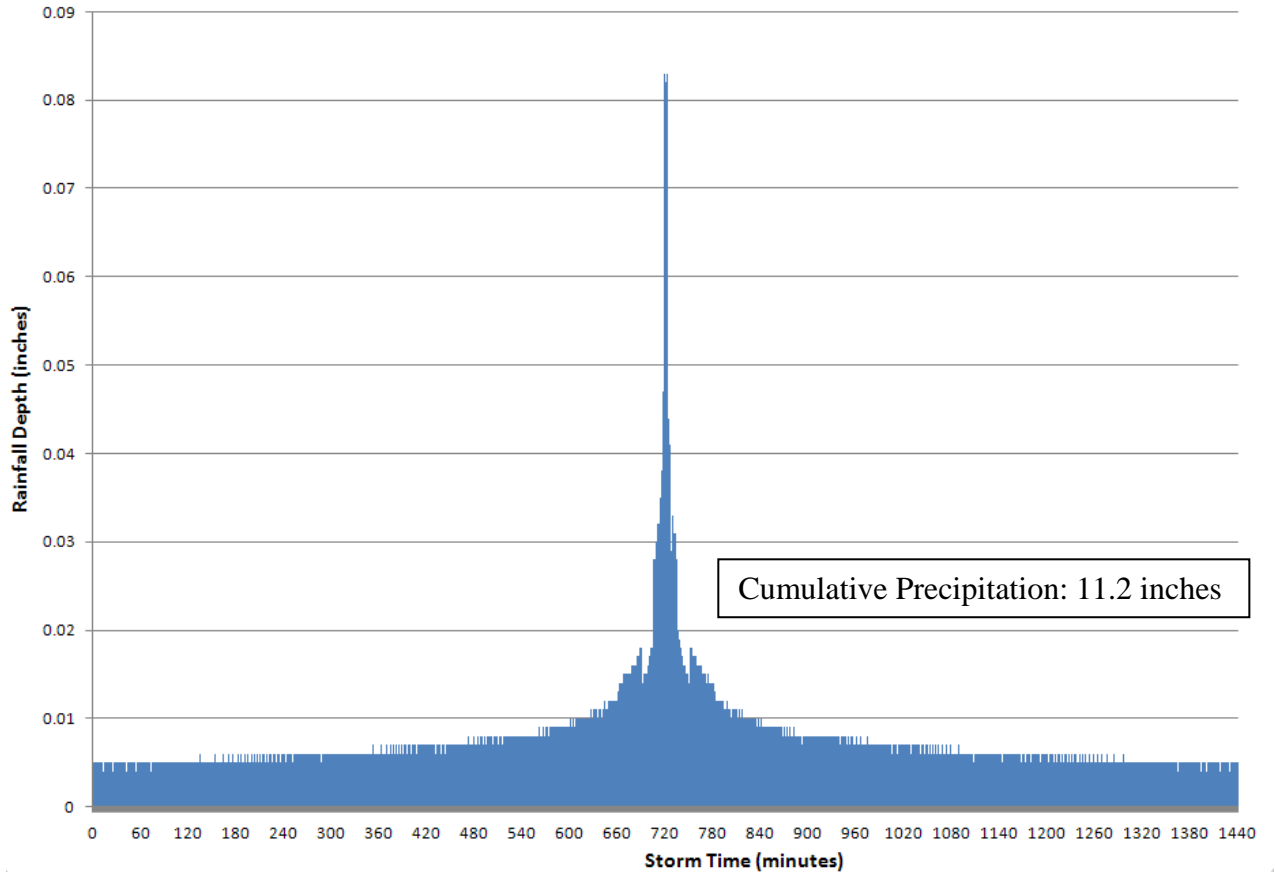


Figure 4.12. Temporal Distribution for the 0.2% 24-hour Design Storm



4.3 Losses

Storm runoff occurs only after a rainfall depth exceeds losses. In other words, the runoff is formed by excess rainfall, which is equal to the rainfall depth minus the losses. In the present study, the Soil Conservation Service (now the Natural Resources Conservation Service) curve number method was used to track the losses during the storm. The method separates the losses into initial abstraction and incremental losses during the storm. The initial abstraction represents the amount of rainfall that must fall before excess rainfall occurs.

In the present analysis, the initial abstraction, denoted as I_a , was estimated as 0.2 times the potential retention (S), which was calculated from the SCS curve number as follows:

$$S = \frac{1000}{CN} - 10 \quad (1)$$

In the above equation, S is the potential retention in inches, and CN is the curve number. The incremental losses represent the infiltration depths during computation time intervals and are calculated as the difference in infiltration volume at the end of two adjacent time intervals. The infiltration loss at the end of each time interval is a function of rainfall depth, runoff volume, initial abstraction, and potential retention and is ultimately a function of rainfall depth and curve number. In other words, the curve number and the design storm together define both initial abstraction and incremental losses during the storm. The Soil Conservation Service (now NRCS) developed a procedure to estimate the curve number based on soil group, the land use/land treatment class, the hydrologic condition, and the antecedent soil moisture condition. They are described in the following sections.

4.3.1 Hydrologic Soil Group Classification

The SCS developed a soil classification system that consists of four different groups identified as A, B, C, and D in the order of decreasing infiltration rate. Soil characteristics associated with each group are as follows:

Group A: Deep sand, deep loess, aggregates silts

Group B: Shallow loess, sandy loam

Group C: Clay loams, shallow sandy loam, soils low in organic content, and soils usually high in clay

Group D: Soils that swell significantly when wet, heavy plastic clays, certain saline soils, and shallow soils over nearly impervious material

Soils data were obtained from the County in GIS format. The soil names were then researched on <http://soils.usda.gov/technical/classification/osd/index.html> (the NRCS website) and TR-55, the NRCS publication documenting the curve number method, to determine hydrologic soil groups for each soil type. Soils in the Las Gallinas watershed are predominately of Group C, with some Group D soils present in the tidal areas and in the steep upper reaches of the watershed, where soils are thinner and poorly developed (**Plate 8**).

4.3.2 Land Use/treatment Classification

The SCS has identified more than 20 general land use/treatment classes for estimating different curve numbers. In this hydrologic analysis, land use data provided by the County of Marin were used to develop the land-use pattern in the watershed and categorized into 8 classes including employment areas, infrastructure, residential, urban open, forest land, rangeland, wetlands, and water. The distribution of land uses is shown in **Plate 9**.

4.3.3 Hydrologic Conditions

The infiltration capacity of a given soil is affected by vegetation/ground cover and quality and density of that cover. To refine the cover type, it is classified into the following hydrologic conditions:

Poor: Heavily grazed or regularly burned areas. Less than 50% of the ground surface is protected by plant or brush and tree canopy.

Fair: Moderate cover with 50 to 75% of the ground surface protected by vegetation.

Good: Heavy or dense cover with more than 75% of the ground surface protected by vegetation.

The hydrologic conditions of the South Fork watershed were determined from a field trip on February 5, 2009 (performed by Noble) and a review of the Google image of the study area. Nearly all of the Las Gallinas watershed can be categorized to be in good hydrologic condition, but a section in the upper northwest corner of the watershed is categorized as fair to poor due to lack of ground cover.

4.3.4 Antecedent Runoff Condition

Antecedent conditions such as soil moisture, vegetative cover and wind have significant effect on the volume and rate of storm runoff. The SCS developed three antecedent runoff conditions (ARC) with the designated values of 1, 2, and 3. They are described as follows:

Condition 1: Soils are dry but not to wilting point, high winds, full vegetative cover.

Condition 2: Average conditions.

Condition 3: Saturated soil; heavy rainfall or light rainfall/low temperatures have occurred within the last 5 days; little vegetative cover.

The curve numbers assigned to each sub-basin vary as a function of ARC. ARC 1 and ARC 3 have been shown to approximately be the 10% and 90% exceedance values, respectively (Van Mullen et. al). Each precipitation event was modeled using all three conditions. The results are shown in a sensitivity analysis presented in **Section 4.7**. ARC 2 is the condition generally accepted for design of flood control structures.

4.3.5 Estimates of SCS Curve Number

The curve numbers within each sub-basin were estimated based on the combined effect of soil group, land use/treatment, hydrologic condition, and antecedent runoff condition, as individually discussed in the previous sections. The spatial distribution of curve number within individual sub-basins is shown in **Plate 10**, assuming ARC 2. It can be seen from the figure that the Gallinas Village, including G-1, G-2, G-3, G-4, and G-5 is predominantly residential with a *CN* of 91, while the hillside south of North San Pedro Road is predominantly forest with a *CN* of 76. Areas with a *CN* greater than 90 are nearly entirely covered in impervious surfaces. This watershed is already highly developed and future development is not expected according to the project sponsor. The information shown in **Plate 10** was used to calculate the composite *CN* values for individual sub-basins by weighting the areas of different *CN* values. The results are shown in **Plate 11**. The composite *CN* values in individual sub-basins for other ARC values are shown in **Table 4.4**.

Table 4.4. Composite curve numbers for each sub-basin and antecedent runoff condition

NAME	ARC 1	ARC 2	ARC 3
G-1	76	88	95
G-2	78	89	95
G-3	76	88	95
G-4	81	91	96
G-5	78	90	95
W310	71	85	93
W310N	57	76	88
W320	87	94	97
W340	80	90	96
W340N	54	73	86
W350N	74	87	94
W370N	72	86	93
W370	55	74	87
W380	61	79	90
W390	34	55	74
W390N	65	81	91
W400	81	91	96
W410	53	73	86
W420N	70	85	93
W430N	52	72	85
W440E	71	85	93
W440W	71	85	93
W460N	63	80	90
W470	70	84	93
W470N	60	78	89
W490N	72	86	93
W510N	73	86	94
W540N	59	78	89
W580N	66	82	91
W590N	58	77	88
W650N	63	80	90
W660N	53	73	86
W670	62	80	90

4.4 Clark Unit Hydrograph

In the runoff simulation of a watershed, the excess rainfall hyetograph is transformed to a runoff hydrograph through a transfer function called the unit hydrograph. In the present hydrologic study, the Clark unit hydrograph was used as the transfer function. The Clark unit hydrograph method first develops a hydrograph based on the time-area curve. It is then routed through a linear reservoir to account for storage attenuation effect of each sub-basin. The Clark unit hydrograph is defined by two parameters including time of concentration and storage coefficient. The time of concentration, denoted by t_c , is defined as the time between the end of excess rainfall and the point of inflection of the falling limb of the runoff hydrograph. Storage coefficient, denoted by R , represents the storage effect of a basin.

4.4.1 Time of Concentration

Times of concentration t_c for sub-basins in the present study were calculated using Kirby Hathaway's formula:

$$t_c = 0.01377 \frac{(nL)^{0.47}}{s^{0.235}} \quad (2)$$

where: L is the length of the flow path in feet; n is Manning's watershed roughness coefficient; and s is the average slope in ft/ft, which is taken as the slope of the flow path between the 25% and 75% points of the path length. Manning's n is taken to be 0.07 for rural sub-basins and 0.03 for urbanized sub-basins. Guidance provided in TR-55 for sheet flow was also referenced to check these assumptions. The aggregate roughness value for a partially developed wooded area with some development (e.g. roads and some connected impervious area) is estimated to be close to 0.07.

4.4.2 Storage Coefficients

The storage coefficient R is often estimated based on an acceptable routing indicator K_C defined as $K_C = R/(t_c + R)$. This indicator affects the peaking characteristics of hydrographs. The larger the value of K_C is, the smaller the peaking of the runoff hydrograph will be. In general, smaller K_C values correspond to more urbanized basins, while larger K_C values correspond to undeveloped rural basins. Since the impervious ratio typically increases with the degree of urbanization within a basin, the K_C values in the present study are assigned smaller values for sub-basins with large impervious ratios. All of the sub-basin parameters pertinent to the HEC-HMS modeling are presented in **Table 4.5**. Assigned K_C values with respect to impervious ratios of sub-basins are presented in **Figure 4.13**.

Table 4.5 Summary of sub-basin parameters used in HEC-HMS modeling

Name	Description of Sub-basin Location and Downstream Drainage	Area (sq.mi.)	CN (ARC 2)	Length (ft)	Slope (ft/ft)	Manning's <i>n</i>	Time of Conc. (hr)	Storage (hr)
G-1	E of G-2 in GV; drains to PS1	0.070	88	2135	0.0005	0.03	0.85	1.57
G-2	SE of G-1 in GV; drains to PS2	0.087	89	2526	0.0022	0.03	0.44	0.82
G-3	W end of GV; drains to PS3	0.037	88	2536	0.0001	0.03	0.63	1.18
G-4	E of G-3 in GV; drains to PS4	0.014	91	799	0.0050	0.03	0.21	0.40
G-5	NE end of GV; drains to PS5	0.059	90	2128	0.0001	0.03	0.85	1.57
W310	S of N. San Pedro Rd; drains to La Pasada Drain	0.030	85	560	0.3956	0.07	0.10	0.22
W310N	N of N. Fork nr confluence; drains to tidal marsh	0.189	76	3150	0.0439	0.03	0.24	0.45
W320	Airfield and low-lying areas upstream of confluence	0.373	94	7610	0.0002	0.07	1.96	4.58
W340	S of N. San Pedro Rd; drains to S. Fork	0.022	90	1755	0.0062	0.07	0.29	0.54
W340N	Headwaters of N. Fork; drains to N. Fork	0.374	73	6690	0.0868	0.03	0.30	0.55
W350N	North of N. Fork nr airfield; drains to N. Fork	0.144	87	2207	0.0551	0.04	0.36	0.85
W370	Bisected by N. San Pedro Rd; drains to S. Fork	0.167	86	6111	0.0741	0.07	0.44	1.02
W370N	North of N. Fork bisected by 101; drains to N. Fork	0.354	74	3987	0.0021	0.07	0.59	1.38
W380	SE of W310; drains to Meadow Dr drain	0.175	79	4899	0.0824	0.07	0.39	1.54
W390	S of W380 ; drains to Meadow Dr drain	0.363	55	6145	0.1191	0.07	0.39	1.57
W390N	N of N. Fork, bisected by Las Gallinas Ave; drains to N. Fork	0.143	81	4509	0.0702	0.03	0.26	0.48
W400	NE of 101, NW of W370; drains to Auditorium Ch.	0.197	91	4771	0.0020	0.03	0.61	1.13
W410	S of W370, bisected by N. San Pedro Rd; drains to Northbridge Ch.	0.748	73	7663	0.0600	0.07	0.51	1.19
W420N	S of W370N, bisected by 101; drains to N. Fork	0.458	85	5084	0.0176	0.07	0.78	1.82
W430N	Upper N. Fork along Freitas Pkwy; drains to N. Fork	0.155	72	5422	0.0757	0.07	0.41	0.96
W440E	E of 101, N of W400; drains to Railroad Ch.	0.333	85	6510	0.0002	0.03	1.22	2.27
W440W	W of 101, W of W440E; drains to culvert under 101	0.130	85	3798	0.0111	0.07	0.55	1.28
W460N	N of N. Fork in upper watershed; drains to N. Fork	0.091	80	3002	0.0994	0.07	0.29	0.68
W470	S end of watershed, W of 101; drains to culvert under 101	0.852	84	7152	0.0378	0.07	0.55	1.29
W470N	E of W430N along Freitas Pkwy; drains to N. Fork	0.172	78	5362	0.0795	0.07	0.40	0.93
W490N	Bisected by N. Fork in upper watershed; drains to N. Fork	0.165	86	4195	0.0795	0.07	0.36	0.84
W510N	S of W490N in upper watershed; drains to N. Fork	0.209	86	5664	0.0750	0.07	0.42	0.98
W540N	E of W510N in upper watershed; drains to N. Fork	0.263	78	7970	0.0788	0.07	0.49	1.14
W580N	S of W510N along Sleepy Hollow Ridge; drains to W540N	0.180	82	4304	0.1277	0.07	0.33	0.76
W590N	S of W580N along Sleepy Hollow Ridge; drains to W540N	0.098	77	4259	0.1292	0.07	0.32	0.76
W650N	E of W340N along Lucas Valley Ridge; drains to N. Fork	0.196	80	5272	0.0805	0.07	0.40	0.94
W660N	S of W340N along Sleepy Hollow Ridge; drains to N. Fork	0.115	73	4518	0.1300	0.03	0.22	0.42
W670	W of W470 in Terra Linda; drains to W440W	0.235	80	4687	0.0820	0.07	0.50	1.05

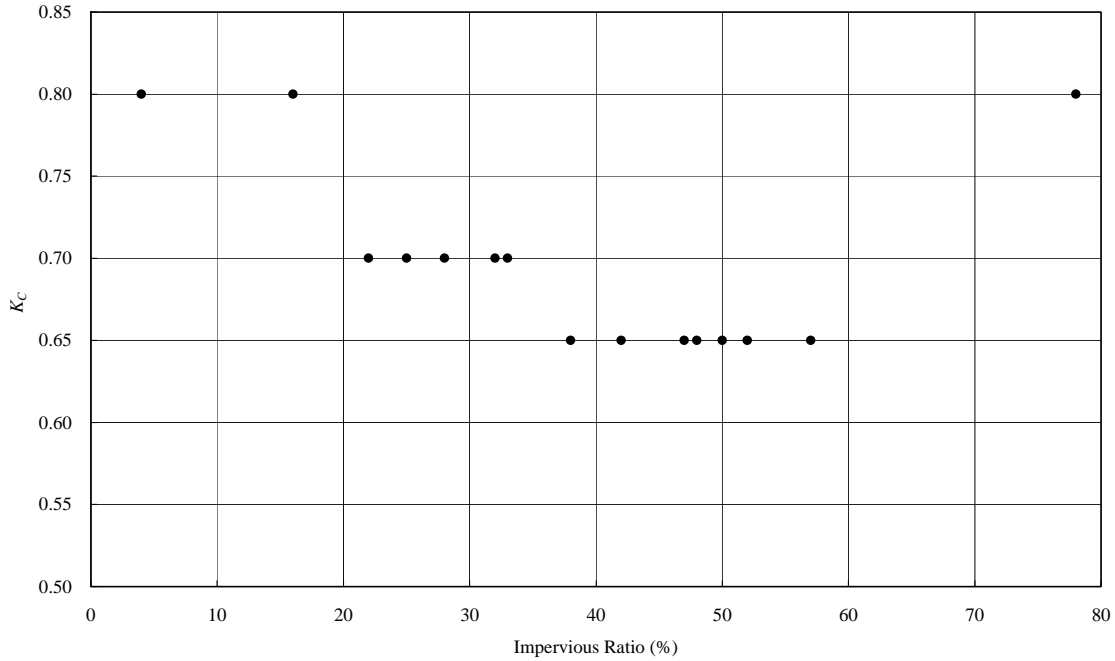


Figure 4.13. Assigned K_C values with Respect to Impervious Ratios of Sub-basins

4.5 Channel Routing

The runoff in channels is subjected to further storage attenuation. In the present study, the Muskingum method was used in the South Fork of Las Gallinas Creek to account for this effect in when appropriate. Flows through all of the North Fork reaches were routed using the Muskingum – Cunge method. The South and North Forks were modeled independently, which accounts for the difference in routing method. For future studies, it is recommended that a consistent routing method (Muskingum) is used throughout the entire basin.

The Muskingum method involves determining the outflow hydrograph at the downstream end of a channel, based on the inflow hydrograph, by solving the following equations:

$$O_2 = C_o I_2 + C_1 I_1 + C_2 O_1 \quad (3)$$

where:

I_1 = Inflow discharge at t_1

I_2 = Inflow discharge at $t_2 = t_1 + \Delta t$

O_1 = Outflow discharge at t_1

O_2 = Outflow discharge at $t_2 = t_1 + \Delta t$

The coefficients in Eq. 3 are expressed as follows:

$$C_o = -\frac{Kx - 0.5\Delta t}{K - Kx + 0.5\Delta t} \quad (4)$$

$$C_1 = \frac{Kx + 0.5\Delta t}{K - Kx + 0.5\Delta t} \quad (5)$$

$$C_2 = \frac{K - Kx - 0.5\Delta t}{K - Kx + 0.5\Delta t} \quad (6)$$

In these equations, x and K are routing coefficients. Specifically, x is a weighting factor for the upstream inflow, while $(1-x)$ is the weighting factor for the downstream outflow; K is the storage coefficient of the channel. C_o , C_1 , and C_2 can be calculated with specified x , K and Δt . In general, x is taken as 0.2 for a natural channel, while K is estimated by the travel time through the channel reach. Number of sub-reaches represents the number of time steps that the hydrograph will be in the reach. In the present hydrologic study, x is taken as 0.2, Δt is taken as 1 minute, and values of K were estimated separately for individual routing reaches as shown in **Table 4.6**.

Table 4.6. Muskingum Channel Routing Coefficients

Reach No	V Ft/sec	L ft	K hr	x	# of Sub-Reaches
1	1.37	3,500	0.71	0.2	43
2	1.24	1,770	0.40	0.2	24
3	4.25	1,620	0.11	0.2	7
4	1.24	860	0.19	0.2	11
5	1.24	851	0.19	0.2	11
6	3.46	1,060	0.09	0.2	5
7	1.24	2,670	0.60	0.2	36
8	1.24	520	0.12	0.2	7
9	1.24	1,700	0.38	0.2	23
11	1.24	865	0.19	0.2	11
18	1.24	1,650	0.35	0.2	21
19	1.24	1,651	0.35	0.2	21

As noted above, the velocities for Reaches 4, 5, 7 – 9, 11, 18 and 19 were assumed to be the same as that for Reach 2. The values for K were then calculated based on individual reach lengths.

As mentioned, flow through all of the North Fork reaches (12 through 17) were routed using the Muskingum – Cunge method, which uses the geometry and roughness of the channel to estimate flood wave attenuation in the channel. Relevant parameters are presented in **Table 4.7**.

Table 4.7. Parameters used to define Muskingum-Cunge routing

<i>Reach No</i>	<i>L ft</i>	<i>Slope ft/ft</i>	<i>Mannings's n</i>	<i>Invert ft</i>	<i>Shape</i>	<i>Width ft</i>	<i>Side Slope xH:1V</i>
12	1400	0.01	0.015	65	Trapezoid	6	2
13	3124	0.011	0.015	48	Trapezoid	6	2
14	4980	0.002	0.015	18	Trapezoid	22	2
15	1600	0.00125	0.025	4	Rectangle	600	N/A
16	5687	0.00035	0.02	4	Trapezoid	60	4
17	4100	0.0004	0.02	7	Trapezoid	17	2

4.6 Hydrologic Simulations

Hydrologic simulations using the HEC-HMS model with parameters developed in this analysis were performed for the 50%, 20%, 10%, 4%, 2%, 1%, 0.5% and 0.2% probability flood events. A time step of 1 minute was used in all simulations due to the small watershed areas (most less than 1 square mile) to accurately define the leading edge of the unit hydrograph. Base flow rates are considered negligible in the present model study (Note: The base flow rates for the 10%, 4%, 2%, 1%, 0.5% and 0.2% floods were previously estimated to be only in the range of 6 cfs to 9 cfs for Las Gallinas Creek downstream of the confluence of the North Fork and the South Fork (USACE-SFD, 1990). Alternate scenarios with antecedent runoff values of 1, 2 and 3 were simulated.

4.7 Present and Future Hydrologic Conditions

Various discussions with County personnel indicate that there will be no further urban development in the Santa Venetia Valley basin. Therefore, the impact of land development will remain unchanged for future conditions. However, there could be effects from global warming (IPCC, 2007). There is no scientific agreement whether the annual precipitation in Northern California will increase in the future, but there exists a general consent that the rainfall intensity for individual storm events will be greater. This would result in alteration of the design storm. Such a change would probably cause an increase in predicted peak flows. Also, the predicted sea level rise ranging from the low end of 0.5 feet to the upper limit of about 2 feet or more at the end of the next 50 years would potentially affect any runoff discharge rate through outfalls that are subject to tidal influence. However, since most of the runoffs in the Gallinas Valley basin are pumped into the creek, the impact due to tidal action will be minimal. On the other hand, the rising temperature resulting from global warming may cause more evapotranspiration. This could result in various degrees of reduction in the antecedent runoff condition (ARC) number. Such a reduction would lower predicted peaks.

4.8 Simulated Results

A 24-hour design storm was used in the HEC-HMS simulations. The HEC-HMS model calculated runoff hydrographs for each sub-basin, reach, pumping station and junction in the entire drainage network. The location of each junction in the watershed is presented in **Plate 12**. Peak flow values at each element in the model for each exceedance probability and ARC assumption are presented in the Appendix. The flood hydrographs at Junction 8 (the confluence of the North and South Forks), for ARC 2 are presented in **Figure 4.14**. Simulations of each precipitation event were run using ARC 1, ARC 2 and ARC 3 curve numbers. A map of 1% discharge values is presented in **Plate 13**.

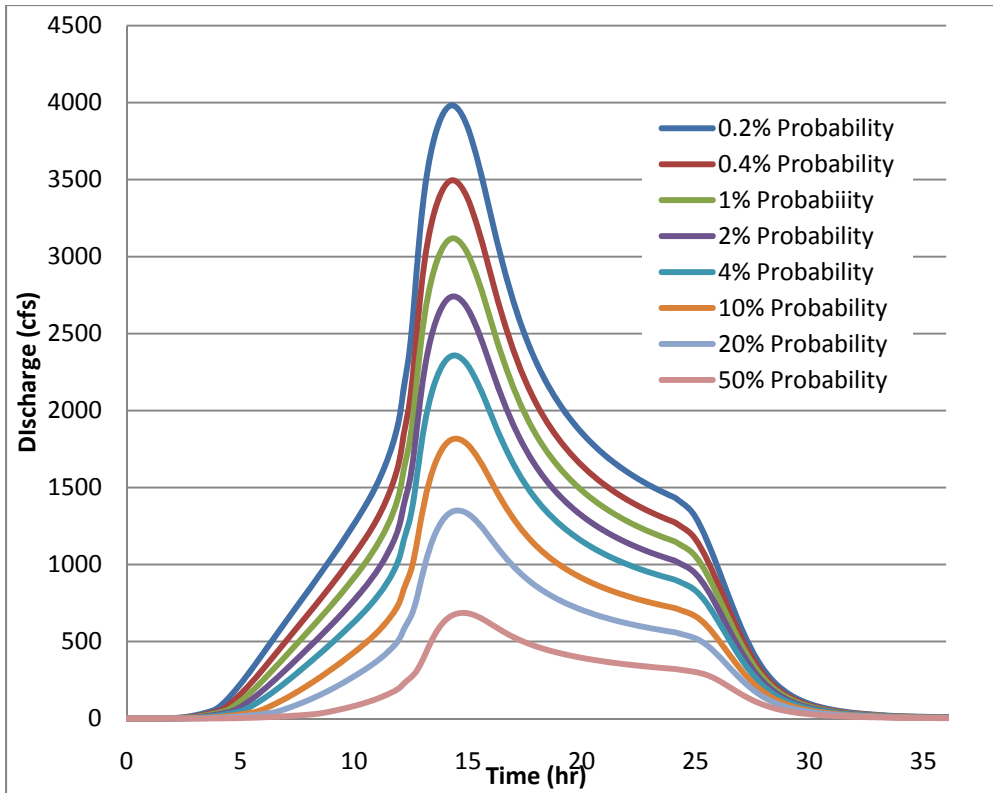


Figure 4.14. Hydrographs calculated by HEC-HMS at Junction 8 (Confluence) for AMC2

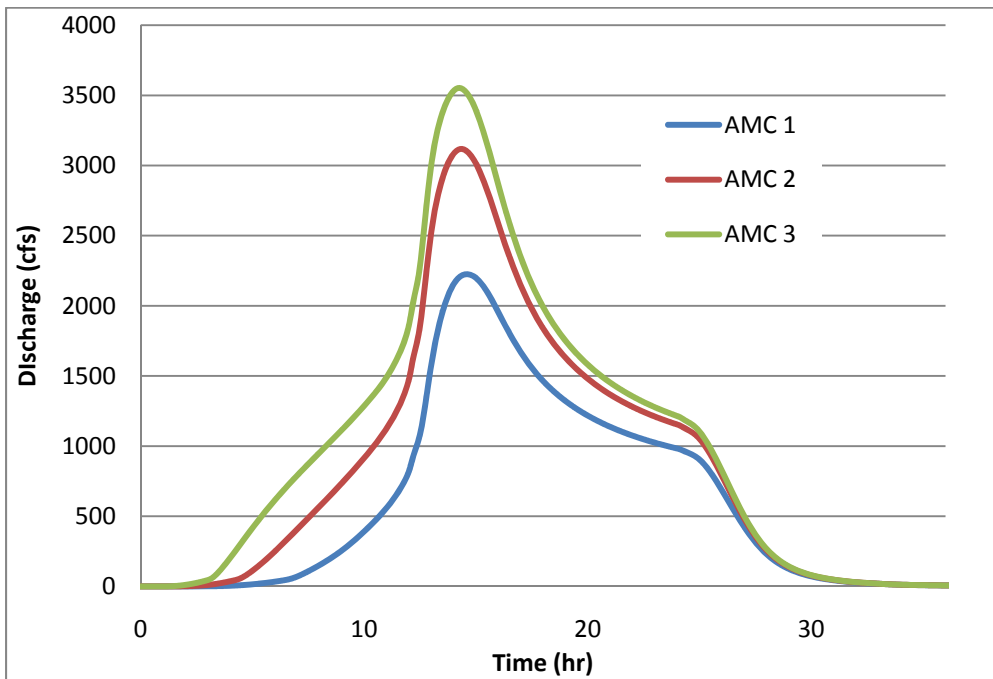


Figure 4.15. Comparison of hydrographs calculated for the three modeled antecedent runoff conditions for the 1% probability event at the junction of North and South Forks.

The 1% event model results were compared with the values predicted by regional equations. Regional flood flow estimates were derived from analysis of FEMA and County flood studies for surrounding watersheds/communities (FEMA 1977, 1989, 1997, and 1997b). This analysis included selecting and tabulating available peak flow estimates for representative floods on area creeks and completing regression analyses between tabulated flow and drainage area (Kamman 2004). That effort yielded the following equation:

$$Q_{1\%} = 2.9317(A)^{0.8084}$$

where $Q_{1\%}$ = 1% probability discharge (cfs) and A = drainage area (ac).

Marin County Department of Public Works developed the following discharge per unit area relationship for the South Fork Las Gallinas watershed in the course of studies for the San Rafael Meadows development:

$$Q_{1\%} = 0.84(A)$$

The U.S. Geological Survey (USGS) also has predictive regression equations for various regions within California (<http://water.usgs.gov/software/NFF/manual/ca/>). The study area is near the regional divide for the Central and Northern Coast Regions, but is overall most similar to the Central Coast Region in aspects related to meteorology and topography. The USGS regression equations derive statistical flows (50, 20, 10, 4, 2, and 1-percent exceedance probabilities) based on basin area (7.2 square miles), mean annual precipitation (34 inches), and an elevation factor (1 for our study, close to sea level). There is also a factor (1.42) for change in flood peak due to impervious area. The equation for the 1% event is presented below:

$$\text{Central Coast Region: } Q_{1\%} = 1.42*(19.7(A)^{0.88}(P)^{0.84}(H)^{0.33})$$

A comparison of the 1% peak flow values at each node predicted by these methods and model results from the present study is presented in **Table 4.8**. The comparison shows that the model results are similar to the values predicted by the other methods. It should be noted that the Marin Flood Control method was developed for use in smaller catchments, which may explain the larger difference in estimates. **Table 4.9** presents a comparison of the USGS Central Coast regression equations for the 50, 20, 10, 4, 2, and 1-percent exceedance events to modeled ARC 2 results. **Figure 4.16** presents a graphical comparison of ARC 2 and the USGS Central Coast estimates. Overall, the results of the model are reasonable compared to the other methods.

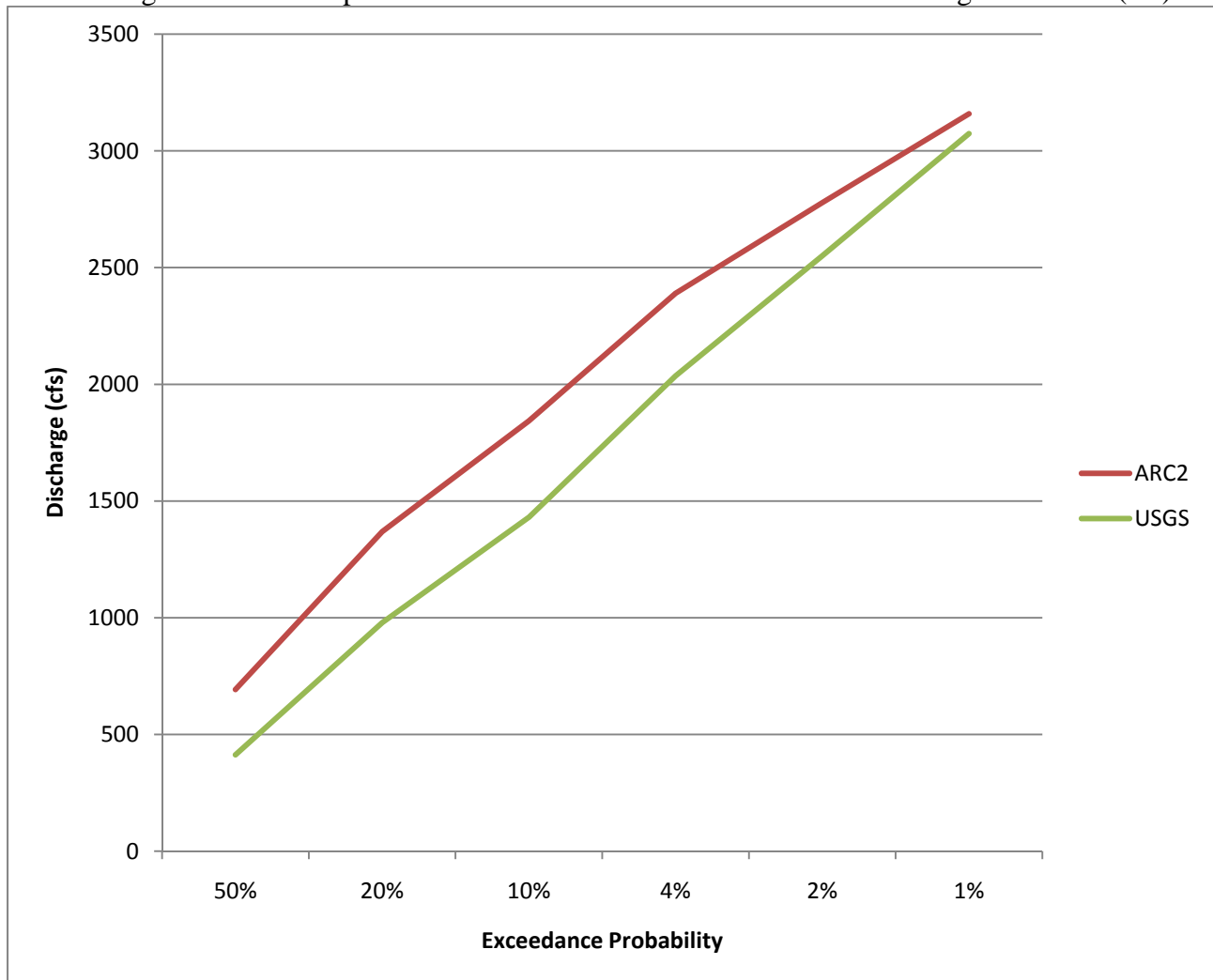
Table 4.8 – Comparison of Estimated 1% Peak Discharge Values, Junction 8

Method	1% Peak Discharge (cfs)	% Difference (Compared to ARC 2)
Present Study (ARC 2)	3159	NA
FEMA Regional Equations	2683	-15%
Marin FC	3870	23%
USGS Central Coast	3074	-2.7%

Table 4.9 – Comparison of Modeled ARC 2 Results to USGS Central Coast Estimated Peak Flow, Junction 8, cfs

Exceedance Probability	Present Study (ARC 2)	USGS Central Coast Regression Equations	% Difference
50%	693	413	-40%
20%	1369	979	-29%
10%	1843	1430	-22%
4%	2390	2036	-15%
2%	2778	2550	-8.2
1%	3159	3074	-2.7%

Figure 4.16 – Comparison of ARC2 and USGS Central Coast Discharge Estimates (cfs)



4.9 Sensitivity Analysis

In general, large precipitation events occur between the months of October and April in the Gallinas watershed. This period is typically cold and wet, so it is likely that a large event will follow a period of low temperatures and some rain showers (ARC 2). However, this region can also experience consecutive weeks of unseasonably warm and dry weather (ARC1), or back-to-back torrential downpours (ARC 3). An examination of the sensitivity of the model to antecedent runoff conditions was performed in order to quantify this uncertainty. A comparison of the 1% peak flows at the watershed outlet is presented in **Table 4.10**, which shows ARC 1 peak flows are 29% less than ARC 2, and ARC 3 flows are expected to be 14% greater than ARC 2.

Table 4.10. Comparison of 1% peak flows at the confluence of the N. and S. Forks (Junction 8)

	ARC 1	ARC 2	ARC 3	ARC 1 vs. ARC 2		ARC 3 vs. ARC 2	
				Diff. (cfs)	Diff. (%)	Diff. (cfs)	Diff. (%)
Outflow (cfs)	2225	3159	3552	-934	-30%	393	11%

5.0 RISK ANALYSIS

Risk analyses were performed for the flood hydrology established for the South Fork at the following three representative locations: (1) the watershed outlet, namely, the confluence of the South and North Forks denoted as Junction 8, (2) the mid-point of the Gallinas Village levee, modeled as Junction 14, and (3) the confluence of the Auditorium Channel and Northbridge Channel where the South Fork begins, denoted as Junction 3. The computed peak discharges for 8 different frequencies at these three identified locations from the HEC-HMS model simulations are shown in **Table 5.1**.

Table 5.1. Peak Discharges of Different Frequencies at Various Index Locations

Location	Q _{50%} cfs	Q _{20%} cfs	Q _{10%} cfs	Q _{4%} cfs	Q _{2%} cfs	Q _{1%} cfs	Q _{0.5%} cfs	Q _{0.2%} cfs
Junction-2	205	410	553	718	837	951	1065	1215
Junction-3	247	504	687	902	1056	1206	1358	1555
Junction-7	286	583	795	1042	1220	1393	1567	1794
Junction-8	693	1369	1843	2390	2778	3159	3540	4030
Reach-11 (Upstream of Junction 8, South Fork)	340	679	920	1200	1401	1596	1793	2049
Junction-14	334	670	908	1185	1383	1577	1772	2025

5.1 Equivalent Length of Record

The equivalent length of record was estimated to be 13 years based on the USACE Risk-Based Analysis for Flood Damage Reduction guidelines as presented in **Table 5.2**. Peak flow values in this study were estimated using a rainfall-runoff model and results were compared with FEMA regional estimates, the Marin Flood Control method, and the USGS Central Coast method. The length of record was used along with the peak flows (**Table 5.1**) to calculate confidence limits for the discharge frequency curve using HEC's Flood Damage Analysis (HEC-FDA) software. A graphical method was used to generate the error bands surrounding the 50-, 20-, 10-, 4-, 2-, 1-, 0.5, and 0.2-percent events. The error band for the higher frequency events was interpolated using the analytical method in FDA to estimate the discharge for the 99.9-percent event.

The 5- and 95-% confidence limits surrounding the 50-, 20-, 10-, 4-, 2-, 1-, 0.5, and 0.2-percent events are shown in **Tables 5.3 through 5.8**. Discharge-Frequency curves at each junction are presented in **Figures 5.1 through 5.6** for Junctions 2, 3, 7, 8, 14, and the outflow of Reach 11 (directly upstream of Junction 8 on the South Fork). A comparison of all discharge-frequency curves is presented in **Plate 14**.

Table 5.2 - Equivalent Record Length Guidelines, USACE EM-1110-2-1619

Method of Frequency Function Estimation	Equivalent Record Length*
Analytical distribution fitted with long-period gauged record available at site.	Systematic record length.
Estimated from analytical distribution fitted for long-period gauge on the same stream, with upstream drainage area within 20% of that point of interest.	90% to 100% of record length of gaged location.
Estimated from analytical distribution fitted for long-period gage within same watershed.	50% to 90% of record length.
Estimated with regional discharge-probability function parameters.	Average length of record used in regional study.
Estimated with rainfall-runoff-routing model calibrated to several events recorded at short-interval event gauge in watershed.	20 to 30 years.
Estimated with rainfall-runoff-routing model with regional model parameters (no rainfall-runoff-routing model calibration).	10 to 30 years.
Estimated with rainfall-runoff-routing model with handbook or textbook model parameters.	10 to 15 years.

* Based on judgment to account for the quality of any data used in the analysis, for the degree of confidence in models, and for previous experience with similar studies.

Table 5.3 - Confidence Limits, Junction 2, South Fork

Exceedance Probability	Discharge (cfs)	Discharge (cfs) of Confidence Limit Curves	
		95%	5%
0.999	3	1	14
0.99	9	2	30
0.95	22	7	64
0.9	36	13	99
0.8	65	24	172
0.7	100	38	263
0.5	205	94	446
0.3	316	175	571
0.2	410	222	757
0.1	553	292	1049
0.04	718	369	1399
0.02	837	423	1658
0.01	951	473	1912
0.005	1065	523	2170
0.004	1101	538	2252
0.002	1215	587	2516
0.001	1333	636	2791

Figure 5.1 - Discharge-Frequency Curve, Junction 2, South Fork

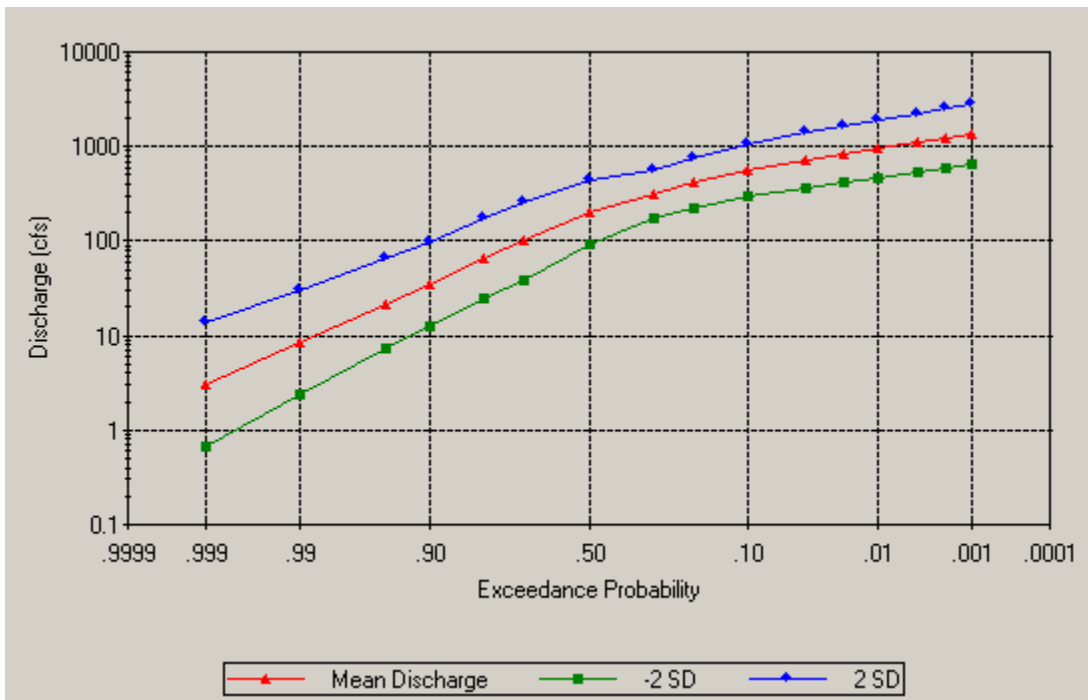


Table 5.4 - Confidence Limits, Junction 3, South Fork (Auditorium and Northbridge Channels)

Exceedance Probability	Discharge (cfs)	Discharge (cfs) of Confidence Limit Curves	
		95%	5%
0.999	3	1	14
0.99	9	2	33
0.95	24	8	73
0.9	40	14	115
0.8	74	27	205
0.7	117	43	320
0.5	247	110	554
0.3	385	209	710
0.2	504	268	948
0.1	687	355	1329
0.04	902	454	1793
0.02	1056	522	2136
0.01	1206	587	2476
0.005	1358	652	2827
0.004	1405	672	2938
0.002	1555	735	3291
0.001	1710	799	3662

Figure 5.2 - Discharge-Frequency Curve, Junction 3 (Auditorium and Northbridge Channels)

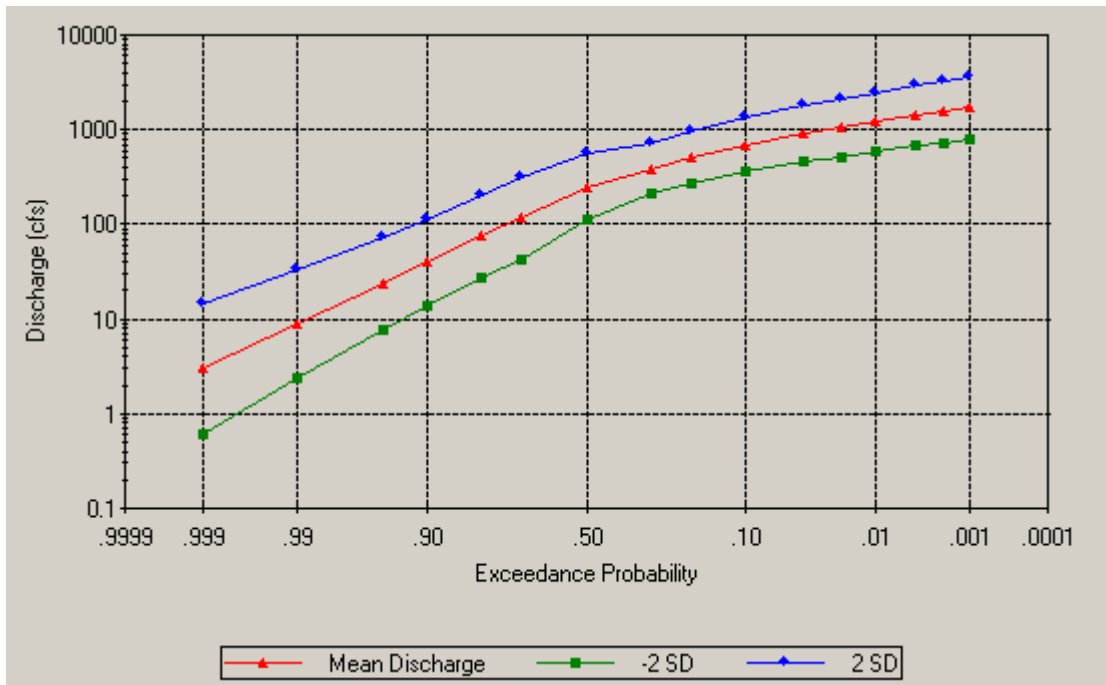


Table 5.5 - Confidence Limits, Junction 7, South Fork (Outlet)

Exceedance Probability	Discharge (cfs)	Discharge (cfs) of Confidence Limit Curves	
		95%	5%
0.999	4	1	18
0.99	11	3	41
0.95	29	10	88
0.9	49	17	137
0.8	89	33	240
0.7	139	52	368
0.5	286	130	630
0.3	446	243	819
0.2	583	311	1094
0.1	795	412	1536
0.04	1042	524	2070
0.02	1220	603	2467
0.01	1393	678	2861
0.005	1567	752	3265
0.004	1621	775	3392
0.002	1794	847	3801
0.001	1973	920	4230

Figure 5.3 - Discharge-Frequency Curve, Junction 7, South Fork of Las Gallinas Creek (Outlet)

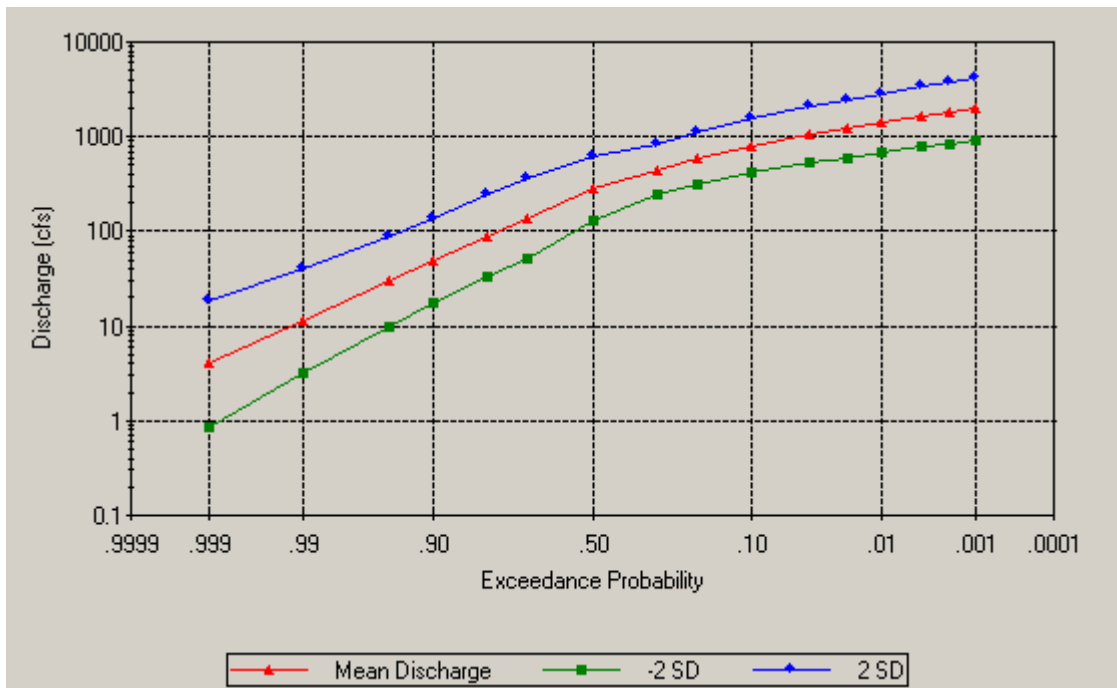


Table 5.6 - Confidence Limits, Junction 8, South Fork (Outlet)

Exceedance Probability	Discharge (cfs)	Discharge (cfs) of Confidence Limit Curves	
		95%	5%
0.999	12	3	51
0.99	33	10	110
0.95	80	28	227
0.9	129	48	344
0.8	230	90	586
0.7	348	138	880
0.5	693	327	1469
0.3	1059	592	1895
0.2	1369	750	2500
0.1	1843	982	3459
0.04	2390	1239	4610
0.02	2778	1416	5450
0.01	3159	1586	6292
0.005	3540	1753	7149
0.004	3658	1804	7417
0.002	4030	1963	8272
0.001	4414	2125	9167

Figure 5.4 - Discharge-Frequency Curve, Junction 8, South Fork of Las Gallinas Creek (Outlet)

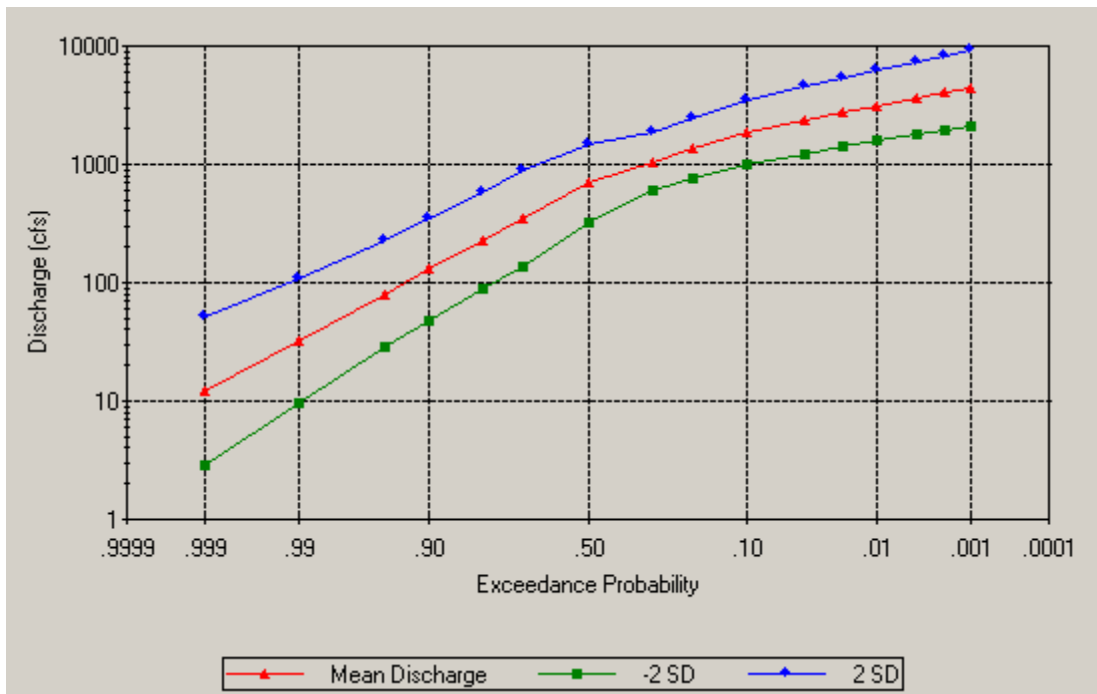


Table 5.7 - Confidence Limits, Reach 11, South Fork (Outlet)

Exceedance Probability	Discharge (cfs)	Discharge (cfs) of Confidence Limit Curves	
		95%	5%
0.999	5	1	23
0.99	14	4	50
0.95	36	12	107
0.9	59	21	164
0.8	108	41	285
0.7	166	63	436
0.5	340	157	738
0.3	523	289	947
0.2	679	368	1254
0.1	920	485	1746
0.04	1200	615	2341
0.02	1401	706	2780
0.01	1596	792	3215
0.005	1793	878	3662
0.004	1854	904	3803
0.002	2049	987	4254
0.001	2250	1071	4727

Figure 5.5 - Discharge-Frequency Curve, Reach 11, South Fork

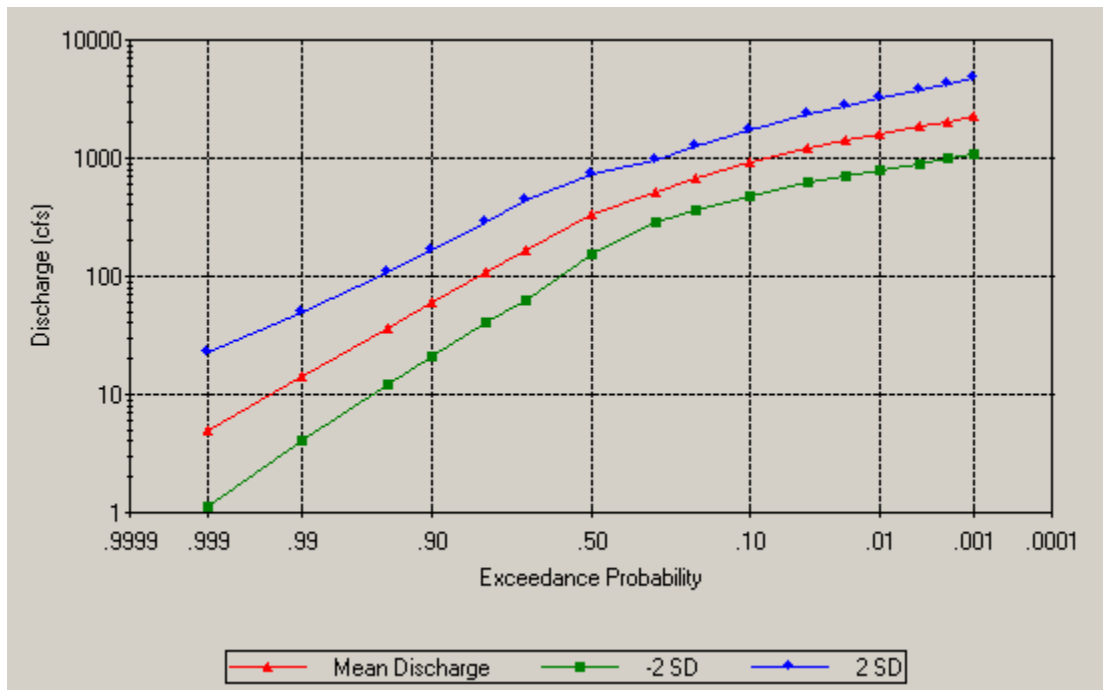
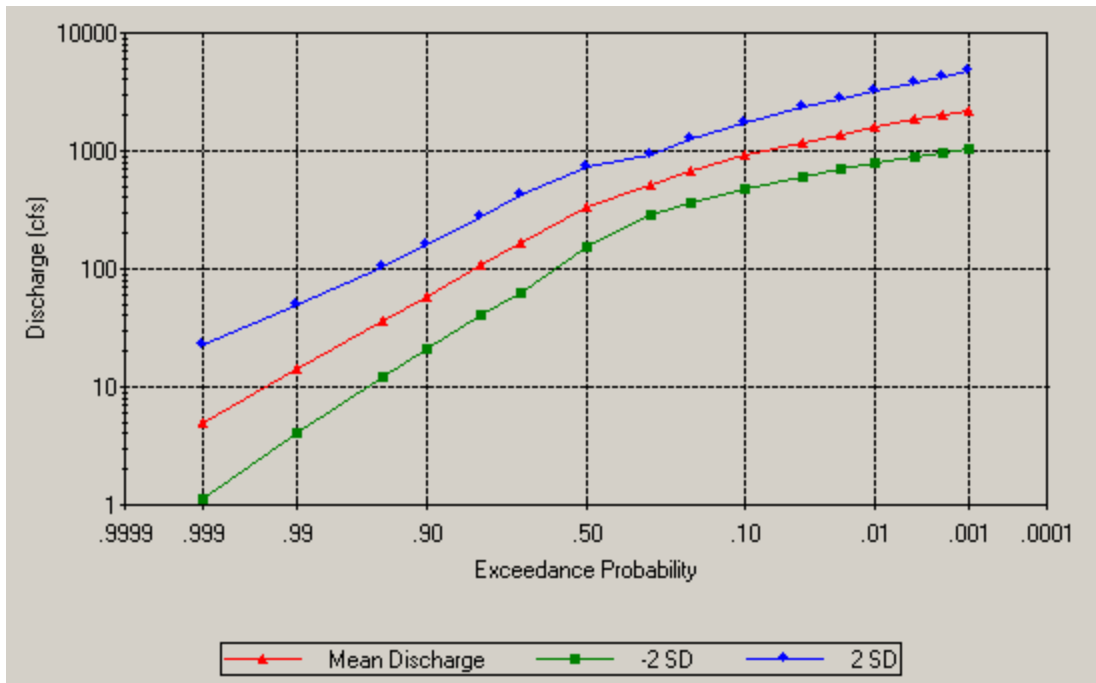


Table 5.8 - Confidence Limits, Junction 14, South Fork (Gallinas Village Levee)

Exceedance Probability	Discharge (cfs)	Discharge (cfs) of Confidence Limit Curves	
		95%	5%
0.999	5	1	22
0.99	14	4	49
0.95	36	12	105
0.9	58	21	162
0.8	106	40	280
0.7	164	63	428
0.5	334	154	725
0.3	515	284	935
0.2	670	362	1241
0.1	908	477	1729
0.04	1185	605	2320
0.02	1383	694	2754
0.01	1577	780	3189
0.005	1772	864	3634
0.004	1833	890	3774
0.002	2025	971	4222
0.001	2224	1054	4692

Figure 5.6 - Discharge-Frequency Curve, Junction 14, South Fork of Las Gallinas Creek



6.0 Summary

A hydrologic analysis using three HEC models (i.e., HEC-GeoHMS, HEC-HMS & HEC-FDA) was performed for the North and South forks of the Las Gallinas Creek watershed to determine peak discharges at various locations along Las Gallinas Creek. A summary is presented below.

- The HEC-GeoHMS was applied to delineate the preliminary drainage sub-basins within the watershed based on the DEM with a grid size of 10 feet by 10 feet and various GIS-based information such as watershed boundary, creek delineation, drainage routes, etc. that were provided by the County of Marin.
- Modification of the deduced preliminary sub-basins was made to reflect human alteration of the drainage pathways for flood control as well as a major corridor (i.e., Highway 101) that interferes in the natural drainage route for the watershed.
- The HEC-HMS model developed for the watershed consists of 34 sub-basins, 21 junctions, and 18 channel reaches.
- Design storms were established based on the rainfall intensity-duration-frequency curves for the rainfall station at San Rafael Civic Center (Station No. E20-7880-20).
- Losses were estimated using the SCS method considering soil group classification, land use/treatment classification, hydrologic conditions, and antecedent runoff conditions.
- Impervious ratios were determined based on the GIS data provided by the County of Marin and were incorporated in the model.
- The Clark unit hydrograph was used to transform excess rainfall into the runoff hydrographs from individual sub-basins.
- Modeled flows were routed through the connecting channels using the Muskingum and Muskingum-Cunge methods to account for channel storage effects.
- It was assumed that the antecedent runoff conditions for the watershed would be average, therefore SCS curve numbers for ARC 2 were used in the final model analysis.
- A sensitivity analysis was conducted to investigate the effect of the ARC condition on peak discharges.
- There will be no further urban development in the Santa Venetia Valley basin and, therefore, the simulation results for the present conditions may be adopted for the future conditions.

7.0 REFERENCES

Coleman, Selmi & Wright (CSW), 1982. “Civic Center North Hydrologic Report for the Upper Reach of the South Fork of Gallinas Creek”, prepared for the First National State Bank of New Jersey, May 26, 1982.

Conatser, Neal. Marin County, 2009. Personal Communication.

Goodridge, Jim. Rainfall Depth-Duration Frequency Analysis for California Rain Gages. Data Compiled with support from the California Department of Water Resources. 2000.

Hydrologic Engineering Center (HEC), 2009. <http://www.hec.usace.army.mil/>

Hydrologic Engineering Center (HEC), 2008. “Hydrologic Modeling System HEC-HMS”, User’s Manual, Version 3.3, January 2008.

Hydrologic Engineering Center (HEC), 2003. “Geospatial Hydrologic Modeling Extension HEC-GeoHMS”, User’s Manual, Version 1.1, December 2003.

Hydrologic Engineering Center (HEC), 1998. “HEC-FDA Flood Damage Reduction Analysis”, User’s Manual, Version 1.0, January 1998.

Intergovernmental Panel on Climate Change (IPCC), 2007. “The Physical Science Basis – Work Group I Report, Chapter 5 Observations: Oceanic Climate Change and Sea Level”, IPCC Fourth Assessment report.

Kamman Hydrology & Engineering, Inc., 2004 “Gallinas Creek Restoration Feasibility Study and Conceptual Design Report, Marin County, California”, prepared for San Pablo Bay Watershed Restoration Program Partners, December 2004..

Marin County, 1998. “Drainage Report for San Rafael Meadows Flood Control Zone 6”, prepared by Marin County Flood Control, September 1998

Nute Engineering, 1999 “Pump Station No.1 and Intertie Pipeline Completion Predesign Study, Marin County Flood Control and Water Conservation District – Zone 7” prepared for Marin County.

Nute Engineering, 1998. “Vendola Driver Intertie Storm Drain and Pump Station Configuration Study, Marin County Flood Control and Water Conservation District – Zone 7” prepared for Marin County.

Nute Engineering, 1971. “Long Range Plan for Drainage and Flood Control, Marin County Flood Control and Water Conservation District – Zone 7, Marin County, California”, prepared for Marin County.

USGS, 2009. Seamless Data Distribution System, <http://seamless.usgs.gov/index.php>

USACE, 1996. “Risk-Based Analysis for Flood Damage Reduction studies”, EM-1110-2-1619, August 1996.

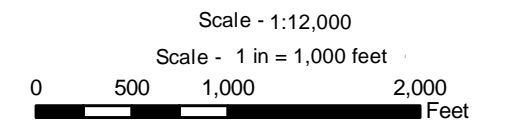
USACE-SFD, 1990. “Fluvial and Tidal Flooding Analysis, Section 205, Reconnaissance Study, Gallinas Creek, Marin County, California”, August 10, 1990.

Van Mullem, J. A., Woodward, D. E., Hawkins, R. H., and Hielfelt, Jr., A. T., [*Runoff Curve Number Method: Beyond the Handbook*](#), Natural Resources Conservation Service, U. S. Department of Agriculture, Washington, D. C.



Las Gallinas Creek Hydrology Study

Plate 1 Project Area - Santa Venetia Valley



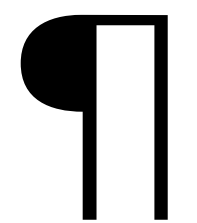
State Plane CA Zone III	Horz. Datum: NAD 83	Horz. Units: feet
	Vert. Datum: NAVD 88	2 June 2010

Regional Reference Map



Legend

 Project Area



Background Map Data Sources:
ESRI World Imagery

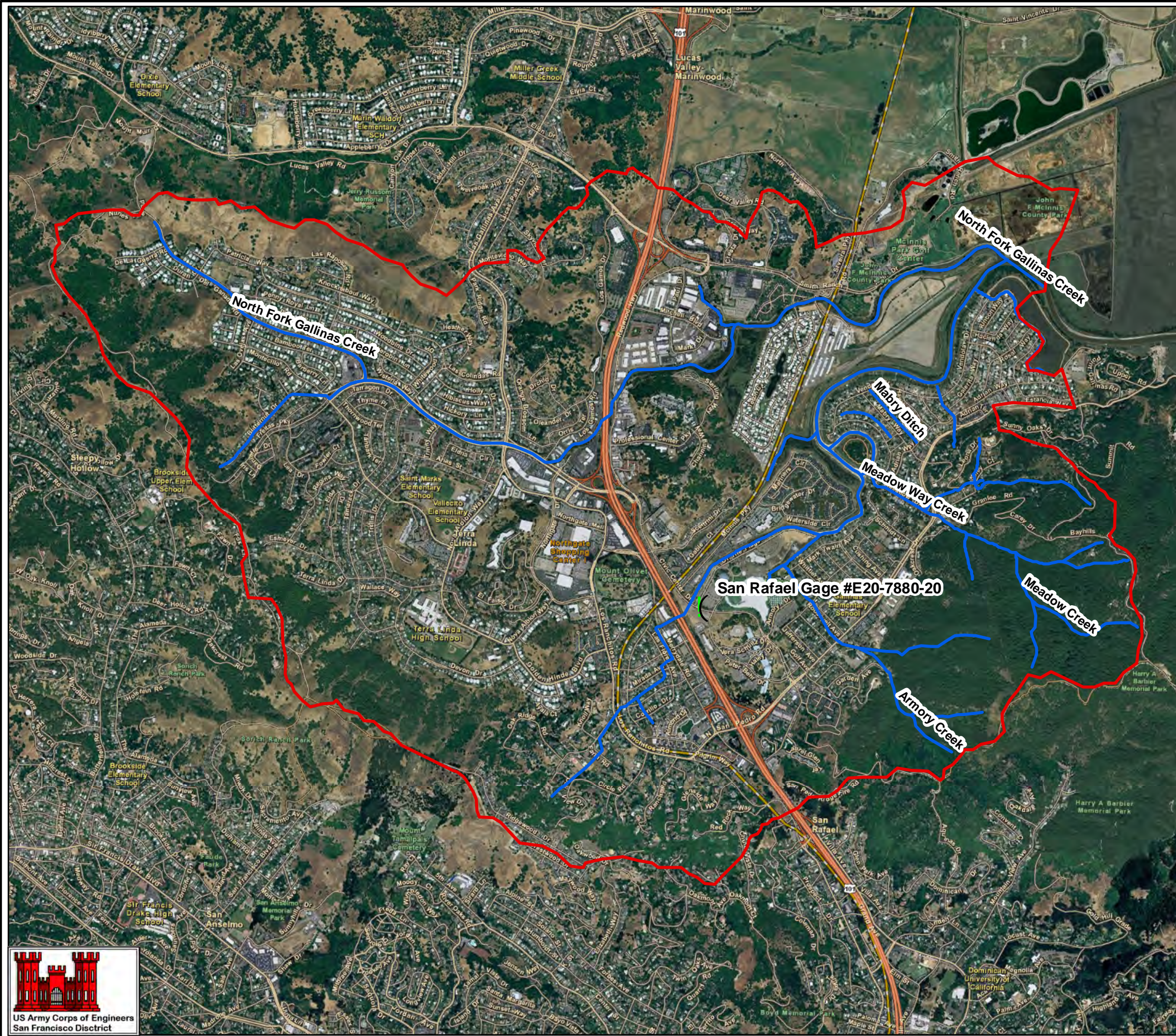
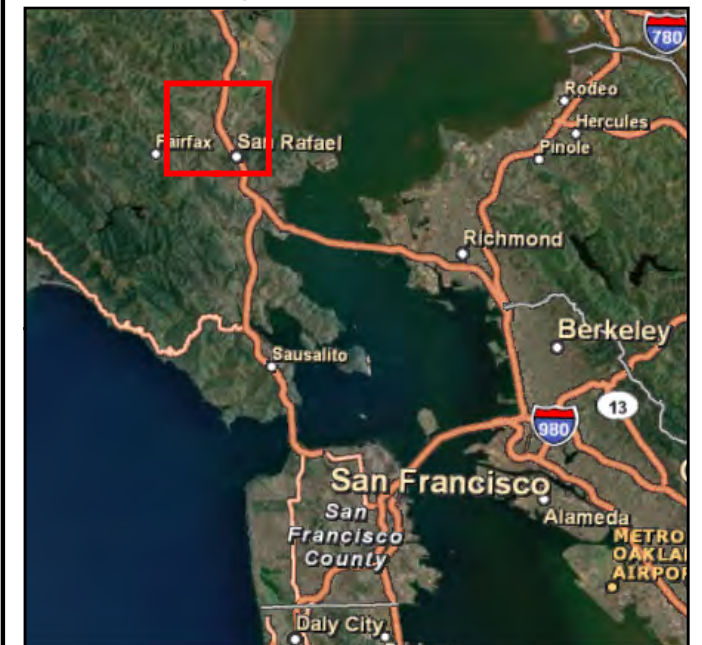
**Las Gallinas Creek
Hydrology Study**

**Plate 2
Gallinas Creek Watershed Aerial View**




Scale - 1:24,000
Scale - 1 in = 2,000 feet
0 1,000 2,000 4,000 Feet

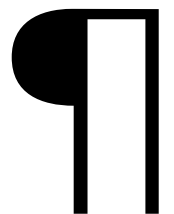
State Plane CA Zone III	Horz. Datum: NAD 83	Horz. Units: feet
	Vert. Datum: NAVD 88	2 June 2010

Regional Reference Map



Legend

-  Rain Gage
-  Watershed Boundary
-  Streams



Background Map Data Sources:
ESRI World Imagery

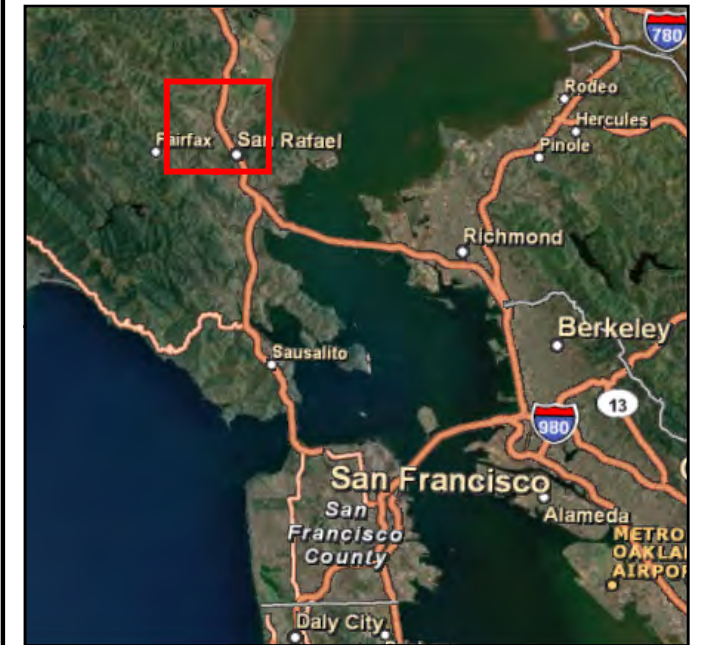
Las Gallinas Creek Hydrology Study

**Plate 3
Gallinas Creek Watershed Street Map**




Scale - 1:24,000
Scale - 1 in = 2,000 feet
0 1,000 2,000 4,000 Feet

State Plane CA Zone III	Horz. Datum: NAD 83	Horz. Units: feet
	Vert. Datum: NAVD 88	2 June 2010

Regional Reference Map

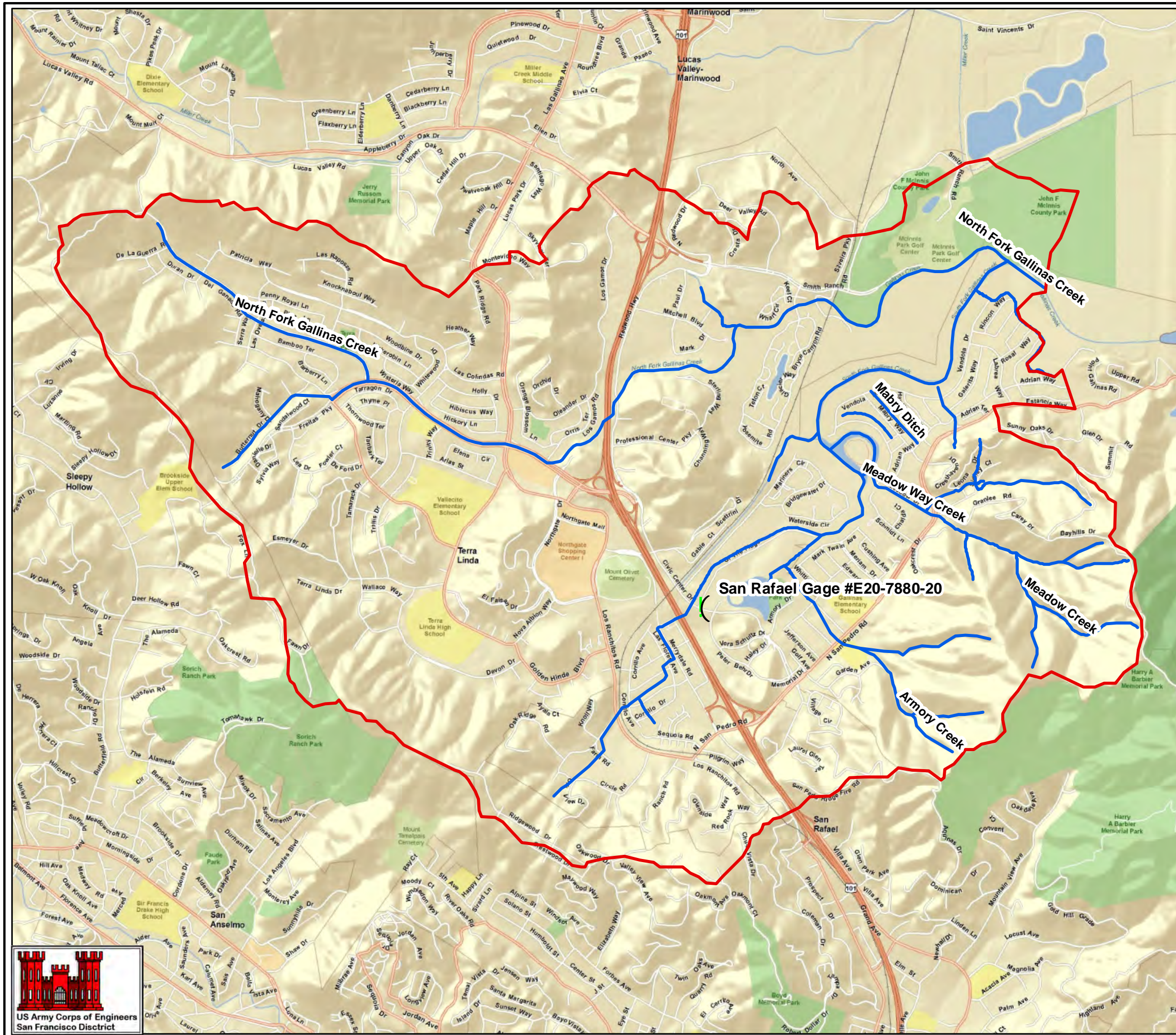


Legend

-  Rain Gage
-  Watershed Boundary
-  Streams



Background Map Data Sources:
ESRI World Imagery



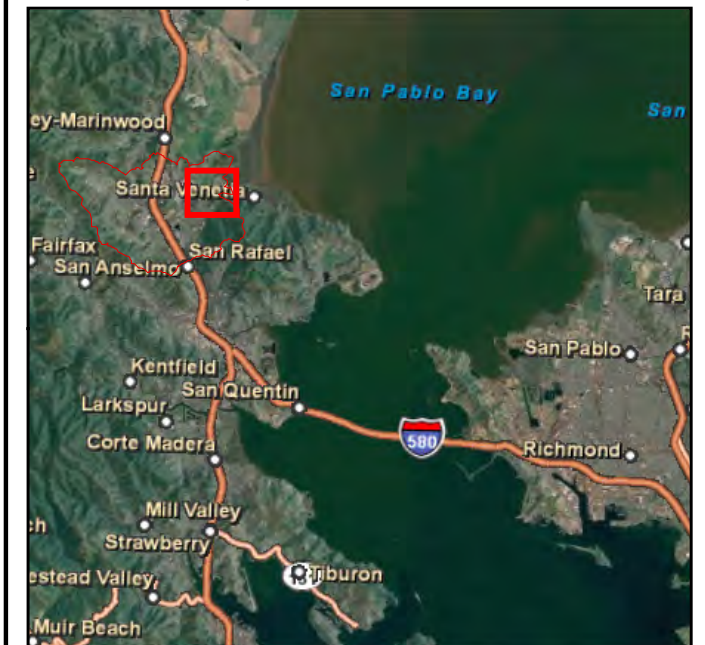
**Las Gallinas Creek
Hydrology Study**

**Plate 4
Santa Venetia Drainage System**



Scale - 1:6,000
Scale - 1 in = 500 feet
0 250 500 1,000 Feet

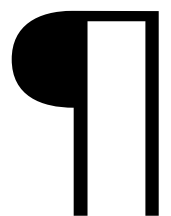
State Plane CA Zone III	Horz. Datum: NAD 83	Horz. Units: feet
	Vert. Datum: NAVD 88	2 June 2010

Regional Reference Map



Legend

-  Interceptor
-  Pump Station



Background Map Data Sources:
ESRI World Imagery

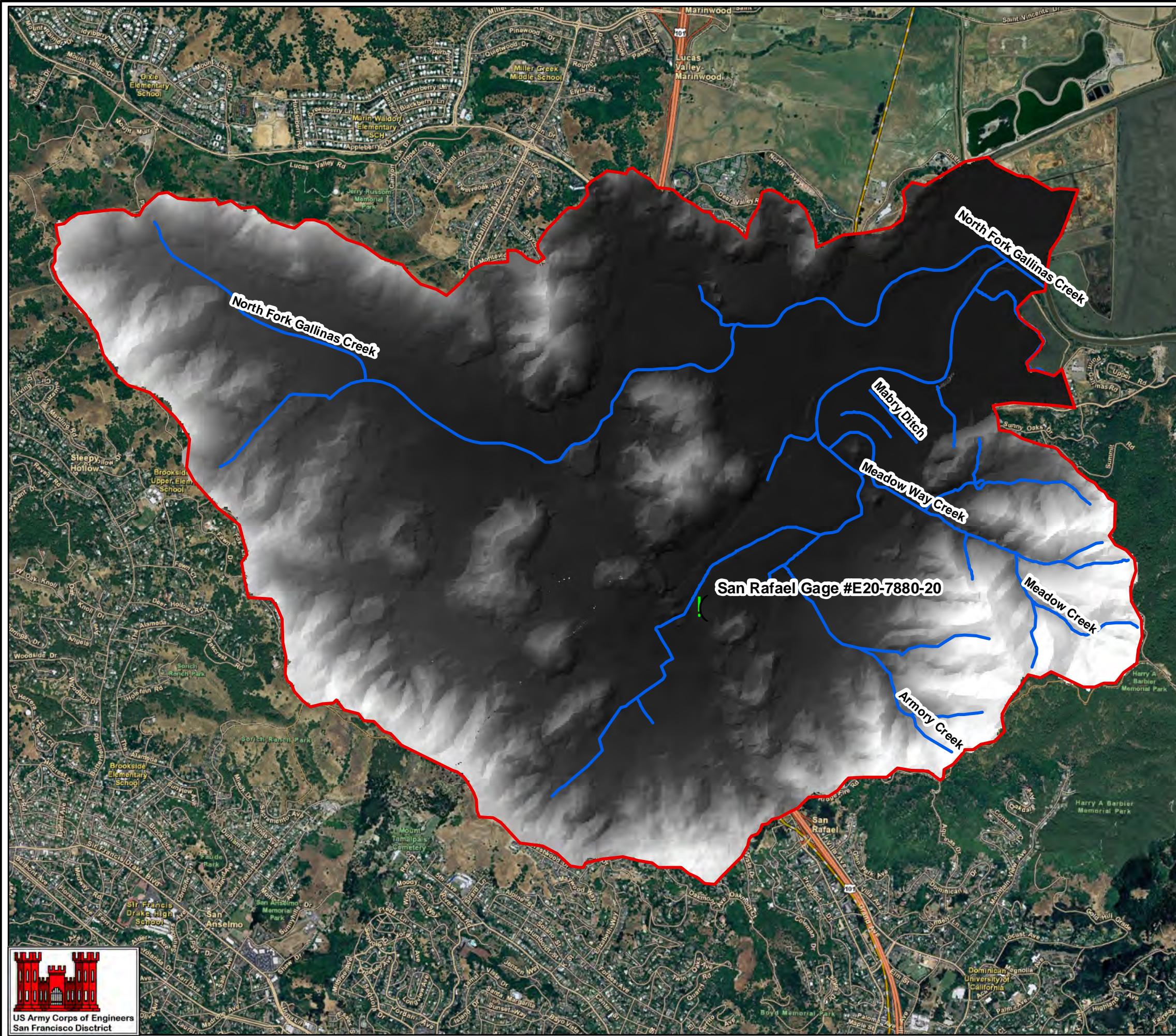
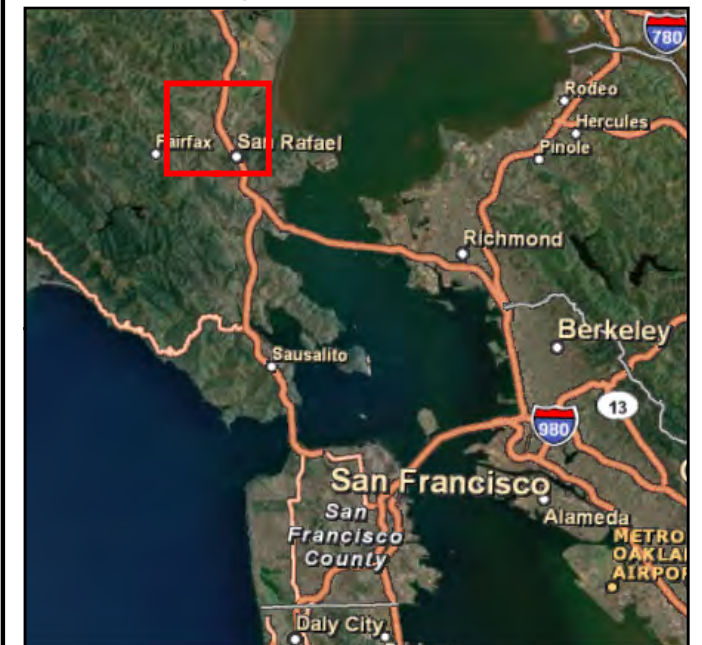
**Las Gallinas Creek
Hydrology Study**

**Plate 5
Gallinas Creek Terrain**

Scale - 1:24,000
Scale - 1 in = 2,000 feet
0 1,000 2,000 4,000 Feet

State Plane CA Zone III	Horz. Datum: NAD 83	Horz. Units: feet
	Vert. Datum: NAVD 88	2 June 2010

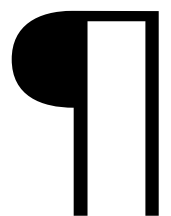
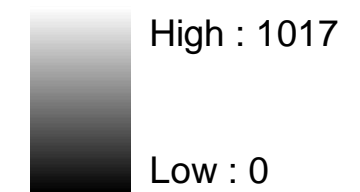
Regional Reference Map



Legend

- Rain Gage
- Watershed Boundary
- Streams

Elevation (ft)



Background Map Data Sources:
ESRI World Imagery

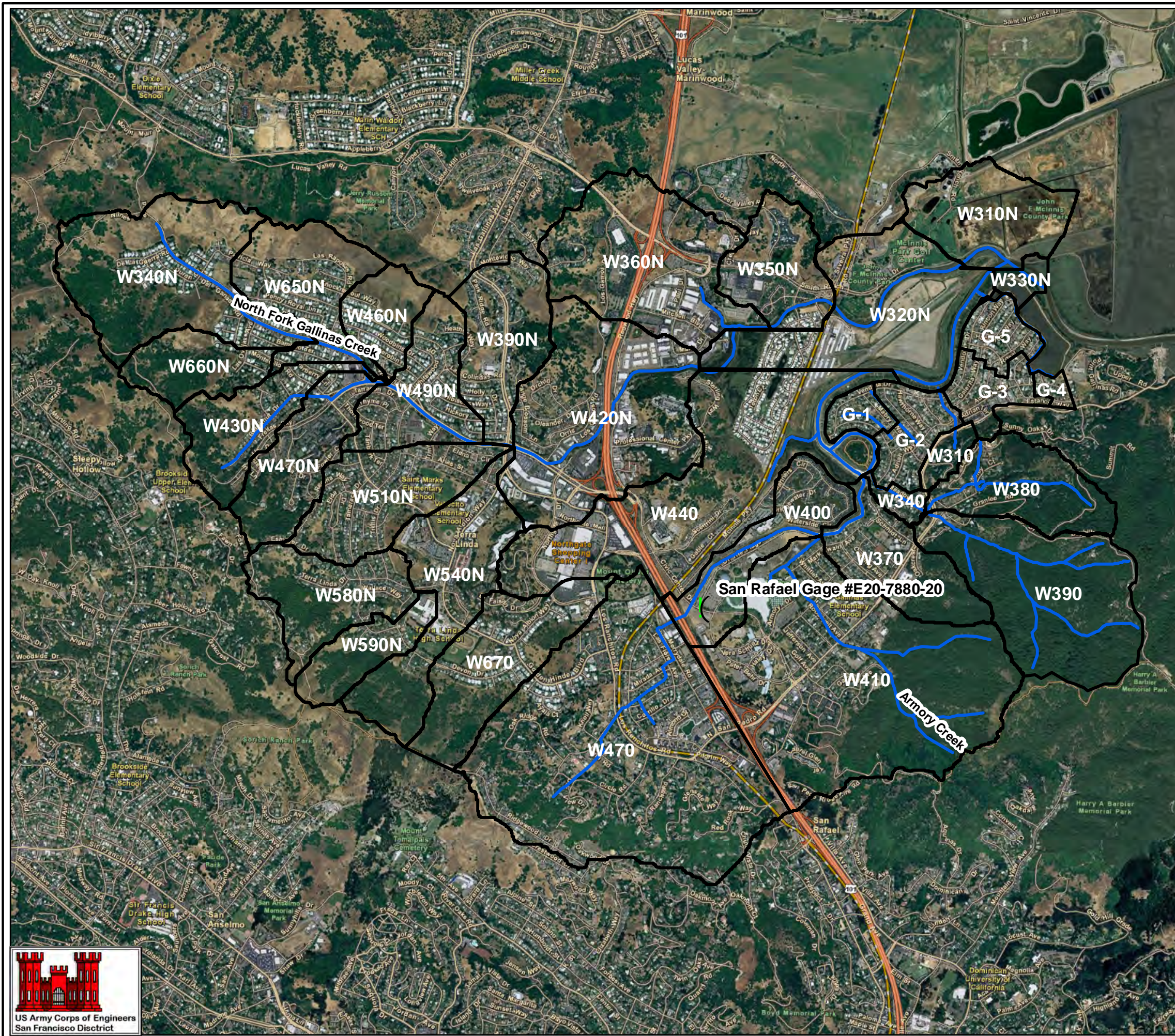
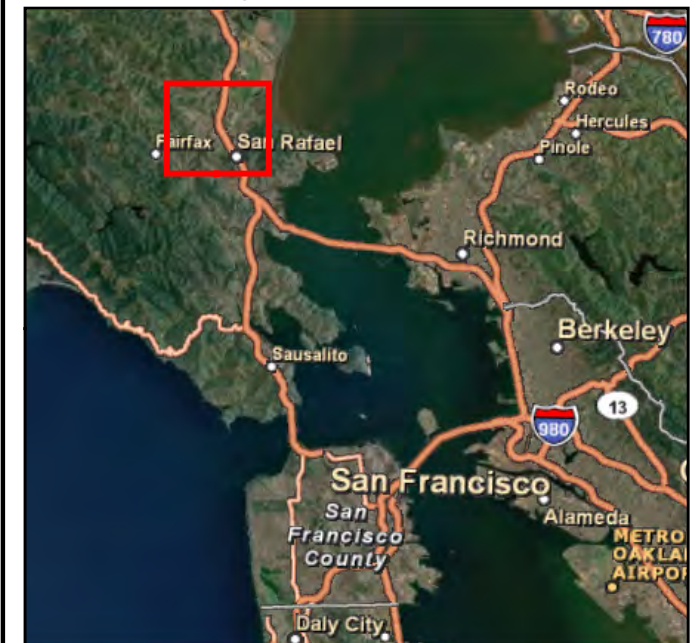
**Las Gallinas Creek
Hydrology Study**

**Plate 6
Final Subbasin Delineation - Aerial View**




Scale - 1:24,000
Scale - 1 in = 2,000 feet
0 1,000 2,000 4,000 Feet

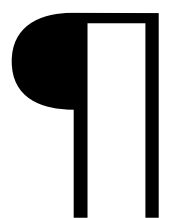
State Plane CA Zone III	Horz. Datum: NAD 83	Horz. Units: feet
	Vert. Datum: NAVD 88	2 June 2010

Regional Reference Map



Legend

-  Rain Gage
-  Streams
-  Subbasins



Background Map Data Sources:
ESRI World Imagery

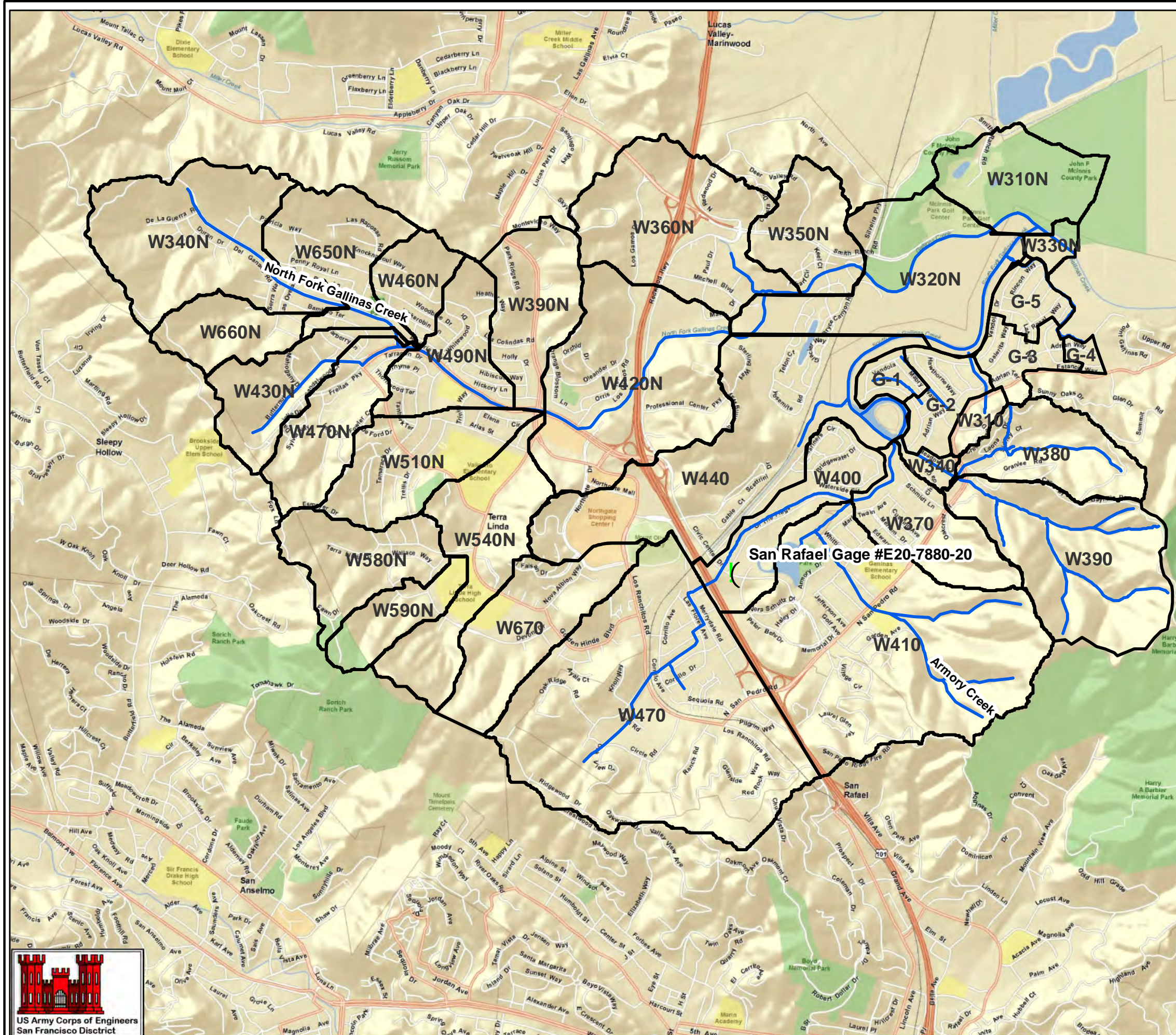
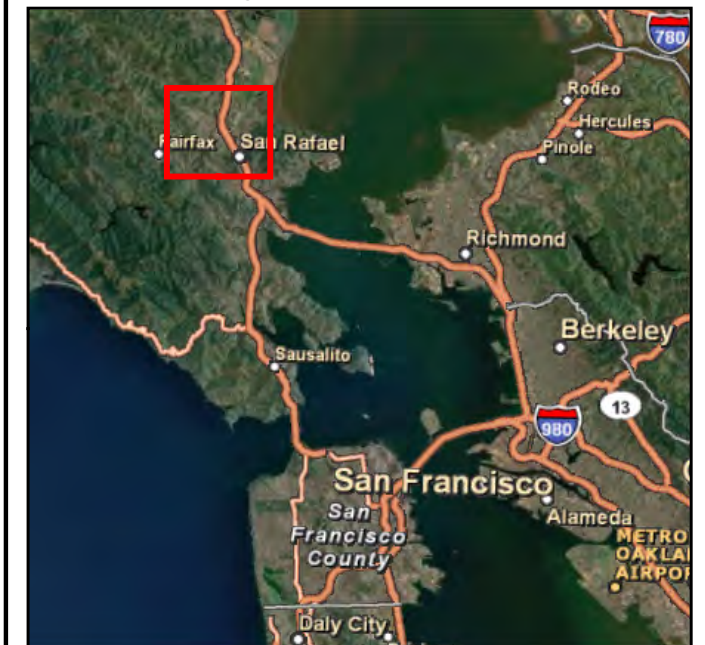
Las Gallinas Creek Hydrology Study

**Plate 7
Final Subbasin Delineation - Street Map**



Scale - 1:24,094
Scale - 1 in = 2,007.8 feet
0 1,000 2,000 4,000 Feet

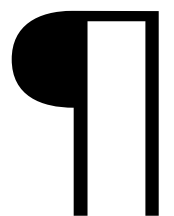
State Plane CA Zone III	Horz. Datum: NAD 83	Horz. Units: feet
	Vert. Datum: NAVD 88	2 June 2010

Regional Reference Map



Legend

-  Rain Gage
-  Streams
- World Street Map
-  Subbasins



Background Map Data Sources:
ESRI World Imagery

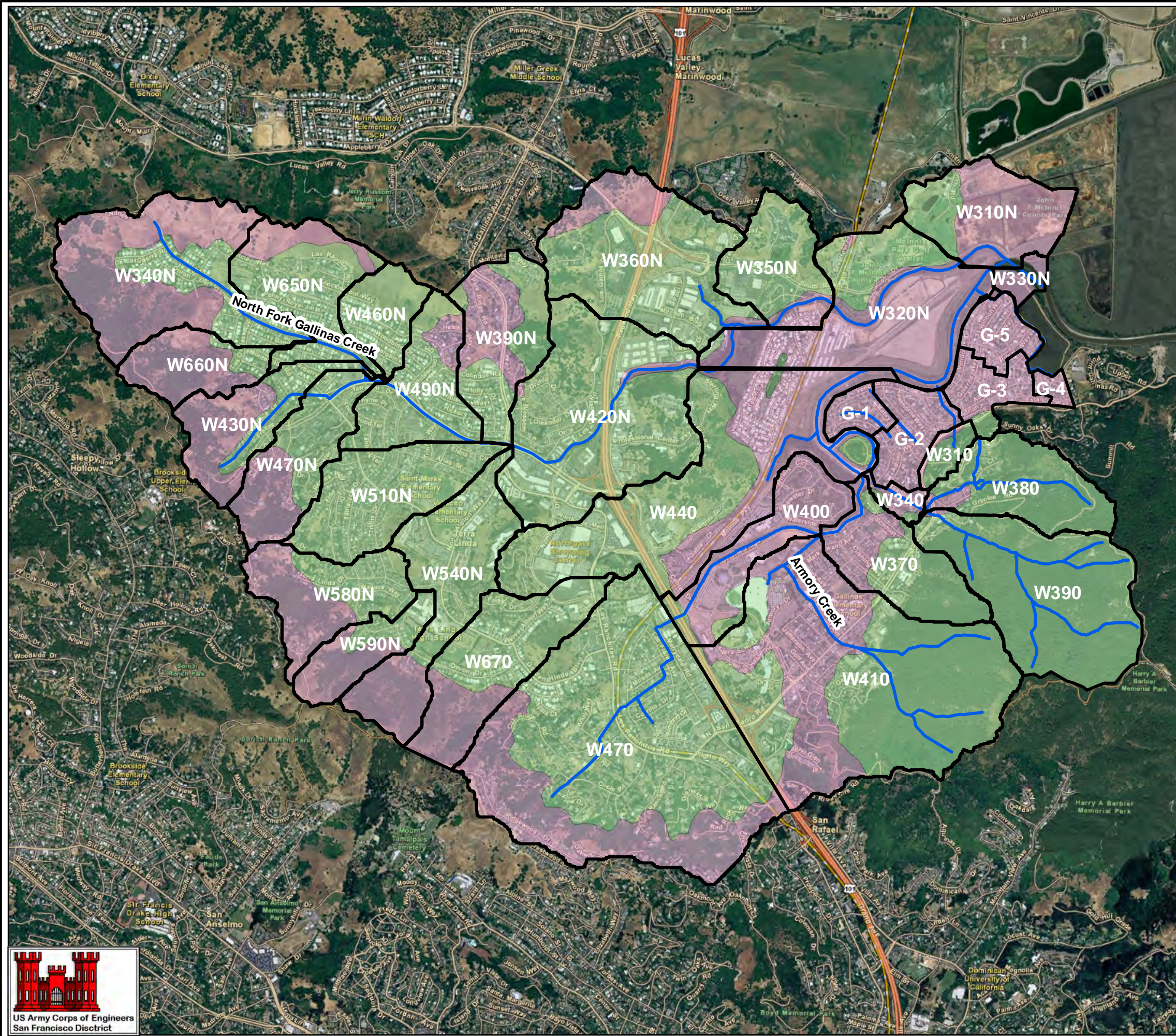
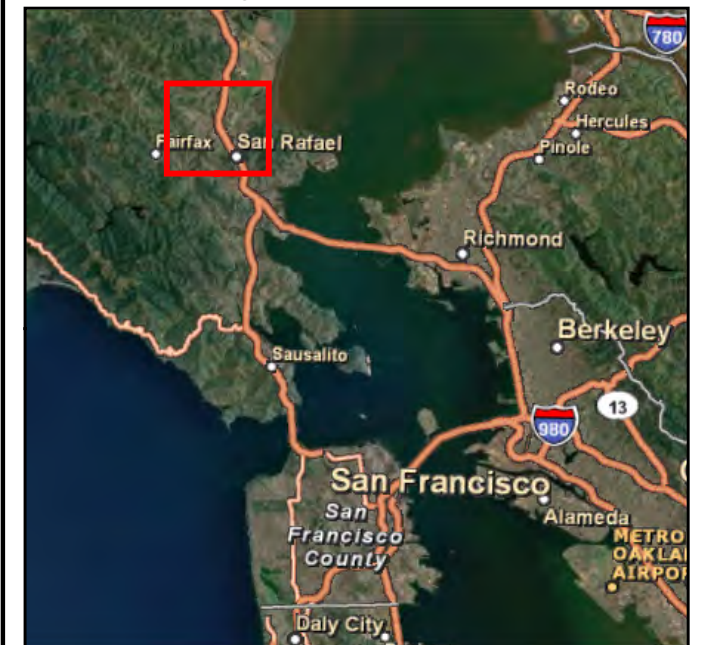
Las Gallinas Creek Hydrology Study

**Plate 8
Hydrologic Soil Group Distribution**





Scale - 1:24,000
Scale - 1 in = 2,000 feet
0 1,000 2,000 4,000 Feet

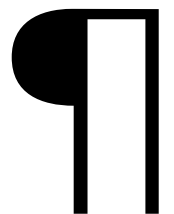
State Plane CA Zone III	Horz. Datum: NAD 83	Horz. Units: feet
	Vert. Datum: NAVD 88	2 June 2010

Regional Reference Map



Legend

-  Streams
-  Subbasins
-  Soil Group C
-  Soil Group D



Background Map Data Sources:
ESRI World Imagery

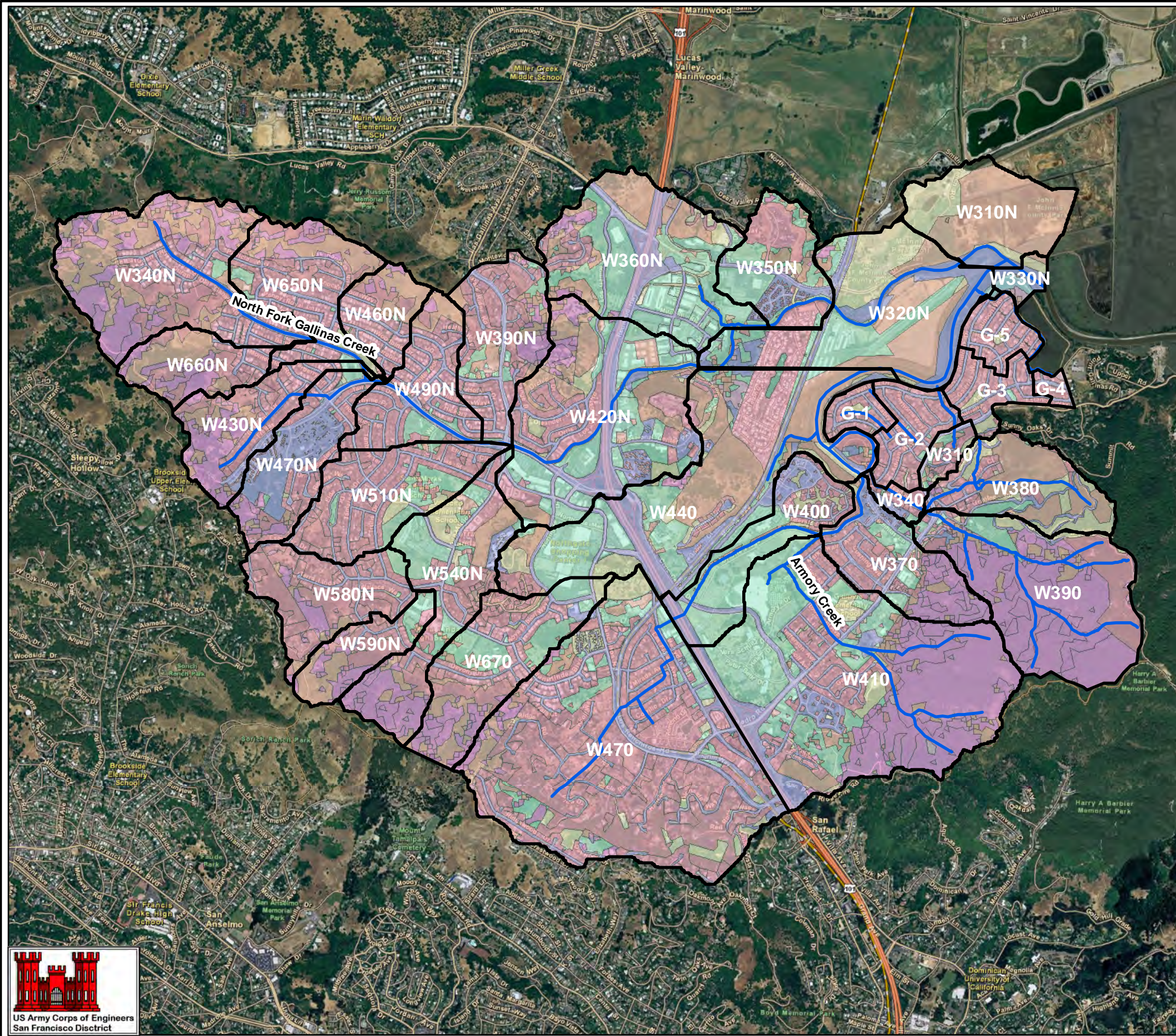
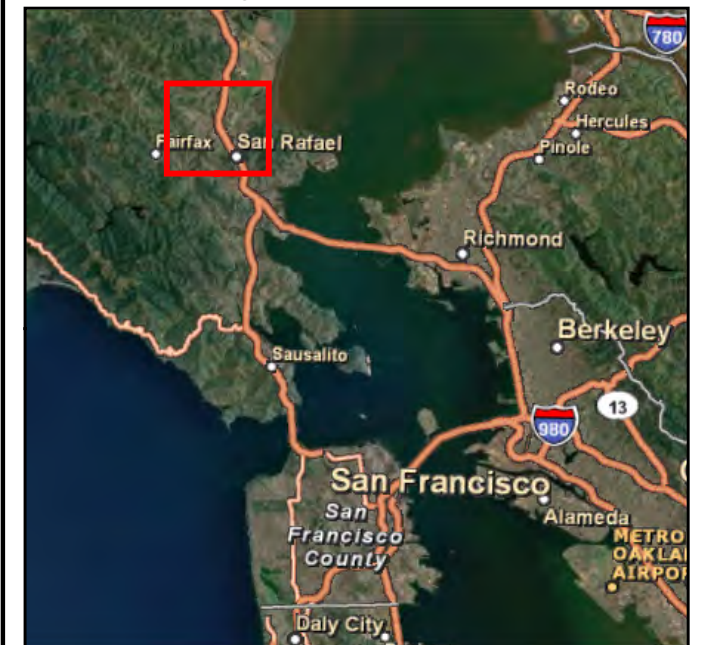
**Las Gallinas Creek
Hydrology Study**

**Plate 9
Land Use Distribution**

Scale - 1:24,000
Scale - 1 in = 2,000 feet
0 1,000 2,000 4,000 Feet

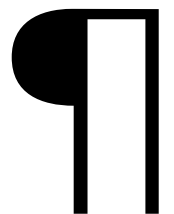
State Plane CA Zone III	Horz. Datum: NAD 83	Horz. Units: feet
	Vert. Datum: NAVD 88	2 June 2010

Regional Reference Map



Legend

- Subbasins
- Streams
- Agriculture
- Employment Areas
- Forest Land
- Infrastructure
- Rangeland
- Residential
- Urban Open
- Water
- Wetlands



Background Map Data Sources:
ESRI World Imagery

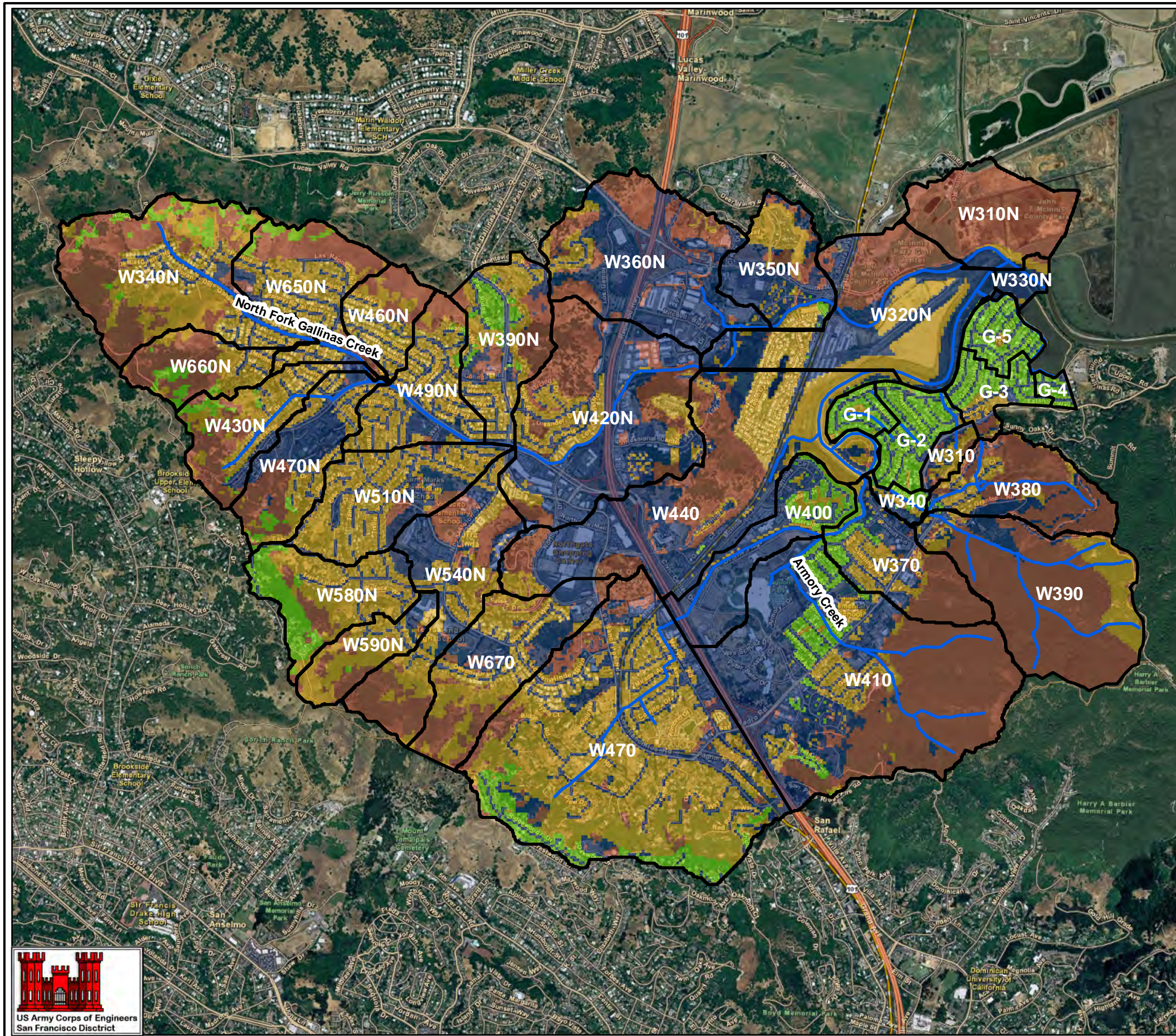
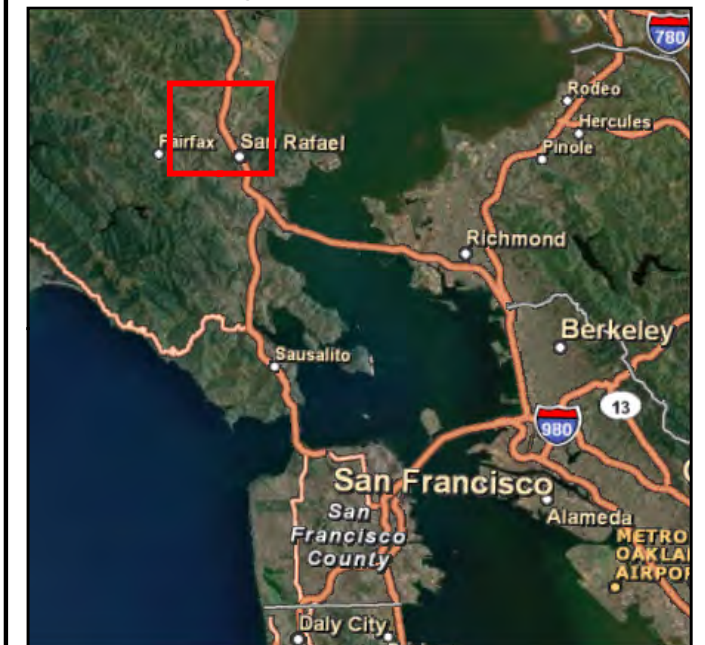


Las Gallinas Creek Hydrology Study
Plate 10
Curve Number Distribution

Scale - 1:24,000
 Scale - 1 in = 2,000 feet
 0 1,000 2,000 4,000 Feet

State Plane CA Zone III | Horz. Datum: NAD 83 | Horz. Units: feet
 | | Vert. Datum: NAVD 88 | 2 June 2010

Regional Reference Map



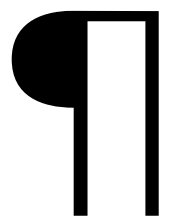
Legend

- Subbasins
- Streams

SCS Curve Number

VALUE

- 52 - 77
- 77 - 84
- 84 - 88
- 88 - 91
- 91 - 93



Background Map Data Sources:
 ESRI World Imagery



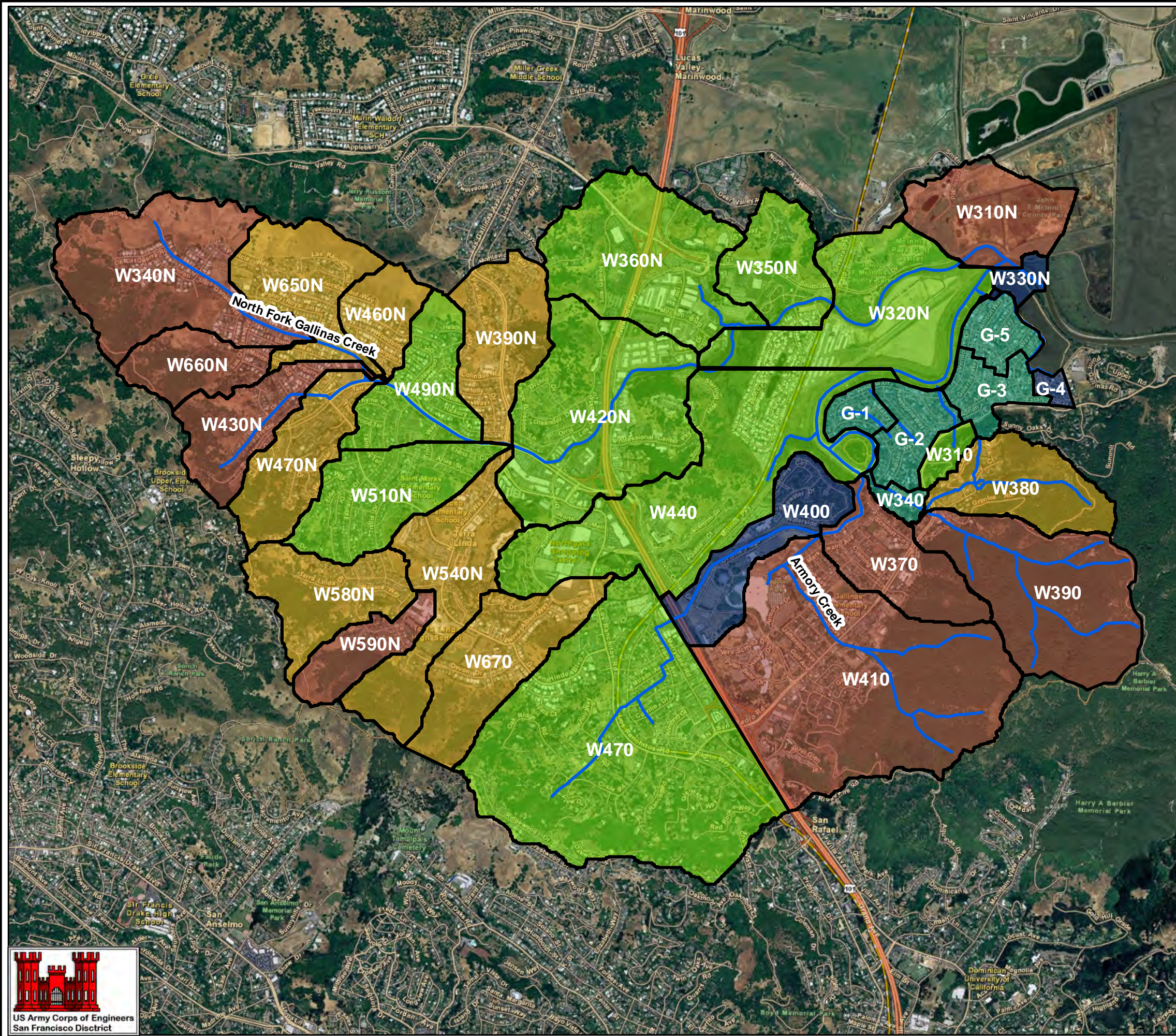
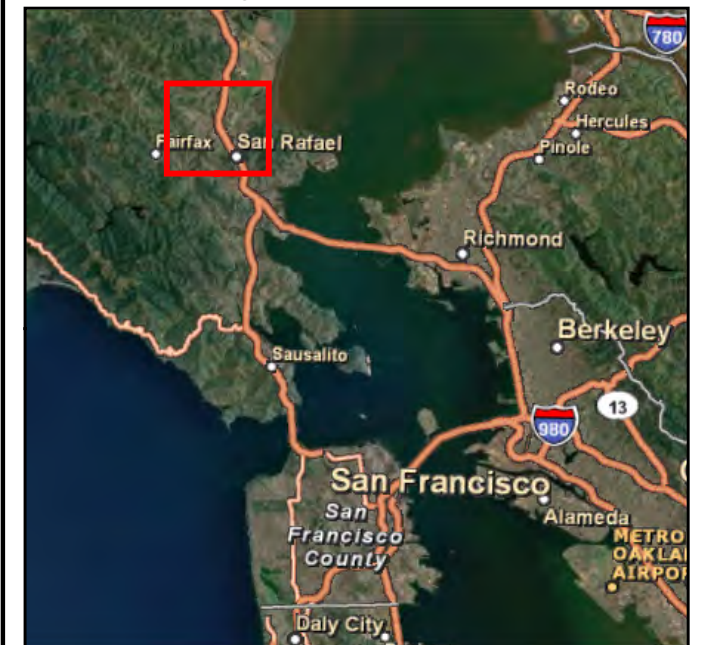
**Las Gallinas Creek
Hydrology Study**

**Plate 11
Composite Subbasin Curve Numbers**

Scale - 1:24,000
Scale - 1 in = 2,000 feet
0 1,000 2,000 4,000 Feet

State Plane CA Zone III	Horz. Datum: NAD 83	Horz. Units: feet
	Vert. Datum: NAVD 88	2 June 2010

Regional Reference Map

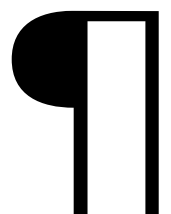


Legend

- Subbasins
- Streams

Composite Curve Number

- 52 - 77
- 77 - 84
- 84 - 88
- 88 - 91
- 91 - 93



Background Map Data Sources:
ESRI World Imagery



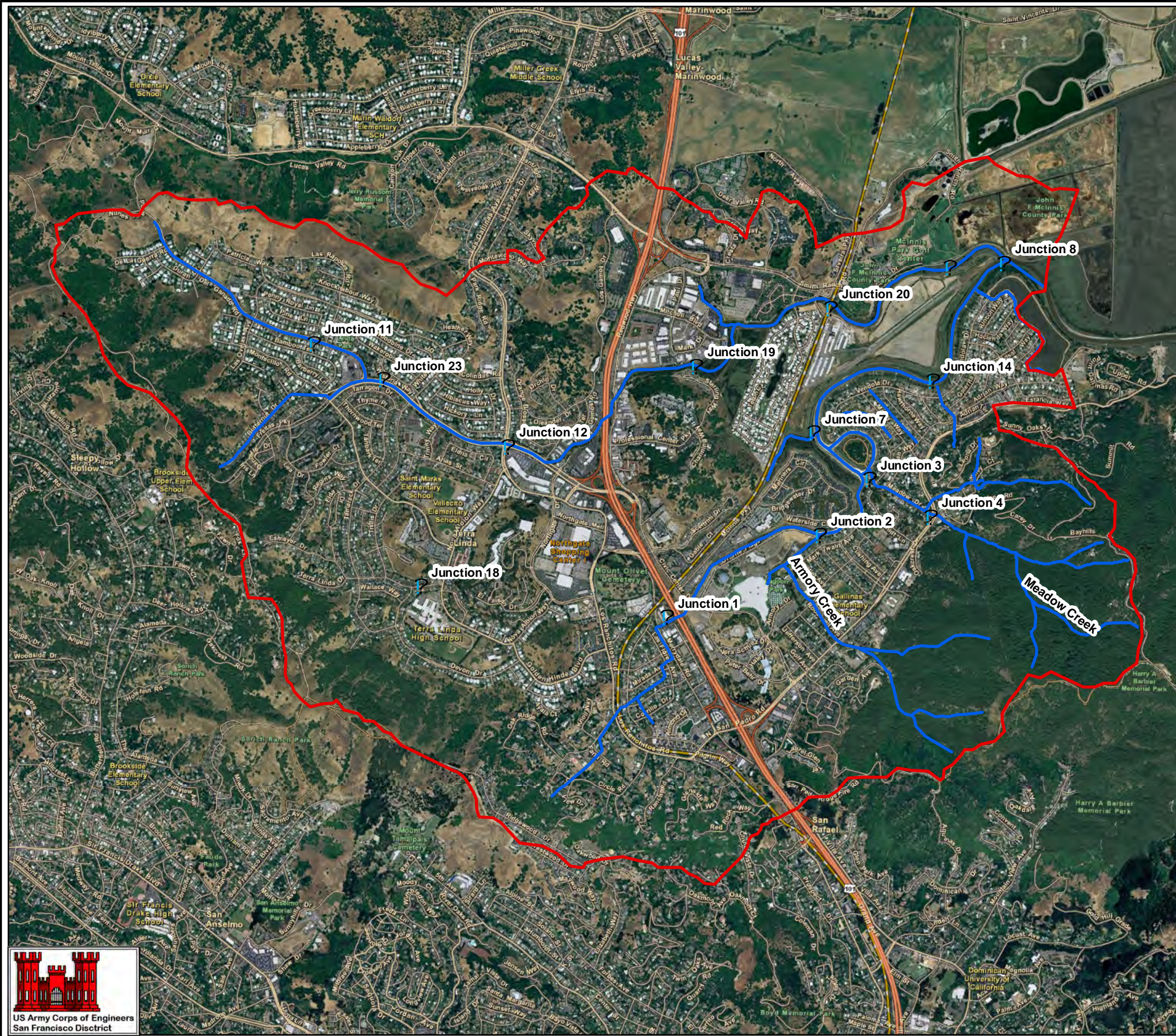
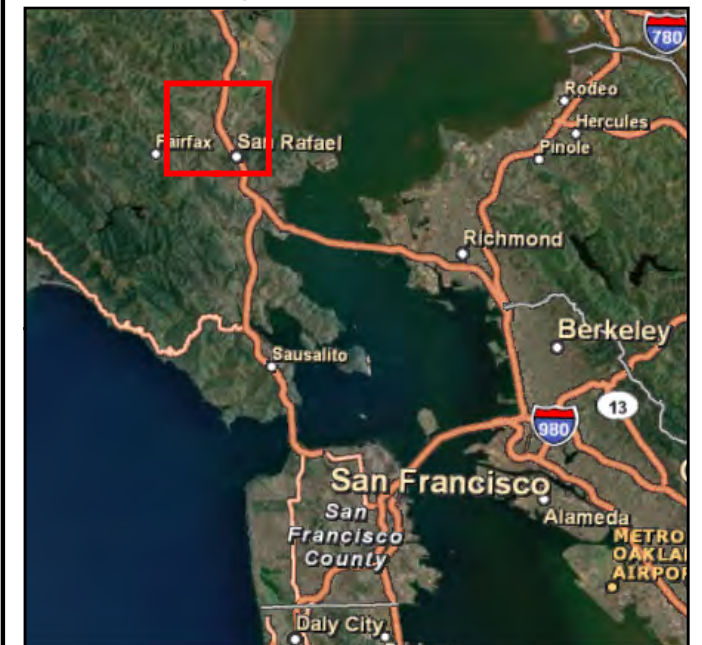
Las Gallinas Creek Hydrology Study

**Plate 12
Junction Location Map**




Scale - 1:24,000
Scale - 1 in = 2,000 feet
0 1,000 2,000 4,000 Feet

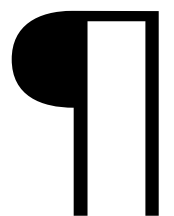
State Plane CA Zone III	Horz. Datum: NAD 83	Horz. Units: feet
	Vert. Datum: NAVD 88	2 June 2010

Regional Reference Map



Legend

-  Junctions
-  Watershed Boundary
-  Streams



Background Map Data Sources:
ESRI World Imagery

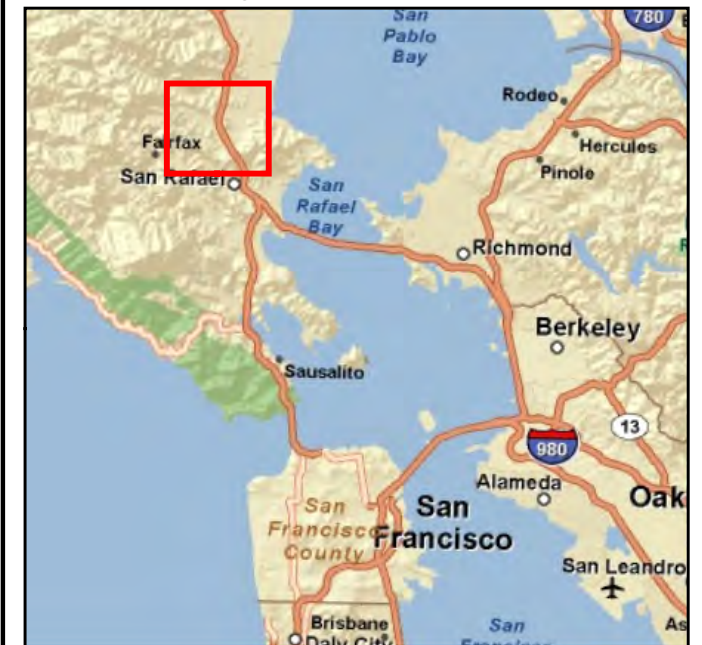
**Las Gallinas Creek
Hydrology Study**

**Plate 13
1% Peak Discharge Map**




Scale - 1:24,000
Scale - 1 in = 2,000 feet
0 1,000 2,000 4,000 Feet

State Plane CA Zone III	Horz. Datum: NAD 83	Horz. Units: feet
	Vert. Datum: NAVD 88	2 June 2010

Regional Reference Map

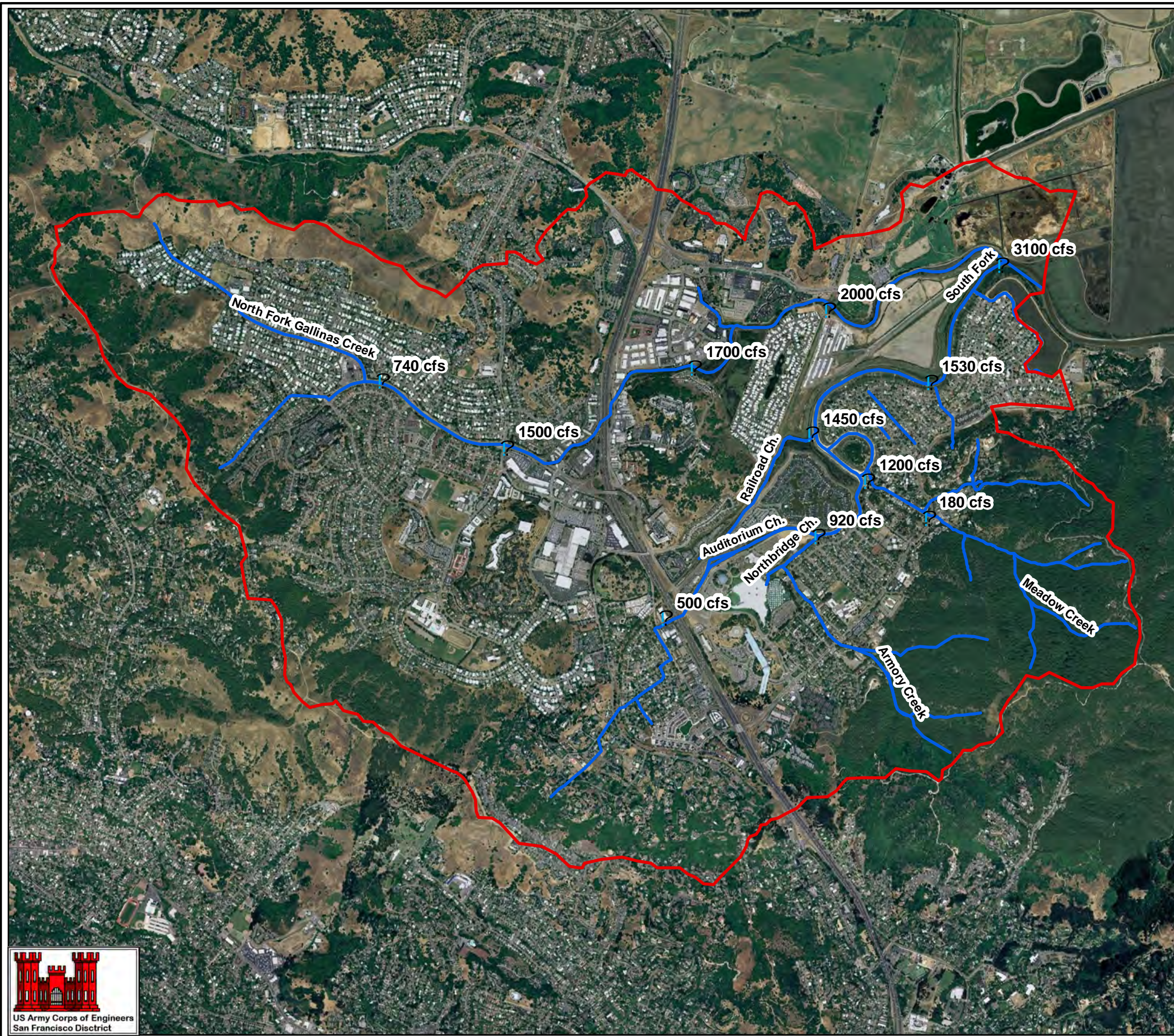


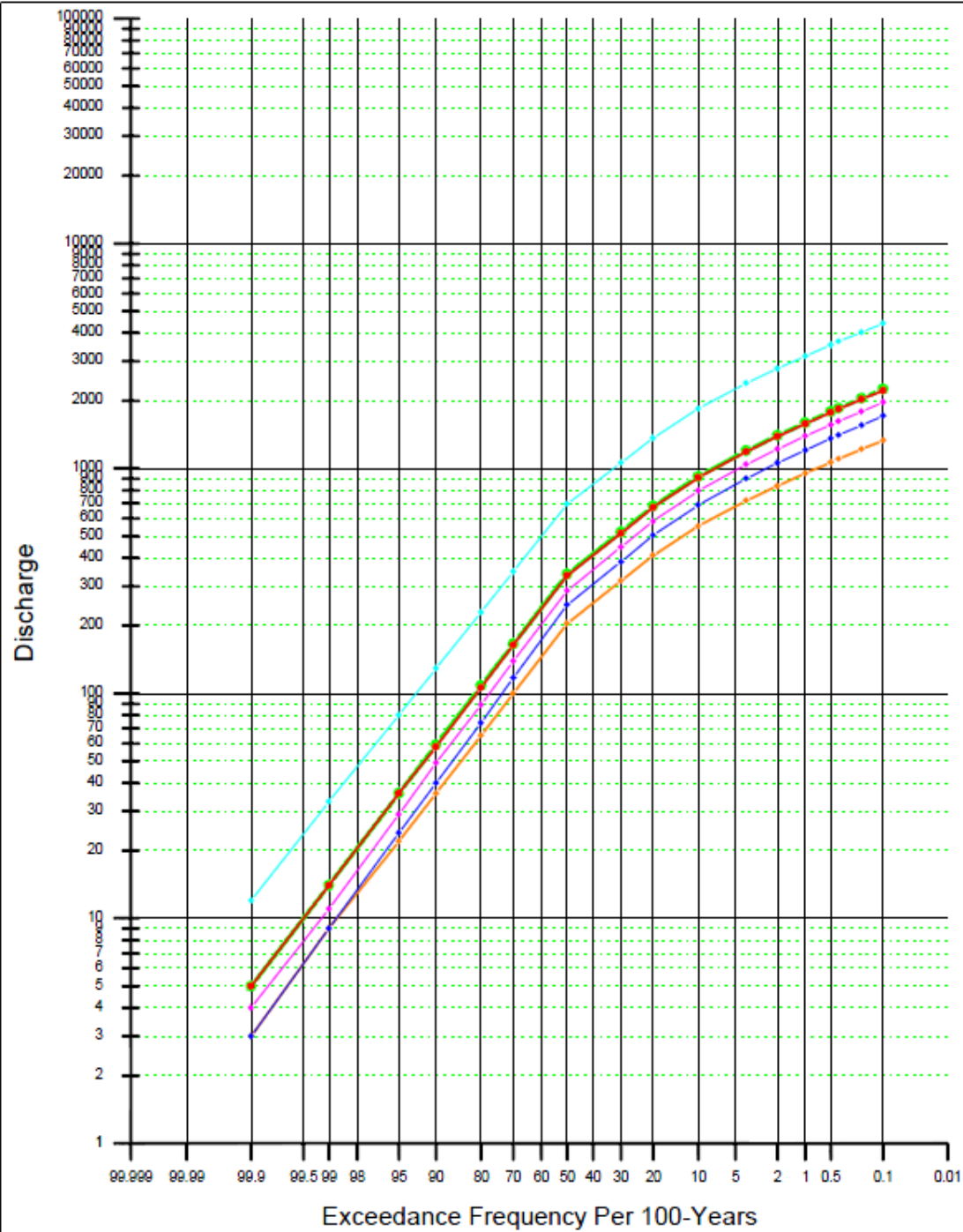
Legend

-  Peak Flow Locations
-  Watershed Boundary
-  Streams



Background Map Data Sources:
ESRI World Imagery





Legend:

- Junction 2 (cfs)
- ▲— Junction 3 (cfs)
- ◆— Junction 7 (cfs)
- Junction 14 (cfs)
- S. Fork Outlet (cfs)
- ▲— Junction 8 (cfs)

Index Point	DA (mi ²)
Junction-2	1.8
Junction-3	2.52
Junction-7	2.96
Junction-14	3.45
Outlet	3.51
Junction-8	7.42

Las Gallinas Hydrology Study Marin County, CA
Flow Frequency Curve Comparison Las Gallinas Creek Plate 14
US Army Corps of Engineers San Francisco District

Appendix D

Final Report

Las Gallinas Creek H&H & Coastal Analysis



Prepared For:
U.S. Army Corps of Engineers
San Francisco District



Prepared By:
Noble Consultants, Inc.



April 20, 2012

TABLE OF CONTENTS

1	INTRODUCTION.....	1
2	HEC-RAS MODEL DEVELOPMENT	3
2.1	DESCRIPTION OF HEC-RAS AND HEC-GEORAS MODELS	3
2.2	CHANNEL GEOMETRY	4
2.2.1	<i>Data Sources</i>	4
2.2.2	<i>Development of DTM</i>	5
2.2.3	<i>Development of Channel Geometry with HEC-GeoRAS</i>	6
2.2.4	<i>Refining of Geometric Data</i>	8
2.3	PEAK FLOW DISCHARGES	11
2.4	TIDAL DATUMS AT GALLINAS	13
2.5	HEC-RAS MODEL CALIBRATION	14
2.6	EXISTING CHANNEL FLOW CAPACITY	18
2.7	SENSITIVITY ANALYSIS.....	20
3	RIVERINE FLOODING ANALYSIS AND FLOODPLAIN DELINEATION	26
3.1	YEAR 0 (2011) CONDITION	26
3.2	YEAR 50 (2061) CONDITION	36
4	RISK AND UNCERTAINTY ANALYSIS	49
4.1	HEC-FDA MODEL	49
4.2	INDEX POINTS	49
4.3	COMPUTED MEDIAN WATER STAGES	51
4.4	UNCERTAINTY IN WATER STAGES	53
4.5	STAGE-DISCHARGE FUNCTIONS WITH UNCERTAINTIES	56
4.6	DISCHARGE EXCEEDANCE PROBABILITY FUNCTIONS WITH UNCERTAINTIES.....	60
4.7	TRANSFORM FLOW RELATIONSHIP FOR SANTA MARGARITA ISLAND RIGHT BRANCH	67
4.8	EVALUATION OF PROJECT PERFORMANCE.....	69
5	COASTAL STILL WATER LEVELS.....	74
5.1	COASTAL STILL WATER LEVEL FREQUENCY ANALYSIS FOR YEAR 0 CONDITION.....	74
5.1.1	<i>Water Level Frequency Analysis for San Francisco</i>	74
5.1.2	<i>Relation of Water Levels between Gallinas and San Francisco</i>	77

5.1.3	<i>Coastal Still Water Level Frequency Curve for Gallinas</i>	82
5.2	SEA LEVEL RISE	84
5.3	COASTAL STILL WATER LEVEL FREQUENCY ANALYSIS FOR YEAR 50 CONDITION	84
6	WAVES, WAVE RUNUP AND WAVE OVERTOPPING	86
6.1	PHYSICAL CHARACTERISTIC OF THE MARSH LEVEES	86
6.1.1	<i>Levee Crest Elevations</i>	87
6.1.2	<i>Inner Marsh Levee Sections</i>	91
6.2	WAVES	95
6.2.1	<i>Wind-Wave Hindcasting for Gallinas (Bay Waves)</i>	95
6.2.2	<i>Waves at the Inner Marsh Levee for Year 0 Condition</i>	102
6.2.3	<i>Waves at the Inner Marsh Levee for Year 50 Condition</i>	105
6.3	WAVE RUNUP AND WAVE OVERTOPPING FOR YEAR 0 CONDITION.....	109
6.3.1	<i>Maximum Wave Runup</i>	109
6.3.2	<i>Wave Overtopping Rates versus Still Water Levels</i>	112
6.3.3	<i>Representative Still Water Level (Tidal Stage) Hydrographs</i>	114
6.3.4	<i>Wave Overtopping during Extreme Storm Flood Events</i>	116
6.4	WAVE RUNUP AND WAVE OVERTOPPING FOR YEAR 50 CONDITION.....	119
6.4.1	<i>Maximum Wave Runup</i>	119
6.4.2	<i>Wave Overtopping Versus Still Water Levels</i>	119
6.4.3	<i>Representative Still Water Level (Tidal Stage) Hydrograph</i>	120
6.4.4	<i>Wave Overtopping During Extreme Coastal Flood Events</i>	120
7	COASTAL FLOODPLAIN MAPPING	131
7.1	STORAGE CAPACITY OF SANTA VENETIA COMMUNITY	131
7.2	COASTAL FLOODPLAIN MAPPING FOR YEAR 0 CONDITION.....	132
7.3	COASTAL FLOODPLAIN MAPPING FOR YEAR 50 CONDITION.....	132
7.4	UNCERTAINTY IN COASTAL FLOODING ANALYSIS	139
8	SUMMARY	141
9	REFERENCES	147

LIST OF FIGURES

Figure 1-1. Gallinas Creek Watershed Map.....2

Figure 2-1. Data Sources for Geometric Data5

Figure 2-2. Stationing of Las Gallinas Creek7

Figure 2-3. River Geometric Schematic.....8

Figure 2-4. Template for the Lower Portion of Channel Cross-Section Near Creek Mouth..... 10

Figure 2-5. Revised Cross-Section versus Raw (Incomplete) Section for Station 6+67 10

Figure 2-6. Flow Change Locations along Las Gallinas Creek..... 11

Figure 2-7. Water Surface Profiles for the February 25, 2004 Flood Event..... 16

Figure 2-8. Example 1: Redwood Flood Wall/Planter Box on Top of the Earthen Levee 17

Figure 2-9. Example 2: Redwood Flood Wall/Planter Box on Top of the Earthen Levee 17

Figure 2-10. Water Surface Profiles for the 1% and 0.2% AEP Flood Events (with MHHW at the Creek Mouth) 19

Figure 2-11. Sensitivity of the 100-Year Water Surface Profile to n-Values (with MHHW at the Creek Mouth)22

Figure 2-12. Sensitivity of the 100-Year Water Surface Profile to Downstream Water Levels ..23

Figure 2-13. Upper and Lower Bounds for 100-Year Water Surface Profile.....24

Figure 2-14. Upper and Lower Bounds for 500-Year Water Surface Profile.....25

Figure 3-1. Computed Water Surface Profiles for Eight Flood Events (Year 0 Condition).....27

Figure 3-2. Riverine Floodplain Map for the 50% AEP Flood Event (Year 0 Condition)28

Figure 3-3. Riverine Floodplain Map for the 20% AEP Flood Event (Year 0 Condition)29

Figure 3-4. Riverine Floodplain Map for the 10% AEP Flood Event (Year 0 Condition)30

Figure 3-5. Riverine Floodplain Map for the 4% AEP Flood Event (Year 0 Condition)31

Figure 3-6. Riverine Floodplain Map for the 2% AEP Flood Event (Year 0 Condition)32

Figure 3-7. Riverine Floodplain Map for the 1% AEP Flood Event (Year 0 Condition)33

Figure 3-8. Riverine Floodplain Map for the 0.4% AEP Flood Event (Year 0 Condition)34

Figure 3-9. Riverine Floodplain Map for the 0.2% AEP Flood Event (Year 0 Condition)35

Figure 3-10. Computed Water Surface Profiles for Eight Flood Events (Year 50 Condition).....37

Figure 3-11. Riverine Floodplain Map for the 50% AEP Flood Event (Year 50 Condition)38

Figure 3-12. Riverine Floodplain Map for the 20% AEP Flood Event (Year 50 Condition)39

Figure 3-13. Riverine Floodplain Map for the 10% AEP Flood Event (Year 50 Condition)40

Figure 3-14. Riverine Floodplain Map for the 4% AEP Flood Event (Year 50 Condition)41

Figure 3-15. Riverine Floodplain Map for the 2% AEP Flood Event (Year 50 Condition)	42
Figure 3-16. Riverine Floodplain Map for the 1% AEP Flood Event (Year 50 Condition)	43
Figure 3-17. Riverine Floodplain Map for the 0.4% AEP Flood Event (Year 50 Condition)	44
Figure 3-18. Riverine Floodplain Map for the 0.2% AEP Flood Event (Year 50 Condition)	45
Figure 3-19. 100-Year Water Surface Profiles for the Year 50 Condition Based on Various Sea Level Rise Scenarios	46
Figure 3-20. Riverine Floodplain Map for the 1% AEP Flood Event (Year 50 Condition, Modified NRC I SLR)	47
Figure 3-21. Riverine Floodplain Map for the 1% AEP Flood Event (Year 50 Condition, Modified NRC III SLR)	48
Figure 4-1. Locations of HEC-FDA Index Points	50
Figure 4-2. Stage-Discharge Function with Uncertainty at Index P3 (Year 0)	56
Figure 4-3. Stage-Discharge Function with Uncertainty at Index P6 (Year 0)	57
Figure 4-4. Stage-Discharge Function with Uncertainty at Index P8 (Year 0)	57
Figure 4-5. Stage-Discharge Function with Uncertainty at Index P13 (Year 0)	58
Figure 4-6. Stage-Discharge Function with Uncertainty at Index P3 (Year 50)	58
Figure 4-7. Stage-Discharge Function with Uncertainty at Index P6 (Year 50)	59
Figure 4-8. Stage-Discharge Function with Uncertainty at Index P8 (Year 50)	59
Figure 4-9. Stage-Discharge Function with Uncertainty at Index P13 (Year 50)	60
Figure 4-10. Discharge-Probability Function at Junction 8 (Index P1 through P4)	61
Figure 4-11. Discharge-Probability Function at Reach 11 (Index P5).....	62
Figure 4-12. Discharge-Probability Function at Junction 14 (Index P6 through P7)	63
Figure 4-13. Discharge-Probability Function at Junction 7 (Index P8 through P9)	64
Figure 4-14. Discharge-Probability Function at Junction 3 (Index P10 through P14)	65
Figure 4-15. Discharge-Probability Function at Junction 2 (Index P15).....	66
Figure 4-16. Transform Flow Relationship with Uncertainty for Santa Margarita Island Right Branch (Year 0 Condition).....	68
Figure 4-17. Transform Flow Relationship with Uncertainty for Santa Margarita Island Right Branch (Year 50 Condition).....	69
Figure 4-18. 90% and 95% CNP Stage Profiles and Right Levee Freeboards for the 1% AEP Flood Event (Year 0 Condition)	72
Figure 4-19. 90% and 95% CNP Stage Profiles and Right Levee Freeboards for the 1% AEP Flood Event (Year 50 Condition)	73

Figure 5-1. Still Water Level Frequency Curve for San Francisco	76
Figure 5-2. Annual Peak Tidal Elevation at San Francisco (Presidio) Station	76
Figure 5-3. Water Level Gauge Locations during the Hydrographic Surveys in February 2009 and in September 2005	78
Figure 5-4. Water Levels Measured in Las Gallinas Creek in February 9-10, 2009 Compared to Measured Water Levels at San Francisco	78
Figure 5-5. Water Levels Measured in Las Gallinas Creek in September 2005 Compared to Measured Water Levels at San Francisco	79
Figure 5-6. Daily Higher-High (HH) Tidal Stages at Richmond Compared to San Francisco	81
Figure 5-7. Difference in Daily Higher-High Water Levels between Richmond and San Francisco (1996-2010)	82
Figure 5-8. Still Water Level Frequency Curve for Gallinas (Year 0 Condition)	83
Figure 5-9. Still Water Level Frequency Curve for Gallinas (Year 50 Condition)	85
Figure 6-1. Inner/Outer Marsh Levees, and Bay front Levee Blocking Bay Waves	86
Figure 6-2. Levee Crest Profile for Outer Santa Venetia Marsh Levee	88
Figure 6-3. Levee Crest Profiles for Inner Santa Venetia Marsh Levee	89
Figure 6-4. Stationing of Inner and Outer Marsh Levees	90
Figure 6-5. Segments of Inner Marsh Levee and Levee Section Surveys	92
Figure 6-6. Cross Sections for Inner Marsh Levee, Segment 1a	93
Figure 6-7. Cross Sections of Inner Marsh Levee, Segment 1b	93
Figure 6-8. Cross Sections of Inner Marsh Levee, Segment 2	94
Figure 6-9. Wind Fetch for Gallinas, Mouth of Las Gallinas Creek	95
Figure 6-10. Hourly Wind Speed at the Hamilton AAF (Blue), Davis Point (Ryan), and Richmond (Black) Stations	99
Figure 6-11. Hourly Wind Speed at the San Francisco International Airport	100
Figure 6-12. Statistical Analysis of Annual Maximum Wave Heights Based on 32-Years Data Record	101
Figure 6-13. Statistical Analysis of Annual Maximum Wave Heights Based on 67-Year Data Record	101
Figure 6-14. Overtopping Flow Rate versus Still Water Levels (Year 0 Condition)	113
Figure 6-15. Water Levels Measured at San Francisco during January 1983 Storm Event	114
Figure 6-16. Templates for 25-Hour Still Water Level Hydrographs	115
Figure 6-17. Representative Still Water Level Hydrographs at Gallinas	115

Figure 6-18. Time Series of SWLs, Overtopping Flow Rates and Cumulated Water Volumes during the 250-Year Coastal Flood Event (Year 0 Condition) 117

Figure 6-19. Time Series of SWLs, Overtopping Flow Rates and Cumulated Water Volumes during the 500-Year Coastal Flood Event (Year 0 Condition) 118

Figure 6-20. Overtopping Flow Rate versus Still Water Levels for Year 50 Condition..... 123

Figure 6-21. Representative Year 50 Still Water Level Hydrographs at Gallinas 124

Figure 6-22. Time Series of SWLs, Overtopping Flow Rates and Cumulated Water Volumes during the 50-Year Coastal Flood Event (Year 50 Condition) 125

Figure 6-23. Time Series of SWLs, Overtopping Flow Rates and Cumulated Water Volumes during the 100-Year Coastal Flood Event (Year 50 Condition) 126

Figure 6-24. Time Series of SWLs, Overtopping Flow Rates and Cumulated Water Volumes during the 250-Year Coastal Flood Event (Year 50 Condition) 127

Figure 6-25. Time Series of SWLs, Overtopping Flow Rates and Cumulated Water Volumes during the 500-Year Coastal Flood Event (Year 50 Condition) 128

Figure 6-26. Time Series of SWLs, Overtopping Flow Rates and Cumulated Water Volumes during the 100-Year Coastal Flood Event (Year 50 Condition, NRC I) 129

Figure 6-27. Time Series of SWLs, Overtopping Flow Rates and Cumulated Water Volumes during the 100-Year Coastal Flood Event (Year 50 Condition, NRC III) 130

Figure 7-1. Water Storage Capacity of Santa Venetia Community 131

Figure 7-2. Coastal Floodplain Map for the 100-Year Coastal Flood Event for Year 50 Condition 134

Figure 7-3. Coastal Floodplain Map for the 250-Year Coastal Flood Event for Year 50 Condition 135

Figure 7-4. Coastal Floodplain Map for the 500-Year Coastal Flood Event for Year 50 Condition 136

Figure 7-5. Coastal Floodplain Map for the 100-Year Coastal Flood Event for Year 50 Condition (NRC I) 137

Figure 7-6. Coastal Floodplain Map for the 100-Year Coastal Flood Event for Year 50 Condition (NRC III) 138

LIST OF TABLES

Table 2-1. Peak Flow Discharges (cfs) Along South Fork, Las Gallinas Creek	12
Table 2-2. Tidal Datums (Feet, 1983-2001 Tidal Epoch)	13
Table 2-3. Uncertainties in HEC-RAS Model Parameters	20
Table 4-1. HEC-FDA Index Points	50
Table 4-2. Flow Discharges at Index Points for the Year 0 Condition.....	51
Table 4-3. Water Levels at Index Points for the Year 0 Condition	52
Table 4-4. Flow Discharges at Index Points for the Year 50 Condition	52
Table 4-5. Water Levels at Index Points for the Year 50 Condition	53
Table 4-6. HEC-RAS Model Parameters Used in Water Stage Uncertainty Analysis.....	54
Table 4-7. Standard Deviation of Error in Stages for the Year 0 Condition	55
Table 4-8. Standard Deviation of Error in Stages for the Year 50 Condition	55
Table 4-9. Discharge-Probability Function at Junction 8 (Index P1 through P4)	61
Table 4-10. Discharge-Probability Function at Reach 11 (Index P5)	62
Table 4-11. Discharge-Probability Function at Junction 14 (Index P6 through P7)	63
Table 4-12. Discharge-Probability Function at Junction 7 (Index P8 through P9)	64
Table 4-13. Discharge-Probability Function at Junction 3 (Index P10 through P14)	65
Table 4-14. Flood Frequency Distribution at Junction 2 (Index P15)	66
Table 4-15. Transform Flow Relationship with Uncertainty for Santa Margarita Island Right Branch (Index P10 through P13).....	68
Table 4-16. Project Performance Evaluation (Year 0 Condition)	70
Table 4-17. Project Performance Evaluation (Year 50 Condition)	71
Table 5-1. Annual Maximum Water Levels at San Francisco	75
Table 5-2. Difference in Peak Tidal Stages between Las Gallinas Creek and NOAA San Francisco Station for a Few Periods of Time	77
Table 5-3. Comparison of MHHW for Different NOAA Tidal Stations	80
Table 5-4. Annual Maximum Water Levels at Gallinas	83
Table 5-5. Annual Maximum Still Water Levels for Year 50 Condition	85
Table 6-1. Levee Characteristics of Inner Marsh Levee	92
Table 6-2. Wind Fetch Lengths and Water Depths at Gallinas	96
Table 6-3. Wind Waves at Gallinas for Eight Return Frequencies.....	98
Table 6-4. Bay Waves Propagating to the Inner Marsh Levee (Year 0 Condition)	103

Table 6-5. Wind-Waves Generated within the Marsh (Year 0 Condition)	104
Table 6-6. Waves at the Inner Marsh Levee (Year 0 Condition).....	105
Table 6-7. Bay Waves Propagating to the Inner Marsh Levee (Year 50 Condition)	106
Table 6-8. Wind-Waves Generated within the Marsh (Year 50 Condition)	107
Table 6-9. Waves at the Inner Marsh Levee (Year 50 Condition).....	108
Table 6-10. Maximum Wave Runup for Year 0 Condition	111
Table 6-11. Wave Overtopping Rate Versus Still Water Levels (Year 0 Condition)	113
Table 6-12. Capacities of Pump Stations.....	116
Table 6-13. Wave Runup for Year 50 Condition	121
Table 6-14. Wave Overtopping Rate for Given Still Water Levels for Year 50 Condition	122
Table 6-15. Coastal Flood Water Volumes in Santa Venetia Community (Year 50 Condition)	124
Table 7-1. Storage Capacity of Santa Venetia Community	132
Table 7-2. Coastal Flood Inundation for Santa Venetia Community (Year 50 Condition).....	133

1 INTRODUCTION

Las Gallinas Creek is located in San Rafael, California. It originates in open space owned by Marin County, above the community of Terra Linda. It has two forks (North and South), which join near the east end of the Smith Ranch Airport. The adjoining creek continues eastward for about 7,000 feet and flows into San Pablo Bay.

The creek basin has a drainage area of approximately 7.2 square miles, and is bounded by San Rafael Creek Basin to the south, Corte Madera Creek Basin to the west, Miller Creek to the north and China Camp State Park to the east. A watershed overview is shown in Figure 1-1. The area of interest for this analysis is the unincorporated area of Santa Venetia, which is located in southeastern Marin County approximately 14 miles north of San Francisco. This study area extends along the South Fork of Las Gallinas Creek from the confluence with Gallinas Creek to approximately 500 feet upstream of Santa Margarita Island.

The purpose of this study is to support the without project condition milestone. The scope of work includes (1) developing the floodplains maps for the without project condition for the Year 0 (2011) condition and for the without project future Year 50 (2061) condition, and (2) evaluating the project performance for the existing flood control system that protects the Santa Venetia community. It is noted that the project area may subject to flooding from a fluvial (riverine) flood event, a coastal storm event, or the combination of the both. For simplicity, the floodplain maps were developed in this analysis separately for the riverine flood events and for the coastal storm events. The riverine flooding analysis focused on the fluvial flood events in Las Gallinas Creek, assuming the still water level at the mouth of the creek was at the Mean Higher High Water level (MHHW). The coastal flooding analysis focused on the coastal storm events alone, neglecting the fluvial flows in Las Gallinas Creek.

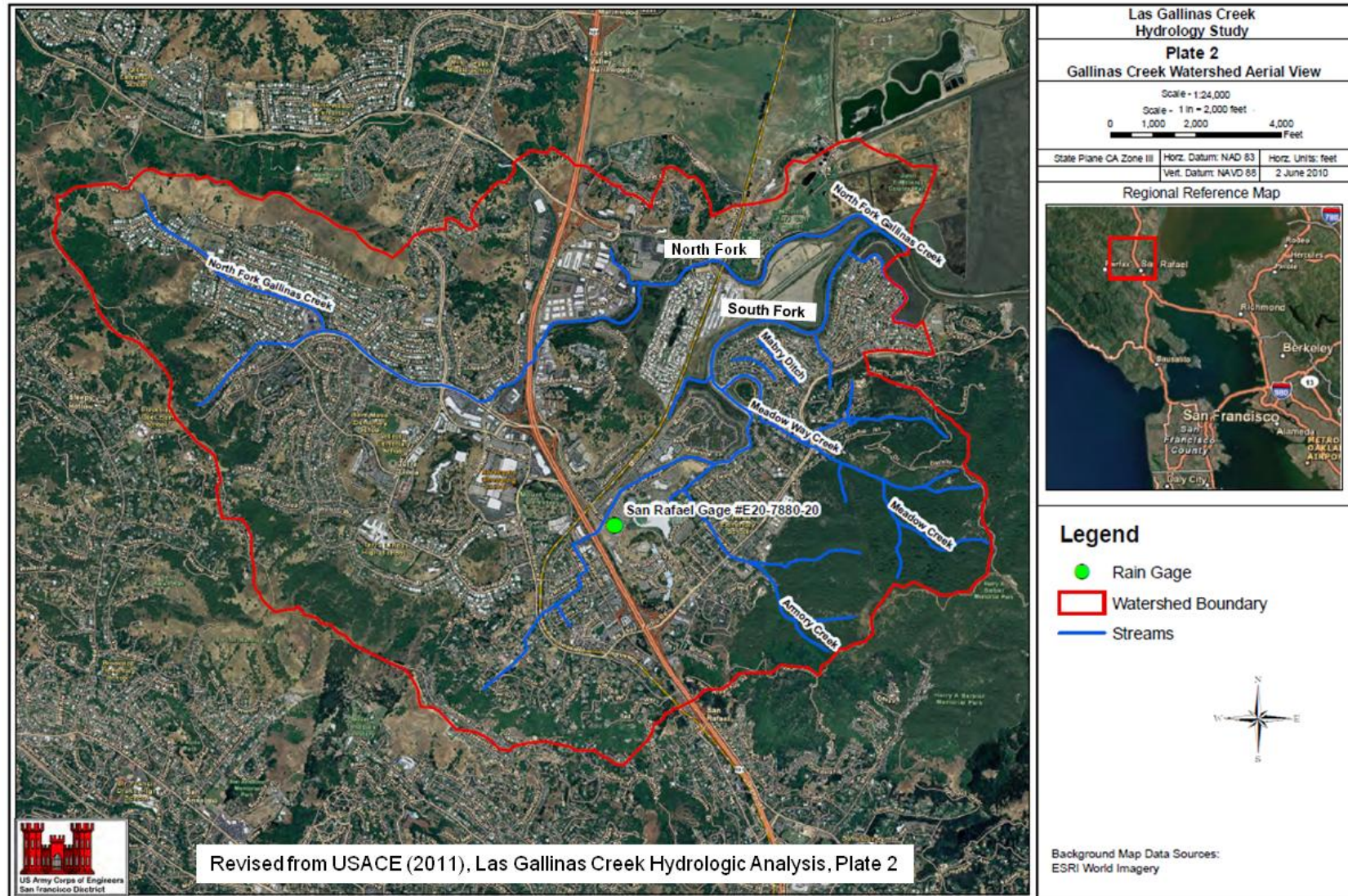


Figure 1-1. Gallinas Creek Watershed Map

2 HEC-RAS MODEL DEVELOPMENT

The U.S. Army Corps of Engineers River Analysis System (HEC-RAS) was used in the fluvial hydraulic analysis. The HEC-RAS model was designed to perform one-dimensional steady flow and unsteady flow calculations, sediment transport/mobile bed computations and water quality modeling (USACE 2008). The steady flow model with HEC-RAS and the ArcGIS tools HEC-GeoRAS were used in this analysis for the channel hydraulic modeling and riverine floodplain mapping.

2.1 Description of HEC-RAS and HEC-GeoRAS Models

The steady flow component of HEC-RAS is capable of modeling subcritical, supercritical, and mixed flow regime water surface profiles. The basic computational procedure is based on the solution of the one-dimensional energy equation. Energy losses are evaluated by friction (Manning's equation) and contraction/expansion (coefficient multiplied by the change in velocity head). The momentum equation is utilized in situations where the water surface profile is rapidly varied. These situations include mixed flow regime calculations, hydraulics of bridges, and evaluating profiles at river confluences. The effects of various hydraulic structures such as levees, bridges, culverts, weirs and other hydraulic structures can be included in the model computations.

Data input requirements for the steady flow model with HEC-RAS include (1) the geometric data for the river system and (2) the flow data and boundary conditions. The geometric data includes the river system connectivity (schematic), the cross-section data (geometry, Manning's roughness, contraction/expansion losses, ineffective flow areas, etc.), and the hydraulic structure data (levees, bridges, culverts, dams, weirs, etc.). The flow data includes the flow discharges at the upstream end of a reach and at the flow change locations. The boundary conditions are necessary to establish the starting water surface elevation at the ends of the river system. The boundary conditions are only required at the downstream ends of the river system for the subcritical flow regime.

HEC-GeoRAS is a set of procedures, tools, and utilities for processing geospatial data in ArcGIS using a graphical user interface (GUI). HEC-GeoRAS creates the geometric data for import into HEC-RAS and processes simulation results exported from HEC-RAS. The

geometric file is created from data extracted from data sets (ArcGIS layers) and from a Digital Terrain Model (DTM). HEC-GeoRAS requires a DTM represented by a triangulated irregular network (TIN) or a GRID. The water surface profile data and velocity data exported from HEC-RAS simulations can also be processed by HEC-GeoRAS for GIS analysis for floodplain mapping, flood damage computations, ecosystem restoration, and flood warning response and preparedness.

2.2 Channel Geometry

The channel geometry used in the HEC-RAS model was developed based on a channel topographic survey conducted for the area of interest in Las Gallinas Creek, the digital terrain model for the Gallinas watershed, and the levee crest elevations survey conducted for the Santa Venetia levee. All of the data was provided to us by the County of Marin. After creating a DTM by merging the channel topographic survey with the County's DTM for the watershed, the HEC-GeoRAS program was used to derive the channel geometric data for import into HEC-RAS, where the geometric data was refined and completed.

2.2.1 Data Sources

The digital terrain model for the Gallinas watershed was provided to us by the County in the format of a single-band floating-point raster image. This DTM was developed from the three sources, including the photogrammetric contours, the breaklines and waterlines, and the FEMA LIDAR points flown by Dewberry in 2007. Part of this DTM is shown in Figure 2-1.

The channel topographic survey covers the area of interest in Las Gallinas Creek, from the mouth of the creek up to approximately 500 feet upstream of Santa Margarita Island. This survey was conducted in February 9 and 10, 2009. The coverage of this survey is shown in Figure 2-1.

The levee crest elevation data for the Santa Venetia levee was surveyed in September and December, 2006. This levee profile survey covered the Santa Venetia levee from the beginning of the Santa Venetia inner marsh levee up to the Santa Margarita Island Bridge. The surveyed points are shown in Figure 2-1.

A bridge survey was conducted by the County in June, 2011 for the pedestrian bridge near Santa Margarita Island, which is referred to the Santa Margarita Island Bridge hereafter. This is the only bridge within the area of interest in Las Gallinas Creek. A spot elevation survey was conducted for multiple points along the high and low chords of the bridge deck. The surveyed points are shown in Figure 2-1.

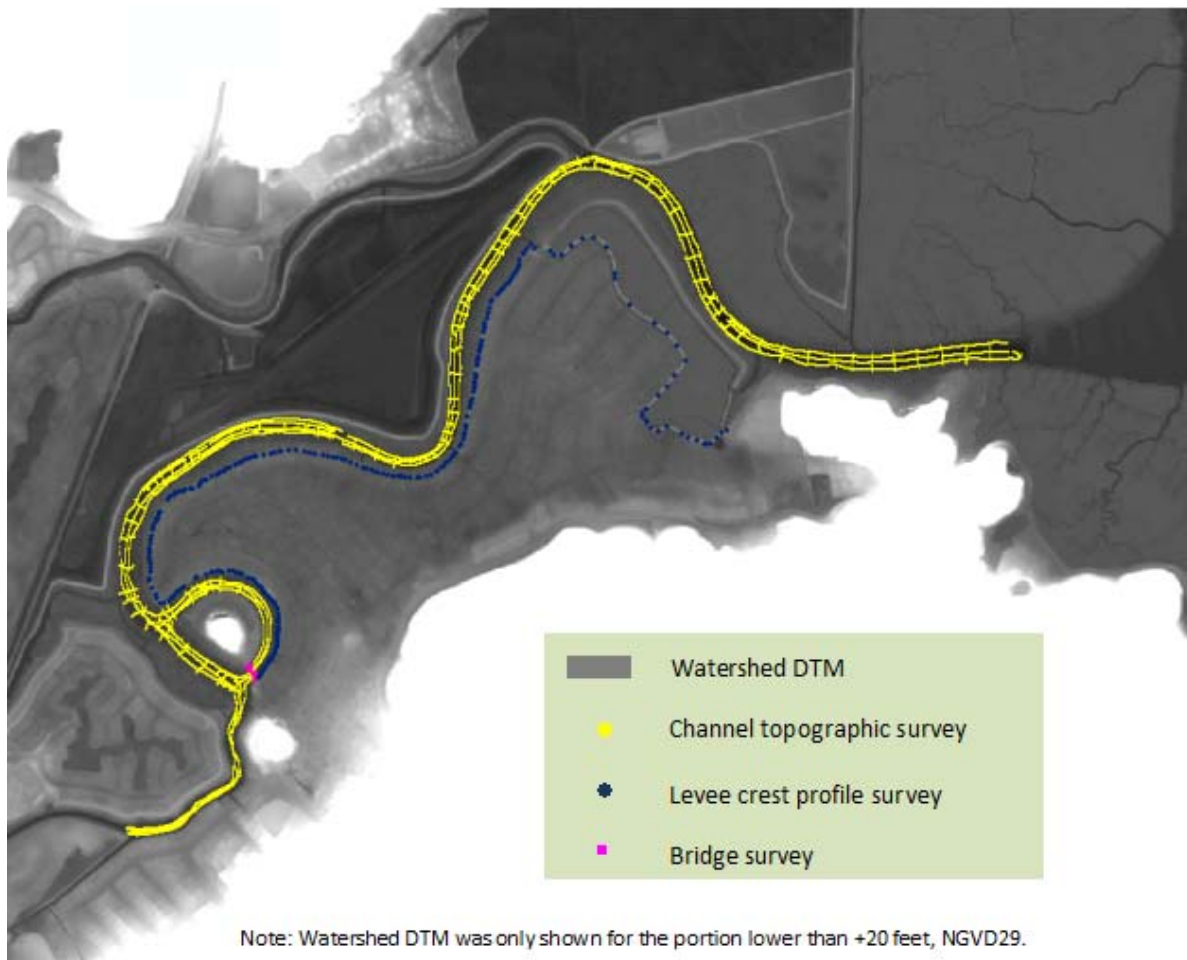


Figure 2-1. Data Sources for Geometric Data

2.2.2 Development of DTM

A DTM was developed in this study to represent the channel and floodplain topography for the project area based on the channel topographic survey and the DTM for the watershed. The channel survey data and the DTM of the watershed were first converted to the same coordinate

system and vertical datum with the same units. The adopted horizontal coordinate system is California State Plane, North American Datum of 1983 (NAD83), Zone 3. The vertical datum is National Geodetic Vertical Datum of 1929 (NGVD29). Project units are US Survey Feet.

The points collected during the channel topographic survey were merged into the DTM of the watershed, which only covers the higher portion of the channel with elevations higher than approximately -0.5 feet, NGVD29. This new DTM was generated in a raster format, as shown in Figure 2-1. This new DTM covered the full extents of the channel geometry for the South Fork and the Gallinas watershed.

2.2.3 Development of Channel Geometry with HEC-GeoRAS

The channel cross section data was created from the DTM using HEC-GeoRAS. The RAS layers created include the stream centerline layer, the XS (cross section) cut lines layer, the bank lines layer, the flow paths centerline layer, the levee alignment layer, and the bridges/culverts layer. The stream center and the river stationing along the centerline is shown in Figure 2-2. The length of the modeled reach is approximately 15,728 feet, or approximately 3 miles. The area of particular interest is from approximately Station 31+14 (east end of the Santa Venetia marsh levee) up to Station 143+13 (approximately 500 feet upstream of the Santa Margarita Island Bridge).

The geometry data generated with the HEC-GeoRAS for import to the HEC-RAS model mainly includes (1) the river reach stream lines and junctions (river system schematic), (2) cross sectional data, including the geometry of the cross sections (station-elevation data), downstream cross sectional reach lengths, main channel bank stations, and the levees locations (stations) and crest elevations, and (3) the preliminary deck information of the bridge.

The levee alignment layer was created to represent the levee systems or the high grounds along the creek. It is noted that the levees exist for the major portion of the modeled reach, except for an approximately 3000-foot long segment at the right bank of the creek mouth area, which is out of the area of interest. The levee alignment and the levee crest elevations were determined based on the levee crest profile survey conducted by the County in 2009 for the Santa Venetia levee, and based on the DTM for the other levees.



Figure 2-2. Stationing of Las Gallinas Creek

Four reaches with two stream junctions, 111 cross sections, and one bridge were used to represent the geometry condition of the 3-mile long channel with floodplains. The river geometric schematic is shown in Figure 2-3. The four reaches include the reach of South Fork upstream of the Santa Margarita Island, two branches around this island, and the reach downstream of this island.

The cross section cut lines were developed to be perpendicular to the direction of flow; therefore, the “dog-leg” shape cut lines were used for Santa Venetia that is located on the right side of the extremely meandering South Fork. As shown in Figure 2-3, the lateral extents of the cross sections extend from approximately the left levee, cross the channel and Santa Venetia, and end at the high ground bounded Santa Venetia on the south that is higher than +20 feet,

NGVD29. As discussed in Section 3, the fluvial flood flow will be conveyed within the channel between the left and right levees, no water will overtop the Santa Venetia levee, and there will be no flow being conveyed within Santa Venetia community during extreme flood events. Therefore, the cross sections used in the HEC-RAS model covered a much wider lateral extent than the waterways, and the right part of the cross sections to represent the Santa Venetia community has no impact on the riverine flooding analysis.

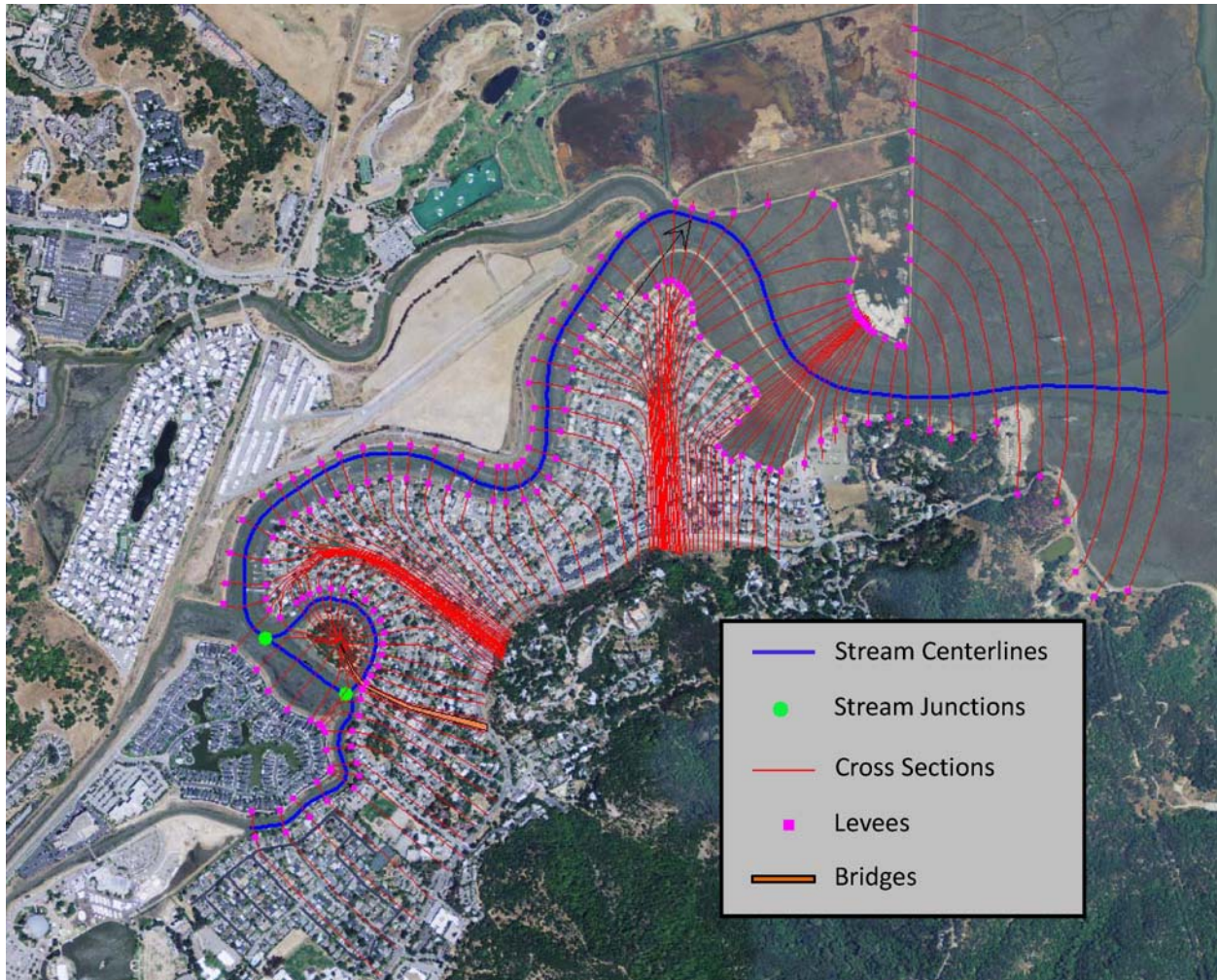


Figure 2-3. River Geometric Schematic

2.2.4 Refining of Geometric Data

After importing the geometry data into HEC-RAS, the data were further completed and refined. These include (1) adding Manning's roughness values, (2) filtering cross-section points and adjusting bank stations, if necessary, and (3) completing the bridge data.

The preliminary bridge data that was derived with HEC-GeoRAS for the Santa Margarita Island Bridge was updated and completed in HEC-RAS based on the bridge survey conducted by the county in June, 2011. The updated or new bridge data includes the bridge deck high chord and low chord profiles and bridge pier and abutment data.

The channel topographic survey conducted for Las Gallinas Creek did not cover the downstream segment of the modeled reach that is approximately 1,100 feet long. Thus, the cross sections derived based on the DTM did not cover the deeper part of the channel that is lower than approximately -0.5 feet, NGVD29 for this segment. In this analysis, the deeper part of the channel was completed for the five cross sections (at stations 0, 2+13, 4+44, 6+67, and 9+14) based on the template derived from the cross section at Station 11+15, which was covered in the channel topographic survey. The template of the lower part of the cross section is shown in Figure 2-4. The base width of the template is approximately 13 feet at the elevation of -6.5 feet, NGVD29, and the side slope is approximately 15 (horizontal) to 1 (vertical). Figure 2-5 shows an example for the original incomplete cross section derived from the DEM, and the updated cross section after completing the deeper channel with the template.

It is noted that the revision to the deeper part of these five cross sections at the 1,100 feet long downstream segment will only have insignificant impact to the water levels at the creek mouth, and will have negligible impact for the area of interest during the extreme flood events. A sensitivity test was conducted by assuming a 3-foot channel shoaling for the five cross-sections within this downstream segment. The resulting difference in the 100-year water level did not exceed 0.04 feet for this downstream segment; and was less than 0.02 feet for the area of interest (upstream of Station 31+14), which is within the resolution tolerance of the model results.

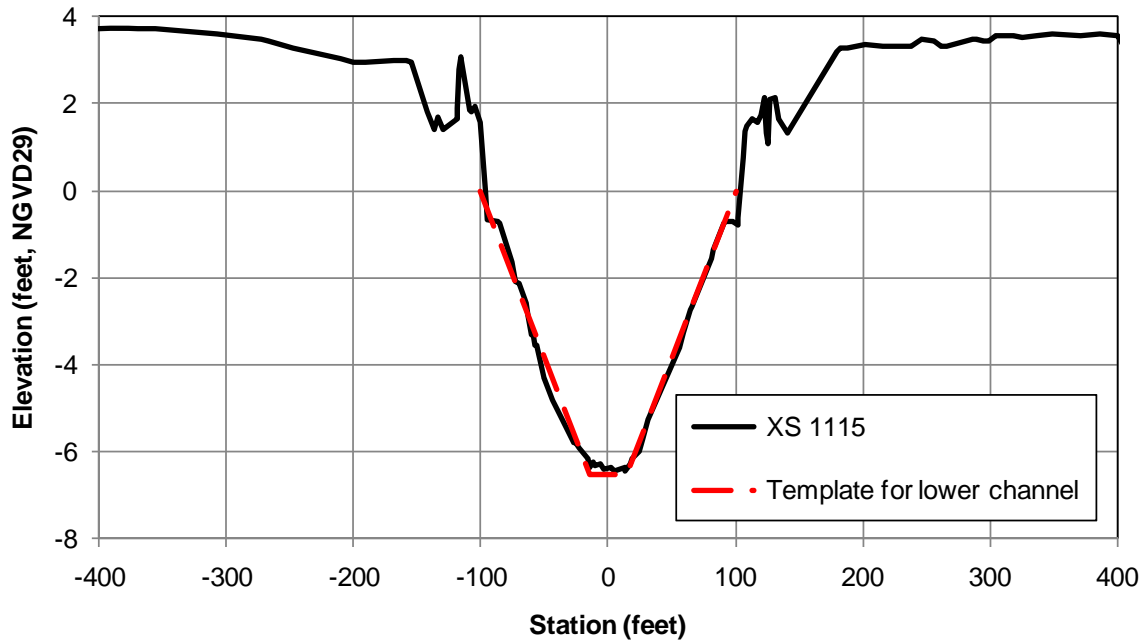


Figure 2-4. Template for the Lower Portion of Channel Cross-Section Near Creek Mouth

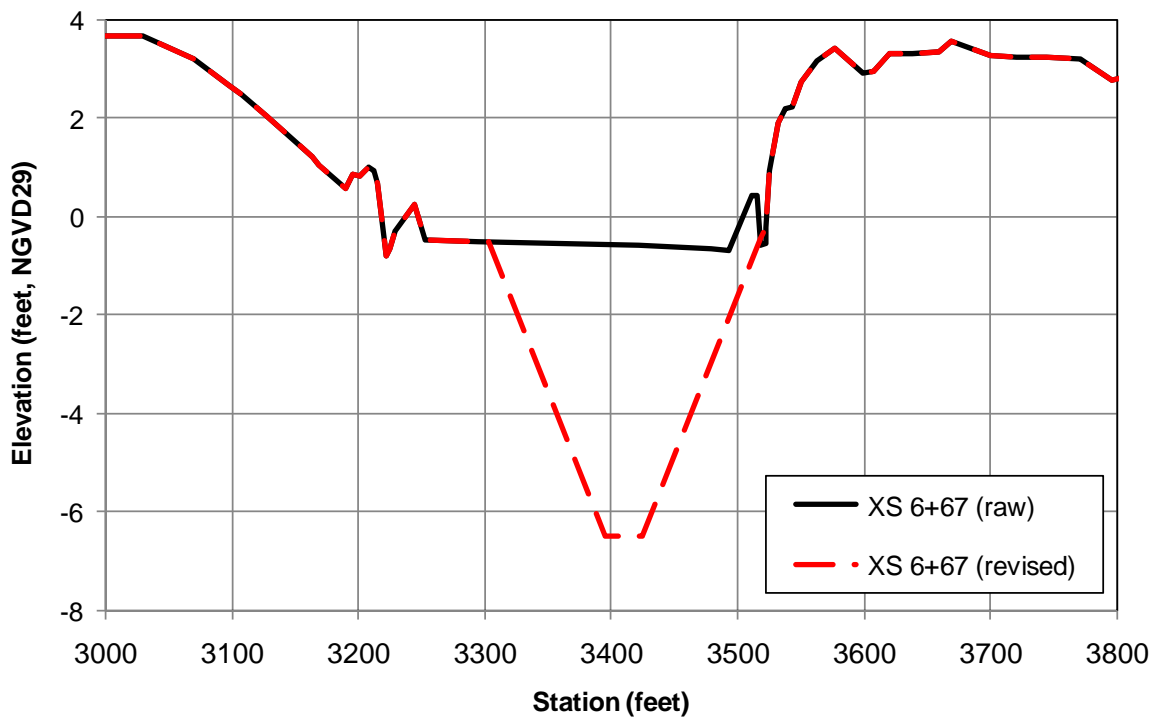


Figure 2-5. Revised Cross-Section versus Raw (Incomplete) Section for Station 6+67

2.3 Peak Flow Discharges

A hydrologic analysis was conducted by Noble Consultants, Inc. (NCI) and et al. in 2009 for the South Fork Drainage Basin. This hydrologic analysis was later updated and expanded to include the entire Las Gallinas Creek watershed by the U.S. Army Corps of Engineers, San Francisco District (USACE-SPN) in 2011. This present hydraulic analysis was conducted based on the updated hydrologic analysis conducted by the Corps (USACE-SPN, 2011).

Six hydrologic junction points were identified along the South Fork of Las Gallinas Creek in the Corps (2011) hydrologic study, which were named Junction 2, Junction 3, Junction 7, Junction 14, Reach 11, and Junction 8, from the upstream to the downstream. The locations of these junction points and the corresponding river stations (in HEC-RAS) are shown in Figure 2-6. The peak flow discharges computed for these junction locations are listed in Table 2-1 for the eight return frequencies. Among these hydrologic junction points, Junction 2 is located at the upstream boundary of the modeled reach, and other junctions were modeled as the flow change locations in the HEC-RAS model.

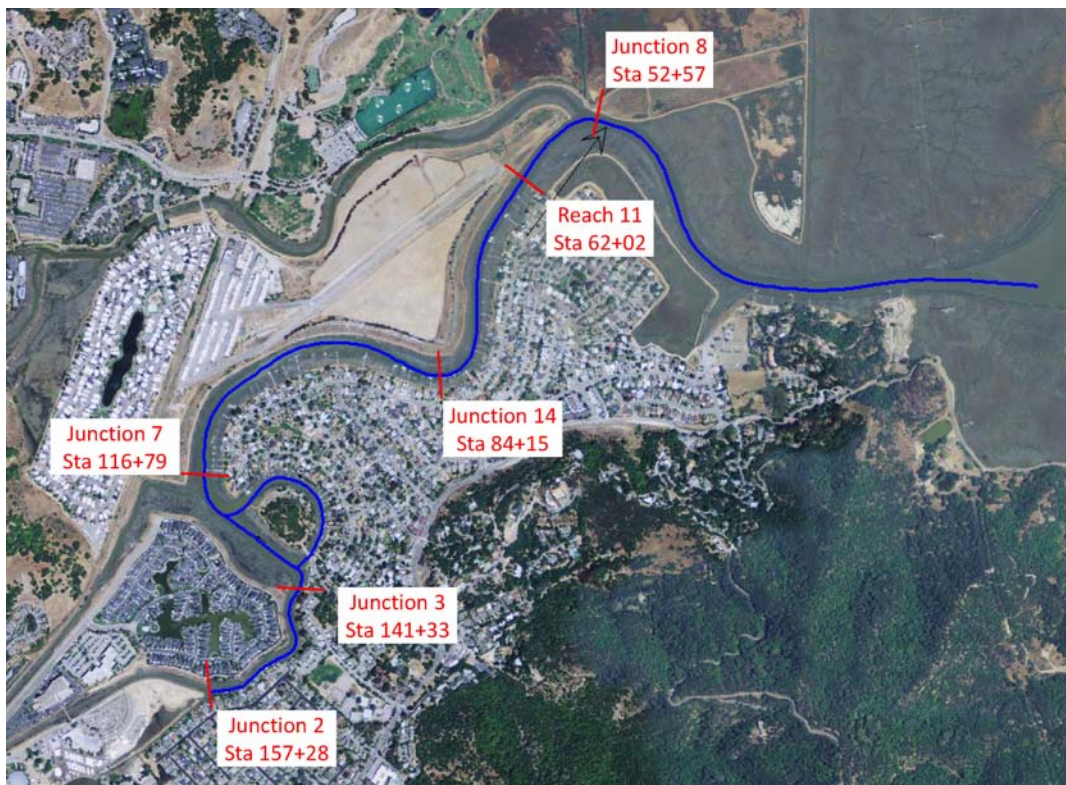


Figure 2-6. Flow Change Locations along Las Gallinas Creek

Table 2-1. Peak Flow Discharges (cfs) Along South Fork, Las Gallinas Creek

Hydrology Junction	Flow Change Location (HEC-RAS River Sta)	0.5 2-yr	0.2 5-yr	0.1 10-yr	0.04 25-yr	0.02 50-yr	0.01 100-yr	0.004 250-yr	0.002 500-yr
Junction 2	14,710	205	410	553	718	837	951	1,101	1,215
Junction 3	13,115	247	504	687	902	1,056	1,206	1,405	1,555
Junction 7	11,679	286	583	795	1,042	1,220	1,393	1,621	1,794
Junction 14	8,415	334	670	908	1,185	1,383	1,577	1,833	2,025
Reach 11	6,202	340	679	920	1,200	1,401	1,596	1,854	2,049
Junction 8	5,257	693	1,369	1,843	2,390	2,778	3,159	3,658	4,030

Source: The peak flow discharges are presented in USACE-SPN (2011). Las Gallinas Creek Hydrologic Analysis. The flow change locations used in the HEC-RAS model are equivalent to the hydrologic junction locations.

2.4 Tidal Datums at Gallinas

The downstream water surface elevation at the mouth of the Las Gallinas Creek was controlled by the water (tidal) level in San Pablo Bay. Among the tidal stations administrated by the National Oceanic and Atmospheric Administration (NOAA), the Gallinas Station (Station ID: 9415052) is located at the mouth of the creek. The tidal datums relative to the Mean Lower Low Water (MLLW) were published by NOAA and are listed in Table 2-2 for this station. However, the relation between MLLW and NGVD29, which was used as the vertical datum in this hydraulic analysis, was not available for this station. Another NOAA tidal station, the Hamilton AFB Station, Outside Gage (Station ID: 9415124) is also located close to the mouth of the creek. The tidal datums relative to MLLW and the relationship between MLLW and NGVD29 were published by NOAA, as also listed in Table 2-2. Therefore, the tidal datums relative to NGVD29 at the Hamilton AFB station were used in this analysis to represent the tidal stages at the mouth of Las Gallinas Creek. Based on the NOAA tidal datums, the MHHW at the mouth of the creek is at approximately +3.58 feet, NGVD29.

Table 2-2. Tidal Datums (Feet, 1983-2001 Tidal Epoch)

Tidal Datums	Gallinas ID: 9415052	Hamilton AFB (Outside) ID: 9415124	San Francisco ID: 9414290
Mean Higher High Water (MHHW)	+5.92	+6.04	+5.84
Mean High Water (MHW)	+5.31	+5.45	+5.23
Mean Tide Level (MTL)	+3.16	+3.28	+3.18
Mean Sea Level (MSL)	+3.13	+3.23	+3.12
National Geodetic Vertical Datum (NGVD29)	N/A	+2.47	+2.63
Mean Low Water (MLW)	+1.01	+1.09	+1.14
Mean Lower Low Water	0.00	0.00	0.00
North American Vertical Datum (NAVD88)	N/A	-0.21	-0.08

2.5 HEC-RAS Model Calibration

The HEC-RAS model calibration involves an adjustment of the Manning's roughness coefficients to obtain reasonable agreement between the measured and computed hydraulic parameters, such as the river stages and flow velocities. However, little information on stream flow and river stage data exists for the South Fork of Las Gallinas Creek during the flood events. As a result, the HEC-RAS model cannot be calibrated with any measured data or high watermarks.

Based on the KHE (2004) study, no significant out-of-bank-flooding was observed during the February 25, 2004 flood event though it was one of the largest observed floods in residents' memory. By comparing the stream flow data measured at Las Pavadas Avenue Bridge in North Gallinas Creek and their hydrologic analysis, KHE(2004) concluded that the February 25, 2004 flood event was approximately a 50-year flood event. This study appears to be the most "complete" information that we can use to conduct a qualitative "calibration" (or a first reality check) of the HEC-RAS model.

The flow discharges along the South Fork of Las Gallinas Creek were not analyzed in the KHE (2004) study. The 50-year flow event determined in the Corps (2011) hydrologic study was used in this analysis to approximate the February 25, 2004 flood event for the South Fork.

Still water level data were not measured at the mouth of the Las Gallinas Creek (Gallinas) during this flood event. Alternatively, the still water level at Gallinas was estimated based on the still water levels measured at San Francisco. The tides at Gallinas are different from San Francisco in phase and in magnitude. The tidal phase lag is approximately one to two hours (a given tidal phase at San Francisco arrives Gallinas in one to two hours). As discussed in Section 5.1.2, the maximum still water level at Gallinas is approximately 0.37 feet higher than San Francisco. The peak flow discharge occurred at approximately 8:00 am during the February 25, 2004 flood event. The water level coincident with the peak flow discharge was thus approximated by the water level measured at San Francisco at 6:30 am (+1.02 feet, NGVD29) by adding 0.37 feet. This estimated water level at +1.39 feet, NGVD29 was used as the downstream (water level) boundary condition for the model calibration with the February 25, 2004 flood event.

The water surface profile computed with the HEC-RAS model for the February 25, 2004 flood event, compared to the levee crest elevation profiles, is shown in Figure 2-7. The adopted Manning's roughness coefficient was 0.035 for the main channel which is bounded by the left and the right levees, was 0.050 for the left floodplain which is located outside of the left levee, and was 0.100 for the right floodplain which is the Santa Venetia community located outside of the right levee.

Based on the HEC-RAS Reference Manual (USACE, 2008b), the Manning's roughness value (n-value) for a winding and sluggish earthen channel ranges between 0.025 and 0.033 with a normal value of 0.030 if grass and some weeds exist in the channel, and ranges between 0.030 and 0.040 with a normal value of 0.035 if dense weeds or aquatic plants exist in the channel. The latter channel condition with a normal n-value of 0.035 was used in this analysis to be conservative.

It is noted that there are more than 50 marina/dock structures in the channel. These structures will reduce the flow areas and increase the resistance to the flow. The impact of these structures was modeled by increasing the roughness value in the HEC-RAS model. This is another reason to use a more conservative n-value (0.035) for the channel.

The Manning's roughness values for the floodplains were also selected based on the HEC-RAS Reference Manual. The left floodplain has scattered brush and heavy woods, which has a n-value ranging from 0.035 to 0.070 with the normal value of 0.050. The right floodplain (Santa Venetia) is equivalent to a floodplain with intensive flow resistance and heavy stand of structures blocking the flow, which has a n-value varying between 0.08 to 0.12 with the normal value of 0.10. As discussed in Section 3, the water will be conveyed within the channel between the left and right levees during the extreme flood events. Therefore, the n-values selected for the left and right floodplains have no impact on the riverine flooding analysis.

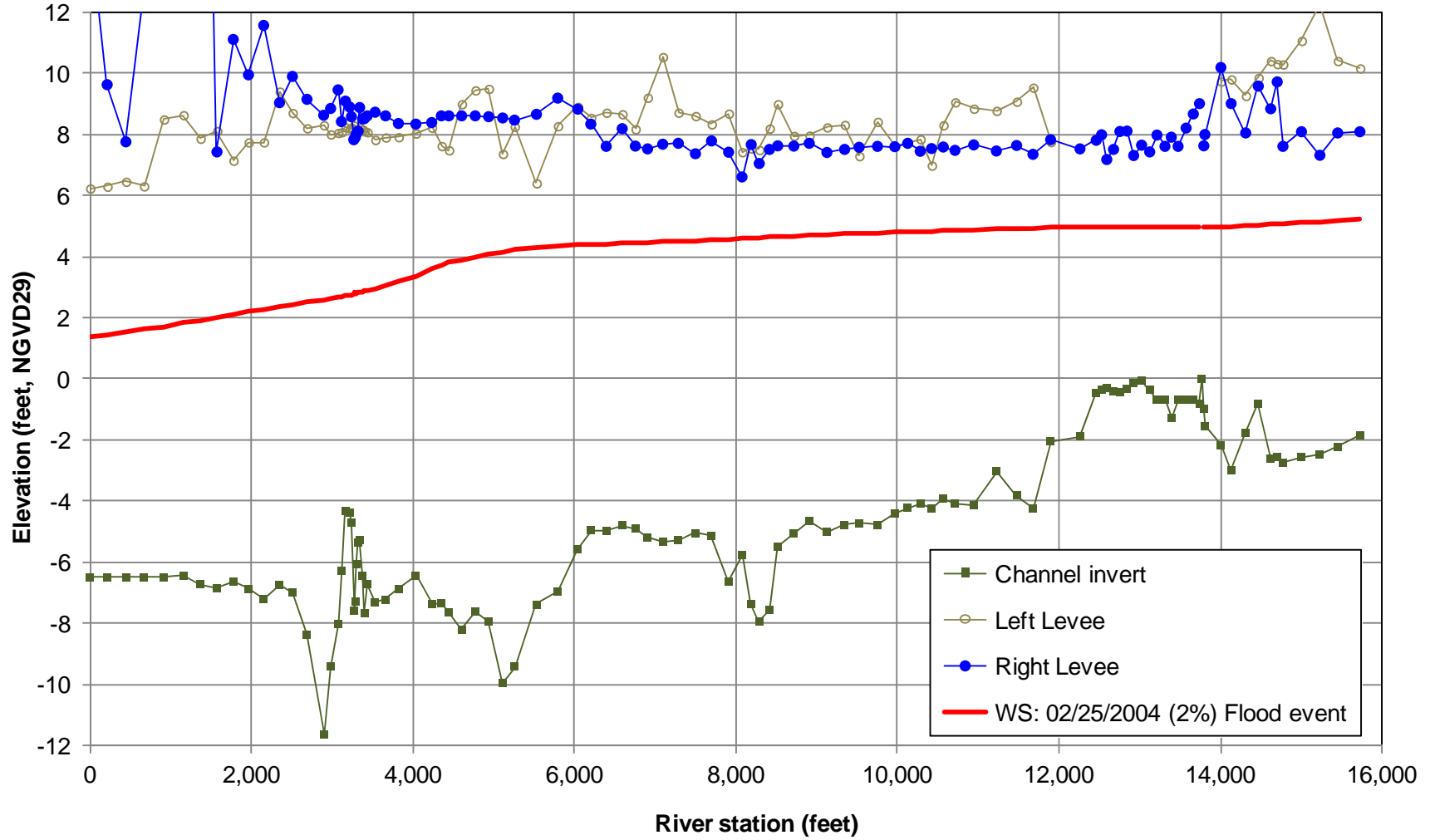


Figure 2-7. Water Surface Profiles for the February 25, 2004 Flood Event

It is noted that the levee crest elevations included in the County's survey (and in the HEC-RAS model) were actually for the top of the redwood floodwalls, or the redwood planter box levees, which were constructed in 1970's to early 1980s on top of the existing earthen levee to add two to three feet of flood protection to the Santa Venetia levee. Examples of the redwood floodwalls/planter box levees are shown in Figure 2-8 and Figure 2-9.



Source: <http://www.marinwatersheds.org/zone-7-levee.html>

Figure 2-8. Example 1: Redwood Flood Wall/Planter Box on Top of the Earthen Levee



Figure 2-9. Example 2: Redwood Flood Wall/Planter Box on Top of the Earthen Levee

The water levels computed for the February 25, 2004 flood event were approximately two to six feet lower than the Santa Venetia levee, as shown in Figure 2-7. This indicates that the water levels during this flood event reached or exceeded the top of the earthen part of the Santa Venetia levee for some segments. The Santa Venetia community would have been flooded during the February 25, 2004 flood event if the redwood floodwalls/planter box levees were not installed.

2.6 Existing Channel Flow Capacity

Eight flood events were modeled in order to determine the existing flow capacity of the creek as well as the capacity for the Santa Margarita Island Bridge. The return frequencies of these eight events ranged from 50% annual exceedance probability (AEP), or 2-year, to 0.2% AEP (or 500-year). The flow discharges along the creek were specified based on results of the Corps' hydrologic analysis, as listed in Table 2-1. The Mean Higher High Water (MHHW), which is at +3.58 feet, NGVD29, was used as the downstream boundary condition at the mouth of the creek in this flow capacity analysis.

The water surface profiles computed for the 1% and the 0.2% AEP flood events were compared to the levee crest elevations, as shown in Figure 2-10. The water levels during the 0.2% AEP flood event are lower than the levee crest elevations for the entire South Fork of Las Gallinas Creek. This indicates that the existing South Fork and the Santa Margarita Island Bridge have the capacity to convey at least the 0.2% AEP (or 500-year) flood event, providing there is no geotechnical or structural failure of the levee and the water level at the mouth of the creek is at MHHW or lower.

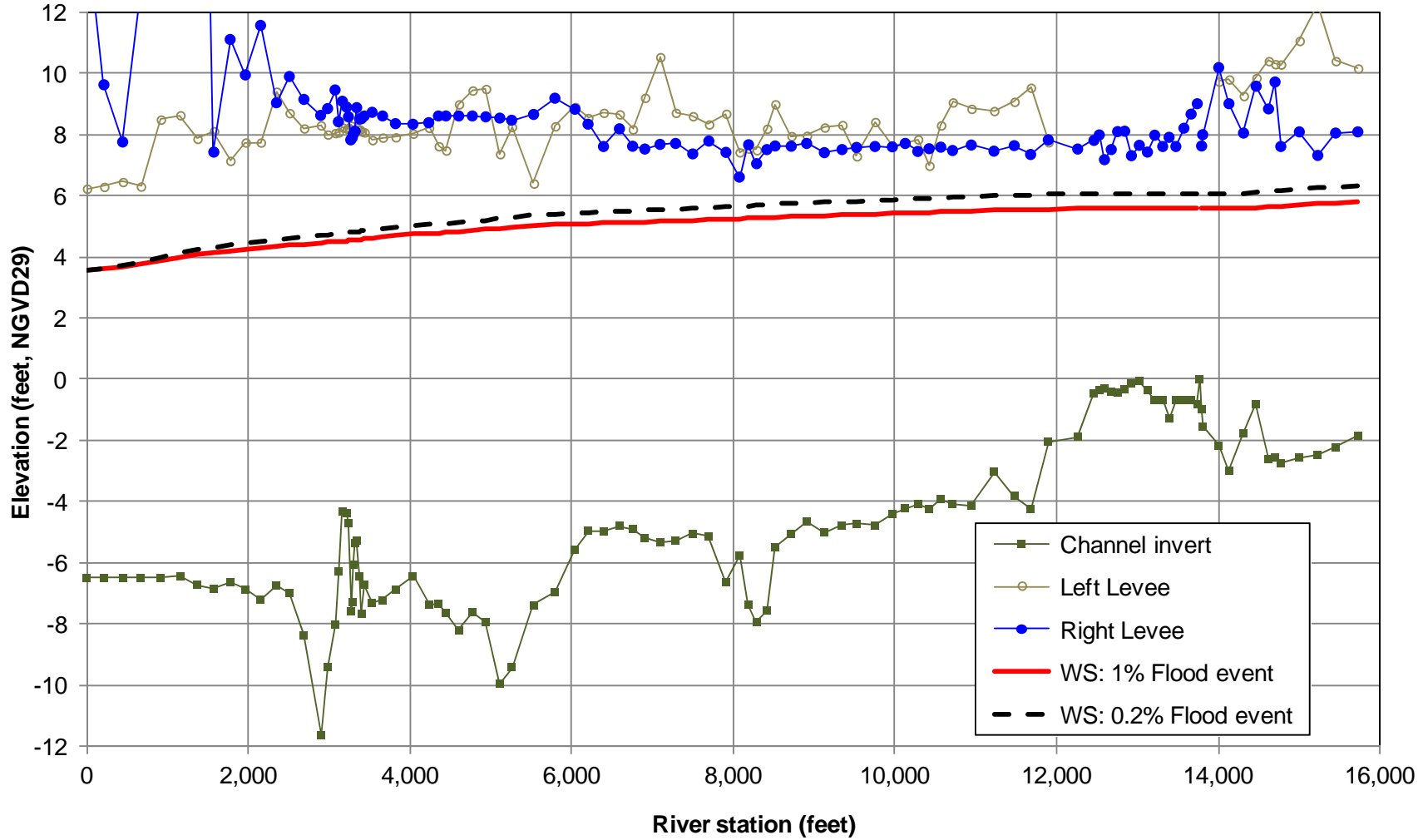


Figure 2-10. Water Surface Profiles for the 1% and 0.2% AEP Flood Events (with MHHW at the Creek Mouth)

2.7 Sensitivity Analysis

The two main sources of uncertainty in the riverine hydraulics analysis were the roughness and the downstream boundary condition. This sensitivity analysis was conducted to test how the Manning's roughness value (n-value), and the downstream water level affect the channel capacity. The analysis was conducted by using combinations of different n-values and different downstream water levels.

The range of the n-values used in this sensitivity analysis was selected based on the values recommended in the HEC-RAS Reference Manual (USACE, 2008), as discussed in Section 2.5. While the MHHW was used as the downstream water level in the evaluation of the flow capacity, the Mean High Water (MHW) was used as the lower limit of the downstream water level, and the 100% AEP (or 1-year) water level was used as the upper limit of the downstream water level. The MHW was used to approximate the averaged maximum water level that occurs every tidal cycle (approximately every 12 hours). The 100% AEP still water level is the maximum water level that may occur every year. The variation ranges and the median values of the n-values and of the downstream water levels are listed in Table 2-3.

Table 2-3. Uncertainties in HEC-RAS Model Parameters

HEC-RAS Model Parameters	Manning's Roughness ^a (Left / Channel / Right)	Downstream Water Level (feet, NGVD29)
Low Limit	0.035 / 0.030 / 0.080	+2.99 ^a
Median Value	0.050 / 0.035 / 0.100	+3.58 ^b
Upper Limit	0.070 / 0.040 / 0.120	+4.39 ^c

Note: a. Mean High Water (MHW).

b. Mean Higher High Water (MHHW).

c. The 1-year maximum (100% AEP) still water level as determined in Section 5.

Figure 2-11 shows the water surface profiles for the 1% annual chance exceedance flood event (100-year flood event) computed with different n-values and with the downstream water level at MHHW. A larger Manning's roughness value yields higher water levels along the creek. The impact of the n-value on the channel hydraulics increases from the downstream to the upstream. The difference in the 100-year water levels between the lower and the larger n-

values varies from 0 feet at the mouth of the creek to approximately 0.5 feet at the upstream end.

Figure 2-12 shows the 100-year water surface profiles computed with different downstream water levels and with the normal n-value. A higher downstream water level yields higher water levels along the creek. The impact of the downstream water level on the channel hydraulics decays from the downstream to the upstream. The difference in the 100-year water levels between the downstream water level at the 1-year still water level and the downstream water level at MHW decreases from 1.4 feet at the mouth of the creek, to approximately 0.7 feet at the east end of the Santa Venetia marsh levee (approximately at Station 31+14), to merely 0.2 feet at the upstream end.

Figure 2-13 shows the computed upper and lower bounds of the 100-year water surface profile. The upper bound of the water surface profile was computed using the higher limit of the n-value with the higher downstream water level (1-year maximum still water level). The lower bound was computed using the lower limit of the n-value with the lower downstream water level (MHW). The difference in the 100-year water levels between the higher and the lower bounds ranges between 0.7 to 1.4 feet.

Figure 2-14 shows the computed upper and lower bounds of the 500-year water surface profile. The upper bound of the 500-year water surface profile is still lower than the levees along the creek. Therefore, it is concluded that the existing South Fork and the Santa Margarita Island Bridge have the capacity to convey at least the 0.2% AEP (or 500-year) flood event, providing there is no geotechnical or structural failure of the levee.

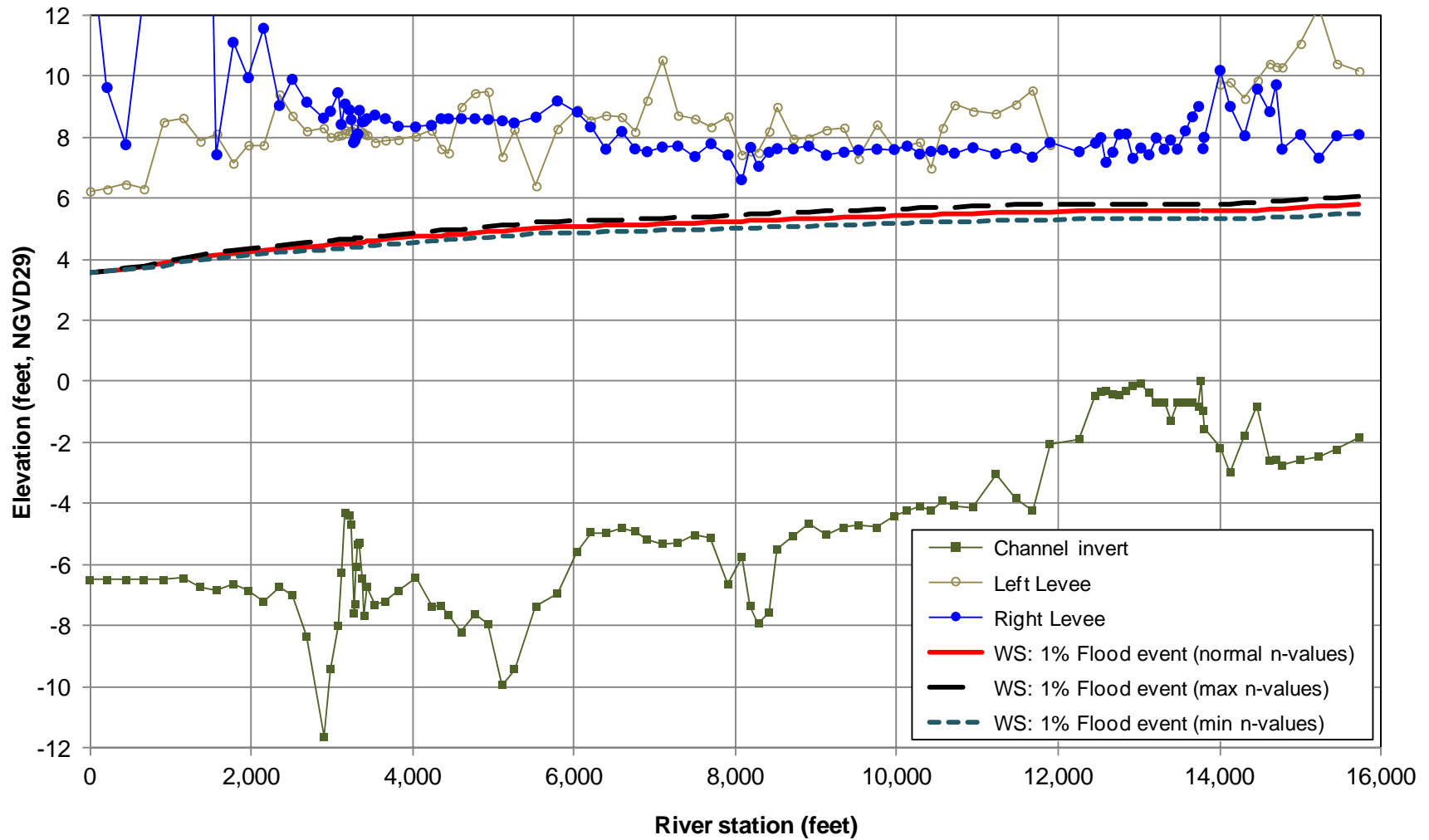


Figure 2-11. Sensitivity of the 100-Year Water Surface Profile to n-Values (with MHHW at the Creek Mouth)

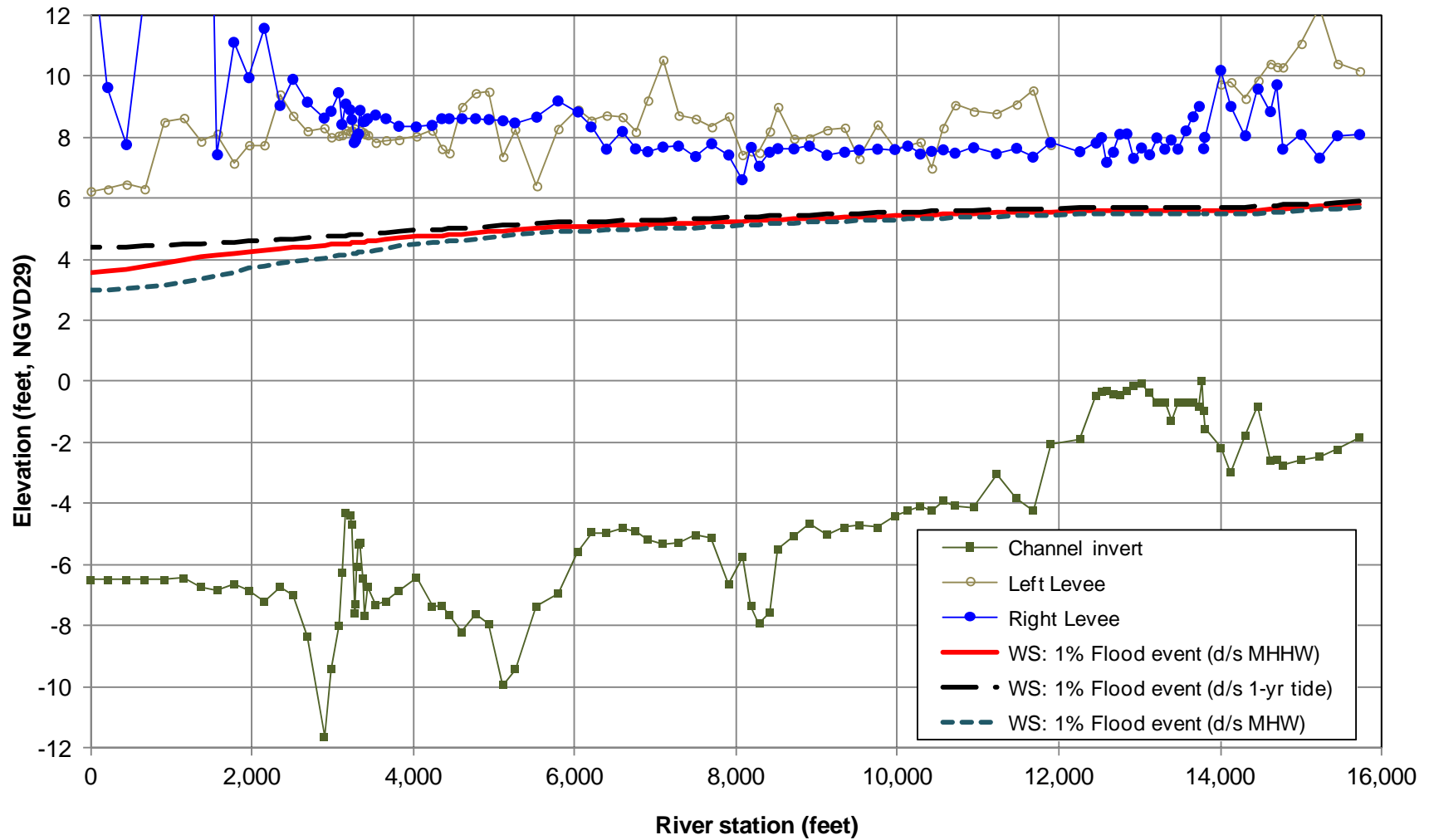


Figure 2-12. Sensitivity of the 100-Year Water Surface Profile to Downstream Water Levels

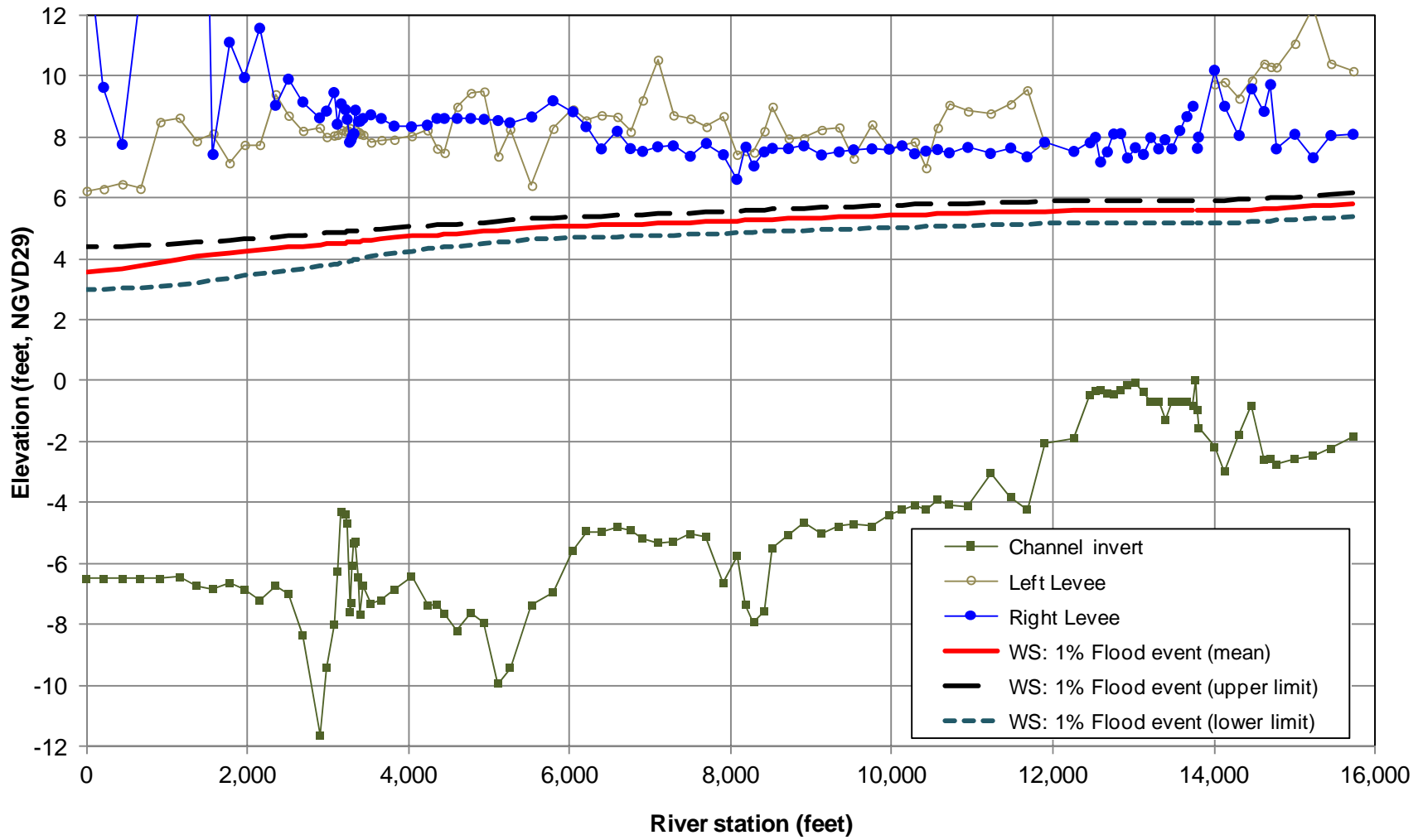


Figure 2-13. Upper and Lower Bounds for 100-Year Water Surface Profile

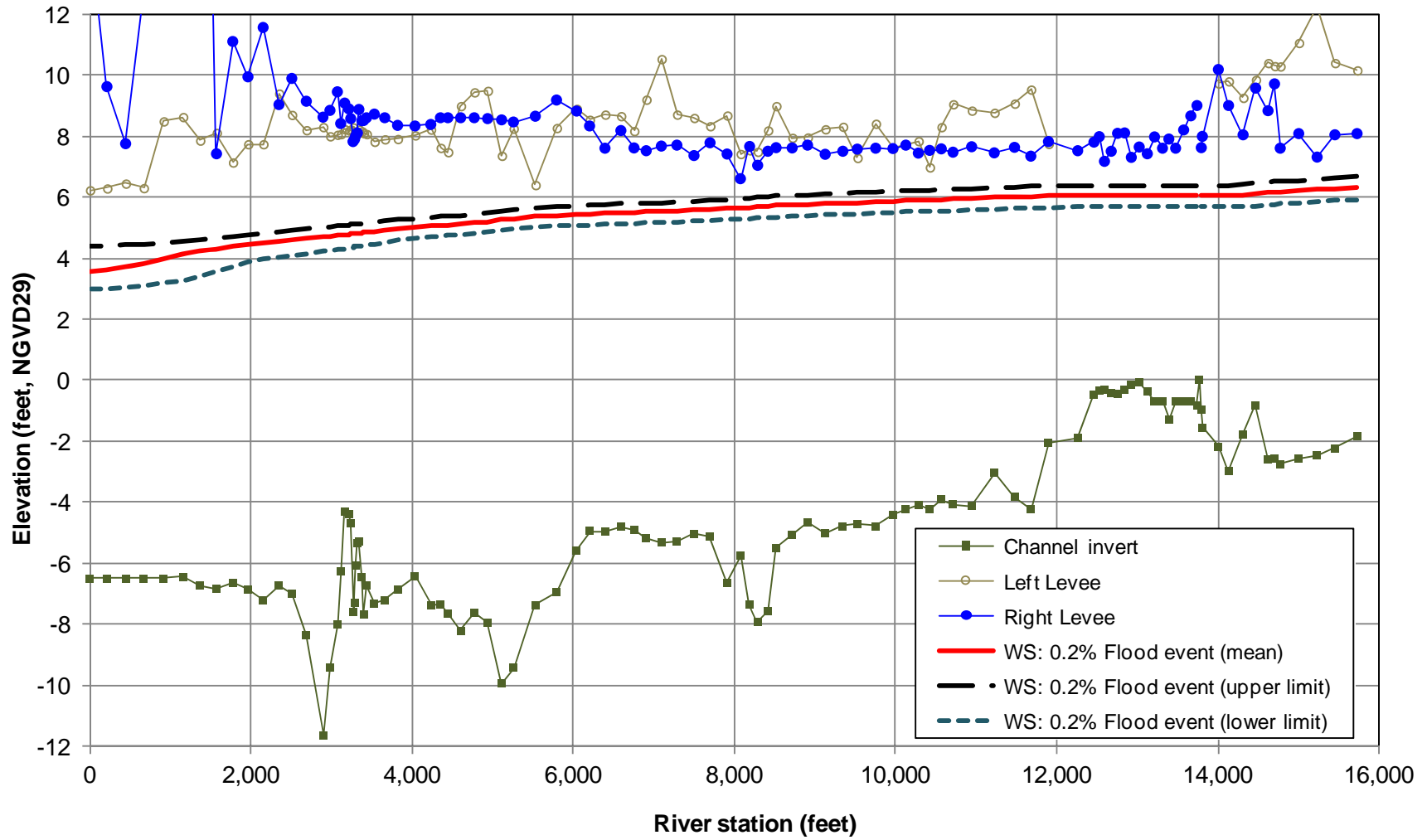


Figure 2-14. Upper and Lower Bounds for 500-Year Water Surface Profile

3 RIVERINE FLOODING ANALYSIS AND FLOODPLAIN DELINEATION

The riverine flooding analysis was conducted for eight riverine flood events. The AEP for these eight flood events are 50% (2-year), 20% (5-year), 10% (10-year), 4% (25-year), 2% (50-year), 1% (100-year), 0.4% (250-year), and 0.2% (500-year), respectively. The water surface profiles for these flood events were computed with the HEC-RAS model. These water surface profiles were then exported for processing in ArcGIS by the HEC-geoRAS program, from which the riverine floodplain maps were generated. The riverine flooding analysis and floodplain delineation were conducted for both the Year 0 (2011) condition and the Year 50 (2061) condition.

3.1 Year 0 (2011) Condition

The riverine flooding analysis for the Year 0 (2011) condition was conducted using the peak flow discharges determined in the Corps' (2011) hydrologic analysis, which are listed in Table 2-1, with the downstream water level at MHHW (+3.58 feet, NGVD29). The water surface profiles computed with HEC-RAS for the eight flood events are shown in Figure 3-1. It is noted that the water levels are lower than the crest elevations of the left and the right levees for these flood events. This indicates that the water will be conveyed within the main channel, and Santa Venetia will not be flooded during these eight flood events.

The floodplain maps for the Year 0 (2011) condition were generated with the ArcGIS / HEC-GeoRAS, and are shown in Figure 3-2 through Figure 3-9 for these eight flood events, respectively. While the inundation depths are different for different flood events, the inundation boundaries do not show significant difference between these eight flood events. The main channel of the creek that is bounded by the left and right levees, and the Santa Venetia marsh will be inundated during these flood events. However, Santa Venetia will not be inundated during these eight flood events.

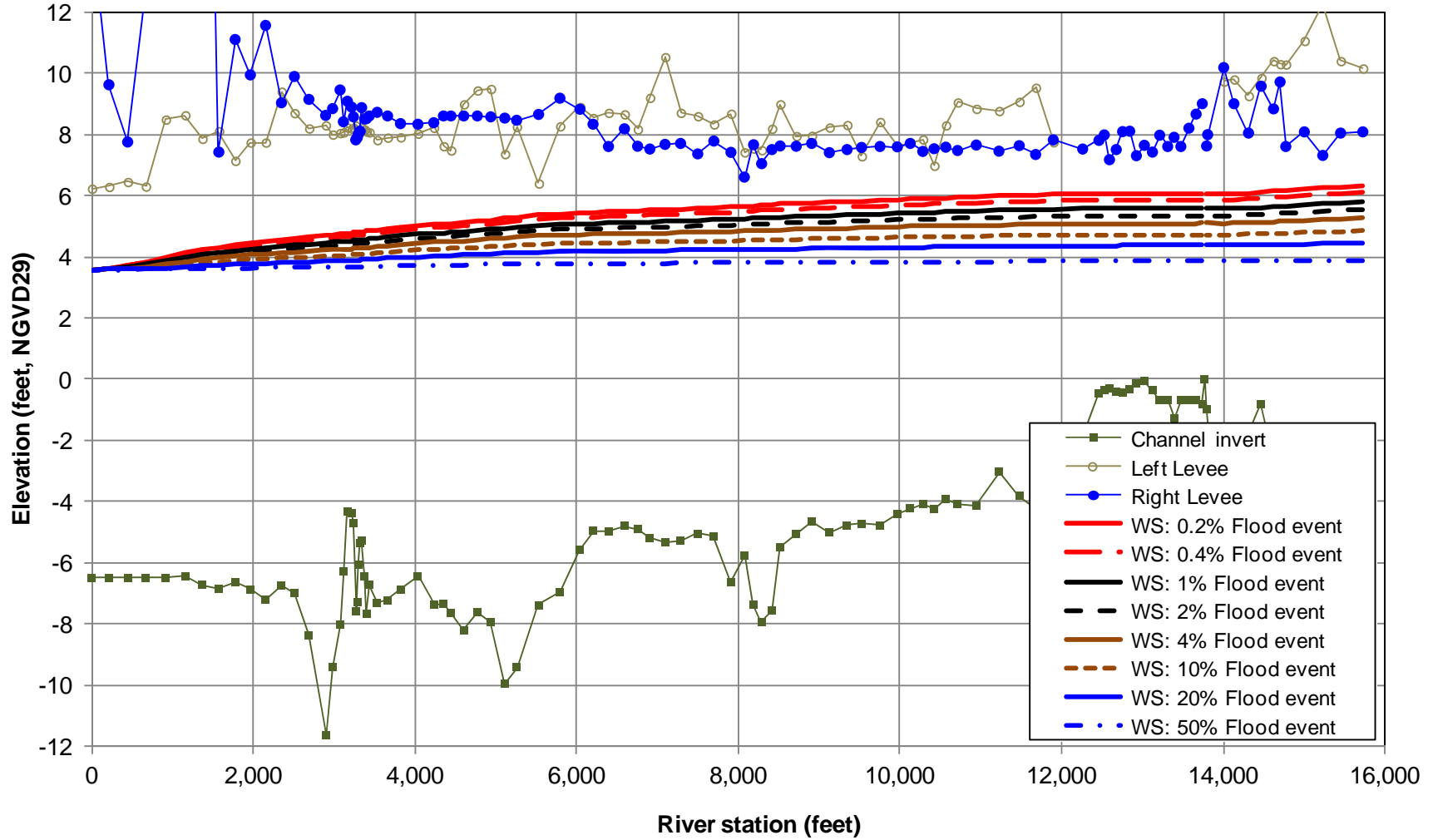


Figure 3-1. Computed Water Surface Profiles for Eight Flood Events (Year 0 Condition)

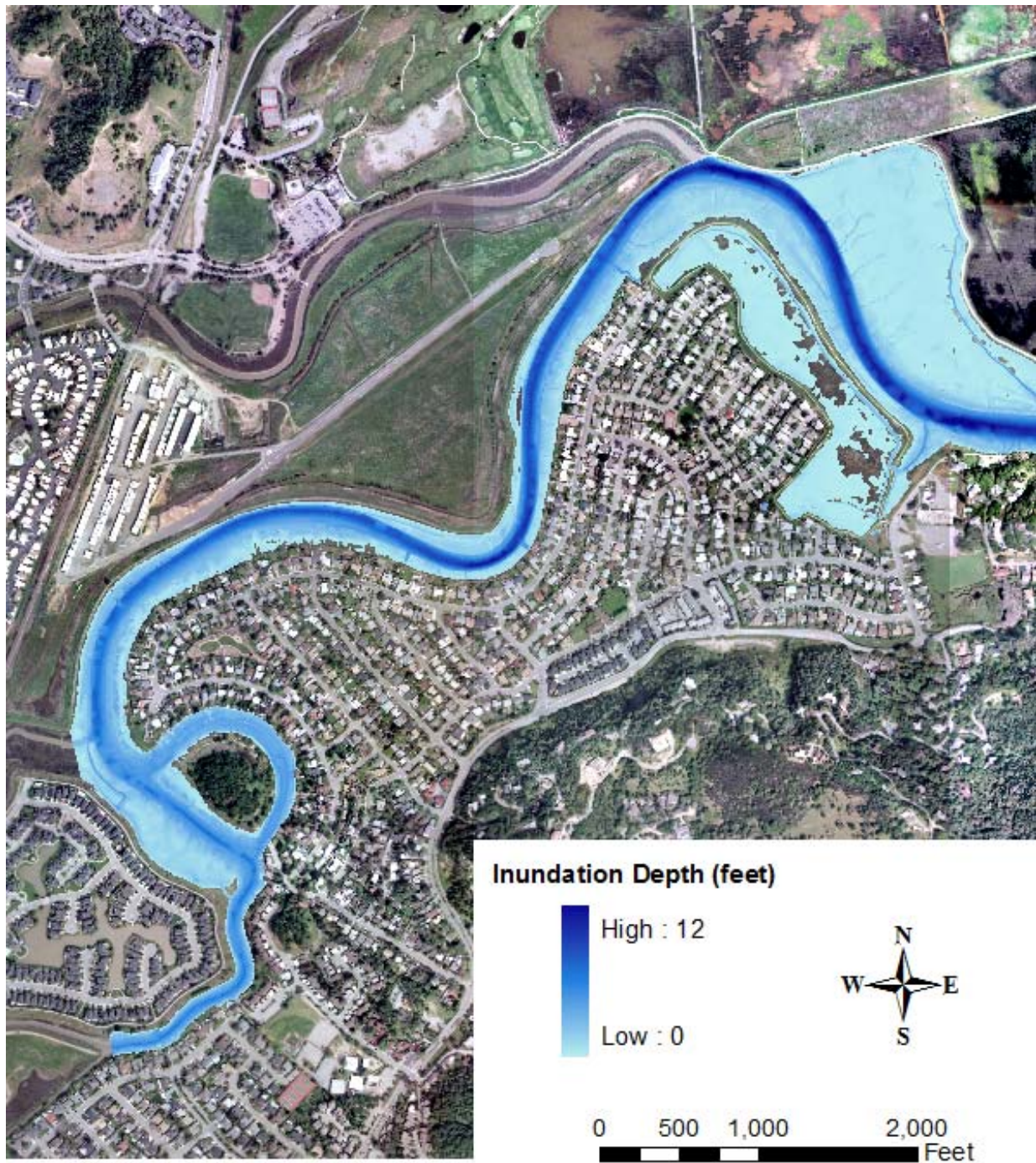


Figure 3-2. Riverine Floodplain Map for the 50% AEP Flood Event (Year 0 Condition)

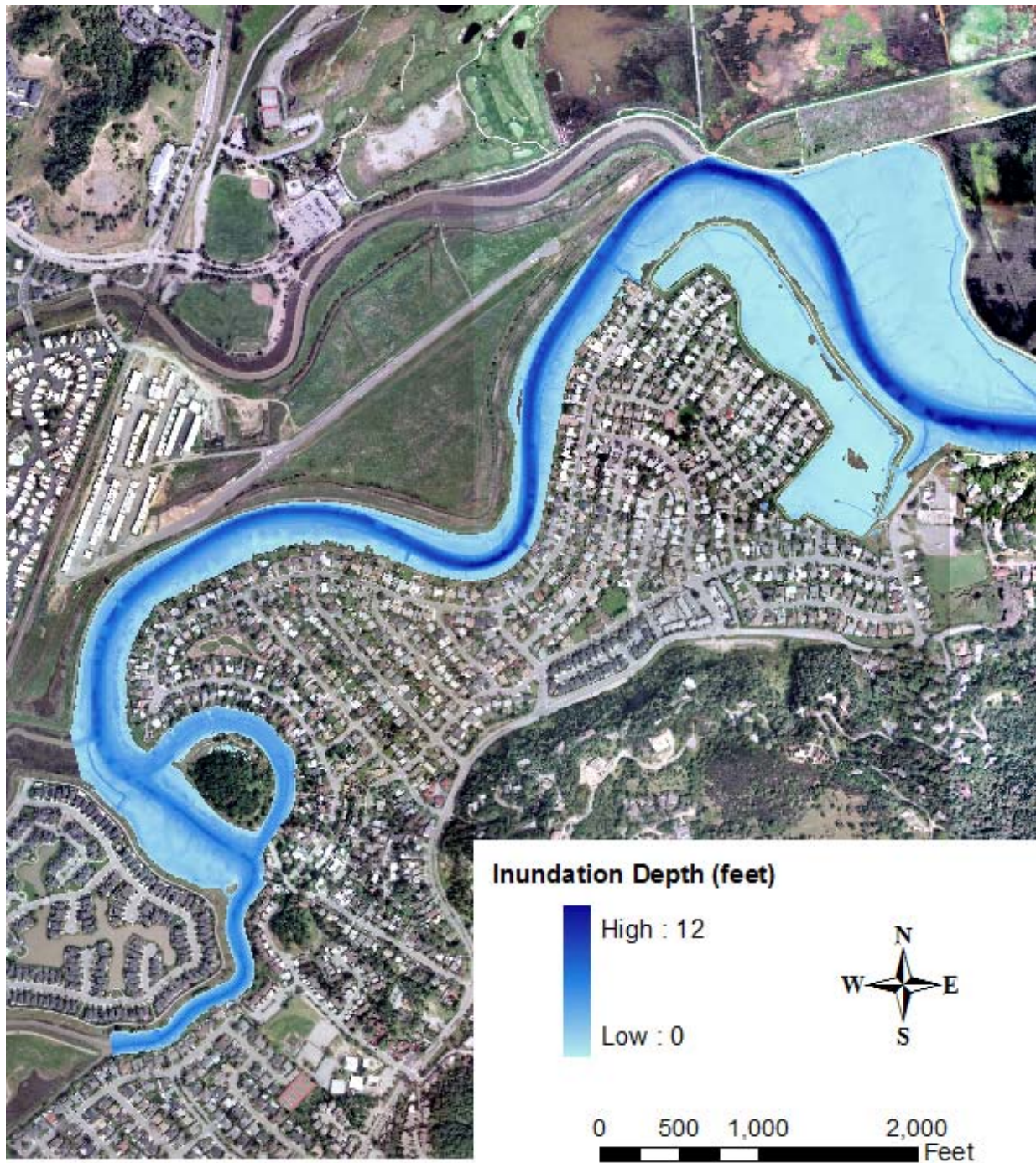


Figure 3-3. Riverine Floodplain Map for the 20% AEP Flood Event (Year 0 Condition)

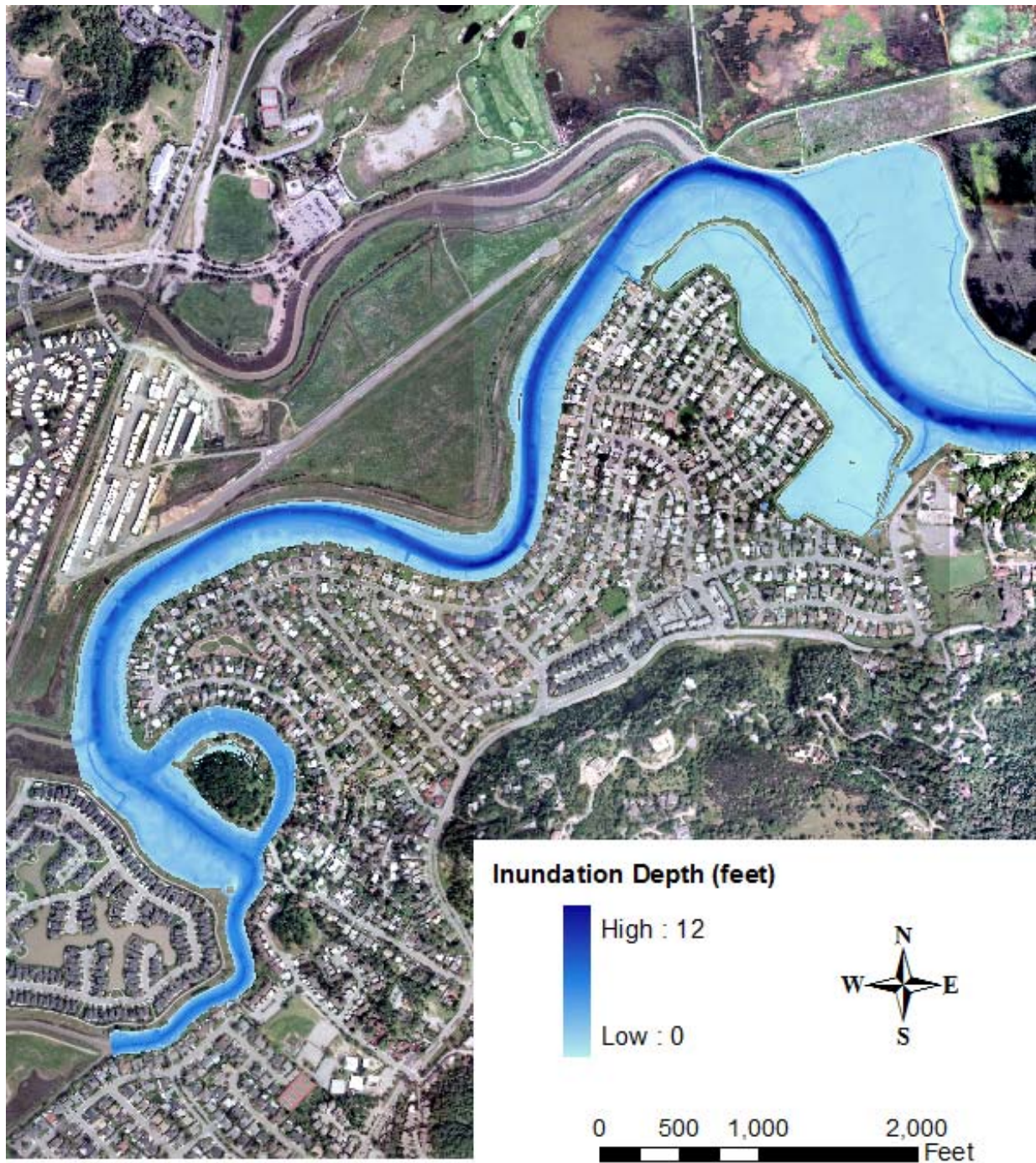


Figure 3-4. Riverine Floodplain Map for the 10% AEP Flood Event (Year 0 Condition)

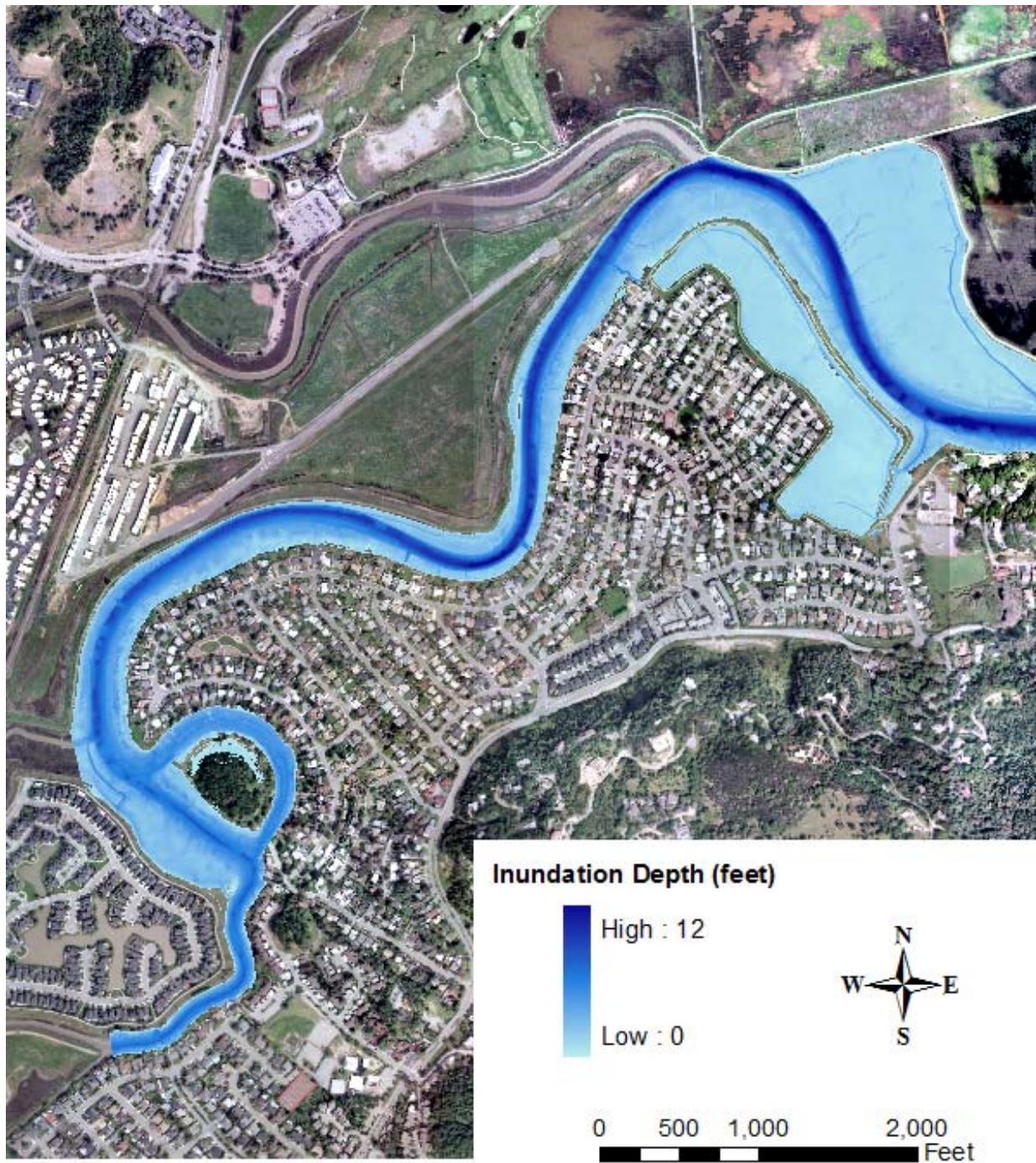


Figure 3-5. Riverine Floodplain Map for the 4% AEP Flood Event (Year 0 Condition)

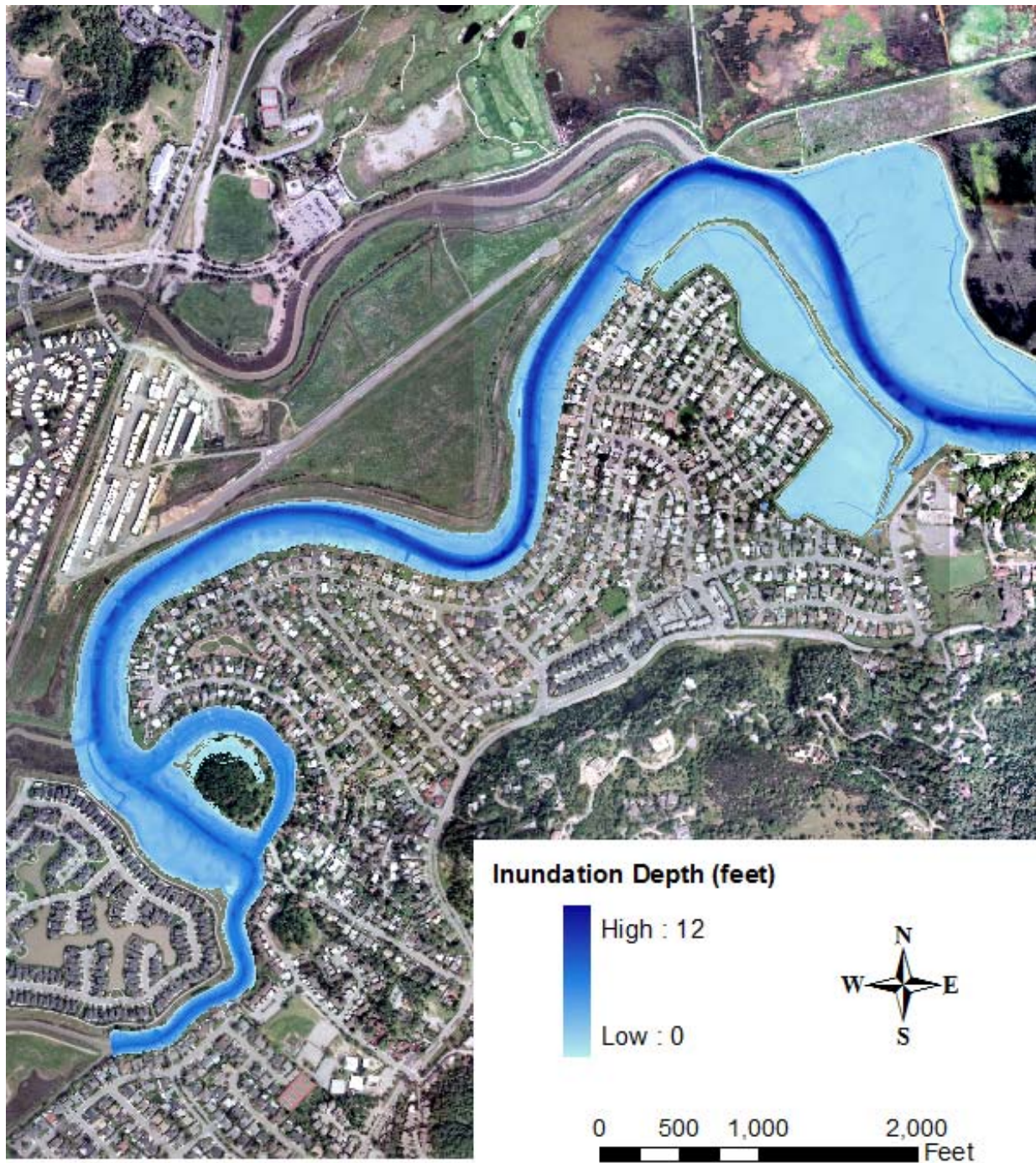


Figure 3-6. Riverine Floodplain Map for the 2% AEP Flood Event (Year 0 Condition)

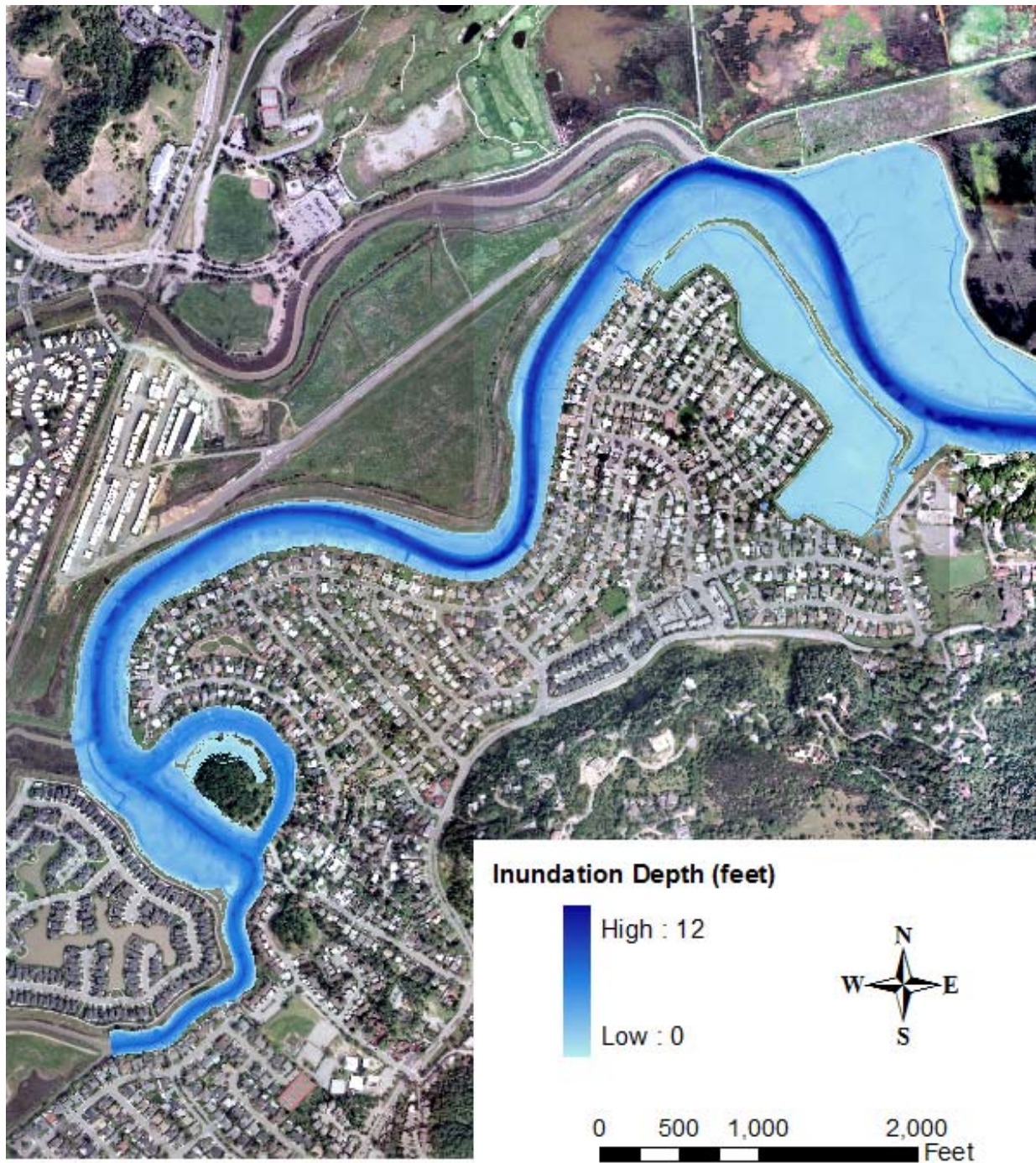


Figure 3-7. Riverine Floodplain Map for the 1% AEP Flood Event (Year 0 Condition)

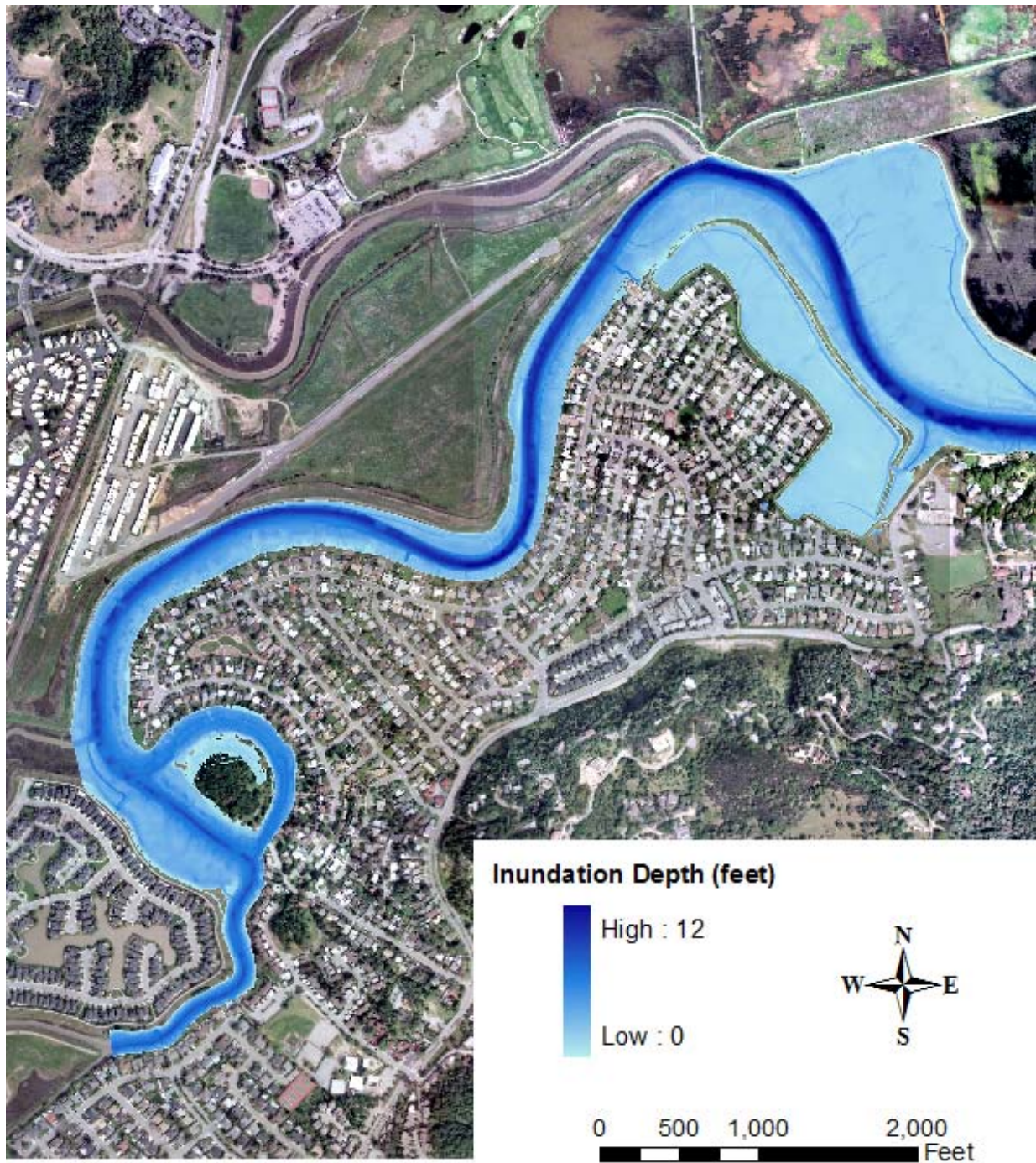


Figure 3-8. Riverine Floodplain Map for the 0.4% AEP Flood Event (Year 0 Condition)

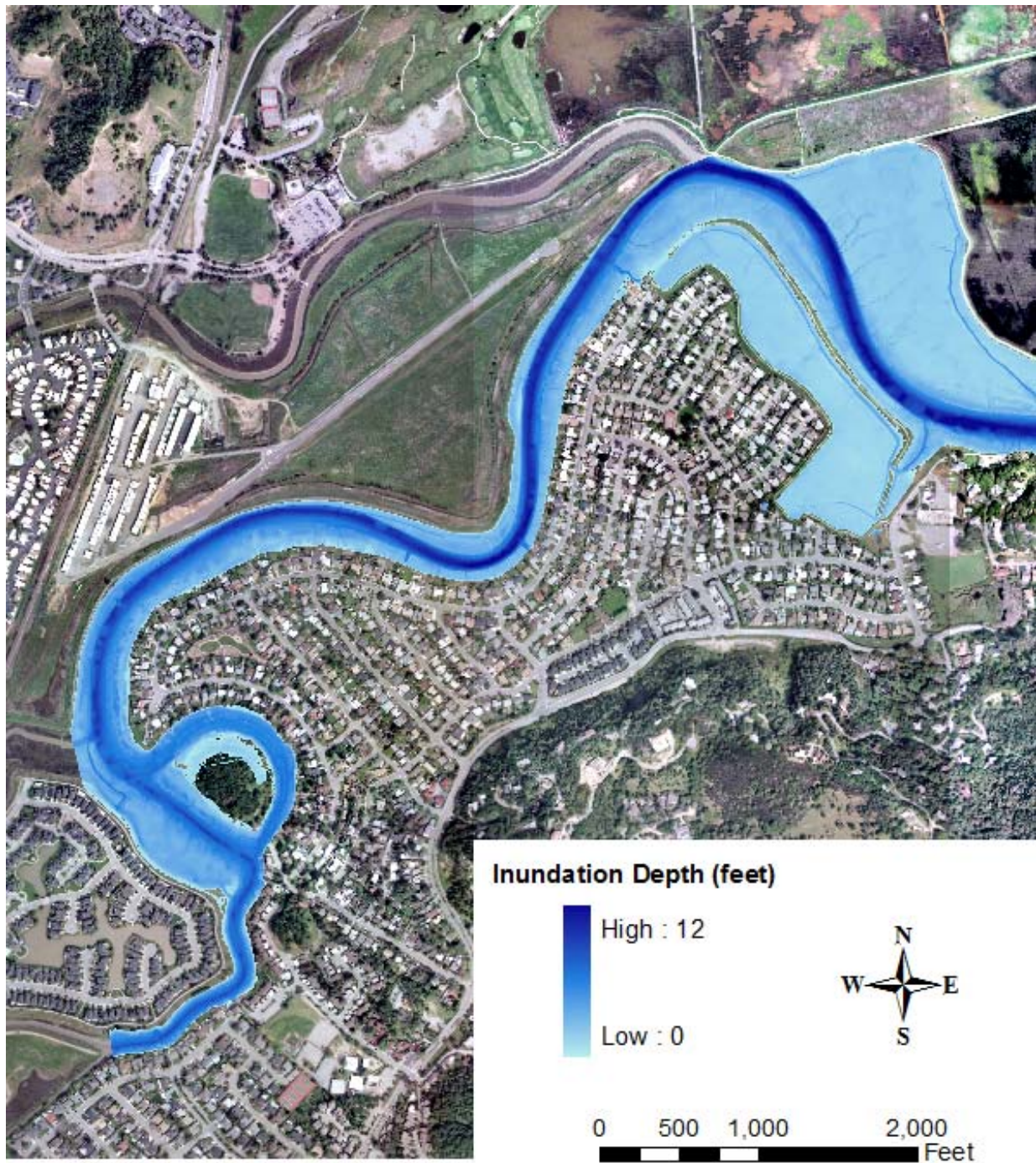


Figure 3-9. Riverine Floodplain Map for the 0.2% AEP Flood Event (Year 0 Condition)

3.2 Year 50 (2061) Condition

The riverine flooding analysis and floodplain delineation were also conducted for the Year 50 (2061) condition. According to the Corps (2011) hydrologic study, the hydrologic condition for the Las Gallinas Creek watershed and the peak flow discharges along the creek were considered the same between the future Year 50 (2061) condition and the existing Year 0 (2011) condition. Therefore, the peak flow discharges for the Year 0 condition were also used in the riverine flooding analysis for the Year 50 condition.

The future sea level change is discussed in Section 5.2. It was estimated that the sea level rise (including the local land movement) in the next 50 years will be approximately 0.5 feet based on the historic sea level rise (SLR) trend, 0.8 feet based on the modified NRC Curve I, and 2.1 feet based on the modified NRC Curve III. The riverine flooding analysis and floodplain delineation for the Year 50 condition focused on the historical sea level rise trend. The existing MHHW is at +3.58 feet, NGVD29. The downstream water level used for the Year 50 was thus set to +4.08 feet, NGVD29 for the Year 50 condition.

The water surface profiles computed for the Year 50 condition are shown in Figure 3-10. The floodplain maps are shown in Figure 3-11 through Figure 3-18 for the eight flood events, respectively. The results indicate that the water will be conveyed within the main channel for the Year 50 (2061) condition. The main channel of the creek and the Santa Venetia marsh will be inundated during the eight flood events. However, Santa Venetia will not be inundated during these flood events.

As a sensitivity test, the riverine flooding analysis and floodplain delineation were also conducted for the 1% AEP (100-year) flood event for the Year 50 condition using the sea level rise values based on the modified NRC curve I and the modified NRC curve III. The computed 100-year water surface profiles with these two SLR scenarios are shown in Figure 3-19. The floodplain maps are shown in Figure 3-20 and Figure 3-21, respectively. Compared to the case with the historic SLR trend, the water levels associated with these two alternative SLR scenarios will be higher and the inundation water depth will be deeper. But the inundation boundaries do not show significant difference. Santa Venetia will not be inundated during the 100-year riverine flood event when considering these two SLR scenarios.

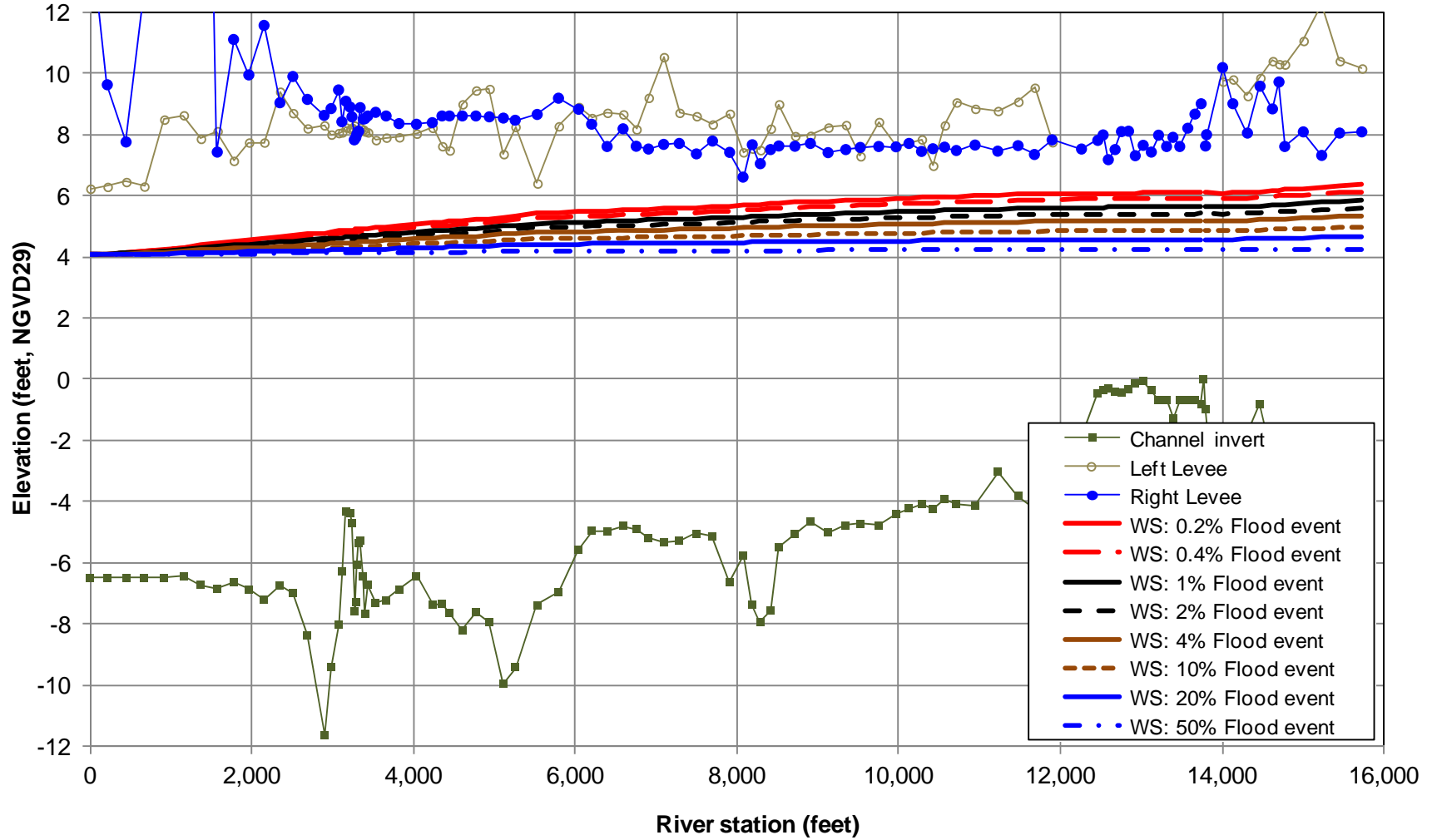


Figure 3-10. Computed Water Surface Profiles for Eight Flood Events (Year 50 Condition)

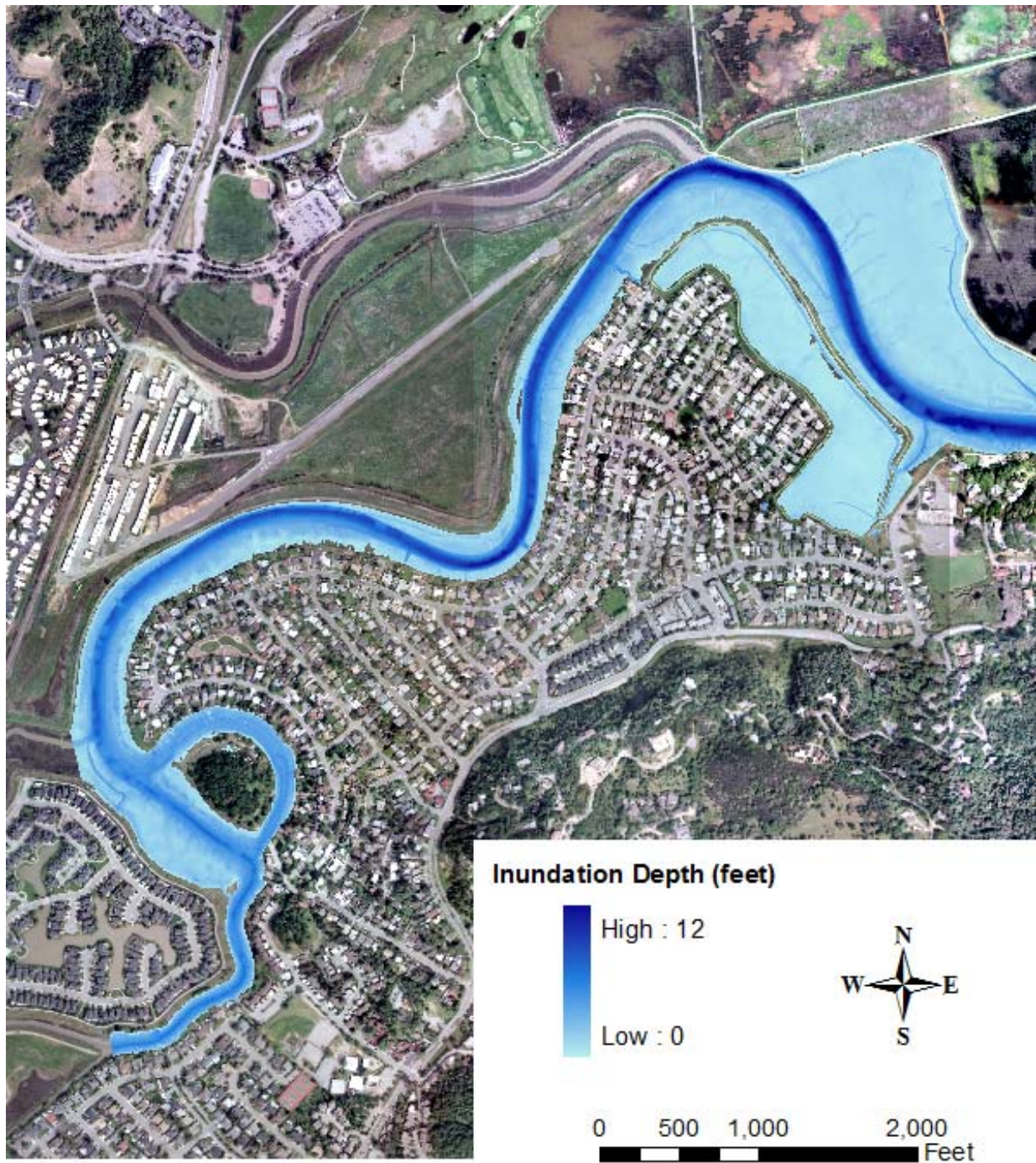


Figure 3-11. Riverine Floodplain Map for the 50% AEP Flood Event (Year 50 Condition)

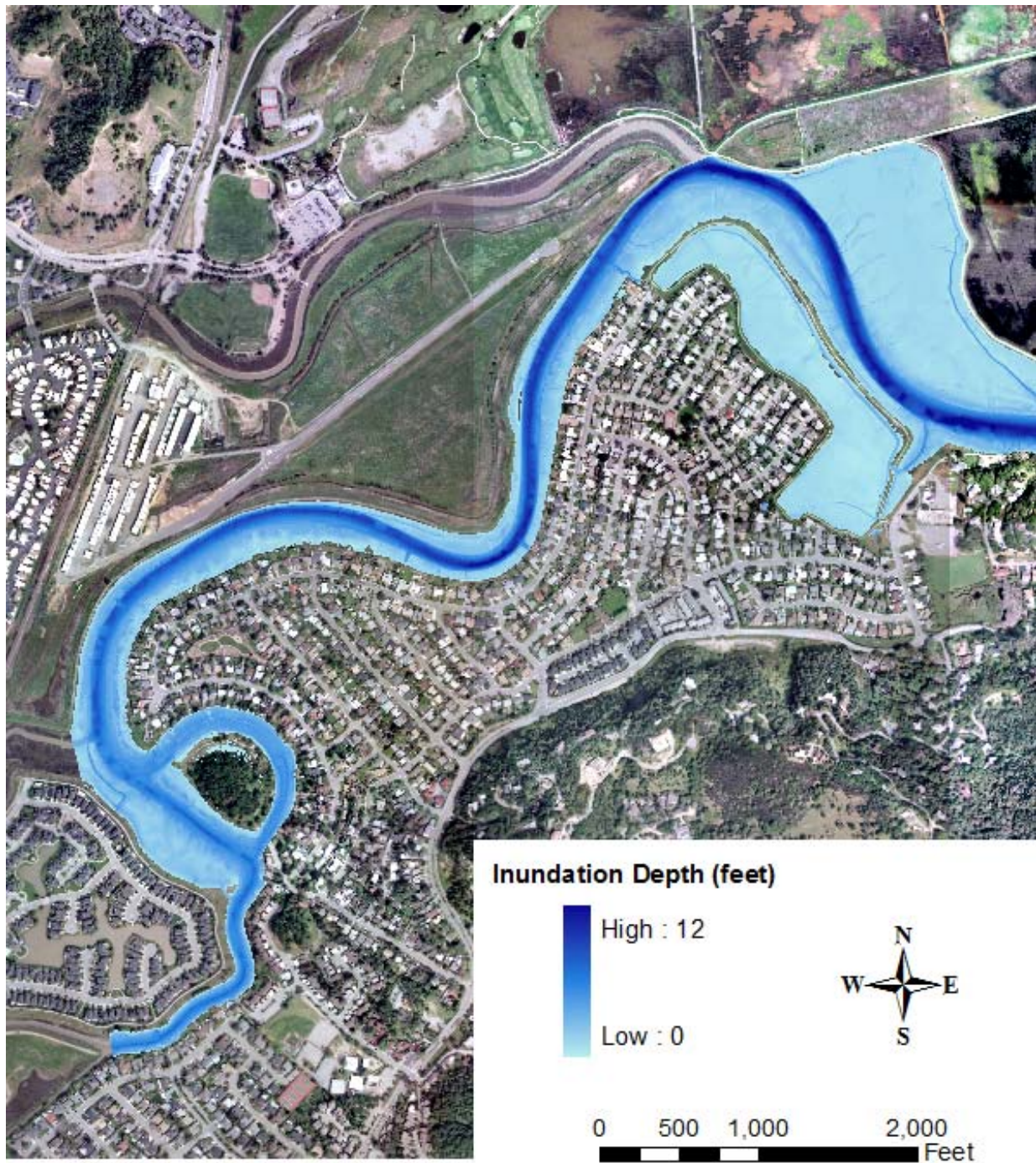


Figure 3-12. Riverine Floodplain Map for the 20% AEP Flood Event (Year 50 Condition)

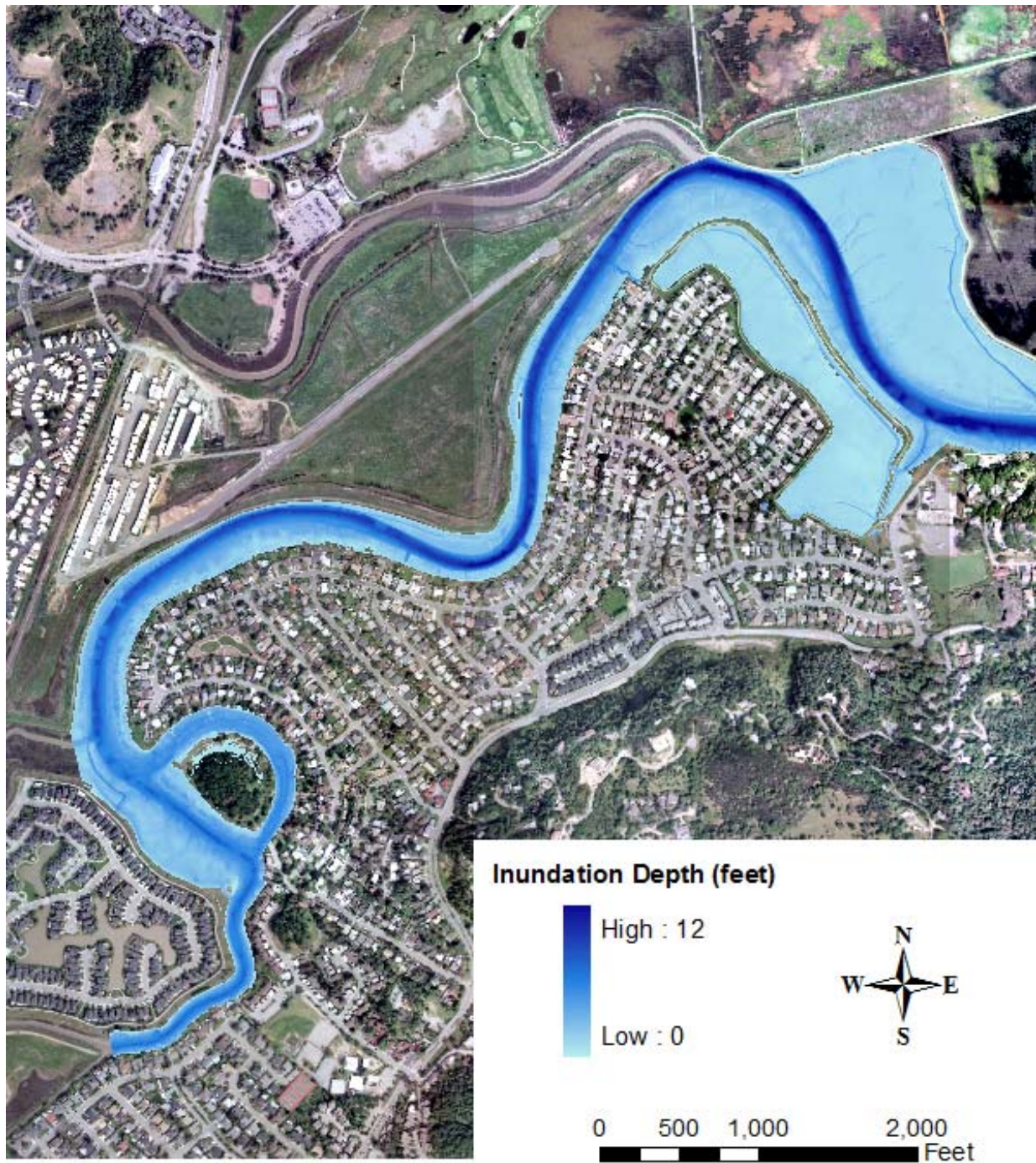


Figure 3-13. Riverine Floodplain Map for the 10% AEP Flood Event (Year 50 Condition)

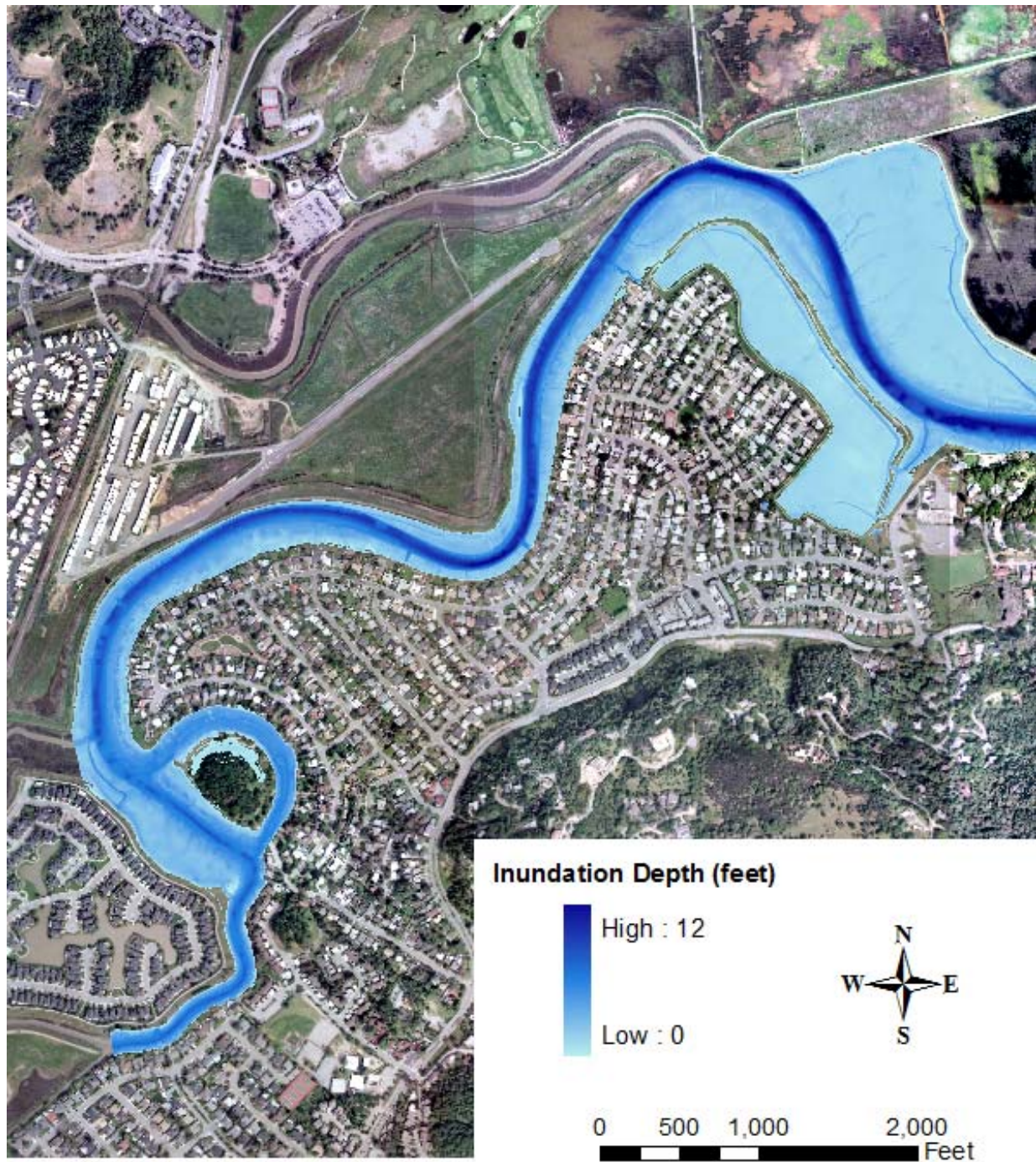


Figure 3-14. Riverine Floodplain Map for the 4% AEP Flood Event (Year 50 Condition)

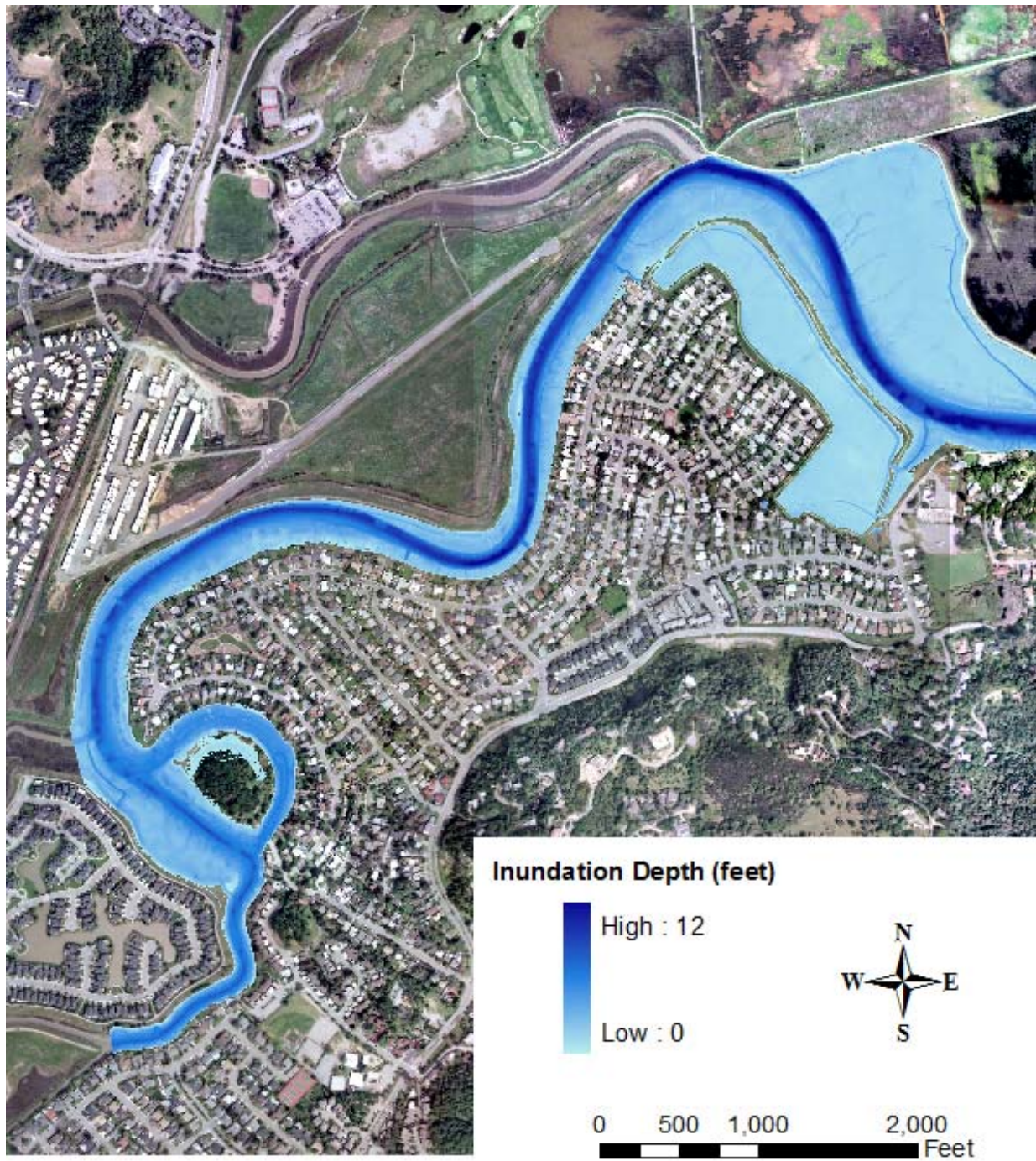


Figure 3-15. Riverine Floodplain Map for the 2% AEP Flood Event (Year 50 Condition)

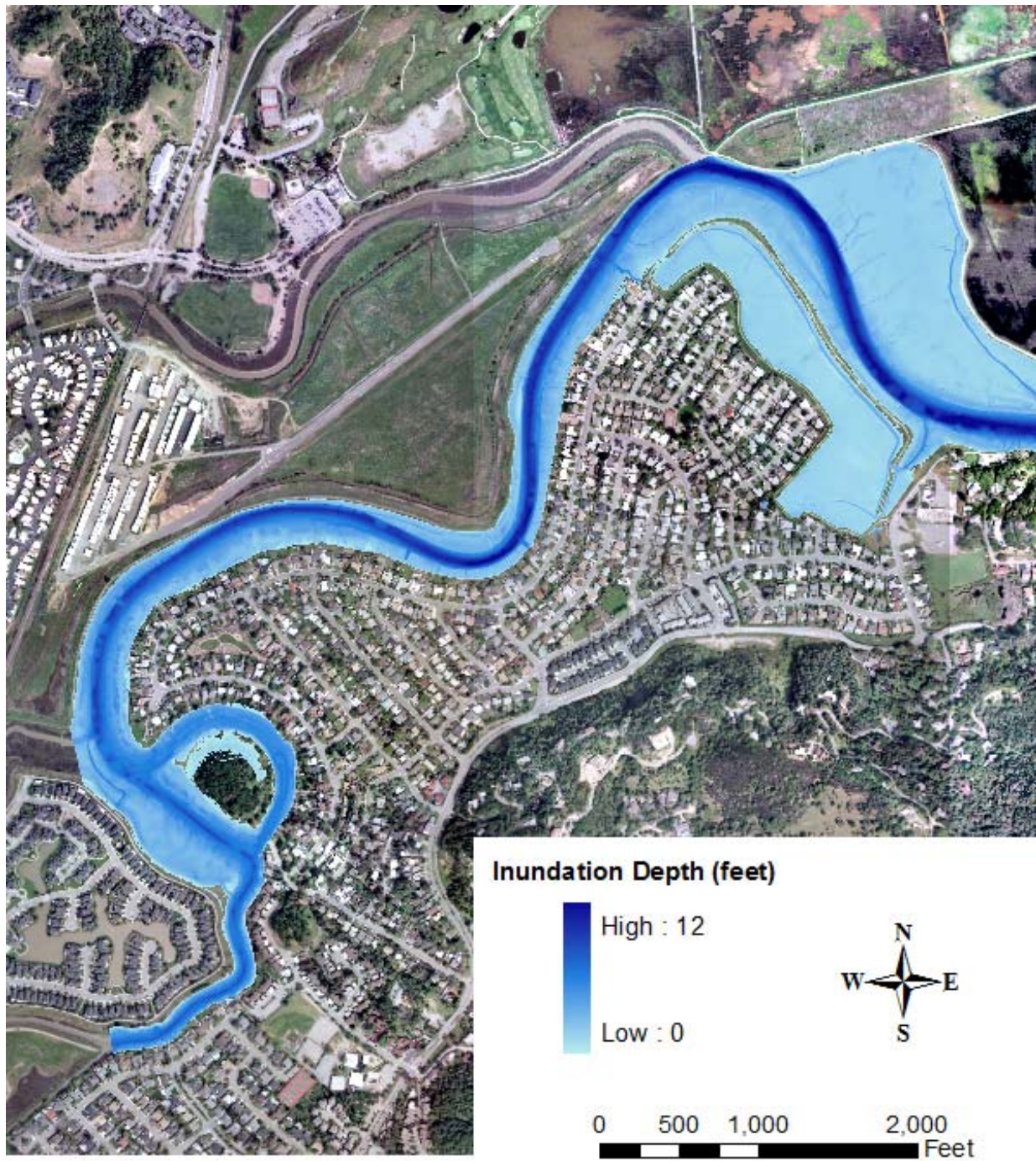


Figure 3-16. Riverine Floodplain Map for the 1% AEP Flood Event (Year 50 Condition)

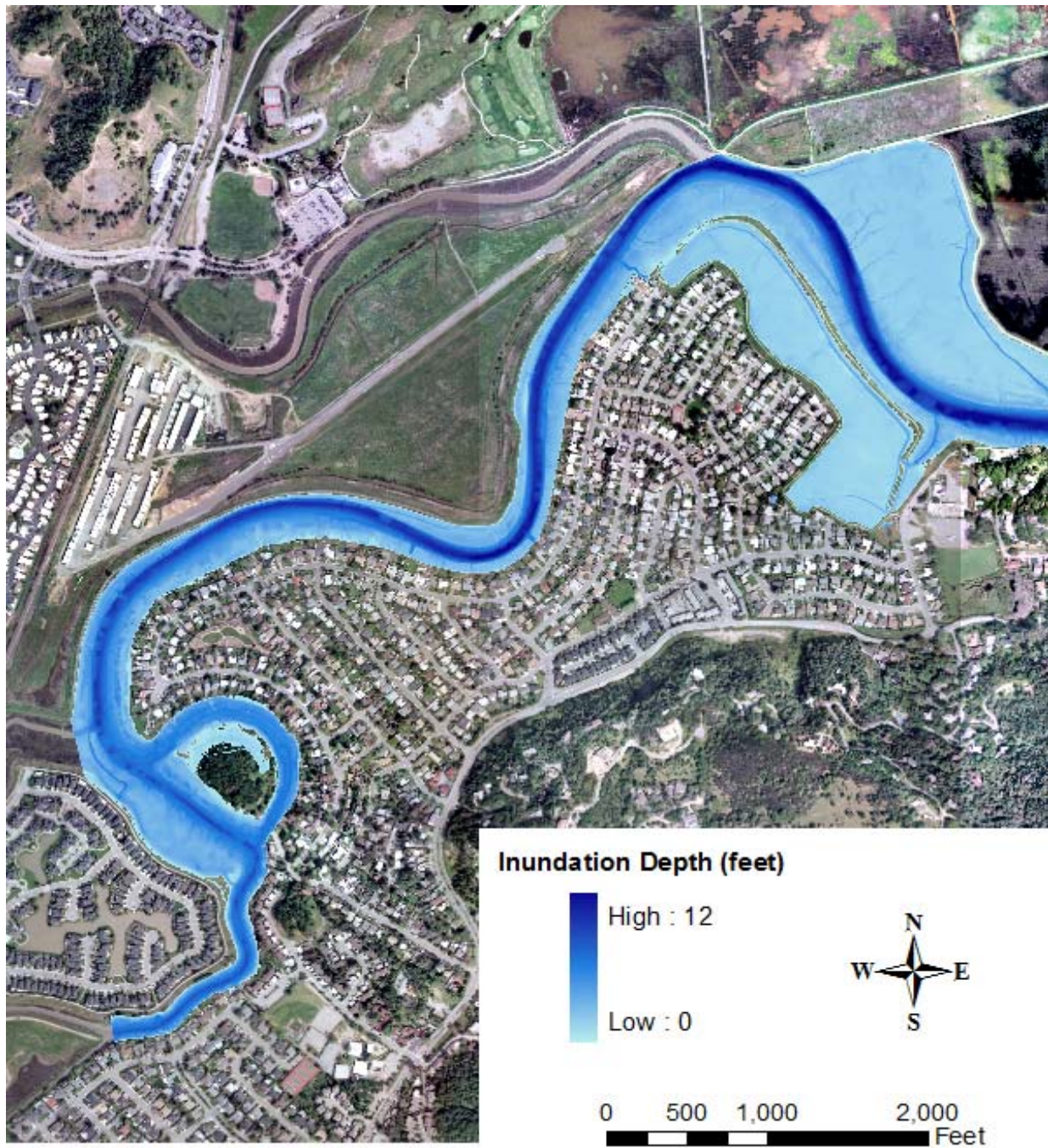


Figure 3-17. Riverine Floodplain Map for the 0.4% AEP Flood Event (Year 50 Condition)

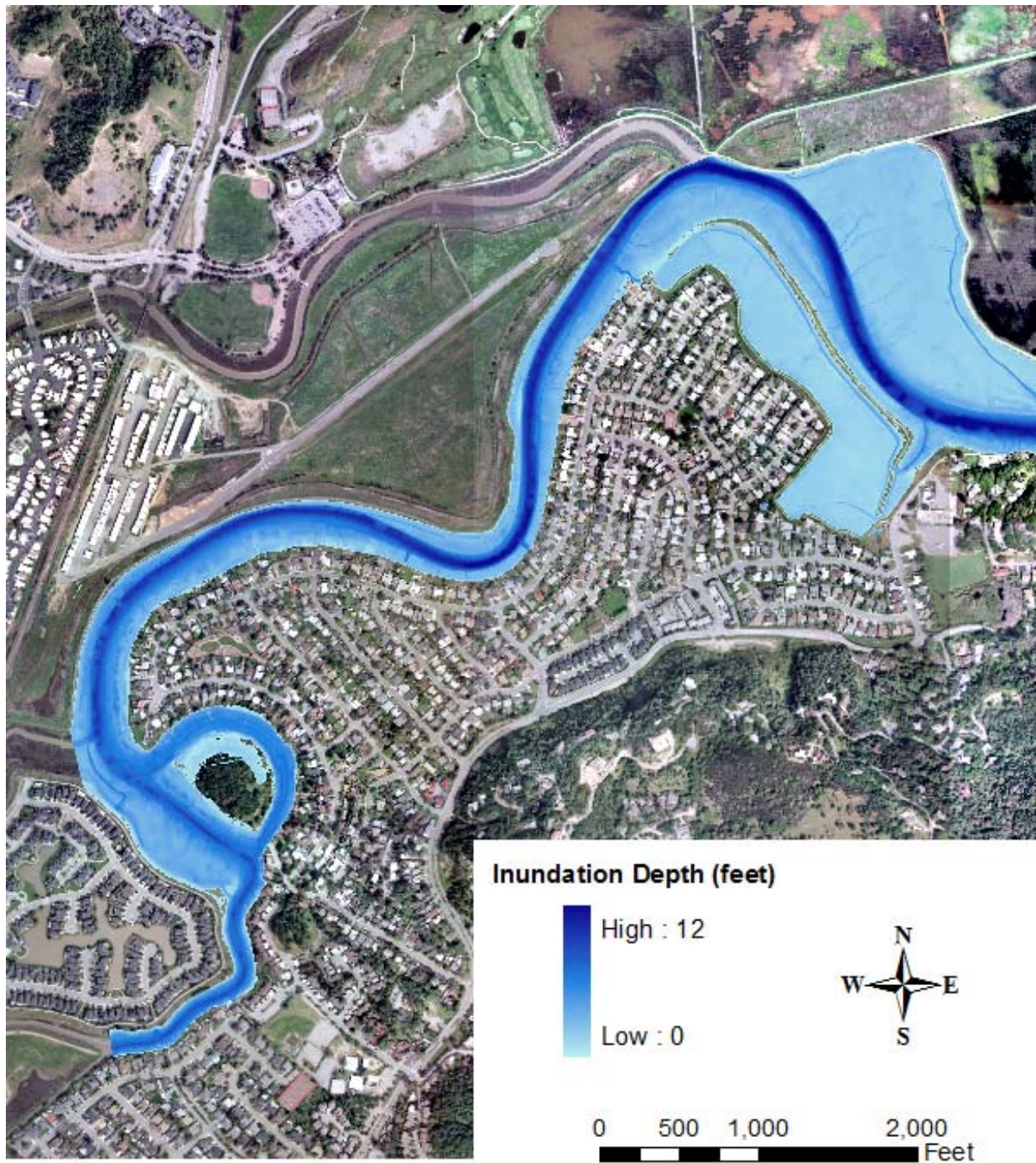


Figure 3-18. Riverine Floodplain Map for the 0.2% AEP Flood Event (Year 50 Condition)

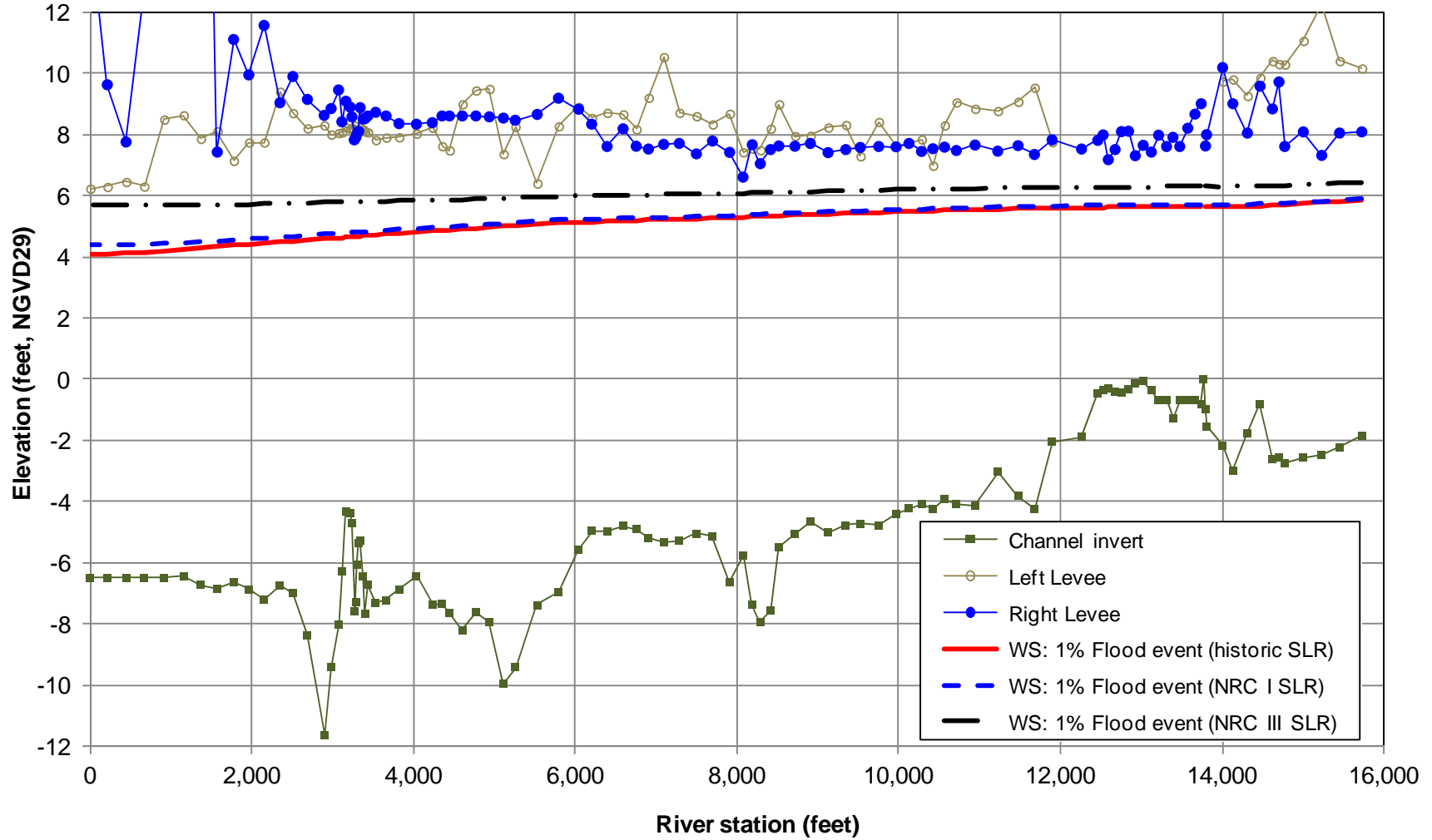


Figure 3-19. 100-Year Water Surface Profiles for the Year 50 Condition Based on Various Sea Level Rise Scenarios

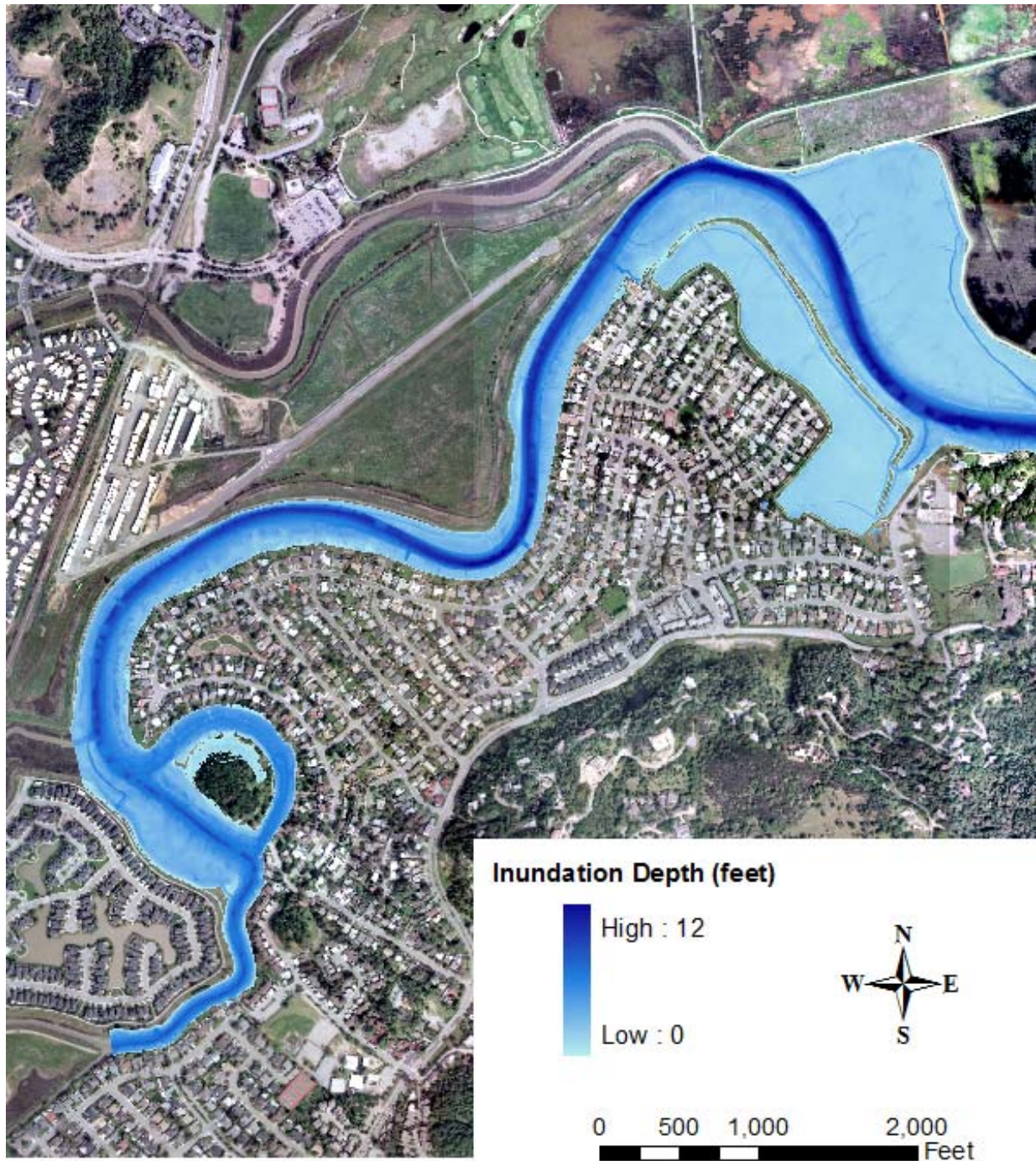


Figure 3-20. Riverine Floodplain Map for the 1% AEP Flood Event (Year 50 Condition, Modified NRC I SLR)

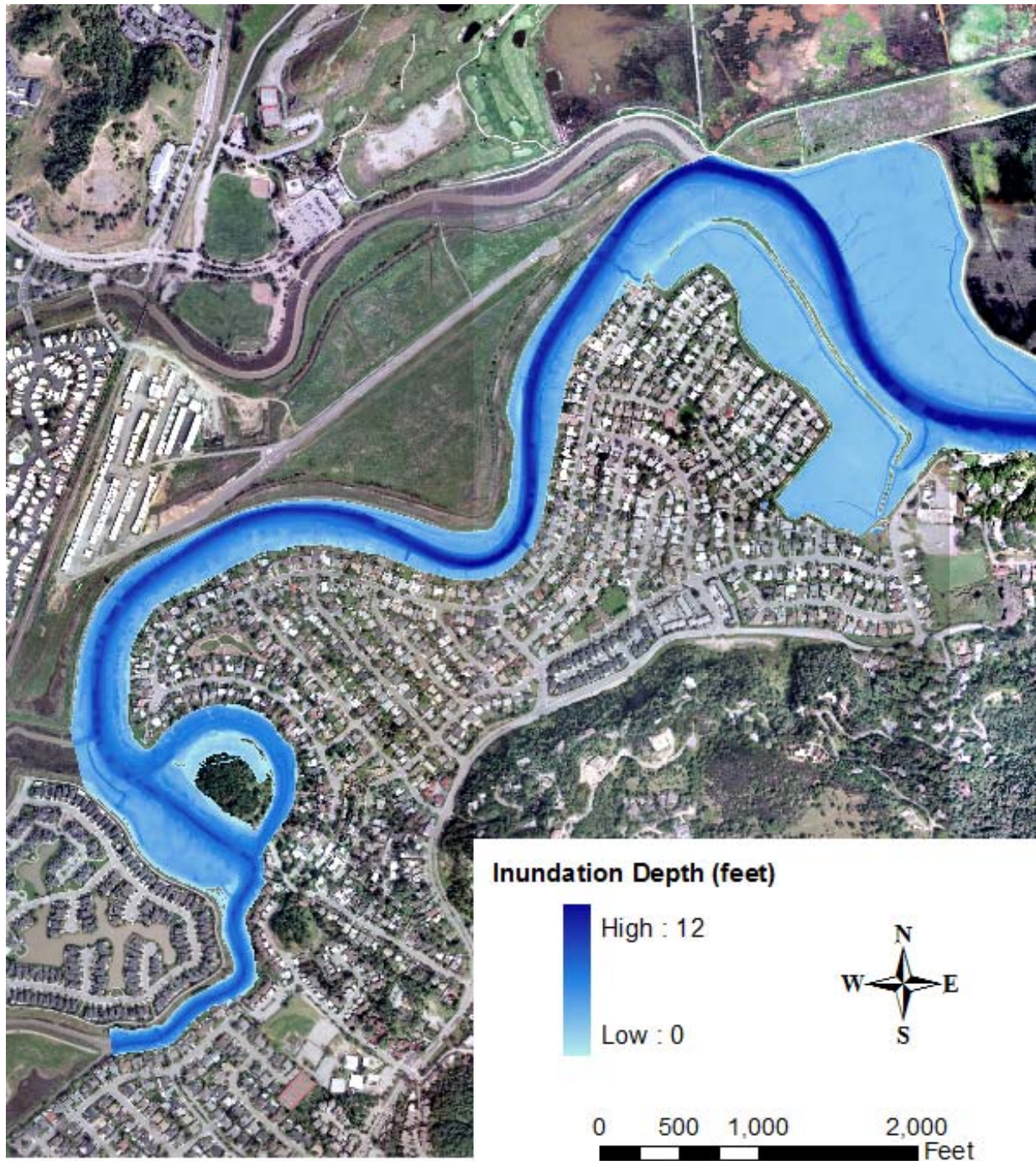


Figure 3-21. Riverine Floodplain Map for the 1% AEP Flood Event (Year 50 Condition, Modified NRC III SLR)

4 RISK AND UNCERTAINTY ANALYSIS

The risk and uncertainty analysis was conducted in order to evaluate the project performance for the existing Santa Venetia levee system that protects the Santa Venetia community. The project performance was evaluated based on the conditional annual non-exceedance probability (CNP) that was computed with the HEC-FDA model together with the freeboard that was determined based on the HEC-RAS results for the 1% AEP flood event.

4.1 HEC-FDA Model

The Hydrologic Engineering Center's Flood Damage Reduction Analysis (HEC-FDA) program provides the capability to perform integrated hydrologic engineering and economic analysis for formulating and evaluation flood damage reduction plans using risk-based analysis. It includes risk analysis methods that follow Federal and Corps of Engineers policy regulations. One capability of HEC-FDA is to compute the conditional annual non-exceedance probability (CNP) for target stages, which can be used as a criterion to evaluate the project performance of a levee system. The HEC-FDA analysis requires the stage-discharge function with uncertainty and the exceedance probability function with uncertainty to be defined for each damage reach index point specified in HEC-FDA.

4.2 Index Points

Fifteen index points were selected along the South Fork of Las Gallinas Creek. They include the flow change locations (hydrologic junctions), upstream and downstream of the Santa Margarita Island Bridge, and other key locations along the creek. The locations of the index points are shown in Figure 4-1, with the description listed in Table 4-1.

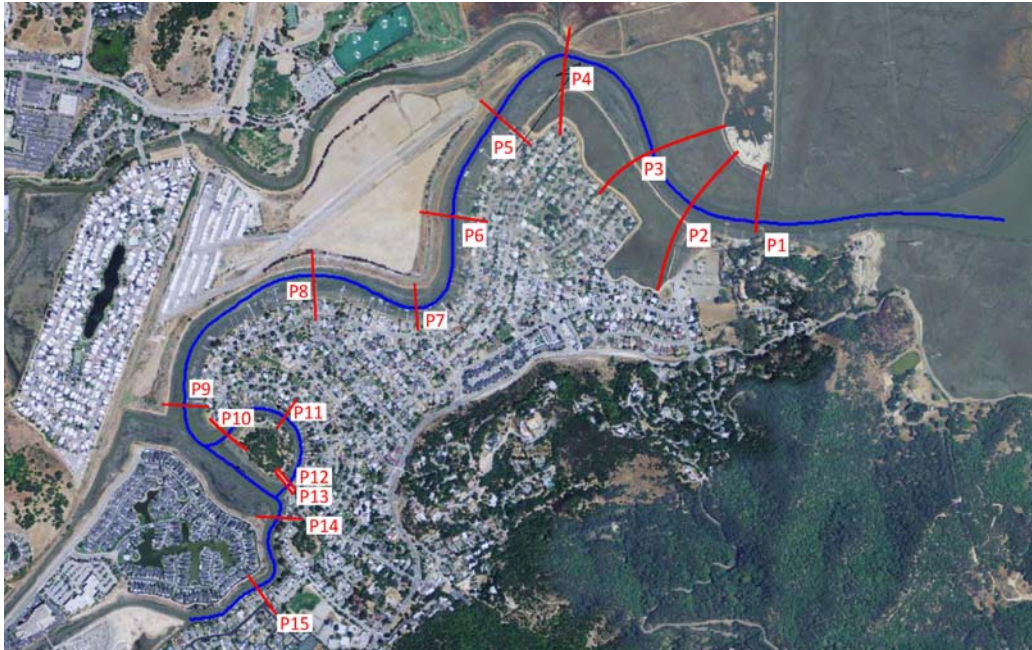


Figure 4-1. Locations of HEC-FDA Index Points

Table 4-1. HEC-FDA Index Points

Index Pts	River Station	Remarks
P1	2,507	East end of Vendola Drive
P2	3,163	South west corner of Inner Marsh Levee
P3	3,820	Middle of Inner Marsh Levee
P4	5,257	Junction 8, confluence of South & North Forks
P5	6,202	Reach 11, outfall of pump station No. 5
P6	7,286	Labrea Way, between Reach 11 and Junction 14
P7	8,415	Junction 14, outfall of pump station No. 1
P8	9,525	Birch Way, between Junction 14 and Junction 7
P9	11,679	Junction 7, confluence of Railroad channel with South Fork
P10	12,261	downstream end of Santa Margarita right branch
P11	13,204	middle of Santa Margarita right branch
P12	13,741	downstream of Santa Margarita Island Bridge
P13	13,794	Upstream of Santa Margarita Island Bridge
P14	14,133	Junction 3, Meadow Drive Hillside drain outfall
P15	15,004	Lowell Ave, between Junction 3 and Junction 2

4.3 Computed Median Water Stages

The stage-discharge function, which is the relationship between the flow discharge at a river cross section and the stage produced by the discharge, is required for each index point as the input to the HEC-FDA model for the calculation of the CNP. This stage-discharge function was derived based on the (median) water surface stages computed for the eight flood events using the median (normal) value of the Manning's roughness coefficient and the normal downstream water level at MHHW, as discussed in Section 3.

The median water surface profiles computed for these eight flood events are shown in Figure 3-1 for the Year 0 condition, and in Figure 3-10 for the Year 50 condition. The flow discharges and the median water levels for the selected index points are listed in Table 4-2 and Table 4-3, respectively, for the Year 0 condition; and in Table 4-4 and Table 4-5, respectively, for the Year 50 condition.

Table 4-2. Flow Discharges at Index Points for the Year 0 Condition

Index point	River Station	Discharge (cfs) for Different Exceedance Probabilities							
		50%	20%	10%	4%	2%	1%	0.4%	0.2%
P1	2,507	693	1,369	1,843	2,390	2,778	3,159	3,658	4,030
P2	3,163	693	1,369	1,843	2,390	2,778	3,159	3,658	4,030
P3	3,820	693	1,369	1,843	2,390	2,778	3,159	3,658	4,030
P4	5,257	693	1,369	1,843	2,390	2,778	3,159	3,658	4,030
P5	6,202	340	679	920	1,200	1,401	1,596	1,854	2,049
P6	7,286	334	670	908	1,185	1,383	1,577	1,833	2,025
P7	8,415	334	670	908	1,185	1,383	1,577	1,833	2,025
P8	9,525	286	583	795	1,042	1,220	1,393	1,621	1,794
P9	11,679	286	583	795	1,042	1,220	1,393	1,621	1,794
P10	12,261	45	103	119	150	194	218	241	264
P11	13,024	45	103	119	150	194	218	241	264
P12	13,741	45	103	119	150	194	218	241	264
P13	13,794	45	103	119	150	194	218	241	264
P14	14,133	247	504	687	902	1,056	1,206	1,405	1,555
P15	15,004	205	410	553	718	837	951	1,101	1,215

Table 4-3. Water Levels at Index Points for the Year 0 Condition

Index point	River Station	Water Stages (ft, NGVD29) for Different Exceedance Probabilities							
		50%	20%	10%	4%	2%	1%	0.4%	0.2%
P1	2,507	3.64	3.82	3.98	4.15	4.27	4.37	4.50	4.59
P2	3,163	3.66	3.87	4.05	4.25	4.39	4.51	4.66	4.77
P3	3,820	3.70	3.97	4.18	4.40	4.55	4.68	4.85	4.96
P4	5,257	3.77	4.13	4.38	4.64	4.81	4.97	5.16	5.30
P5	6,202	3.79	4.18	4.45	4.73	4.91	5.08	5.29	5.44
P6	7,286	3.80	4.21	4.49	4.79	4.98	5.17	5.39	5.55
P7	8,415	3.81	4.25	4.55	4.87	5.09	5.28	5.53	5.70
P8	9,525	3.82	4.29	4.61	4.95	5.17	5.38	5.64	5.82
P9	11,679	3.85	4.35	4.70	5.07	5.31	5.54	5.82	6.02
P10	12,261	3.85	4.36	4.71	5.09	5.34	5.57	5.85	6.05
P11	13,024	3.85	4.37	4.72	5.09	5.34	5.57	5.85	6.06
P12	13,741	3.85	4.37	4.72	5.10	5.35	5.58	5.86	6.06
P13	13,794	3.85	4.37	4.72	5.10	5.35	5.58	5.86	6.06
P14	14,133	3.86	4.37	4.72	5.10	5.34	5.57	5.86	6.06
P15	15,004	3.87	4.41	4.79	5.18	5.44	5.68	5.98	6.19

Table 4-4. Flow Discharges at Index Points for the Year 50 Condition

Index point	River Station	Discharge (cfs) for Different Exceedance Probabilities							
		50%	20%	10%	4%	2%	1%	0.4%	0.2%
P1	2,507	693	1,369	1,843	2,390	2,778	3,159	3,658	4,030
P2	3,163	693	1,369	1,843	2,390	2,778	3,159	3,658	4,030
P3	3,820	693	1,369	1,843	2,390	2,778	3,159	3,658	4,030
P4	5,257	693	1,369	1,843	2,390	2,778	3,159	3,658	4,030
P5	6,202	340	679	920	1,200	1,401	1,596	1,854	2,049
P6	7,286	334	670	908	1,185	1,383	1,577	1,833	2,025
P7	8,415	334	670	908	1,185	1,383	1,577	1,833	2,025
P8	9,525	286	583	795	1,042	1,220	1,393	1,621	1,794
P9	11,679	286	583	795	1,042	1,220	1,393	1,621	1,794
P10	12,261	46	87	120	151	173	219	250	265
P11	13,024	46	87	120	151	173	219	250	265
P12	13,741	46	87	120	151	173	219	250	265
P13	13,794	46	87	120	151	173	219	250	265
P14	14,133	247	504	687	902	1,056	1,206	1,405	1,555
P15	15,004	205	410	553	718	837	951	1,101	1,215

Table 4-5. Water Levels at Index Points for the Year 50 Condition

Index point	River Station	Water Stages (ft, NGVD29) for Different Exceedance Probabilities							
		50%	20%	10%	4%	2%	1%	0.4%	0.2%
P1	2,507	4.11	4.19	4.26	4.36	4.43	4.51	4.61	4.68
P2	3,163	4.12	4.22	4.32	4.44	4.54	4.63	4.76	4.85
P3	3,820	4.14	4.27	4.40	4.55	4.67	4.78	4.92	5.03
P4	5,257	4.17	4.38	4.55	4.76	4.90	5.04	5.21	5.34
P5	6,202	4.18	4.42	4.61	4.83	4.99	5.14	5.34	5.48
P6	7,286	4.19	4.44	4.65	4.89	5.06	5.23	5.43	5.58
P7	8,415	4.20	4.47	4.70	4.97	5.16	5.34	5.57	5.73
P8	9,525	4.21	4.51	4.75	5.04	5.24	5.43	5.67	5.85
P9	11,679	4.23	4.56	4.83	5.15	5.37	5.59	5.85	6.05
P10	12,261	4.23	4.57	4.85	5.17	5.40	5.61	5.88	6.08
P11	13,024	4.23	4.57	4.85	5.17	5.40	5.62	5.89	6.09
P12	13,741	4.23	4.57	4.85	5.18	5.41	5.62	5.90	6.09
P13	13,794	4.23	4.57	4.85	5.18	5.41	5.63	5.90	6.09
P14	14,133	4.23	4.57	4.85	5.18	5.41	5.62	5.89	6.09
P15	15,004	4.24	4.61	4.91	5.26	5.50	5.73	6.01	6.22

4.4 Uncertainty in Water Stages

As discussed in Section 2.7 (Sensitivity Analysis), the uncertainty in this hydraulic analysis attributes to the uncertainty in the Manning's roughness value (n-value) and the uncertainty in the downstream boundary condition (water level). The calibrated n-value and the downstream water level at MHHW were used to determine the median water stages. The lower and the upper bounds of these two model input parameters, which were also discussed in Section 2.7, were used to determine the uncertainty in the water stages.

The lower limit of the n-value with the lower limit of the downstream boundary condition was used to generate the lower bound of the water stages. The upper limit of the n-value with the upper limit of the downstream boundary condition was used to generate the upper bound of the water stages. The model parameters used in the computation of the upper and lower bounds of the water stages are summarized in Table 4-6.

Table 4-6. HEC-RAS Model Parameters Used in Water Stage Uncertainty Analysis

WSEL Profiles	Manning's Roughness (Left / Channel / Right)	Downstream Water Level (feet, NGVD29)
Median SWEL	0.050 / 0.035 / 0.100	+3.58 ^a
Upper bound of WSEL	0.070 / 0.040 / 0.120	+4.39 ^b
Lower bound of WSEL	0.035 / 0.030 / 0.080	+2.99 ^c

Note: a. Mean Higher High Water (MHHW).

b. The 1-year (100% annual chance) maximum still water level as determined in Section 5.

c. Mean High Water (MHW).

As examples, the computed upper and lower bounds of the water stages for the Year 0 condition are shown in Figure 2-13 for the 1% AEP flood event, and in Figure 2-14 for the 0.2% AEP flood event. By assuming the stage difference between the upper bound and the lower bound to be the “reasonable bounds”, e.g., 95% of the stage uncertainty range, the standard deviation was computed by dividing this stage range by four, as recommended in the EM 1110-2-1619 (USACE, 1996). The computed standard deviation of error in water stages is listed in Table 4-7 for the Year 0 condition and in Table 4-8 for the Year 50 condition.

It is noted that a minimum value of the standard deviation of error in stages was considered in this analysis. The computed standard deviation that was less than the minimum value was adjusted to this minimum value. The cross sections used in the HEC-RAS models were based on field survey, and the reliability of the n-value was deemed good. The minimum value of the standard deviation was set to 0.3 feet in this analysis based on Table 5-2 of EM 1110-2-1619.

Table 4-7. Standard Deviation of Error in Stages for the Year 0 Condition

Index point	River Station	Standard Deviation for Different Exceedance Probabilities							
		50%	20%	10%	4%	2%	1%	0.4%	0.2%
P1	2,507	0.35	0.34	0.34	0.32	0.30	0.30	0.30	0.30
P2	3,163	0.35	0.34	0.33	0.31	0.30	0.30	0.30	0.30
P3	3,820	0.35	0.33	0.30	0.30	0.30	0.30	0.30	0.30
P4	5,257	0.34	0.31	0.30	0.30	0.30	0.30	0.30	0.30
P5	6,202	0.34	0.30	0.30	0.30	0.30	0.30	0.30	0.30
P6	7,286	0.34	0.30	0.30	0.30	0.30	0.30	0.30	0.30
P7	8,415	0.34	0.30	0.30	0.30	0.30	0.30	0.30	0.30
P8	9,525	0.34	0.30	0.30	0.30	0.30	0.30	0.30	0.30
P9	11,679	0.33	0.30	0.30	0.30	0.30	0.30	0.30	0.30
P10	12,261	0.33	0.30	0.30	0.30	0.30	0.30	0.30	0.30
P11	13,024	0.33	0.30	0.30	0.30	0.30	0.30	0.30	0.30
P12	13,741	0.33	0.30	0.30	0.30	0.30	0.30	0.30	0.30
P13	13,794	0.33	0.30	0.30	0.30	0.30	0.30	0.30	0.30
P14	14,133	0.33	0.30	0.30	0.30	0.30	0.30	0.30	0.30
P15	15,004	0.33	0.30	0.30	0.30	0.30	0.30	0.30	0.30

Table 4-8. Standard Deviation of Error in Stages for the Year 50 Condition

Index point	River Station	Standard Deviation for Different Exceedance Probabilities							
		50%	20%	10%	4%	2%	1%	0.4%	0.2%
P1	2,507	0.34	0.32	0.30	0.30	0.30	0.30	0.30	0.30
P2	3,163	0.34	0.31	0.30	0.30	0.30	0.30	0.30	0.30
P3	3,820	0.33	0.30	0.30	0.30	0.30	0.30	0.30	0.30
P4	5,257	0.32	0.30	0.30	0.30	0.30	0.30	0.30	0.30
P5	6,202	0.32	0.30	0.30	0.30	0.30	0.30	0.30	0.30
P6	7,286	0.32	0.30	0.30	0.30	0.30	0.30	0.30	0.30
P7	8,415	0.32	0.30	0.30	0.30	0.30	0.30	0.30	0.30
P8	9,525	0.32	0.30	0.30	0.30	0.30	0.30	0.30	0.30
P9	11,679	0.32	0.30	0.30	0.30	0.30	0.30	0.30	0.30
P10	12,261	0.32	0.30	0.30	0.30	0.30	0.30	0.30	0.30
P11	13,024	0.32	0.30	0.30	0.30	0.30	0.30	0.30	0.30
P12	13,741	0.32	0.30	0.30	0.30	0.30	0.30	0.30	0.30
P13	13,794	0.32	0.30	0.30	0.30	0.30	0.30	0.30	0.30
P14	14,133	0.32	0.30	0.30	0.30	0.30	0.30	0.30	0.30
P15	15,004	0.32	0.30	0.30	0.30	0.30	0.30	0.30	0.30

4.5 Stage-Discharge Functions with Uncertainties

The stage-discharge function with uncertainty is needed as an input to the HEC-FDA model when the exceedance probability function is defined in terms of discharge. These functions were determined for the selected fifteen index points. As examples, the stage-discharge function with uncertainty is shown in Figure 4-2 through Figure 4-5 for index points P3, P6, P8 and P13, respectively, for the Year 0 condition. The examples for the Year 50 condition are shown in Figure 4-6 through Figure 4-9.

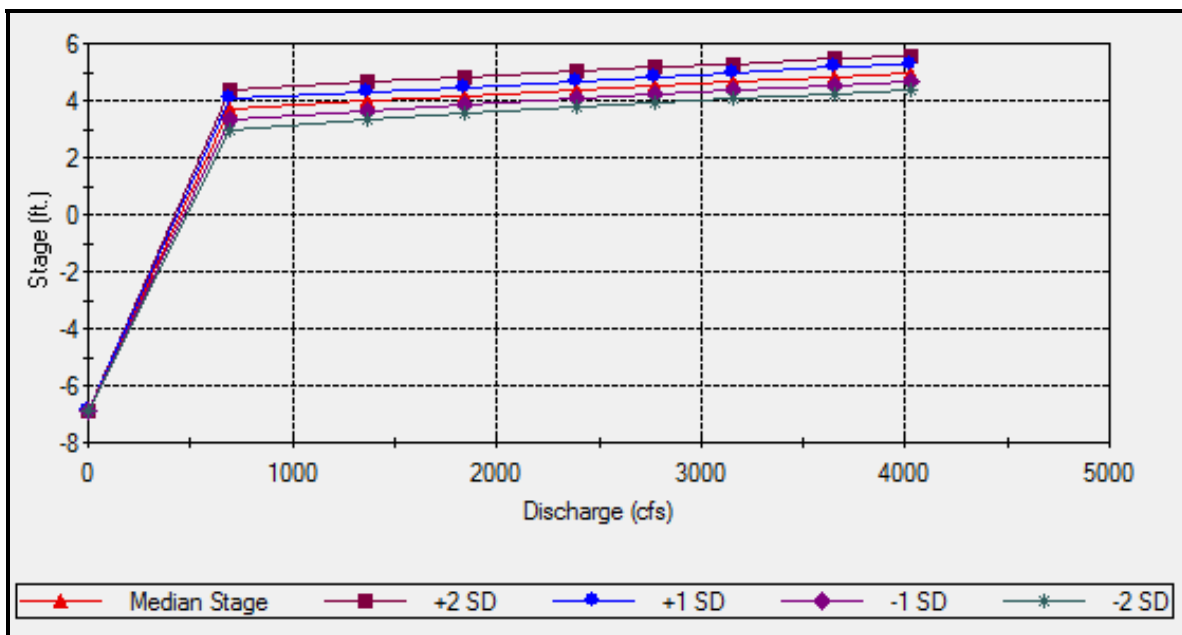


Figure 4-2. Stage-Discharge Function with Uncertainty at Index P3 (Year 0)

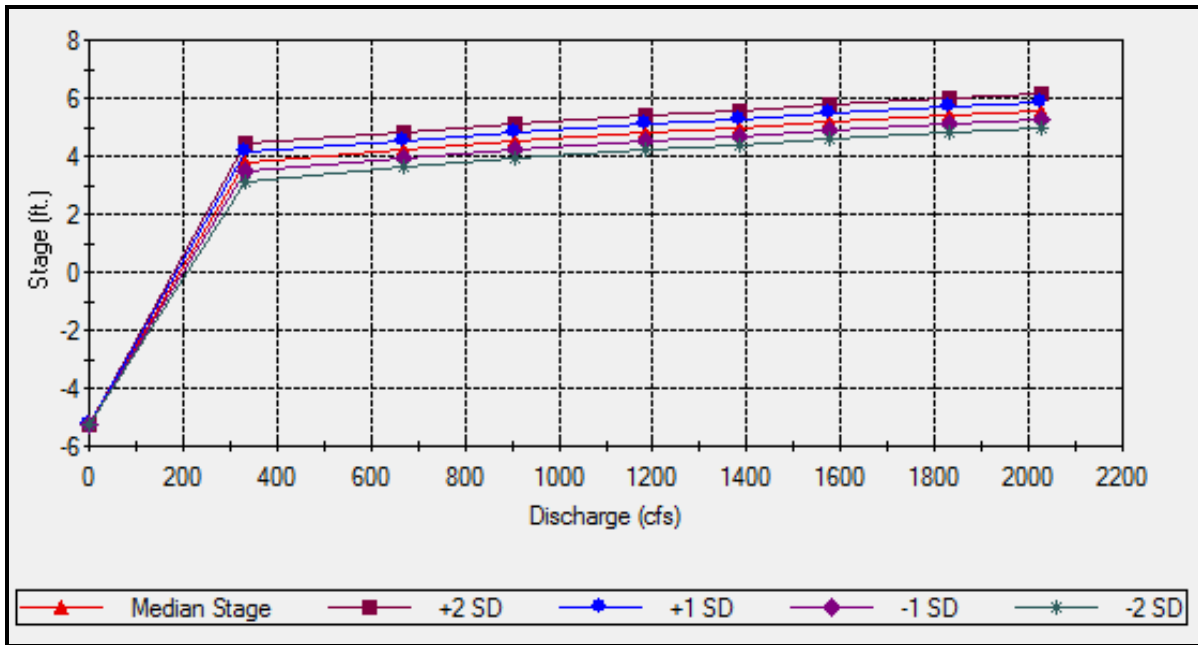


Figure 4-3. Stage-Discharge Function with Uncertainty at Index P6 (Year 0)

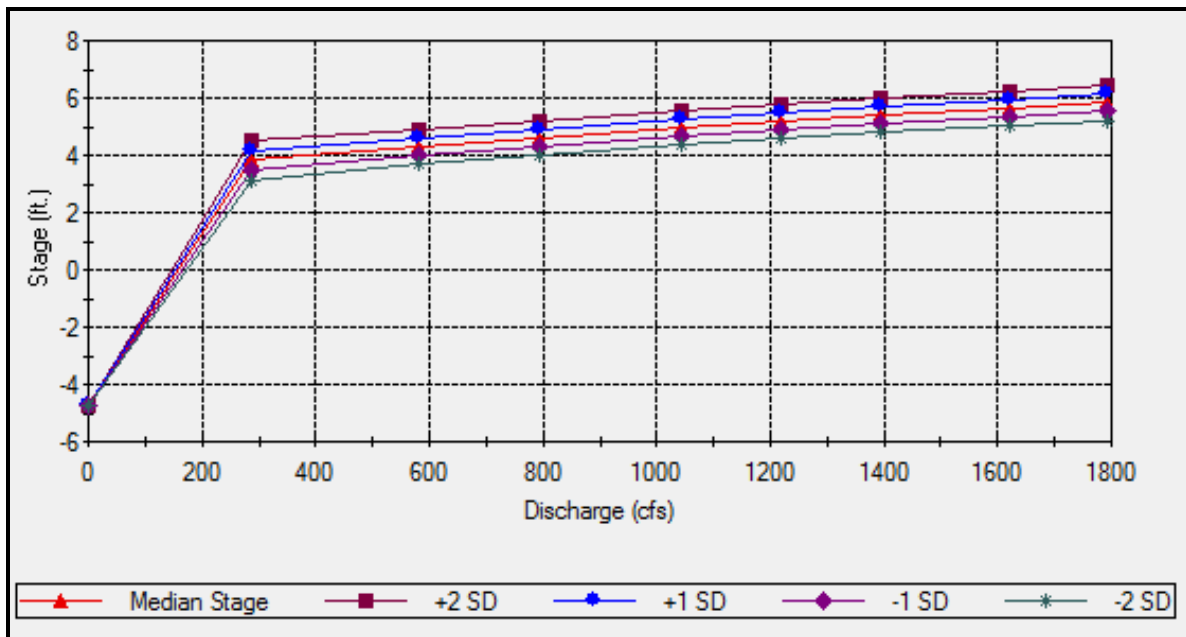


Figure 4-4. Stage-Discharge Function with Uncertainty at Index P8 (Year 0)

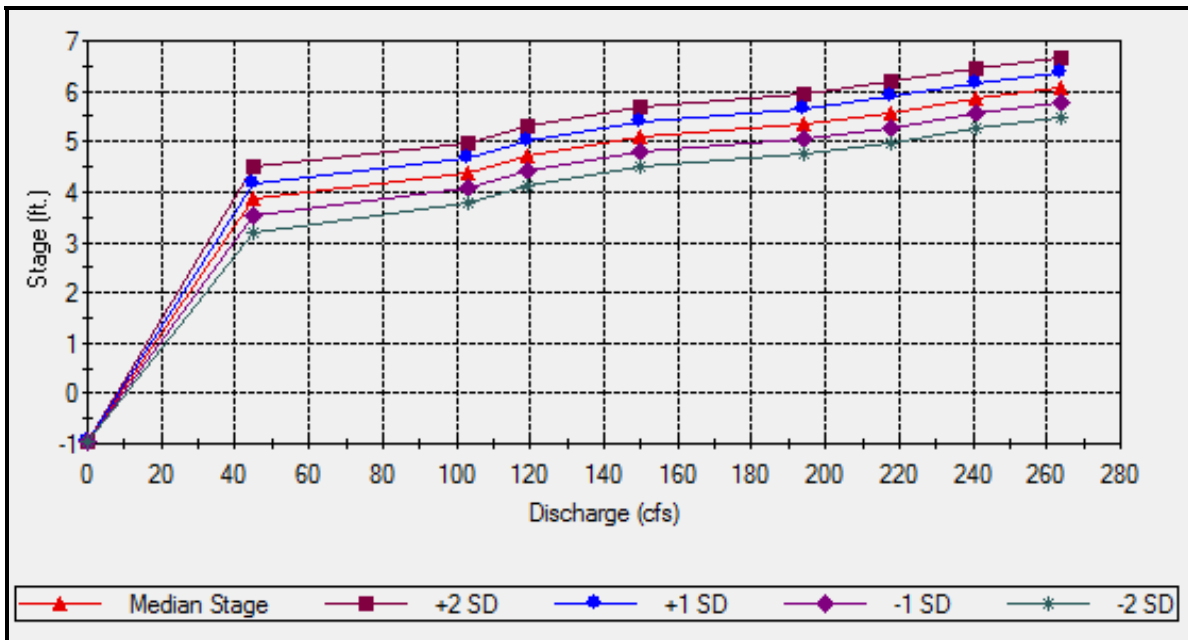


Figure 4-5. Stage-Discharge Function with Uncertainty at Index P13 (Year 0)

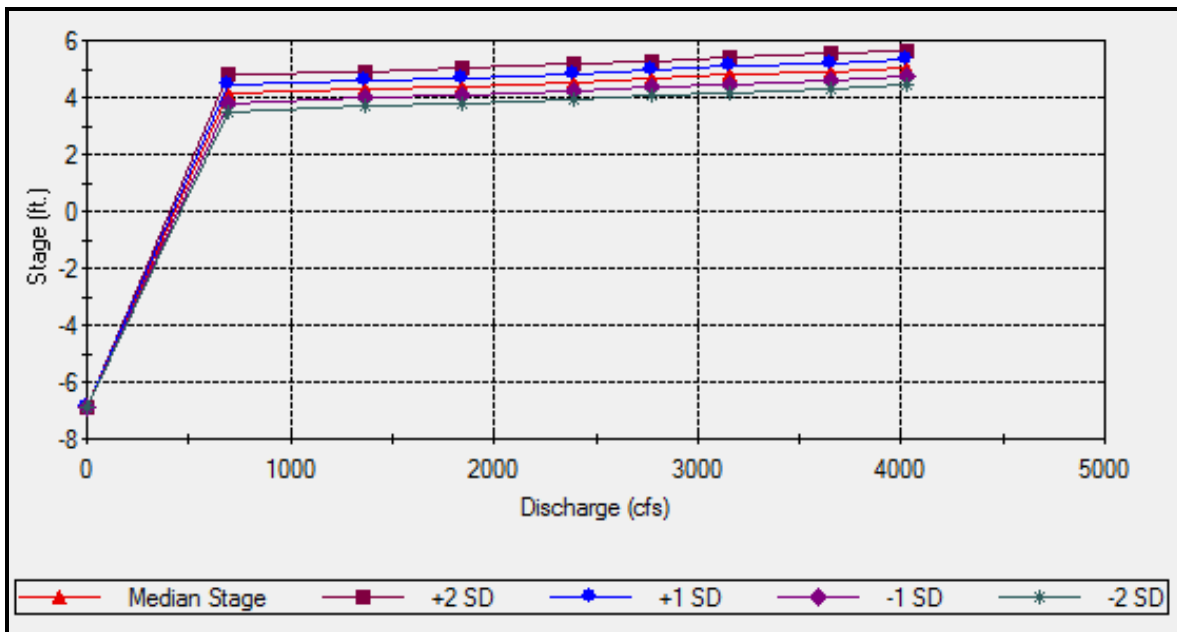


Figure 4-6. Stage-Discharge Function with Uncertainty at Index P3 (Year 50)

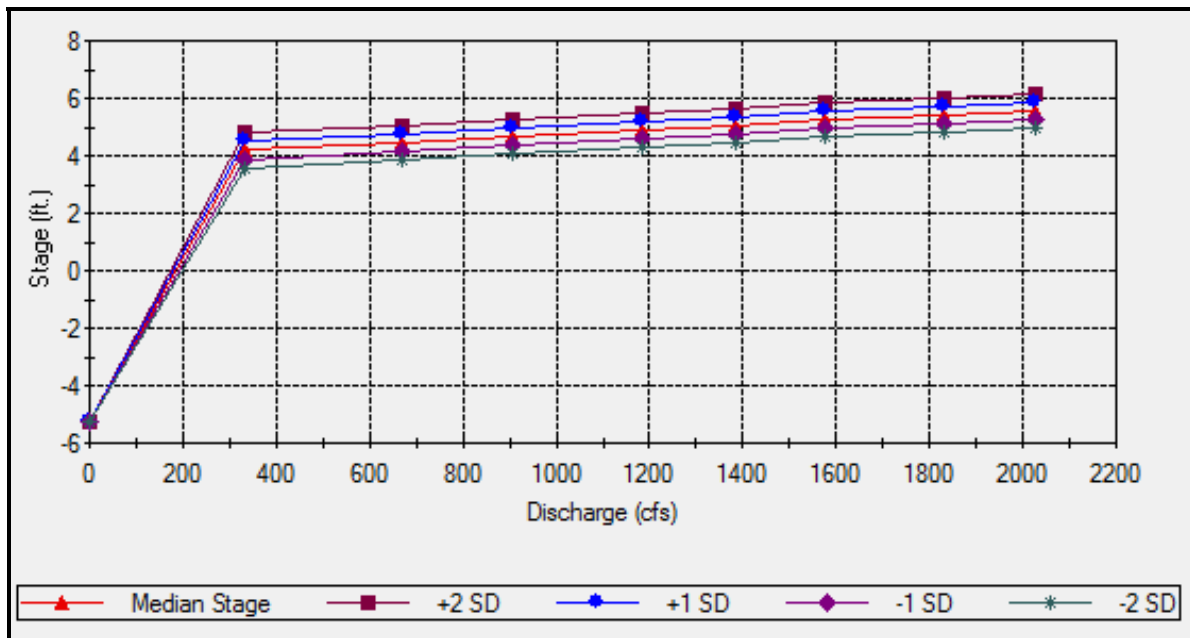


Figure 4-7. Stage-Discharge Function with Uncertainty at Index P6 (Year 50)

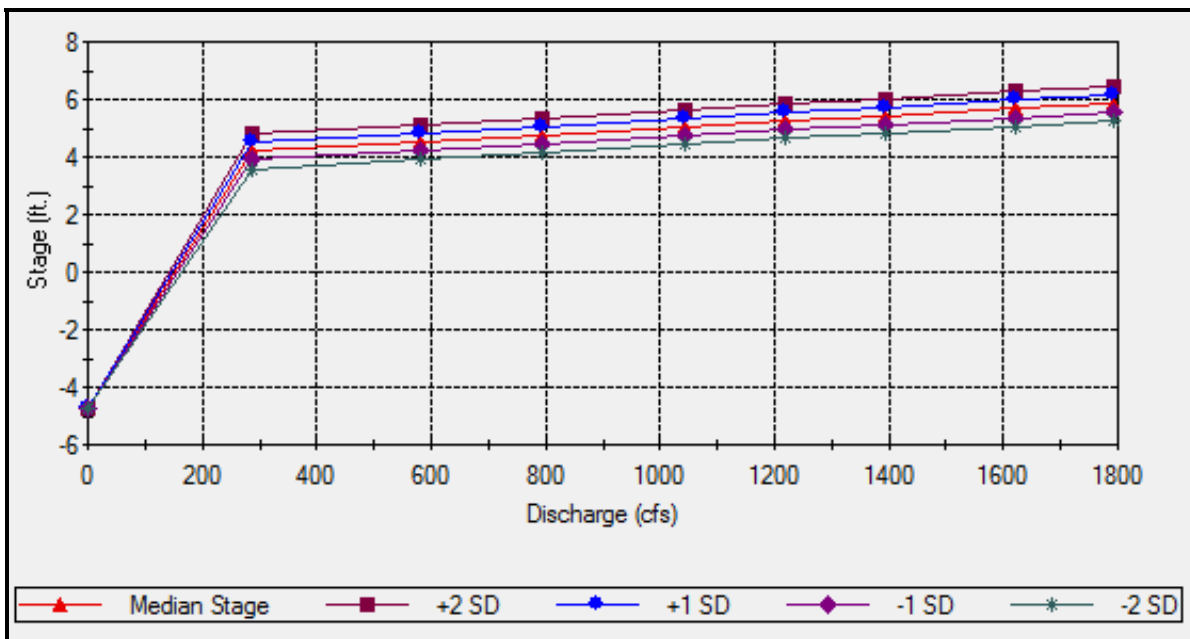


Figure 4-8. Stage-Discharge Function with Uncertainty at Index P8 (Year 50)

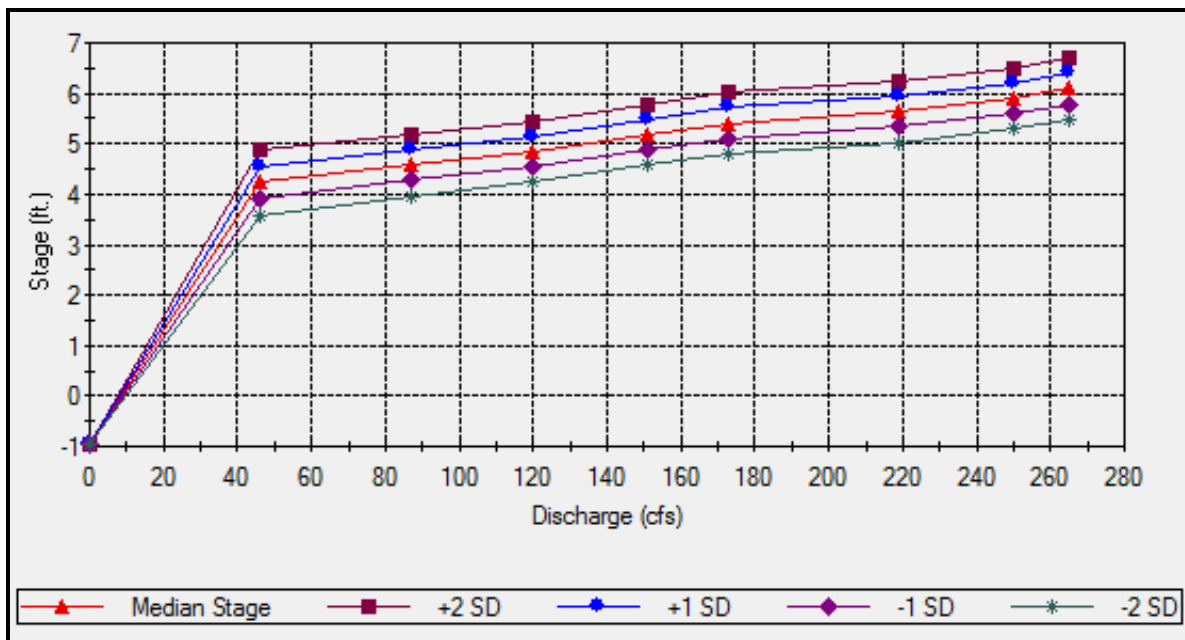


Figure 4-9. Stage-Discharge Function with Uncertainty at Index P13 (Year 50)

4.6 Discharge Exceedance Probability Functions with Uncertainties

The HEC-FDA analysis requires a discharge exceedance probability function with uncertainty to be defined for each index point. The discharge exceedance probability functions with uncertainties were determined in the Corps (2011) hydrologic analysis for the six flow change locations along the creek. In this analysis, these functions were directly assigned to the fifteen index points based on the locations of these index points.

The discharge exceedance probability functions with uncertainties assigned for the index points are tabulated in Table 4-9 through Table 4-14, and are also shown in Figure 4-10 through Figure 4-15. According to the Corps (2011) hydrologic study, the hydrologic condition for the Las Gallinas Creek watershed and the discharge exceedance probability functions were considered the same between the Year 50 condition and the Year 0 condition. Therefore, the same discharge exceedance probability functions were used for the Year 0 condition and for the Year 50 condition.

Table 4-9. Discharge-Probability Function at Junction 8 (Index P1 through P4)

Exceedance Probability	Discharge (cfs)	Confidence Limit Curves (standard error)			
		Discharge (cfs)			
		-2 SD	-1 SD	+1 SD	+2 SD
0.9990	12	3	6	25	51
0.9900	33	10	18	60	110
0.9500	80	28	47	135	227
0.9000	129	48	79	211	344
0.8000	230	90	144	367	586
0.7000	348	138	219	554	880
0.5000	693	327	476	1009	1469
0.3000	1059	592	792	1417	1895
0.2000	1369	750	1013	1850	2500
0.1000	1843	982	1345	2525	3459
0.0400	2390	1239	1721	3319	4610
0.0200	2778	1416	1983	3891	5450
0.0100	3159	1586	2238	4458	6292
0.0040	3658	1804	2569	5208	7417
0.0020	4030	1963	2813	5774	8272
0.0010	4414	2125	3063	6361	9167

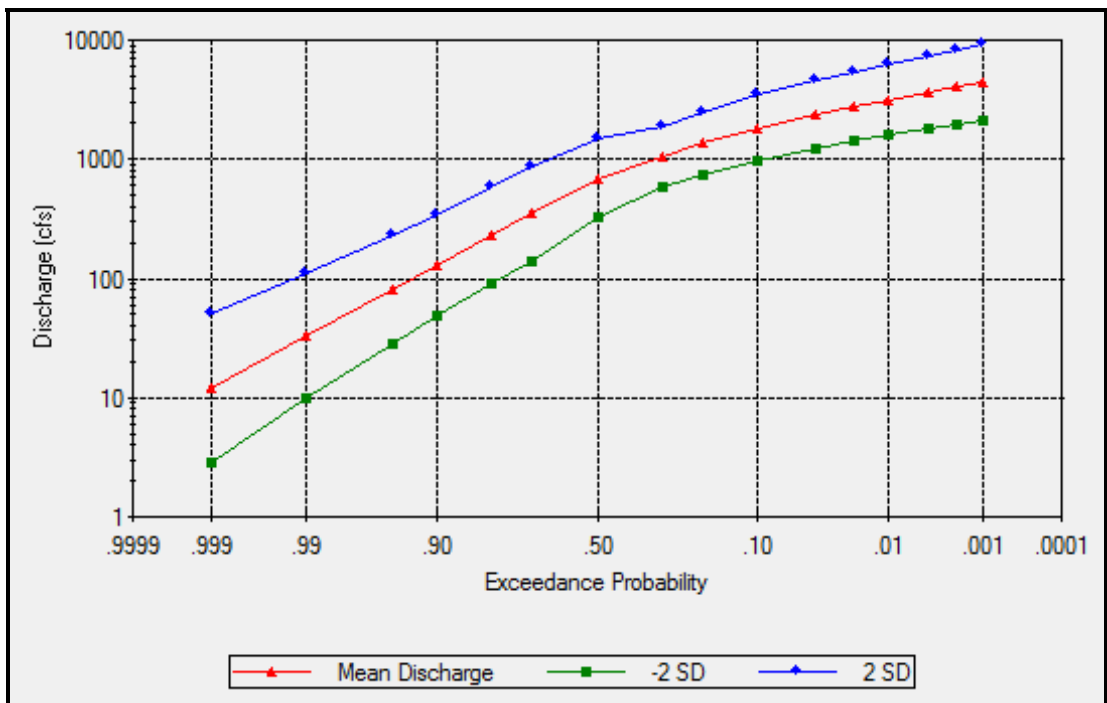


Figure 4-10. Discharge-Probability Function at Junction 8 (Index P1 through P4)

Table 4-10. Discharge-Probability Function at Reach 11 (Index P5)

Exceedance Probability	Discharge (cfs)	Confidence Limit Curves (standard error)			
		Discharge (cfs)			
		-2 SD	-1 SD	+1 SD	+2 SD
0.9990	12	3	6	25	51
0.9900	33	10	18	60	110
0.9500	80	28	47	135	227
0.9000	129	48	79	211	344
0.8000	230	90	144	367	586
0.7000	348	138	219	554	880
0.5000	693	327	476	1009	1469
0.3000	1059	592	792	1417	1895
0.2000	1369	750	1013	1850	2500
0.1000	1843	982	1345	2525	3459
0.0400	2390	1239	1721	3319	4610
0.0200	2778	1416	1983	3891	5450
0.0100	3159	1586	2238	4458	6292
0.0040	3658	1804	2569	5208	7417
0.0020	4030	1963	2813	5774	8272
0.0010	4414	2125	3063	6361	9167

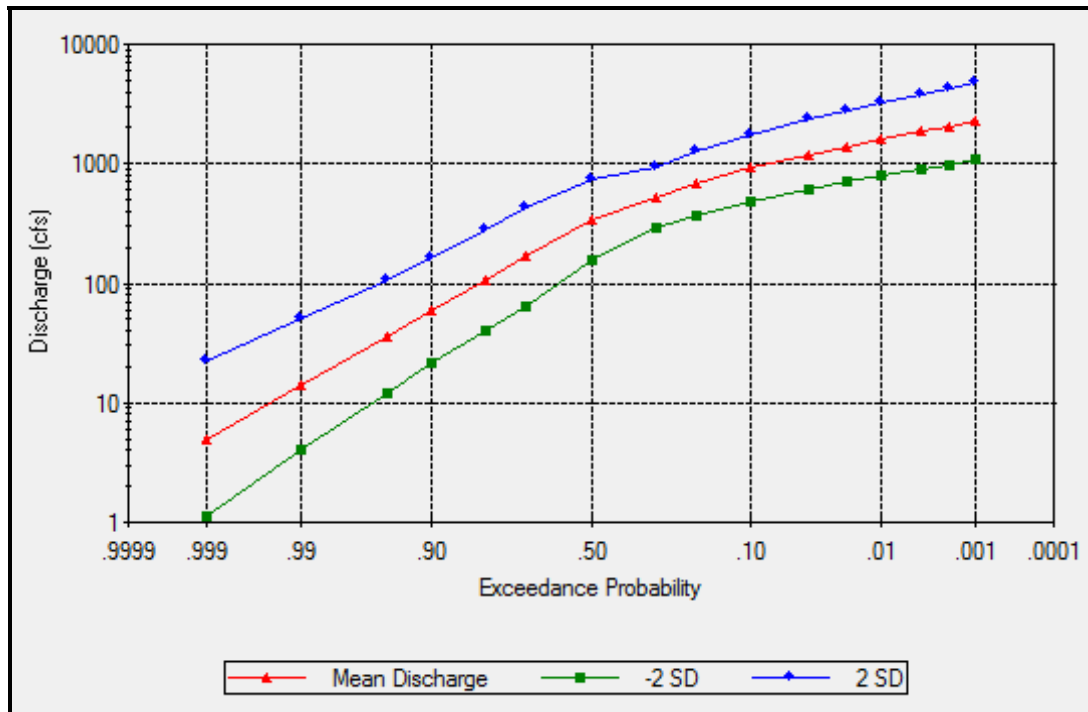


Figure 4-11. Discharge-Probability Function at Reach 11 (Index P5)

Table 4-11. Discharge-Probability Function at Junction 14 (Index P6 through P7)

Exceedance Probability	Discharge (cfs)	Confidence Limit Curves (standard error)			
		Discharge (cfs)			
		-2 SD	-1 SD	+1 SD	+2 SD
0.9990	5	1	2	11	22
0.9900	14	4	8	26	49
0.9500	36	12	21	61	105
0.9000	58	21	35	97	162
0.8000	106	40	65	173	280
0.7000	164	63	101	265	428
0.5000	334	154	227	492	725
0.3000	515	284	383	694	935
0.2000	670	362	492	912	1241
0.1000	908	477	658	1253	1729
0.0400	1185	605	847	1658	2320
0.0200	1383	694	980	1952	2754
0.0100	1577	780	1109	2243	3189
0.0040	1833	890	1277	2630	3774
0.0020	2025	971	1402	2924	4222
0.0010	2224	1054	1531	3230	4692

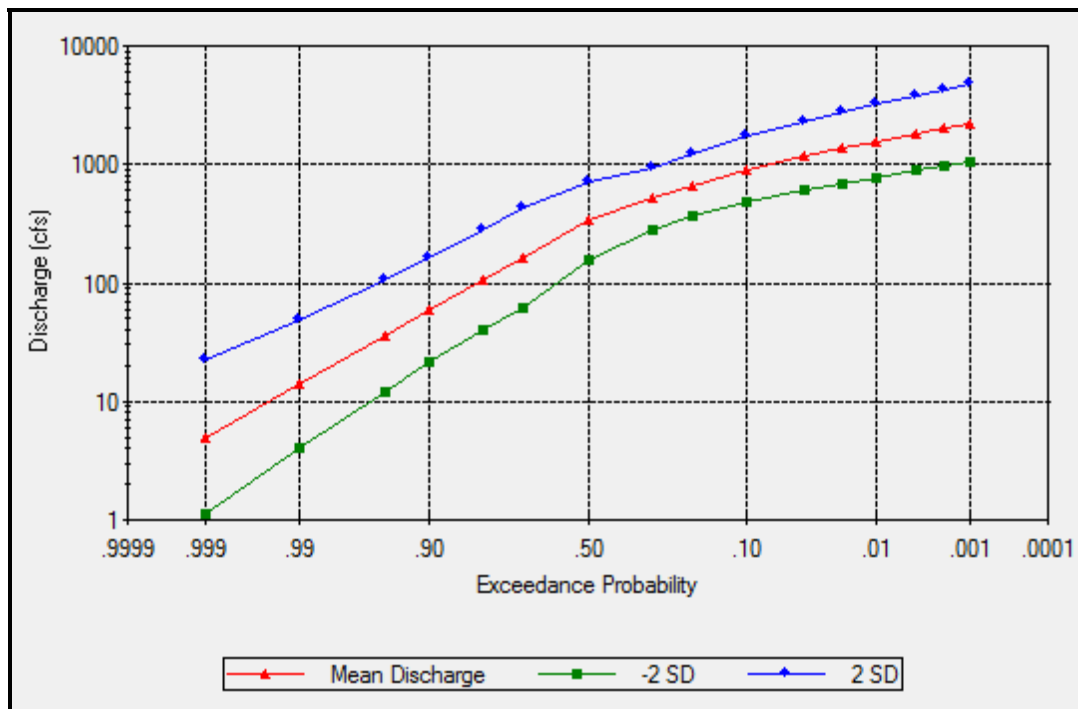


Figure 4-12. Discharge-Probability Function at Junction 14 (Index P6 through P7)

Table 4-12. Discharge-Probability Function at Junction 7 (Index P8 through P9)

Exceedance Probability	Discharge (cfs)	Confidence Limit Curves			
		Discharge (cfs)			
		-2 SD	-1 SD	+1 SD	+2 SD
0.9990	4.00	0.87	1.87	8.57	18.35
0.9900	11.49	3.21	6.08	21.73	41.09
0.9500	29.47	9.81	17.01	51.07	88.49
0.9000	48.68	17.32	29.04	81.62	136.84
0.8000	89.40	33.36	54.62	146.35	239.56
0.7000	138.58	52.22	85.07	225.75	367.74
0.5000	286.00	129.89	192.74	424.39	629.74
0.3000	445.75	242.53	328.79	604.30	819.25
0.2000	583.00	310.57	425.52	798.77	1,094.39
0.1000	795.00	411.57	572.01	1,104.91	1,535.64
0.0400	1,042.00	524.45	739.24	1,468.76	2,070.29
0.0200	1,220.00	603.28	857.91	1,734.92	2,467.18
0.0100	1,393.00	678.22	971.99	1,996.37	2,861.07
0.0040	1,621.38	775.00	1,120.97	2,345.19	3,392.11
0.0020	1,794.00	846.72	1,232.48	2,611.34	3,801.07
0.0010	1,972.58	919.78	1,346.97	2,888.77	4,230.48

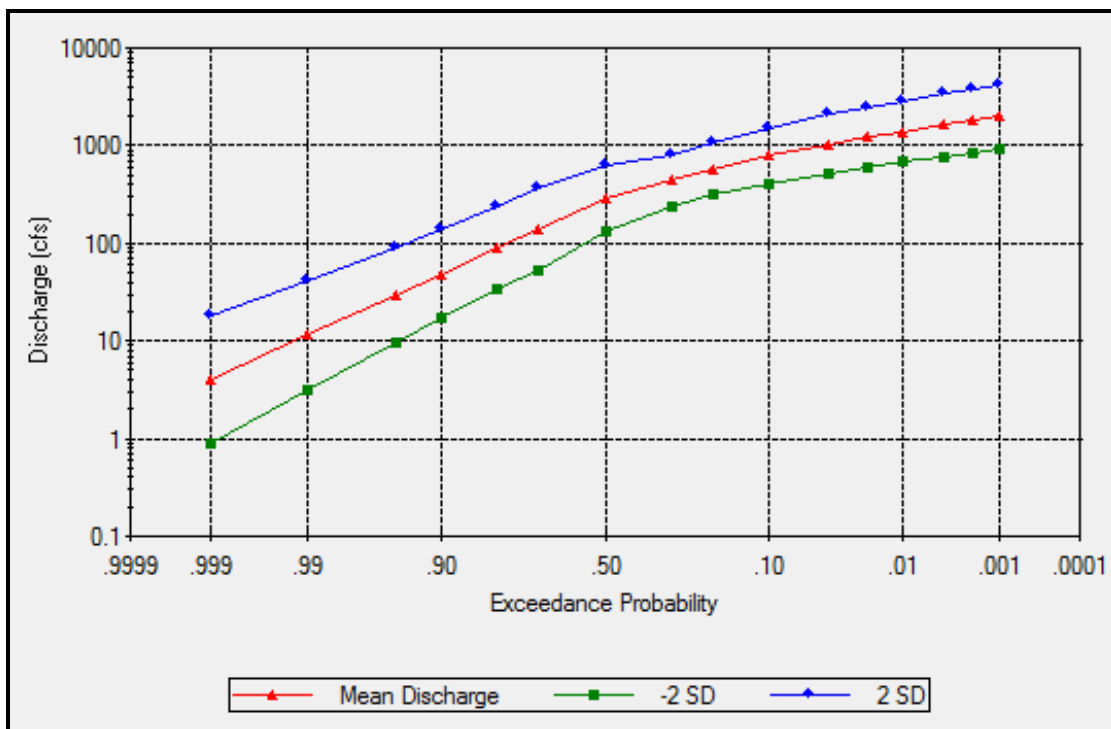


Figure 4-13. Discharge-Probability Function at Junction 7 (Index P8 through P9)

Table 4-13. Discharge-Probability Function at Junction 3 (Index P10 through P14)

Exceedance Probability	Discharge (cfs)	Confidence Limit Curves (standard error)			
		Discharge (cfs)			
		-2 SD	-1 SD	+1 SD	+2 SD
0.9990	3	1	1	7	14
0.9900	9	2	5	17	33
0.9500	24	8	13	42	73
0.9000	40	14	23	68	115
0.8000	74	27	45	124	205
0.7000	117	43	71	193	320
0.5000	247	110	165	370	554
0.3000	385	209	284	523	710
0.2000	504	268	367	691	948
0.1000	687	355	494	955	1329
0.0400	902	454	640	1272	1793
0.0200	1056	522	743	1502	2136
0.0100	1206	587	842	1728	2476
0.0040	1405	672	972	2032	2938
0.0020	1555	735	1069	2262	3291
0.0010	1710	799	1169	2502	3662

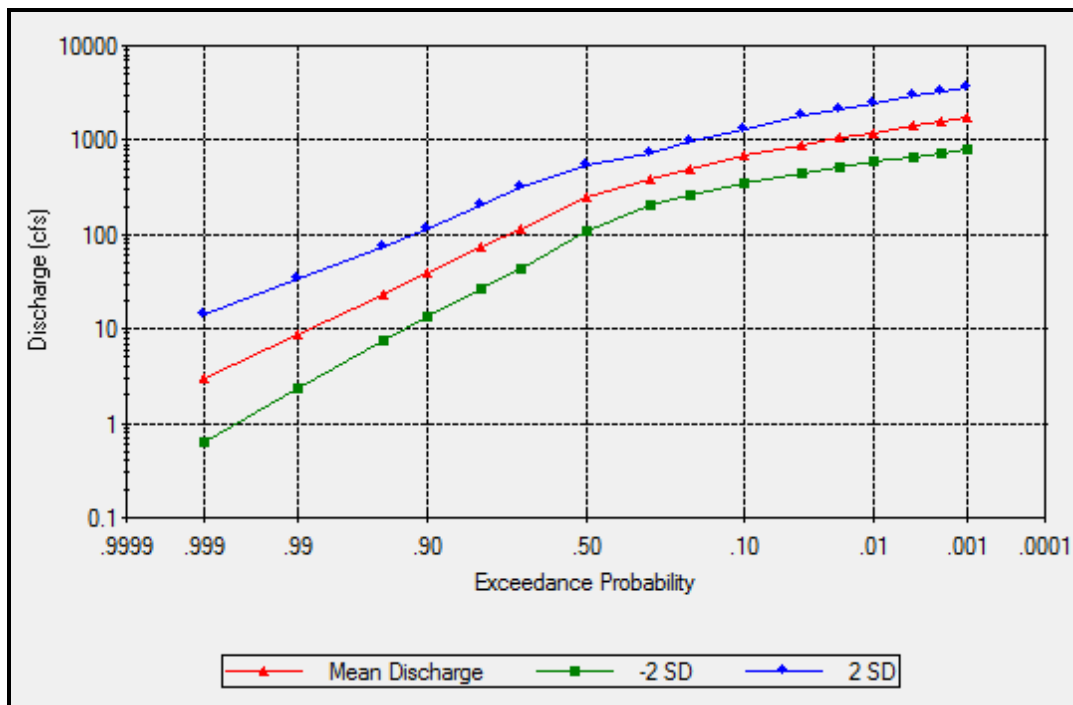


Figure 4-14. Discharge-Probability Function at Junction 3 (Index P10 through P14)

Table 4-14. Flood Frequency Distribution at Junction 2 (Index P15)

Exceedance Probability	Discharge (cfs)	Confidence Limit Curves (standard error)			
		Discharge (cfs)			
		-2 SD	-1 SD	+1 SD	+2 SD
0.9990	3	1	1	6	14
0.9900	9	2	5	16	30
0.9500	22	7	13	37	64
0.9000	36	13	21	59	99
0.8000	65	24	40	106	172
0.7000	100	38	62	162	263
0.5000	205	94	139	302	446
0.3000	316	175	235	425	571
0.2000	410	222	302	557	757
0.1000	553	292	402	762	1049
0.0400	718	369	514	1002	1399
0.0200	837	423	595	1178	1658
0.0100	951	473	671	1348	1912
0.0040	1101	538	770	1575	2252
0.0020	1215	587	844	1748	2516
0.0010	1333	636	921	1929	2791

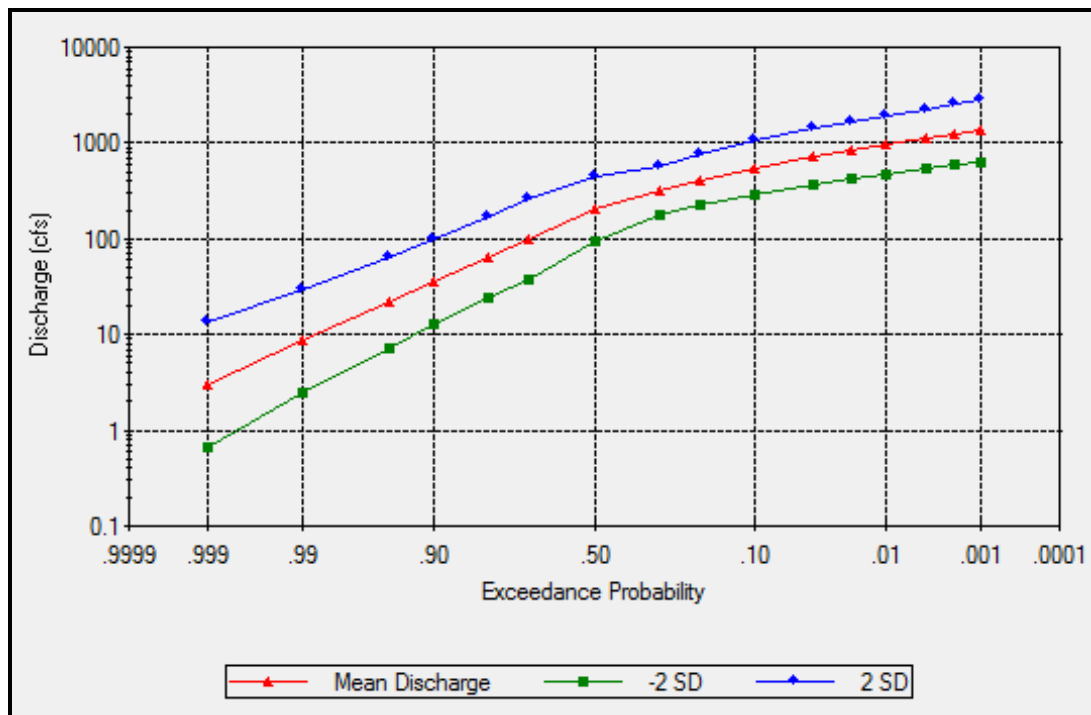


Figure 4-15. Discharge-Probability Function at Junction 2 (Index P15)

4.7 Transform Flow Relationship for Santa Margarita Island Right Branch

The South Fork is divided into two branches by the Santa Margarita Island, with the Santa Venetia levee located along the right bank of the right branch. Therefore, the risk and uncertainty analysis focused on the right branch in order to evaluate the project performance of the Santa Venetia levee system for this area. The four index points selected for this right branch, P10 through P13, are shown in Figure 4-1.

The transform flow relationship was used in the model to define the relationship between the flow defined with the discharge-probability function based on the Corps (2011) hydrology study, which is referred to as inflow in FEC-FDA, and the flow in the right branch, which is referred to as outflow in HEC-FDA. The inflow is the flow discharge at Junction 3 before the flow split at Santa Margarita Island. The outflow is the true flow discharge conveyed in the right branch. The difference between the inflow and the outflow is the flow discharge conveyed in the left branch.

Based on the HEC-RAS model results for the eight flood events, the transform flow relationship was derived for both the Year 0 condition and the Year 50 condition. The mean outflows of the transform flow relationship are the flow discharges associated with the median water surface profiles. The minimum and the maximum outflows are the lower and the upper limits of the flow discharges that can occur within the variation bounds of the water surface profiles. The uncertainty of the transform flow relationship was represented by the uncertainty of the outflow, which was assumed to follow a triangular distribution.

The transform flow relationship with uncertainty for the right branch, which was represented by index points P10 through P13, is summarized in Table 4-15. This relationship is also shown in Figure 4-16 for the Year 0 condition and in Figure 4-17 for the Year 50 condition. It is noted that uncertainty in the transform flow relationship is negligible, and the transform flow relationship show negligible difference between the Year 0 condition and the Year 50 condition.

Table 4-15. Transform Flow Relationship with Uncertainty for Santa Margarita Island Right Branch (Index P10 through P13)

Frequency	Inflow ^a (cfs)	Outflow ^b (cfs)					
		Year 0 Condition			Year 50 Condition		
		Mean	Minimum	Maximum	Mean	Minimum	Maximum
50%	247	45	45	53	46	45	46
20%	504	103	86	105	87	87	102
10%	687	119	112	140	120	115	120
4%	902	150	150	168	151	144	151
2%	1056	194	172	194	173	173	176
1%	1206	218	203	218	219	196	220
0.4%	1405	241	239	241	250	223	252
0.2%	1555	264	262	264	265	265	266

Note: a. Flow discharge before flow split at Santa Margarita Island.
 b. Flow discharge in the Santa Margarita Island right branch.

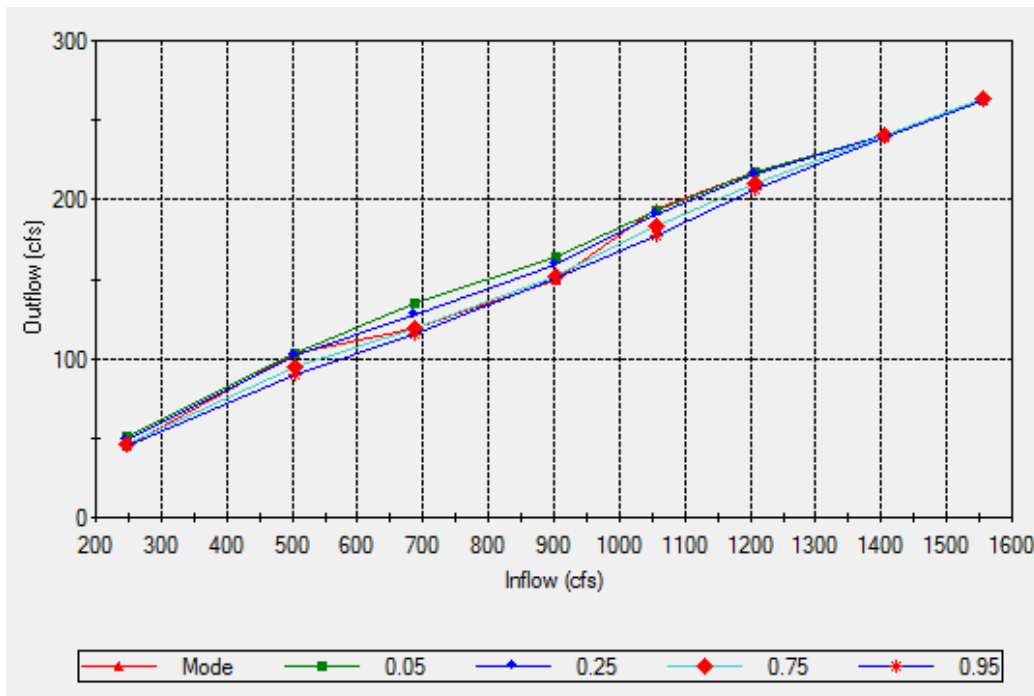


Figure 4-16. Transform Flow Relationship with Uncertainty for Santa Margarita Island Right Branch (Year 0 Condition)

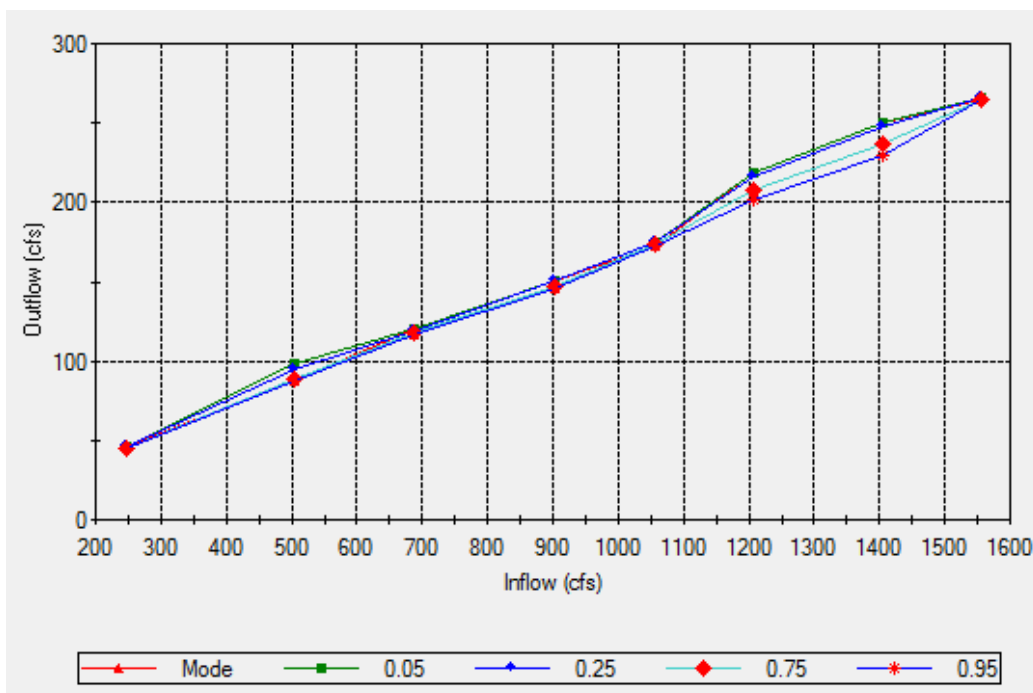


Figure 4-17. Transform Flow Relationship with Uncertainty for Santa Margarita Island Right Branch (Year 50 Condition)

4.8 Evaluation of Project Performance

The stage-discharge function with uncertainty and the discharge exceedance probability function with uncertainty were inputted to the HEC-FDA model for each index point. The conditional annual non-exceedance probability (CNP) was computed with HEC-FDA for a series of target stages for these index points, from which the target stages with the 90% CNP and with the 95% CNP were interpolated.

The 90% CNP stages and the 95% CNP stages calculated for the fifteen index points are listed in Table 4-16 for the Year 0 condition. The profiles for the 90% CNP stages and for the 95% CNP stages were estimated based on the results for these fifteen index points, as shown in Figure 4-18 for the Year 0 condition. The freeboard of the Santa Venetia levee for the 1% AEP flood event was also determined. The freeboard was defined as the vertical distance between the levee crest elevation and the median water stage computed with HEC-RAS for the 1% AEP

flood. The freeboards for these fifteen index points are listed in Table 4-16, and the freeboards for the entire creek are shown in Figure 4-18 for the Year 0 condition.

Table 4-16. Project Performance Evaluation (Year 0 Condition)

Index Point	River Station (feet)	Channel Type	Right Levee Crest El (ft, NGVD)	1% WSEL (ft, NGVD)	Freeboard (feet)	90% CNP Stage (ft, NGVD)	95% CNP Stage (ft, NGVD)	Meet Performance Requirements
P1	2,507	Incised	9.89	4.37	5.52	4.86	5.01	Yes
P2	3,163	Levee	9.08	4.51	4.57	4.98	5.10	Yes
P3	3,820	Levee	8.35	4.68	3.67	5.17	5.28	Yes
P4	5,257	Levee	8.46	4.97	3.49	5.49	5.62	Yes
P5	6,202	Levee	8.33	5.08	3.25	5.62	5.75	Yes
P6	7,286	Levee	7.70	5.17	2.53	5.72	5.86	Yes
P7	8,415	Levee	7.50	5.28	2.22	5.87	6.00	Yes
P8	9,525	Levee	7.57	5.38	2.19	5.98	6.12	Yes
P9	11,679	Levee	7.34	5.54	1.80	6.17	6.32	No
P10	12,261	Levee	7.52	5.57	1.95	6.19	6.34	No
P11	13,204	Levee	7.64	5.57	2.07	6.20	6.35	Yes
P12	13,741	Levee	9.00	5.58	3.42	6.20	6.35	Yes
P13	13,794	Levee	7.62	5.58	2.04	6.20	6.35	Yes
P14	14,133	Levee	9.00	5.57	3.43	6.21	6.36	Yes
P15	15,004	Levee	8.08	5.68	2.40	6.34	6.48	Yes

The computed 90% CNP and 95% CNP stages for the Year 50 condition are listed in Table 4-17 for the fifteen index points. Figure 4-19 shows the 90% CNP and 95% CNP stage profiles. The freeboards for the Year 50 condition are listed in Table 4-17 for the fifteen index points, and are shown in Figure 4-19 for the entire creek.

The project performance of the Santa Venetia levee system was evaluated in this analysis based on the Corps certification criteria. The criteria require that (1) the project provides a minimum of 3 feet of freeboard with a 90% CNP for the 1% AEP flood event, or (2) the project provides a minimum of 2 feet of freeboard with a 95% CNP for the 1% AEP flood event.

Table 4-17. Project Performance Evaluation (Year 50 Condition)

Index Point	River Station (feet)	Channel Type	Right Levee Crest El (ft, NGVD)	1% WSEL (ft, NGVD)	Freeboard (feet)	90% CNP Stage (ft, NGVD)	95% CNP Stage (ft, NGVD)	Meet Performance Requirements
P1	2,507	Incised	9.89	4.51	5.38	4.94	5.15	Yes
P2	3,163	Levee	9.08	4.63	4.45	5.08	5.30	Yes
P3	3,820	Levee	8.35	4.78	3.57	5.25	5.47	Yes
P4	5,257	Levee	8.46	5.04	3.42	5.54	5.76	Yes
P5	6,202	Levee	8.33	5.14	3.19	5.66	5.89	Yes
P6	7,286	Levee	7.70	5.23	2.47	5.76	5.99	Yes
P7	8,415	Levee	7.50	5.34	2.16	5.90	6.04	Yes
P8	9,525	Levee	7.57	5.43	2.14	6.01	6.25	Yes
P9	11,679	Levee	7.34	5.59	1.75	6.20	6.35	No
P10	12,261	Levee	7.52	5.61	1.91	6.22	6.46	No
P11	13,204	Levee	7.64	5.62	2.02	6.23	6.47	Yes
P12	13,741	Levee	9.00	5.62	3.38	6.23	6.47	Yes
P13	13,794	Levee	7.62	5.63	1.99	6.23	6.47	No
P14	14,133	Levee	9.00	5.62	3.38	6.24	6.48	Yes
P15	15,004	Levee	8.08	5.73	2.35	6.37	6.51	Yes

The results of the project performance evaluation for the fifteen index points are listed in Table 4-16 for the Year 0 condition, and in Table 4-17 for the Year 50 Condition. Thirteen of the fifteen index points (or damage reaches) meet the Corps levee certification criteria for the Year 0 condition. Twelve of the fifteen index points (or damage reaches) meet the criteria for the Year 50 condition.

As shown in Figure 4-18 and Figure 4-19, the 90% CNP and 95% CNP stage profiles for the 1% AEP flood event are lower than the crest elevation profile of Santa Venetia levee system for both the Year 0 and the Year 50 conditions. This indicates that the entire Santa Venetia levee system meet the CNP requirement for the certification. However, some portions of the Santa Venetia levee do not meet the required minimum freeboard of 2 feet, and thus do not meet the Corps levee certification criteria.

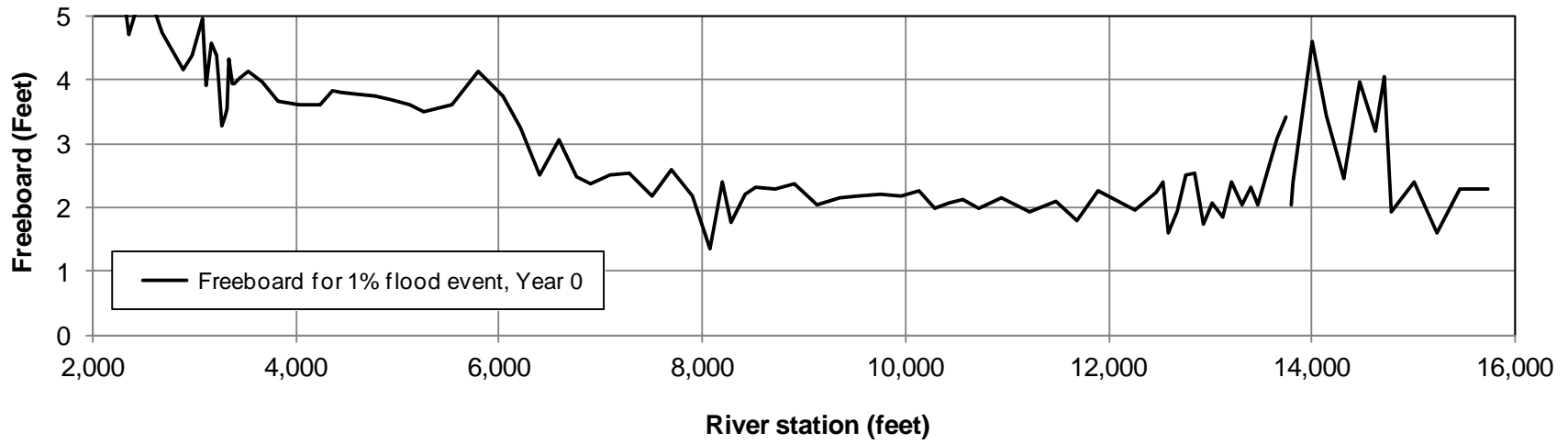
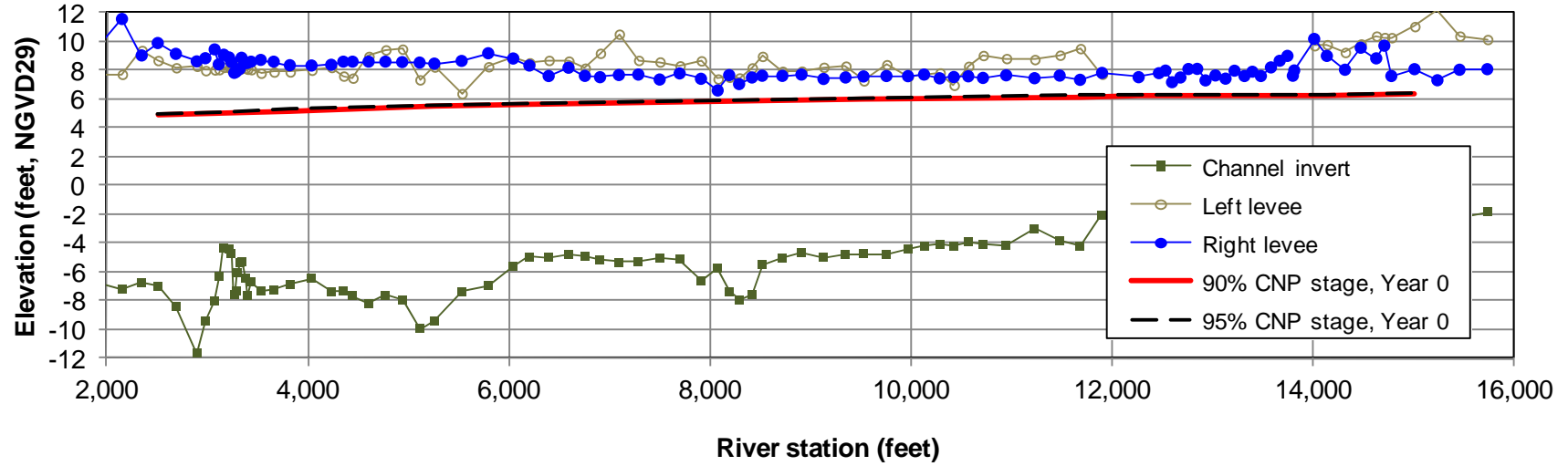


Figure 4-18. 90% and 95% CNP Stage Profiles and Right Levee Freeboards for the 1% AEP Flood Event (Year 0 Condition)

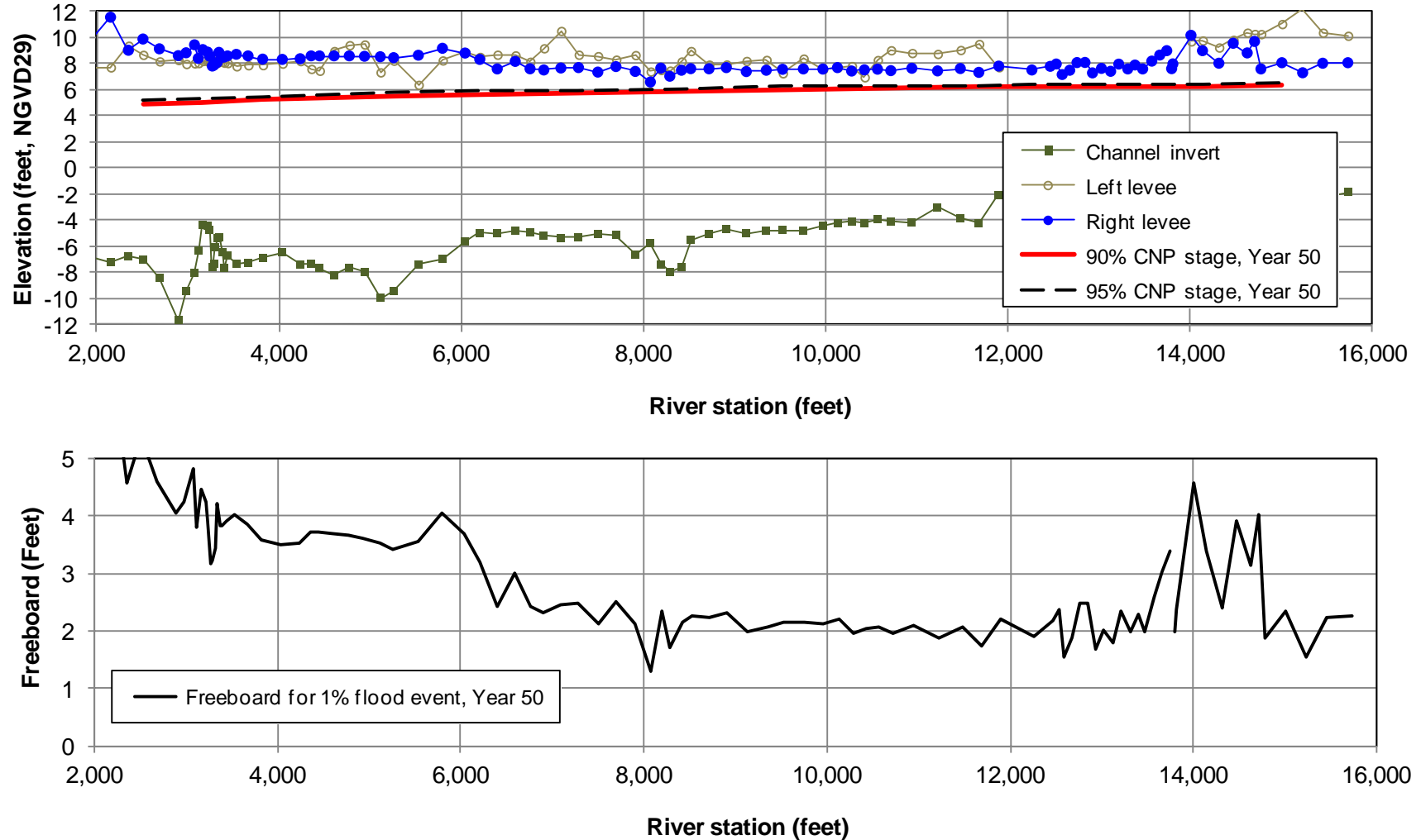


Figure 4-19. 90% and 95% CNP Stage Profiles and Right Levee Freeboards for the 1% AEP Flood Event (Year 50 Condition)

5 COASTAL STILL WATER LEVELS

The is no long-term data record of the still water levels available for the mouth of the Las Gallinas Creek (Gallinas) at the San Pablo Bay. A water level frequency analysis was conducted for the NOAA San Francisco Station, where the tidal stages were measured since 1855. Based on the correlation relation of the still water levels between Gallinas and San Francisco, the coastal still water level frequency curve was developed for Gallinas for the existing Year 0 (2011) condition.

Three scenarios for sea level change were considered for the Year 50 (2061) condition based on the Corps' guidance EC 1165-2-211 (USACE, 2009). After including the future sea level change and the local land movements (uplift and subsidence), the coastal still water level frequency curve was developed for the Year 50 (2061) without project condition.

5.1 Coastal Still Water Level Frequency Analysis for Year 0 Condition

5.1.1 Water Level Frequency Analysis for San Francisco

The water levels have been measured at the NOAA tidal gauge at the San Francisco Station (Station ID: 9414290) since 1855. The annual maximum water levels were downloaded from the NOAA website for the period between 1900 through 2010. The data prior to 1900 were not published in NOAA's website, but were presented in the report titled "San Francisco Bay Tidal Stage vs. Frequency Study" that was prepared by USACE-SPN in 1984. The annual maximum water level data for the period between 1990 and 2010 were used in this analysis. The data for the period prior to 1900 were not used because of the three reasons: (1) the quality of the data for this period cannot be confirmed as they are no longer published by NOAA; (2) the gauge datum might be affected by the 1906 San Francisco Earthquake; and (3) the data for this period, which is more than 110 years ago, may be too obsolete to reasonably represent the reoccurrence of extreme water levels under the existing condition, particularly when considering the sea level change in the past. The water level frequency curve, which was determined based on data measured between 1900 and 2010, is shown in Figure 5-1. Both the data and the curve-fitting of the data using the Weibull distribution are shown in this figure.

The water levels in San Francisco Bay have been rising. The annual maximum water levels at San Francisco have shown fairly consistent rise in the past, as shown in Figure 5-2. The mean annual maximum water level averaged over the past 55 years (from 1956 to 2010) is approximately 4.87 feet, NGVD29, which is 0.24 feet higher than the mean value averaged the 111-year period (1900 to 2010). Therefore, the original water level frequency curve, which was determined based on the 111-year data, was moved upward by 0.24 feet to represent the water level frequency curve under the existing condition in this analysis. It is noted that a similar methodology was also used in USACE (1984) tidal study. The adopted water level frequency curve, compared to the original curve, is shown in Figure 5-1. The annual maximum still water levels for different recurrent frequencies are listed in Table 5-1. The 1-percent annual maximum water level at San Francisco is at approximately +6.1 feet, NGVD29, which is about 0.1 feet higher than the value determined in the USACE (1984) study.

Table 5-1. Annual Maximum Water Levels at San Francisco

Return Frequency	Annual Peak Tidal Stage (ft, NGVD29)	
	Computed	Adopted
0.50	4.57	4.81
0.20	4.99	5.23
0.10	5.22	5.46
0.04	5.49	5.73
0.02	5.66	5.90
0.01	5.82	6.06
0.004	6.01	6.25
0.002	6.15	6.39

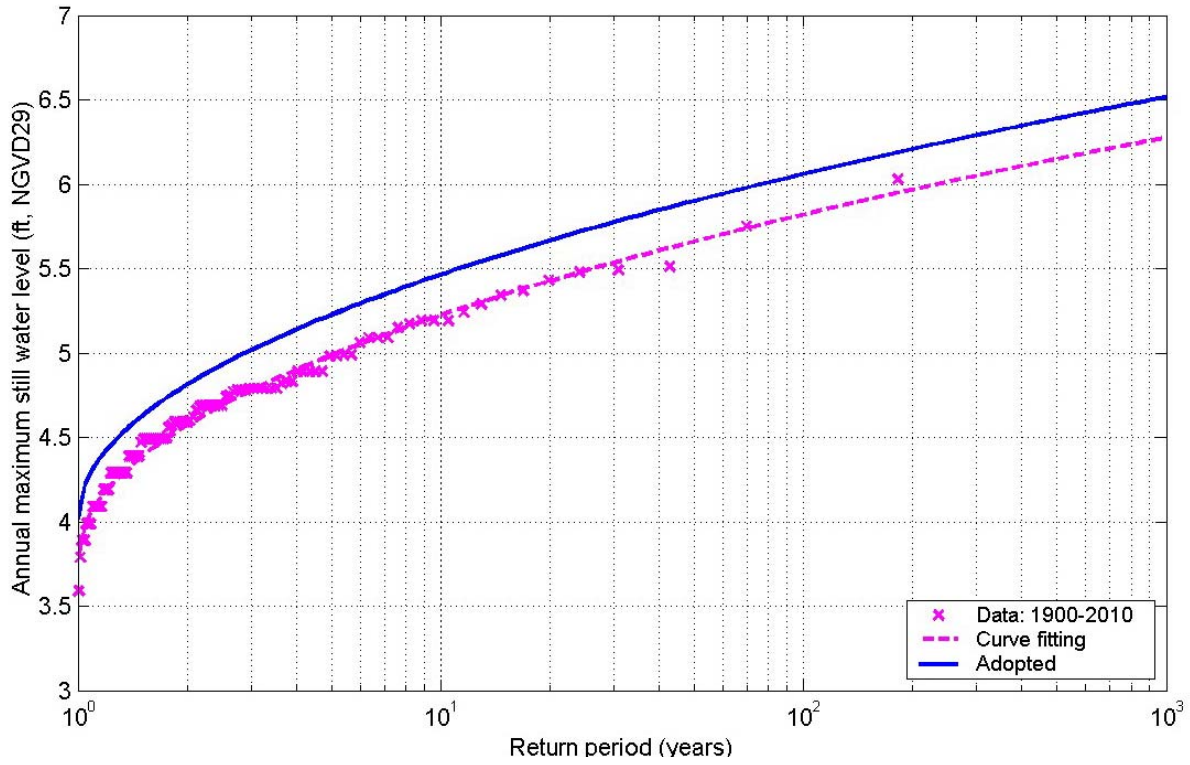


Figure 5-1. Still Water Level Frequency Curve for San Francisco

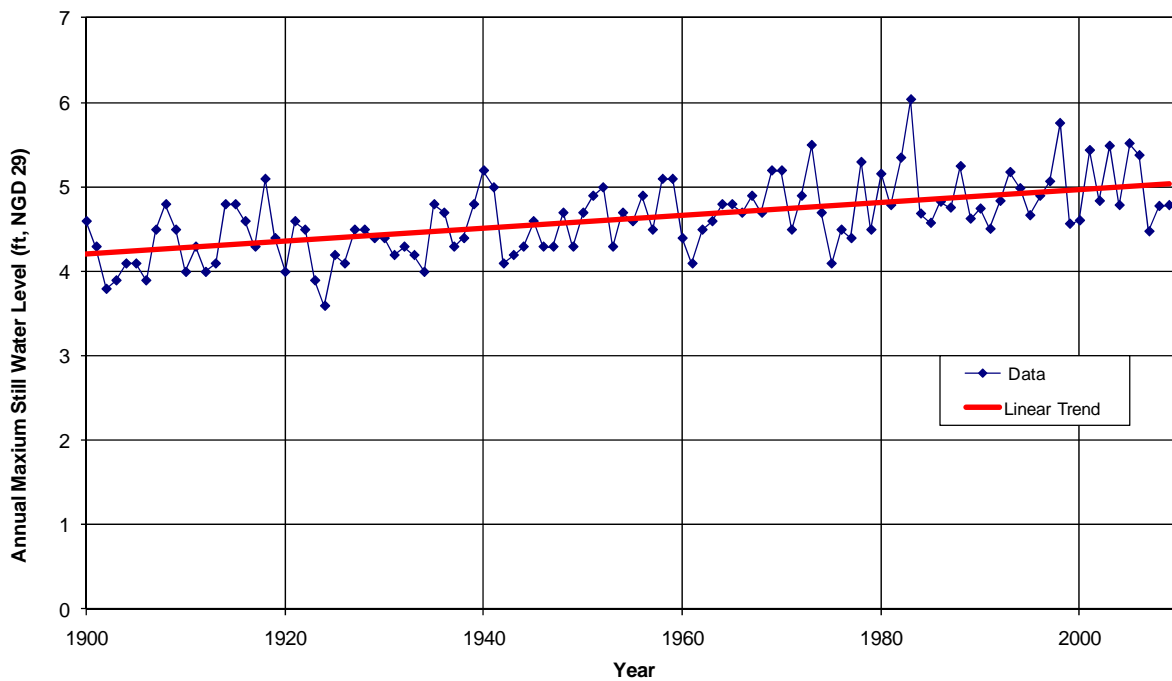


Figure 5-2. Annual Peak Tidal Elevation at San Francisco (Presidio) Station

5.1.2 Relation of Water Levels between Gallinas and San Francisco

The data from several sources were investigated to determine the relationship of the still water levels between Gallinas and San Francisco. The water level frequency curve at Gallinas for the Year 0 (2011) condition was then developed by adjusting the frequency curve for San Francisco with this relationship.

Measured Water Levels in Las Gallinas Creek

The water level data were collected at two locations in Las Gallinas Creek for a few short periods of time when the hydrographic surveys were conducted in February 2009 and in September 2005, respectively. The locations of these two gauges are shown in Figure 5-3. The data are shown in Figure 5-4 through Figure 5-5, compared with the measured tidal stage at San Francisco. The difference in the peak tides between these two gauges and San Francisco is listed in Table 5-2. It is noted that the gauge at Buck's Launching is close to the mouth of the creek, and thus the measured data at this gauge can be used as a preliminary indicator of the water levels at the mouth of the creek. The peak tidal stages at Buck's Launching are 0.06 feet to 0.24 feet higher than San Francisco for these short periods of time.

Table 5-2. Difference in Peak Tidal Stages between Las Gallinas Creek and NOAA San Francisco Station for a Few Periods of Time

Time	Buck's Launching	Meadow drive
02/09/2009	0.06	-0.02
02/10/2009	0.21	0.13
09/07/2005	0.24	0.07
09/08/2005	0.11	-0.03
09/12/2005	>0.19	N/A

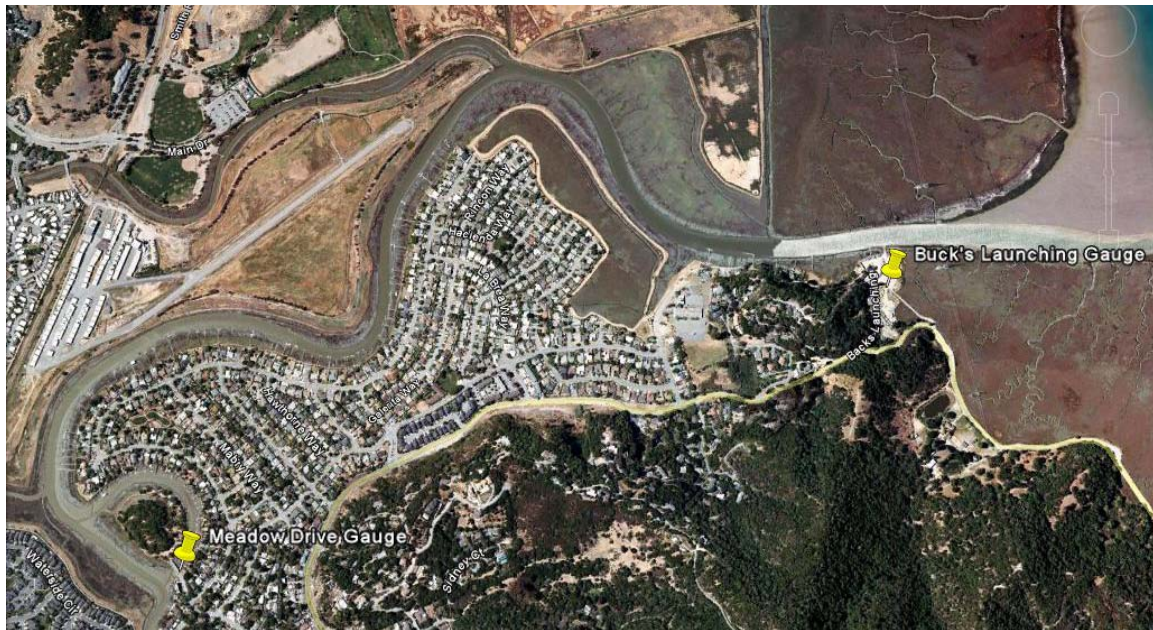


Figure 5-3. Water Level Gauge Locations during the Hydrographic Surveys in February 2009 and in September 2005

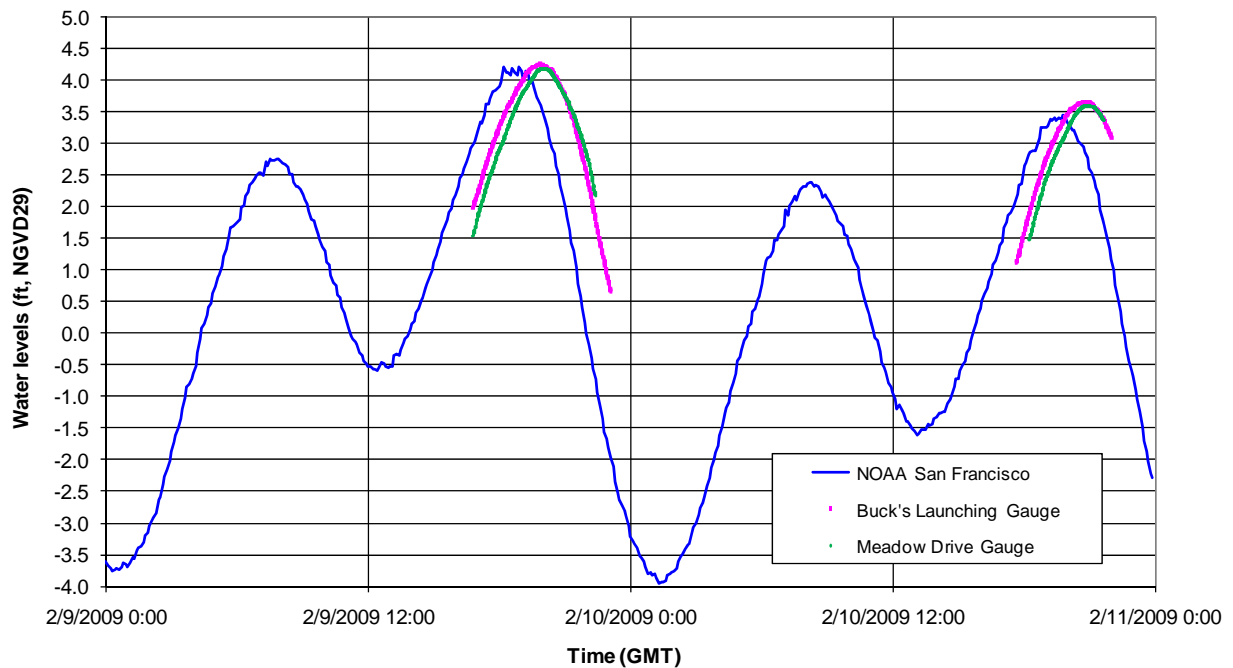


Figure 5-4. Water Levels Measured in Las Gallinas Creek in February 9-10, 2009 Compared to Measured Water Levels at San Francisco

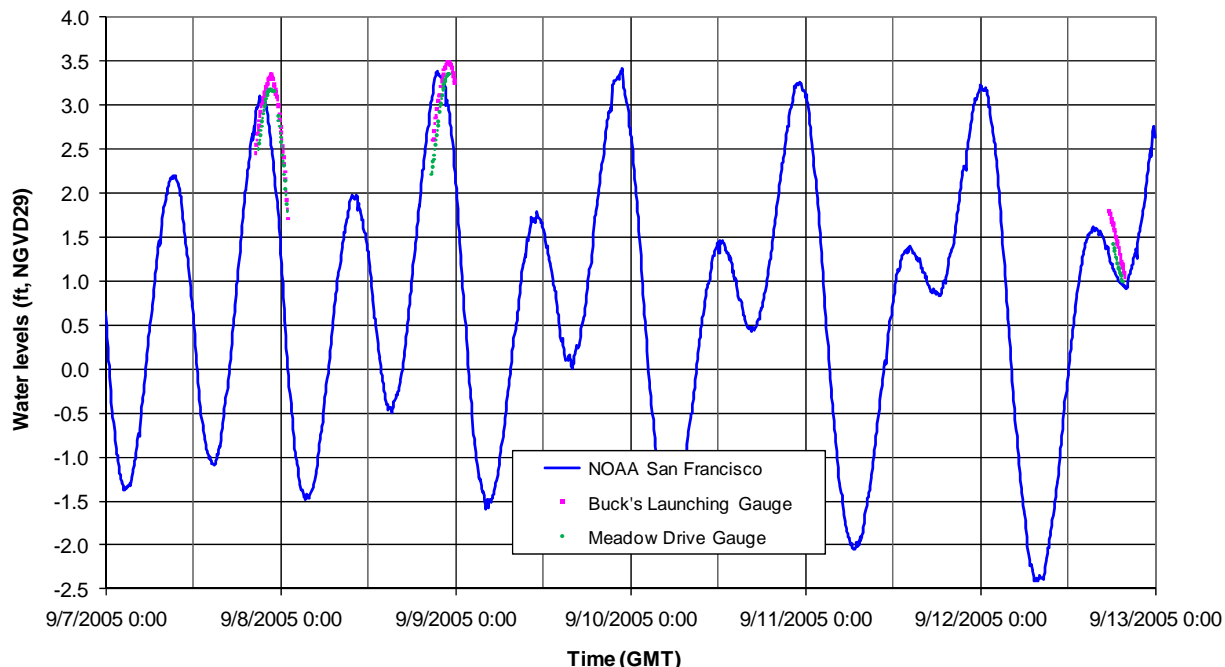


Figure 5-5. Water Levels Measured in Las Gallinas Creek in September 2005 Compared to Measured Water Levels at San Francisco

NOAA Tidal Datum

The tidal datum published on NOAA website was investigated for San Francisco and other NOAA stations close to the project site, as summarized in Table 5-3. The Mean Higher-High Water (MHHW) is 3.21 feet above NGVD29 for San Francisco, and is 3.58 feet above NGVD29 for Hamilton AFB station. This indicated that the MHHW at Hamilton AFB is approximately 0.37 feet above the MHHW at San Francisco. The MHHW relative to NGVD29 is not available for Gallinas, but the Hamilton AFB Station is close to Gallinas. Therefore, the MHHW at Gallinas was also considered be approximately 0.37 feet higher than San Francisco.

Daily Peak Tides

Among the NOAA tidal stations, the Richmond station is the station that is close to the project site and that has the longest record of tide data. The tidal stage has been measured at this station since 1996. The daily higher-high (HH) tidal stages measured at Richmond were compared to the HH tides at San Francisco, as shown in Figure 5-6. The difference in the HH tides between these two stations is shown in Figure 5-7. The daily HH tides in Richmond are

generally higher than San Francisco. As shown in Figure 5-7, the average difference is approximately 0.11 feet, but shows low correlation with the daily HH tides (the correlation coefficient $R = 0.046$, or $R^2 = 0.0021$). It is noted that the difference in MHHW between Richmond and San Francisco is approximately 0.13 feet (listed in Table 5-3), which is close to the difference in the HH tides between 1996 and 2010.

Table 5-3. Comparison of MHHW for Different NOAA Tidal Stations

NOAA Tidal Station	Mean Higher-High Water (MHHW) ¹ (feet, NGVD29)
San Francisco	+3.21
Richmond	+3.34 ²
Hamilton AFB	+3.58
Gallinas, Gallinas Creek	Not Available

Note: ¹ For 1983-2001 tidal epoch.

² Assuming 0 feet, NGVD29 = +2.70 feet, NAVD 88.

Adopted Difference in Water Levels between Gallinas and San Francisco

After analyzing the water levels from these various data sources, the difference in the MHHW between NOAA Hamilton AFB station and the San Francisco station, i.e., 0.37 feet, was adopted as the difference in the annual maximum water levels between Gallinas and San Francisco. This relation was adopted because of the following reasons: (1) the Hamilton AFB station is much closer to the project site compared to Richmond, (2) the quality of the data at this NOAA station is much better than the two gauges in the creek that only measured tidal stage for a few hours in five days, and (3) it is more conservative compared to the values derived from the other two sources.

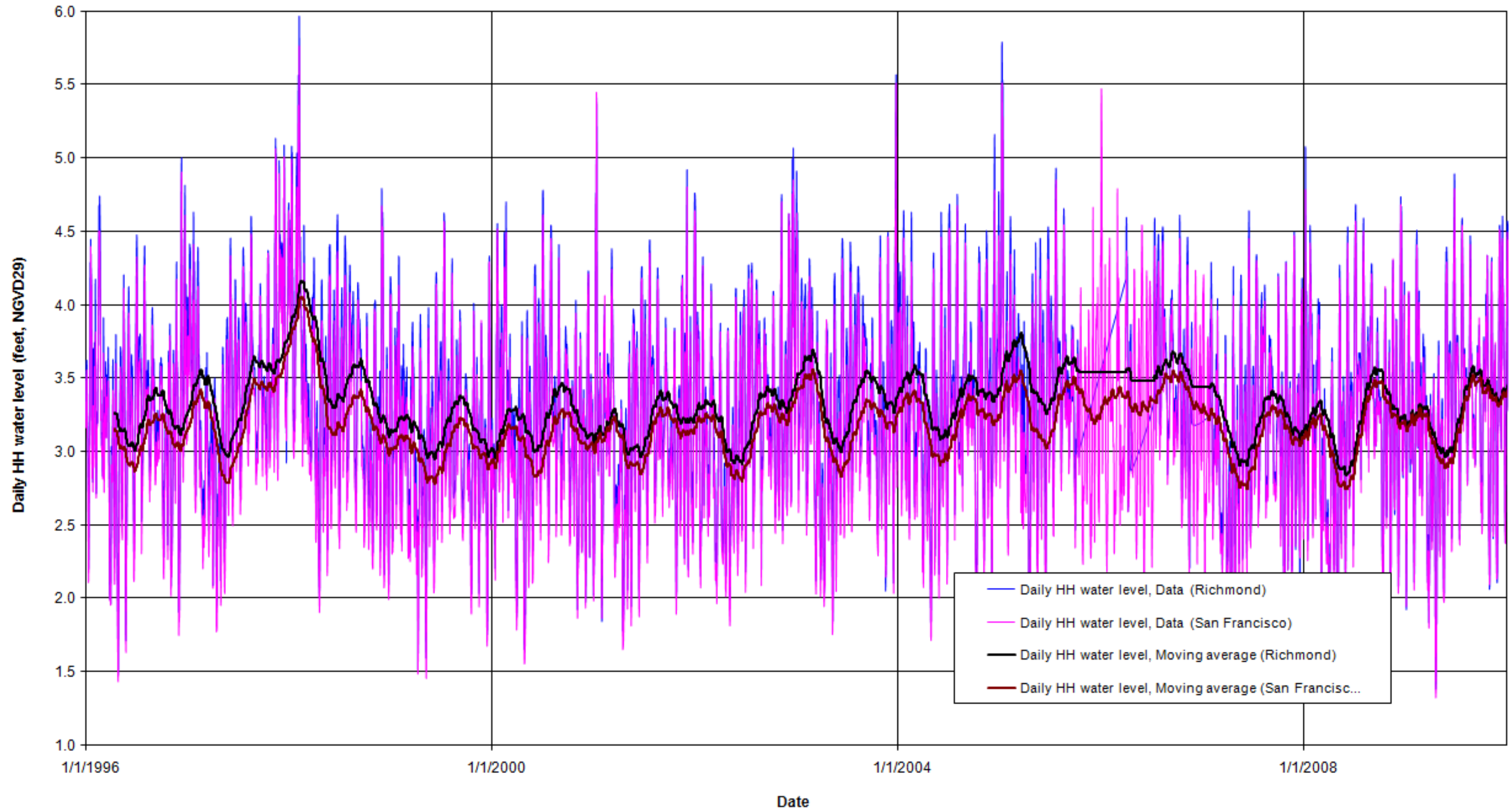


Figure 5-6. Daily Higher-High (HH) Tidal Stages at Richmond Compared to San Francisco

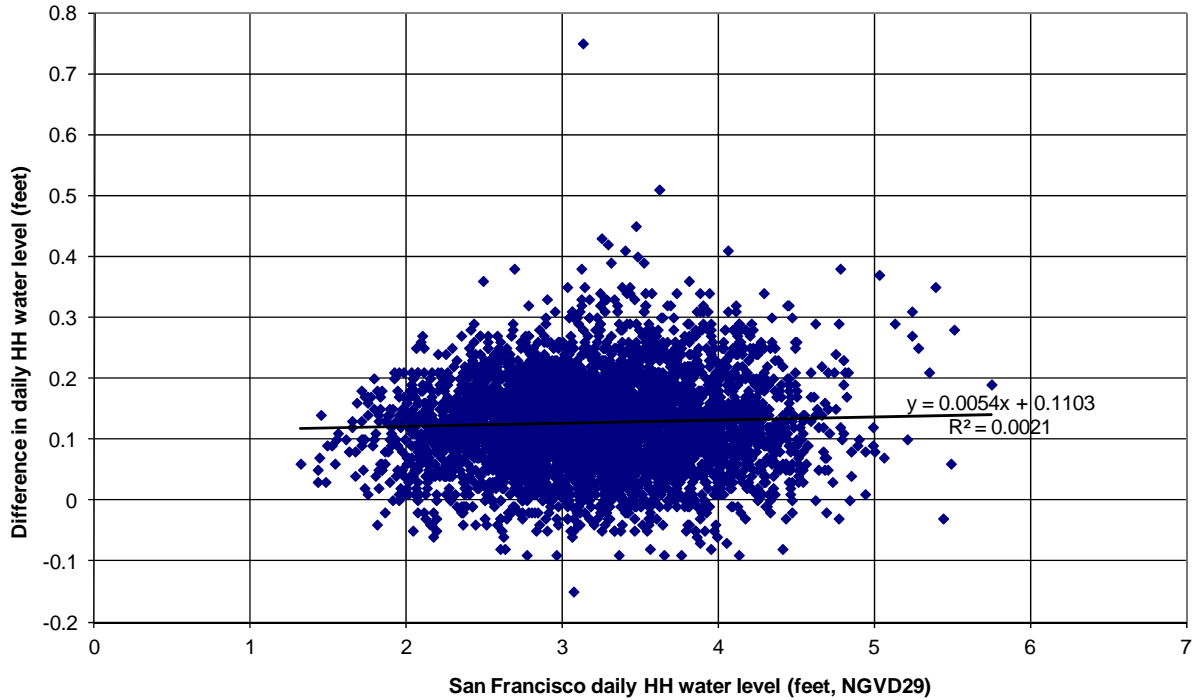


Figure 5-7. Difference in Daily Higher-High Water Levels between Richmond and San Francisco (1996-2010)

5.1.3 Coastal Still Water Level Frequency Curve for Gallinas

Based on the relationship of extreme water levels between Gallinas and San Francisco, the water level frequency curve at Gallinas was derived by moving the adopted water level frequency curve for San Francisco upward by 0.37 feet for the existing (2011) condition. The water level frequency for Gallinas, compared to the curve for San Francisco, is shown in Figure 5-8. The annual maximum water levels for eight return frequencies are listed in Table 5-4. It is noted that the 1-percent annual maximum water level at Gallinas is approximately +6.4 feet, NGVD29, which is approximately the same as the value determined in the USACE (1984) study.

Table 5-4. Annual Maximum Water Levels at Gallinas

Return Frequency	Annual Maximum Water Level (ft, NGVD29)	
	San Francisco	Gallinas
0.50	4.81	5.18
0.20	5.23	5.60
0.10	5.46	5.83
0.04	5.73	6.10
0.02	5.90	6.27
0.01	6.06	6.43
0.004	6.25	6.62
0.002	6.39	6.76

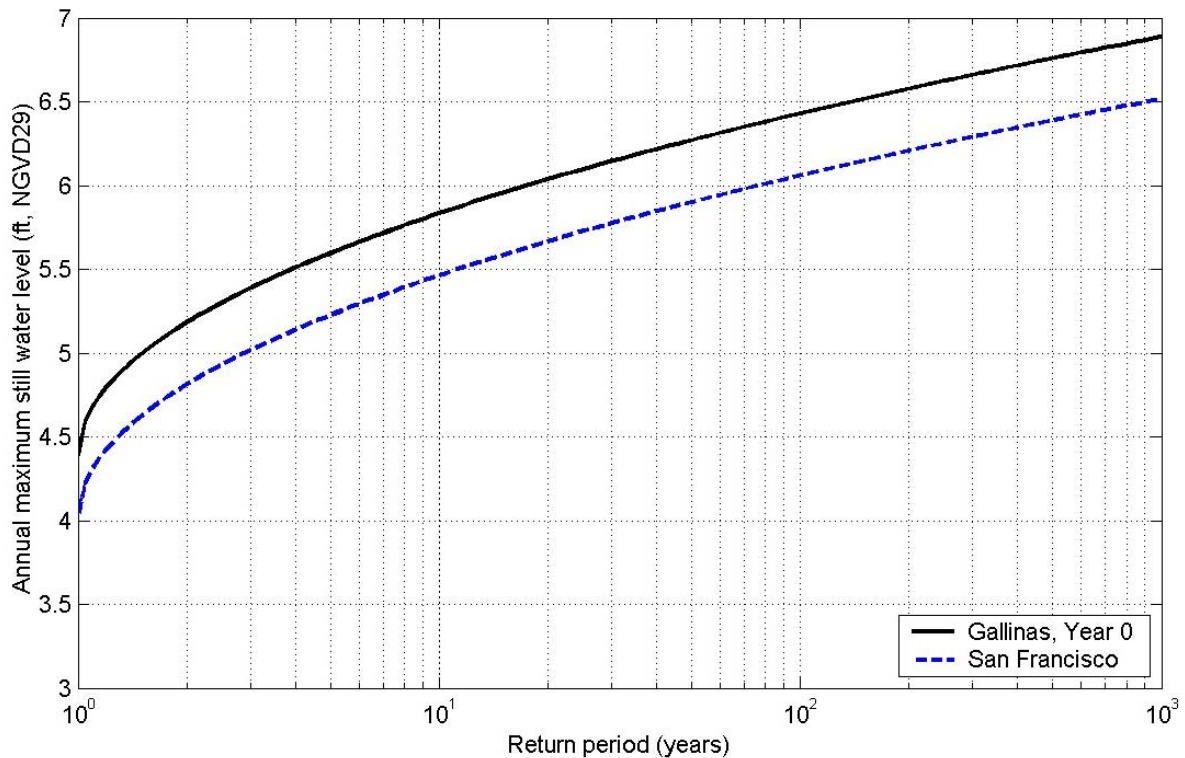


Figure 5-8. Still Water Level Frequency Curve for Gallinas (Year 0 Condition)

5.2 Sea Level Rise

The water levels in San Francisco Bay have been rising. Three sea level rise (SLR) scenarios were considered in this analysis based on the Corps' guidance EC 1165-2-211 (USACE, 2009). The three SLR scenarios included: (1) the "low" SLR rate using the historic rate of sea level change, (2) the "intermediate" SLR rate using the modified NRC Curve I, and (3) the "high" rate using the modified NRC Curve III. Based on this guidance, the increases in the water levels of the San Francisco Bay in the next 50 years (from 2011 to 2061) will be approximately 0.33 feet, 0.67 feet, and 1.93 feet for the "low", "intermediate", and "high" rates, respectively.

Based on the USACE-SPN (2010) analysis, the local land settlement was estimated to be 2 inches, or 0.17 feet, between 2011 and 2061. After including the local land settlement, the equivalent sea level rise in the next 50 years will be approximately 0.5 feet based on the historic sea level rise trend, 0.8 feet based on the modified NRC Curve I, and 2.1 feet based on the modified NRC Curve III. It is noted that this analysis focused on historic rates of sea level change, with the other two scenarios being addressed through sensitivity tests.

5.3 Coastal Still Water Level Frequency Analysis for Year 50 Condition

The still water level frequency curve for the Year 50 (2061) condition was derived by moving the frequency curve for the Year 0 (2011) condition upward by the equivalent sea level rise values in 50 years. The curves are shown in Figure 5-9 for different SLR scenarios. The annual maximum still water levels are listed in Table 5-5 for eight return frequencies.

Table 5-5. Annual Maximum Still Water Levels for Year 50 Condition

Return Period (years)	Year 0 Condition (ft, NGVD29)	Year 50 Condition (ft NGVD29)		
		Historic SLR	NRC I	NRC III
2	5.2	5.7	6.0	7.3
5	5.6	6.1	6.4	7.7
10	5.8	6.3	6.6	7.9
25	6.1	6.6	6.9	8.2
50	6.3	6.8	7.1	8.4
100	6.4	6.9	7.2	8.5
250	6.6	7.1	7.4	8.7
500	6.8	7.3	7.6	8.9

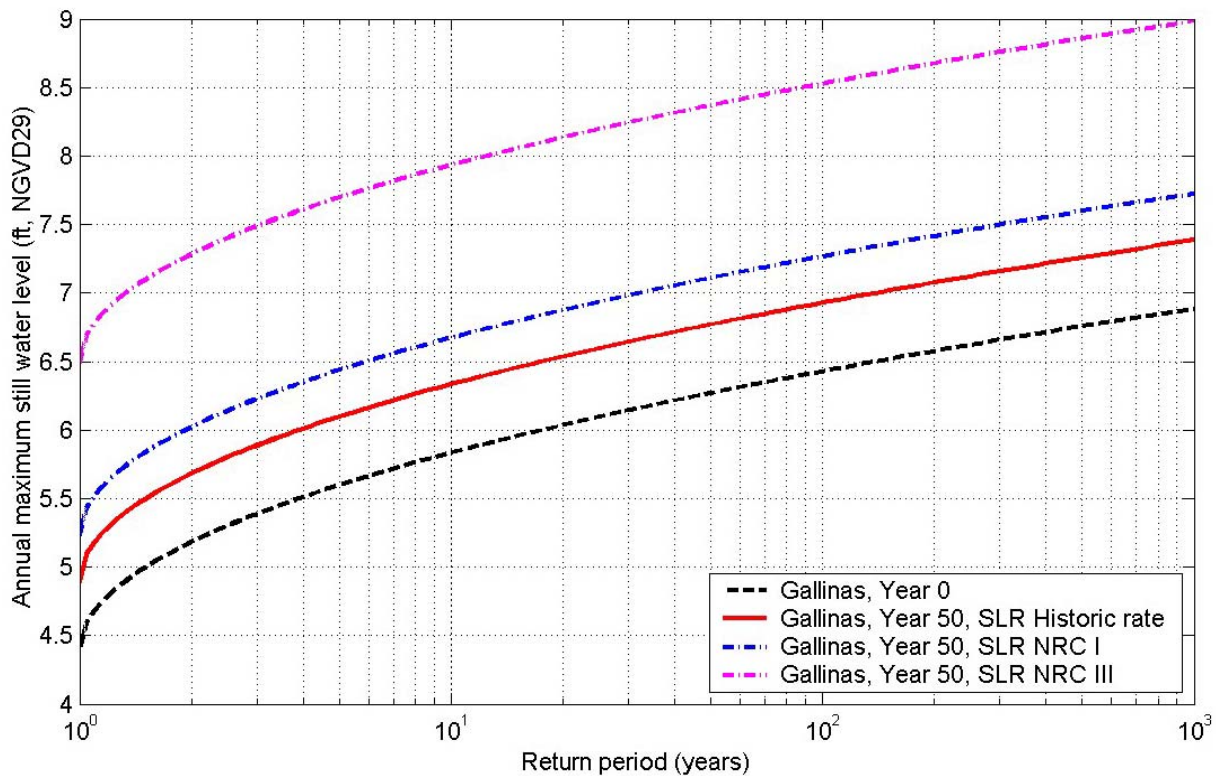


Figure 5-9. Still Water Level Frequency Curve for Gallinas (Year 50 Condition)

6 WAVES, WAVE RUNUP AND WAVE OVERTOPPING

The Santa Venetia community is protected by levees along the Las Gallinas Creek, which is a tidally influenced creek. The (San Pablo) Bay front levee system blocks the bay waves being propagated to the project site from most directions. As a result, only the lower portion of the Las Gallinas levee system, which is also named the Santa Venetia Marsh perimeter levee (referred to marsh levee hereafter), is exposed to wave action within a narrow band of directions. The wave action on the upper portion of the Las Gallinas levee system, which is upstream of the Santa Venetia Marsh (referred to creek levee hereafter), is negligible. The flooding of Santa Venetia resulting from coastal storm events is mainly caused by wave overtopping of the marsh levee. Therefore, the coastal flooding analysis was only conducted for the marsh levee. Figure 6-1 shows the locations of the outer and inner marsh levees as well as the Bay front levee.



Figure 6-1. Inner/Outer Marsh Levees, and Bay front Levee Blocking Bay Waves

6.1 Physical Characteristic of the Marsh Levees

The characteristics of the marsh levee impact the wave condition propagating to the inner marsh levee, the wave runup and wave overtopping on this levee, and the coastal flooding

condition in Santa Venetia. These levee characteristic include the levee crest elevations, side slopes and toe elevations.

6.1.1 Levee Crest Elevations

The levee crest elevation profiles were determined based on the DTM and/or the levee crest elevations survey conducted for the Santa Venetia levee by the County. This data source was discussed in Section 2.2.1. The crest elevation profile for the bay front levee on the north side of the Las Gallinas Creek was derived from the DTM. The crest elevation of the bay front levee varies from +7.4 to +9.4 feet NGVD29, which is higher than the 500-year still water level with the historic sea level rise trend. This indicates that this bay front levee will thus block the waves from the north direction clockwise to the northeast direction.

The levee profiles are shown in Figure 6-2 for the outer marsh levee, and in Figure 6-3 for the inner marsh levee. Both the crest profile determined from the DTM and that determined from the County's levee crest elevation profile survey are shown in Figure 6-3 for the inner marsh levee. No levee profile survey was conducted for the outer marsh levee. The stationing of the inner and outer marsh levees is shown in Figure 6-4.

Due to the orientation of the levee alignment, the northwest portion of the outer and inner marsh levees are exposed to negligible wave action. The outer marsh levee that is exposed to the bay waves is approximately 2,250 feet long, with the crest elevation varying from +5.9 feet to +7.8 feet NGVD29. There are two levee breaches at the southwest corners of the outer marsh levee for two narrow tidal channels. The size of the two breaches are too limited to allow significant energy of bay waves to propagate into the marsh through these small breach openings. The inner marsh levee that subjects to the bay wave action is about 2,550 feet long, with the crest elevation varying between +7.8 feet and +9.4 feet NGVD based on the levee profile survey, and between +7.3 feet to +9.6 feet NGVD based on the DTM. Compared to the DTM that was derived from the LiDAR data, the County's levee profile survey is expected to have better accuracy. The levee profile survey was used in this analysis to represent the crest elevations for the inner marsh levee.

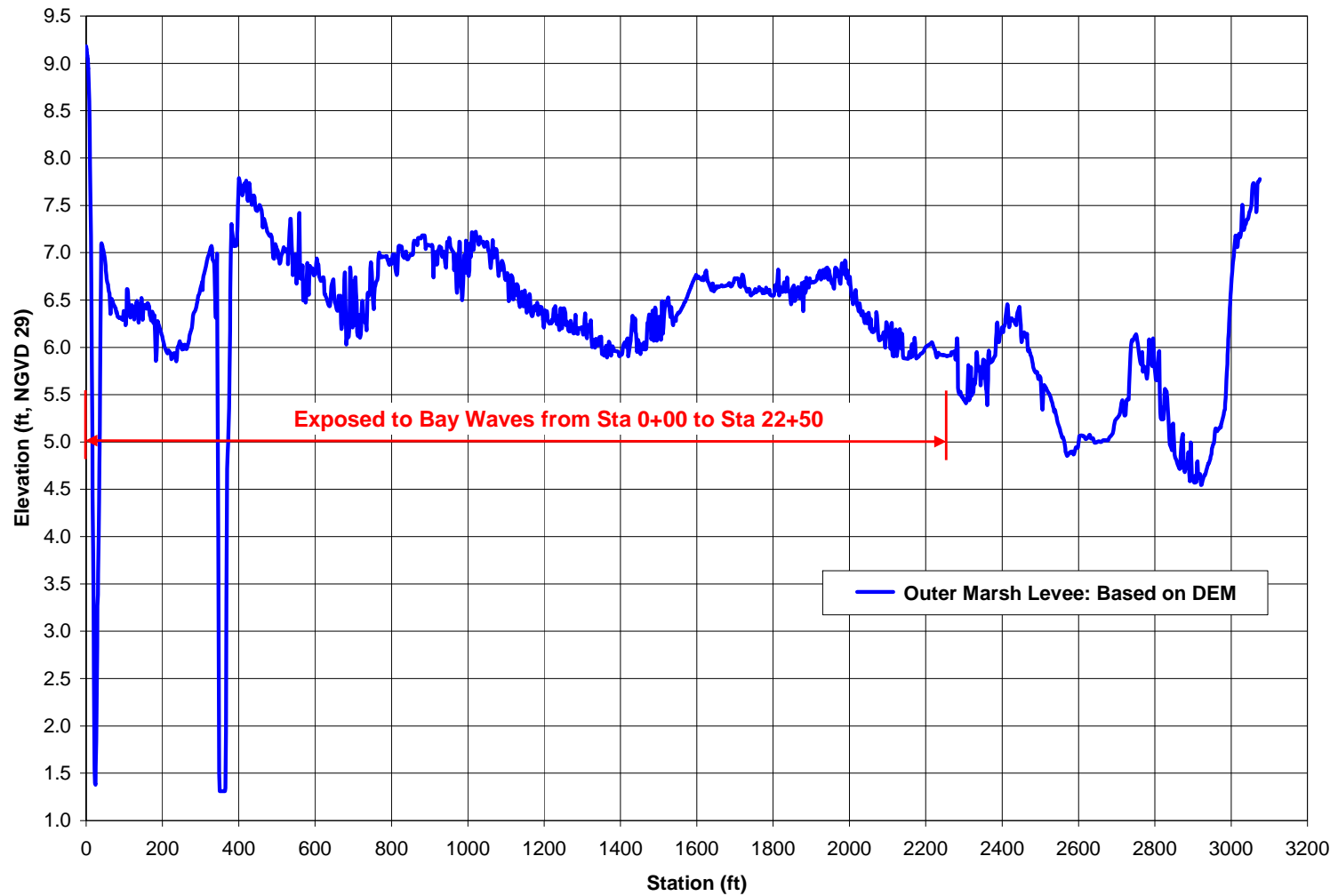


Figure 6-2. Levee Crest Profile for Outer Santa Venetia Marsh Levee

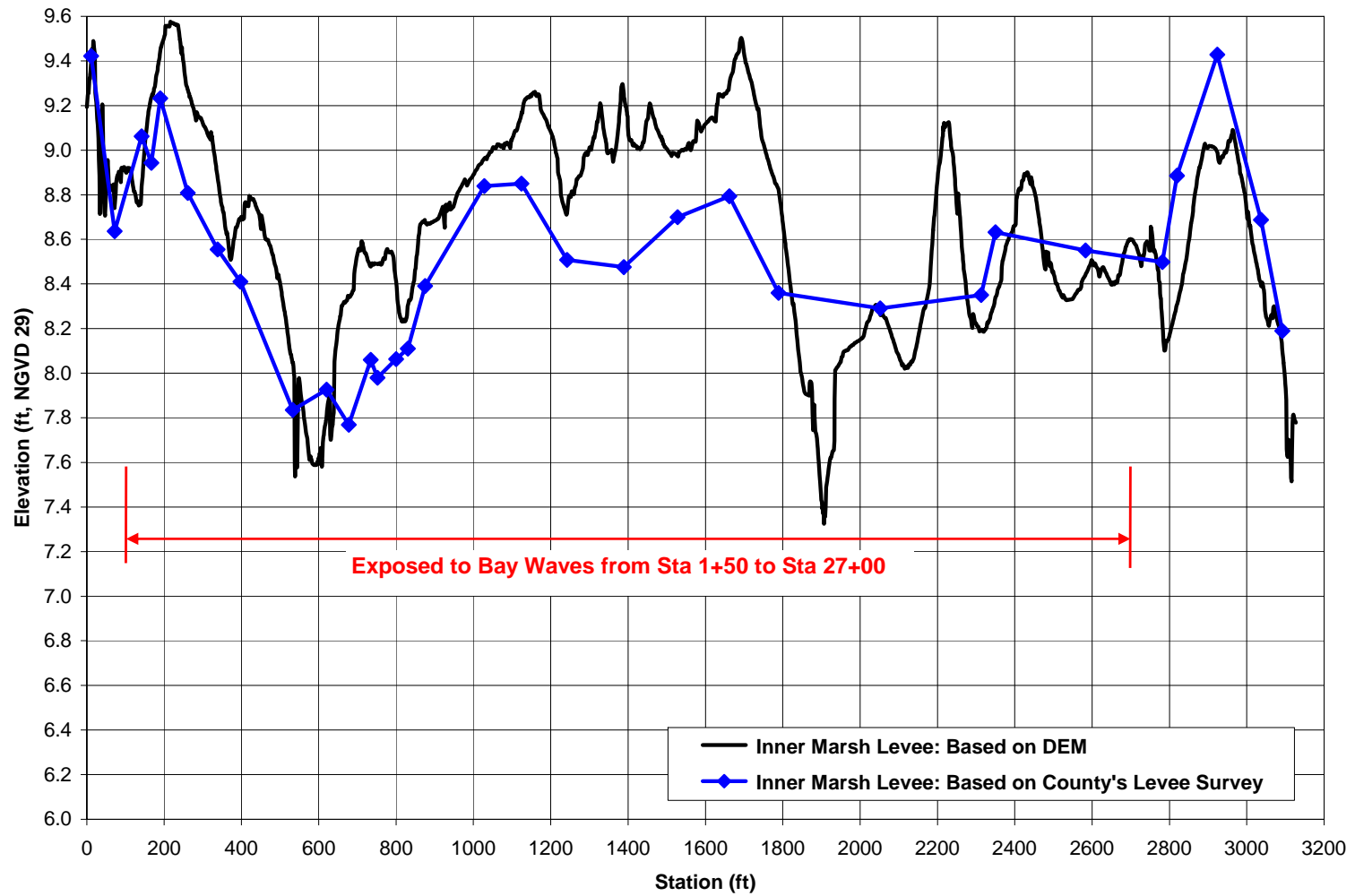


Figure 6-3. Levee Crest Profiles for Inner Santa Venetia Marsh Levee



Figure 6-4. Stationing of Inner and Outer Marsh Levees

6.1.2 Inner Marsh Levee Sections

In addition to the crest elevation, other characteristics of the inner marsh levee, such as the side slopes and the toe elevations, will also impact the wave runup elevation and the wave overtopping on the inner marsh levee which was designed to provide flood protection of Santa Venetia. The inner marsh levee that is exposed for wave action can be divided into three major segments base on the orientation of levee alignment, as show in Figure 6-5.

A series of levee cross-sections were derived based on the County's DEM for the three segments of the inner marsh levee, as shown in Figure 6-6 through Figure 6-8, respectively. A couple of transects were also surveyed by the County for the marsh levees, the creek levee and the bay front levee. The levee sections based on this survey are also shown in Figure 6-6 through Figure 6-8 for the inner marsh levee, and the locations of these transects are shown in Figure 6-5. Based on the sections derived from the DEM and from the County's levee transect survey, the representative levee sections, which were used in the wave runup/overtopping computation, were determined for the three segments of the inner marsh levee. The representative levee sections are also shown in Figure 6-6 through Figure 6-8.

The representative levee sections for segments 1a and 1b have approximately the same toe elevations and side slopes on the marsh side. These two segments were thus considered as one segment (Segment 1) in this analysis. The characteristics of the representative levee sections, including the levee toe elevations and side slopes on the marsh side, are summarized in Table 6-1 for the two segments of the inner marsh levee. It is noted that the crest elevation of the inner marsh levee varies from +7.8 feet to +9.4 feet, NGVD29. The length of the levee segments with different crest elevations were determined based on the County's levee profile survey, and the results are also listed in Table 6-1.

Table 6-1. Levee Characteristics of Inner Marsh Levee

Segments	Segment 1	Segment 2
Toe Elevation (ft, NGVD29)	+3.0	+3.5
Slope (H:V)	2.3	2.3
Levee Length (ft) for Various Crest Elevations		
7.8 ± 0.1 feet, NGVD29	160	0
8.0 ± 0.1 feet, NGVD29	190	0
8.2 ± 0.1 feet, NGVD29	90	80
8.4 ± 0.1 feet, NGVD29	230	520
8.6 ± 0.1 feet, NGVD29	240	540
8.8 ± 0.1 feet, NGVD29	90	160
9.0 ± 0.1 feet, NGVD29	210	0
9.2 ± 0.1 feet, NGVD29	40	0



Figure 6-5. Segments of Inner Marsh Levee and Levee Section Surveys

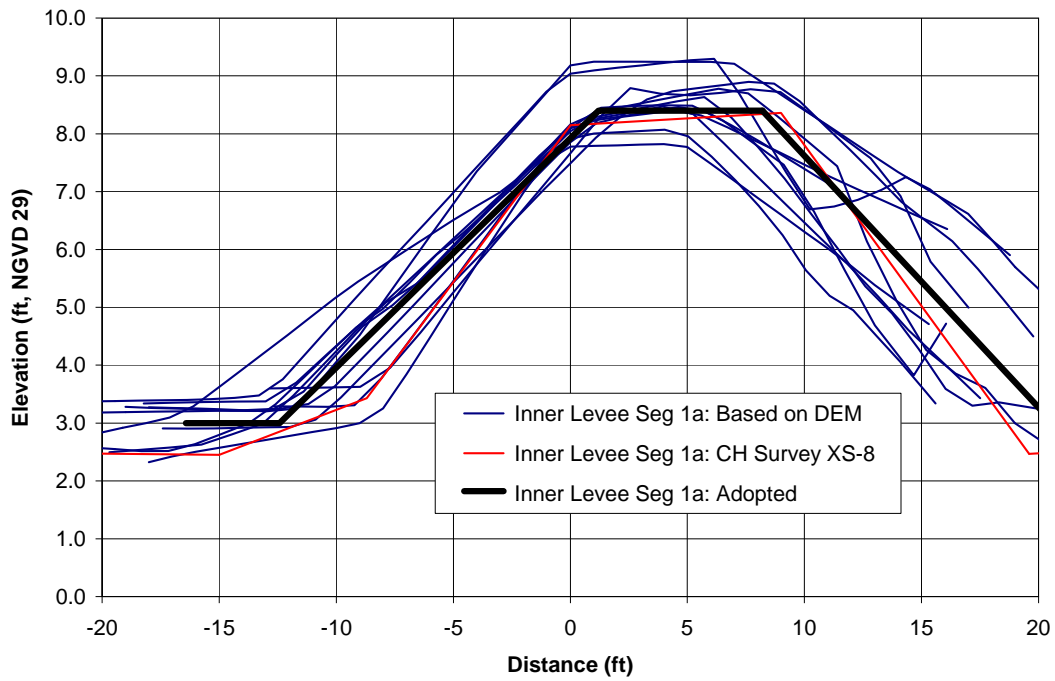


Figure 6-6. Cross Sections for Inner Marsh Levee, Segment 1a

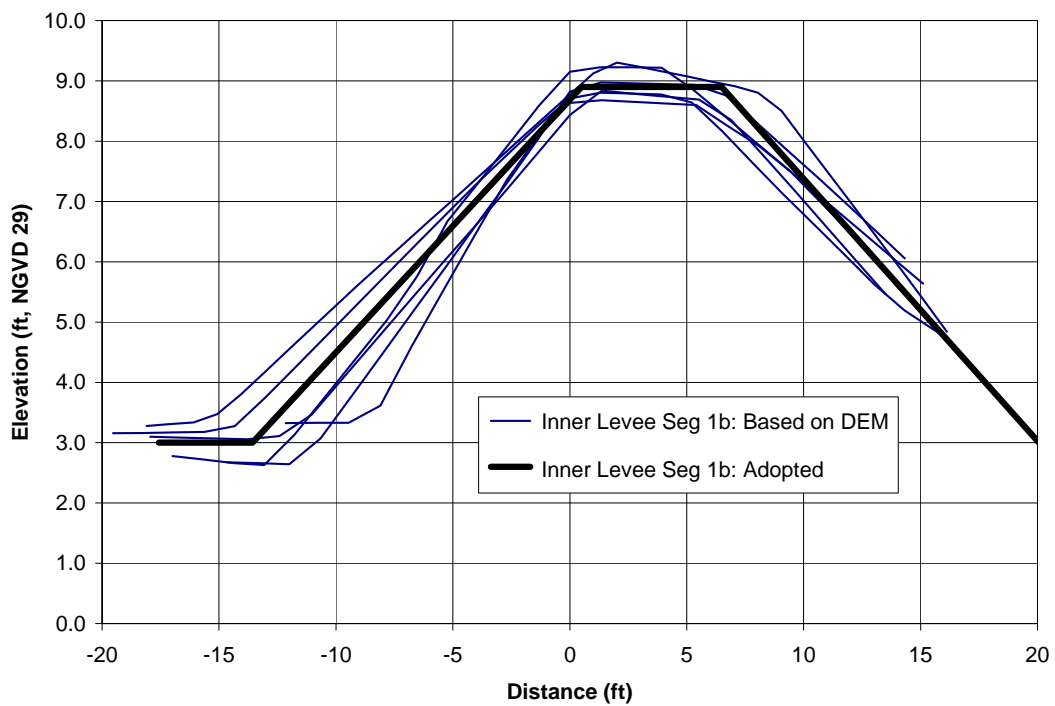


Figure 6-7. Cross Sections of Inner Marsh Levee, Segment 1b

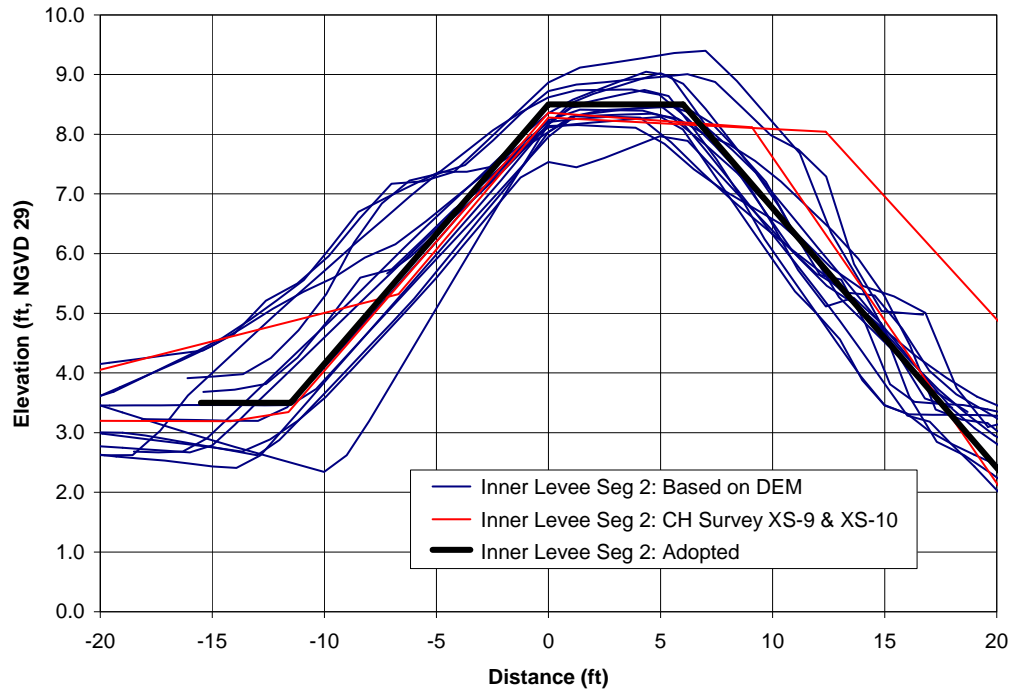


Figure 6-8. Cross Sections of Inner Marsh Levee, Segment 2

6.2 Waves

6.2.1 Wind-Wave Hindcasting for Gallinas (Bay Waves)

The wind-wave hindcasting was conducted to determine the wave conditions at the San Pablo near the mouth of the Las Gallinas Creek, or Gallinas. The directions from which waves can be generated at Gallinas by the winds blowing over the San Pablo Bay, and the wind fetches for these directions are shown in Figure 6-9. The MHHW water depth averaged over each fetch was determined based on the NOAA nautical charts. The fetch lengths and the MHHW water depths are summarized in Table 6-2.

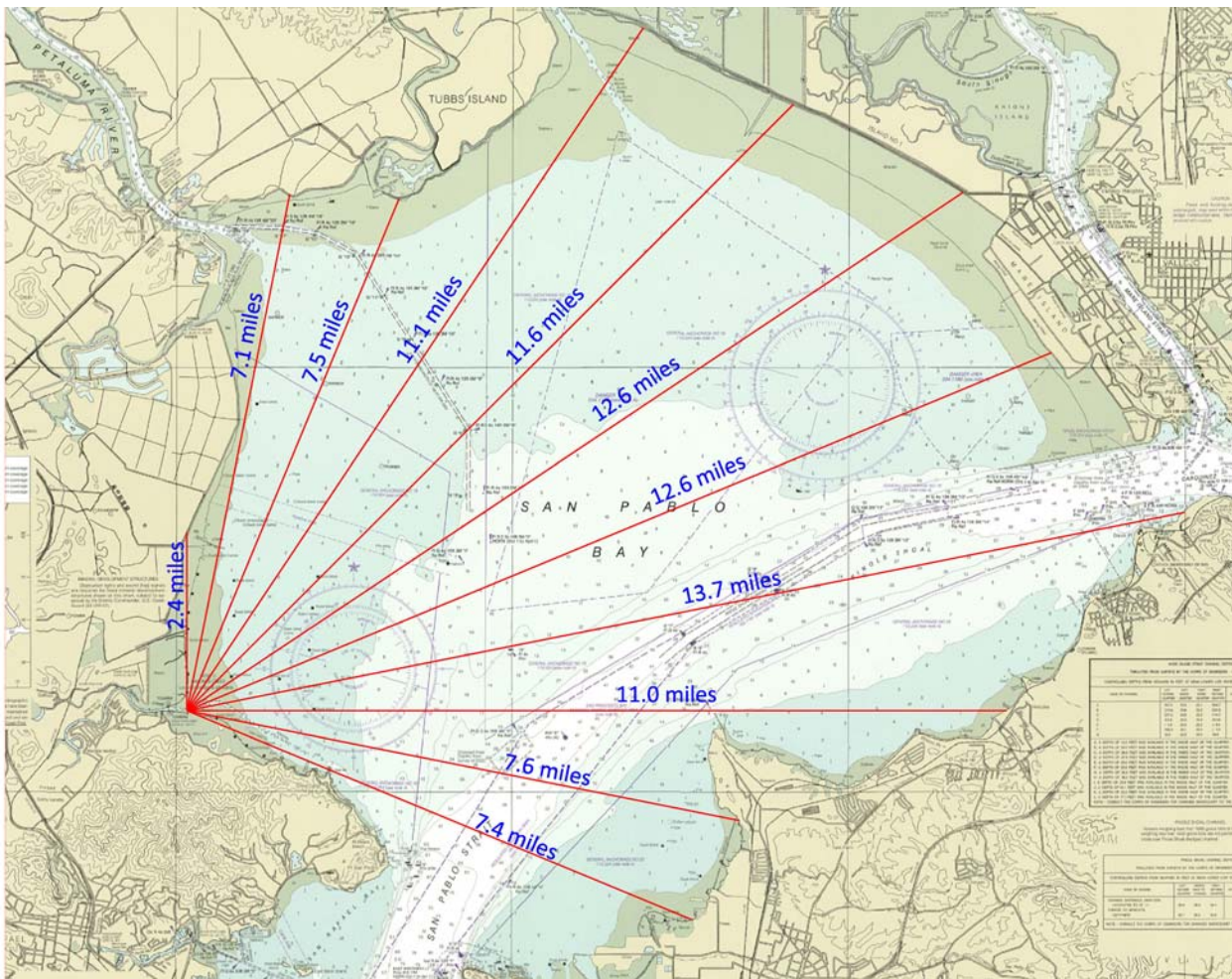


Figure 6-9. Wind Fetch for Gallinas, Mouth of Las Gallinas Creek

Table 6-2. Wind Fetch Lengths and Water Depths at Gallinas

Wind Direction	Fetch Length (Miles)	MHHW Water Depth (ft)
0 (North)	2.4	4
11.25	7.1	6
22.5	7.5	7
33.75	11.1	8
45 (NE)	11.6	9
56.25	12.6	10
67.5	12.6	11
78.75	13.7	22
90 (East)	11.0	17
101.25	7.6	17
112.5	7.4	17

The wind data that were acquired from the National Climate Data Center (NCDC) for three stations in the San Pablo Bay (Hamilton AAF, Davis Point, and Richmond), the Alameda NAS station and the San Francisco International Airport station were analyzed. The wind data record covered the periods of 1943-1971 and 1973-1975 for the Hamilton AAF station (32 years in total), the periods of 1976-1981 and 1983-1984 for the Davis Point station (8 years in total), the period of 2008-2009 for the Richmond station (2 years), the period of 1973-1996 for the Alameda NAS station (24 years), and the period of 1948-present for the San Francisco International Airport station. As examples, Figure 6-10 shows the hourly wind speed measured at the three NCDC stations in the San Pablo Bay, and Figure 6-11 shows the hourly wind speed measured at the San Francisco International Airport.

Two sets of wind data were used to hindcast the wind wave at Gallinas, respectively. One data set is the 32 years of wind data collected at NCDC Hamilton AAF station. This station is closest to the project site compared to other NCDC stations. The second data set was developed for the purpose of covering a longer period of record. This data set included the data record for the three NCDC station in the San Pablo Bay, with the data record for the Alameda NAS and the San Francisco International Airport stations being added to the data gaps where no wind data are available for the three stations in the San Pablo Bay. By doing that, the coverage of the

wind data was extended to 67 years between 1943 and 2009. The data set used in this 67-year period is listed in Table 6-3. The higher waves computed based on these two sets of wind data were adopted in this analysis in order to be conservative.

The wind-wave hindcasting was conducted using the wave prediction application within the Automated Coastal Engineering System (ACES), which is a module within the Coastal Engineering Design and Analysis System (CEDAS) that was developed by the U.S. Army Corps of Engineers. ACES is a comprehensive set of software programs for applying a broad spectrum of coastal engineering design and analysis technologies, which includes applications for wave prediction, wave theory, wave transformation, structural design, wave runup, transmission and overtopping, littoral processes, and inlet processes. The methodologies included in the wave prediction application of ACES provide quick and simple estimates for wave growth over open-water and restricted fetches in deep and shallow water. Also, improved methods (over those given in the Shore Protection Manual (SPM), 1984) are included for adjusting the observed winds to those required by wave growth formulas. The shallow water restricted wind fetch option was used in this analysis.

The significant wave heights and wave periods were first computed with ACES for a series of given wind speeds ranging from 0 to 70 miles per hour blowing from the different fetch directions between 0 degrees and 112.5 degrees. The hourly wave conditions at the site were then calculated by interpolating these computed wave-wind relations with each of the hourly wind data.

The annual maximum wave heights were determined based on the interpolated hourly waves for each year of the data record. The statistical analysis was then conducted based on these annual maximum waves to determine the wave heights for different recurrent frequency coastal storm events. The results are shown in Figure 6-12 for the case using the 32-year wind data record, and in Figure 6-13 for the case using 67-year wind data record. Both the data for the annual maximum wave heights and the Weibull curve fitting are shown in these figures. The wave heights for the eight return frequencies are summarized in Table 6-3. The larger values of the return wave heights using the two different wind data sets were adopted in this analysis in order to be conservative. However, the difference in return wave heights using these two wind data sets is merely 0.1 feet or less, which is considered negligible.

Table 6-3. Wind Waves at Gallinas for Eight Return Frequencies

Return period (Years)	Significant Wave Height (ft)			Significant Wave Period (seconds)
	Based on 32- Year Wind Data ¹	Based on 67- Year Wind Data ²	Adopted	
2	2.0	1.9	2.0	3.0
5	2.4	2.4	2.4	3.3
10	2.7	2.6	2.7	3.5
25	2.9	2.9	2.9	3.7
50	3.1	3.1	3.1	3.8
100	3.3	3.3	3.3	3.9
250	3.5	3.5	3.5	4.1
500	3.6	3.7	3.7	4.2

Note: 1. Based on hindcasted waves using the 32-year (1943-1971, 1973-1975) wind data collected at NCDC Hamilton AAF station;

2. Based on hindcasted waves using the 67-year (1943-2009) wind data collected at NCDC Hamilton AAF station (1943-1971, 1973-1975), at Davis Point Station (1976-1981, 1983-1984), at Richmond Station (2008-2009), at Alameda NAS Station (1982, 1985-1996), and at San Francisco Intl. Airport Station (1972, 1977-2007);

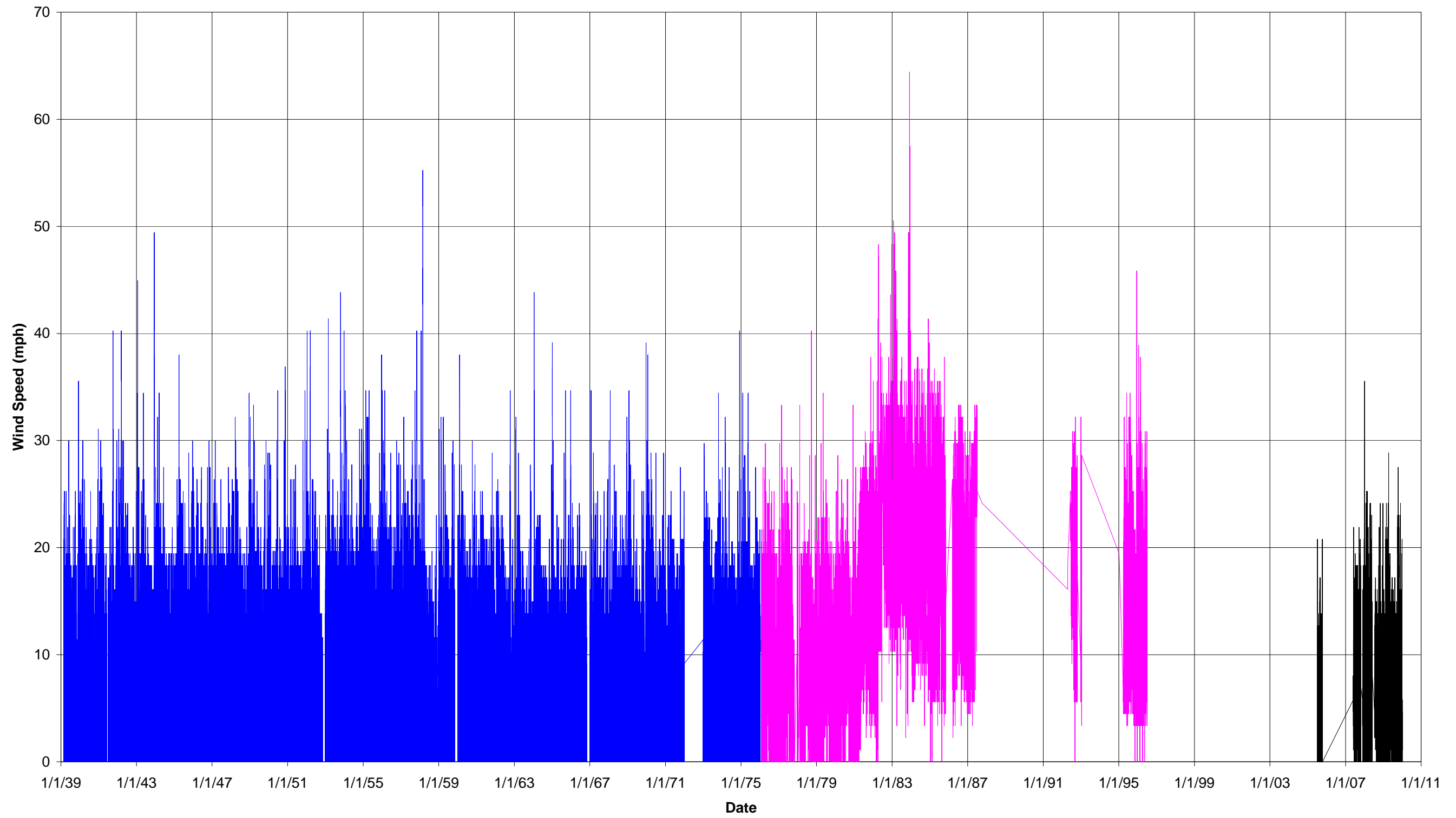


Figure 6-10. Hourly Wind Speed at the Hamilton AAF (Blue), Davis Point (Ryan), and Richmond (Black) Stations

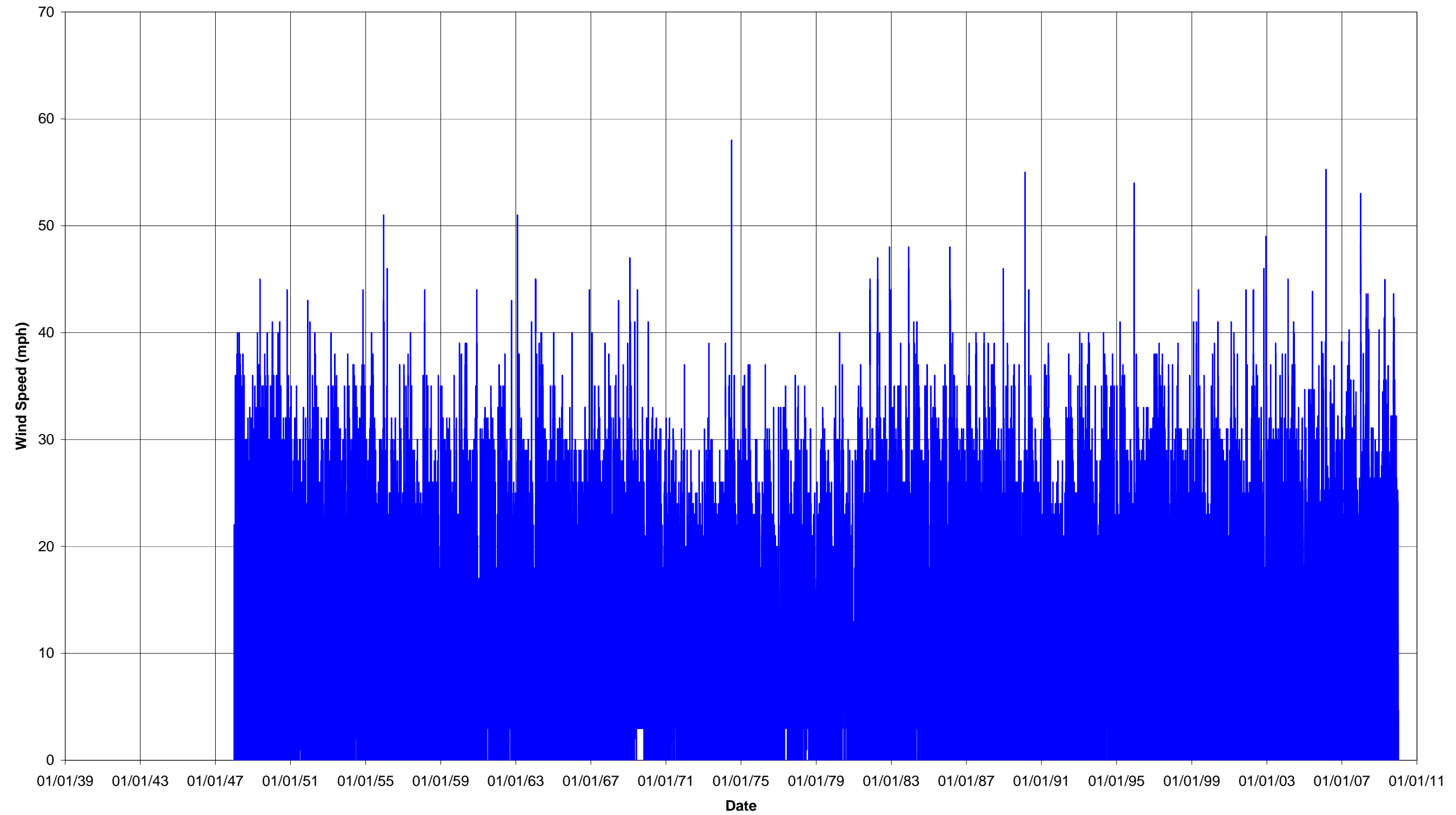


Figure 6-11. Hourly Wind Speed at the San Francisco International Airport

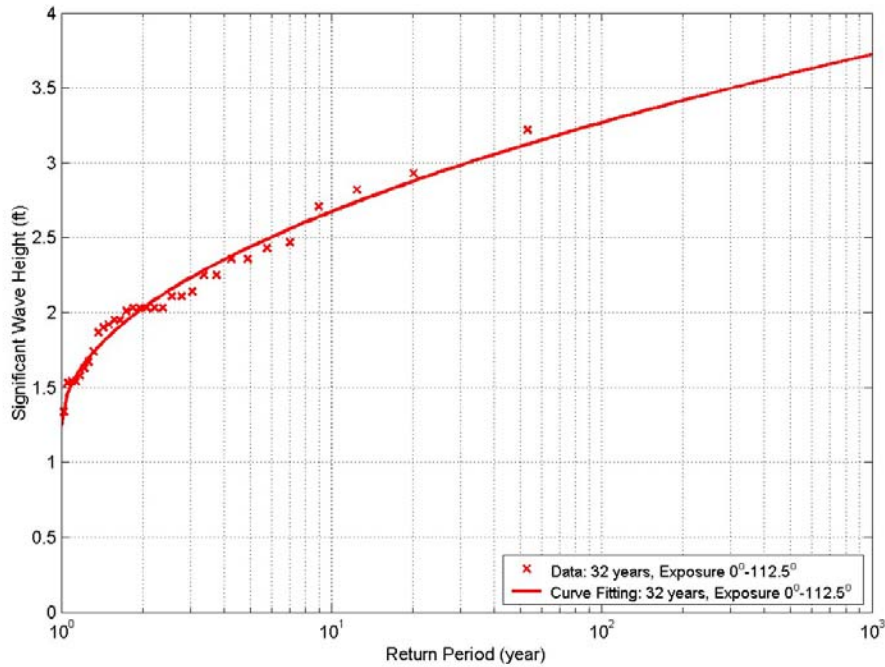


Figure 6-12. Statistical Analysis of Annual Maximum Wave Heights Based on 32-Years Data Record

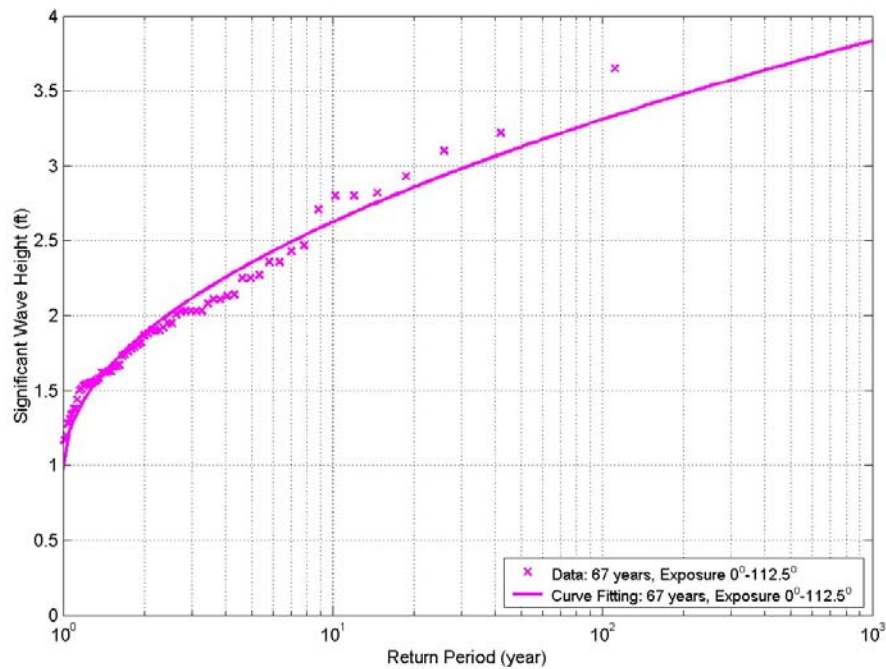


Figure 6-13. Statistical Analysis of Annual Maximum Wave Heights Based on 67-Year Data Record

6.2.2 Waves at the Inner Marsh Levee for Year 0 Condition

Bay Waves Propagating to the Inner Marsh Levee

When the bay waves, which are generated at Gallinas by winds blowing over the San Pablo Bay, propagate towards the project site, wave transformation occurs as the bathymetry varies. When the still water level is lower than the outer levee of the Santa Venetia marsh, waves are blocked by this outer marsh levee and no bay waves propagate to the inner marsh levee. When the still water level exceeds the crest elevation of the outer marsh levee, waves can pass over the outer marsh levee, propagate through the marsh, and reach to the inner marsh levee.

The crest elevation of the outer marsh levee that is exposed to the bay waves varies between +5.9 feet to +7.8 feet, NGVD29, as shown in Figure 6-2. The 500-year still water level is approximately +6.8 feet, NGVD29 for the Year 0 (2011) condition, as listed in Table 5-4. As a result, the still water depth associated with the 500-year tidal storm event is less than 1 feet on the outer marsh levee. This indicates that the outer marsh levee will act as a submerged breakwater when the bay waves propagate from the San Pablo Bay to the inner marsh levee during the extreme storm events. In other words, the wave heights of the bay waves that can propagate from the Bay to the inner marsh levee is controlled (limited) by water depth on the outer marsh levee, rather than by the wave heights in the Bay or the wave transformation process from the bay to the outer marsh levee.

The wave heights of the Bay waves that can propagate from the Bay to the inner marsh levee was determined based on the traditional depth-limited wave criterion:

$$H_b = 0.78d$$

Where H_b is the wave height of the bay waves at the inner marsh levee, and d is the still water depth on the outer marsh levee. This depth-limited wave criterion is commonly used in engineering practice as a first estimate of the wave heights for the depth-limited waves. The still water levels, the water depths on the outer marsh levee, and the computed wave heights of the depth-limited bay waves at the inner marsh levee are summarized in Table 6-4.

It is noted that the wave period approximately remains unchanged when the waves propagate from the Bay to the inner marsh levee. The significant wave periods of the bay waves are listed in Table 6-3. The mean wave periods, which can be approximated as 0.85 times the significant

wave periods, are listed in Table 6-4. The mean wave condition (the mean wave height and the mean wave period) instead of the significant wave condition is recommended by Federal Emergency Management Agency (FEMA, 2003) for the coastal flood hazard analysis.

Table 6-4. Bay Waves Propagating to the Inner Marsh Levee (Year 0 Condition)

Return period (Year)	SWL (ft, NGVD29)	Water Depth ¹ (ft)	Mean Wave Height ² (ft)	Mean Wave Period ³ (sec)
2	5.2			
5	5.6			
10	5.8			
25	6.1	0.2	0.2	3.1
50	6.3	0.4	0.3	3.2
100	6.4	0.5	0.4	3.3
250	6.6	0.7	0.5	3.5
500	6.8	0.9	0.7	3.6

- Note: 1. The water depth equals the still water level minus the minimum crest elevation of the outer marsh levee (+5.9 feet, NGVD29) to be conservative.
 2. Depth-limited wave height equals water depth times 0.78.
 3. The wave period remains unchanged during propagation. The mean wave period equals 0.85 times the significant wave period based on FEMA (2003) guidelines.

Local Wind-Waves Generated within Santa Venetia Marsh

In addition to the bay waves propagating to the inner marsh levee during the extreme storm events, waves can also be generated locally when the wind blows on the water body within the Santa Venetia marsh from the outer marsh levee to the inner marsh levee. The average wind fetch length within the marsh ranges from 400 to 600 feet for different wind directions. The average bottom elevation of the marsh is approximately +3.5 feet, NGVD29. The 500-year water depth will be approximately 3.3 feet under the existing condition. The wave generation for this small scale of domain is typically neglected in the coastal analysis because the waves that can be generated will be very mild. However, it was considered in this analysis in order to be conservative.

The wind data used in this local wind-wave hindcasting and the procedure to determine the wave conditions for different return frequencies are the same as those used for determining the Bay waves at Gallinas. The results of the computed local wind-waves are summarized in Table 6-5. Both the significant wave condition, which were determined in the wind-wave hindcasting, and the mean wave condition are listed in this table.

Table 6-5. Wind-Waves Generated within the Marsh (Year 0 Condition)

Return Period (Years)	Significant Wave Height (ft)	Significant Wave Period (sec)	Mean Wave Height ¹ (ft)	Mean Wave Period ² (sec)
2	0.2	0.7	0.1	0.6
5	0.3	0.8	0.2	0.6
10	0.3	0.8	0.2	0.7
25	0.4	0.9	0.2	0.7
50	0.4	0.9	0.3	0.7
100	0.5	0.9	0.3	0.8
250	0.5	0.9	0.3	0.8
500	0.5	0.9	0.3	0.8

Note: 1. The mean wave height equals 0.626 times the significant wave height based on the FEMA (2003) guidelines.

2. The mean wave period equals 0.85 times the significant wave period height based on the FEMA (2003) guidelines.

Waves at the Inner Marsh Levee

The wave energy at the inner marsh levee can be approximated by the energy of the Bay waves propagating from the Bay adding the energy of the local waves generated within the marsh. The wave energy is proportional to the wave height squared. Therefore, the wave height of the combined wave at the inner levee was approximated in this analysis as the square root of the sum of the wave height squared for the Bay wave and the wave height squared for the local wind-wave. The results are summarized in Table 6-6. The longer wave period between the Bay wave and the local wind-wave was used as the representative wave period for the combined wave. The combined wave condition was used in the coastal flooding analysis. It is noted that the difference in the wave heights between the combined waves and the Bay Waves alone is approximately 0.1 feet for the extreme storm events, which is considered negligible. In other

words, including the local wind-wave generated within the Santa Venetia marsh has negligible impact on the coastal flooding analysis.

Table 6-6. Waves at the Inner Marsh Levee (Year 0 Condition)

Return Period (Years)	Mean Wave Height (ft)			Mean Wave Period (sec)		
	Bay Waves	Waves Generated in Marsh	Combined ¹	Bay Waves	Waves Generated in Marsh	Combined ²
2		0.1	0.1		0.6	0.6
5		0.2	0.2		0.6	0.6
10		0.2	0.2		0.7	0.7
25	0.2	0.2	0.3	3.1	0.7	3.1
50	0.3	0.3	0.4	3.2	0.7	3.2
100	0.4	0.3	0.5	3.3	0.8	3.3
250	0.5	0.3	0.6	3.5	0.8	3.5
500	0.7	0.3	0.8	3.6	0.8	3.6

Note: 1. Wave height at the inner levee equals the square root of the sum of the wave height squared for the Bay wave and the wave height squared for the local wind-wave.

2. The wave period at the inner levee equals the larger value of the wave periods of the Bay wave and of the local wave generated within the marsh.

6.2.3 Waves at the Inner Marsh Levee for Year 50 Condition

As discussed in Section 5.2, the still water level will rise in the future. The still water levels for the Year 50 condition are listed in Table 5-5. The increase in the still water depth will be approximately 0.5 feet based on the historic SLR trend, 0.8 feet based on the modified NRC Curve I, and 2.1 feet based on the modified NRC Curve III.

Bay Waves Propagating to the Inner Marsh Levee

The increase in the water depth is relatively limited compared to the average water depths in the San Palo Bay for the wind fetches from different directions, and will induce insignificant change to the wave climate in the Bay. However, this increase in the water depth on the outer marsh levee is relatively significant compared to the existing condition. The increase in water depth on the outer marsh levee will allow higher waves propagating from the Bay to inner marsh levee,

while the waves are still controlled by the water depth on the outer marsh levee for the Year 50 condition. The methodologies used to determine the wave condition for the bay waves propagating to the inner marsh levee for the Year 50 condition is the same as that used for the Year 0 condition. The results are listed in Table 6-7. It is noted that the waves for the Year 50 condition will be significantly higher than the Year 0 condition.

Table 6-7. Bay Waves Propagating to the Inner Marsh Levee (Year 50 Condition)

Return period (Year)	Equivalent SWL (ft, NGVD29)	Water Depth ¹ (ft)	Mean Wave Height ² (ft)	Mean Wave Period ³ (sec)
2	5.7			
5	6.1	0.2	0.2	2.8
10	6.3	0.4	0.3	2.9
25	6.6	0.7	0.5	3.1
50	6.8	0.9	0.7	3.2
100	6.9	1.0	0.8	3.3
250	7.1	1.2	0.9	3.5
500	7.3	1.4	1.1	3.6
100 (NRC I)	7.2	1.3	1.0	3.3
100 (NRC III)	8.5	2.6	2.0	3.3

Note: 1. The water depth equals the equivalent still water level minus the minimum crest elevation of the outer marsh levee (+5.9 feet, NGVD29).

2. Depth limited wave height equals water depth times 0.78.

3. Wave period is assumed to remain unchanged during wave propagation.

Local Wind-Waves Generated within Santa Venetia Marsh

The water depth within the Santa Venetia Marsh will also be increased for the Year 50 condition because of the elevated still water level. Wind-wave hindcasting was conducted for the Year 50 condition based on the increased water depth. The results are summarized in Table 6-8. It is noted that the local wind-waves generated within the marsh for the Year 50 condition will be essentially the same as the existing condition. This indicates that the increase in water depth from Year 0 to Year 50 has negligible impact on the wave generation within the marsh.

Table 6-8. Wind-Waves Generated within the Marsh (Year 50 Condition)

Return Period (Years)	Significant Wave Height ¹ (ft)	Significant Wave Period (sec)	Mean Wave Height ² (ft)	Mean Wave Period ³ (sec)
2	0.2	0.7	0.1	0.6
5	0.3	0.8	0.2	0.6
10	0.3	0.8	0.2	0.7
25	0.4	0.9	0.2	0.7
50	0.4	0.9	0.3	0.7
100	0.5	0.9	0.3	0.8
250	0.5	0.9	0.3	0.8
500	0.5	0.9	0.3	0.8
100 (NRC I)	0.5	0.9	0.3	0.8
100 (NRC III)	0.5	0.9	0.3	0.8

Note: 1. Waves generated in the marsh for the Year 50 condition are essentially the same as the existing condition.

2. The mean wave height equals 0.626 times the significant wave height based on the FEMA (2003) guidelines.

3. The Mean wave period equals 0.85 times the significant wave period based on the FEMA (2003) guidelines.

Waves at the Inner Marsh Levee

The wave condition at the inner marsh levee was determined by combining the Bay waves propagating to the site and the local wind-waves generated within the Santa Venetia marsh, as done for the Year 0 condition. The results are summarized in Table 6-9. It is noted that the waves at the inner marsh levee for the Year 50 condition will be significantly higher than the Year 0 condition, which will lead to more serious coastal flooding hazard.

Table 6-9. Waves at the Inner Marsh Levee (Year 50 Condition)

Return Period (Years)	Mean Wave Height (ft)			Mean Wave period (sec)		
	Bay Waves	Generated in Marsh	Inner Levee ¹	Bay Waves	Generated in Marsh	Inner Levee ²
2		0.1	0.1		0.6	0.6
5	0.2	0.2	0.3	2.8	0.6	2.8
10	0.3	0.2	0.4	2.9	0.7	2.9
25	0.5	0.2	0.5	3.1	0.7	3.1
50	0.7	0.3	0.8	3.2	0.7	3.2
100	0.8	0.3	0.9	3.3	0.8	3.3
250	0.9	0.3	0.9	3.5	0.8	3.5
500	1.1	0.3	1.1	3.6	0.8	3.6
100 (NRC I)	1.0	0.3	1.0	3.3	0.8	3.3
100 (NRC III)	2.0	0.3	2.0	3.3	0.8	3.3

Note: 1. Wave height at the inner levee equals the square root of the sum of the wave height squared for the Bay wave and the wave height squared for the local wind-wave.

2. The wave period at the inner levee equals the larger value of the wave periods of the Bay wave and of the local wave generated within the marsh.

6.3 Wave Runup and Wave Overtopping For Year 0 Condition

When the waves propagate to the inner marsh levee, the waves will run up on the marsh-side face of the levee. This uprush of water from wave action on the levee is called wave runup. When the wave runup elevation exceeds the crest elevation of the levee, wave overtopping will occur. The water overtopping the inner marsh levee will flow into the Santa Venetia Community, causing coastal flooding within the community. The wave runup and overtopping analysis was conducted to investigate the coastal flooding potential in Santa Venetia community and determine the coastal inundation levels if the coastal flooding occurs.

The wave runup and wave overtopping on the inner marsh levee were computed using the wave runup and overtopping on impermeable structures application of ACES. This application of ACES provides estimates of wave runup and overtopping on rough and smooth slope structures that are assumed to be impermeable. Runup heights and overtopping rates are estimated independently or jointly for monochromatic or irregular waves specified at the toe of the structure. The empirical equations suggested by Ahrens and McCartney (1975), Ahrens and Titus (1985), and Ahrens and Burke (1987) are used to predict runup, and Weggel (1976) to predict overtopping.

6.3.1 Maximum Wave Runup

The wave runup on the levee depends on the incident wave condition, the water depth at the toe of the levee, the side slope and the roughness of the levee side slope, and the bottom slope in front of the levee. The wave condition was discussed in Section 6.2.2, the still water levels were discussed in Section 5.1.3, and the levee characteristics were discussed in 6.1. The results of the wave runup and the input parameters for ACES are listed in Table 6-10 for these coastal flood events for the Year 0 condition.

It is noted that the FEMA (2003) guidelines were used in this analysis to define the coastal flood events. Based on these Guidelines, the p -percent-annual-chance coastal flood is defined as the p -percent-annual-change still water levee coinciding with the mean wave condition of the p -percent-annual-chance storm wave event. As an example, the 100-year coastal flood is defined as the 100-year still water level coinciding with the mean wave condition associated with the 100-year wave event. Therefore, the maximum wave runup was computed using the mean

wave condition, and the wave runup elevation was determined by adding the wave runup to the annual maximum still water level.

The results indicate that the maximum wave runup elevations will be lower than the crest elevation of the inner levee during most coastal flood events under the Year 0 condition. Wave overtopping or coastal flooding will only occur during the 250- and 500-year coastal flood events.

Table 6-10. Maximum Wave Runup for Year 0 Condition

Return Period (Years)	Still Water Level (ft,NGVD)	Mean Wave Height (ft)	Mean Wave Period (sec)	Segment 1 (H:V=2.3:1, Toe EI +3.0 ft NGVD, Min Crest EI +7.8 ft NGVD)			Segment 2 (H:V=2.3:1, Toe EI +3.5 ft NGVD, Min Crest EI +8.2 ft NGVD)		
				Wave Runup (ft)	Wave Runup EI (ft, NGVD)	Overtopping Potential	Wave Runup (ft)	Wave Runup EI (ft, NGVD)	Overtopping Potential
2	+5.2	0.1	0.6	0.2	+5.4	No	0.2	+5.4	No
5	+5.6	0.2	0.6	0.3	+5.9	No	0.3	+5.9	No
10	+5.8	0.2	0.7	0.3	+6.1	No	0.3	+6.1	No
25	+6.1	0.3	3.1	0.7	+6.8	No	0.7	+6.8	No
50	+6.3	0.4	3.2	0.9	+7.2	No	0.9	+7.2	No
100	+6.4	0.5	3.3	1.1	+7.5	No	1.1	+7.5	No
250	+6.6	0.6	3.5	1.3	+7.9	Yes	1.3	+7.9	No
500	+6.8	0.8	3.6	1.8	+8.6	Yes	1.8	+8.6	Yes

6.3.2 Wave Overtopping Rates versus Still Water Levels

The still water levels vary with tides during a coastal flood event. As a result, the wave runup elevation and the wave overtopping rate also vary with tides. In this analysis, the wave overtopping rates were first calculated for a series of given still water levels. The derived relation between the wave overtopping rates versus the still water levels were then used as the basis to interpolate the overtopping rates for the still water hydrographs during these two coastal flood events.

It is noted that the wave heights at the inner marsh levee also vary with the still water levels during a storm event. This is because the wave heights of the Bay waves that propagate to the inner marsh levee are controlled by the water depths on the outer marsh levee, as discussed in Section 6.2.2. The variation of the wave heights with the still water levels during a storm event was thus included in the wave overtopping analysis. During each storm event, the wave height for a given water level was determined by combining the Bay wave (associated with this still water level) with the local marsh wave using the same methodology as used for determining the maximum wave heights (Section 6.2.2).

The wave overtopping rate per unit length was calculated using the wave runup and overtopping on impermeable structures application of ACES. For each given still water level, this computation was conducted for each of the sections (with a 0.2-foot crest elevation increment) of the two segments of the inner marsh levee. The lengths of these sections are listed in Table 6-1. The total wave overtopping rate of a segment for this given still water level was then determined as the sum of the overtopping rate of all the sections within this segment.

The wave heights, the wave periods, and the computed wave overtopping flow rates for different still water levels are summarized in Table 6-11 for the 250- and 500-year coastal flood events. The relationship between the overtopping flow rates versus the still water levels are also shown in Figure 6-14.

Table 6-11. Wave Overtopping Rate Versus Still Water Levels (Year 0 Condition)

Return Period (Years)	SWL (ft, NGVD)	Wave Height (ft)	Wave Period (sec)	Overtopping Flow Rate (ft ³ /s)		
				Segment 1	Segment 2	Total
250	+6.6	0.6	3.5	1.5	0.0	1.5
	+6.4	0.5	3.5	0.0	0.0	0.0
500	+6.8	0.8	3.6	57.7	13.2	70.9
	+6.6	0.6	3.6	1.5	0.0	1.5
	+6.4	0.5	3.6	0.0	0.0	0.0
	+6.2	0.4	3.6	0.0	0.0	0.0

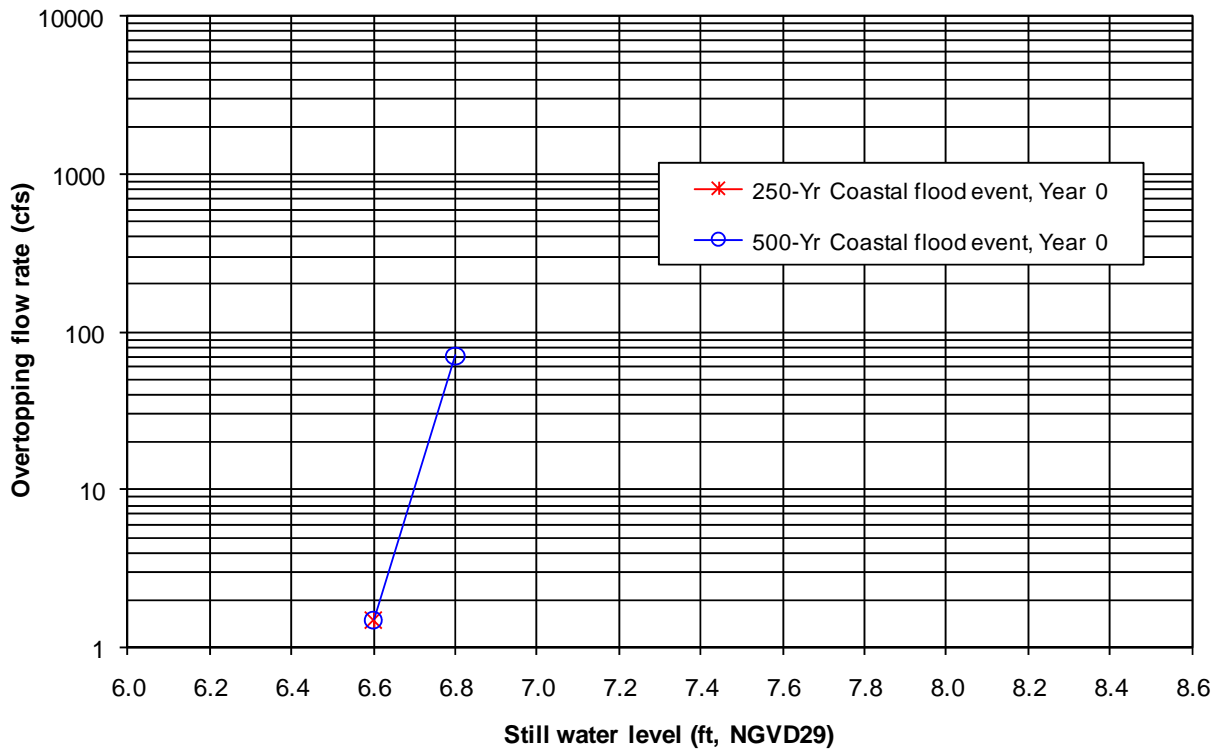


Figure 6-14. Overtopping Flow Rate versus Still Water Levels (Year 0 Condition)

6.3.3 Representative Still Water Level (Tidal Stage) Hydrographs

As the wave runup elevations and the wave overtopping rates vary with still water levels during a coastal flood event, the still water level hydrographs are required to determine the hydrograph of the wave overtopping flow rate and the total water volume of the wave overtopping. In this analysis, the 25-hour still water level (tidal stage) data measured at San Francisco during the January 1983 storm event, as shown in Figure 6-15, was used as the base to derive the typical still water level hydrograph. This measured tidal stage hydrograph was amplified by 1% to obtain a template for the tidal fluctuation at Gallinas, as shown in Figure 6-16. This amplification factor was determined based on the difference in MHHW-MLLW tidal range between the NOAA Gallinas station and the San Francisco station. The representative still water level hydrographs for the 250- and 500-year coastal flood events were then derived by moving the template upward to match the peak still water levels determined for these two storm events, respectively. The results are shown in Figure 6-17.

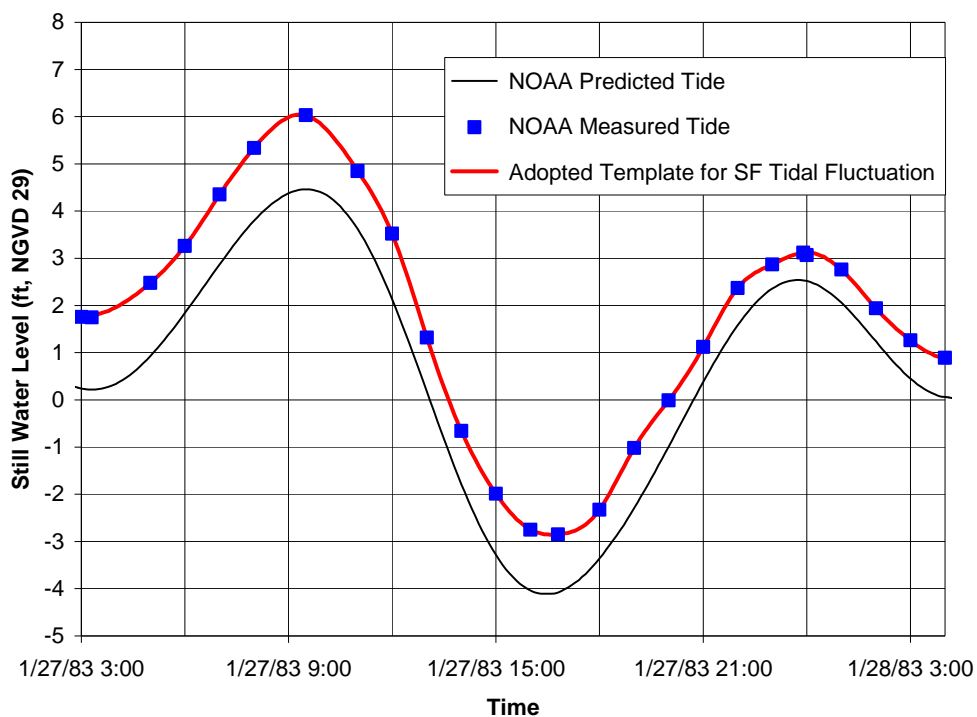


Figure 6-15. Water Levels Measured at San Francisco during January 1983 Storm Event

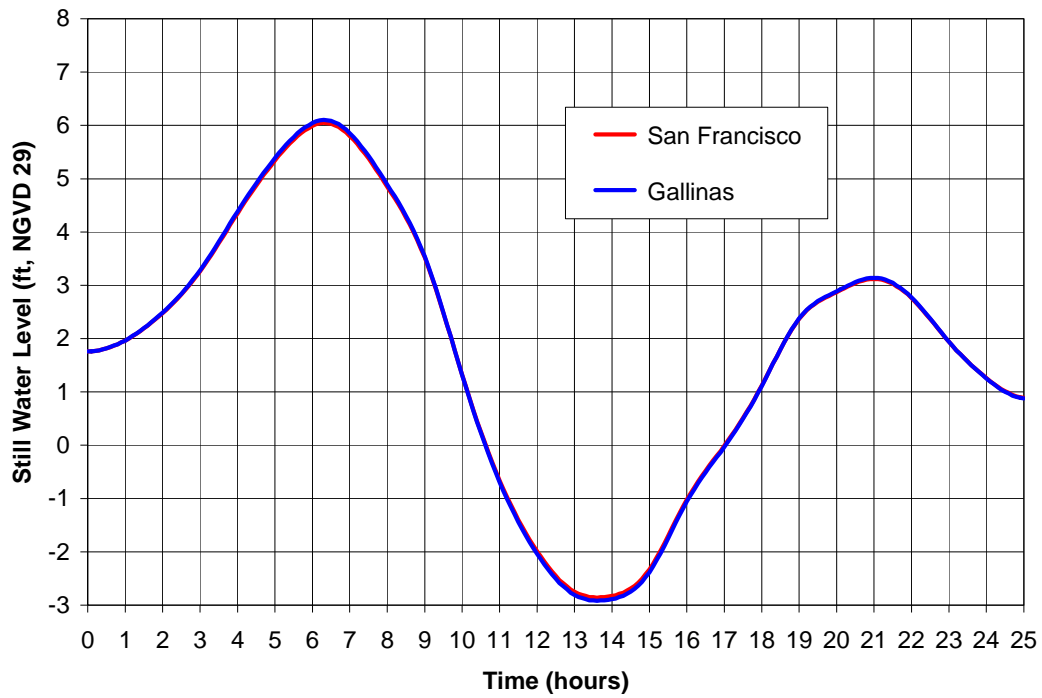


Figure 6-16. Templates for 25-Hour Still Water Level Hydrographs

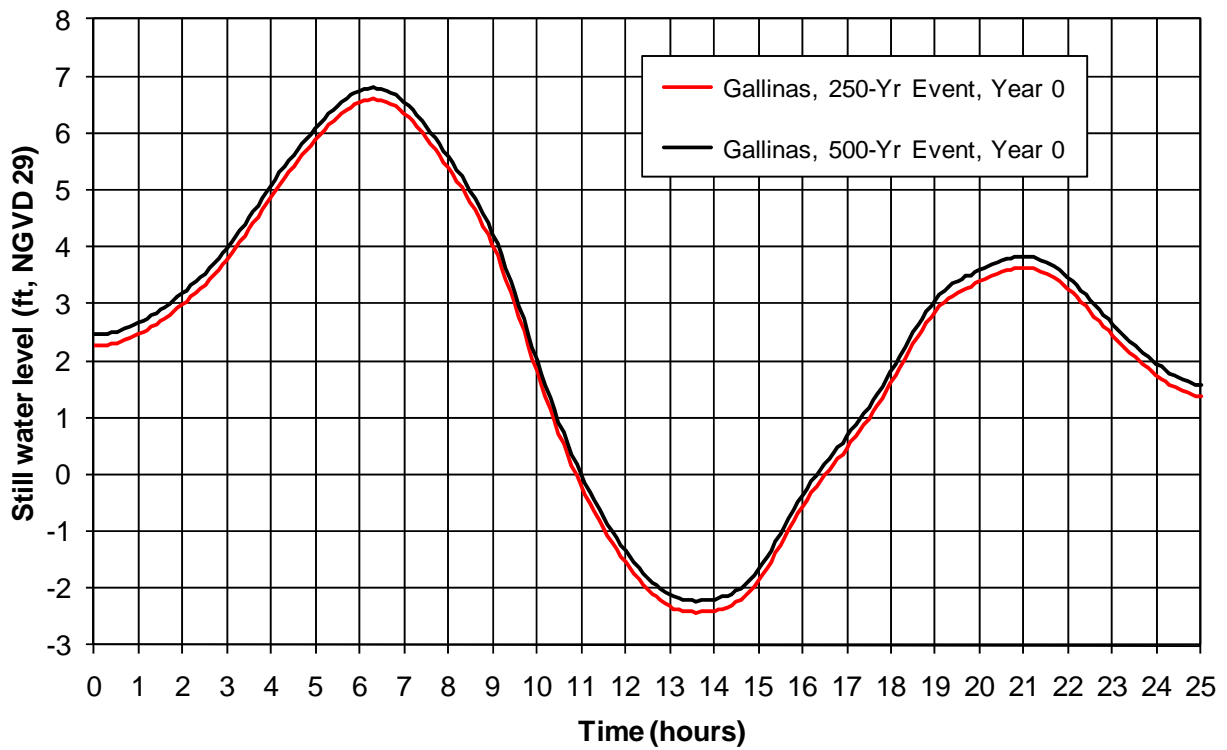


Figure 6-17. Representative Still Water Level Hydrographs at Gallinas

6.3.4 Wave Overtopping during Extreme Storm Flood Events

The wave overtopping flow rates were computed for the 250- and 500-year coastal flood events, the only two coastal flood events during which the wave overtopping will occur under the Year 0 condition. The hydrograph of the wave overtopping flow rates for a given flood event was computed by interpolating the relationship of the wave overtopping rates versus the still water levels using the representative still water level hydrograph for this event. The representative still water level hydrographs and the computed hydrographs of the wave overtopping flow rates are shown in Figure 6-18 for the 250-year coastal flood event, and in Figure 6-19 for the 500-year coastal flood event. The maximum overtopping flow rate was estimated to be 71 cfs during the 500-year coastal flood event, and is negligible for the 250-year coastal flood event.

Five permanent pump stations are situated along the South Fork, with 2 to 3 small portable pump stations (USACE, 2011). The discharge capacity of each permanent pump station is listed in Table 6-12. The total capacity of these five permanent pump stations is approximately 192 cfs. It noted that the coastal flooding and the riverine flooding were analyzed separately in this study by assuming that the coastal storm events will not coincide with the fluvial flood events. As a result, it was assumed that the five permanent pump stations could be operated in their full capacities, if needed, to pump out the coastal inundation water during coastal flooding events.

Table 6-12. Capacities of Pump Stations

Pump Station ID	Capacity (cfs)
1	63.4
2	40.5
3	38.0
4	5.0
5	45.0
Total	192

Since the total capacity of the five permanent pump stations (192 cfs) is higher than the maximum wave overtopping flow rate (71 cfs), coastal flooding is considered negligible for the Year 0 condition.

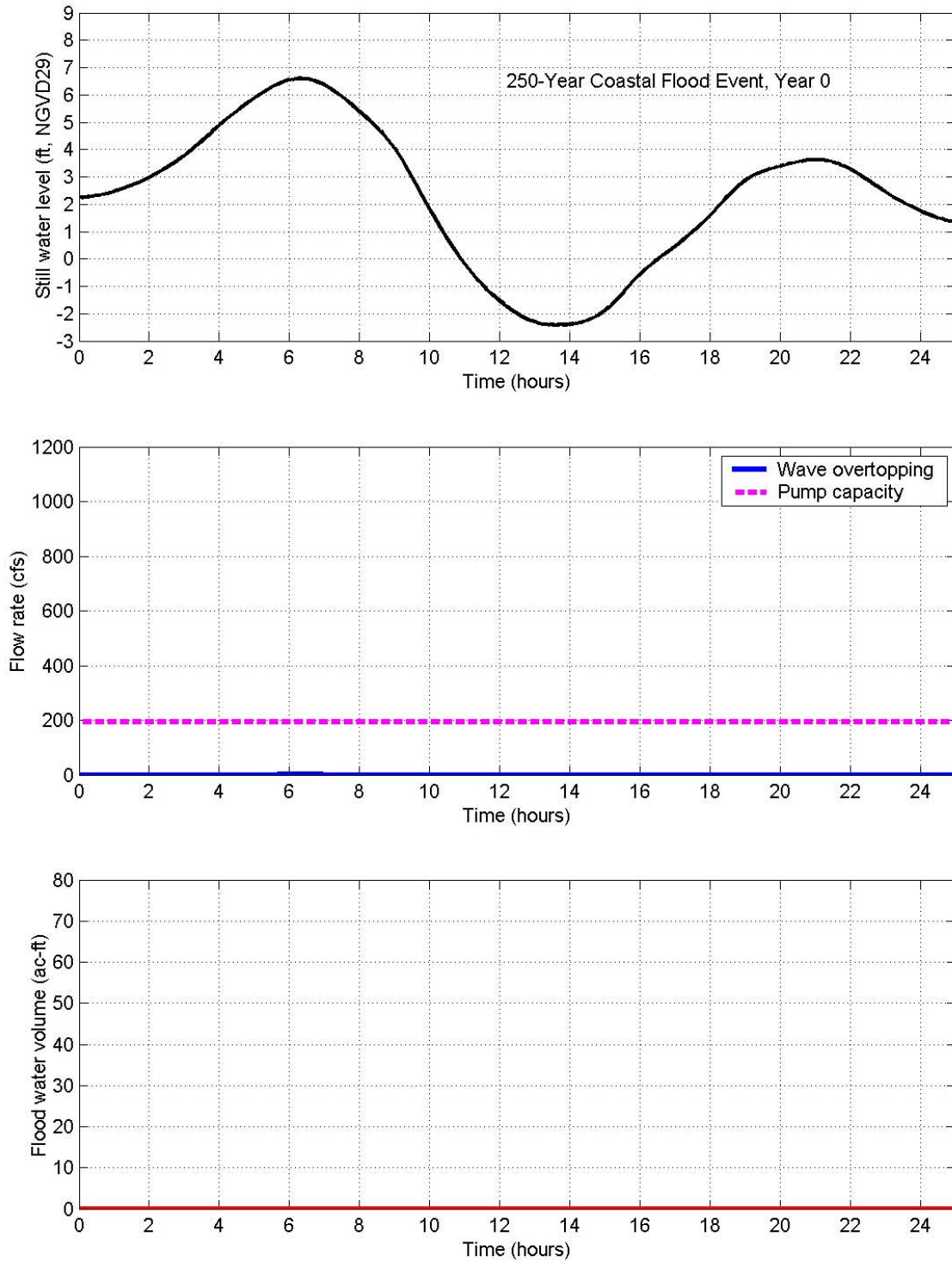


Figure 6-18. Time Series of SWLs, Overtopping Flow Rates and Cumulated Water Volumes during the 250-Year Coastal Flood Event (Year 0 Condition)

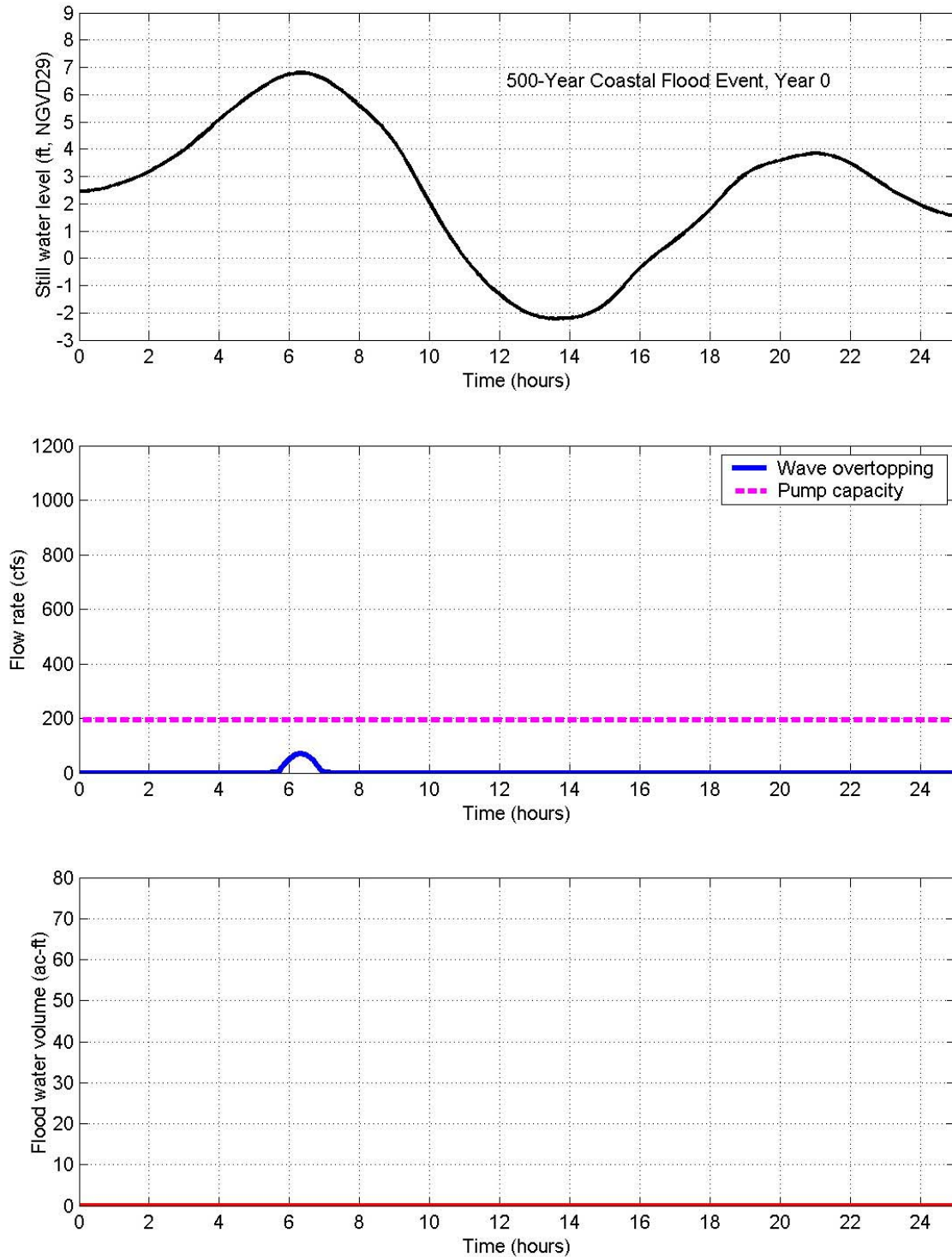


Figure 6-19. Time Series of SWLs, Overtopping Flow Rates and Cumulated Water Volumes during the 500-Year Coastal Flood Event (Year 0 Condition)

6.4 Wave Runup and Wave Overtopping For Year 50 Condition

Both the still water levels and the wave heights for the Year 50 (2061) condition will be higher than the Year 0 (2011) condition because of the sea level rise and the local land settlement. As a result, the wave runup elevations for the Year 50 condition will be higher, and the wave overtopping volumes will be larger than the Year 0 condition. The increase to the still water levels was discussed in Section 5.2. The storm wave condition for the Year 50 was discussed in Section 6.2.3. It is noted that the same procedures and methodologies were used to calculate the wave runup elevations and the wave overtopping for the Year 50 condition as used for the Year 0 condition. The difference in the wave overtopping condition is caused by the differences in the still water levels and the depth-limited wave condition between the Year 50 and the Year 0 conditions.

6.4.1 Maximum Wave Runup

The wave runup was computed using the ACES/CEDAS model for the eight coastal storm events for the Year 50 condition. The results of the maximum wave runup and the input parameters for the wave runup computation are listed in Table 6-13 for the Year 50 condition for the eight coastal flood events based on the historic SLR rate (0.50 feet in 50 years), and for the 100-year coastal flood event based on the modified NRC I SLR rate (0.8 feet in 50 years) and on the modified NRC III SLR rate (2.1 feet in 50 years), respectively. The results indicate that wave overtopping and potential coastal flooding will only occur during the 50-, 100-, 250- and 500-year coastal flood events for the Year 50 condition. The wave runup elevations will not exceed the existing inner marsh levee for the coastal flood events with the return periods of 25 years or shorter.

6.4.2 Wave Overtopping Versus Still Water Levels

The wave overtopping rates versus still water levels were calculated for the Year 50 condition for the six coastal flood events during which wave overtopping will occur. These six coastal flood events include the 50-, 100-, 250- and 500-year events based on the historical SLR trend, and the 100-year event based on the modified NRC-I and NRC-III SLR, respectively. As done for the Year 0 condition, the variation of the wave heights with the still water levels was included in the wave overtopping analysis for each storm event. The wave heights, the wave periods, and the computed wave overtopping flow rates for different still water levels are summarized in

Table 6-14 for the six coastal flood events. The relationship between the overtopping flow rates versus the still water levels are also shown in Figure 6-20.

6.4.3 Representative Still Water Level (Tidal Stage) Hydrograph

The representative still water level hydrographs for the Year 50 condition were derived by shifting the hydrographs for the Year 0 condition upward by the equivalent SLR values as determined in Section 5.2. The derived still water level hydrographs are shown in Figure 6-21 for the six coastal flood events for the Year 50 condition.

6.4.4 Wave Overtopping During Extreme Coastal Flood Events

The wave overtopping flow rates were computed for the six extreme coastal flood events for the Year 50 condition. The hydrograph of the wave overtopping flow rates for a given flood event was computed by interpolating the relationship of the wave overtopping flow rates versus the still water levels with the representative still water level hydrograph for this event. The representative still water level hydrographs and the computed hydrographs of the wave overtopping flow rates are shown in Figure 6-22 through Figure 6-27 for the six coastal flood events, respectively. The total capacity of the existing five permanent pump stations in Santa Venetia, which is approximately 192 cfs, is also shown in these figures.

The coastal flood water volumes accumulated within the Santa Venetia community were computed by integrating the time series of the net wave overtopping flow rates, which are the differences between the overtopping flow rates and the pump capacity. The time series of the water volume are shown in Figure 6-22 through Figure 6-27 for the six coastal flood events, respectively. As shown in these figure, the coastal flood water will start to accumulate within the community when the wave overtopping flow rates exceed the total pump capacity until the overtopping flow rates drop to below the pumping capacity. The maximum water volumes within the community are listed Table 6-15. It is noted that the total pump capacity exceeds the maximum overtopping flow rate for the 50-year flood event, and thus no coastal flood water will be stored in Santa Venetia during this flood event for the Year 50 condition.

Table 6-13. Wave Runup for Year 50 Condition

Return Periods (Years)	Equivalent SWL (ft NGVD)	Wave Height (ft)	Wave Period (sec)	Segment 1 (H:V=2.3:1, Toe EI +3.0 ft NGVD, Min Crest EI +7.8 ft NGVD)			Segment 2 (H:V=2.3:1, Toe EI +3.5 ft NGVD, Min Crest EI +8.2 ft NGVD)		
				Wave Runup (ft)	Wave Runup EI (ft, NGVD)	Overtopping Potential	Wave Runup (ft)	Wave Runup EI (ft, NGVD)	Overtopping Potential
2	+5.7	0.1	0.6	0.2	+5.9	No	0.2	+5.9	No
5	+6.1	0.3	2.8	0.6	+6.7	No	0.7	+6.8	No
10	+6.3	0.4	2.9	0.9	+7.2	No	0.9	+7.2	No
25	+6.6	0.5	3.1	1.1	+7.7	No	1.1	+7.7	No
50	+6.8	0.8	3.2	1.8	+8.6	Yes	1.8	+8.6	Yes
100	+6.9	0.9	3.3	2.1	+9.0	Yes	2.1	+9.0	Yes
250	+7.1	0.9	3.5	2.0	+9.1	Yes	2.0	+9.1	Yes
500	+7.3	1.1	3.6	2.6	+9.9	Yes	2.6	+9.9	Yes
100 (NRC I)	+7.2	1.0	3.3	2.4	+9.6	Yes	2.4	+9.6	Yes
100 (NRC III)	+8.5	2.0	3.3	4.6	+13.1	Yes	4.6	+13.1	Yes

Table 6-14. Wave Overtopping Rate for Given Still Water Levels for Year 50 Condition

Return Period (Years)	Equivalent SWL (ft, NGVD)	Wave Height (ft)	Wave Period (sec)	Overtopping Flow Rate (ft ³ /s)		
				Segment 1	Segment 2	Total
50	+6.8	0.8	3.2	55.9	12.0	67.9
	+6.6	0.6	3.2	1.4	0.0	1.4
	+6.4	0.5	3.2	0.0	0.0	0.0
100	+6.9	0.9	3.3	143.8	86.0	229.8
	+6.7	0.7	3.3	17.7	0.2	17.9
	+6.5	0.6	3.3	0.1	0.0	0.1
	+6.3	0.4	3.3	0.0	0.0	0.0
250	+7.1	0.9	3.5	220.9	147.4	368.3
	+6.9	0.9	3.5	138.7	78.0	216.7
	+6.7	0.7	3.5	17.6	0.2	17.8
	+6.5	0.6	3.5	0.1	0.0	0.1
	+6.3	0.4	3.5	0.0	0.0	0.0
500	+7.3	1.1	3.6	605.1	534.0	1,139.1
	+7.1	0.9	3.6	225.4	142.5	367.9
	+6.9	0.9	3.6	141.6	75.8	217.4
	+6.7	0.7	3.6	17.5	0.3	17.8
	+6.5	0.6	3.6	0.1	0.0	0.1
	+6.3	0.4	3.6	0.0	0.0	0.0
100 (NRC I)	+7.2	1.0	3.3	420.6	343.2	763.8
	+7.0	0.9	3.3	181.0	118.1	299.1
	+6.8	0.8	3.3	54.8	12.5	67.3
	+6.6	0.6	3.3	1.4	0.0	1.4
	+6.4	0.5	3.3	0.0	0.0	0.0
100 (NRC III)	+8.5	2.0	3.3	4,854.0	4,677.9	9,531.9
	+8.3	1.9	3.3	4,053.9	3,845.8	7,899.7
	+8.1	1.7	3.3	3,063.9	2,922.7	5,986.6
	+7.9	1.6	3.3	2,441.6	2,347.8	4,789.4
	+7.7	1.4	3.3	1,738.2	1,548.8	3,287.0

	+7.5	1.2	3.3	1,026.1	882.4	1,908.5
	+7.3	1.1	3.3	649.3	546.2	1,195.5
	+7.1	0.9	3.3	225.6	151.1	376.7
	+6.9	0.9	3.3	143.8	83.3	227.1
	+6.7	0.7	3.3	16.8	0.2	17.0
	+6.5	0.6	3.3	0.1	0.0	0.1
	+6.3	0.4	3.3	0.0	0.0	0.0

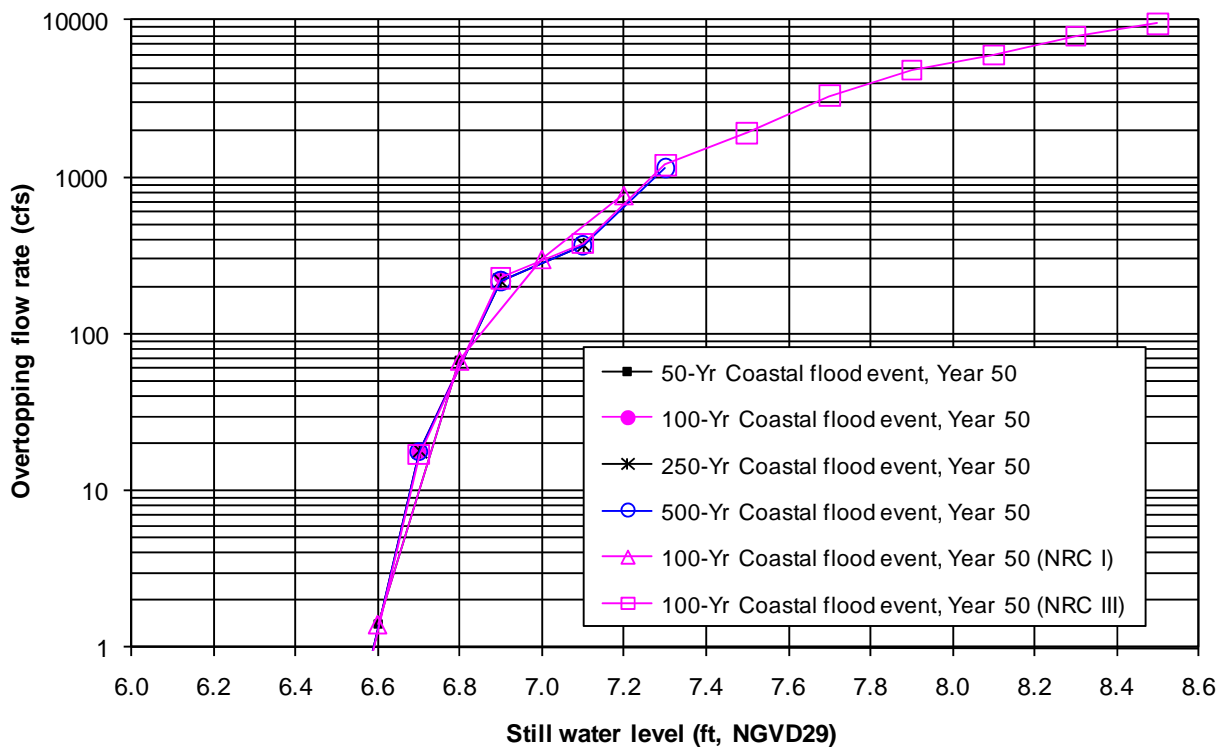


Figure 6-20. Overtopping Flow Rate versus Still Water Levels for Year 50 Condition

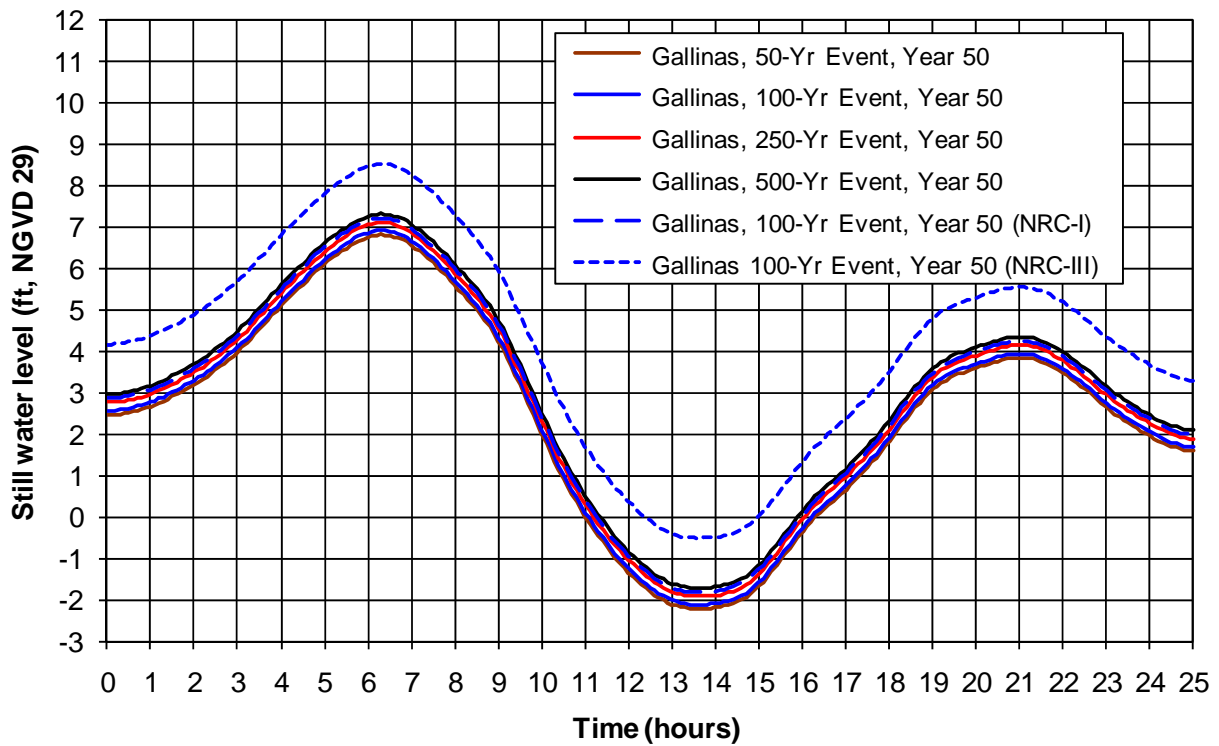


Figure 6-21. Representative Year 50 Still Water Level Hydrographs at Gallinas

Table 6-15. Coastal Flood Water Volumes in Santa Venetia Community (Year 50 Condition)

Return Period (Years)	Maximum Water Volume at Santa Venetia Community (ac-ft)
50	0
100	1
250	13
500	74
100 (NRC I)	43
100 (NRC III)	1,699

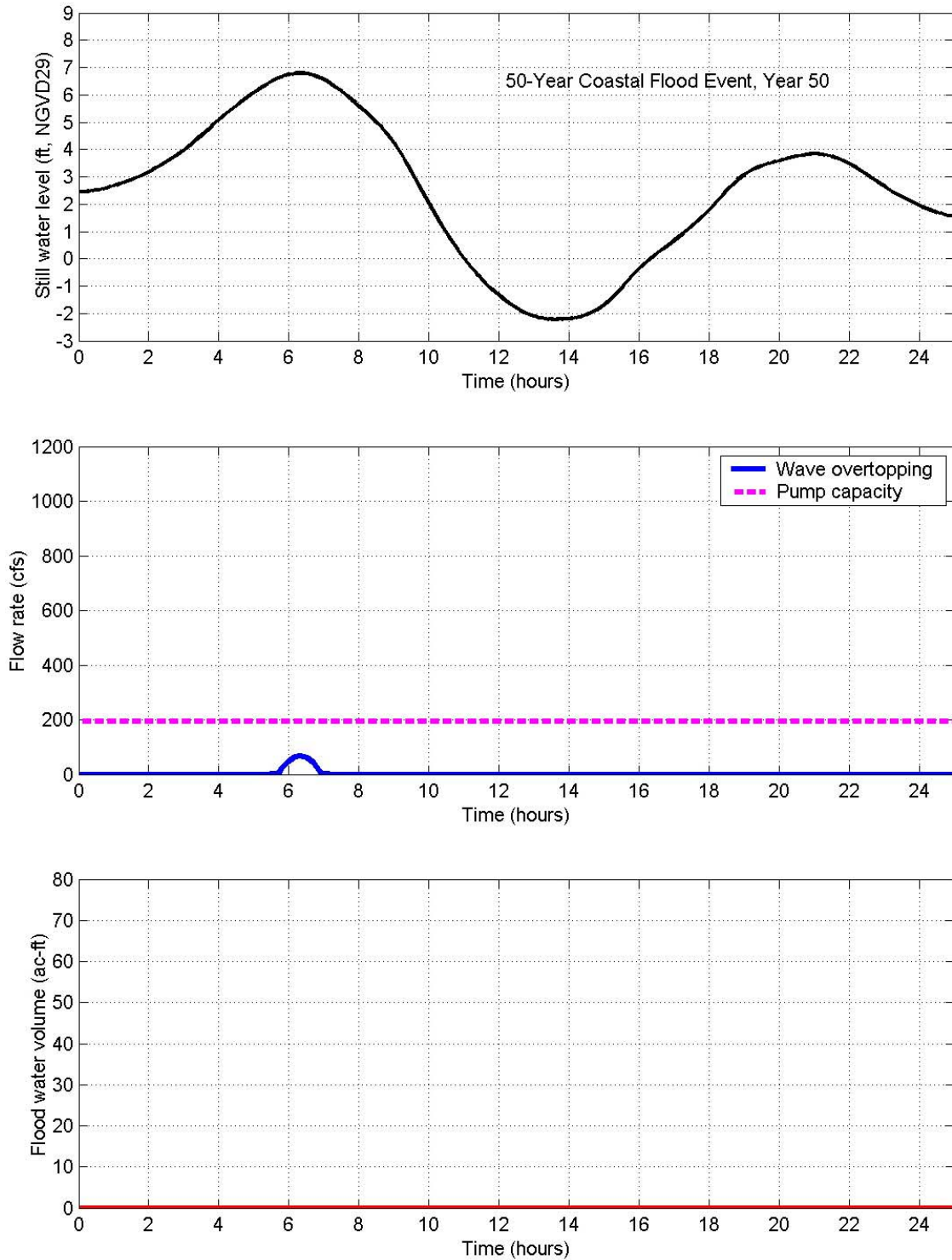


Figure 6-22. Time Series of SWLs, Overtopping Flow Rates and Cumulated Water Volumes during the 50-Year Coastal Flood Event (Year 50 Condition)

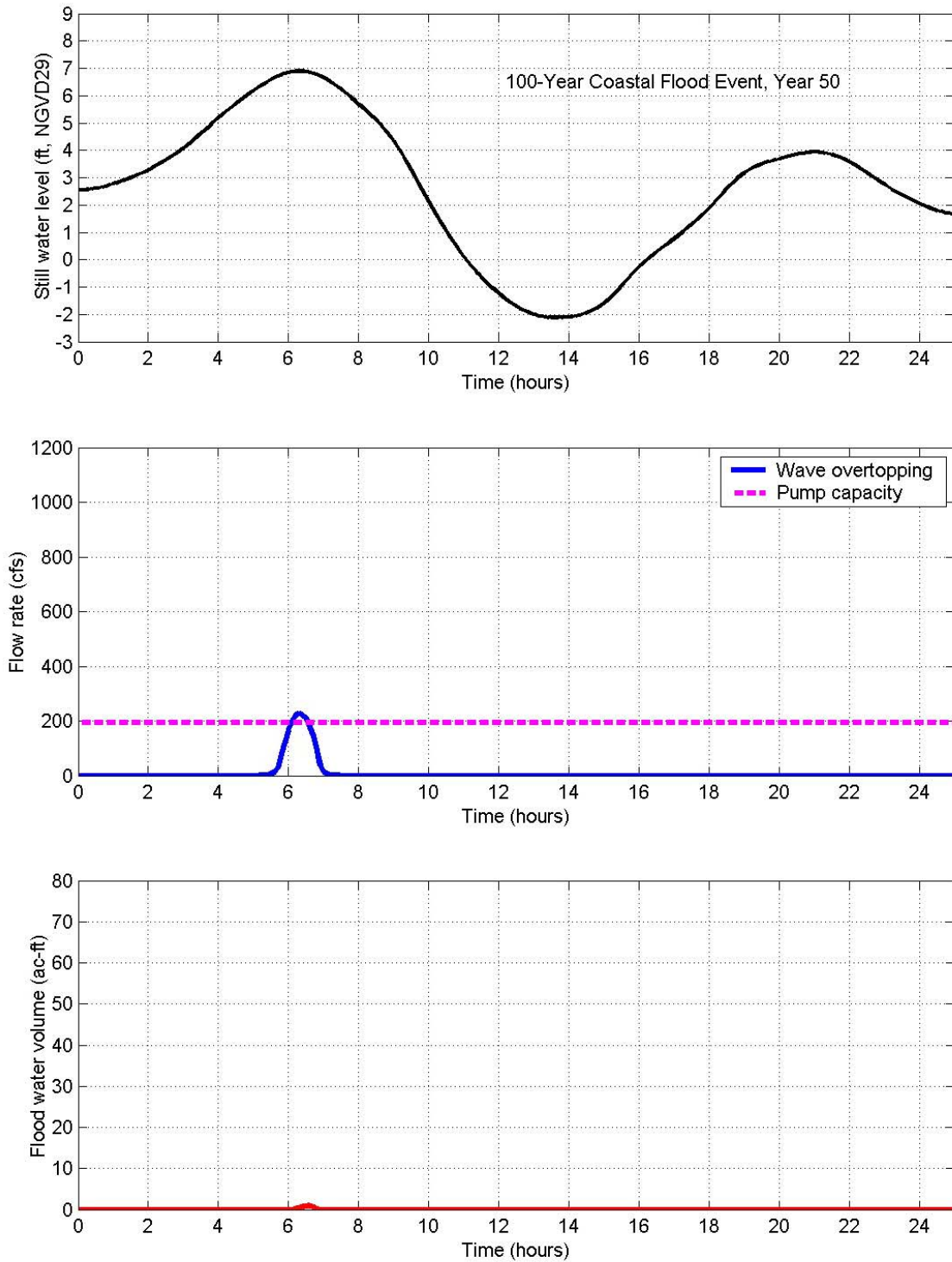


Figure 6-23. Time Series of SWLs, Overtopping Flow Rates and Cumulated Water Volumes during the 100-Year Coastal Flood Event (Year 50 Condition)

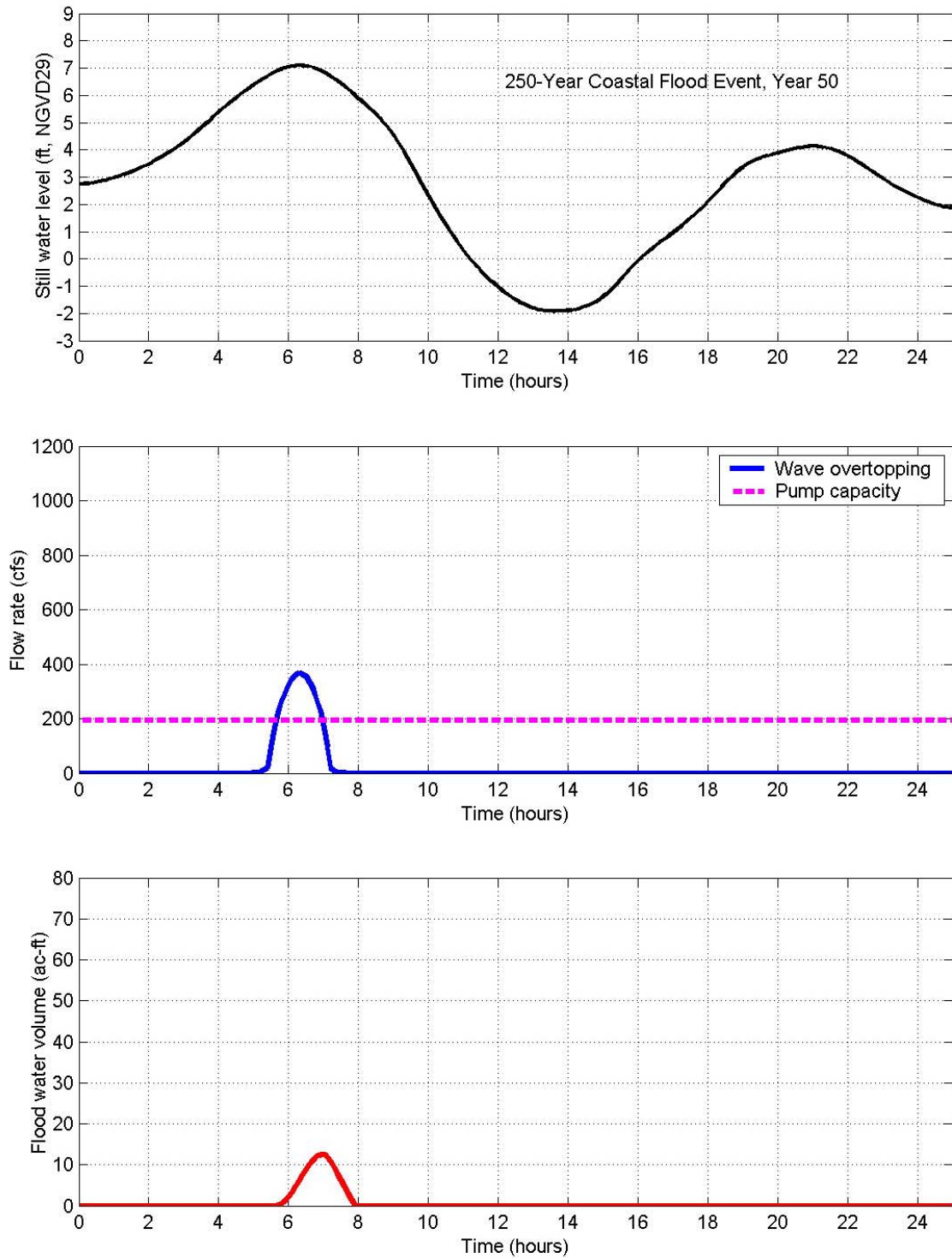


Figure 6-24. Time Series of SWLs, Overtopping Flow Rates and Cumulated Water Volumes during the 250-Year Coastal Flood Event (Year 50 Condition)

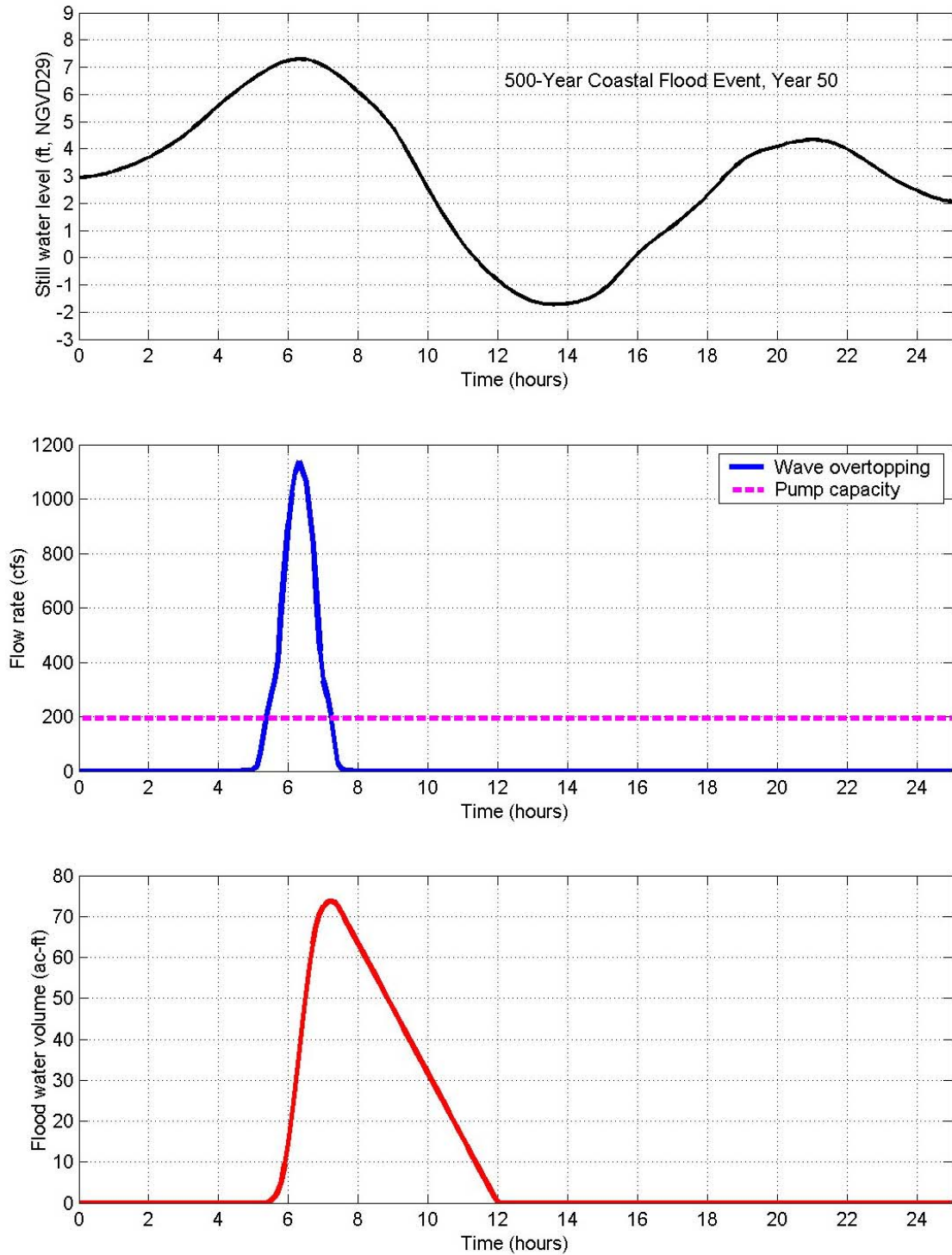


Figure 6-25. Time Series of SWLs, Overtopping Flow Rates and Cumulated Water Volumes during the 500-Year Coastal Flood Event (Year 50 Condition)

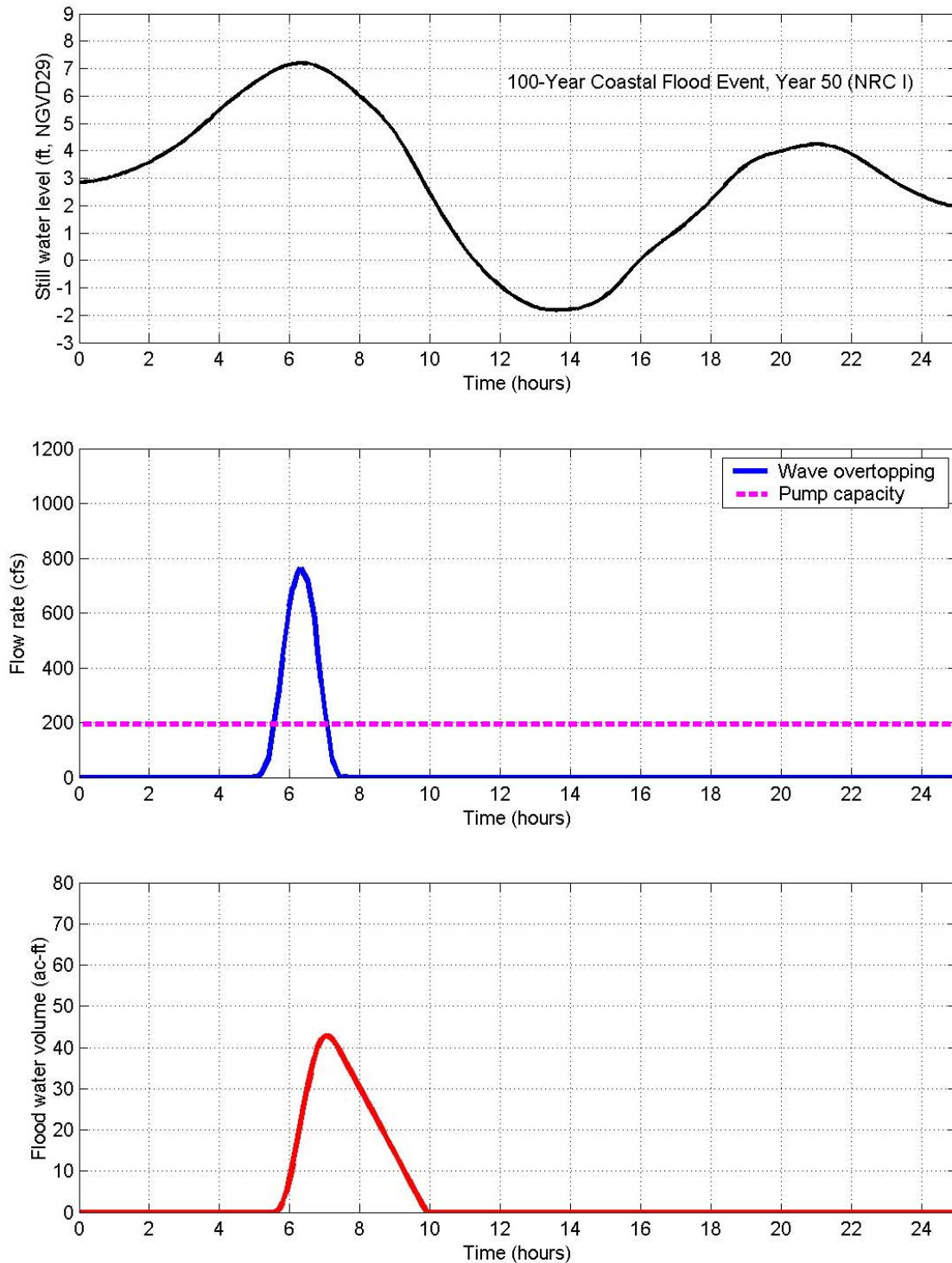


Figure 6-26. Time Series of SWLs, Overtopping Flow Rates and Cumulated Water Volumes during the 100-Year Coastal Flood Event (Year 50 Condition, NRC I)

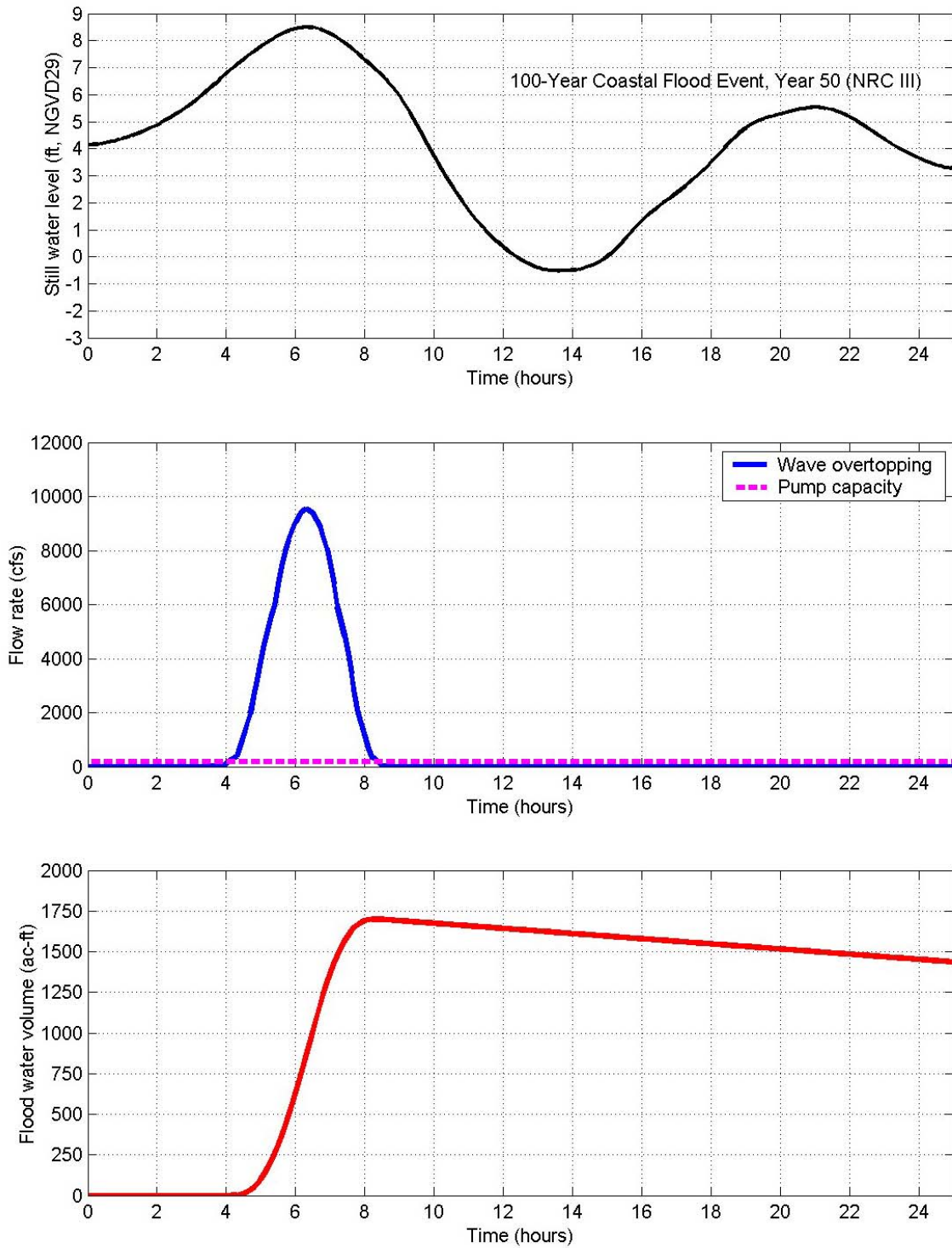


Figure 6-27. Time Series of SWLs, Overtopping Flow Rates and Cumulated Water Volumes during the 100-Year Coastal Flood Event (Year 50 Condition, NRC III)

7 COASTAL FLOODPLAIN MAPPING

The coastal flood water volumes stored in the Santa Venetia community, after taking into account the drainage capacity of the five pump stations situated in this community, were presented in Sections 6.3 and 6.4 for the Year 0 and Year 50 conditions, respectively. The inundation water levels of this community were determined based on the coastal flood water volumes and the storage capacity of the community. The floodplain maps due to the coastal flood inundation were then produced for extreme coastal flood events based on the inundation water levels and the County’s DEM for this community.

7.1 Storage Capacity of Santa Venetia Community

The Santa Venetia community was modeled as a storage basin for the coastal flood analysis. The storage curve of the community, which was defined as the storage capacities (water volumes) for various water levels, was derived based on the County’s DEM. The storage curve is shown in Figure 7-1 and is tabulated in Table 7-1.

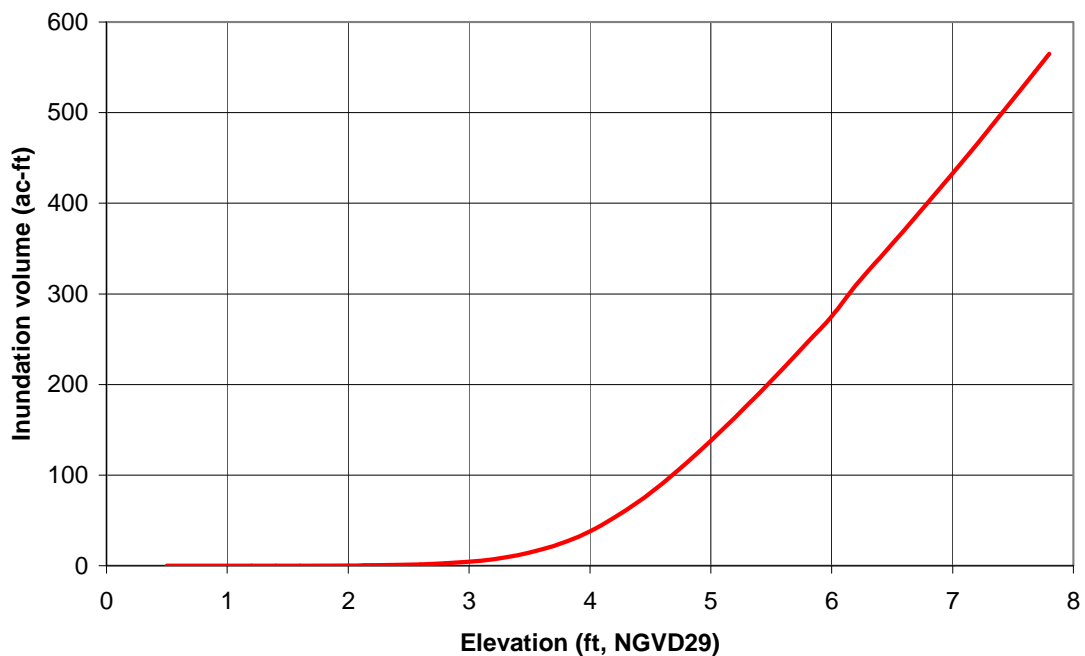


Figure 7-1. Water Storage Capacity of Santa Venetia Community

Table 7-1. Storage Capacity of Santa Venetia Community

Water Level (ft, NGVD29)	Water Surface Area (acre)	Water Storage Volume (ac-ft)
+1.0	0.02	0.01
+2.0	0.9	0.2
+3.0	10.9	4.5
+4.0	64.0	38.0
+5.0	125.8	138.0
+6.0	144.3	275.2
+7.0	159.0	433.1
+7.8	170.8	565.0

7.2 Coastal Floodplain Mapping for Year 0 Condition

As discussed in Section 6.3.4, no coastal flood water is stored within the community for the Year 0 condition, after taking into account the drainage capacity of the five pump stations situated within the community. In other words, the community does not experience coastal flood inundation for the Year 0 condition as long as the pump stations do not fail. Therefore, no coastal floodplain inundation maps were generated for the Year 0 condition.

7.3 Coastal Floodplain Mapping for Year 50 Condition

The maximum coastal flood water volumes stored within the Santa Venetia community are listed Table 6-15 for the Year 50 condition, based on which the inundation water levels were determined using the storage curve developed for Santa Venetia. The results are listed in Table 7-2 for the five coastal flood events for the Year 50 condition, during which the community will be inundated by coastal flood water.

It is noted that the computed maximum water volume for the 100-year coastal flood event based on the NRC III SLR scenario will yield an inundation water level that exceeds the inner levee crest elevation (+7.8 to +9.4 feet, NGVD29) and that exceeds the still water level at the San Pablo Bay (+8.5 ft, NGVD29). This indicate that the inner marsh levee will be submerged, and

Santa Venetia will become a part of the San Pablo Bay water body for this event. Therefore, the inundation water level of Santa Venetia was approximated by the still water level of the Bay, or +8.5 ft, NGVD29, for the 100-year coastal flood event with NRC III SLR scenario.

Table 7-2. Coastal Flood Inundation for Santa Venetia Community (Year 50 Condition)

Return Period (Years)	Equivalent Tidal Stage (ft, NGVD29)	Maximum Water Volume (ac-ft)	Inundation Water Level (ft, NGVD29)	
			Computed	Adopted
100	+6.9	1	2.4	2.4
250	+7.1	13	3.4	3.4
500	+7.3	74	4.4	4.4
100 (NRC I)	+7.2	43	4.1	4.1
100 (NRC III)	+8.5	1,699	13.2	8.5

The coastal floodplain maps within the Santa Venetia community were generated with ArcGIS by intercepting the County's DEM with the inundation water levels for the extreme coastal flood events for the Year 50 condition. The maps are shown in Figure 7-2 through Figure 7-4 for the 100-, 250-, and 500-year coastal flood events based on the historic SLR trend, in Figure 7-5 for the 100-year coastal flood event based on the modified NRC I SLR scenario, and in Figure 7-6 for the 100-year coastal flood event based on the modified NRC III SLR scenario.

The coastal flood inundation for Santa Venetia will be negligible for the Year 50 condition during the 100-year coastal flood event based on the historic sea level rise trend, with only the ditches and some lower spots being flooded. However, most portions of Santa Venetia will be inundated during the 500-year coastal flood event (with the historic sea level rise trend) and during the 100-year coastal flood event if considering the conservative sea level rise scenario (modified NRC III).

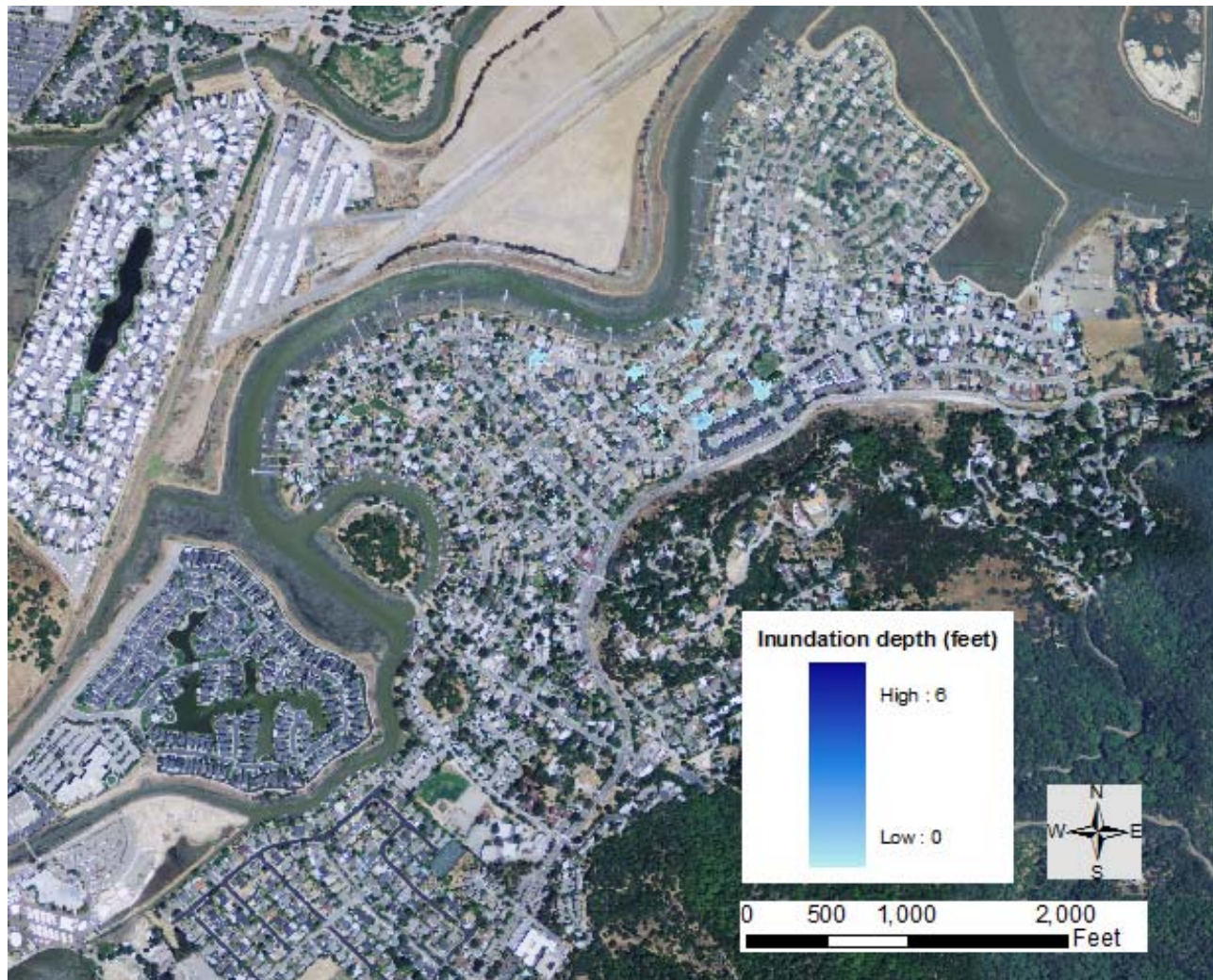


Figure 7-2. Coastal Floodplain Map for the 100-Year Coastal Flood Event for Year 50 Condition

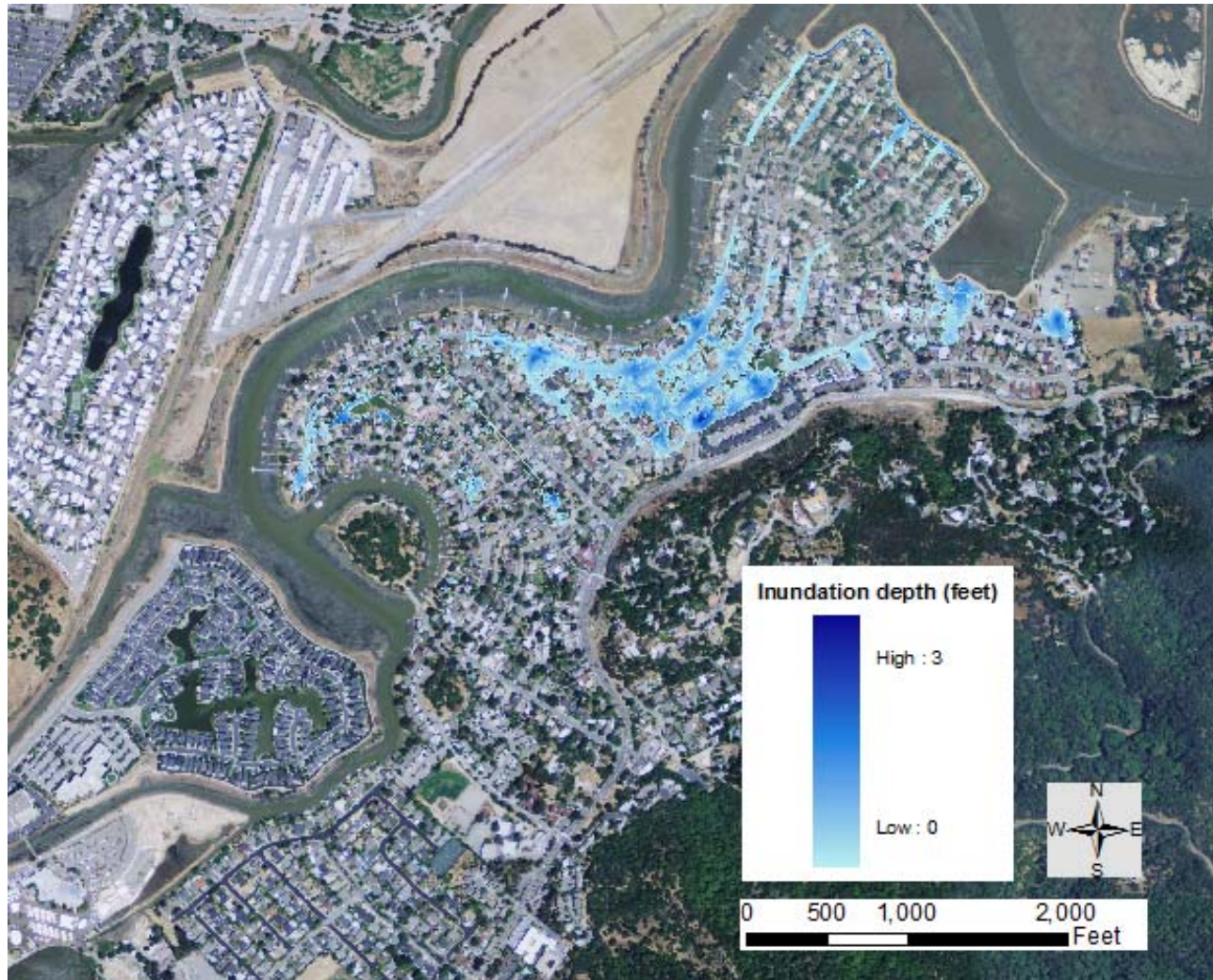


Figure 7-3. Coastal Floodplain Map for the 250-Year Coastal Flood Event for Year 50 Condition

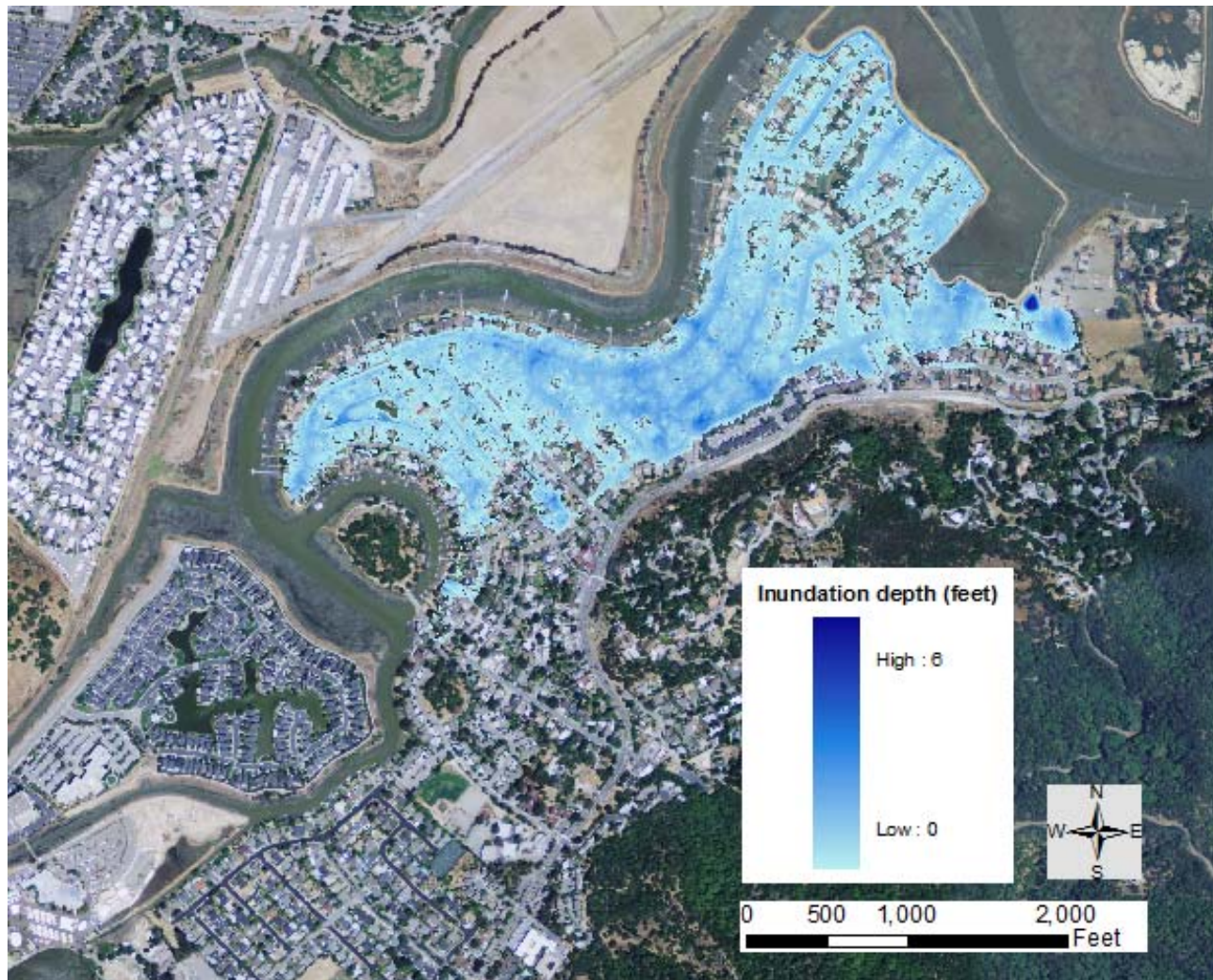


Figure 7-4. Coastal Floodplain Map for the 500-Year Coastal Flood Event for Year 50 Condition

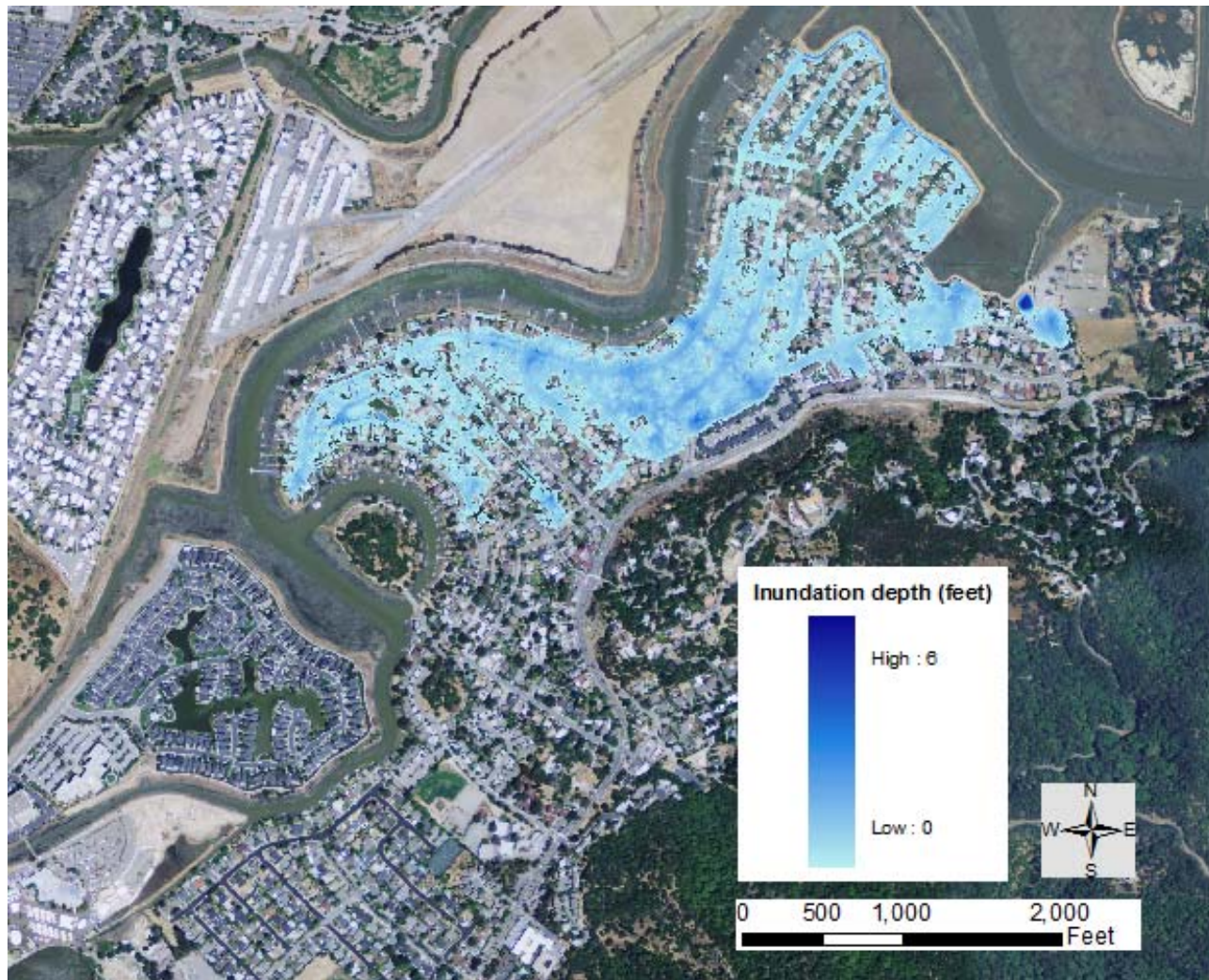


Figure 7-5. Coastal Floodplain Map for the 100-Year Coastal Flood Event for Year 50 Condition (NRC I)

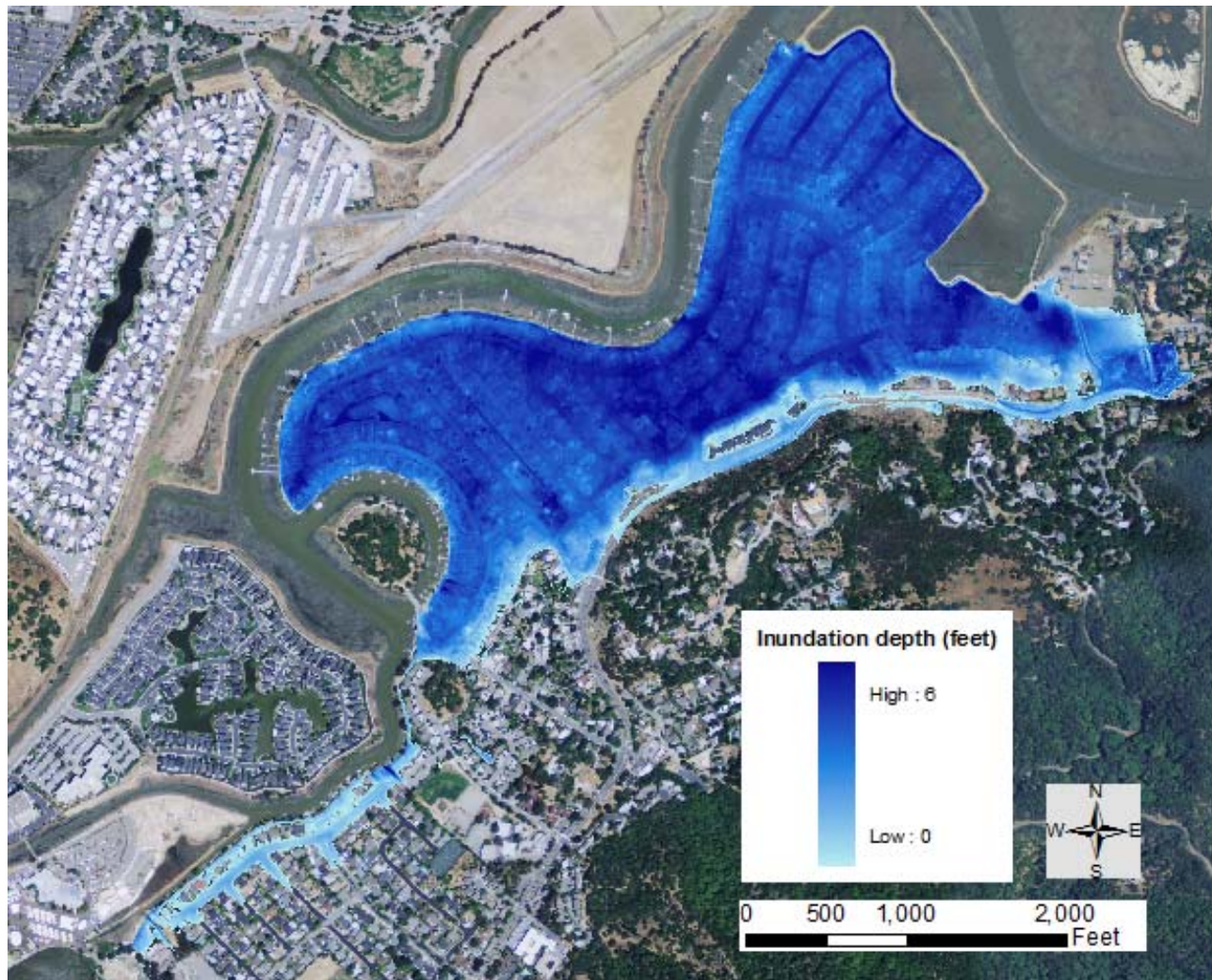


Figure 7-6. Coastal Floodplain Map for the 100-Year Coastal Flood Event for Year 50 Condition (NRC III)

7.4 Uncertainty in Coastal Flooding Analysis

As discussed in Section 6.2, the wave height at the inner marsh levee is mainly controlled by the water depth on the outer marsh levee. Therefore, the wave condition (particularly the wave height) at San Pablo Bay has limited impact on the wave overtopping on the inner marsh levee and coastal flooding in Santa Venetia. The uncertainty in coastal flooding analysis caused by the uncertainty in the wind-wave hindcasting is considered limited.

The characteristics of the inner marsh levee impact the wave overtopping rates and thus the inundation water levels in Santa Venetia. The levee characteristics used in the coastal flooding analysis were developed mainly based on County's levee crest profile survey and the survey for a couple of levee transects. The uncertainty in the survey is considered limited. In other words, the uncertainty in the coastal flooding analysis caused by the uncertainty in the levee characteristics data is limited.

The coastal still water level not only determines the still water level at the inner marsh levee, but also impacts the wave condition at the inner marsh levee that is controlled by the water depth on the outer marsh levee. The still water level and the wave condition are the most important factors to impact the wave overtopping flow rates and the coastal inundation depth in Santa Venetia. Therefore, the uncertainty in the coastal still water level is the major cause for the uncertainty in the coastal flooding analysis.

The still water levels for the Year 0 condition were developed in this analysis based on the historic tidal data, which were deemed relatively liable. The uncertainty in the flooding analysis for the Year 0 condition is thus considered limited.

However, the uncertainty in the still water levels for the Year 50 condition is considered significant because of the great uncertainty in the future sea level rise (SLR). While SLR has been extensively investigated, there is no general agreement about the SLR rate. According to the Corps guidance EC 1165-2-211, the SLR in the next 50 years (including the local land settlement) ranges from approximately 0.5 feet based on the historic SLR trend to 2.1 feet based on the modified NRC Curve III. Other agencies may estimate/adopt even higher sea level rise values.

As discussed in Section 7.3, the Year 50 coastal inundation depths in Santa Venetia show significant difference for different SLR scenarios. This implies that the uncertainty in the future SLR will be the major cause for the uncertainty in the coastal flooding analysis for the Year 50 condition.

8 SUMMARY

Las Gallinas Creek is located in San Rafael, California. It has two forks (North and South), which join near the east end of the Smith Ranch Airport. The area of interest for this analysis extends along the South Fork of Las Gallinas Creek from the confluence with Gallinas Creek to approximately 500 feet upstream of Santa Margarita Island.

The purpose of this study is to support the without project condition milestone. The scope of work includes (1) developing the floodplains maps for the without project condition for Year 0 (2011) and for the without project future Year 50 (2061) condition, and (2) evaluating the project performance for the existing levee system that protect the Santa Venetia community. The floodplain maps were developed separately for the riverine flood events and for the coastal flood events. The riverine flooding analysis focused on the fluvial flood events in Las Gallinas Creek, assuming the still water level at the mouth of the creek was at the Mean Higher High Water level (MHHW). The coastal flooding analysis focused on the coastal storm events alone, neglecting the fluvial flows in Las Gallinas Creek. It is noted that the uncertainty in the geotechnical condition of the levees or the levee damage/failure was not included in this flooding analysis due to project constrain.

H&H Analysis

The steady flow model with HEC-RAS and the ArcGIS tools HEC-GeoRAS were used for the channel hydraulic modeling and riverine floodplain mapping. The channel geometry used in the HEC-RAS model was developed based on a channel topographic survey, the digital terrain model (DTM) for the Gallinas watershed, and the levee crest elevation survey conducted for the Santa Venetia Levee. A DTM was developed by merging the channel survey into the DTM of the watershed. The HEC-geoRAS model was used to create the channel geometry data including the levees. The pedestrian bridge near Santa Margarita Island was also included in the HEC-RAS model.

The peak flow discharges at six junctions along the South Fork were estimated for eight flood events in the Corps (2011) hydrologic study. These were directly used in the hydraulic analysis as the inflow condition. The downstream water surface elevation at the mouth of the Las Gallinas Creek was controlled by the water level in San Pablo Bay. The tidal datums relative to

NGVD29 at the NOAA Hamilton AFB Station, Outside Gage were used to represent the tidal stages at the mouth of Las Gallinas Creek. The MHHW at this station is at approximately +3.58 feet, NGVD29.

Little information on stream flow and river stage data exists for the South Fork of Las Gallinas Creek during the historic flood events, and thus the HEC-RAS model cannot be calibrated with any measured data or high watermarks. A qualitative “calibration”, or a first reality check, was conducted based on the February 25, 2004 flood event, which is deemed a 50-year flood event. The adopted Manning’s roughness value (n-value) was 0.035 for the main channel bounded by the levees, 0.050 for the left floodplain, and 0.100 for the right floodplain. The adopted n-values are the normal values recommended in the HEC-RAS Reference Manual for the similar types of channels and floodplains.

The existing flow capacity of the creek as well as the capacity for the Santa Margarita Island Bridge were evaluated based on the HEC-RAS model results for the eight flood events. The results indicated that the existing South Fork and the Santa Margarita Island Bridge have the capacity to convey at least the 0.2% AEP (or 500-year) flood event, providing there is no geotechnical or structural failure of the levee.

A sensitivity analysis was conducted to test how the n-values and the downstream water levels affect the channel capacity. The results indicate that the impact of the n-value is very limited because of the relatively short length of the creek. The impact of the downstream water levels is also limited. Based on the computed upper bounds of the water surface profiles, it is concluded that the existing South Fork and the Santa Margarita Island Bridge have the capacity to convey at least the 0.2% AEP flood based on the conservative consideration.

The riverine flooding analysis and riverine floodplain delineation were conducted using the HEC-RAS model and the HEC-geoRAS program in ArcGIS for both the Year 0 (2011) condition and the Year 50 (2061) condition. Eight flood events, with the 50%, 20%, 10%, 4%, 2%, 1%, 0.4% and 0.2% AEPs, respectively, were analyzed for Year 0 condition. These eight flood events were also analyzed for the Year 50 condition after considering future sea level rise (based on the historic sea level rise trend) and the local land movement. The results indicate that while the inundation water depths are different, the inundation boundaries do not show significant difference between different flood events or between the Year 0 condition and the Year 50

condition. The main channel of the creek that is bounded by the left and right levees, and the Santa Venetia marsh will be inundated, but Santa Venetia will not be inundated during these flood events.

A risk and uncertainty analysis was conducted using HEC-FDA in order to evaluate the project performance for the existing Santa Venetia levee system that protects the Santa Venetia community. Fifteen index points were selected along the South Fork of Las Gallinas Creek. The stage-discharge functions with uncertainties were determined for these index points. The exceedance probability functions with uncertainties were determined in Corps (2011) hydrologic analysis for the hydrologic junctions, and were assigned to the index points in this analysis. The transform flow relationship was used in the model to represent the flow split around the Santa Margarita Island.

The 90% and 95% CNP stages for the 1% AEP flood event were computed using HEC-FDA for the fifteen index points for both the Year 0 and Year 50 conditions, based on which the 90% and 95% CNP profiles were developed for the entire creek. The freeboard of the Santa Venetia levee for the 1% AEP flood event was also determined based on the HEC-RAS model results.

The project performance of the Santa Venetia levee system was evaluated based on the Corps certification criteria. The criteria require that (1) the project provides a minimum of 3 feet of freeboard with a 90% conditional annual non-exceedance probability (CNP) for the 1% AEP flood event, or (2) the project provides a minimum of 2 feet of freeboard with a 95% CNP for the 1% AEP flood event. Based on the criteria, thirteen of the fifteen index points (or damage reaches) meet the Corps levee certification criteria for the Year 0 condition. Twelve of the fifteen index points (or damage reaches) meet the criteria for the Year 50 condition. Overall, major portions of the Santa Venetia levee system meet the CNP certification criteria. Some short segments of the levee do not meet the criteria because of the insufficient freeboard that is less than the minimum freeboard requirement of 2 feet.

Coastal Analysis

A coastal still water level frequency analysis was conducted for the NOAA San Francisco Station based on the annual maximum water level data for the period between 1990 and 2010. The correlation relationship of the still water levels between Gallinas (the mouth of the Las Gallinas Creek) and San Francisco was developed. The annual maximum water level at Gallinas was estimated to be approximately 0.37 feet higher than San Francisco. The coastal still water level frequency curve for the Year 0 (2011) condition was developed for Gallinas by moving the water level frequency curve for San Francisco upward by 0.37 feet. The maximum water level at Gallinas was estimated to be approximately +6.4 feet, NGVD29 for the 1% AEP flood, and approximately +6.8 feet, NGVD29 for the 0.2% AEP flood.

The still water level frequency curve for the Year 50 (2061) condition was derived by moving the frequency curve for the Year 0 (2011) condition upward by the future sea level rise (SLR), including the local land movement, in the next 50 years. This analysis focused on the historic rate of SLR, which was estimated to be approximately 0.50 feet between 2011 and 2061, including the local land settlement. Two other SLR scenarios were also addressed through sensitivity tests.

The San Pablo Bay front levee system blocks the bay waves being propagated to the project site from most directions. Only the lower portion of the Las Gallinas levee system, which is also named the Santa Venetia Marsh perimeter levee, is exposed to wave action within a narrow band of directions. The flooding of Santa Venetia resulted from the coastal storm events is caused by the wave overtopping over the Santa Venetia Marsh levee.

A wind-wave hindcasting was conducted using CEDAS/ACES to determine the wave conditions at Gallinas. The wind data acquired from the National Climate Data Center (NCDC) for multiple locations were used in the wind-wave hindcasting. The significant wave heights and periods were determined for different return frequencies.

A wave transformation was conducted to propagate the Bay waves from Gallinas to the project site. When the water level is lower than the outer Santa Venetia Marsh levee, this outer marsh levee blocks the Bay waves being propagated to the inner marsh levee that protects Santa Venetia. When the water level is higher than the outer marsh levee, this outer marsh levee acts

as a submerged breakwater for wave propagation from the Bay to the inner marsh levee because of the shallow water depth on the outer marsh levee. The wave heights of the Bay waves that can propagate from the Bay to the inner marsh levee were determined based on the traditional depth-limited wave criterion.

A wind-wave hindcasting was also conducted to estimate the local waves generated within the Santa Venetia Marsh. The wave condition at the inner marsh levee was determined by combining the depth-limited Bay waves propagating to the inner marsh and the local waves generated within the marsh based on the conservation of wave energy. It is noted that the local waves have negligible contribution to the combined wave condition, which was used in the wave runup and wave overtopping analysis for the inner marsh levee.

The wave runup elevation and wave overtopping, if any, were computed using CEDAS/ACES for the inner marsh levee. The levee characteristics of the inner marsh levee, such as the crest elevations, side slopes and toe elevations, were considered in the wave runup and wave overtopping analysis. Representative still water level (tidal stage) hydrographs were used in the wave overtopping computation. The flow hydrographs for the wave overtopping flow rates were computed for the extreme coastal storm. The total capacity of the existing five permanent pump stations in Santa Venetia, which was estimated to be approximately 192 cfs, was included in the coastal flooding analysis.

The coastal flood water volumes accumulated within the Santa Venetia community during the extreme coastal storm events were computed by integrating the time series of the net wave overtopping flow rates, which are the differences between the overtopping flow rates and the pump capacity. The coastal inundation water levels of Santa Venetia were determined based on the maximum coastal flood water volumes and the storage capacity of the community. The floodplain maps due to the coastal flood inundation were produced based on the inundation water levels and the County's DEM for the watershed.

The coastal flooding analysis were conducted for both the Year 0 condition and for the Year 50 condition. The future sea level change, including the local land movement, was considered for the Year 50 condition, with the primary focus on the historic rates of sea level rise (SLR). Other two SLR scenarios were addressed through sensitivity tests.

Wave overtopping will occur for the 250- and 500-year coastal flood events under the Year 0 condition. The maximum overtopping flow rates during these two events are lower than the total capacity of the five permanent pump stations. Therefore, coastal flooding is considered negligible for the Year 0 condition if the pump stations do not fail.

Wave overtopping will occur for the 50-, 100-, 250-, and 500-year coastal storm events during the Year 50 condition, after considering the historic sea level rise trend. The maximum overtopping rate for the 50-year storm event will be less than the total pump capacity. Therefore, coastal flooding will occur in Santa Venetia during the 100-, 250- and 500-year coastal flood events. As shown in the coastal floodplain maps, Santa Venetia will be flooded at some scatter locations during the 100-year coastal flood event, and will be flooded for most places during the 500-year event.

The coastal flooding analysis was also conducted and the coastal floodplain maps were produced for the 100-year coastal flood event for the Year 50 condition based on two additional sea level rise scenarios: the modified NRC curve I and the modified NRC curve III. Waves will overtop the inner marsh levee and coastal flooding will occur in Santa Venetia for the 100-year coastal flood considering these two sea level rise scenarios.

This sensitivity analysis indicated that the coastal inundation water level in Santa Venetia is very sensitive to the coastal still water level. This is because the coastal still water level not only impacts the still water level at the inner marsh levee, but also impacts the depth-limited Bay waves that propagate to the inner marsh levee. The still water level and the wave condition are the most important factors to impact the wave overtopping flow rate and thus the coastal inundation water level in Santa Venetia.

9 REFERENCES

Ahrens, J. P., and Burke, C. E. 1987. Unpublished report of modifications to "Prediction of Irregular Wave Overtopping," CERC CETA 77-7, prepared by Ahrens, J. P., US Army Engineer Waterways Experiment Station, Vicksburg, MS, 1977.

Ahrens, J. P., and McCartney B. L. 1975. "Wave Period Effect on the Stability of Riprap," Proceedings of Civil Engineering in the Oceans/III, American Society of Civil Engineers, pp. 1019-1034.

Ahrens, J. P., and Titus, M. F. 1985. "Wave Runup Formulas for Smooth Slopes," Journal of Waterway, Port, Coastal and Ocean Engineering, American Society of Civil Engineers, Vol. 111, No. 1, pp. 128-133.

Federal Emergency Management Agency (FEMA), 2003. Guidelines and Specifications for Flood Hazard Mapping Partners. Prepared in April 2003.

Kamman Hydrology & Engineering, Inc. (KHE), 2004. Gallinas Creek Restoration Feasibility Study and Conceptual Design Report, Marin County, California. Prepared for San Pablo Bay Watershed Restoration Program Partners: U.S. Army Corps of Engineers, San Francisco District and California Coastal Conservancy. Prepared in December 2004.

Noble Consultants, Inc. (NCI) and Multech Engineering Consultants, Inc. (MEC), 2009. Las Gallinas Creek Hydrologic Analysis, South Fork Drainage Basin. Prepared for USACE, San Francisco District.

Prunuske Chatham, Inc. (2010). Draft Report, Gallinas Creek Existing Conditions. Prepared for the Marin County Flood Control and Water Conservation District. Prepared in February 2010.

USACE, San Francisco District (USACE-SPN), 2011. Las Gallinas Creek Hydrologic Analysis. Prepared in August 2011.

USACE, San Francisco District (USACE-SPN), 2010. Las Gallinas Levee System Settlement Estimates. Project Memorandum. Prepared on July 16, 2010.

USACE, 2009. EC 1165-2-211, Incorporating Sea-Level Change Considerations in Civil Works Programs, Water Resource Policies and Authorities, July 2009.

USACE, 2008a. HEC-FDA, Flood Damage Reduction Analysis, User's Manual, Version 1.2.4, November 2008.

USACE, 2008b. HEC-RAS River Analysis System, Hydraulic Reference Manual, Version 4.0.

USACE, 2006. ER 1105-2-101, Risk Analysis for flood Damage Reduction Studies, January 2006.

USACE, 1996. EM 1110-2-1619, Risk-based Analysis for Flood Damage Reduction Studies, August 1996.

USACE, 1991. EM 1110-2-1601, Engineering and Design - Hydraulic Design of Flood Control Channels, Original Document - 1 July 1991, Change 1 - 30 June 1994.

USACE, San Francisco District (USACE-SPN), 1984. San Francisco Bay Tidal Stage vs. Frequency Study.

Weggel, J. R. 1976. "Wave Overtopping Equation," Proceedings of the 15th Coastal Engineering Conference, American Society of Civil Engineers, Honolulu, HI, pp. 2737-2755.

Appendix E

Las Gallinas Creek –
Downstream Boundary Condition (DSBC) Analysis
February, 2013



Photo courtesy of ArcGis

EXECUTIVE SUMMARY

Las Gallinas Creek inlet is located on the west side of San Pablo Bay within San Francisco Bay (Figure 1-1). The objective of this report is to establish a downstream boundary condition (DSBC) at the inlet to Las Gallinas Creek for hydraulic modeling. The *Las Gallinas Creek H&H & Coastal Analysis* used the mean higher high water (MHHW) as the DSBC (USACE, 2011). This report updates the downstream boundary condition, or coastal water surface elevation (WSE), to account for the full range of tide, including astronomical and residual tide contributions, and wave setup than can contribute to combined coastal and fluvial flooding at tidally influenced portions of the creek.

Site specific historical data was not available for use in this analysis. Accordingly, engineering judgment was used to identify representative and proximal historical datasets from each controlling parameter. Tide information used in this analysis was obtained from the San Francisco tide station. Wind information used in this analysis was obtained from the Hamilton Army Air Field. Fluvial flow information was obtained from the Corte Madera Creek, Ross Valley Watershed.

Two approaches were used to evaluate the coastal DSBC. The first approach presents a time-series based methodology. The time-series method assumes all of the controlling coastal parameters are statistically independent of fluvial flow. This assumption suggests that the entire time series of each controlling coastal parameter can be used to generate a probability distribution function (PDF). The PDFs were combined using joint probability to establish a combined PDF. The combined PDF was further developed into a combined cumulative distribution function (CDF) curve. The combined CDF is presented as the DSBC for hydraulic modeling in this approach.

The second approach presents event-based methodology. The event-based approach decouples measured tide into two parts: predicted tide and residual tide. Predicted tide is a predictable WSE based on lunar and solar constituents and residual tide includes weather effects that may cause an elevated WSE, such as storm surge, sea level rise and El Niño contributions. Measured tide was decoupled to investigate the statistical relationship of fluvial flow at the inlet and residual tide, i.e. coastal surge, using a linear relationship. The computed correlation coefficient, R , is very small. The small correlation coefficient indicates that this linear relationship is not valid. However, a qualitative relationship between residual tide, coastal surge, and fluvial flow was observed. Based on this observation, a database of coincident residual tide, or the residual tide at the time of the fluvial peak, was developed. A second database was developed to estimate the full range of predicted tide at the time of each fluvial peak event. The third database of the wave setup contribution was included as described in the first approach. Similar to the first approach, PDFs of the event-based datasets of predicted tide, residual tide, wave setup were developed, combined using joint probability, and presented as a CDF as the DSBC for hydraulic modeling.

Future sea level rise scenarios including, eustatic historical, Curve I and Curve III, were also considered in both DSBC approaches. The sea level rise contribution was included in the astronomical tide contribution of the DSBC analysis for both approaches.

The second approach estimates a slightly higher DSBC, on the order of 0.1-0.6 feet. Both coastal DSBC approaches can be used to evaluate combined WSE of coastal and fluvial WSE in tidally influenced reaches of Las Gallinas Creek. Using the event based approach provides a slightly more conservative estimate of the coastal DSBC.

TABLE OF CONTENTS

1.0 Study Purpose	1
2.0 Coastal Flooding Potential of Las Gallinas Creek.....	2
3.0 <i>Approach 1: Time Series Based Analysis for the Establishment of Downstream Boundary Condition (DSBC) at Las Gallinas Creek Inlet</i>	4
3.1 Tidal WSE – Data Analysis and PDF Development.....	4
3.2 Offshore Wave Parameters – Data Analysis and PDF Development	7
3.3 Combined Measured WSE and Wave Setup PDF – Year 0 (2011).....	11
3.4 Combined Measured WSE and Wave Setup PDF – Year 50 (2061).....	14
4.0 <i>Approach 2: Event Based Analysis for Establishment of Down Stream Boundary Conditions</i>	18
4.1 Significant Fluvial Flow Events and Correlation with Residual Tide	18
4.2 Event Based, Coincident, Residual Tide Database and Development of PDF	21
4.3 Event Based Predicted Tide Database and Development of PDF.....	22
4.4 Combined Predicted Tide, Residual Tide and Wave Setup PDF – Year 0 (2011)	23
4.5 Combined Predicted Tide, Residual Tide and Wave Setup PDF – Year 50 (2061)	26
5.0 Summary and Conclusions	30
6.0 References.....	31
Appendix A- Tidal Amplification between the San Francisco Tide Station and Las Gallinas Creek Inlet.....	33
Appendix B – San Francisco Tide Station – Tidal Datums	36
Appendix C – Descritized PDF of Measured Tide	37
Appendix D – Computed Wave Height Comparision	39
Appendix E – Wave Set-Up Equations.....	41
Appendix F – Time Series Plots of Residual Tide and Fluvial Flow	43
Appendix G – Descritized PDF of Event Based Residual Tide.....	52
Appendix H – Descritized PDF of Event Based Predicted Tide	54

1.0 STUDY PURPOSE

Previous hydraulic modeling efforts described in the *Las Gallinas Creek H&H & Coastal Analysis* used the mean higher high water (MHHW) as the downstream boundary condition (DSBC) at Las Gallinas Creek (USACE, 2011). The objective of this report is to establish a DSBC at the inlet to Las Gallinas Creek for hydraulic modeling (Figure 1-1) that considers the full range of coastal water surface elevations (WSEs) and their statistical probabilities. This study was conducted as part of the Las Gallinas Creek Marin County, California Section 205 Study.

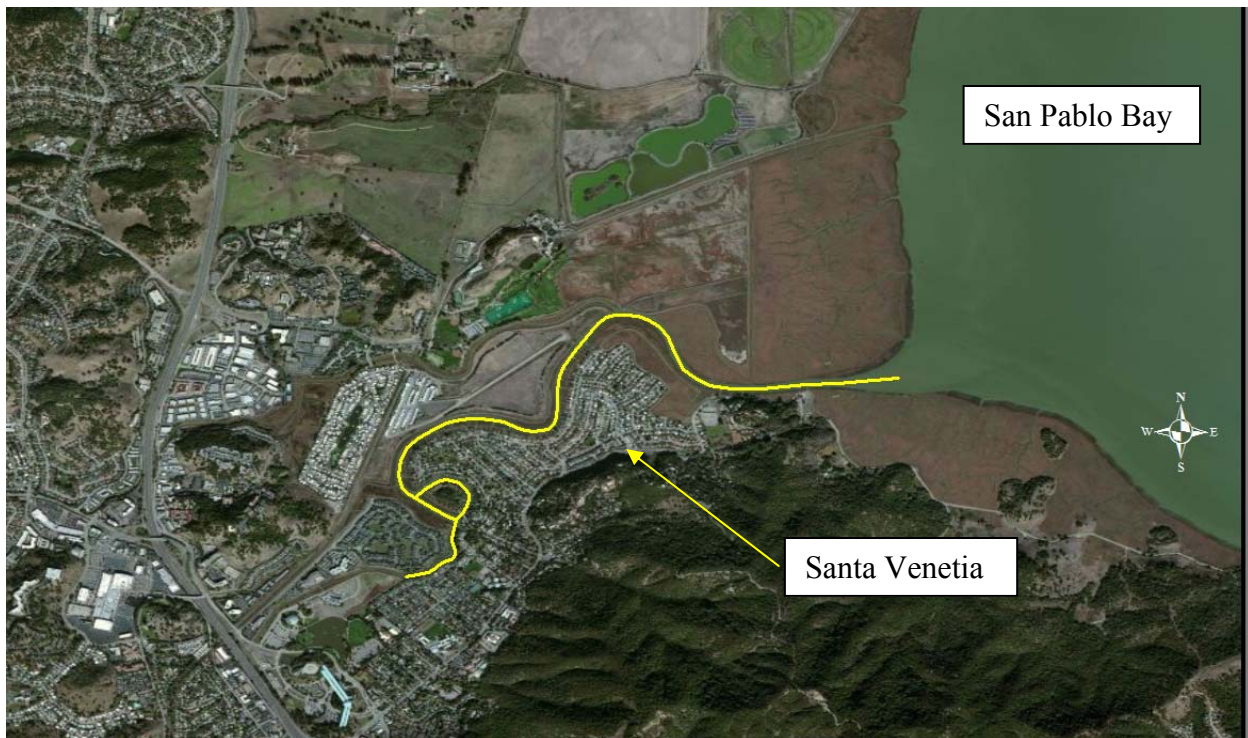


Figure 1-1. Las Gallinas Creek modeled reach (yellow line)

In tidally influenced river reaches, such as the downstream portion of the Las Gallinas Creek, flood stage may be affected by coastal WSE. Therefore, it is necessary to incorporate both fluvial and coastal effects into a combined fluvial and coastal flood stage frequency analysis. Limited data is available at the Las Gallinas Creek inlet to establish a database of peak fluvial flow events to be used to evaluate the interaction of fluvial and coastal processes that could contribute to a combined coastal and fluvial flood event. Accordingly, available and proximal fluvial flow data from an adjacent watershed was used to estimate the statistical relationship between fluvial flow and the coastal parameters that contribute to the DSBC at the Las Gallinas Creek inlet. Fluvial flow information, which had an 8 year record, from Corte Madera Creek,

located in the Ross Valley Watershed was used. This watershed was selected for use in this analysis based on a recommendation by the project sponsor, Marin County.

The controlling parameters of coastal WSE to be used in the DSBC analysis have been identified as measured tide and wave setup. Tide information, for a 112 year record, was obtained from the San Francisco tide station. A 36 years of wind information was used as input to compute wave setup was obtained from the Hamilton Army Airfield wind station.

To establish the DSBC two approaches have been implemented, which are presented in Section 3.0 and Section 4.0. The methodology developed for these approaches is based on a collaborative effort with USACE teams, namely the Hydrologic Engineering Center and the San Francisco District, to develop a risk and uncertainty based analysis to statistically combine both fluvial and coastal contributions to the flood stage frequency curve.

The approaches use a database of measured WSE and wave setup derived from the data sets described above. The developed databases are used to generate a cumulative distribution function (CDF) for use as the DSBC.

2.0 COASTAL FLOODING POTENTIAL OF LAS GALLINAS CREEK

Las Gallinas Creek inlet is located on the west side of San Pablo Bay within San Francisco Bay (Figure 1-1 and Figure 2-1). Three historic flood events, two in 1982 and one in 1983, damaged between 50 and 160 homes per flood event in the Santa Venetia area.

Levee improvements were made, shortly after the December 1983 flood event, to decrease the flooding potential. Coastal levee crest elevations reported in the *Las Gallinas Creek H&H & Coastal Analysis* range from 7.82 and 9.18 feet National Geodetic Vertical Datum of 1929 (NGVD29) or 10.50 and 11.86 feet North American Vertical Datum of 1988 (NAVD88). The levee crest elevations were surveyed in 2006. To convert between NGVD29 and NAVD88 a datum conversion factor of 2.68 feet was used (i.e. NAVD88=NGVD29-2.68) (Restoration, 2008 and Leventhal, 2013).

In 2012, the U.S. Army Corps of Engineers, San Francisco District completed a coastal flood frequency analysis at the San Francisco tide station. From this analysis, the 100 year coastal flood elevation was found to be 9.0 feet above NAVD88 or 6.32 feet above NGVD29. This analysis suggests levee elevations less than 9.0 feet NAVD88 have the potential to be overtopped during a 100 year tidal WSE event. The current survey indicates that all coastal levee crest elevations are above the 100 year coastal flood elevation.

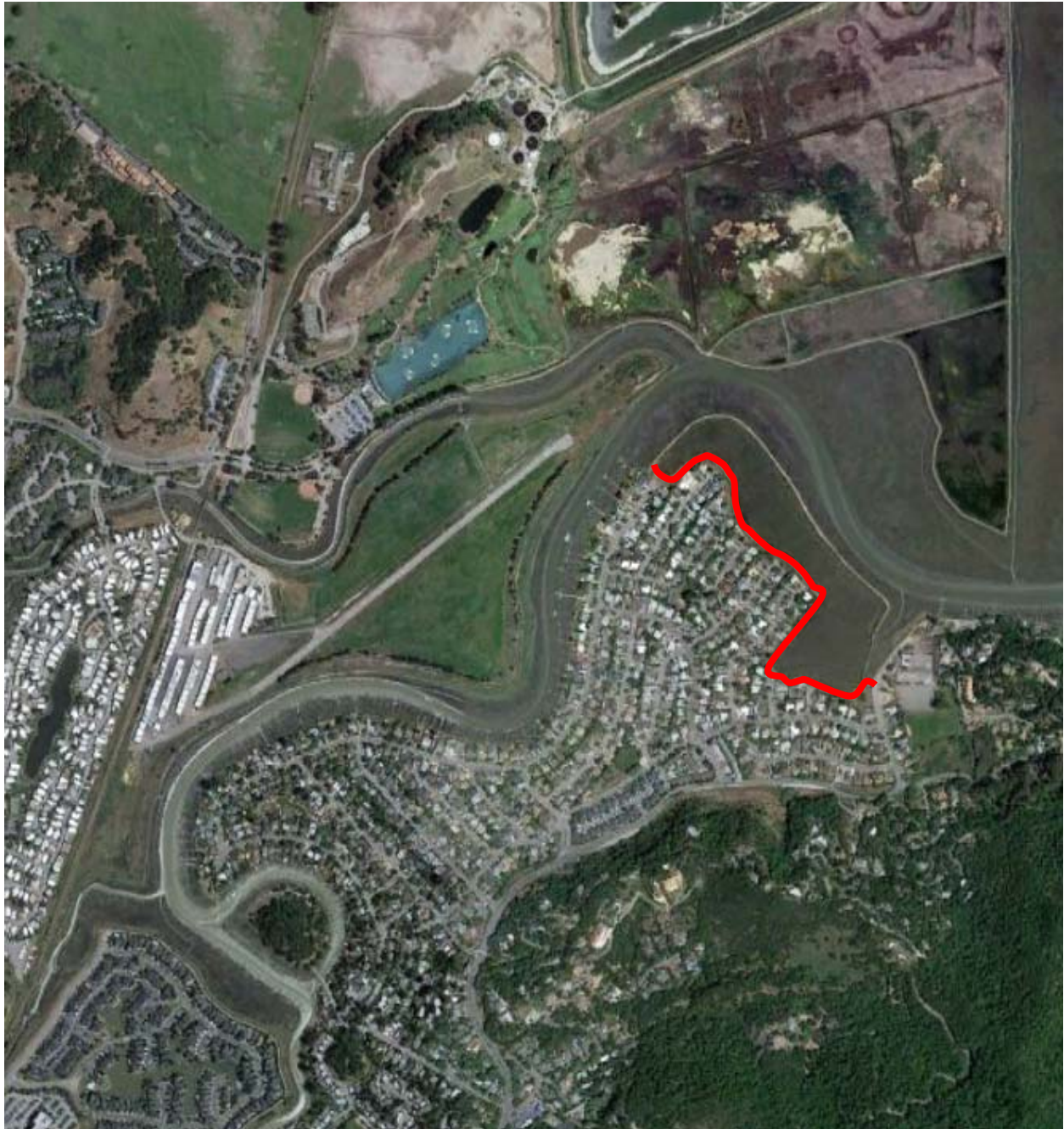


Figure 2-1. Coastal Levee, outlined in red (Google Earth, 2013).

3.0 APPROACH 1: TIME SERIES BASED ANALYSIS FOR THE ESTABLISHMENT OF DOWNSTREAM BOUNDARY CONDITION (DSBC) AT LAS GALLINAS CREEK INLET

The time series approach assumes all of the controlling coastal parameters, i.e. measured tide and wave setup, are statistically independent of fluvial flow. This assumption suggests that the entire time series of each controlling coastal parameter can be used to generate a probability distribution function (PDF). In other words, the entire time series of measured tide was used to generate a measured tide PDF and the entire time series of wave setup was used to generate a wave setup PDF. Measured tide (measured WSE) is the most significant coastal parameter to contribute to the DSBC. Measured tide is the instantaneous, measured WSE at the San Francisco tide station. Measured WSE includes both astronomical (predicted) tide and weather affects. Wave set-up effects are not included in the measured tide record because the gage is located outside of the breaker zone. The wave induced set-up will be included in the combined distribution curve.

The PDFs can be combined using joint probability to establish a combined PDF. The combined PDF is further developed to establish a combined cumulative distribution function (CDF) curve. The combined CDF is used as the DSBC in hydraulic modeling for the baseline, Year 0, condition. The baseline condition is set as 2011. Future sea level rise (SLR) added to the DSBC to consider project Year 50 or Year 2061.

3.1 Tidal WSE – Data Analysis and PDF Development

Measured WSE data was not available at the project site for use in this analysis. Tidal WSE data from the San Francisco tide station was selected for use in this analysis. The San Francisco tide station is a National Oceanic and Atmospheric Administration (NOAA) tide station 9414290 located in San Francisco, CA. The San Francisco tide station is located near the southern end of the Golden Gate Bridge, approximately 9 miles and 14 miles south of the inlets of Corte Madera and Las Gallinas Creeks (Figure 3-1).

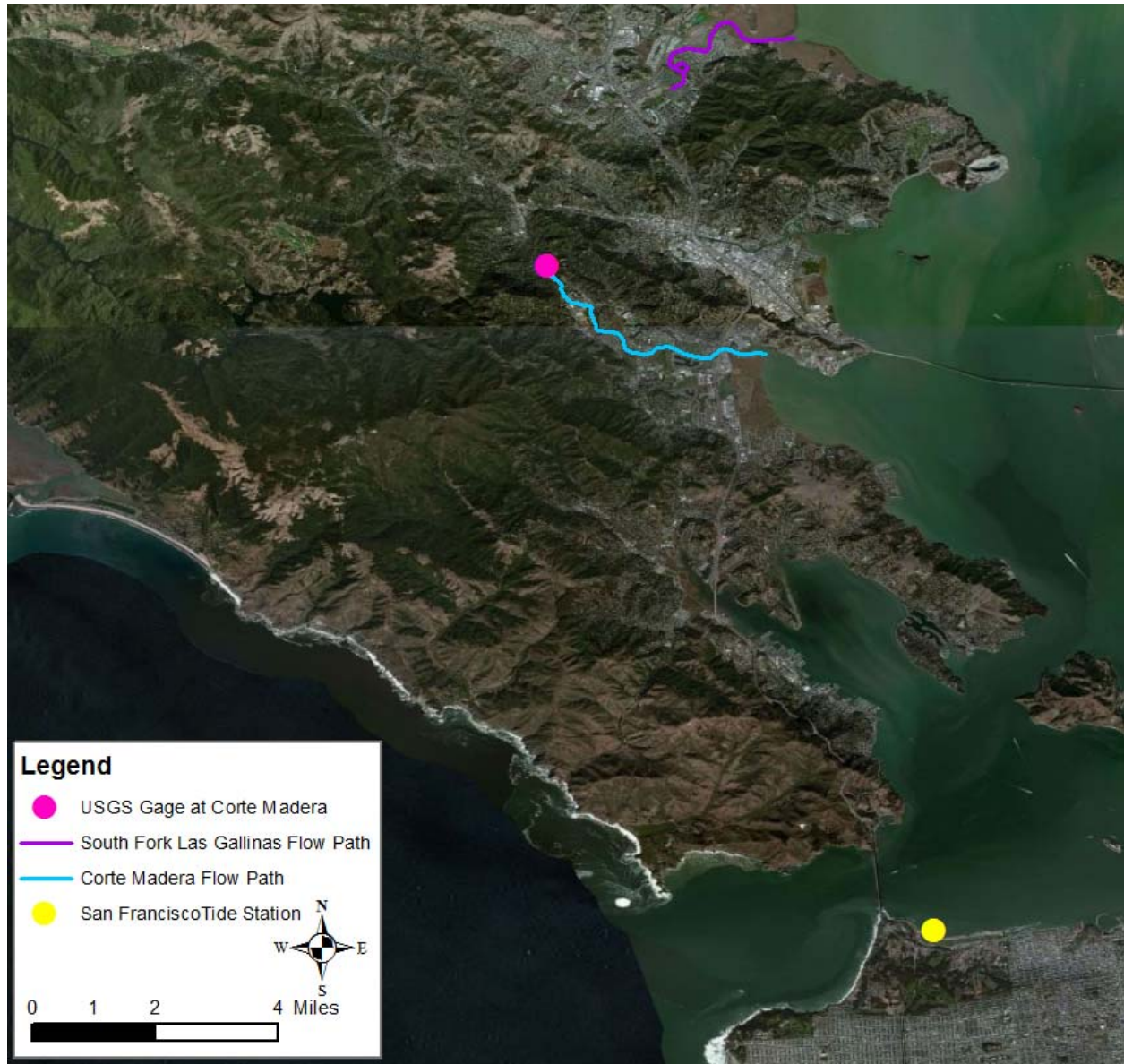


Figure 3-1. Las Gallinas (South Fork) and Corte Madera Creek locations

NOAA tide tables indicate tidal amplitude between San Francisco tide station and the Las Gallinas Creek inlet are approximately one percent. This small change in tidal amplitude is assumed to be minor and not included in this analysis (USACE, 2010). Appendix A discusses the tidal amplification in more detail. Tidal datum information from the San Francisco tide station is presented in Appendix B.

Hourly water level data was downloaded between 1901 and 2005 for a duration of 105 years. Figure 3-2 presents a representative tidal data set of predicted, measured and residual WSE from December 1 to 31, 2002. Based on the 105 year record, a PDF of measured WSE was developed. The measured WSE PDF is presented in Figure 3-3. Tabulated PDF information can be found in Appendix C.

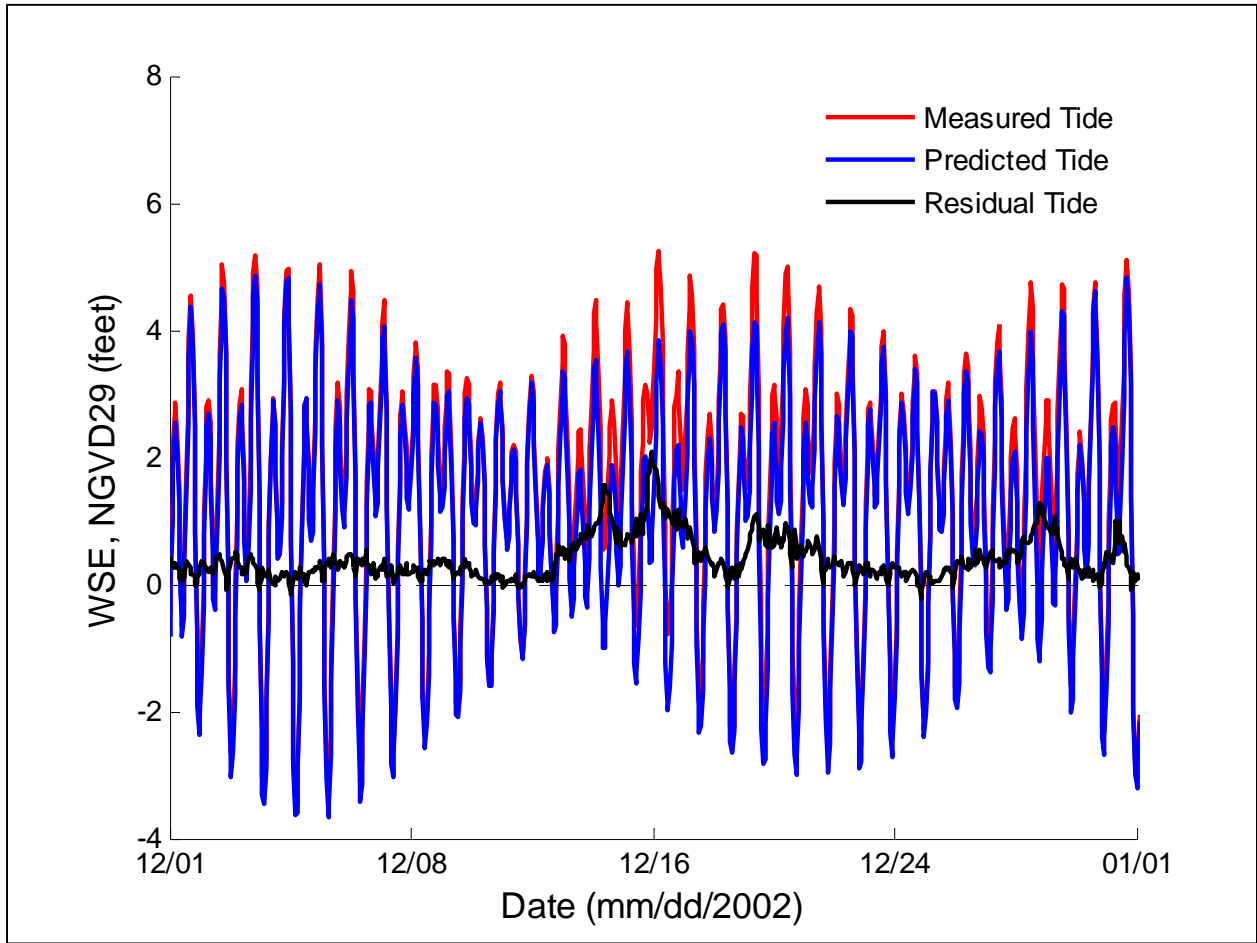


Figure 3-2. Time series of San Francisco tide station (9414290) data from 12/2002

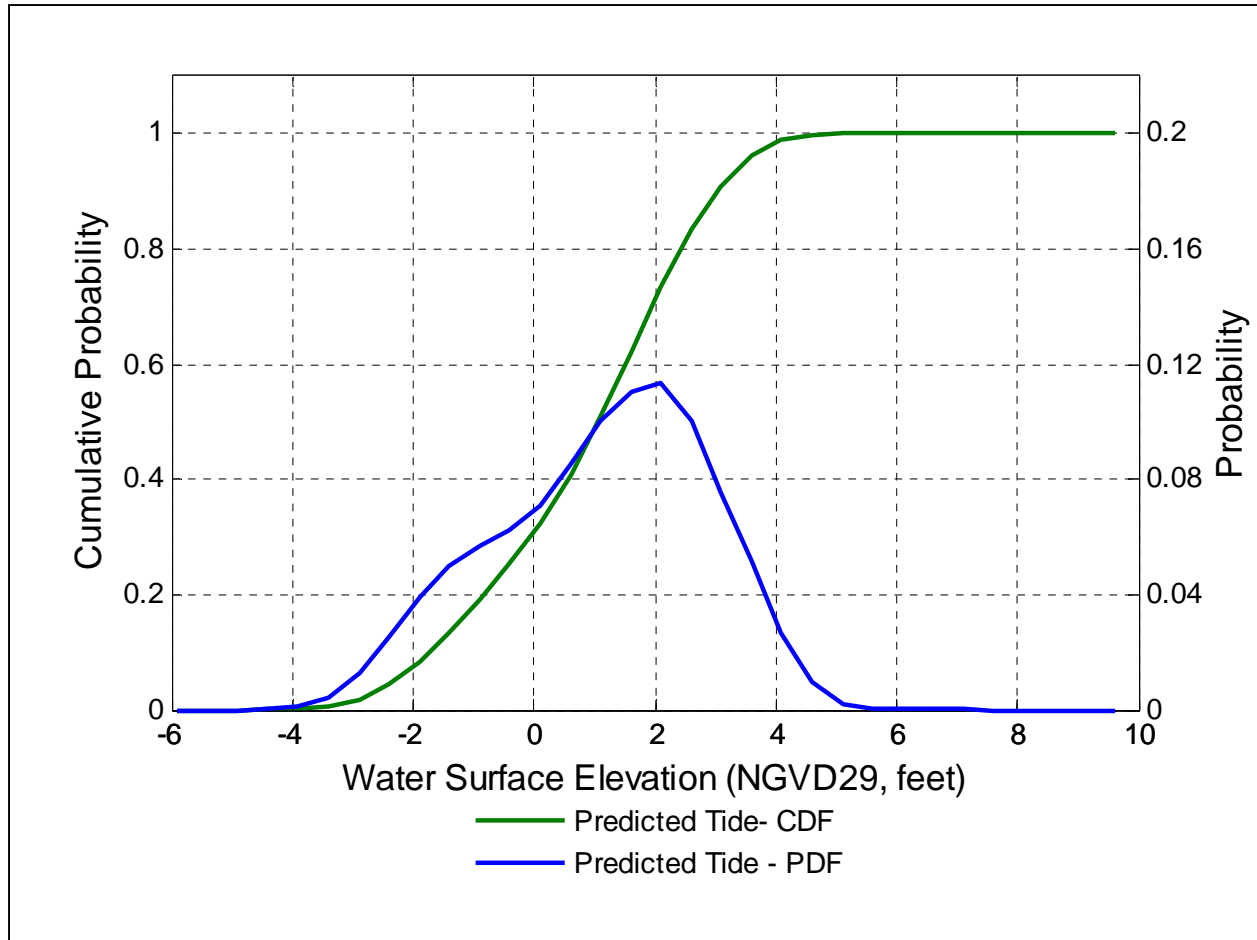


Figure 3-3. Year 0 probability distributions

3.2 Offshore Wave Parameters – Data Analysis and PDF Development

Wind data at the project site was not available for use in this analysis. However, over 34 years of historical wind data, speed and direction, was available for use at the Hamilton Army Airfield (HAAF). The HAAF is located approximately 3 miles north of the inlet to Las Gallinas Creek (Figure 3-4). Wind information was obtained from the Climate Services 14th Weather Squadron (CSWS) station 23211. This is one of the most proximal wind stations to the creek inlet and assumed as representative of wind conditions at the project site.

Hourly wind data, speed and direction, was recorded for 36 years (1939 and 1975). After 1975, wind data was not recorded. Although no wind data has been collected at this site since 1975, this data set is widely used for engineering analysis in this region. Figure 3-5 presents the wind rose of the 36 year data set. Wind approach to the project site is predominately from the northwest and southeast directions; however, there are recorded wind approaches from nearly all directions.

The wind data was used to compute wind wave height and subsequent wave setup based on equations in the USACE Coastal Engineering Manual (EM 1110-2-1100). Methodology for this calculation is presented in Appendix D. Based on the 36 year record a PDF of wave setup (η_{setup}) was developed for use in the computation of DSBC (Figure 3-6). Tabulated PDF information is presented in Appendix E, Table E-1.

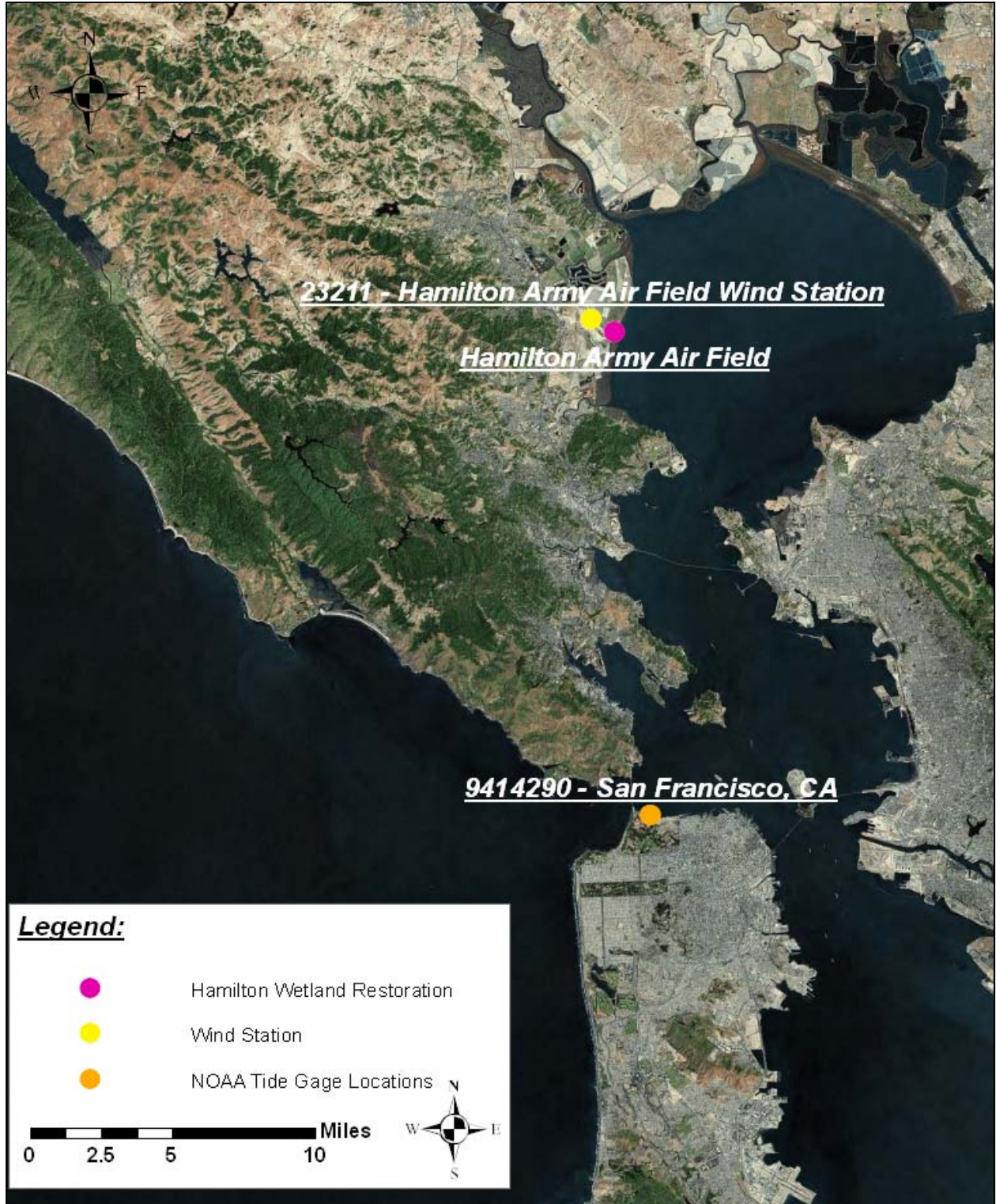


Figure 3-4. Location of NOAA tide station 9414290 in San Francisco, CA and the CSWS wind station located in HAAF.

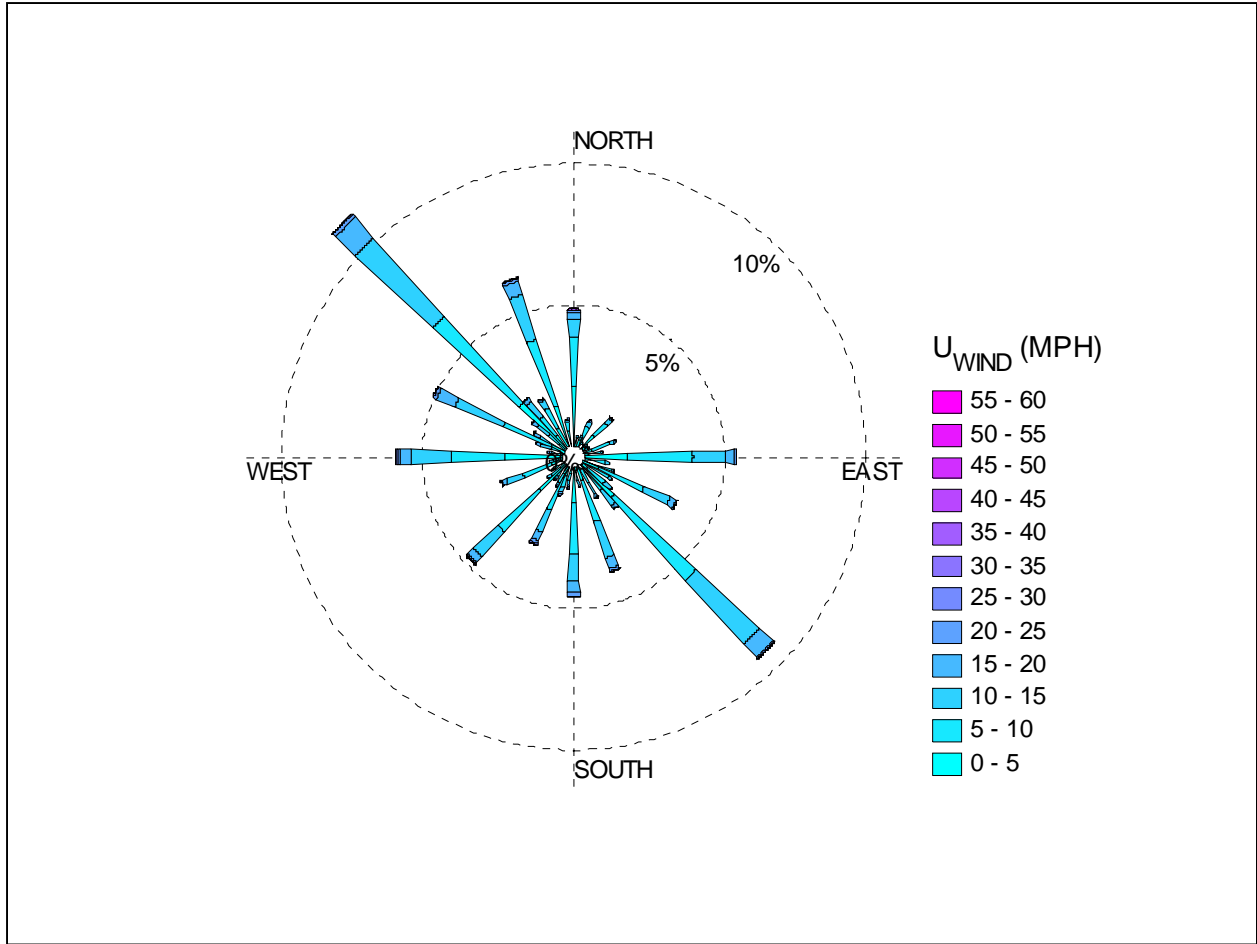


Figure 3-5. Wind rose of HAAF wind station (23211) data from 1939 to 1975

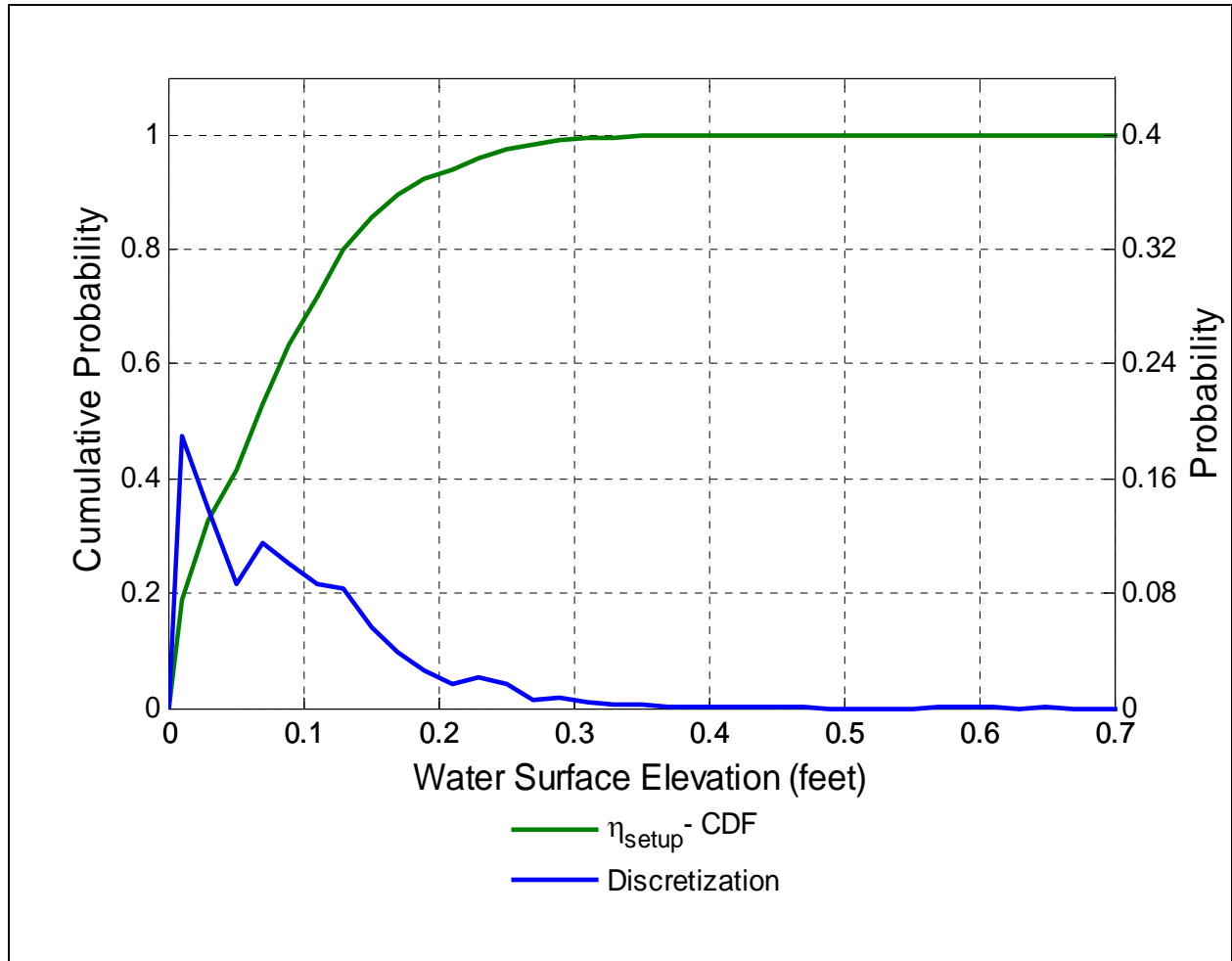


Figure 3-6. Probability distribution of wave setup

3.3 Combined Measured WSE and Wave Setup PDF – Year 0 (2011)

The PDFs of measured WSE (Figure 3-3) and wave setup (Figure 3-6) were combined using joint probability to establish a combined PDF. The combined PDF is presented in Figure 3-7.

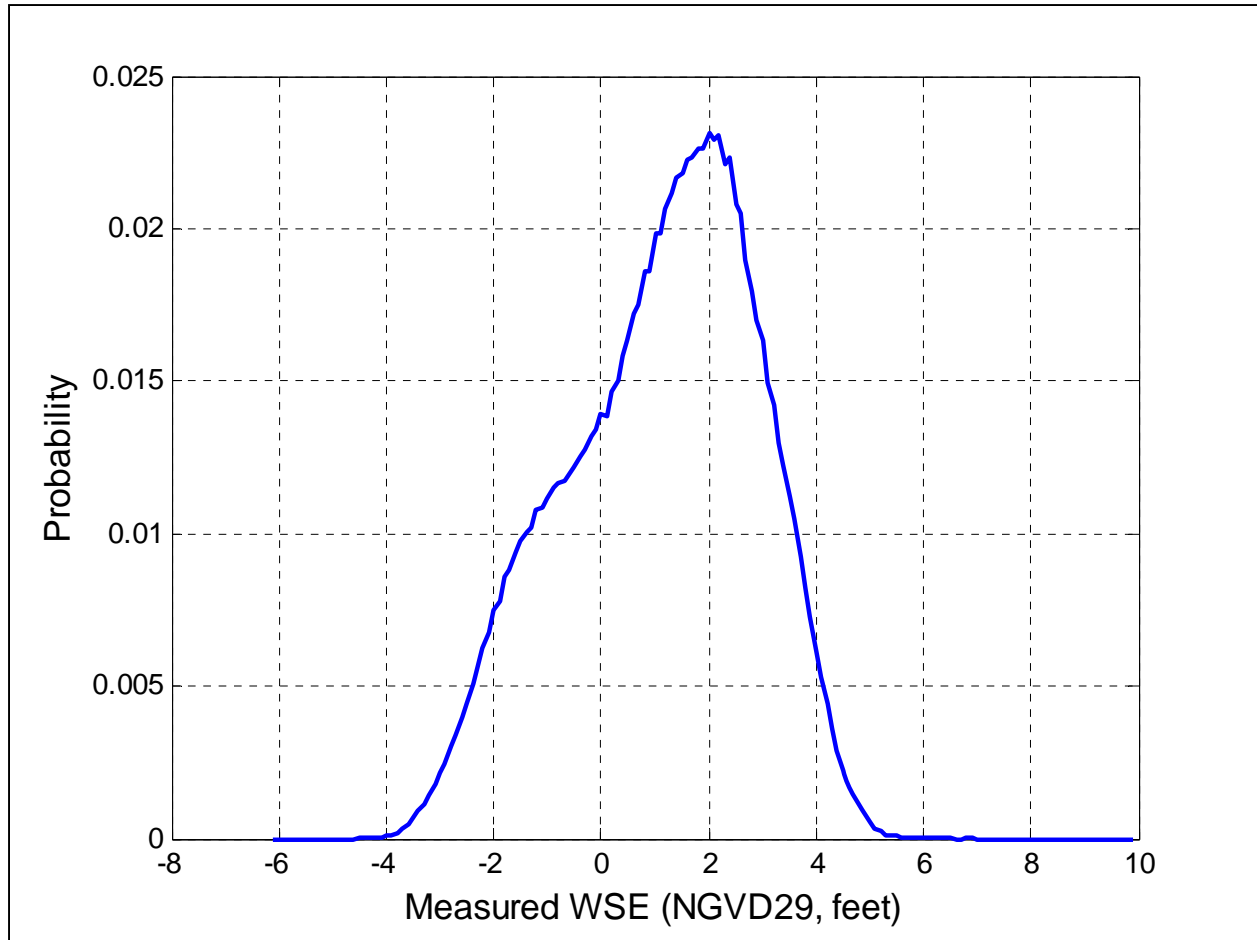


Figure 3-7. Probability distribution of combined WSE

The combined PDF is further analyzed to create a combined CDF curve presented in Figure 3-8 and Table 3-1. The combined CDF curve was discretized into probability bins. The discretized, divided, WSEs provided to be used as input as the DSBC in the hydraulic model simulations. The CDF was divided into 0.20 probability bins, i.e. WSE corresponding to the median probability value of the distribution curve was recorded between 0.20 and 0.40, 0.40 and 0.60, and etc. Additional binning was completed to provide finer resolution of the distribution curve for large WSEs occurring between 0.95 and 1.00. The median value in each probability bin of the distribution curve was selected as a representative WSE. The magenta boxes in presented in Figure 3-8 represent the median value of each probability bin.

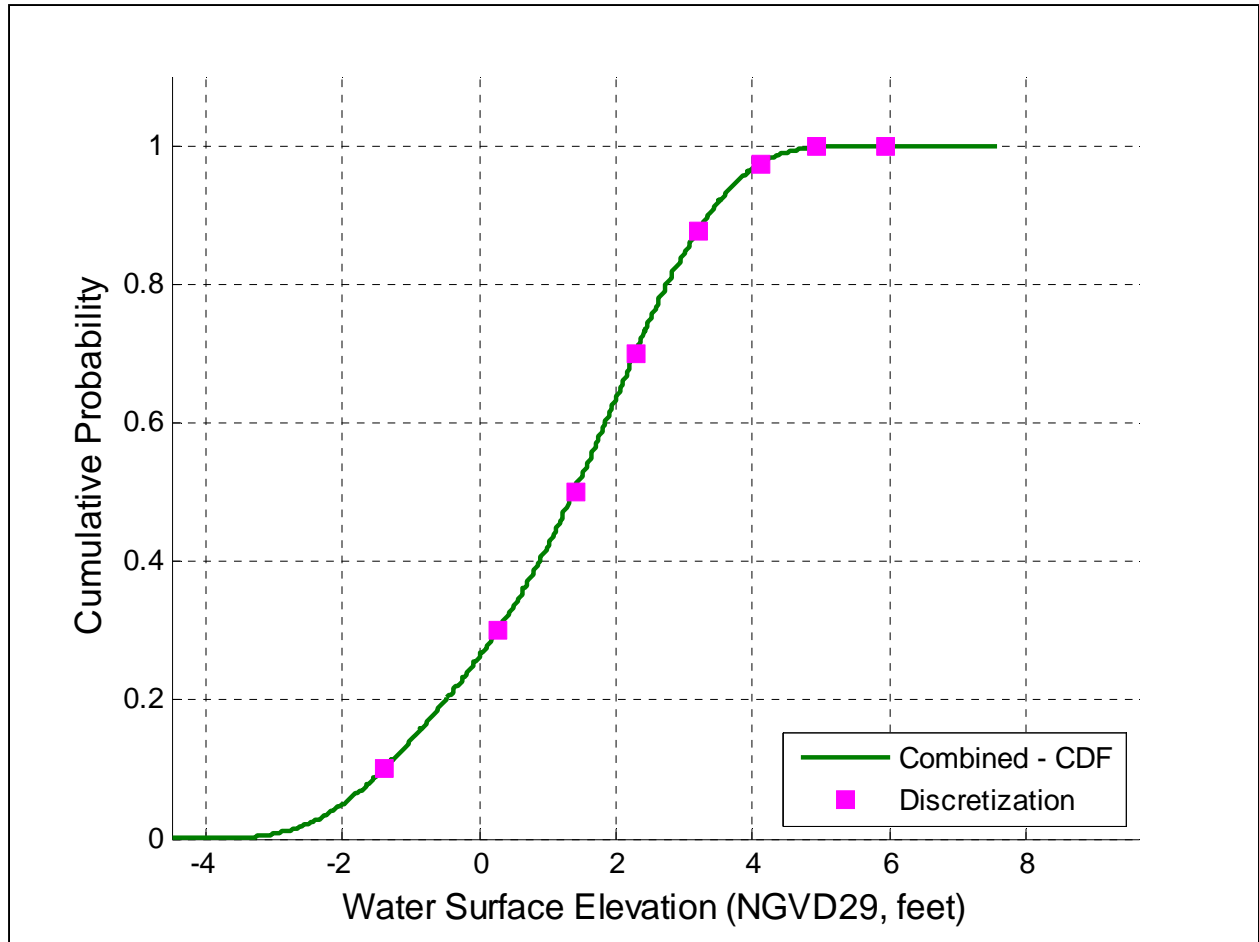


Figure 3-8. Combined cumulative probability distribution of Combined WSE

Table 3-1. Discretized water surface elevation for the combined Year 0 Conditions

Index	Cumulative Probability	Probability of Occurrence	Combined WSE (feet)
1	0.00 - 0.20	0.20	-1.39
2	0.20 - 0.40	0.20	0.27
3	0.40 - 0.60	0.20	1.41
4	0.60 - 0.80	0.20	2.29
5	0.80 - 0.95	0.15	3.19
6	0.95 - 0.995	0.045	4.11
7	0.995 - 0.9999	0.0049	4.93
8	0.9999 - 1.00	0.0001	5.93

3.4 Combined Measured WSE and Wave Setup PDF – Year 50 (2061)

To consider a DSBC for 50 years beyond the baseline conditions (future Yr 50 or 2061). SLR projections were computed based on National Research Council's (NRC) three different accelerating eustatic SLR scenarios (EC1165-2-212) and local land settlement. The *Las Gallinas Creek H&H & Coastal Analysis* reported local land settlement between 2011 and 2061 to be 0.17 feet (USACE, 2011). This value was used in the analysis. The U.S. Army Corps guidance suggests eustatic historical (0.45 feet), NRC Curve I (0.84 feet), and NRC Curve III (2.08 feet) rates are appropriate minimum, intermediate, and maximum SLR projections to consider eustatic SLR plus local land subsidence. Sea level rise elevations were computed with equations provided in EC 1165-2-212, local land subsidence was added separately.

Figure 3-9 through Figure 3-11 and Table 3-2 through Table 3-4 present the discretized combined DSBC distribution curves for Year 50 conditions under Historical, Curve I and Curve III SLR scenarios, respectively. These reported values are provided to be used as downstream tidal boundary conditions.

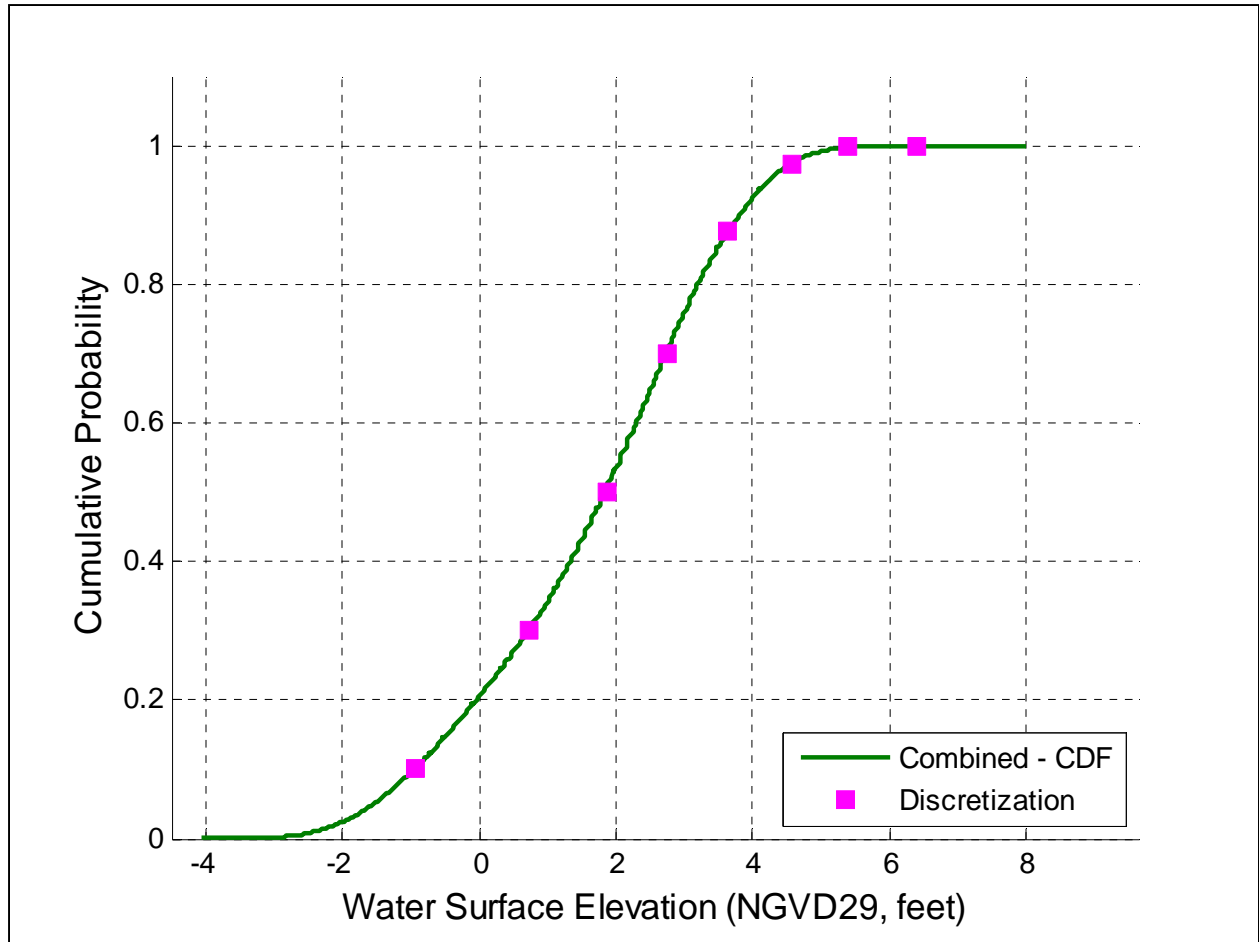


Figure 3-9. Combined Year 50 Historical cumulative probability distributions

Table 3-2. Discretized water surface elevation for the combined Year 50 Historical SLR

Index	Cumulative Probability	Probability of Occurrence	Combined WSE (feet)
1	0.00 - 0.20	0.20	-0.94
2	0.20 - 0.40	0.20	0.72
3	0.40 - 0.60	0.20	1.86
4	0.60 - 0.80	0.20	2.74
5	0.80 - 0.95	0.15	3.64
6	0.95 - 0.995	0.045	4.56
7	0.995 - 0.9999	0.0049	5.38
8	0.9999 - 1.00	0.0001	6.38

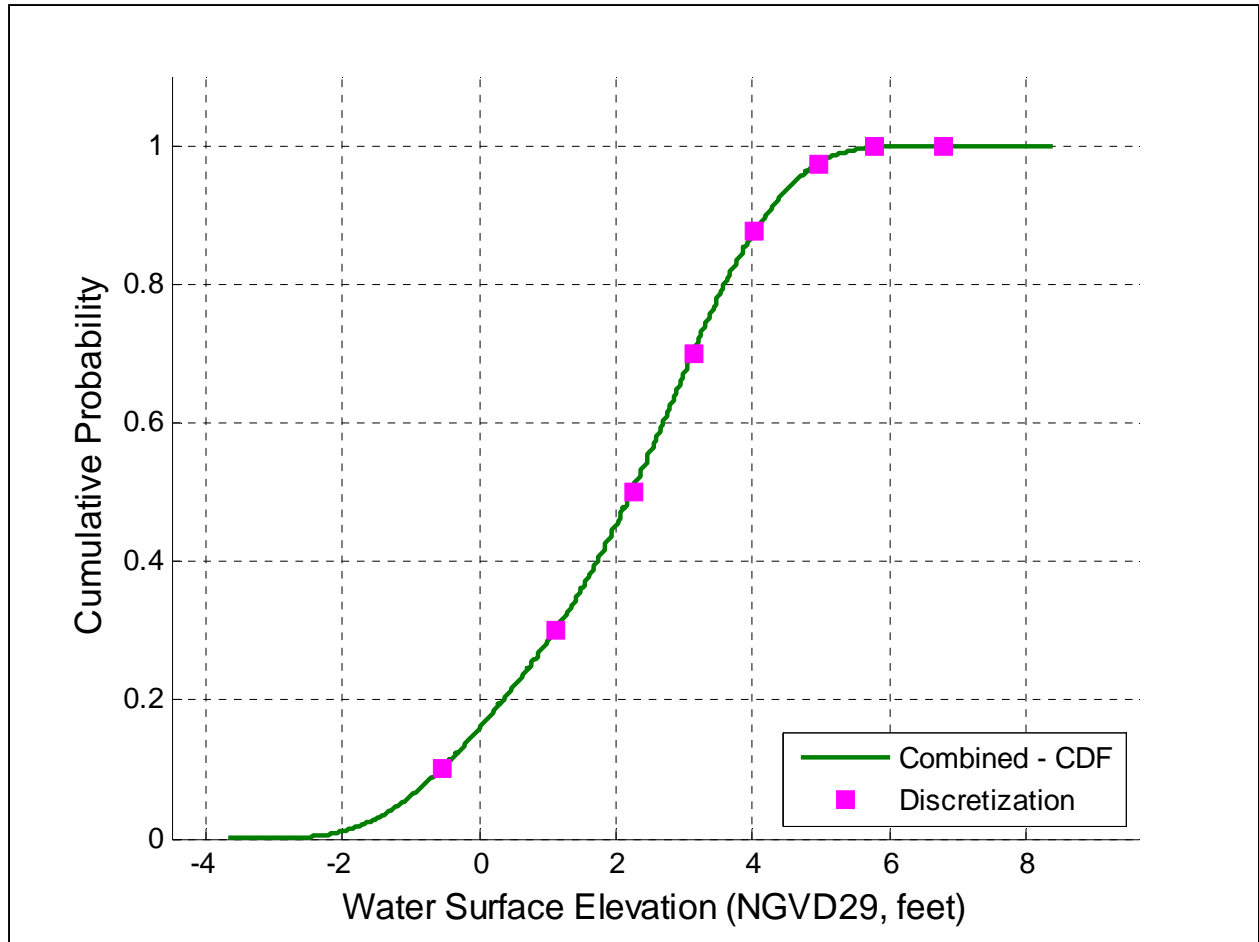


Figure 3-10. Combined Year 50 Curve I cumulative probability distributions

Table 3-3. Discretized water surface elevation for the combined Year 50 Curve I SLR

Index	Cumulative Probability	Probability of Occurrence	Combined WSE (feet)
1	0.00 - 0.20	0.20	-0.55
2	0.20 - 0.40	0.20	1.11
3	0.40 - 0.60	0.20	2.25
4	0.60 - 0.80	0.20	3.13
5	0.80 - 0.95	0.15	4.03
6	0.95 - 0.995	0.045	4.95
7	0.995 - 0.9999	0.0049	5.77
8	0.9999 - 1.00	0.0001	6.77

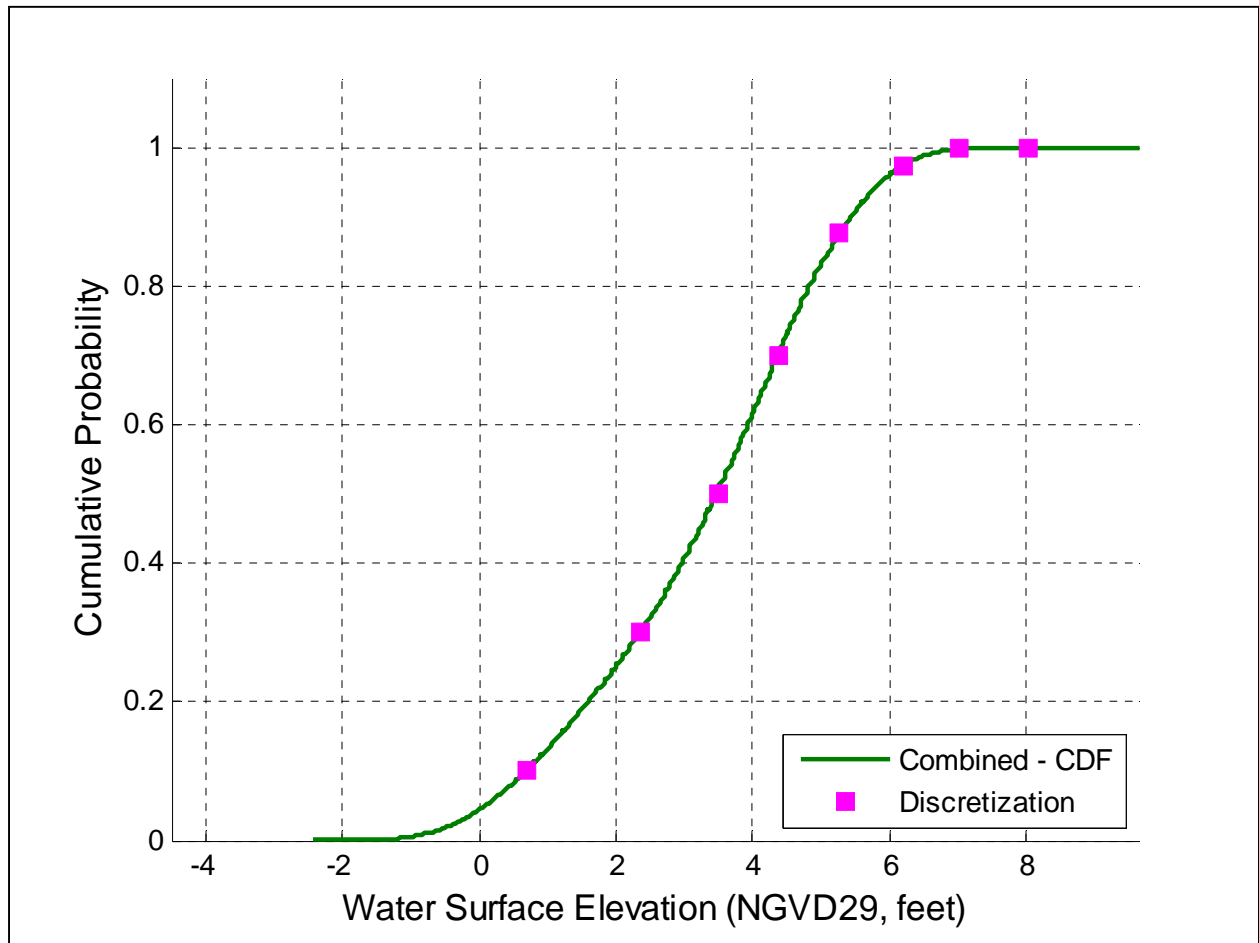


Figure 3-11. Combined Year 50 Curve III cumulative probability distributions

Table 3-4. Discretized water surface elevation for the combined Year 50 Curve III SLR

Index	Cumulative Probability	Probability of Occurrence	Combined WSE (feet)
1	0.00 - 0.20	0.20	0.69
2	0.20 - 0.40	0.20	2.35
3	0.40 - 0.60	0.20	3.49
4	0.60 - 0.80	0.20	4.37
5	0.80 - 0.95	0.15	5.27
6	0.95 - 0.995	0.045	6.19
7	0.995 - 0.9999	0.0049	7.01
8	0.9999 - 1.00	0.0001	8.01

4.0 APPROACH 2: EVENT BASED ANALYSIS FOR ESTABLISHMENT OF DOWN STREAM BOUNDARY CONDITIONS

The event based approach decouples measured tide into two parts: predicted tide and residual tide. Predicted tide is a predictable WSE based on tidal constituents, the most common being lunar and solar. Residual tide includes weather effects, such as storm surge, sea level rise and El Niño contributions that can contribute to elevated WSE at the creek inlet. Measured tide was decoupled to investigate the statistical relationship of fluvial flow at the inlet and residual tide, i.e. coastal surge, using a linear correlation.

To develop this relationship peak fluvial flow events greater than 1,500 cfs were used as a basis for comparison. Fluvial flow events greater than 1,500 cfs were selected because it seemed to be a reasonable threshold, based on evaluation of peak fluvial storm flows ranging between 1,000 cfs and 1,700 cfs. Coincident residual tide was compared to the peak flow in each identified storm event. The computed correlation coefficient, R , is very small suggesting both physical processes are statistically independent. However, a qualitative relationship between residual tide, coastal surge, and fluvial flow was observed (Appendix F). Based on the qualitative observation of a relationship between residual tide and fluvial flow, event based databases were developed of residual tide and predicted tide.

The residual tide database was formed by using the coincident, the residual tide WSE that occurred simultaneously with fluvial flow. A second database was developed to estimate the full range of predicted tide at the time of each fluvial peak event. The wave setup contribution to the DSBC was included as described in Section 3.2. The event based data sets of predicted tide, residual tide and wave setup were combined using joint probability.

These databases were combined using joint probability to develop a combined DSBC for hydraulic modeling of the baseline, Year 0, condition. The combined DSBC was also updated to consider future SLR to project Year 50 or Year 2061.

4.1 Significant Fluvial Flow Events and Correlation with Residual Tide

The Las Gallinas Watershed has very limited stream gage information available for use to determine the statistical relationship between residual tide and peak fluvial flow events. Marin County, the project sponsor, recommended use of stream gage data from the Ross Valley Watershed (Figure 4-1), bordering the eastern edge of the Las Gallinas Watershed for use in this analysis. Therefore, fluvial flow from U.S. Geological Survey (USGS) stream gage 11460000, located along Corte Madera Creek, was assumed to be representative of the fluvial flow at the Las Gallinas Creek inlet (Figure 3-1). Because of the close proximity of these watersheds it is likely that the same storm systems might impact both watersheds simultaneously.

According to the Marin County Watershed Program (2012), the Ross Valley Watershed is 28 square miles. The Corte Madera stream gage has a drainage area of 18.1 square miles and

captures 65% of the runoff from the watershed. This gage has been in operation since 1951, and implemented an electronic data logger in 1987. Prior to 1987, mean daily flows were recorded. The data analyzed for the study was from October 1987 to December 2011. The gage was not in operation between 1993 and 2009 resulting in no data available for use during this period. The historical record used in this analysis is 8 years (Figure 4-2). Data was also reviewed from the Corte Madera stream gage maintained by Marin County from 1995 through 2012. This additional data set was not used in the analysis; however, further confirmed the statistical relationship between peak fluvial flow and residual tide.



Figure 4-1. Marin County watershed map with Ross Valley/Corte Madera Watershed (pink) and Las Gallinas Watershed (brown) (Marin County Watershed Program, 2012)

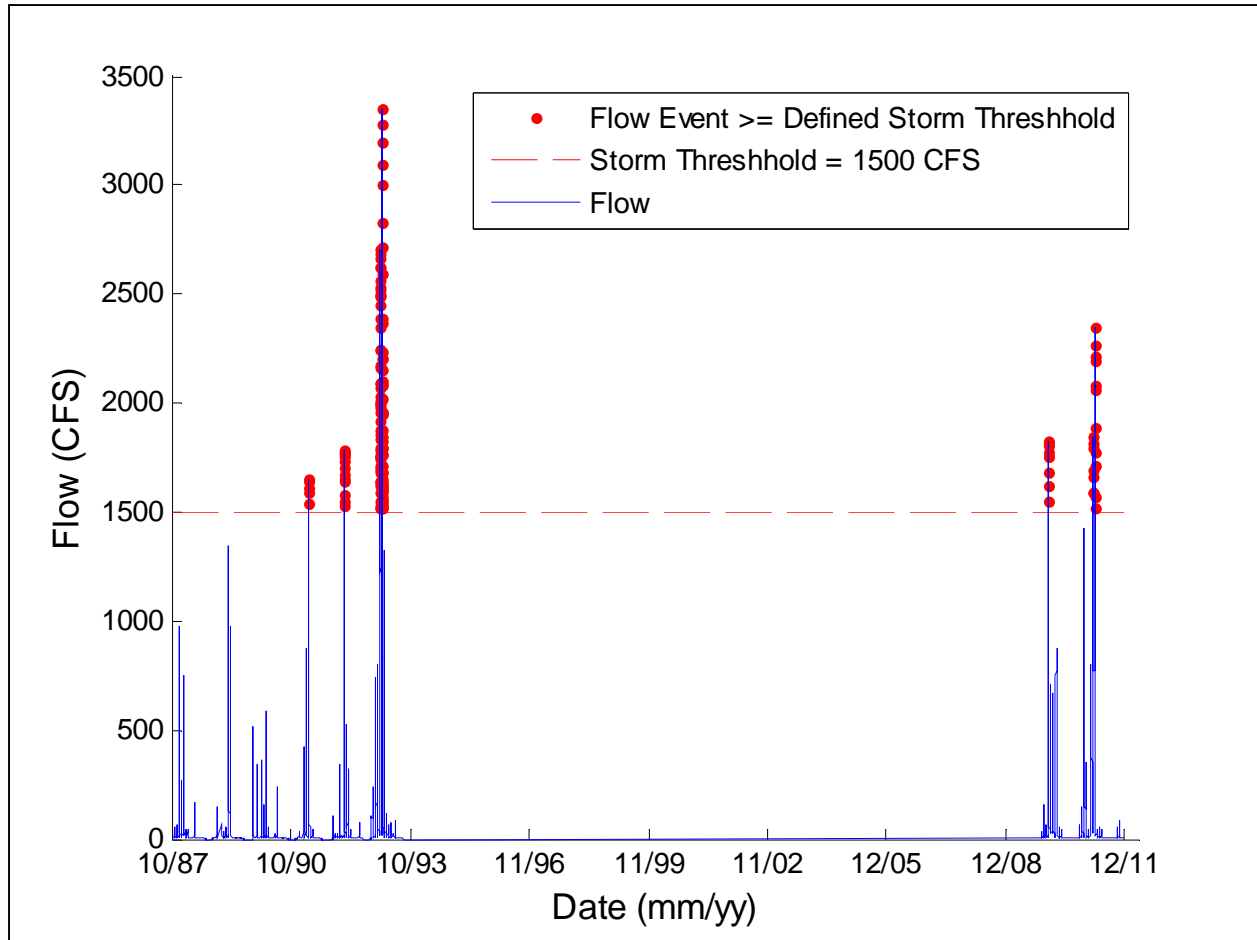


Figure 4-2. Flow record from the USGS Station 11460000

Prior to the correlation analysis, fluvial flow and tidal residual WSE were plotted together to qualitatively review the coincidence, namely timing and magnitude, of both fluvial and residual tide peak events (Appendix F). The timing of both peaks, fluvial and tidal, appeared to qualitatively coincide or at least partially overlap.

To determine the statistical dependence of fluvial flow from the Corte Madera Creek stream gage and residual tide WSE, a correlation was developed considering large fluvial discharge events. To establish a criterion for large events, or peak fluvial discharges, were evaluated between 1,000 cfs (cubic feet per second) and 1,750 cfs. All peak fluvial discharge thresholds indicated similar results, and a peak fluvial discharge threshold 1,500 cfs was selected as a reasonable engineering limit to justify a storm event. Nine events greater than 1,500 cfs occurred during the 8 year historical record. Peak fluvial flow from each storm event and the corresponding coincident residual tide were selected to develop the databases used to create a linear correlation between both parameters. The analysis yielded a small correlation coefficient, $R=0.01$, and a negative sloping the trend line (Figure 4-3). The low correlation coefficient and negatively sloping trend line suggest that the two physical processes are a statistical independent. However, a qualitative relationship between residual tide, coastal surge, and fluvial flow was observed.

Based on the qualitative observation of a relationship between residual tide and fluvial flow, event based databases were developed of residual tide and predicted tide.

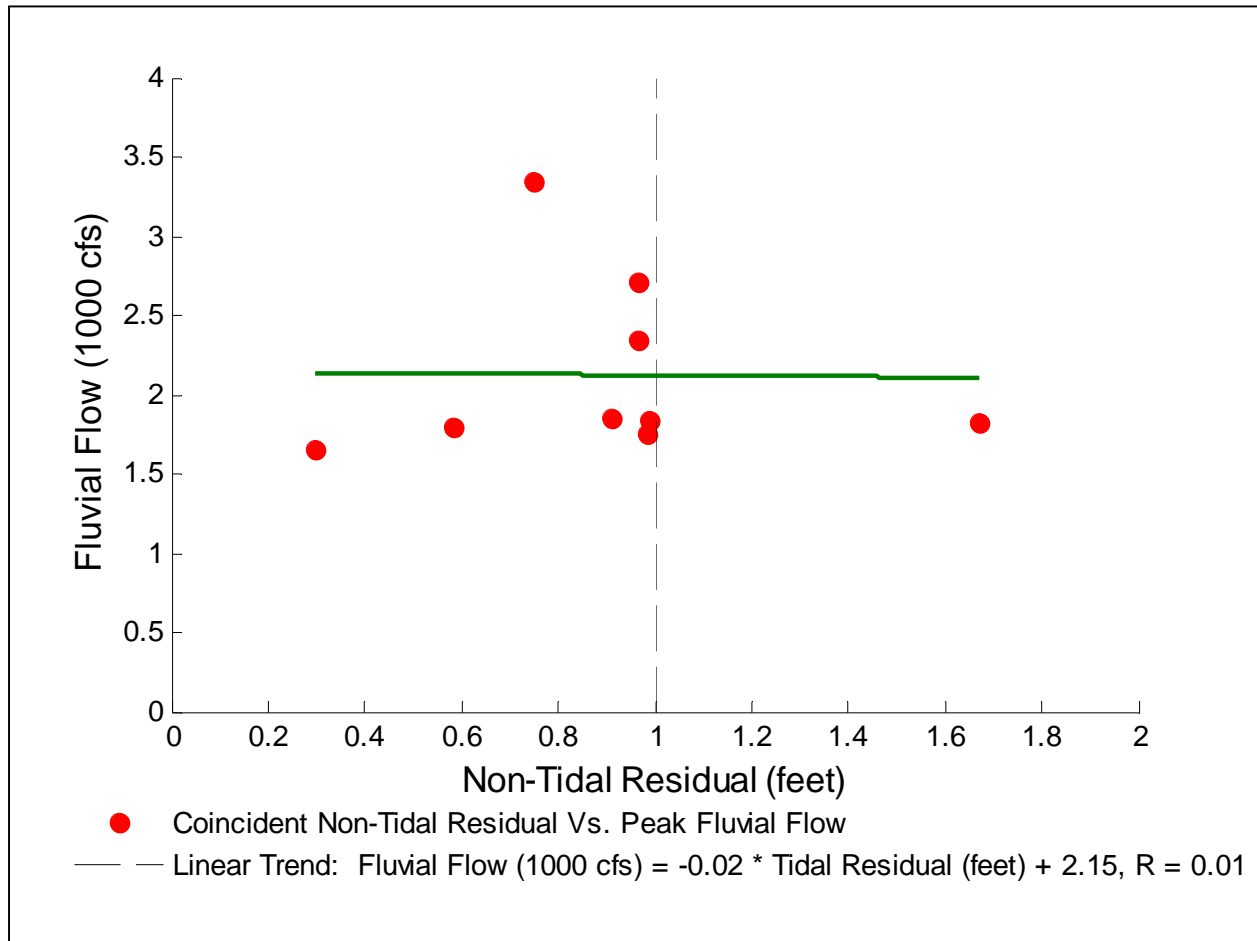


Figure 4-3. Linear Relationship and Correlation Coefficient of Coincident Non-Tidal Residual and Fluvial Flow

4.2 Event Based, Coincident, Residual Tide Database and Development of PDF

The database of residual tide was developed by using the coincident residual tide, i.e. the residual tide that occurred at the time of peak fluvial flow, during the 9 storm events selected for this analysis. The PDF of these values are presented in Figure 4-3 and tabulated in Appendix G. This database was used to develop a PDF of residual tide presented in Figure 4-4.

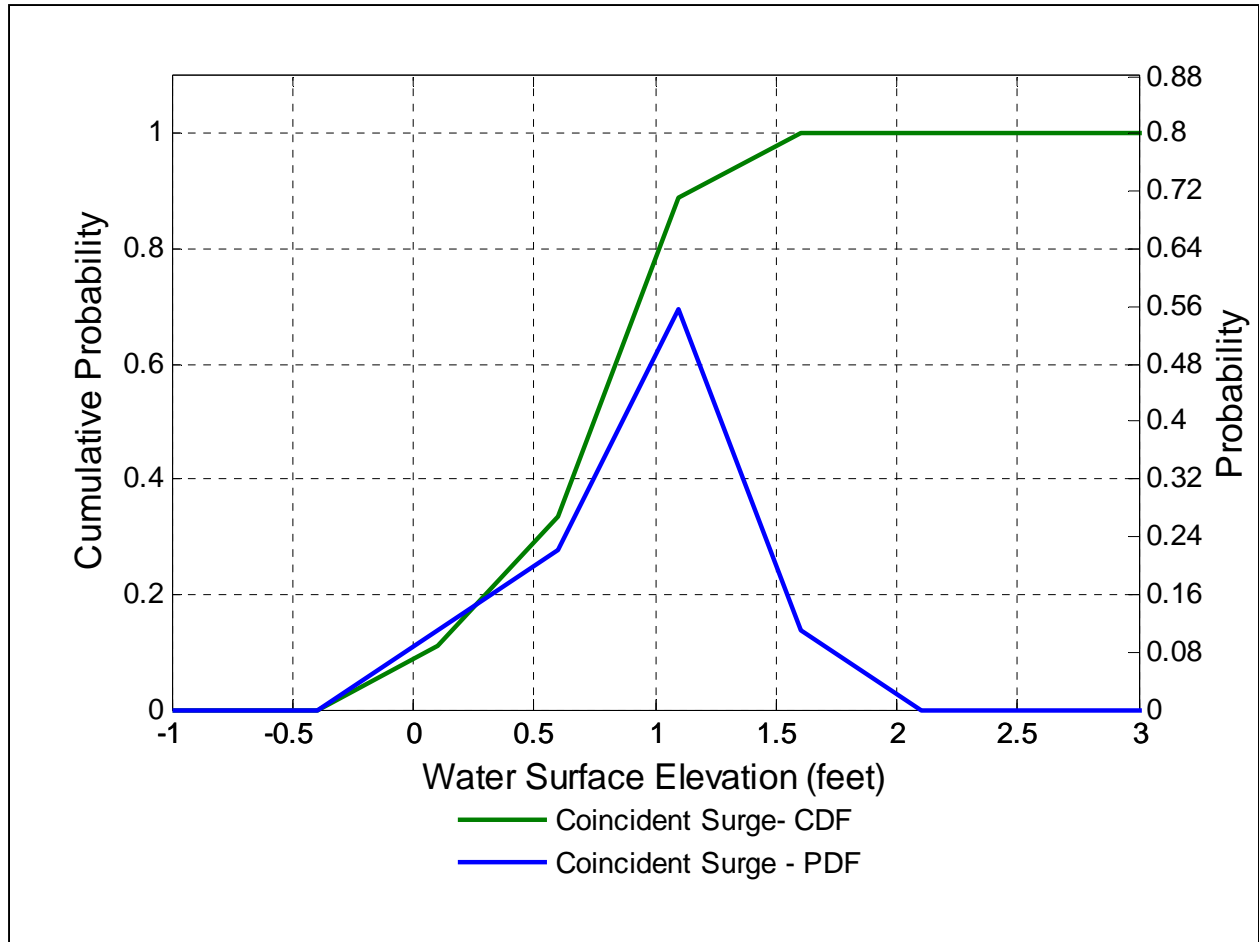


Figure 4-4. Event based Year 0 probability distributions of coincident surge (residual tide)

4.3 Event Based Predicted Tide Database and Development of PDF

To capture the full range of predicted tide for the development of DSBC, a four day record of predicted tide centered on the peak fluvial flow for each storm event was selected for analysis. In other words, the predicted tide used to form the predicted tide database began two days before the fluvial peak and ended two days after the fluvial peak of each event. This predicted tide record was selected because a four day period covered multiple cycles of high and low tide. This database was used to develop a PDF of predicted tide presented in Figure 4-5 and tabulated in Appendix H.

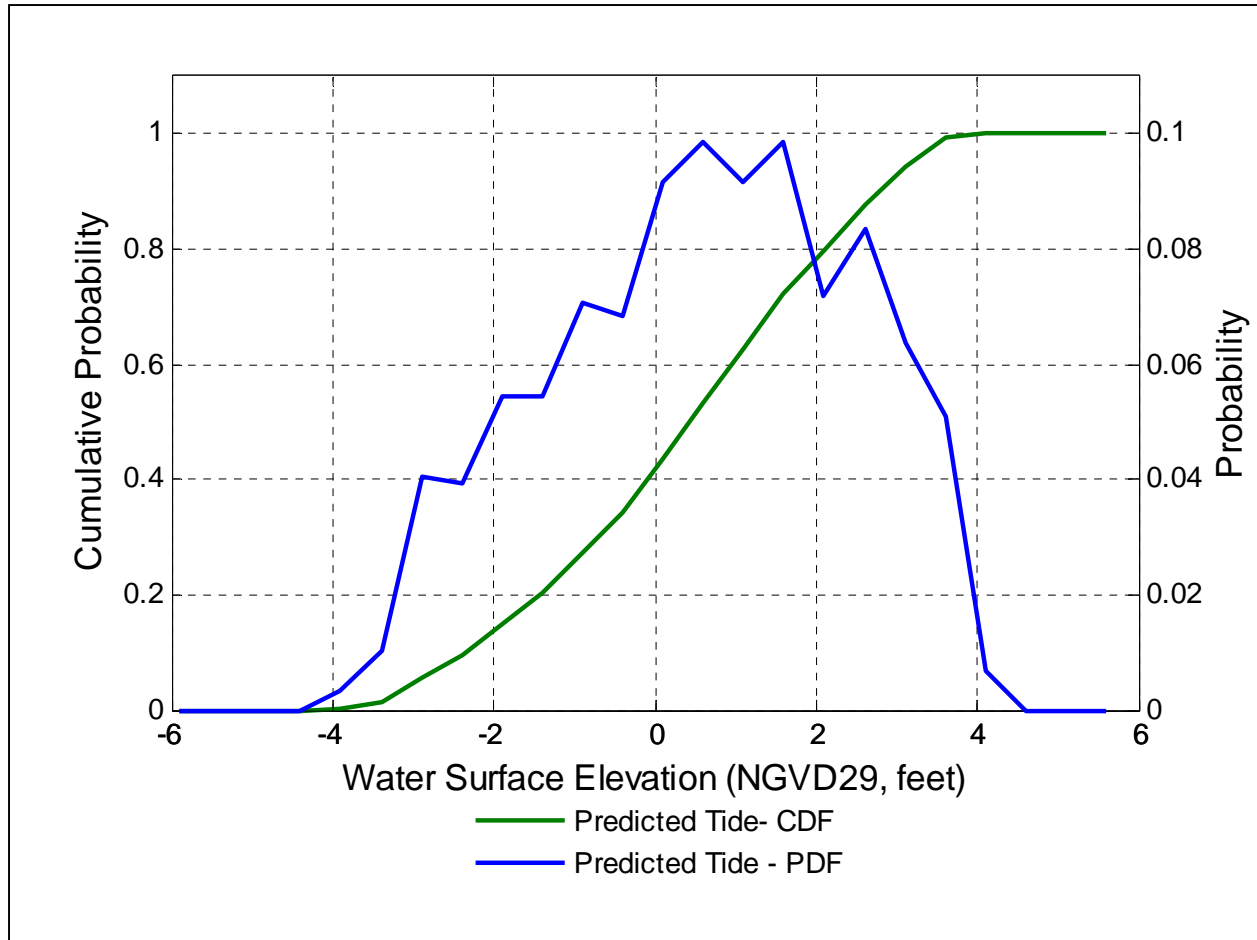


Figure 4-5. Event based Year 0 probability distributions of predicted tide

4.4 Combined Predicted Tide, Residual Tide and Wave Setup PDF – Year 0 (2011)

The PDFs of the event based databases of residual tide (Figure 4-4) and predicted tide (Figure 4-5) were combined using joint probability to establish a combined PDF. The combined PDF is presented in Figure 4-6.

The combined PDF is further analyzed to create a combined cumulative distribution function (CDF) curve presented in Figure 4-7 and Table 4-1. The combined CDF curve was discretized into probability bins. The discretized, divided, WSEs will be used as input as the DSBC in the hydraulic model simulations. The cumulative distribution curve was divided into 0.20 probability bins, i.e. the WSE corresponding to the median probability value of the distribution curve was recorded between 0.20 and 0.40, 0.40 and 0.60, and etc. Additional binning was completed to provide finer resolution of the distribution curve for large WSEs occurring between 0.95 and 1.00. The median value in each probability bin of the distribution curve was selected as a representative WSE. The magenta boxes presented in Figure 4-7 represent the median value of each probability bin.

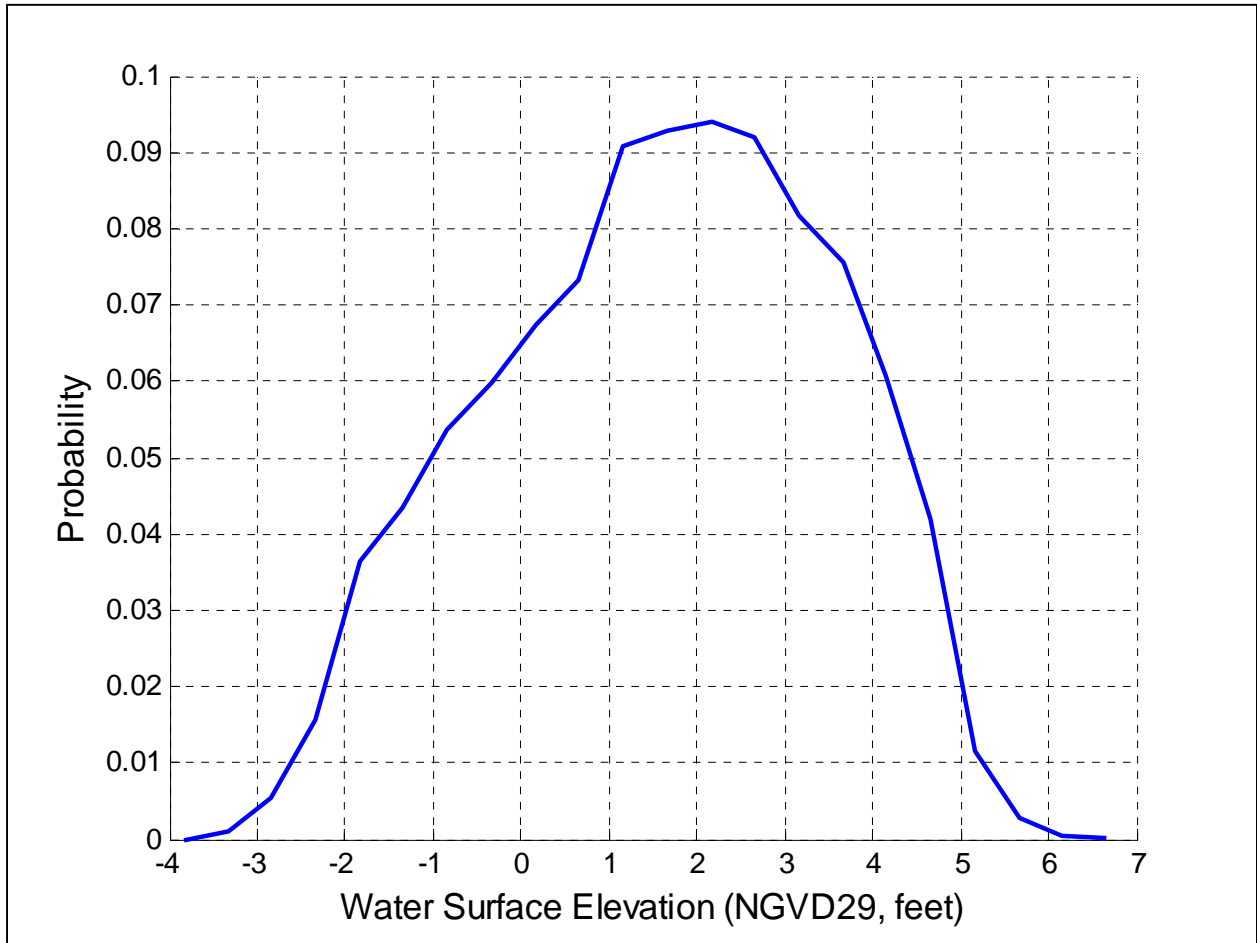


Figure 4-6. Event based joint probability distribution of Combined WSE

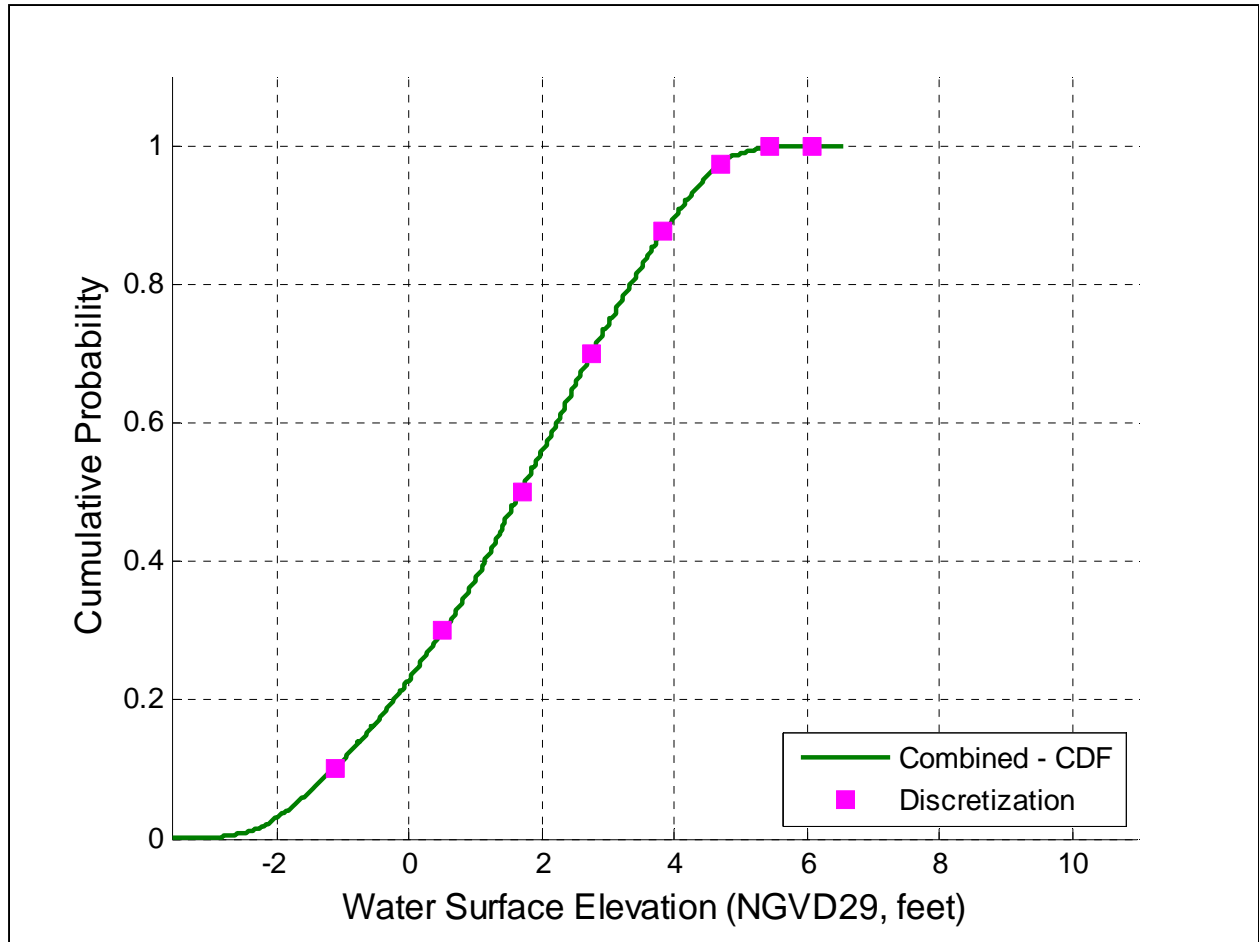


Figure 4-7. Combined cumulative probability distribution of Combined WSE

Table 4-1. Discretized water surface elevation for the combined Year 0 Conditions

Index	Cumulative Probability	Probability of Occurrence	Combined WSE (feet)
1	0.00 - 0.20	0.20	-1.11
2	0.20 - 0.40	0.20	0.53
3	0.40 - 0.60	0.20	1.69
4	0.60 - 0.80	0.20	2.75
5	0.80 - 0.95	0.15	3.83
6	0.95 - 0.995	0.045	4.71
7	0.995 - 0.9999	0.0049	5.43
8	0.9999 - 1.00	0.0001	6.07

4.5 Combined Predicted Tide, Residual Tide and Wave Setup PDF – Year 50 (2061)

To consider a DSBC for 50 years beyond the baseline conditions (future Yr 50 or 2061). SLR projections were computed based on National Research Council's (NRC) three different accelerating eustatic SLR scenarios (EC1165-2-212) and local land settlement. The *Las Gallinas Creek H&H & Coastal Analysis* reported local land settlement between 2011 and 2061 to be 0.17 feet. This value was used in the analysis. The U.S. Army Corps guidance suggests eustatic historical (0.45 feet), NRC Curve I (0.84 feet), and NRC Curve III (2.08 feet) rates are appropriate minimum, intermediate, and maximum SLR projections to consider eustatic SLR and local land subsidence. Sea level rise elevations were computed with equations provided in EC 1165-2-212.

Figure 4-8 through Figure 4-10 and Table 4-2 through Table 4-4 present the discretized combined DSBC distribution curves for Year 50 conditions under eustatic historical, Curve I and Curve III SLR scenarios. These reported values can be used as downstream tidal boundary conditions.

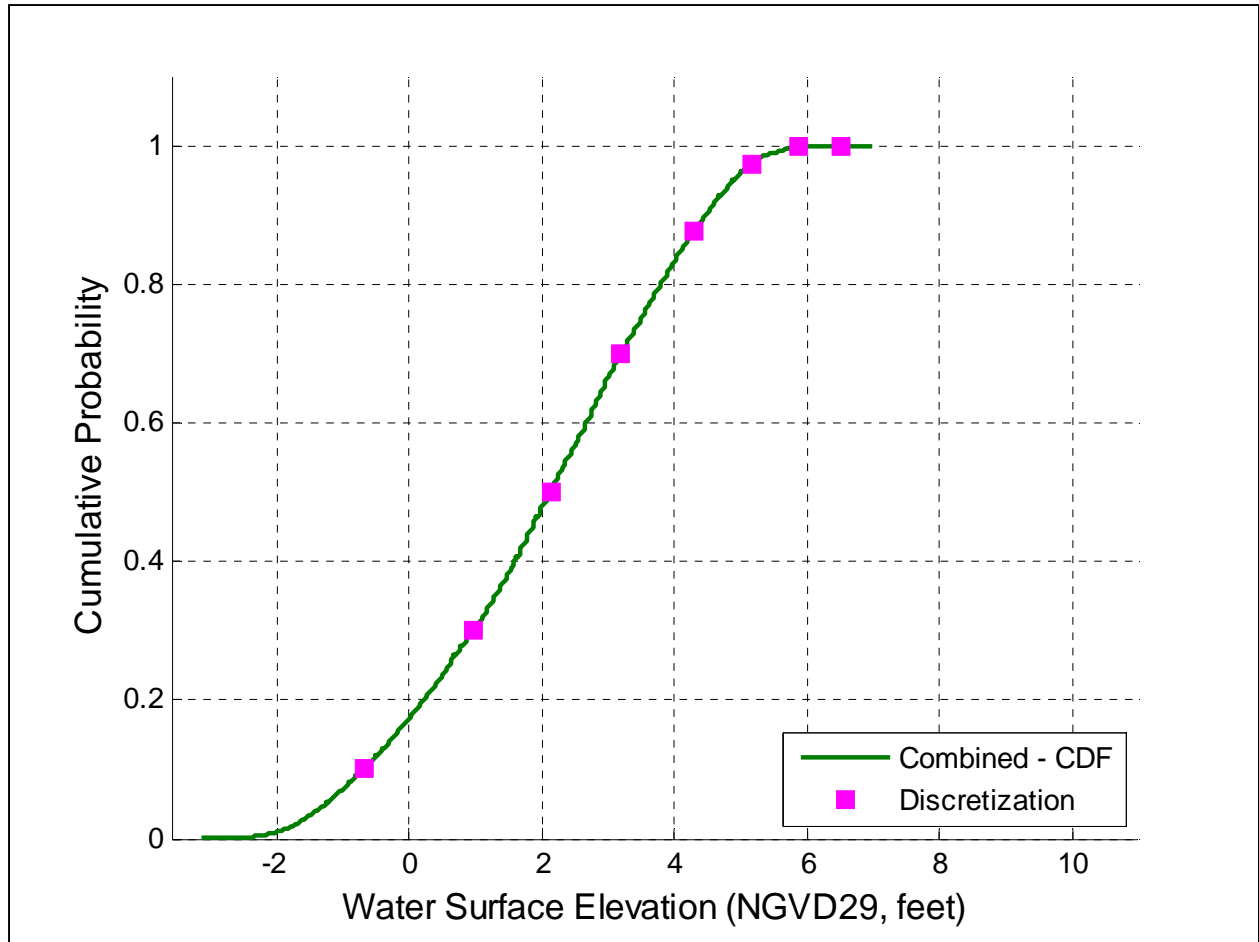


Figure 4-8. Combined Year 50 Historical cumulative probability distributions

Table 4-2. Discretized water surface elevation for the combined Year 50 Historical SLR

Index	Cumulative Probability	Probability of Occurrence	Combined WSE (feet)
1	0.00 - 0.20	0.20	-0.66
2	0.20 - 0.40	0.20	0.98
3	0.40 - 0.60	0.20	2.14
4	0.60 - 0.80	0.20	3.20
5	0.80 - 0.95	0.15	4.28
6	0.95 - 0.995	0.045	5.16
7	0.995 - 0.9999	0.0049	5.88
8	0.9999 - 1.00	0.0001	6.52

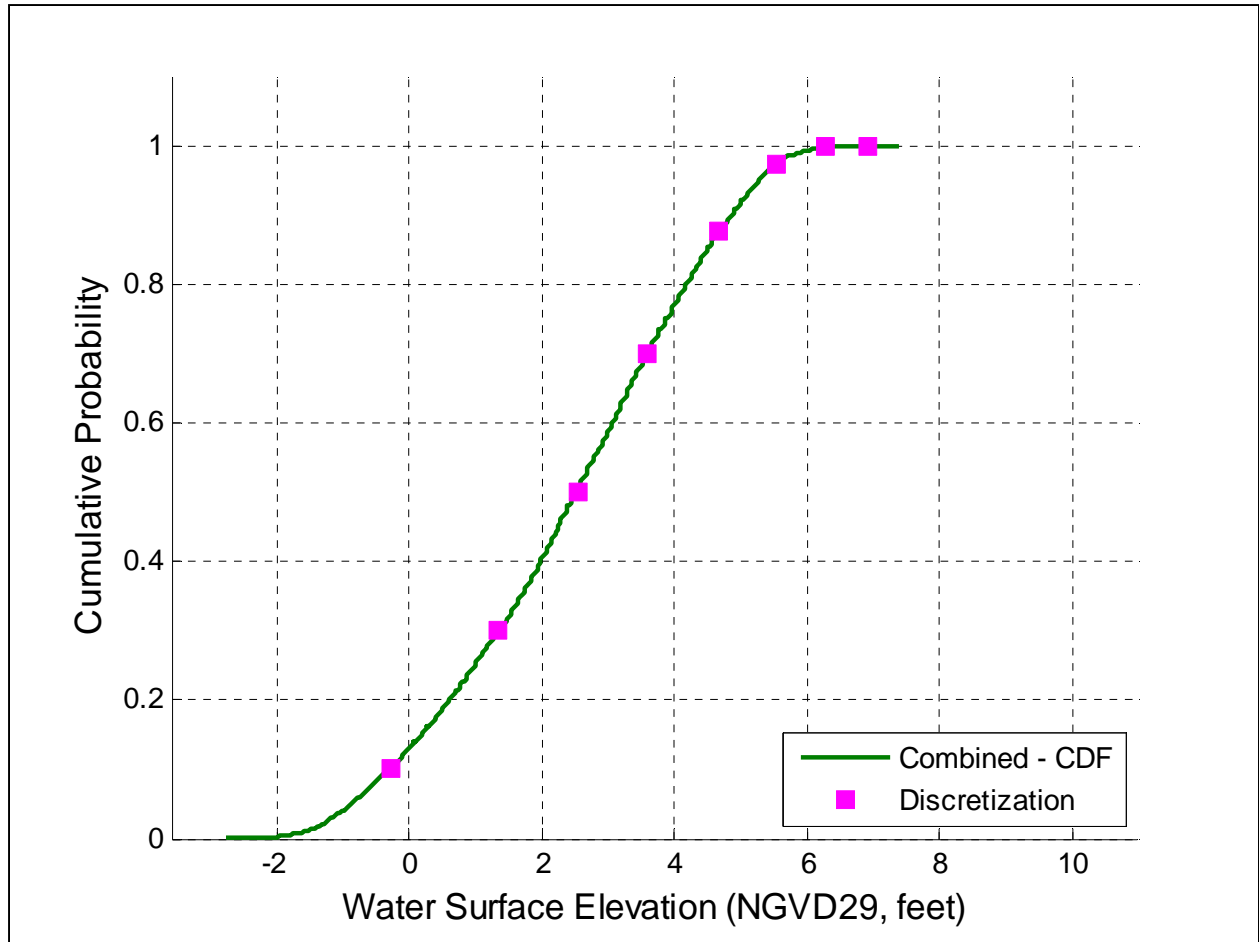


Figure 4-9. Combined Year 50 Curve I cumulative probability distributions

Table 4-3. Discretized water surface elevation for the combined Year 50 Curve I SLR

Index	Cumulative Probability	Probability of Occurrence	Combined WSE (feet)
1	0.00 - 0.20	0.20	-0.27
2	0.20 - 0.40	0.20	1.37
3	0.40 - 0.60	0.20	2.53
4	0.60 - 0.80	0.20	3.59
5	0.80 - 0.95	0.15	4.67
6	0.95 - 0.995	0.045	5.55
7	0.995 - 0.9999	0.0049	6.27
8	0.9999 - 1.00	0.0001	6.91

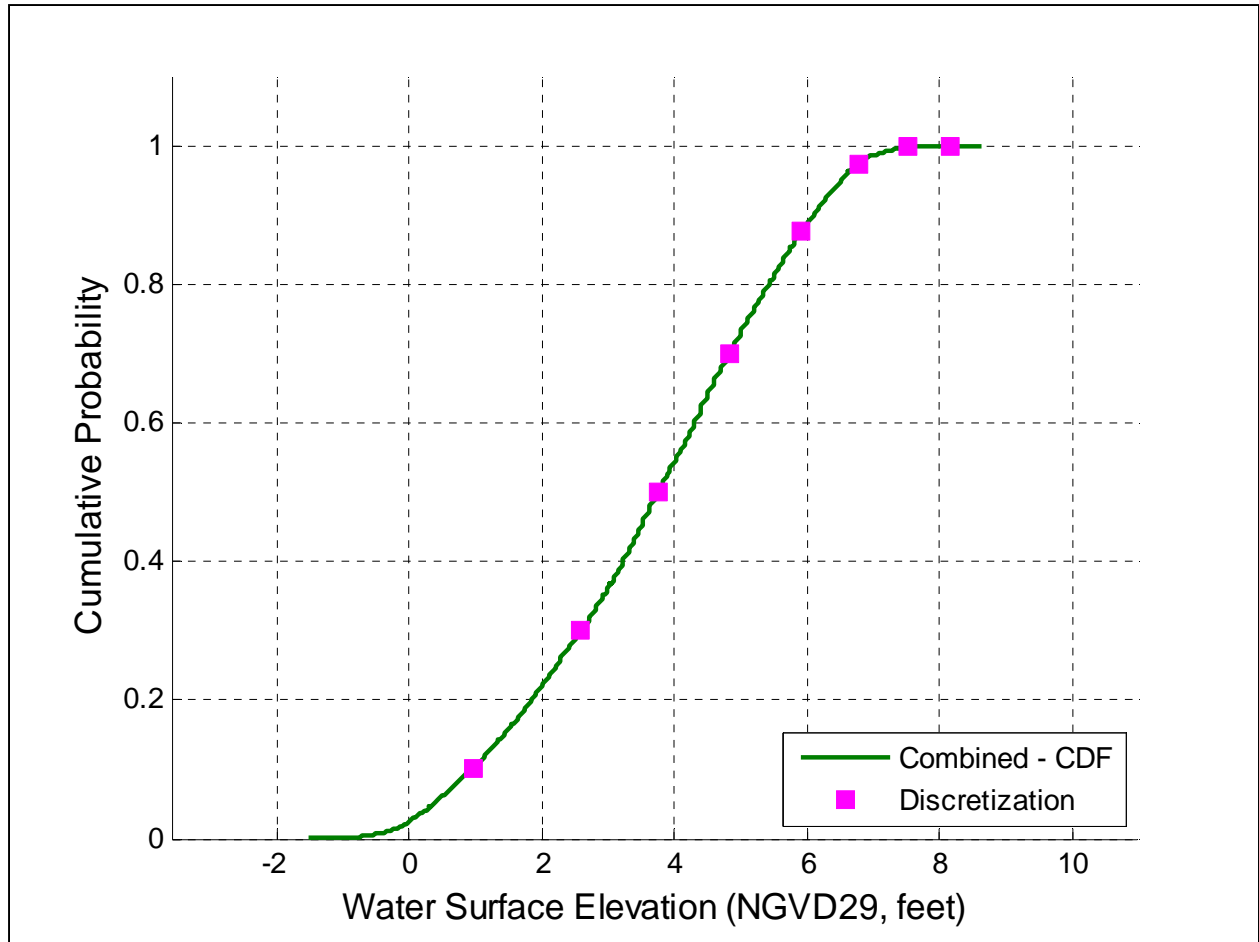


Figure 4-10. Combined Year 50 Curve III cumulative probability distributions

Table 4-4. Discretized water surface elevation for the combined Year 50 Curve III SLR

Index	Cumulative Probability	Probability of Occurrence	Combined WSE (feet)
1	0.00 - 0.20	0.20	0.97
2	0.20 - 0.40	0.20	2.61
3	0.40 - 0.60	0.20	3.77
4	0.60 - 0.80	0.20	4.83
5	0.80 - 0.95	0.15	5.91
6	0.95 - 0.995	0.045	6.79
7	0.995 - 0.9999	0.0049	7.51
8	0.9999 - 1.00	0.0001	8.15

5.0 SUMMARY AND CONCLUSIONS

This report documents the statistical analysis used to estimate the coastal DSBC for hydraulic modeling at the Las Gallinas Creek Inlet. This effort was conducted as part to the Las Gallinas Creek Phase 1 Feasibility Study. The DSBC analysis will be used to estimate combined fluvial and coastal water surface elevation (WSE) in the tidally influenced portion of Las Gallinas Creek.

Very little data was available for use to estimate the coastal DSBC at Las Gallinas Creek. Reasonable and proximal data to the project site was assumed to be representative and used in this analysis. Tidal WSE information from the San Francisco tide station was used, for a 112 year record. This database was used to estimate the tidal contribution to the DSBC. Wind information from the Hamilton Army Air Field, for a 36 year record, was used to compute the wave setup contribution to the DSBC.

To establish the DSBC two approaches have been implemented. Both approaches use a database of measured WSE and wave setup derived from the data sets described above. The developed databases are used to generate a probability distribution function (PDF).

The first approach presents a time-series based methodology. The time-series approach assumes all of the controlling coastal parameters are statistically independent of fluvial flow and the entire time series of the each controlling coastal parameter can be used to generate PDFs. The PDFs can be combined using joint probability to establish a combined PDF. The combined PDF was further developed to establish a combined CDF. The combined CDF is used as the DSBC in hydraulic modeling.

The second approach presents an event-based methodology, narrowly focusing the time series on peak flow events. The event-based approach decouples measured tide into two parts: predicted tide and residual tide. Predicted tide is a predictable WSE based on tidal constituents, the most common are lunar and solar. Residual tide includes weather effects, such as storm surge, sea level rise and El Niño contributions that may elevate the WSE. Measured tide was decoupled to investigate the statistical relationship of fluvial flow at the inlet and residual tide, i.e. coastal surge, using a linear relationship. The computed correlation coefficient, R , is very small. However, a qualitative relationship between residual tide, coastal surge, and fluvial flow was observed. Based on this observation, a database of coincident residual tide, or the residual tide at the time of the fluvial peak, was developed. A second database was developed to estimate the full range of predicted tide at the time of each fluvial peak event. The wave setup contribution was included. The event-based datasets of predicted tide, residual tide and wave setup were combined using joint probability.

Both approaches estimated the combined DSBC for the baseline condition, Year 0 (2011), and considering future sea level rise for project Year 50 or Year 2061.

The second approach estimates a slightly higher DSBC, on the order of 0.1-0.6 feet higher than the first approach. Both coastal DSBC approaches can be used to evaluate combined WSE of

coastal and fluvial WSE in tidally influenced reaches of Las Gallinas Creek. The event based approach provides a more conservative estimate of the coastal DSBC.

6.0 REFERENCES

Conatser, N. and R. Leventhal. Personal Communication. August 31, 2012.

Climate Services 14th Weather Squadron. April, 2011.
<https://notus2.afccc.af.mil/SCIS/services/pickupSAR.asp>

Dean, Robert and Robert A. Dalrymple. Coastal Processes with Engineering Applications. United Kingdom: Cambridge Press, 2002.

Dean, Robert and Robert A. Dalrymple. Water Wave Mechanics for Engineers and Scientists. Salem, MA: World Scientific Publishing, 1991.

ESRI, ArcMap, GIS, Version 10.0.

Restoration Design Report Seasonal and Tidal Wetlands Hamilton Wetland Restoration Project Novato, California. January, 2008.

Hinds, A. B. Crawford, M. Rodriguez, F. Vogler, D. Dawson, K. Drumm, B. Collins, L. Roznowski, S. Silver. Technical Flooding Background Report. Clearwater Hydrology. November, 2005.

Marin County Watershed Program. Ross Valley Watershed. Watershed Overview. Accessed September 13, 2012. http://www.marinwatersheds.org/ross_valley.html

Mathworks, Matlab 2012a.

Leventhal, Roger. Las Gallinas Creek - Conversion between NAVD88 and NGVD29. Personal Email. 4 Jan. 2013.

National Oceanic and Atmospheric Administration (NOAA) San Francisco, CA 9414290 (November, 2010). <http://tidesandcurrents.noaa.gov/geo.shtml?location=9414290>

U.S. Army Corps of Engineers (USACE), San Francisco District. 2011a. Las Gallinas Creek H&H & Coastal Analysis. Prepared for USACE by Noble Consultants, Inc.

U.S. Army Corps of Engineers (USACE), San Francisco District. 2010. Tides and Currents San Francisco Bay & Tributaries. San Francisco, CA.

U.S. Army Corps of Engineers (USACE), San Francisco District. Las Gallinas Creek Marin County California Section 205 Reconnaissance Study Report of Negative Findings (1991). San Francisco, CA.

U.S. Army Corps of Engineers (USACE). 2011b. Sea-Level Change Considerations for Civil Works Programs, EC 1165-2-212. San Francisco, CA.

U.S. Geological Survey (USGS) USGS 11460000 Corte Madera C A Ross CA. September, 2012. <http://waterdata.usgs.gov/usa/nwis/uv?11460000>

U. S. Army Corps of Engineers (USACE), San Francisco District. 2012. "Statistical Analysis Report – South San Francisco Bay Shoreline Study". San Francisco, CA.

U.S. Army Corps of Engineers (USACE). 31 July 2003. *Coastal Engineering Manual: Part III, Chapter 2 – Longshore Sediment Transport (EM1110-2-1100)*.

APPENDIX A- TIDAL AMPLIFICATION BETWEEN THE SAN FRANCISCO TIDE STATION AND LAS GALLINAS CREEK INLET

Travel time and phase shift from the San Francisco tide station to the Corte Madera and Las Gallinas Creek inlets is presented in Table A-1 and Figure A-1. Predicted tidal amplitude changes are considered minor and not included in this analysis.



Figure A-1. San Francisco, Richmond and Mare Island tide stations

Table A-1. Tidal amplification and phase shift to Las Gallinas and Corte Madera Creeks from San Francisco tide station (ID 9414290)

	High Water Amplification Factor*	Phase Shift* (minutes)
Las Gallinas Creek	1.01	71
Corte Madera Creek	1.00	37
*Tidal amplifications factors and phase shifts were obtained from <i>Tides and Currents San Francisco Bay & Tributaries</i> , published by USACE, San Francisco District in 2010.		

Travel time and phase shift were also investigated for residual tide. This analysis was used to evaluate if residual tide changed as it propagated into the north San Francisco Bay. To evaluate the changes in the residual tide, residual tide information from the Richmond and Mare Island tide stations were compared to the residual tide from the San Francisco tide station. The Richmond and Mare Island tide stations were selected for this comparison because they are both north of the San Francisco tide station (Figure A-1). Figure A-2 presents the comparison and illustrates nearly no change in residual tide peak residual tide at any of the three stations used for comparison. This comparison suggests that it is appropriate to assume that residual tide remains unchanged from the San Francisco tide station to as far north as the Mare Island tide station, which includes the inlet to Las Gallinas. Adjustments were made to measured tide values to remove the SLR trend prior to computing residual WSE.

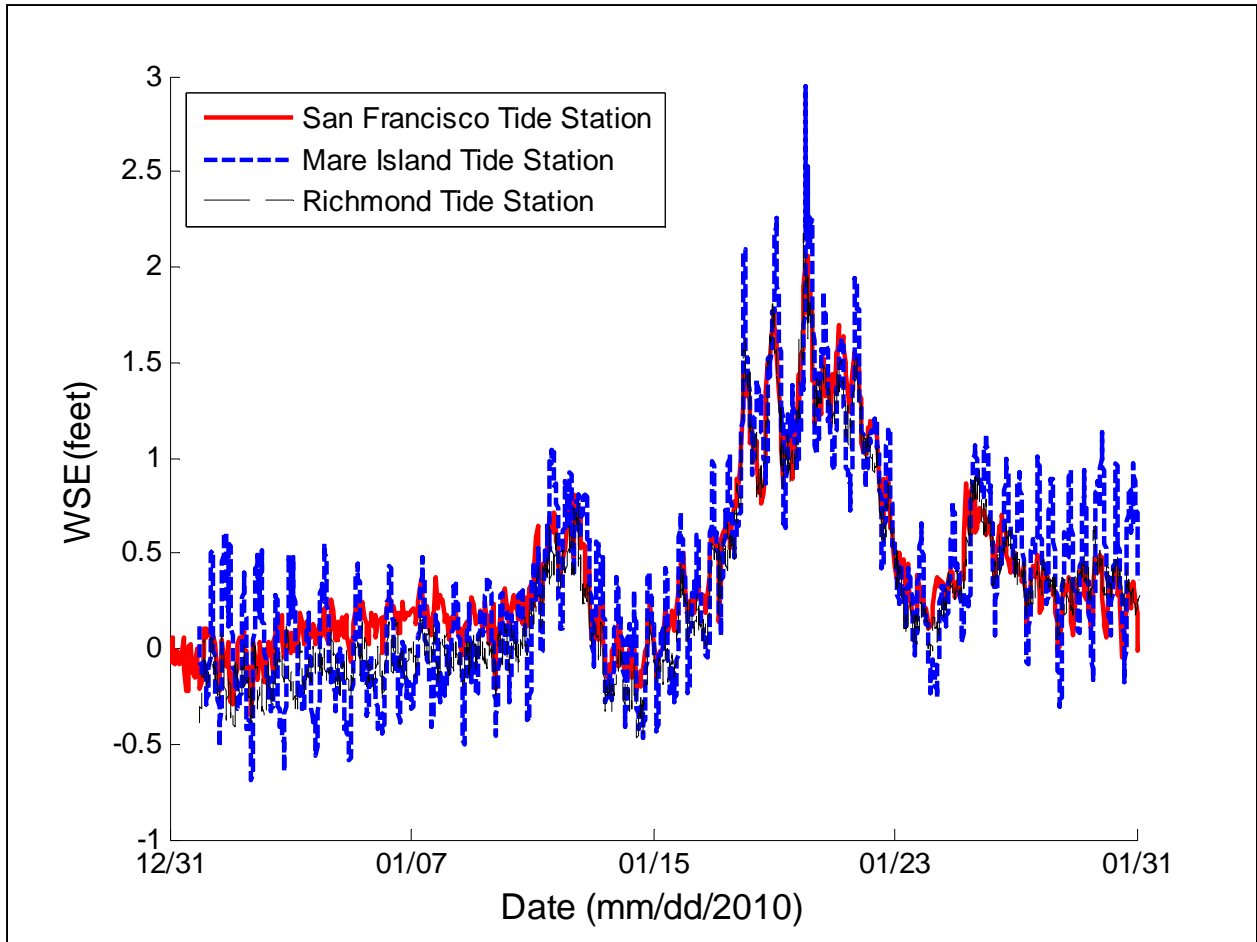


Figure A-2. Comparison of residual tide at the San Francisco, Richmond and Mare Island NOAA tide stations

APPENDIX B – SAN FRANCISCO TIDE STATION – TIDAL DATUMS

Table B-1 presents tidal datum information from the San Francisco tide station using the most recent tidal epoch, 1983 – 2001.

Table B-1. Tidal datum of San Francisco tide station (ID 9414290)

Datum	Value* (feet, NAVD88)	Value* (feet, MLLW)	Value* (feet, NGVD29)
Highest Observed Water Level (01/27/1983)	8.72	8.66	6.04
Mean Higher-High Water	5.90	5.84	3.22
Mean High Water	5.29	5.23	2.61
Mean Tide Level	3.24	3.18	0.56
Mean Sea Level	3.18	3.12	0.50
Mean Diurnal Tide Level	2.98	2.92	0.30
National Geodetic Vertical Datum of 1929 (NGVD29)	2.68	2.62	0.0
Mean Low Water	1.19	1.13	-1.49
Mean Lower-Low Water	0.06	0.00	-2.62
North American Vertical Datum of 1988 (NAVD88)	0.00	-0.06	-2.68
Lowest Observed Water Level (12/17/1933)	-2.82	-2.88	-5.50
*Tidal Datum information was obtained from: http://tidesandcurrents.noaa.gov/geo.shtml?location=9414290			

APPENDIX C – DESCRIPTED PDF OF MEASURED TIDE

The measured tide has the most significant contribution to the downstream WSE when compared to the wave setup contributions. The tidal phase (i.e. timing of high tide and low tide) occurring at the arrival time of peak flood flow to the river mouth plays an important role for flood stage calculation. The peak flood flow can coincide with any phase of tide. In other words, there is equal probability of occurrence of tide elevation to meet with peak flood flow. Measured tide from the San Francisco tide station was used to create a discretized distribution curve of the tidal WSE probability distribution at the mouth of Las Gallinas Creek for the current baseline condition (i.e. Year 0 or 2011).

The 105 year predicted tide, covering multiple cycles of neap and spring tide, was analyzed to obtain the probability distribution of tidal elevation at the creek inlet. Figure C-1 and Table C-1 present the cumulative probability, the tide elevation selected, and their assigned probability to serve as the downstream water elevation boundary condition for HEC-RAS simulation.

To discretize the distribution curve, measured WSE values were presented in 0.20 probability bins. For example, measured WSE is presented between 0.20 and 0.40, 0.40 and 0.60, and etc. Additional binning was completed to provide finer resolution of the distribution curve for large measured WSE occurring between 0.95 and 1.00. The median value in each probability bin of the distribution curve was selected as a representative WSE. The magenta boxes presented in Figure C-1 represent the median value of each probability bin.

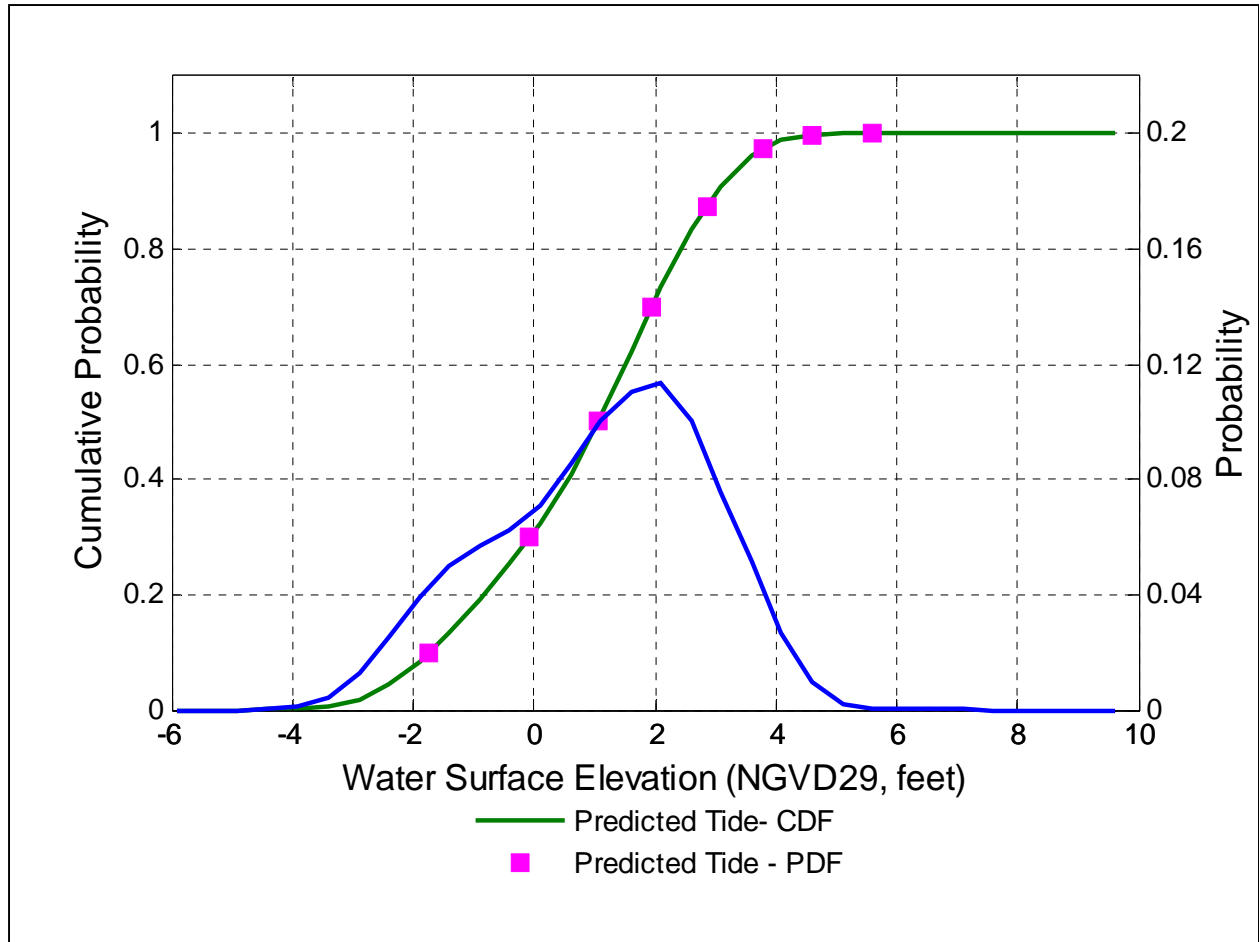


Figure C-1. Year 0 probability distributions

Table C-1. Discretized water surface elevation for Year 0 Conditions

Index	Cumulative Probability	Probability of Occurrence	Tidal WSE (feet)
1	0.00 - 0.20	0.20	-1.52
2	0.20 - 0.40	0.20	0.14
3	0.40 - 0.60	0.20	1.25
4	0.60 - 0.80	0.20	2.15
5	0.80 - 0.95	0.15	3.05
6	0.95 - 0.995	0.045	3.96
7	0.995 - 0.9999	0.0049	4.78
8	0.9999 - 1.00	0.0001	5.79

APPENDIX D – COMPUTED WAVE HEIGHT COMPARISON

A wave height was computed, fit to a distribution as described in the *Draft Report Las Gallinas Creek H&H & Coastal Analysis* (USACE, 2011a). The wave height frequency curves are compared and presented Figure D-1 and Table D-1. The computed wave height presented is approximately 0.5 feet larger than that of what was reported in the *Draft Report Las Gallinas Creek H&H & Coastal Analysis*. This was discussed with Noble Consultants and decided to be acceptable within the engineering uncertainty of this project.

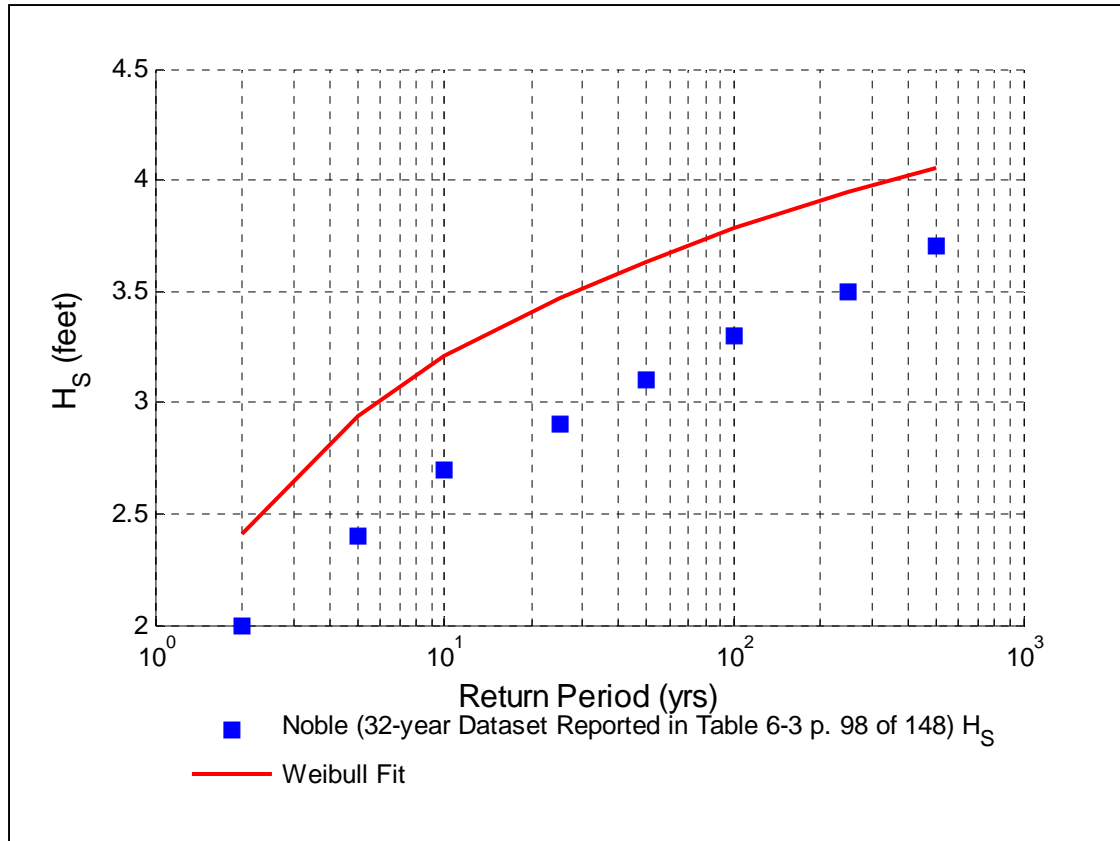


Figure D-1. Wave height frequency curve

Table D-1. Comparison of computed wave height frequency

Return Period	H _s Computed	H _s (USACE, 2011a)	Difference (H _s Computed - H _s (USACE, 2011a))
2	2.4	2.0	0.41
5	2.9	2.4	0.54
10	3.2	2.7	0.50
25	3.5	2.9	0.57
50	3.6	3.1	0.53
100	3.8	3.3	0.48
250	3.9	3.5	0.44
500	4.1	3.7	0.36

APPENDIX E – WAVE SET-UP EQUATIONS

Linear wave theory was used to compute wave setup WSE at the creek inlet. To compute wave breaker height the computed hourly wave height was used as input, two key assumptions were made: parallel bathymetric bottom contours and wave energy is conserved between the wave buoy and the depth at which wave breaking occurs.

Equation 1 describes the approach used to compute breaking wave height, H_b , where H_s , C_1 (Equation 1A), C_{g1} (Equation 1B) and α_1 are the offshore wave height, wave celerity, wave group velocity and wave approach angle relative to the shore normal, approximately 87° from true north, respectively. Constant values of g and k are also included in Equation 1, where k and g are the wave breaking criterion ($g=0.60$) and gravity (9.81 m/s^2 or 32.2 ft/s^2), respectively. Each storm case was evaluated individually by iterating Equation 1 until the maximum difference between iterations of H_b was less than 0.0001 feet. H_b is used as input into Equation 2 to compute wave set-up. All computations were made in Matlab.

$$H_b = H_{s1}^{\frac{4}{5}} (C_{g1} \cos \alpha_1)^{\frac{2}{5}} \left[\frac{g}{\gamma} - \frac{H_b g^2 \sin^2(\alpha_1)}{\gamma^2 C_1^2} \right]^{\frac{-1}{5}} \quad \text{Equation 1 (CEM, 2008, Equation III-2-16)}$$

$$C_1 = \frac{T_p g}{2\pi} \quad \text{Equation 1A (Dean, 1991)}$$

$$C_{g1} = \frac{1}{2} \left(1 + \frac{2kh}{\sin 2kh} \right) * \frac{L_1}{T_p} \quad \text{Equation 1B (Dean, 1991)}$$

$$\eta_{setup} = 0.188 H_b \quad \text{Equation 2 (Dean, 2002)}$$

Figure 3-6. Figure E-1 and Table E-1 present the PDF and CDF of wave setup. The distribution will be used as input to obtain a joint probability distribution of predicted tide and wave setup.

To discretize the distribution curve, wave setup values were presented in 0.20 probability bins, i.e. a median value of the distribution curve was recorded between 0.20 and 0.40, 0.40 and 0.60, and etc. Additional binning was completed to provide finer resolution of the distribution curve for large wave setup occurring between 0.95 and 1.00. The median value in each probability bin of the distribution curve was selected as a representative WSE. The magenta boxes in presented in Figure E-1 represent the median value of each probability bin is the magenta boxes.

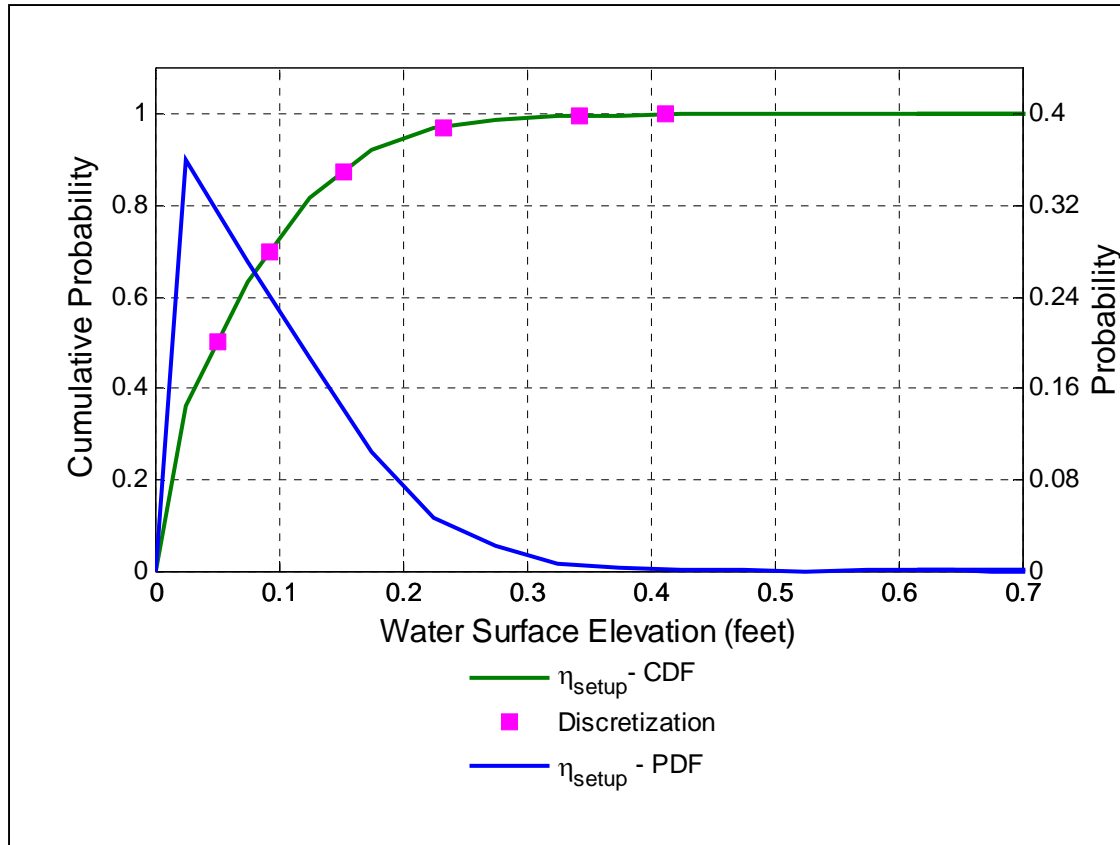


Figure E-1. Probability distribution of wave setup

Table E-1. Discretized probability distribution wave setup

Index	Cumulative Probability	Probability of Occurrence	Wave Setup (feet)
1	0.00 - 0.20	0.20	0.01
2	0.20 - 0.40	0.20	0.02
3	0.40 - 0.60	0.20	0.07
4	0.60 - 0.80	0.20	0.11
5	0.80 - 0.95	0.15	0.17
6	0.95 - 0.995	0.045	0.25
7	0.995 - 0.9999	0.0049	0.35
8	0.9999 - 1.00	0.0001	0.64

APPENDIX F – TIME SERIES PLOTS OF RESIDUAL TIDE AND FLUVIAL FLOW

Table F-1. Selected fluvial flow events and the corresponding residual tide

Storm ID	Date	Peak Fluvial Flow (CFS)	Coincident Residual Tide (feet)
1	03/24/91	1650	0.30
2	02/19/92	1790	0.58
3	01/06/93	1760	0.99
4	01/13/93	2710	0.97
5	01/15/93	1840	0.99
6	01/20/93	3350	0.75
7	01/20/10	1830	1.67
8	03/20/11	1850	0.91
9	03/24/11	2350	0.97

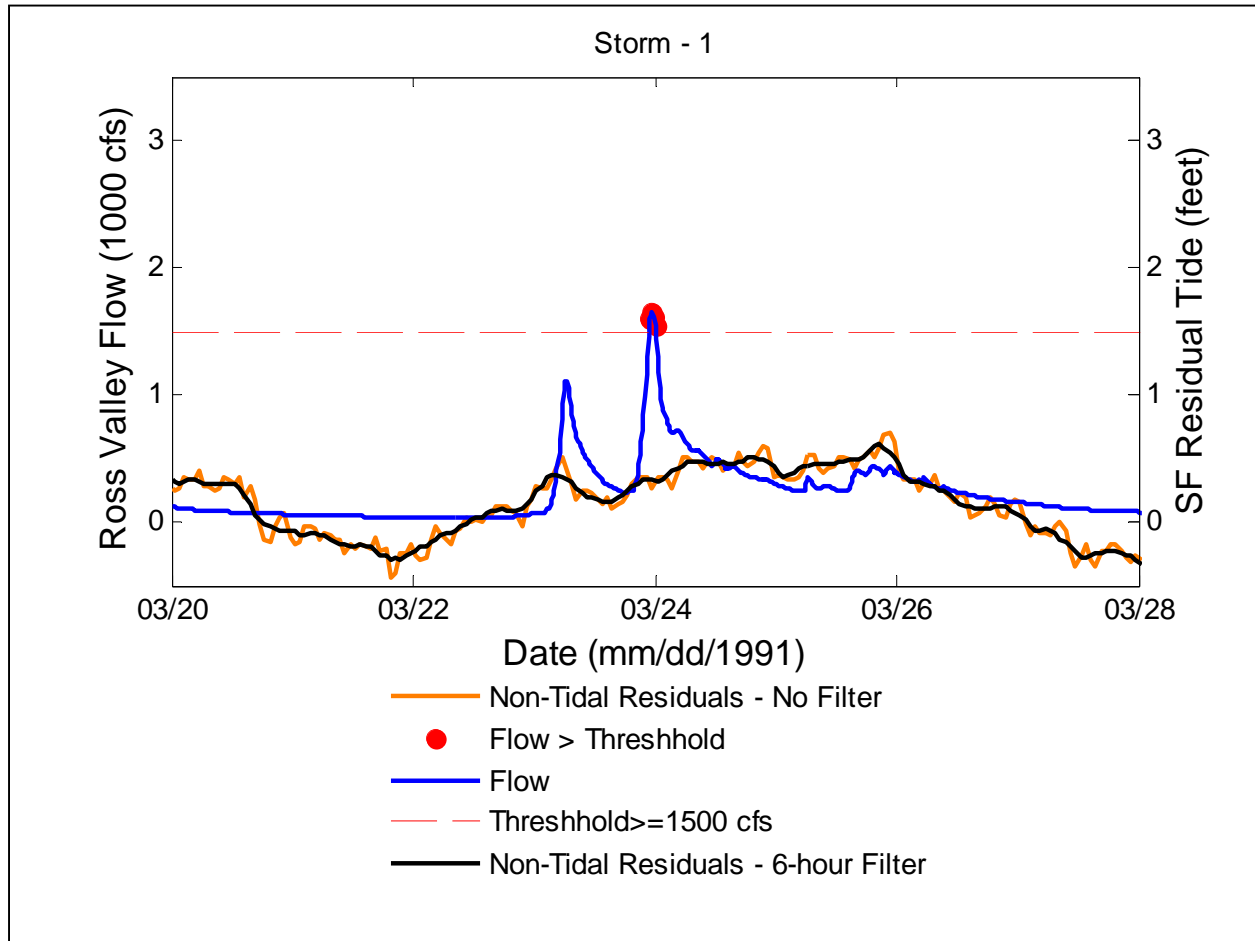


Figure F-1. Fluvial Flow and Coincident Non-Tidal Residual for Storm Event ID 1

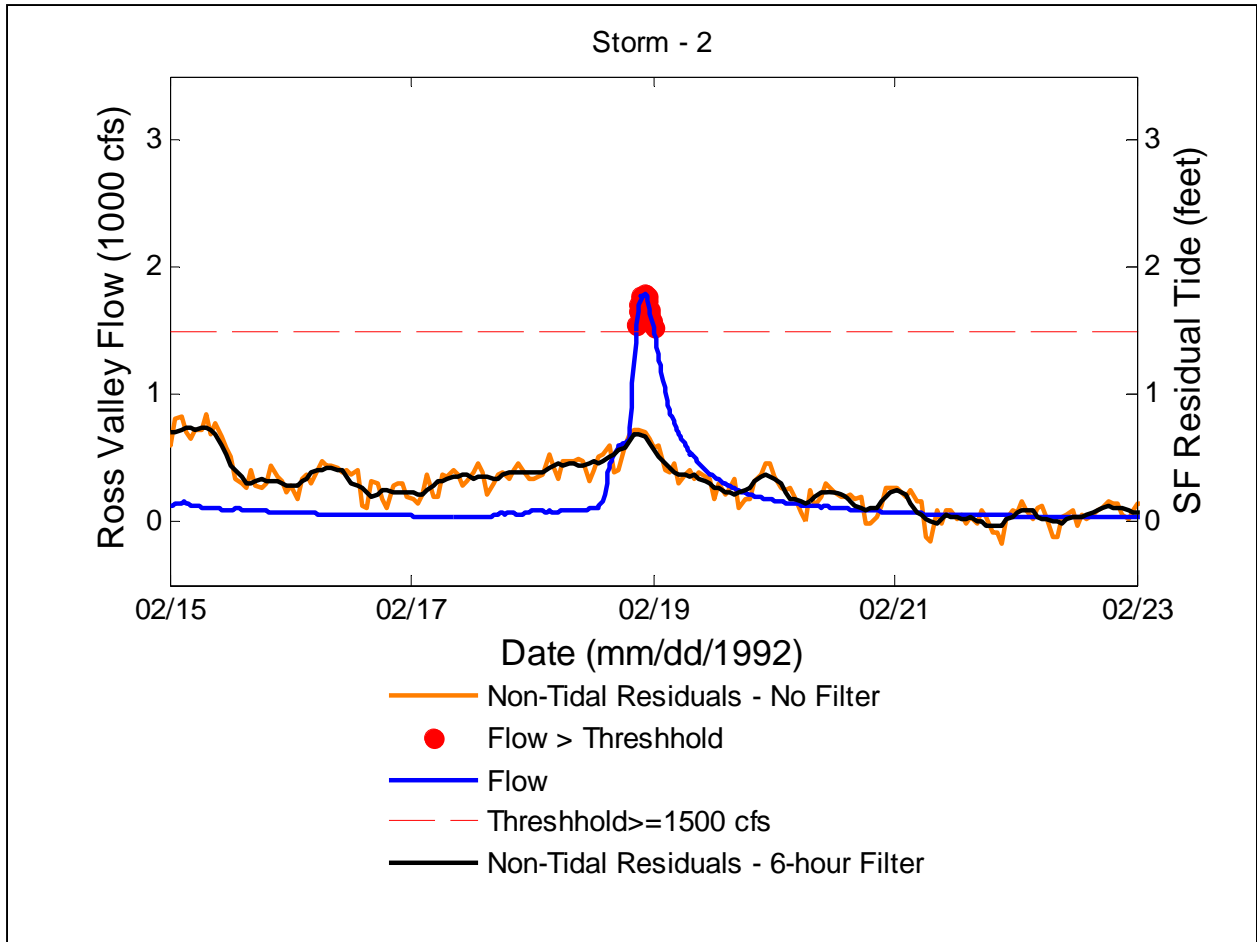


Figure F-2. Fluvial Flow and Coincident Non-Tidal Residual for Storm Event ID 2

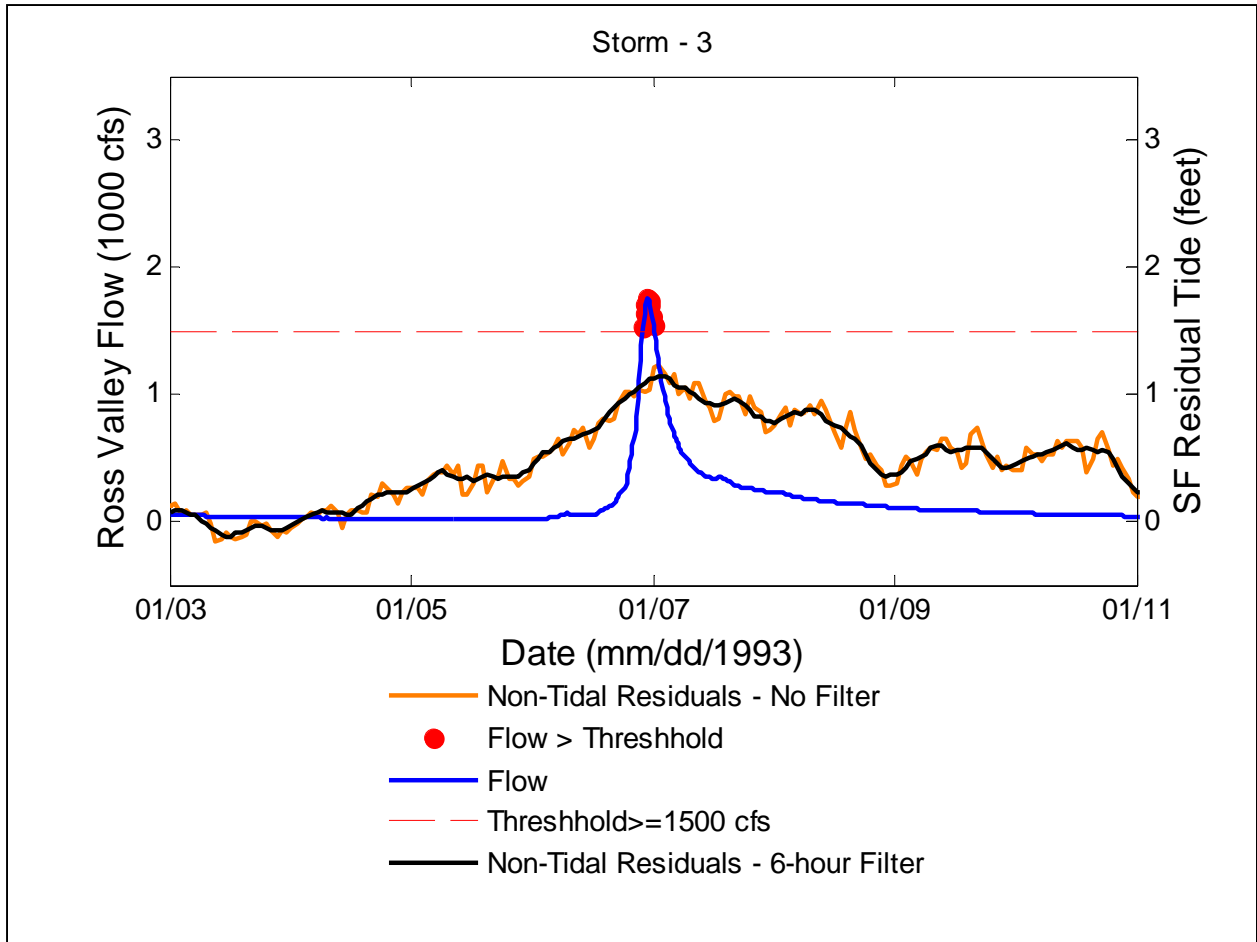


Figure F-3. Fluvial Flow and Coincident Non-Tidal Residual for Storm Event ID 3

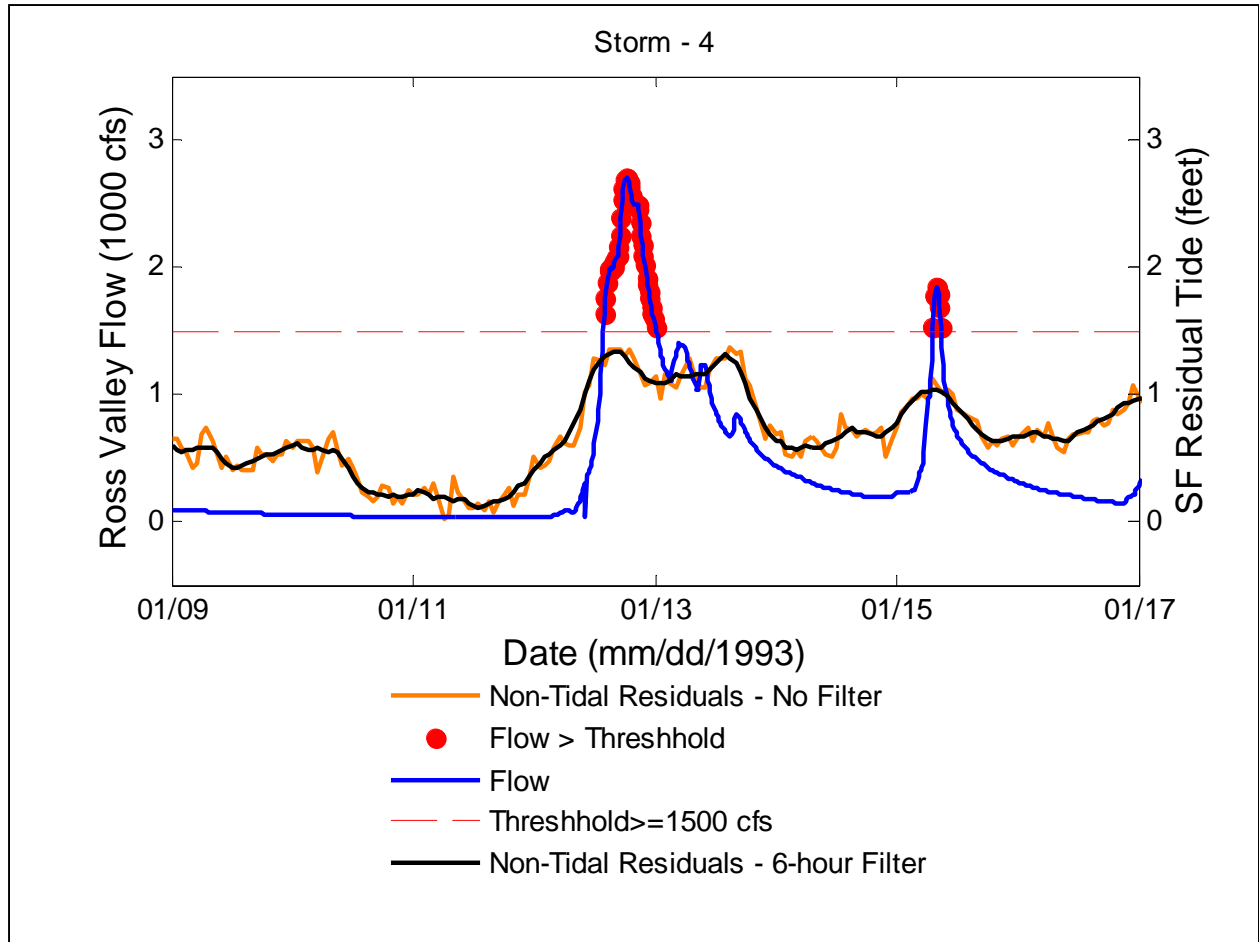


Figure F-4. Fluvial Flow and Coincident Non-Tidal Residual for Storm Event ID 4

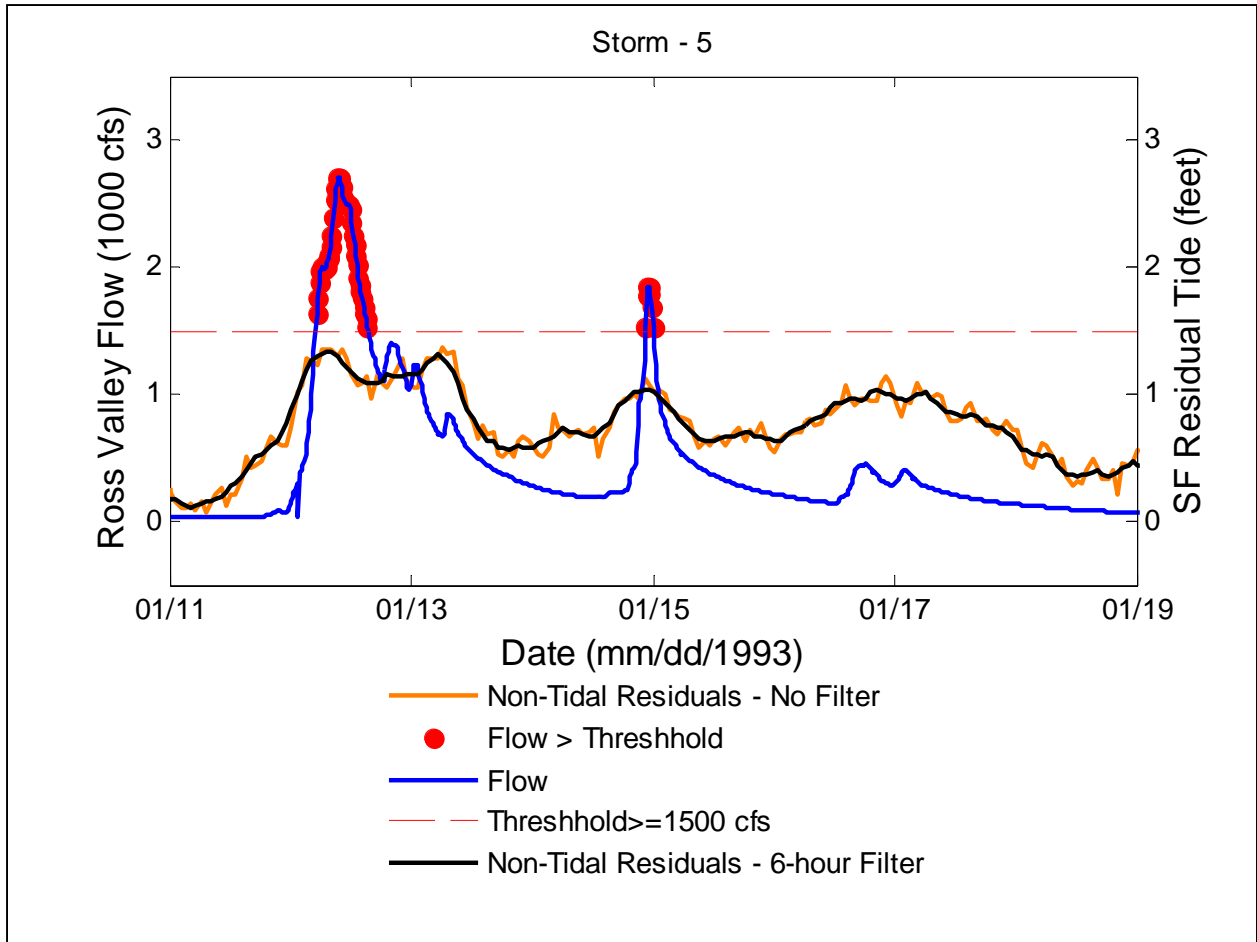


Figure F-5. Fluvial Flow and Coincident Non-Tidal Residual for Storm Event ID 5

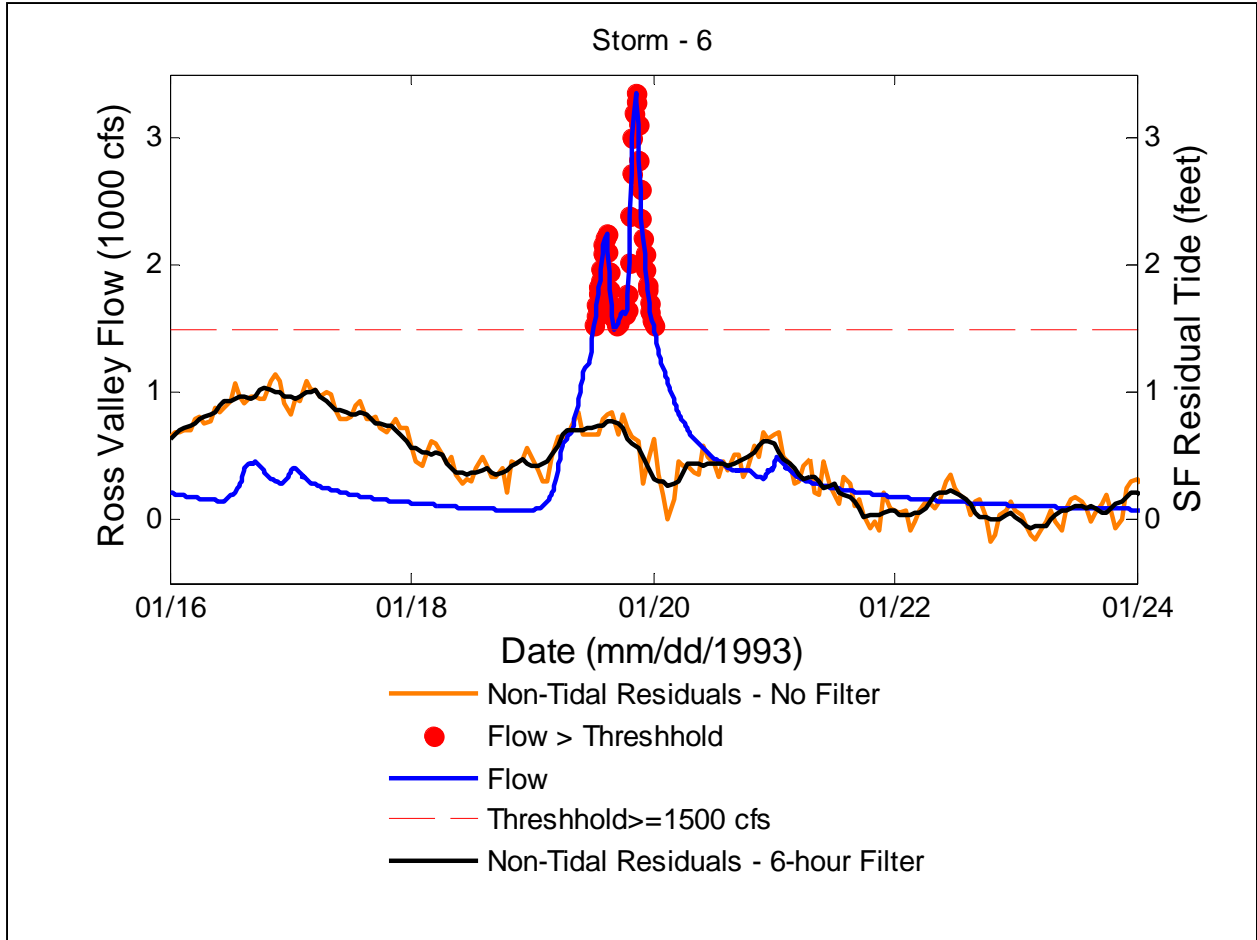


Figure F-6. Fluvial Flow and Coincident Non-Tidal Residual for Storm Event ID 6

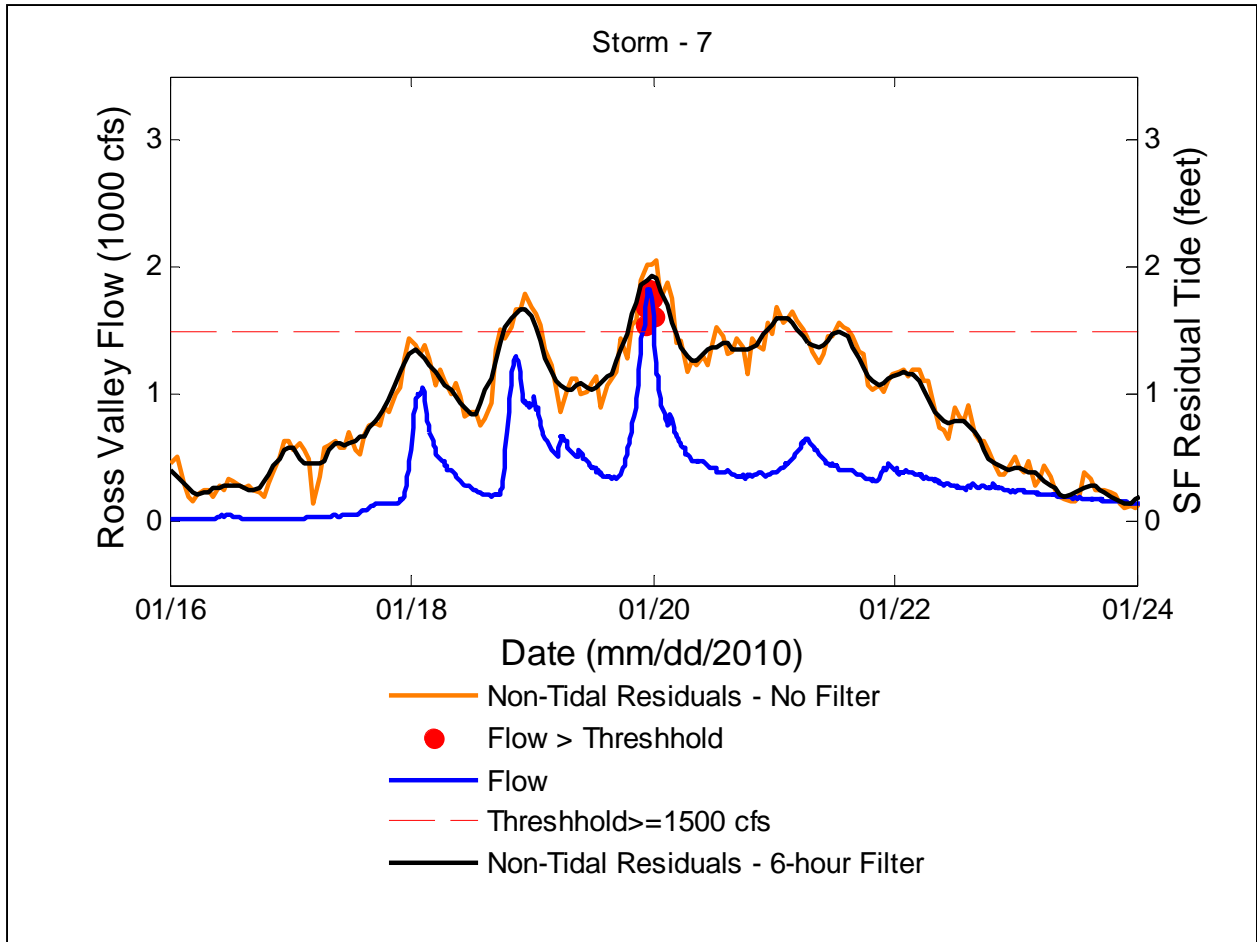


Figure F-7. Fluvial Flow and Coincident Non-Tidal Residual for Storm Event ID 7

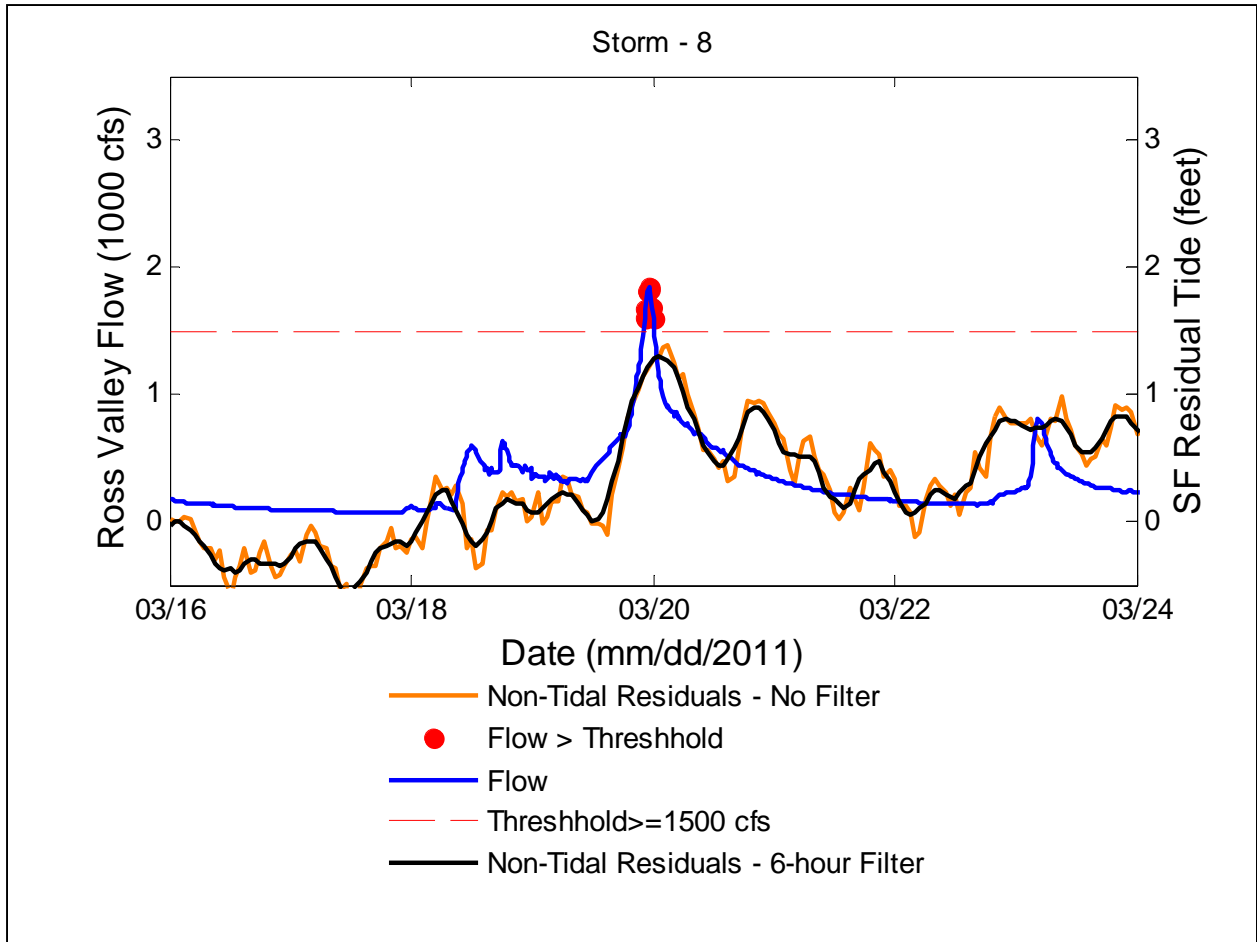


Figure F-8. Fluvial Flow and Coincident Non-Tidal Residual for Storm Event ID 8

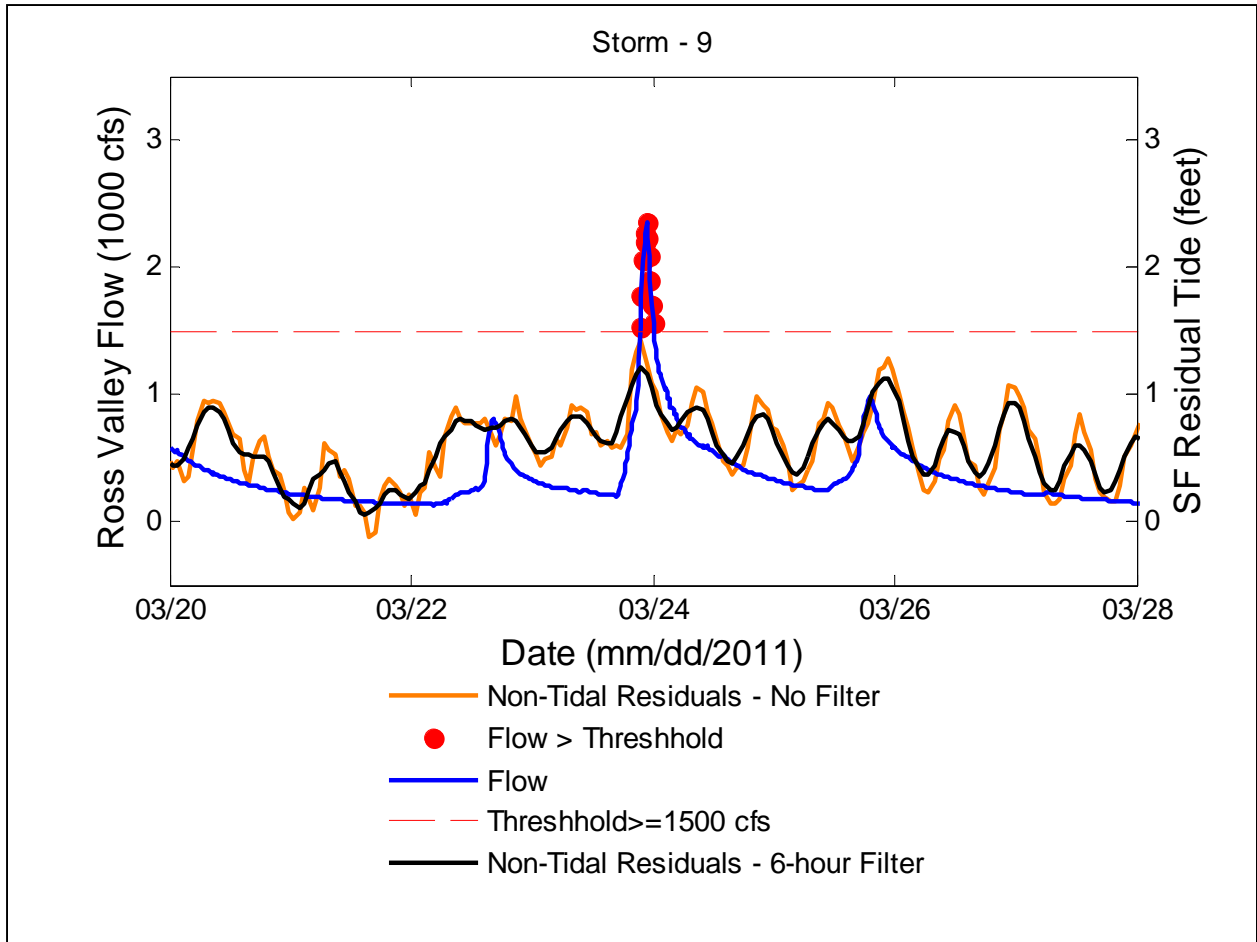


Figure F-9. Fluvial Flow and Coincident Non-Tidal Residual for Storm Event ID 9

APPENDIX G – DESCRITIZED PDF OF EVENT BASED RESIDUAL TIDE

The coincident residual tide from the 9 selected fluvial flow events was used to form the database for residual tide. This database was analyzed to obtain the probability distribution of residual tide elevation at the creek inlet. Figure G-1 and Table G-1 present the cumulative probability, the tide elevation selected, and their assigned probability to serve as the downstream water elevation boundary condition for HEC-RAS simulation.

To discretize the distribution curve, residual tide values were presented in 0.20 probability bins. For example, residual tide is presented between 0.20 and 0.40, 0.40 and 0.60, and etc. Additional binning was completed to provide finer resolution of the distribution curve for large residual tide occurring between 0.95 and 1.00. The median value in each probability bin of the distribution curve was selected as a representative WSE. The magenta boxes in presented in Figure G-1 represent the median value of each probability bin.

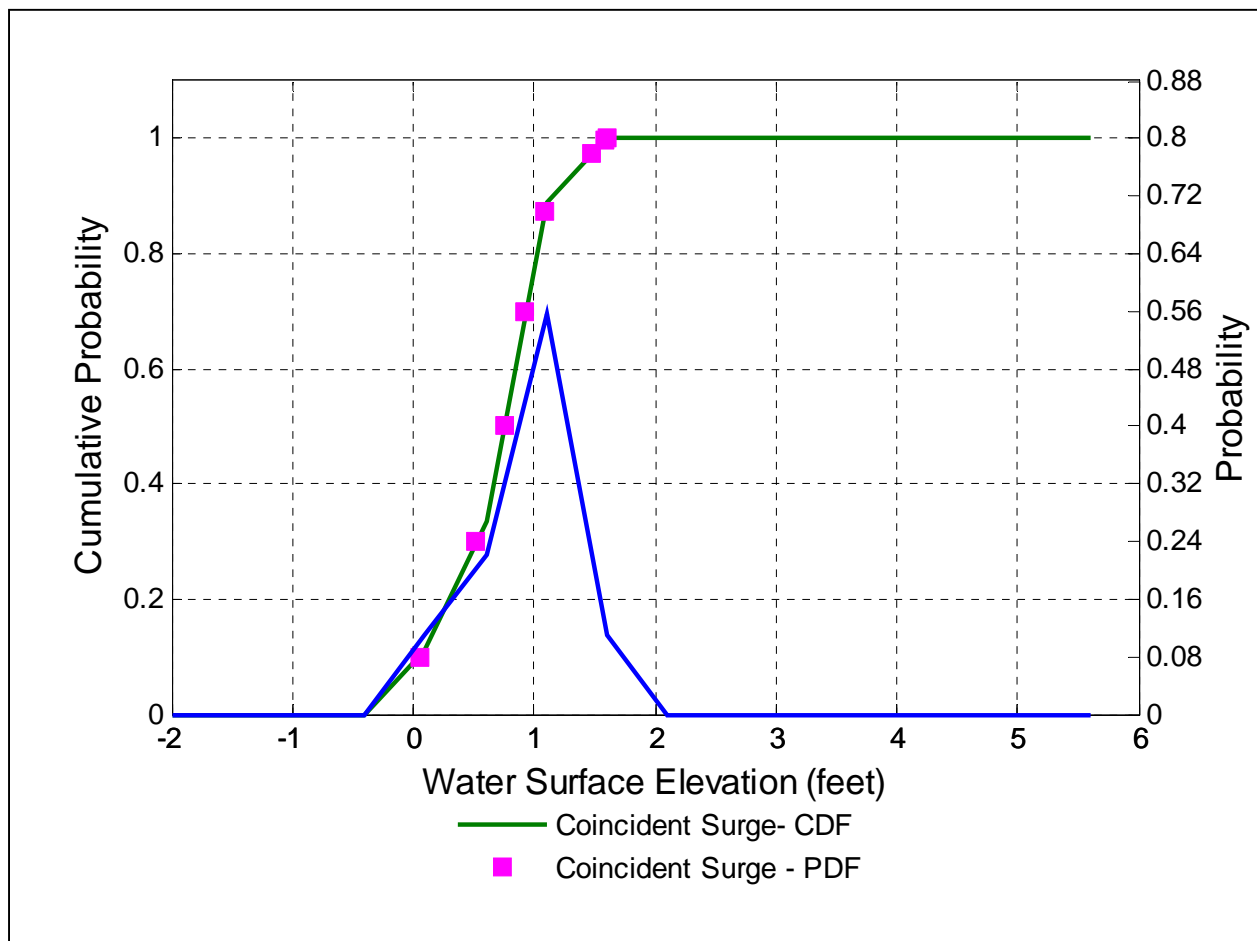


Figure G-1. Year 0 probability distributions

Table G-1. Discretized water surface elevation for Year 0 Conditions

Index	Cumulative Probability	Probability of Occurrence	$\eta_{\text{residual tide}}$ (feet)
1	0.00 - 0.20	0.20	0.05
2	0.20 - 0.40	0.20	0.53
3	0.40 - 0.60	0.20	0.75
4	0.60 - 0.80	0.20	0.93
5	0.80 - 0.95	0.15	1.09
6	0.95 - 0.995	0.045	1.48
7	0.995 - 0.9999	0.0049	1.59
8	0.9999 - 1.00	0.0001	1.60

APPENDIX H – DESCRITIZED PDF OF EVENT BASED PREDICTED TIDE

To capture the full range of predicted tide for the development of DSBC, a four day record of predicted tide record centered on the peak fluvial flow for each storm event was selected for analysis. In other words, the predicted tide used to form the predicted tide database occurred between two days before the fluvial peak and two days after the fluvial peak of each event. This predicted tide record was selected because a four day period covered multiple cycles of high and low tide.

To discretize the distribution curve, predicted tide values were presented in 0.20 probability bins. For example, residual tide is presented between 0.20 and 0.40, 0.40 and 0.60, and etc. Additional binning was completed to provide finer resolution of the distribution curve for large residual tide occurring between 0.95 and 1.00. The median value in each probability bin of the distribution curve was selected as a representative WSE. The magenta boxes in presented in Figure H-1 represent the median value of each probability bin.

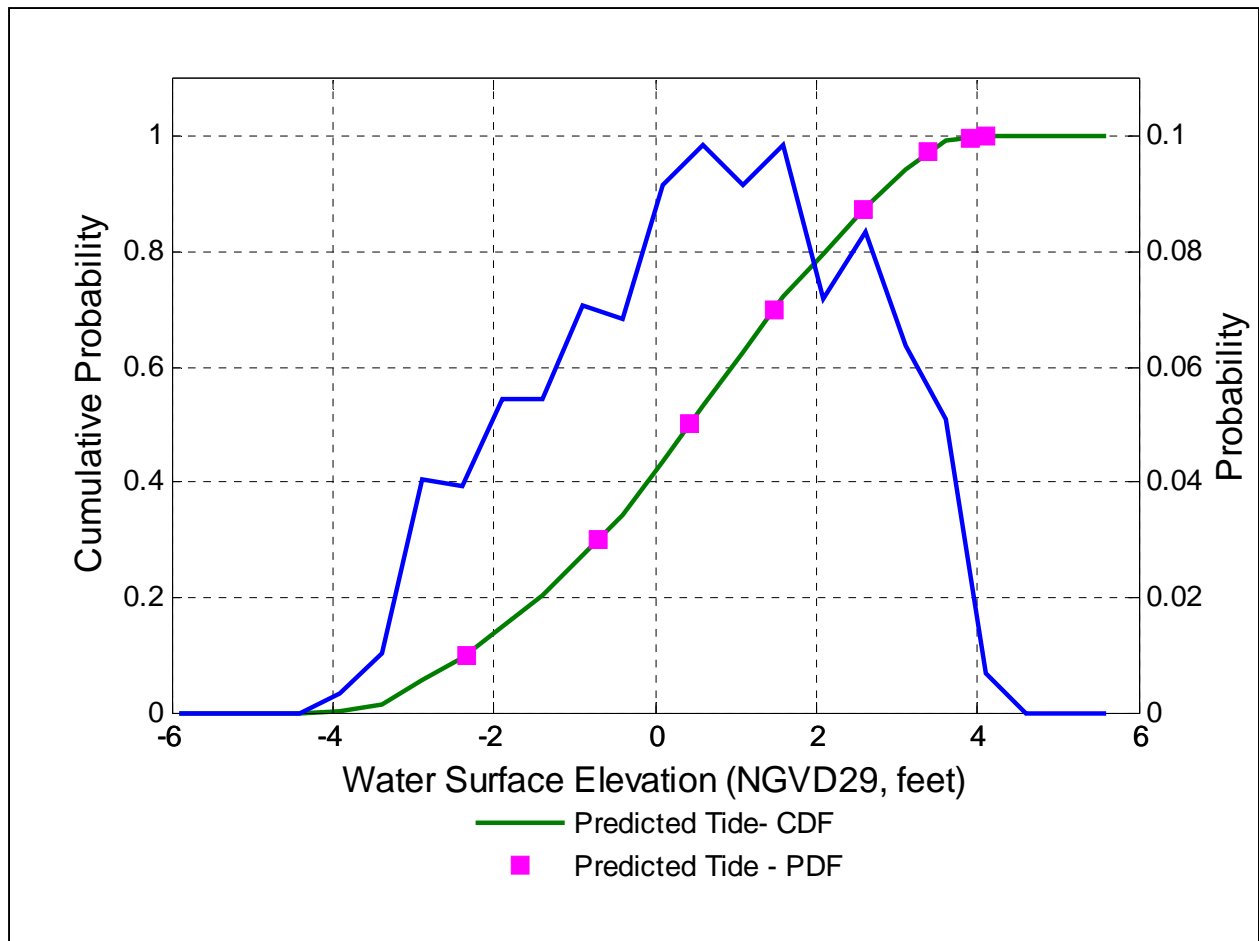


Figure H-1. Year 0 probability distributions

Table H-1. Discretized water surface elevation for Year 0 Conditions

Index	Cumulative Probability	Probability of Occurrence	$\eta_{\text{predicted tide}}$ (feet)
1	0.00 - 0.20	0.20	-2.15
2	0.20 - 0.40	0.20	-0.53
3	0.40 - 0.60	0.20	0.62
4	0.60 - 0.80	0.20	1.68
5	0.80 - 0.95	0.15	2.76
6	0.95 - 0.995	0.045	3.55
7	0.995 - 0.9999	0.0049	4.09
8	0.9999 - 1.00	0.0001	4.20

Appendix F

Las Gallinas Creek

Marin County, CA

Hydraulic Loading Analysis

Prepared By:

U.S. Army Corps of Engineers

San Francisco District

September 16, 2013

Contents

INTRODUCTION	1
COINCIDENT FREQUENCY ANALYSIS.....	2
JOINT STAGE PROBABILITY	18
LEVEED AREA INTERIOR STAGE PROBABILITY.....	22
DISCUSSION	26
SUMMARY	26
REFERENCES.....	28

Tables

TABLE 1. PEAK FLOW VALUES IN LAS GALLINAS CREEK	6
TABLE 2. DISCRETIZED TIDAL VALUES, REPRESENTING LAS GALLINAS CREEK OUTLET, INCLUDING YEAR 50 NRC CURVES FOR SEA LEVEL RISE.....	15
TABLE 3. RIVERINE STAGE-PROBABILITY VALUES (COINCIDENT FREQUENCY ANALYSIS RESULTS).....	18
TABLE 4. COASTAL (AND JOINT) STAGE-PROBABILITY VALUES.....	19

Figures

FIGURE 1. EXAMPLE OF SITUATION REQUIRING COINCIDENT FREQUENCY ANALYSIS.....	3
FIGURE 2. AERIAL VIEW OF SANTA VENETIA AREA AND LOCATION OF INDEX POINT, STA 80+75.....	4
FIGURE 3. SAMPLE PROBABILITY DISTRIBUTION OF VARIABLE A, FLOW (CFS) IN LAS GALLINAS CREEK (AT OUTLET)...	6
FIGURE 4. VARIABLE C AS A FUNCTION OF VARIABLES A AND B	7
FIGURE 5. PROBABILITY DISTRIBUTION OF VARIABLE B.....	7
FIGURE 6. CONDITIONAL PROBABILITY DISTRIBUTION OF VARIABLE C GIVEN VARIABLE B	8
FIGURE 7. CUMULATIVE PROBABILITY DISTRIBUTIONS FOR VARIABLE B, TIDAL BOUNDARY CONDITION FOR VARIOUS SEA LEVEL RISE SCENARIOS.....	11
FIGURE 8. YEAR 0 TIDAL DISCRETIZATIONS.....	12
FIGURE 9. YEAR 50 - HISTORIC TREND SEA LEVEL RISE TIDAL DISCRETIZATIONS	13
FIGURE 10. YEAR 50 CURVE 1 SEA LEVEL RISE TIDAL DISCRETIZATIONS	14
FIGURE 11. YEAR 50 CURVE 3 SEA LEVEL RISE TIDAL DISCRETIZATIONS	15
FIGURE 12. STAGE-PROBABILITY CURVES AT STA 80+75	17
FIGURE 13. JOINT, RIVERINE AND COASTAL-ONLY STAGE-PROBABILITY CURVES FOR YEAR 0 (EXISTING CONDITIONS)	19
FIGURE 14. JOINT, RIVERINE AND COASTAL-ONLY STAGE-PROBABILITY CURVES, YEAR 50 HISTORIC SEA LEVEL RISE 20	
FIGURE 15. JOINT, RIVERINE AND COASTAL-ONLY STAGE-PROBABILITY CURVES, YEAR 50 NRC CURVE 1 SEA LEVEL RISE.....	21

FIGURE 16. JOINT, RIVERINE AND COASTAL-ONLY STAGE-PROBABILITY CURVES, YEAR 50 NRC CURVE 3 SEA LEVEL RISE.....	21
FIGURE 17. VOLUME-ELEVATION CURVE FOR SANTA VENETIA NEIGHBORHOOD	22
FIGURE 18. TIDAL BOUNDARY CONDITION USED DURING LEVEE BREACH ANALYSIS	24

Introduction

Earthen Levees and wooden floodwalls currently protect the Santa Venetia neighborhood in Marin County, CA from flood waters in Las Gallinas Creek. The structures are subject to periodic hydraulic loading from both high tide events and high flows in Las Gallinas Creek. The actual level of protection the structures provide was studied by the US Army Corps of Engineers, San Francisco District (SPN). The probability of the structure being loaded and/or overtopped was assessed, while taking into consideration both riverine and coastal influences.

Detailed Corps studies related to hydrology, hydraulics, and coastal processes preceded this analysis. A geotechnical investigation has been performed by Kleinfelder, Inc for Marin County (Kleinfelder 2013). The Las Gallinas Creek Hydrologic Analysis is included as Appendix B. Precipitation, topography, soil type, land use, impervious area and channel geometry data were integrated using a geographic information system (GIS) and hydrologic modeling software (HEC-HMS). Stormwater runoff hydrographs and peak flow values were determined for a number of locations in the Gallinas Creek watershed and along Las Gallinas Creek.

Peak flow values from the hydrology study were used in hydraulic modeling, which quantified the probability of a water surface elevation (or stage) being exceeded in any given year due to stormwater runoff. The original hydraulic modeling study, Las Gallinas Creek Hydrology, Hydraulics and Coastal Study, which is included as Appendix D, assumed the tidal boundary condition to be mean higher high water (MHHW, 3.58 ft NGVD 29), as defined by the National Oceanic and Atmospheric Administration (NOAA) for the gage at Hamilton (Station ID: 9415124). Although MHHW is a commonly-used, conservative assumption in hydraulic modeling, anecdotal evidence from the study area suggested that the coincidence of a storm event with a high tide and storm surge event was likely, and should therefore be studied explicitly. A range of downstream boundary conditions for use in a coincident frequency analysis were developed by analyzing local tide gage records. The report of that analysis, Las

Gallinas Creek Downstream Boundary Condition Analysis is included in this report as Appendix E.

The levees along Las Gallinas Creek are required to withstand hydraulic loading during riverine events (stormwater runoff) coastal events (king tide, storm surge, etc), and combinations thereof. The probability of loading due to a riverine event coinciding with a coastal event was determined using a coincident frequency analysis in the present study. The probability of loading due to a coastal event was determined by a tide gage analysis, described in Appendix B. The combined probability of hydraulic loading due to a stormwater runoff event, a coastal event, or a combination thereof, was calculated using the law of total probability. Coastal stillwater elevations are significantly higher than the river stage elevations, and therefore represent the greater risk to the leveed area.

If the levee were to fail, whether due to a breach prior to overtopping or due to the erosive force of flows overtopping the levee crest, inundation will occur in the leveed area. Hydraulic modeling was performed to estimate how deep the flooding would be in the leveed area in relation to the stage in Las Gallinas Creek. The final product of this analysis was a set of stage-probability curves which will be used to determine the overall risk and economic impact of flooding in the levee-protected area.

Coincident Frequency Analysis

Flooding is often the result of multiple factors working together. Usually the probability of a flood event itself will be unknown, even if the contributing factors have known probability distributions. Examples of flooding affected by coinciding conditions include:

- Confluence flooding: the water level in a tributary upstream of a confluence will be affected both by the flow in the tributary itself and the backwater from the flow in the mainstem. See Figure 1.

- Interior flooding: water levels on the landside (i.e., interior) of a levee can be affected not only by interior storm runoff, but also an inability to pass flows through the levee via pipes or pumps when the river stage on the waterside of the levee is high.
- Situations involving storms and obstructed flow: ice jams, debris yield, or mud

A pictographic example of a situation requiring a coincident frequency analysis is presented in Figure 1. Variables A and B, the tributary flow rate and the stage in the mainstem, have known probability distributions. The unknown variable of interest is the tributary stage, Variable C, which is a function of both the flow in the tributary and the stage of the mainstem. This is analogous to the situation in the current study, where Gallinas Creek is the “tributary” to the San Pablo Bay, and San Pablo Bay is the “mainstem”. The purpose of the CFA was to determine Variable C, the “tributary” stage at an index point where flood damage may occur.

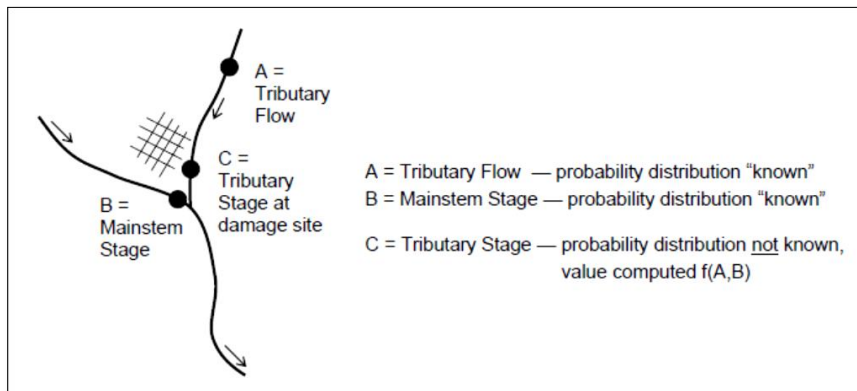


Figure 1. Example of situation requiring coincident frequency analysis

For purposes of this report, river station 80+75 was selected as the location to determine stage (Variable C). This is the lowest point of the redwood floodwall, as identified by the 2006 Marin County survey. Station 80+75 is therefore the location of incipient overtopping of the levee along Las Gallinas Creek. The location of Sta 80+75 is shown in Figure 2.

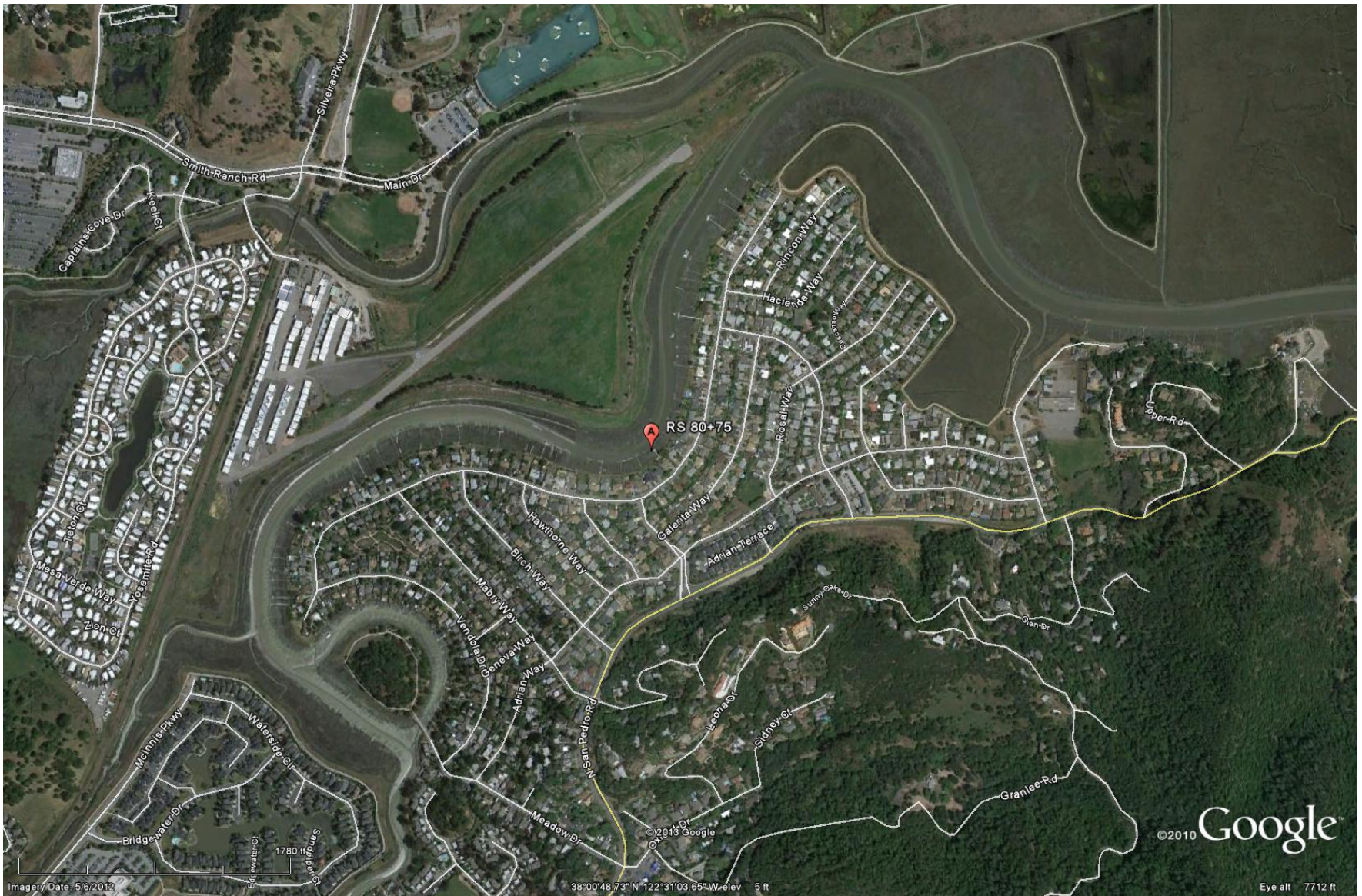


Figure 2. Aerial view of Santa Venetia area and location of index point, Sta 80+75

In some cases it is clear that several conditions will contribute to a flood stage, but their statistical relationship may not be apparent. These simultaneous or “coincident” causes may be perfectly correlated, that is, statistically more likely to occur together, or they may be independent. However, because the variable of interest, flood level, is a function of each of the contributing causes, their joint probability must be used to predict flooding frequency. Therefore, the purpose of a coincident frequency analysis is to calculate the joint probability of two or more variables, the effects of which coincide at a particular location of interest.

A stage frequency curve can be developed for a stream if there is a stream gage in the stream and sufficient historical observations. However, in a tidally influenced system the occurrence of the “100 year” or, more accurately, the 1% exceedance storm (or any other storm), may not directly correlate to the same frequency flood because of the potential for a tidal backwater effect. A statistical relationship between the flow, tide, and corresponding river stage must be developed to accurately determine the stage frequency curve for the stream.

Variable A is often used to represent flow in a creek or tributary as the result of a storm event with a particular probability. Storms with the following annual probabilities are of interest for this analysis: 0.5, 0.2, 0.1, 0.04, 0.02, 0.01, 0.004, and 0.002. Figure 3 shows the exceedance probability distribution for Variable A, flow (cfs), on Las Gallinas Creek; peak flow values used in the hydraulic model at four locations are presented in Table 1.

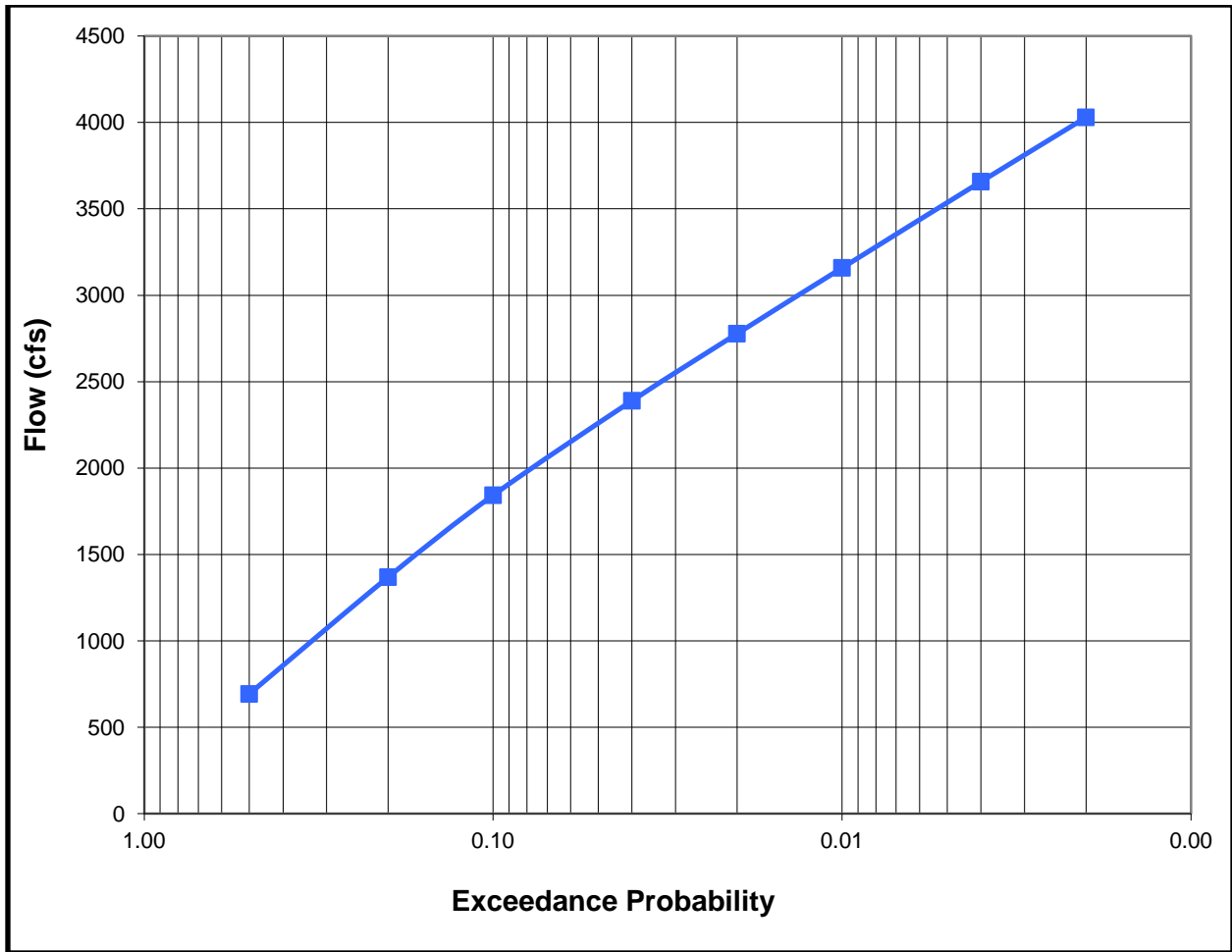


Figure 3. Sample probability distribution of Variable A, flow (cfs) in Las Gallinas Creek (at outlet)

Table 1. Peak flow values in Las Gallinas Creek

Location	Peak Flow Rates by Exceedance Probability (cfs)							
	0.5	0.2	0.1	0.04	0.02	0.01	0.004	0.002
Las Gallinas Creek @ outlet, RS 52+57	693	1369	1843	2390	2778	3159	3658	4030
Las Gallinas Creek @ RS 62+02	340	679	920	1200	1401	1596	1854	2049
Las Gallinas Creek @ RS 84+15	334	670	908	1185	1383	1577	1833	2025
Las Gallinas Creek @ RS 116+79	286	583	795	1042	1220	1393	1621	1794

It is reasonable and resource-efficient to calculate only the values for Variable A that have meaning to us (typically the eight probabilities, 0.5 to 0.002, listed above) and for which we have data. Therefore, the data for Variable B must span the full range of probability of B so that any value of C can be found by interpolating across B for a specific A. Figure 4 shows that when representing a relationship between three variables on a 2-dimensional plot, each B results in a new A vs. C curve.

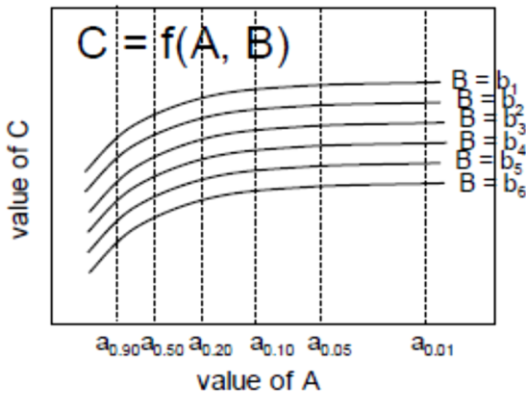


Figure 4. Variable C as a function of Variables A and B

The full range of B can be discretized for easier processing and calculations. Figure 5 shows a duration curve for a generic Variable B that has been discretized into ranges b1 through b6, where b1 and b6 each represent 10% of the range and b2 through b5 represent 20% each.

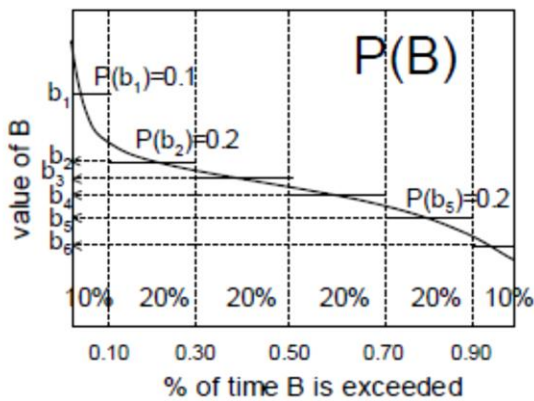


Figure 5. Probability distribution of Variable B

Since B, the tidal stage at the mouth of Las Gallinas Creek, has a full duration curve spanning its probability (Figure 6), the conditional probability of C (example: $c_{0.01}$ is the flood stage, C, with an exceedance probability of 0.01 or 1%), given a particular value of A ($a_{0.01}$), can be found for any B. Hence, the value of C computed from $A = a_{0.01}$ and $B = b_1$ is $C = c_{0.01}|b_1$ (read as the 1% exceedance value of C, given that $B = b_1$.) The combination of the frequency curve for A and the computations of C given A and B produce an array of conditional probability curves for “C given B”, such as the one shown in Figure 6.

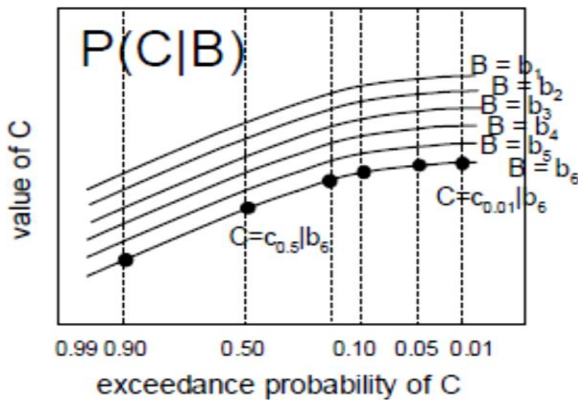


Figure 6. Conditional probability distribution of Variable C given Variable B

Before we can find the probability distribution of C, we must first determine the relationship between tidal stage (B) and stream flow (A) that determine river stage (C). If the two are found to be independent, we can use the Total Probability Method as discussed below to calculate the probability of a certain river stage at a given index location.

According to USACE Engineering Manual (EM) 1110-2-1413, the relationship between two events can vary from completely non-coincident (i.e. they never coincide) to completely coincident (i.e. they always coincide). In the middle of these two extremes, the two events are completely independent (i.e. they may or may not coincide, with no correlation), as shown below:

Completely Non-Coincident ----- Independent ----- Completely Coincident

The stage in the bay is in large part determined by the completely independent astronomical tidal cycle, but may also experience surges due to meteorological effects such as wind and low pressure. The difference between the astronomically predicted tide elevation and the observed value is known as the non-tidal residual. Flow in Las Gallinas Creek is not affected at all by the astronomical tidal cycle, but likely would be affected by storms or other meteorological events that also have an effect on stage in the bay. Conceptually, we can see that there may be some coincidence between tidal stage and flow due to meteorological events, but because the tidal cycle is the primary driver of stage in the bay, the relationship between the tidal stage and flow in Las Gallinas Creek is likely closer to being independent than to being completely coincident. The stage in the bay fluctuates significantly even where there is no change in the flow of Las Gallinas Creek.

Flow records from Las Gallinas Creek were insufficient to statistically quantify the local correlation between streamflow and tidal boundary condition, but an extensive record exists at nearby Corte Madera Creek. As described in detail in Appendix E, the correlation coefficient (R value) between the non-tidal residual and flow in Corte Madera Creek is 0.01, indicating that the variables are independent. Therefore, the Total Probability Method can be used to determine the probability distribution of C.

The goal of the coincident frequency analysis is to find the single-variate probability distribution of C, stage at an index point along the stream. In Figure 5, we know the probability of C for a given B, but the conversion from a multi-variate distribution, such as the distribution shown in Figure 5, to a single-variate distribution requires a weighted summation over Variable B.

The Total Probability Method uses the Law of Total Probability to determine the probability distribution of the variable of interest, C. The Law of Total Probability is defined as:

$$P(C) = \sum_B [P(C | B) * P(B)]$$

C represents the stage at an index point. For purposes of this report, an index point was selected for analysis at river station 80+75, the lowest point identified by the 2006 Marin

County survey. Station 80+75 is the location of incipient overtopping of the levee along Las Gallinas Creek. $P(C)$ represents the probability of a particular stage occurring, and calculating $P(C)$ for every B is the purpose of doing the coincident frequency analysis.

$P(C|B)$ is the probability of a particular C, given that a particular B exists. This can also be called the conditional probability of C given B. So for each B, the probability of C is found and multiplied by the probability of B and these values are summed over the full range of B. This is why Variable B requires a full duration probability curve: so that it can be summed across for every value of B.

Variable B must be a contributing variable with a known probability duration curve. In this case, B represents the tidal stage in the San Pablo Bay at the outlet of Las Gallinas Creek. $P(B)$ is the probability of a particular B. Four alternative tidal distributions were evaluated in this analysis: existing conditions (Year 0) and three sea level rise scenarios for future conditions (Year 50) from EC 1165-2-212 (2011), the official USACE guidance on sea level rise. Cumulative probability distributions for Variable B for the four tide scenarios are shown in Figure 7.

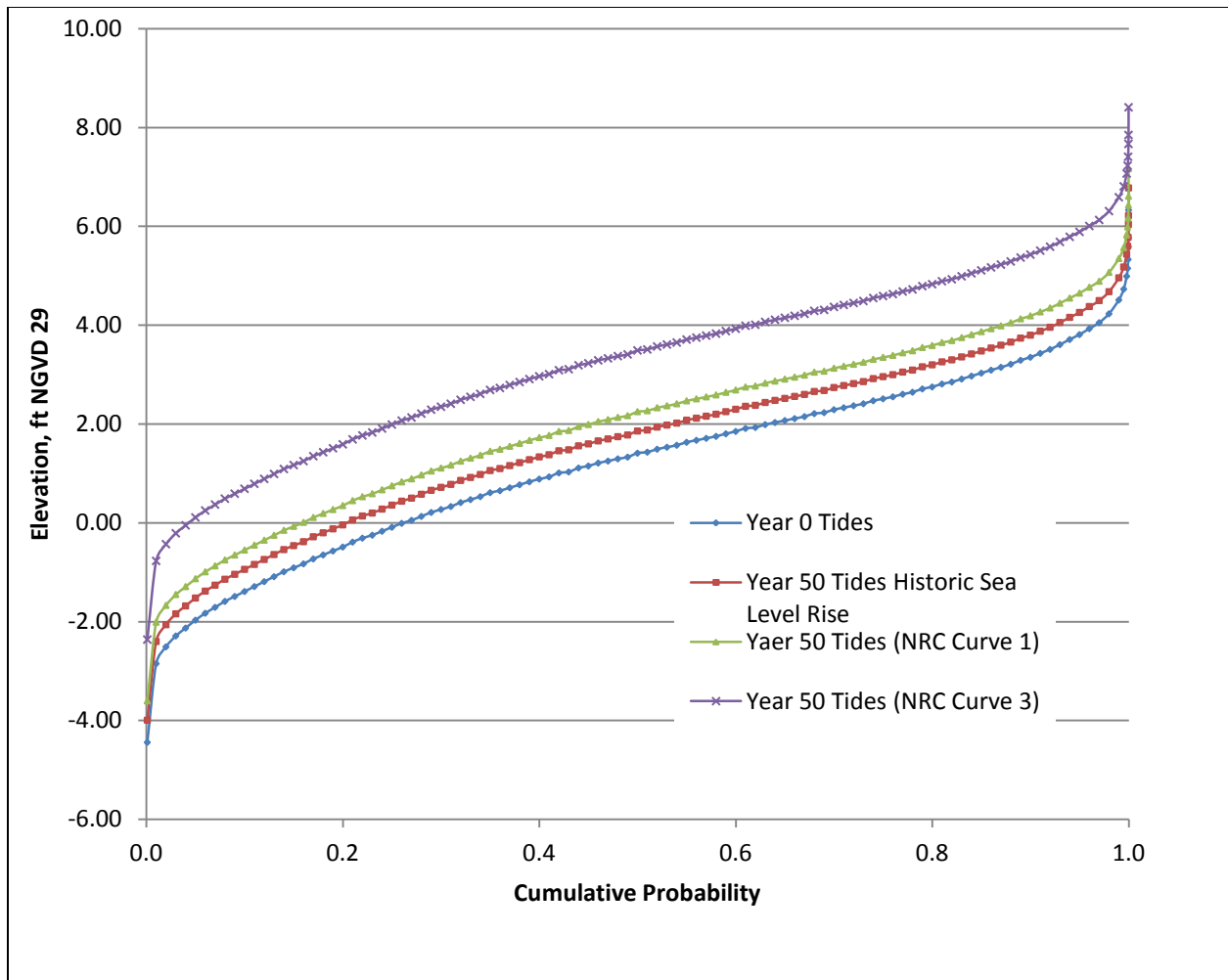


Figure 7. Cumulative probability distributions for Variable B, tidal boundary condition for various sea level rise scenarios

A one-dimensional hydraulic modeling program known as HEC-RAS was used to determine river stage at an index location (C) for a given A (flow) and B (tidal stage). It would be impossible to run a HEC-RAS model to determine river stage for every value of B, as there could be infinite values, so the stage-probability curve of B must be discretized into a manageable number of B values. The discretization of B must span the range of B and the sections must not overlap. In the case of Las Gallinas Creek, the tidal range was divided into 8 ranges. With the 8 storm frequencies, having 8 tidal ranges resulted in 64 flow-tide combinations, which is a manageable number to model in HEC-RAS. Pink bars in Figures 8 - 11 show how the San Pablo Bay tidal range at the Las Gallinas Creek outlet was discretized for each of the tidal sea level rise

scenarios. These discretized values, presented in Table 2, were incorporated into the HEC-RAS model for Las Gallinas Creek to obtain stages at the index point.

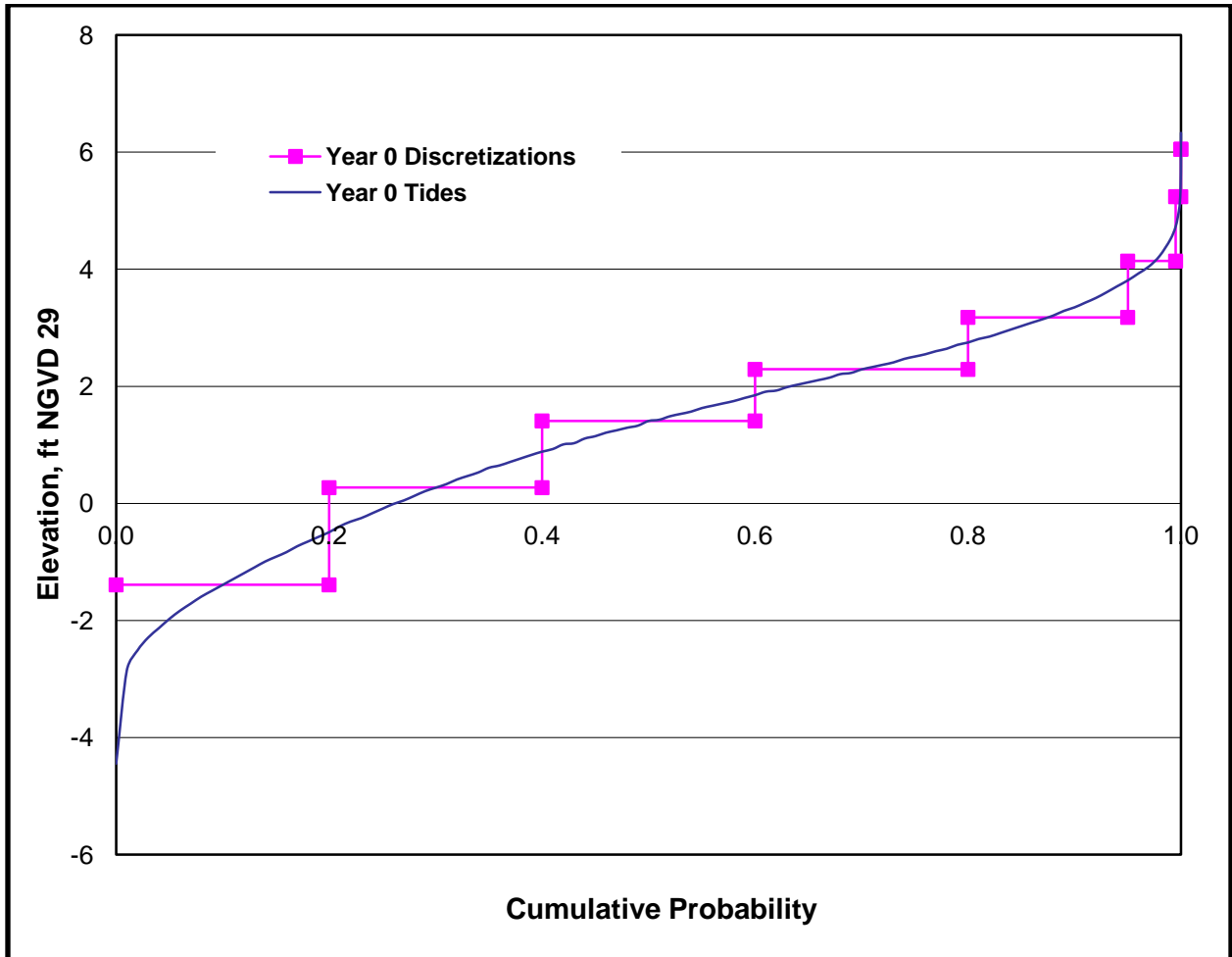


Figure 8. Year 0 tidal discretizations

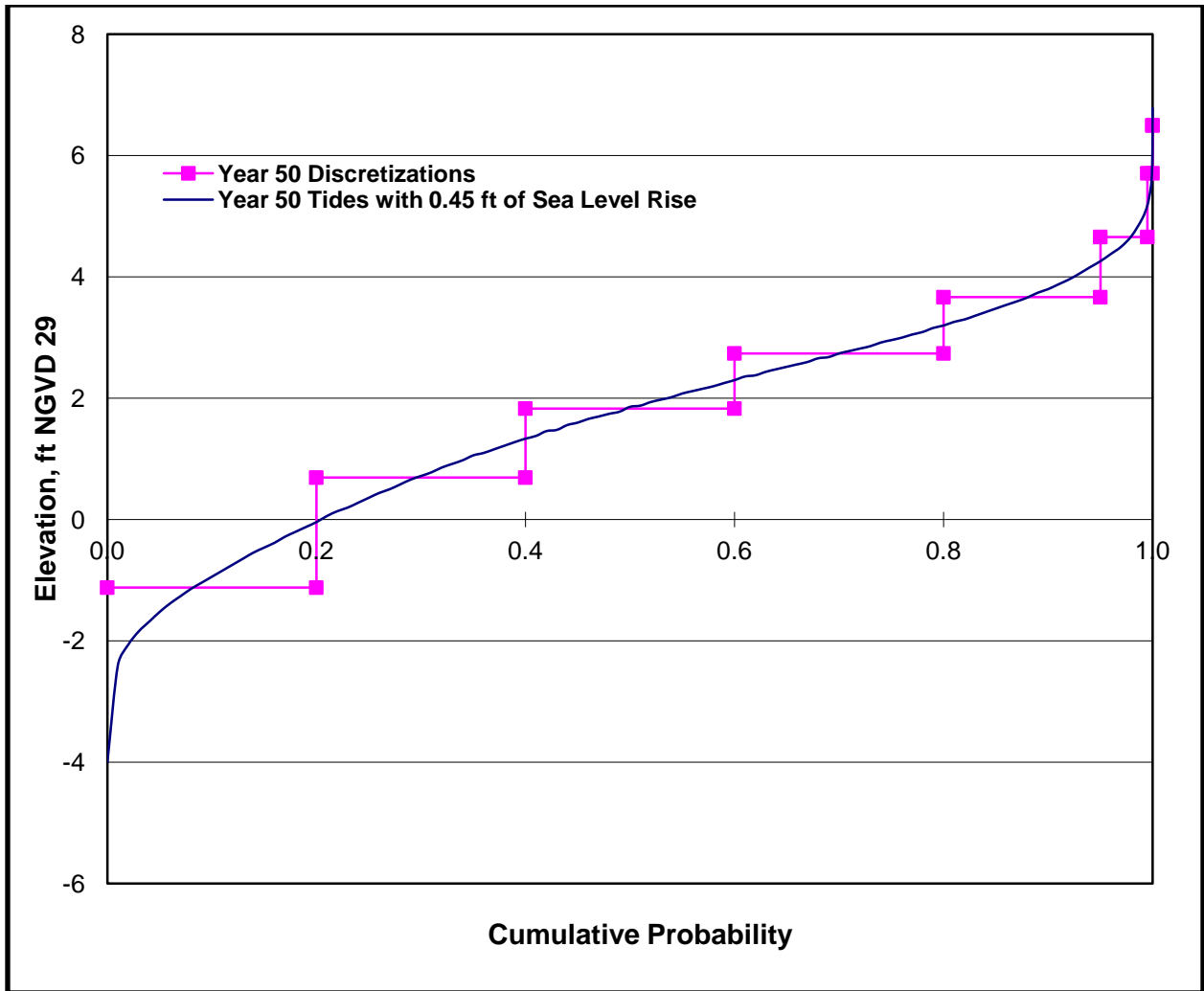


Figure 9. Year 50 - Historic Trend sea level rise tidal discretizations

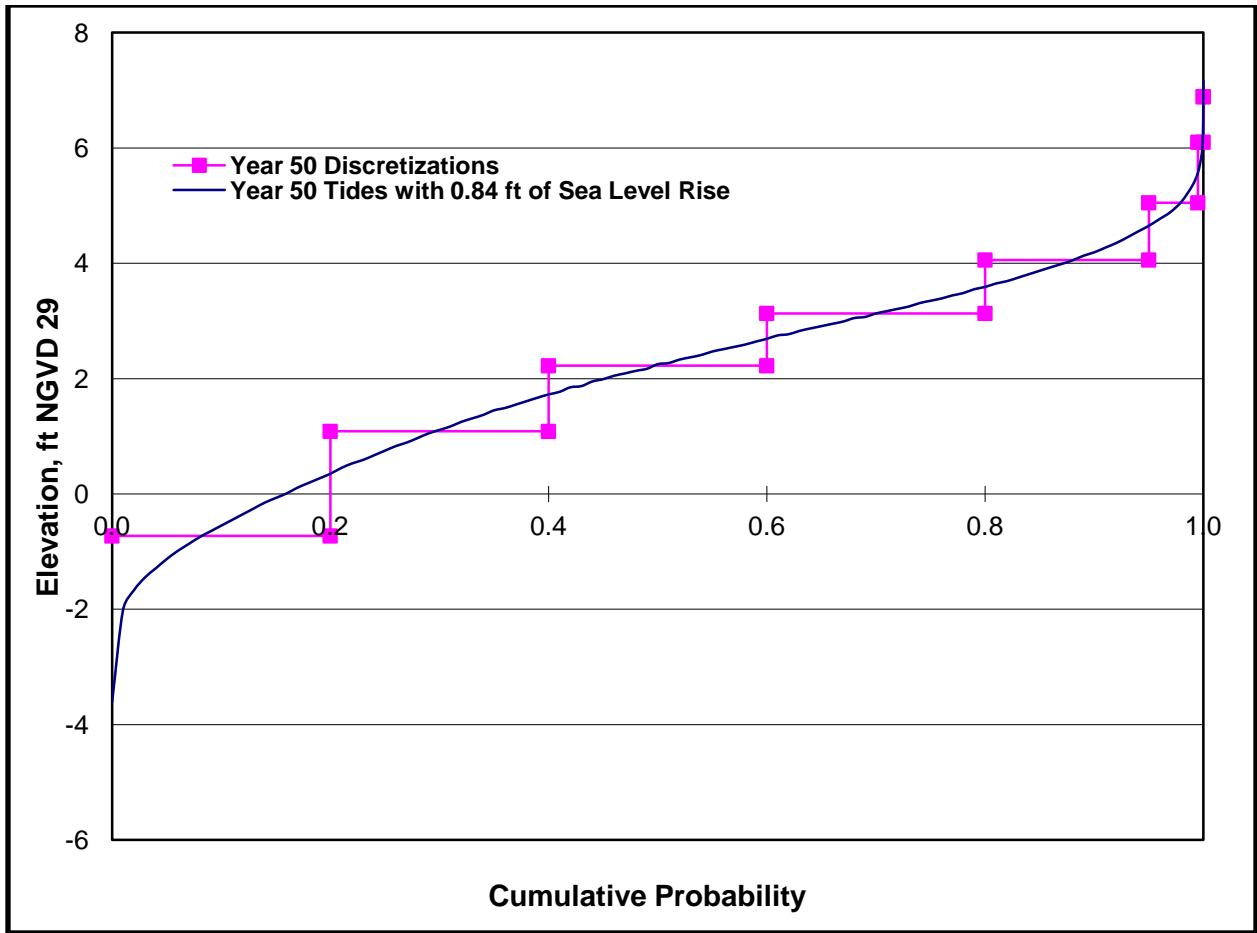


Figure 10. Year 50 Curve 1 sea level rise tidal discretizations

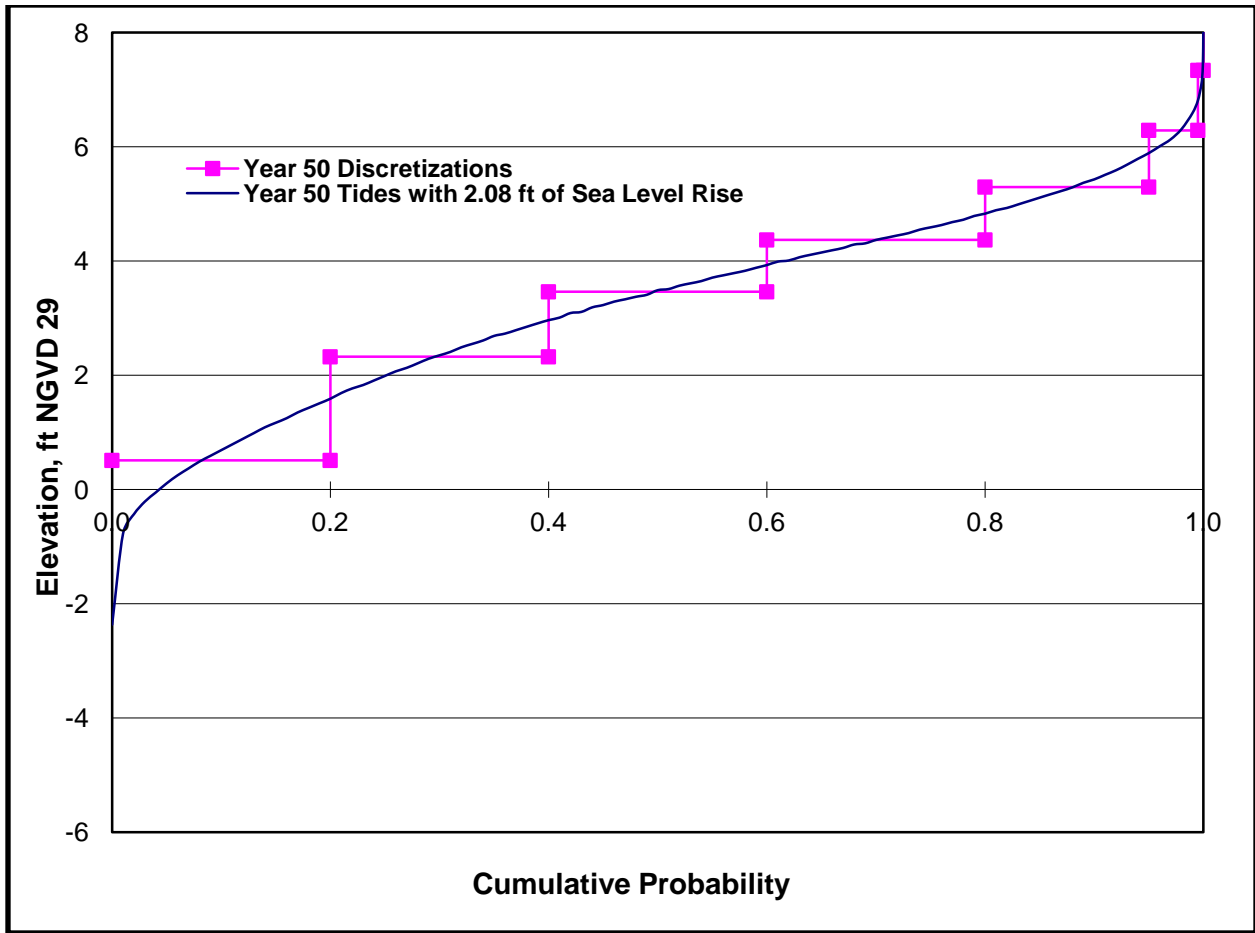


Figure 11. Year 50 Curve 3 sea level rise tidal discretizations

Table 2. Discretized Tidal Values, representing Las Gallinas Creek outlet, Including Year 50 NRC Curves for Sea Level Rise

Cumulative Probability Upper Limit (% of Time Not Exceeded)	Range of Probability Represented (b _i)	Year 0 (NGVD 29, ft)	Yr 50, Historic (NGVD 29, ft)	Yr 50, Curve I (NGVD 29, ft)	Yr 50, Curve III (NGVD 29, ft)
20	20%	-1.39	-1.12	-0.73	0.51
40	20%	0.27	0.69	1.09	2.33
60	20%	1.41	1.83	2.22	3.46
80	20%	2.29	2.74	3.13	4.37
95	15%	3.18	3.67	4.06	5.30
99.5	4.5%	4.14	4.66	5.05	6.29
99.99	0.49%	5.24	5.71	6.10	7.34
100	0.01%	6.05	6.50	6.89	8.13

$P(C|B)$ is called the conditional probability of C given B. So for each B, the probability of C is found and multiplied by the probability of B and these values are summed over the full range of B. This is why Variable B requires a full duration probability curve: so that it can be summed across for every value of B.

The relationship between the multiple $P(C|B)$ curves and the $P(C)$ curve is the Law of Total Probability. Here is an example of the law as applied to a value of C, c_1 :

$$P(c_1) = [P(c_1|b_1)*P(b_1)] + [P(c_1|b_2)*P(b_2)] + [P(c_1|b_3)*P(b_3)] \dots$$

$$\dots + [P(c_1|b_4)*P(b_4)] + [P(c_1|b_5)*P(b_5)] + [P(c_1|b_6)*P(b_6)] + [P(c_1|b_7)*P(b_7)] + [P(c_1|b_8)*P(b_8)]$$

Where:

Probability $P(c_i|b_i)$ is read from the horizontal axis in Figure 6

Probability $P(b_i)$ is noted in the tidal discretization table (Table 2)

In summary, the steps of the process were as follows:

Step 1: Define annual frequency curve for flow in Las Gallinas Creek (Figure 3)

$$A = a_{0.9}, a_{0.5}, a_{0.1} \dots a_{0.002}$$

Step 2: Define duration-based probability distributions of the tidal boundary condition, section the probability range and choose index values, each assuming the probability of its section (Figures 8-11, Table 1)

$$B = b_1, b_2, b_3 \dots b_8$$

Step 3: Compute the stage for every combination of flow and tidal boundary condition using HEC-RAS. These results define the conditional probability curves $C|b_i$ for each b_i

Step 4: Compute the marginal probability for each stage using the Law of Total Probability and a spreadsheet.

The result of the analysis, four stage-probability curves at the Index Point (base condition plus one for each sea level rise scenario), is shown in Figure 12 and Table 3. Stage values in Table 3 highlighted in red exceed the lowest levee crest elevation of 6.6 ft NGVD 29 (Sta 80+75).

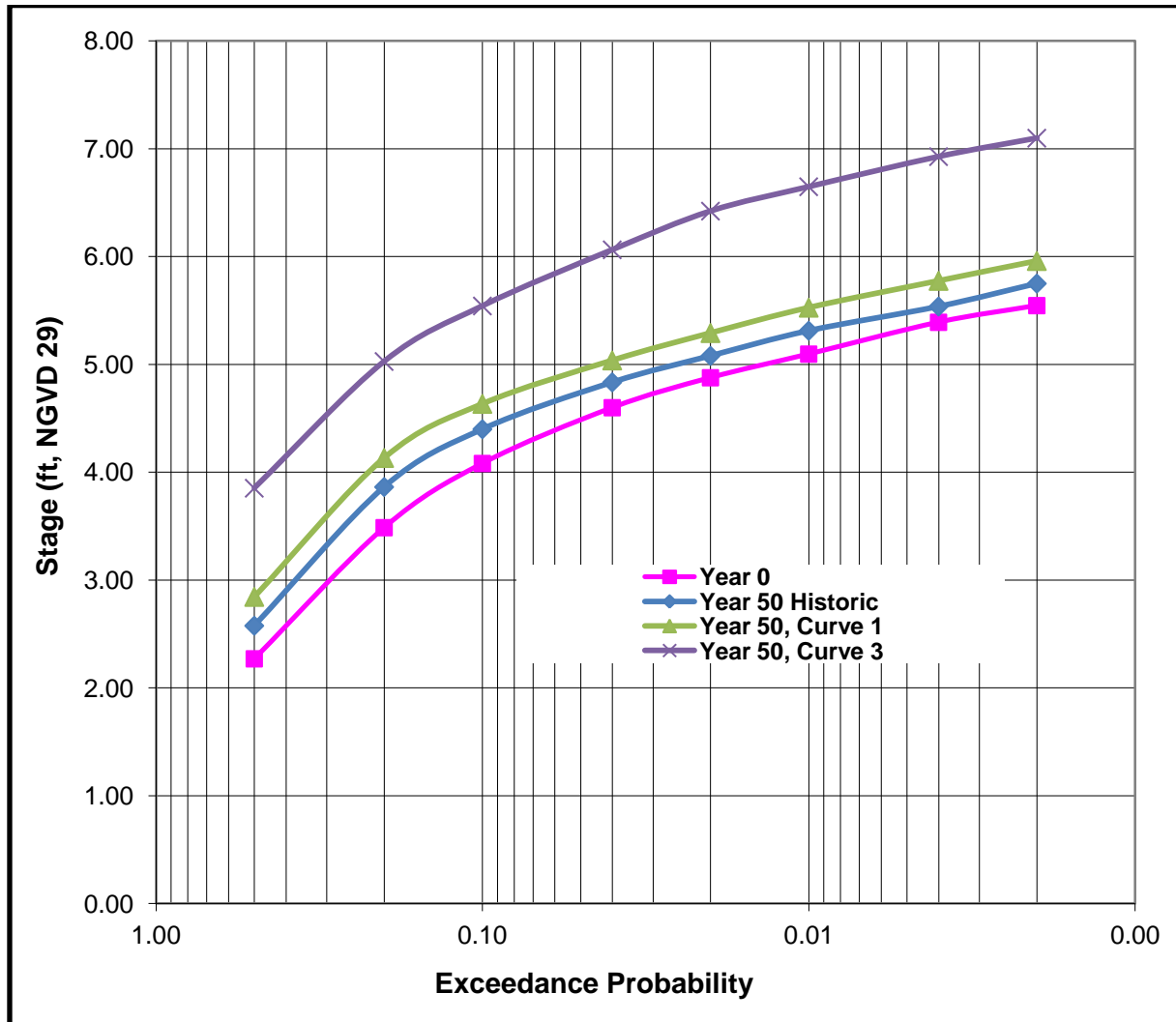


Figure 12. Stage-probabilty curves at Sta 80+75

Table 3. Riverine stage-probability values (coincident frequency analysis results)

Exceedance Probability (%)	Year 0 Condition (ft, NGVD 29)	Year 50 Condition (ft NGVD 29)		
		Historic SLR	NRC 1	NRC 3
50	2.2	2.5	2.8	3.8
20	3.5	3.9	4.1	5.0
10	4.1	4.4	4.6	5.5
4	4.6	4.8	5.0	6.1
2	4.9	5.1	5.3	6.4
1	5.1	5.3	5.5	6.7
0.4	5.4	5.5	5.8	6.9
0.2	5.6	5.8	6.0	7.1

Joint Stage Probability

The joint probability was calculated to determine the likelihood of the levee being loaded from *either* a riverine or a coastal event:

$$P(C,D) = P(C) + P(D) - P(C)P(D)$$

where P(C) is the annual maximum stage-probability at the index point due to a riverine event, and P(D) is the annual maximum stage-probability at the index point due to coastal influences. Coastal still water elevations were determined during a previous study (USACE-SPN, 2012), which used local tide gage data to define Year 0 maxima and USACE guidance to project sea level rise values (Table 4). Comparing Tables 3 and 4, it’s clear that there is a much greater probability of levee loading due to a coastal event than a riverine event in any given year. The contribution of the riverine component is so small that the difference between the coastal and combined stage-probability values is negligible. In Figures 13-16 below, the joint riverine and coastal stage-probability curves are essentially identical to the underlying coastal-only stage-probability curves, therefore the blue still water stage plots are not visible.

Table 4. Coastal (and joint) stage-probability values

Exceedance Probability (%)	Year 0 Condition (ft, NGVD 29)	Year 50 Condition (ft NGVD 29)		
		Historic SLR	NRC 1	NRC 3
50	5.2	5.7	6.0	7.3
20	5.6	6.1	6.4	7.7
10	5.8	6.3	6.6	7.9
4	6.1	6.6	6.9	8.2
2	6.3	6.8	7.1	8.4
1	6.4	6.9	7.2	8.5
0.4	6.6	7.1	7.4	8.7
0.2	6.8	7.3	7.6	8.9

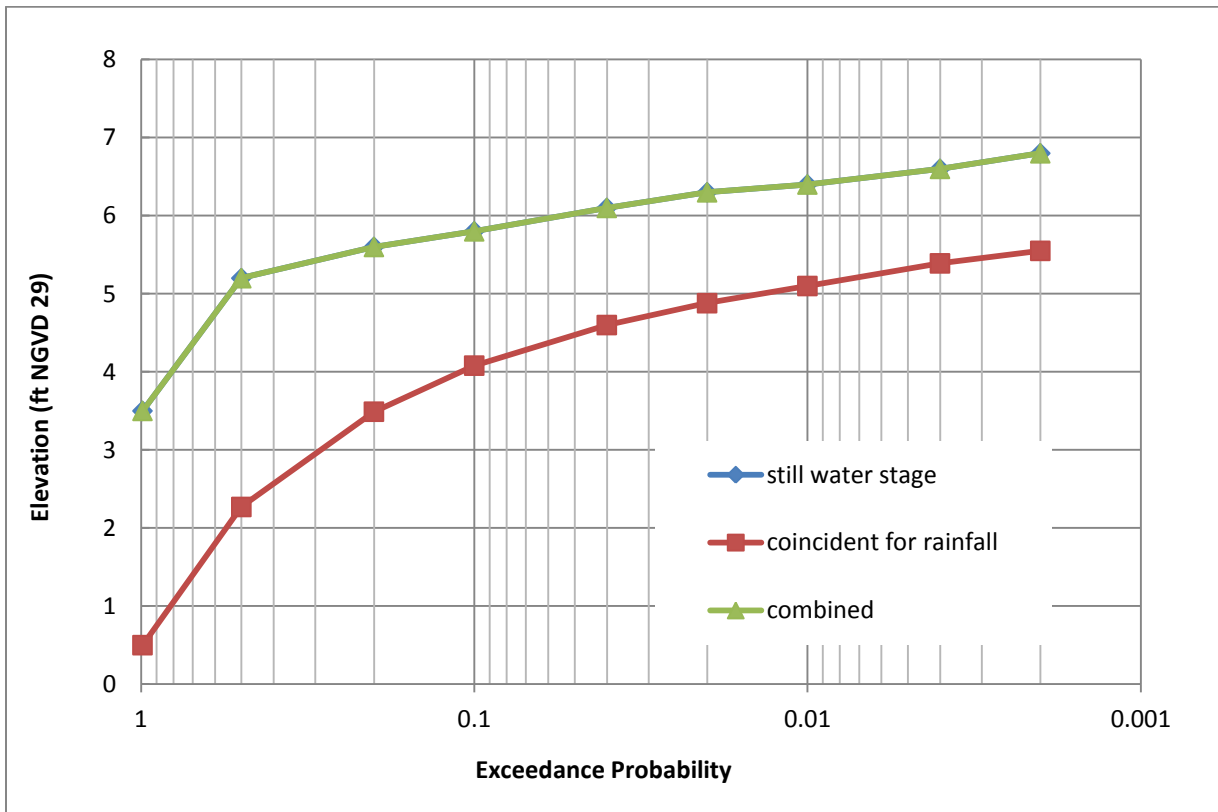


Figure 13. Joint, riverine and coastal-only stage-probability curves for Year 0 (Existing Conditions)

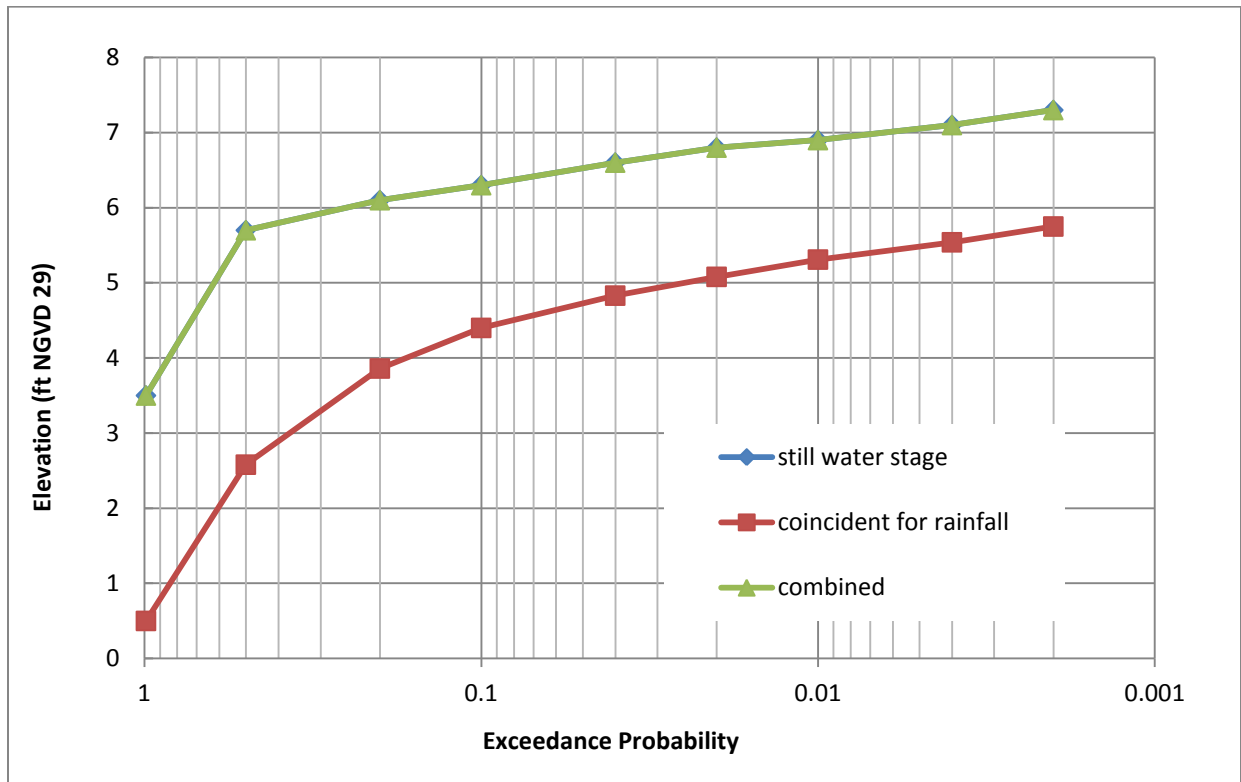


Figure 14. Joint, riverine and coastal-only stage-probability curves, Year 50 Historic Sea Level Rise

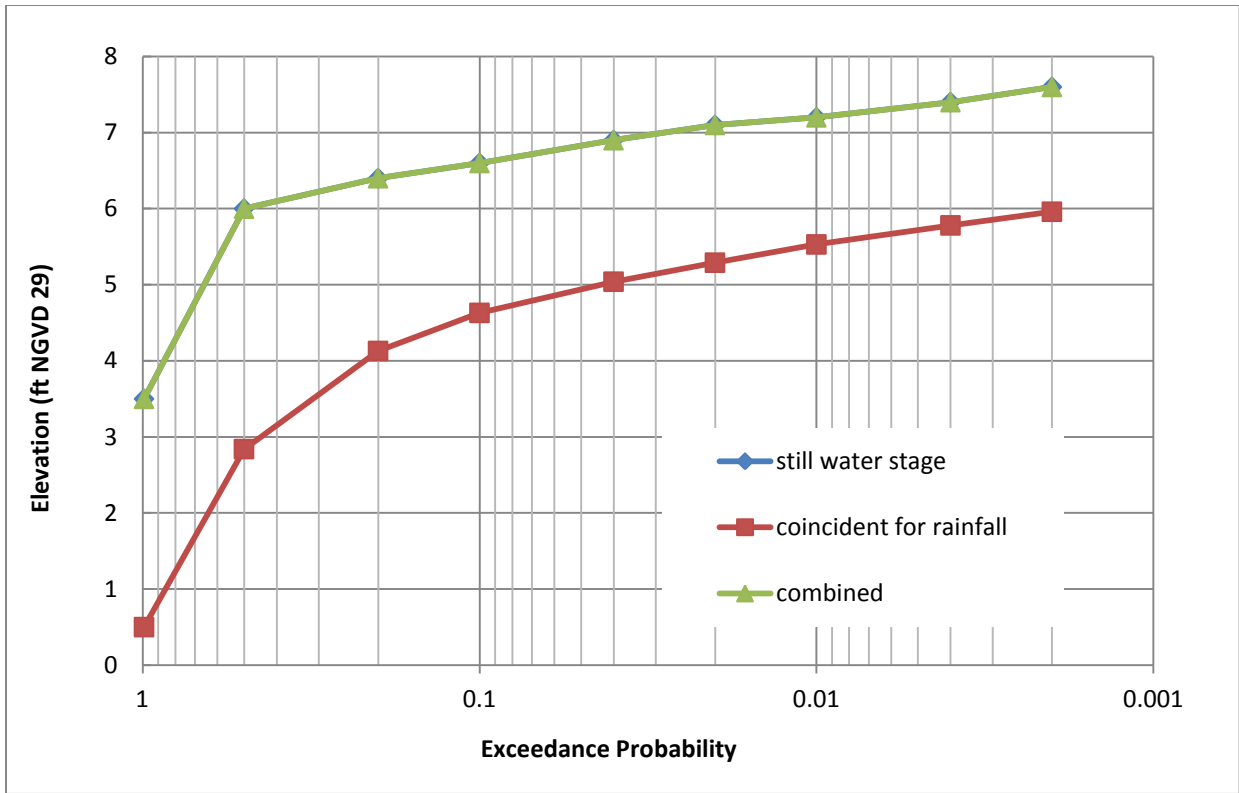


Figure 15. Joint, riverine and coastal-only stage-probability curves, Year 50 NRC Curve 1 Sea Level Rise

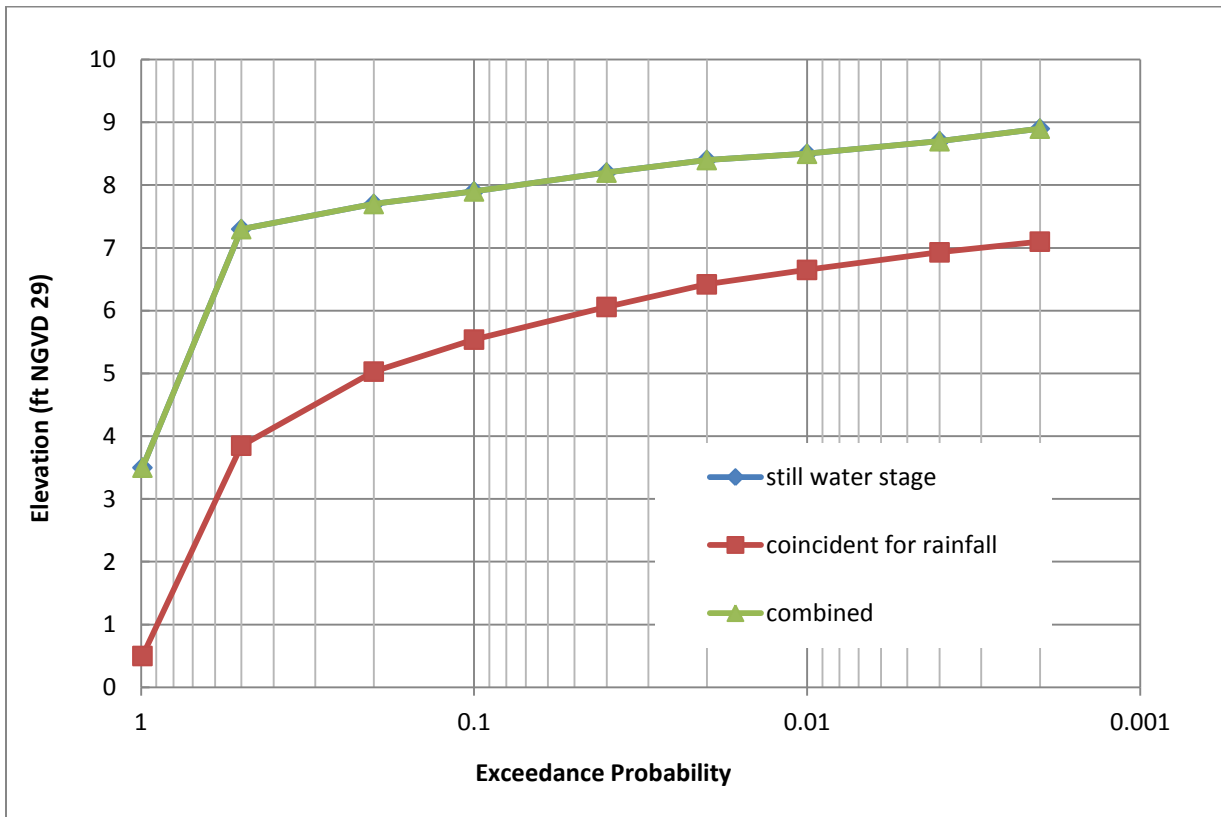


Figure 16. Joint, riverine and coastal-only stage-probability curves, Year 50 NRC Curve 3 Sea Level Rise

Leveed Area Interior Stage Probability

For the purposes of flood modeling, it was assumed that levees and redwood floodwalls separating the Santa Venetia neighborhood from Las Gallinas Creek could potentially fail when subjected to hydraulic loading. The probability of geotechnical failure was recently studied by Marin County (Kleinfelder 2013). The resulting depth of water in the leveed area could be a function of several factors, including the failure mode (overtopping vs. breach prior to overtopping), geometry of the breach, the timing relative to the passage of the flood wave or high tide event, and the performance of the interior drainage pump system. A conservative assumption would be that the interior stage would be equal to the stage in Las Gallinas Creek for any levee failure mode. In reality, the stage in the leveed area is likely to be somewhat lower. For example, the flood wave or tide cycle may be receding when the breach occurs, the pumps may function perfectly, and the breach may be relatively small.

A range of levee breach scenarios were simulated using HEC-RAS to define the interior stage-probability curves. The Santa Venetia neighborhood was simulated by adding a storage area to the one-dimensional HEC-RAS model. Volume of the storage area was calculated as a function of elevation using a geographic information system and LiDAR provided by Marin County for the 2011 USACE hydrology study. The volume elevation curve is presented in Figure 17.

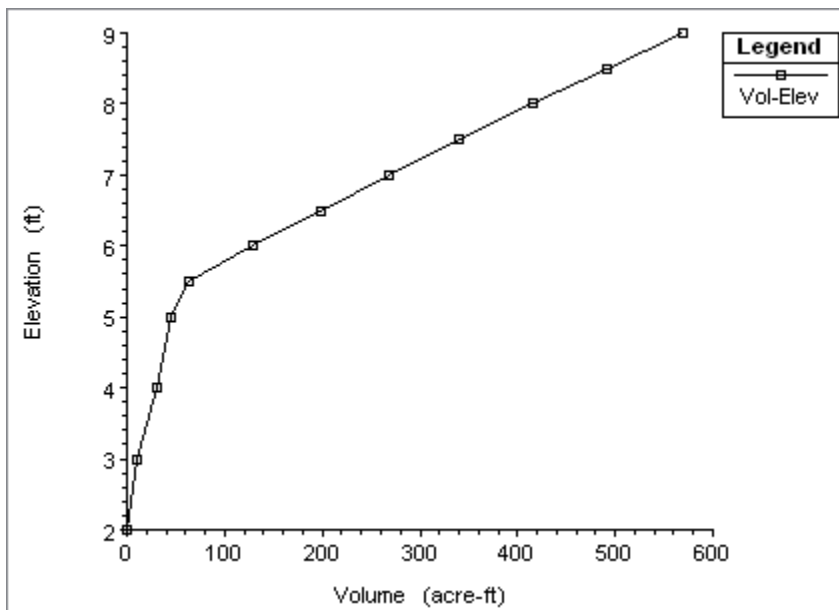


Figure 17. Volume-elevation curve for Santa Venetia neighborhood

The Las Gallinas Creek levee/floodwall structure was represented as a lateral structure connecting the creek to the neighborhood. The actual number of possible breach scenarios is practically limitless, so to make the analysis practical, a set of four events representing a reasonable range of possible events were simulated: (1) Year 0 tide cycle assuming a 10 foot wide breach due to piping failure, with levee breaching to the elevation of the levee toe near the beginning of the tide cycle, (2) a 20 foot wide breach with all other model parameters being the same as Scenario #1, (3) a 100 foot wide breach with all other model parameters being the same as Scenario #1, and (4) Year 50 Curve 3 tide cycle with levee breach due to overtopping. All scenarios assumed that the levee would breach to the ground elevation of 5 ft NGVD 29, have side slopes of 2:1 horizontal to vertical, a weir coefficient of 2.6, breach formation time of 15 minutes, and no immediate repairs would be made.

The joint stage probability analysis showed that coastal processes are the main drivers of flood risk to the leveed area. Therefore, the flow Las Gallinas Creek was held constant at 500 cfs and the tidal boundary condition varied following the astronomical tide cycle, with maximum values defined by the coastal still water analysis (Table 4). The flow value of 500 cfs was selected using engineering judgment. It is slightly less than the average annual maximum peak flow and represents a reasonable flow rate to occur during a coastal flow event based on stormwater runoff probability. The timing of the levee breach during the breach-prior-to-overtopping scenarios is shown relative to the tide cycle in Figure 18.

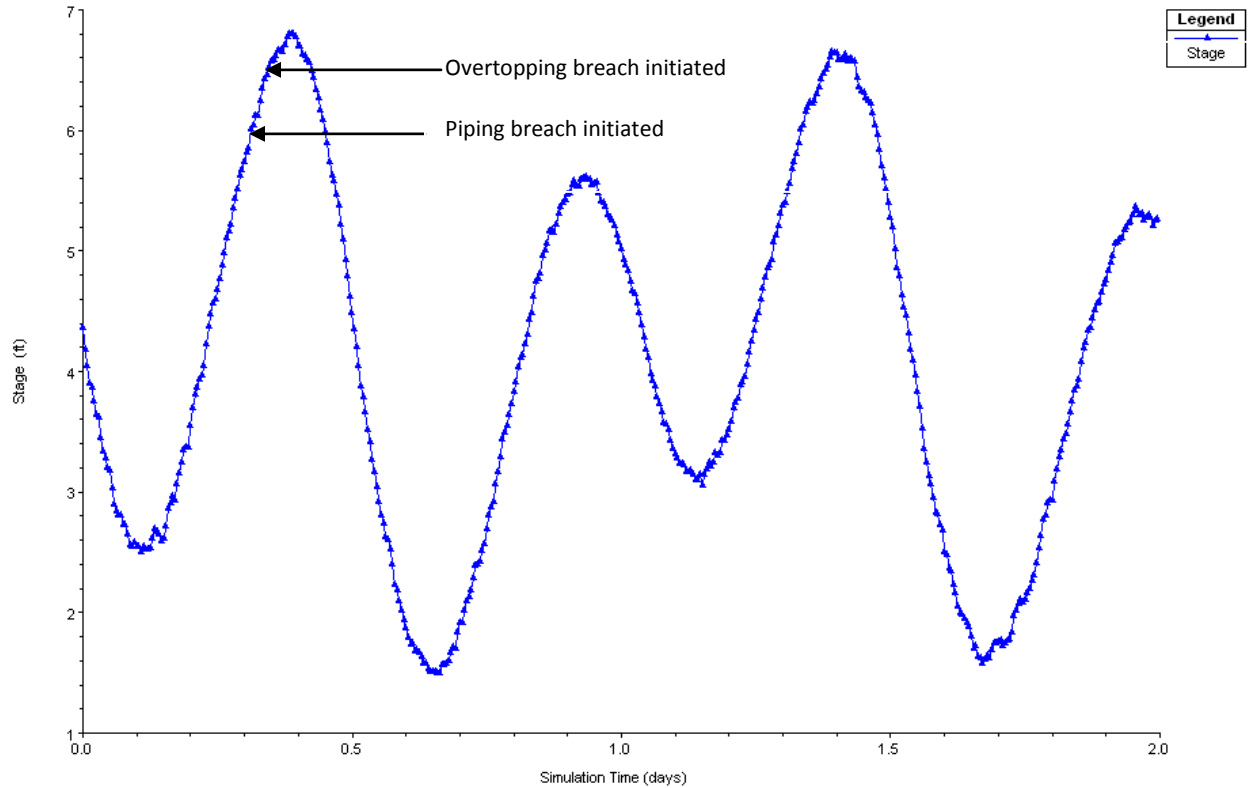


Figure 18. Tidal boundary condition used during levee breach analysis

Interior stage would be dependent on the size of the breach and failure mode. Piping breaches 100 feet wide and greater occurring under these conditions can be expected to result in interior flooding of equivalent elevation as the source. A 20 foot wide breach may result in an interior stage one foot less than the exterior stage; a 10 foot wide breach may result in an interior stage 1.5 feet less than the exterior stage. Failures due to overtopping resulted in interior stages equal to exterior stages. Based on this basic analysis, it is recommended that an existing-conditions economic analysis of likely flood damage assume that interior stage be one foot less than the exterior stage when the hydraulic loading is less than the redwood floodwall crest elevation of 6.6 ft NGVD 29; interior stage should be assumed to be equal to exterior stage when the exterior stage exceeds 6.6 ft NGVD 29. See Table 5.

Table 5. Predicted water stages in Las Gallinas Creek and Santa Venetia in the event of levee failure

Year 50 NRC Curve 1 Exceedance Probability (%)	Water Stage in Las Gallinas Creek (ft NGVD 29)	Water Stage in Santa Venetia in Event of Levee Failure (ft NGVD 29)
50	6.0	5.0
20	6.4	5.4
10	6.6	5.6
4	6.9	6.9
2	7.1	7.1
1	7.2	7.2
0.4	7.4	7.4
0.2	7.6	7.6

Note: The purpose of table 5 is to show the relationship between water stage in Santa Venetia and Las Gallinas Creek. It doesn't matter whether it's 50 year Curve 1, Historic or curve 3. Once the levee is overtopped, the water level can be assumed to be the same. If it fails prior to overtopping, the levee breach model shows that water levels in the levee protected area will be about one foot less than in the creek.

Discussion of Statistical Analysis Approaches

One aspect of this analysis that deserves some further discussion is the concept of coincident frequency versus that of joint probability: what makes the two unique, and how the statistics were applied for this analysis. One might assume that a coincident frequency analysis would yield the annual maximum stage probability for a tidal slough like the study reach of Las Gallinas Creek, by taking into consideration both riverine and coastal influences. However, this is not the case. The coincident frequency analysis yields the annual maximum riverine stage probability, which takes into account the probability of the tidal condition *at any given moment*. The probability associated with the tidal boundary condition used in the riverine analysis is based on nearly instantaneous tide observations. As a result, the tidal elevations used in the coincident frequency analysis are much lower than the annual maximum coastal still water elevations. Coastal still water elevations are based on only the highest tides observed in each year during the gage record. That is why the joint probability must be calculated in addition to the coincident frequency. The joint probability is the total annual probability of maximum water surface elevation occurring in the study area from *either*, (1) an annual maximum riverine event coinciding with any number of independent tidal boundary conditions, *or* (2) a coastal high tide event. The dominant flood risk is from coastal processes, which makes sense because the study area is in the tidal zone.

Summary

Three analyses were performed to increase understanding of flood risk in the Santa Venetia area: a coincident frequency analysis, joint probability analysis, and levee breach modeling. Risk due to coastal processes such as king tide, storm surge and sea level rise is generally much greater than risk due to stormwater runoff in Las Gallinas Creek. The joint stage-probability curve is virtually identical to the annual maximum coastal stage probability curve. In the event of levee failure prior to overtopping, the elevation of flood waters within the leveed area can be expected to be only marginally lower than the exterior water level due to the relatively small size of the leveed area. The interior flood depth will likely be the same as the exterior depth if the levee fails due to overtopping.

The results of this analysis will be used in conjunction with the levee fragility data developed by Kleinfelder (2013) to assess the probability of flooding occurring in the Santa Venetia neighborhood. A Monte Carlo-type analysis will be performed using Hydrologic Engineering Center Flood Damage Reduction Analysis (HEC-FDA) software, taking into account probabilities associated with water surface elevations, levee failure, structural, economic, and life-safety data. The economics evaluation will be reported in a separate document, Las Gallinas Preliminary Flood Damage Analysis (2013), which will provide information for helping assess whether or not federal interest may exist for a further study and development of an improvement project along Las Gallinas Creek.

References

Faber, Beth (Corps of Engineers, Hydrologic Engineering Center). Emails, October 2009 and in-person conversation, 19 October 2009. Topic: How to use statistics in coincident frequency analysis.

Faber, Beth (Corps of Engineers, Hydrologic Engineering Center). Microsoft Excel spreadsheet with basis of 3D diagrams and use of interpolation for coincident frequency analysis.

Faber, B. and S. Gibson. *Coincident Frequency Analysis for Planning and Design in Urban Areas*. Davis, CA: Army Corps of Engineers Institute for Water Resources, Hydrologic Engineering Center.

Foxgrover, A.C. and Jaffe, B.E., 2005, *South San Francisco Bay 2004 topographic lidar survey: Data overview and preliminary quality assessment*, U.S. Geological Survey Open-File Report OFR-2005-1284 [URL: <http://pubs.usgs.gov/of/2005/1284/>]

Foxgrover, A.C., Jaffe, B.E., Hovis, G.T., Martin, C.A., Hubbard, J.R., Samant, M.R., and Sullivan, S.M., 2007, *2005 Hydrographic Survey of South San Francisco Bay, California*, U.S. Geological Survey Open-File Report 2007-1169, 113 p. [URL: <http://pubs.usgs.gov/of/2007/1169/>]

Kleinfelder, Inc. 2013. *Final Geotechnical Data Report, Las Gallinas Levee System*. San Rafael, California

Letter, Joseph V (2011). *US Army Corps Response to Sea Level Rise*. Workshop on Sea Level Rise and Climate Change Impacts on Florida's Coastal Rivers. Vicksburg, MS: U.S. Army Corps of Engineers, Engineer Research and Development Center.

National Research Council. *Responding to Changes in Sea Level: Engineering Implications*. Washington, DC: The National Academies Press, 1987.

National Research Council. *Sea-Level Rise for the Coasts of California, Oregon, and Washington: Past, Present, and Future*. Washington, DC: The National Academies Press, 2012.

USACE. (1993). *EM 1110-2-1415, Hydrologic Frequency Analysis*. Department of the Army, US Army Corps of Engineers, Washington DC.

USACE. (1996). *EM 1110-2-1417, Flood-Runoff Analysis*. Department of the Army, US Army Corps of Engineers, Washington DC.

USACE. (1996). *EM 1110-2-1619, Risk-Based Analysis for Flood Damage Reduction Studies*. Department of the Army, US Army Corps of Engineers, Washington DC.

USACE. (2011). *EM 1165-2-211, Incorporating Sea-Level Change Considerations in Civil Works Programs*.

USACE-HEC. (2000). *HEC-RAS, River Analysis System, Version 4.0*. Davis, CA: US Army Corps of Engineers Institute for Water Resources, Hydrologic Engineering Center.

USACE-HEC. (2000). *HEC-FDA, Flood Damage Analysis, Version 1.2*. Davis, CA: US Army Corps of Engineers Institute for Water Resources, Hydrologic Engineering Center.

USACE-SPN. (2013). *Las Gallinas Creek Downstream Boundary Condition Analysis*. US Army Corps of Engineers, San Francisco District.

